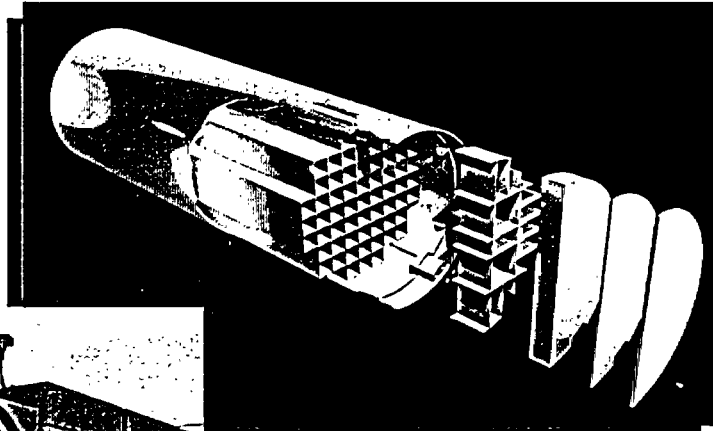
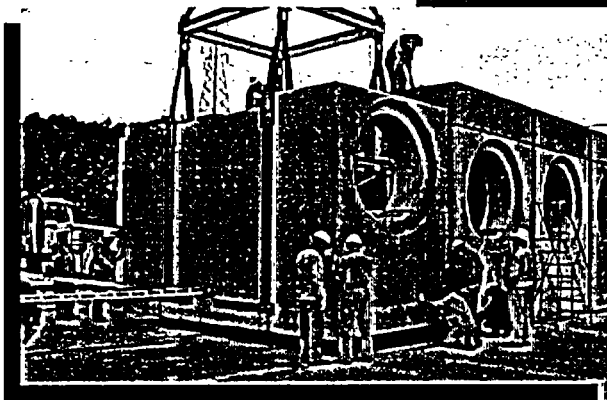


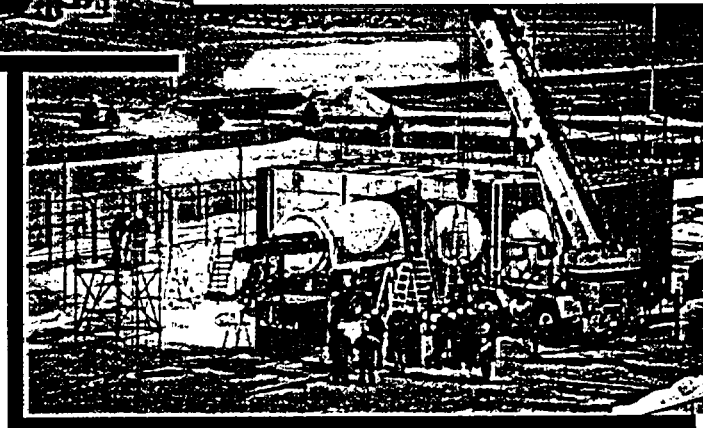
Standardized NUHOMS[®] Horizontal Modular Storage System for Irradiated Nuclear Fuel



61BT Dry Shielded Canister



HSM Placement



HSM Loading

NON-PROPRIETARY
FOR INFORMATION ONLY

FINAL SAFETY ANALYSIS REPORT

Volume 3 of 4

Appendix M

A
TRANSNUCLEAR

A
TRANSNUCLEAR

APPENDIX M,
Rev. 8
of
NUHOMS[®] FSAR
NON-PROPRIETARY

TABLE OF CONTENTS

	<u>Page</u>
M.1	General Discussion.....M.1-1
M.1.1	Introduction.....M.1-2
M.1.2	General Description of the NUHOMS [®] -32PT DSC.....M.1-3
M.1.2.1	NUHOMS [®] -32PT DSC CharacteristicsM.1-3
M.1.2.2	Operational Features.....M.1-4
M.1.2.3	Cask Contents.....M.1-5
M.1.3	Identification of Agents and Contractors.....M.1-6
M.1.4	Generic Cask Arrays.....M.1-7
M.1.5	Supplemental Data.....M.1-8
M.1.6	References.....M.1-9
M.2	Principal Design CriteriaM.2-1
M.2.1	Spent Fuel To Be StoredM.2-2
M.2.1.1	General Operating Functions.....M.2-3
M.2.2	Design Criteria for Environmental Conditions and Natural Phenomena.....M.2-4
M.2.2.1	Tornado Wind and Tornado Missiles.....M.2-4
M.2.2.2	Water Level (Flood) Design.....M.2-4
M.2.2.3	Seismic Design.....M.2-4
M.2.2.4	Snow and Ice Loading.....M.2-4
M.2.2.5	Combined Load Criteria.....M.2-4
M.2.3	Safety Protection Systems.....M.2-8
M.2.3.1	GeneralM.2-8
M.2.3.2	Protection By Multiple Confinement Barriers and SystemsM.2-8
M.2.3.3	Protection By Equipment and Instrumentation SelectionM.2-8
M.2.3.4	Nuclear Criticality Safety.....M.2-8
M.2.3.5	Radiological Protection.....M.2-9
M.2.3.6	Fire and Explosion Protection.....M.2-9
M.2.4	Decommissioning ConsiderationsM.2-10
M.2.5	Summary of NUHOMS [®] -32PT DSC Design Criteria.....M.2-11
M.2.6	References.....M.2-12
M.3	Structural Evaluation.....M.3.1-1
M.3.1	Structural DesignM.3.1-1
M.3.1.1	DiscussionM.3.1-1
M.3.1.2	Design CriteriaM.3.1-4
M.3.2	Weights and Centers of Gravity.....M.3.2-1
M.3.3	Mechanical Properties of MaterialsM.3.3-1
M.3.3.1	Material PropertiesM.3.3-1
M.3.3.2	Materials DurabilityM.3.3-2
M.3.4	General Standards for Casks.....M.3.4-1
M.3.4.1	Chemical and Galvanic Reactions.....M.3.4-1
M.3.4.2	Positive Closure.....M.3.4-7
M.3.4.3	Lifting Devices.....M.3.4-7
M.3.4.4	Heat and Cold.....M.3.4-7
M.3.5	Fuel RodsM.3.5-1

TABLE OF CONTENTS

(Continued)

		<u>Page</u>
M.3.6	Structural Analysis (Normal and Off-Normal Operations)	M.3.6-1
M.3.6.1	Normal Operation Structural Analysis	M.3.6-1
M.3.6.2	Off-Normal Load Structural Analysis	M.3.6-10
M.3.7	Structural Analysis (Accidents)	M.3.7-1
M.3.7.1	Reduced HSM Air Inlet and Outlet Shielding.....	M.3.7-1
M.3.7.2	Tornado Winds/Tornado Missile.....	M.3.7-2
M.3.7.3	Earthquake.....	M.3.7-2
M.3.7.4	Flood.....	M.3.7-6
M.3.7.5	Accidental Cask Drop	M.3.7-7
M.3.7.6	Lightning	M.3.7-14
M.3.7.7	Blockage of Air Inlet and Outlet Openings.....	M.3.7-14
M.3.7.8	DSC Leakage.....	M.3.7-14
M.3.7.9	Accident Pressurization of DSC.....	M.3.7-15
M.3.7.10	Load Combinations	M.3.7-15
M.3.7.11	Evaluation of Poison Rod Assemblies	M.3.7-16
M.3.7.12	LS-DYNA Finite Element Model Analysis	M.3.7-17
M.3.8	References.....	M.3.8-1
M.4	Thermal Evaluation	M.4-1
M.4.1	Discussion.....	M.4-1
M.4.2	Summary of Thermal Properties of Materials	M.4-4
M.4.3	Specifications for Components	M.4-9
M.4.4	Thermal Evaluation for Normal Conditions of Storage (NCS) and Transfer (NCT)	M.4-10
M.4.4.1	NUHOMS [®] -32PT DSC Thermal Models	M.4-10
M.4.4.2	Maximum Temperatures	M.4-17
M.4.4.3	Minimum Temperatures	M.4-18
M.4.4.4	Maximum Internal Pressures.....	M.4-18
M.4.4.5	Maximum Thermal Stresses	M.4-21
M.4.4.6	Evaluation of Cask Performance for Normal Conditions	M.4-21
M.4.5	Thermal Evaluation for Off-Normal Conditions	M.4-22
M.4.5.1	Off-Normal Maximum/Minimum Temperatures during Storage.....	M.4-23
M.4.5.2	Off-Normal Maximum/Minimum Temperatures during Transfer	M.4-24
M.4.5.3	Off-Normal Maximum and Minimum Temperatures During Storage/Transfer	M.4-24
M.4.5.4	Off-Normal Maximum Internal Pressure During Storage/Transfer	M.4-25
M.4.5.5	Maximum Thermal Stresses.....	M.4-25
M.4.5.6	Evaluation of Cask Performance for Off-Normal Conditions	M.4-25
M.4.6	Thermal Evaluation for Accident Conditions.....	M.4-26
M.4.6.1	Blocked Vent Accident Evaluation	M.4-26

TABLE OF CONTENTS
(Continued)

		<u>Page</u>
	M.4.6.2 Transfer Accident Evaluation.....	M.4-27
	M.4.6.3 Hypothetical Fire Accident Evaluation	M.4-27
	M.4.6.4 Fuel Cladding and Basket Materials	M.4-28
	M.4.6.5 Maximum Internal Pressures.....	M.4-29
	M.4.6.6 Evaluation of Cask Performance During Accident Conditions	M.4-29
M.4.7	Thermal Evaluation for Loading/Unloading Conditions	M.4-30
	M.4.7.1 Maximum Fuel Cladding Temperatures During Vacuum Drying.....	M.4-30
	M.4.7.2 Evaluation of Thermal Cycling of Fuel Cladding During Vacuum Drying, Helium Backfilling and Transfer Operations	M.4-30
	M.4.7.3 Reflooding Evaluation.....	M.4-31
M.4.8	Determination of Minimum Effective Fuel Conductivity	M.4-33
	M.4.8.1 Determination of Bounding Effective Fuel Thermal Conductivity	M.4-33
	M.4.8.2 Calculation of Fuel Effective Specific Heat and Density.....	M.4-36
M.4.9	Derivation of Effective Thermal Conductivity of Water Within the Neutron Shield of the OS197/OS197H Transfer Cask	M.4-38
	M.4.9.1 Validation of the Methodology Used to Determine Keff for OS197 Cask Neutron Shield.....	M.4-43
M.4.10	References.....	M.4-46
M.4.11	Example Input Files	M.4-48
	M.4.11.1 Example ANSYS Input File for Applying Heat Generation.....	M.4-48
	M.4.11.2 Example ANSYS Input File for Solar Heat Flux Application	M.4-50
M.5	Shielding Evaluation	M.5-1
	M.5.1 Discussion and Results	M.5-3
	M.5.2 Source Specification	M.5-4
	M.5.2.1 Gamma Source	M.5-5
	M.5.2.2 Neutron Source Term	M.5-6
	M.5.2.3 Axial Peaking	M.5-6
	M.5.2.4 ANISN Evaluation for Bounding Source Terms.....	M.5-6
	M.5.3 Model Specification.....	M.5-9
	M.5.3.1 Material Densities.....	M.5-9
M.5.4	Shielding Evaluation.....	M.5-10
	M.5.4.1 Computer Programs.....	M.5-10
	M.5.4.2 Spatial Source Distribution	M.5-10
	M.5.4.3 Cross Section Data	M.5-11
	M.5.4.4 Flux-to-Dose-Rate Conversion.....	M.5-11
	M.5.4.5 Methodology	M.5-11
	M.5.4.6 Assumptions	M.5-12
	M.5.4.7 Source Region Homogenization.....	M.5-13

TABLE OF CONTENTS
(Continued)

	<u>Page</u>
M.5.4.8 HSM Dose Rates for the 32PT-S125/32PT-L125 Configuration.....	M.5-15
M.5.4.9 HSM Models for the 32PT-S100/32PT-L100 DSC Configuration.....	M.5-16
M.5.4.10 Data Reduction and HSM Dose Rate Results for the 32PT-S125/32PT-L125 DSC Configuration	M.5-16
M.5.4.11 HSM Dose Rates for the 32PT-S100/32PT-L100 DSC Configuration.....	M.5-17
M.5.4.12 TC Dose Rates for the 32PT-S125/32PT-L125 DSC Configuration.....	M.5-18
M.5.4.13 Cask Dose Rates for 32PT-S100/32PT-L100 DSC Configuration.....	M.5-19
M.5.4.14 Supporting 3-D Analysis	M.5-20
M.5.5 Appendix.....	M.5-21
M.5.5.1 Sample SAS2H/ORIGEN-S Input File	M.5-21
M.5.5.2 Sample HSM DORT Model (RZ Roof Neutron Model).....	M.5-23
M.5.5.3 Sample TC DORT Model (RZ Transfer Configuration).....	M.5-29
M.5.5.4 Sample MCNP Model	M.5-34
M.5.5.5 Sample ANISN Model (HSM -1.2 kW - 3.3 wt%/45,000MWd/MTU 6-yr cooled).....	M.5-56
M.5.6 References.....	M.5-61
M.6 Criticality Evaluation.....	M.6-1
M.6.1 Discussion and Results	M.6-2
M.6.2 Package Fuel Loading.....	M.6-3
M.6.3 Model Specification	M.6-4
M.6.3.1 Description of Calculational Model	M.6-4
M.6.3.2 Package Regional Densities	M.6-5
M.6.4 Criticality Calculations	M.6-6
M.6.4.1 Calculational Method	M.6-6
M.6.4.2 Fuel Loading Optimization	M.6-8
M.6.4.3 Studies with Radial Variation of Enrichment.....	M.6-10
M.6.4.4 Determination of the Maximum Initial Enrichment for each Fuel Class and PRA Configuration	M.6-10
M.6.4.5 Criticality Results	M.6-12
M.6.5 Critical Benchmark Experiments.....	M.6-13
M.6.5.1 Benchmark Experiments and Applicability	M.6-13
M.6.5.2 Results of the Benchmark Calculations.....	M.6-14
M.6.6 Appendix.....	M.6-15
M.6.6.1 References	M.6-15
M.6.6.2 KENO Plots of Various Cases.....	M.6-16
M.6.6.3 Example CSAS25 Input Files (based on the 20 poison plate basket configuration).....	M.6-16
M.6.6.4 Design Basis Case CSAS25 Input Deck	M.6-25

TABLE OF CONTENTS
(Continued)

		<u>Page</u>
	M.6.6.5	Example CSAS25 Input Files (based on the 16 poison plate basket configuration (we1734bP-16P250-0065.in).....M.6-29a
	M.6.6.6	Example CSAS25 Input Files WE 15x15 in (based on the 24 poison plate basket configuration – worst case WE 15x15 with no BPRAs and 8 PRAs) (we1546-var-08pra-0080.in).....M.6-29e
M.7	Confinement	M.7-1
	M.7.1	Confinement Boundary.....M.7-2
	M.7.1.1	Confinement Vessel.....M.7-2
	M.7.1.2	Confinement Penetrations.....M.7-3
	M.7.1.3	Seals and Welds.....M.7-3
	M.7.1.4	Closure.....M.7-3
	M.7.2	Requirements for Normal Conditions of Storage.....M.7-4
	M.7.2.1	Release of Radioactive Material.....M.7-4
	M.7.2.2	Pressurization of Confinement Vessel.....M.7-4
	M.7.3	Confinement Requirements for Hypothetical Accident Conditions.....M.7-5
	M.7.3.1	Fission Gas Products.....M.7-5
	M.7.3.2	Release of Contents.....M.7-5
	M.7.4	References.....M.7-6
M.8	Operating Systems.....	M.8-1
	M.8.1	Procedures for Loading the Cask.....M.8-2
	M.8.1.1	Preparation of the TC and DSC.....M.8-2
	M.8.1.2	DSC Fuel Loading.....M.8-3
	M.8.1.3	DSC Drying and Backfilling.....M.8-5
	M.8.1.4	DSC Sealing Operations.....M.8-7
	M.8.1.5	TC Downending and Transport to ISFSI.....M.8-8
	M.8.1.6	DSC Transfer to the HSM.....M.8-9
	M.8.1.7	Monitoring Operations.....M.8-10
	M.8.2	Procedures for Unloading the Cask.....M.8-15
	M.8.2.1	DSC Retrieval from the HSM.....M.8-15
	M.8.2.2	Removal of Fuel from the DSC.....M.8-15
	M.8.3	Identification of Subjects for Safety Analysis.....M.8-24
	M.8.4	Fuel Handling Systems.....M.8-24
	M.8.5	Other Operating Systems.....M.8-24
	M.8.6	Operation Support System.....M.8-24
	M.8.7	Control Room and/or Control Areas.....M.8-24
	M.8.8	Analytical Sampling.....M.8-24
	M.8.9	References.....M.8-25
M.9	Acceptance Tests and Maintenance Program.....	M.9-1
	M.9.1	Acceptance Tests.....M.9-1
	M.9.1.1	Visual Inspection.....M.9-1
	M.9.1.2	Structural Tests.....M.9-1
	M.9.1.3	Leak Tests.....M.9-1

TABLE OF CONTENTS

(Continued)

	<u>Page</u>
M.9.1.4	Component Tests.....M.9-2
M.9.1.5	Shielding Integrity TestsM.9-2
M.9.1.6	Thermal Acceptance TestsM.9-2
M.9.1.7	Poison AcceptanceM.9-2
M.9.2	Maintenance ProgramM.9-10
M.9.3	References.....M.9-11
M.10	Radiation Protection.....M.10-1
M.10.1	Occupational ExposureM.10-1
M.10.2	Off-Site Dose CalculationsM.10-3
M.10.2.1	Activity Calculations.....M.10-5
M.10.2.2	Dose Rates.....M.10-5
M.10.3	References.....M.10-7
M.11	Accident Analyses.....M.11-1
M.11.1	Off-Normal Operations.....M.11-2
M.11.1.1	Off-Normal Transfer Loads.....M.11-2
M.11.1.2	Extreme TemperaturesM.11-3
M.11.1.3	Off-Normal Releases of Radionuclides.....M.11-3
M.11.1.4	Radiological Impact from Off-Normal OperationsM.11-4
M.11.2	Postulated Accidents.....M.11-5
M.11.2.1	Reduced HSM Air Inlet and Outlet Shielding.....M.11-5
M.11.2.2	Earthquake.....M.11-5
M.11.2.3	Extreme Wind and Tornado Missiles.....M.11-6
M.11.2.4	Flood.....M.11-7
M.11.2.5	Accidental TC DropM.11-7
M.11.2.6	LightningM.11-8
M.11.2.7	Blockage of Air Inlet and Outlet Openings.....M.11-8
M.11.2.8	DSC Leakage.....M.11-9
M.11.2.9	Accident Pressurization of DSC.....M.11-9
M.11.2.10	Fire and Explosion.....M.11-10
M.11.3	References.....M.11-12
M.12	Conditions for Cask Use - Operating Controls and Limits or Technical SpecificationsM.12-1
M.13	Quality AssuranceM.13-1
M.14	Decommissioning.....M.14-1

LIST OF TABLES

	<u>Page</u>
Table M.1-1	Nominal Dimensions and Weight of the NUHOMS [®] -32PT DSCM.1-10
Table M.2-1	Intact PWR Fuel Assembly CharacteristicsM.2-13
Table M.2-2	PWR Fuel Assembly Design CharacteristicsM.2-14
Table M.2-3	Initial Enrichment and Number of PRAs for Various Fuel Assembly TypesM.2-15
Table M.2-4	Poison Rod Assembly (PRA) DescriptionM.2-16
Table M.2-5	PWR Fuel Qualification Table for 1.2 kW per Assembly for the NUHOMS [®] -32PT DSC (Fuel w/o BPRAs)M.2-17
Table M.2-6	PWR Fuel Qualification Table for 0.87 kW per Assembly for the NUHOMS [®] -32PT DSC (Fuel w/o BPRAs)M.2-18
Table M.2-7	PWR Fuel Qualification Table for 0.7 kW per Assembly for the NUHOMS [®] -32PT DSC (Fuel w/o BPRAs)M.2-19
Table M.2-8	PWR Fuel Qualification Table for 0.63 kW per Assembly for the NUHOMS [®] -32PT DSC (Fuel w/o BPRAs)M.2-20
Table M.2-9	PWR Fuel Qualification Table for 0.6 kW per Assembly for the NUHOMS [®] -32PT DSC (Fuel w/o BPRAs)M.2-21
Table M.2-10	PWR Fuel Qualification Table for 1.2 kW per Assembly for the NUHOMS [®] -32PT DSC (Fuel w/ BPRAs)M.2-22
Table M.2-11	PWR Fuel Qualification Table for 0.87 kW per Assembly for the NUHOMS [®] -32PT DSC (Fuel w/ BPRAs)M.2-23
Table M.2-12	PWR Fuel Qualification Table for 0.7 kW per Assembly for the NUHOMS [®] -32PT DSC (Fuel w/ BPRAs)M.2-24
Table M.2-13	PWR Fuel Qualification Table for 0.63 kW per Assembly for the NUHOMS [®] -32PT DSC (Fuel w/ BPRAs)M.2-25
Table M.2-14	PWR Fuel Qualification Table for 0.6 kW per Assembly for the NUHOMS [®] -32PT DSC (Fuel w/ BPRAs)M.2-26
Table M.2-15	Summary of 32PT-DSC Load Combinations.....M.2-27
Table M.2-16	Summary of Stress Criteria for Subsection NB Pressure Boundary Components.....M.2-31
Table M.2-17	Summary of Stress Criteria for Subsection NG ComponentsM.2-32
Table M.2-18	Classification of NUHOMS [®] -32PT DSC Components.....M.2-33
Table M.2-19	Additional Design Criteria for NUHOMS [®] -32PT DSCM.2-34
Table M.2-20	Summary of NUHOMS [®] -32PT Component Design Loadings ⁽¹⁾M.2-35
Table M.3.1-1	Alternatives to the ASME Code for the NUHOMS [®] -32PT DSC Confinement BoundaryM.3.1-6
Table M.3.1-2	Alternatives to the ASME Code Exceptions for the NUHOMS [®] -32PT DSC Basket AssemblyM.3.1-8
Table M.3.2-1	Summary of the NUHOMS [®] -32PT System Component Nominal Weights.....M.3.2-2
Table M.3.3-1	ASME Code Materials Data For SA-240 Type 304 Stainless SteelM.3.3-3
Table M.3.3-2	Materials Data For ASTM A36 Steel.....M.3.3-4
Table M.3.3-3	ASME Code Materials Data For SA-240 Type XM-19 Stainless Steel.....M.3.3-5
Table M.3.3-4	ASME Code Properties for 6061 AluminumM.3.3-6
Table M.3.3-5	Analysis Properties for Aluminum Transition RailsM.3.3-7

LIST OF TABLES
(Continued)

		<u>Page</u>
Table M.3.3-6	Additional Material Properties	M.3.3-8
Table M.3.4-1	Summary of Thermal Stress Results - 32PT Basket with Steel Transition Rails	M.3.4-13
Table M.3.4-2	Summary of Thermal Stress Results - 32PT Basket with Aluminum Transition Rails	M.3.4-14
Table M.3.6-1	NUHOMS [®] Normal Operating Loading Identification.....	M.3.6-13
Table M.3.6-2	Maximum NUHOMS [®] -32PT DSC Shell Assembly Stresses for Normal and Off-Normal Loads	M.3.6-14
Table M.3.6-3	NUHOMS [®] -32PT Basket Model Components, Element Types and Materials	M.3.6-16
Table M.3.6-4	Material Properties Used in Normal Condition 32PT Basket Analyses	M.3.6-17
Table M.3.6-5	Summary of Results for 32PT Basket Assembly Deadweight Analyses	M.3.6-18
Table M.3.6-6	Summary of Results for 32PT Basket Assembly On-Site Handling (2.0g Loads).....	M.3.6-19
Table M.3.6-7	32PT Basket Analyses Used to Determine On-Site Handling Loads	M.3.6-20
Table M.3.6-8	NUHOMS [®] Off-Normal Operating Loading Identification.....	M.3.6-21
Table M.3.7-1	Maximum NUHOMS [®] -32PT DSC Stresses for Drop Accident Loads	M.3.7-18
Table M.3.7-2	List of Drop Condition ANSYS Stress Analyses of the 32PT Basket Assembly	M.3.7-19
Table M.3.7-3	Summary of Material Properties for Drop Accident Analyses of the 32PT Basket Assembly	M.3.7-20
Table M.3.7-4	32PT Basket, Enveloping Stress Results - 75g Side Drops	M.3.7-21
Table M.3.7-5	32PT Basket, Enveloping Stress Results - 60g Part 71 End Drop	M.3.7-22
Table M.3.7-6	Drop Condition Stability Analyses for the 32PT Basket Assembly	M.3.7-23
Table M.3.7-7	Summary of 32PT Basket Stability Analysis -- Side Drops	M.3.7-24
Table M.3.7-8	NUHOMS [®] -32PT DSC Enveloping Load Combination Results for Normal and Off-Normal Loads	M.3.7-25
Table M.3.7-9	NUHOMS [®] -32PT DSC Enveloping Load Combination Results for Accident Loads.....	M.3.7-26
Table M.3.7-10	NUHOMS [®] -32PT DSC Enveloping Load Combination Results for Accident Loads.....	M.3.7-27
Table M.3.7-11	DSC Enveloping Load Combination Table Notes	M.3.7-28
Table M.4-1	Fuel Cladding Long-Term Storage Temperatures.....	M.4-52
Table M.4-2	Fuel Cladding Short-Term Normal Condition Maximum Temperatures.....	M.4-53
Table M.4-3	DSC Basket Assembly Maximum Normal Operating Component Temperatures; Configuration 1	M.4-54
Table M.4-4	DSC Basket Assembly Maximum Normal Operating Component Temperatures; Configuration 2	M.4-55
Table M.4-5	DSC Basket Assembly Maximum Normal Operating Component Temperatures; Configuration 3	M.4-56
Table M.4-6	32PT DSC Initial Helium Fill Molar Quantities	M.4-57
Table M.4-7	32PT DSC Maximum Normal Operating Condition Pressures	M.4-58
Table M.4-8	Off-Normal Event Fuel Cladding Maximum Temperatures.....	M.4-59

LIST OF TABLES
(Continued)

		<u>Page</u>
Table M.4-9	Off-Normal Event DSC Basket Assembly Maximum Component Temperatures; Configuration 1	M.4-60
Table M.4-10	Off-Normal Event DSC Basket Assembly Maximum Component Temperatures; Configuration 2	M.4-61
Table M.4-11	Off-Normal Event DSC Basket Assembly Maximum Component Temperatures; Configuration 3	M.4-62
Table M.4-12	32PT DSC Maximum Off-Normal Operating Condition Pressures.....	M.4-63
Table M.4-13	Accident Fuel Cladding Maximum Temperatures	M.4-64
Table M.4-14	DSC Basket Assembly Maximum Accident Condition Component Temperatures;.....	M.4-65
Table M.4-15	32PT DSC Maximum Accident Condition Pressures	M.4-66
Table M.4-16	Maximum Component Temperatures for the Hypothetical Fire Accident Case for the NUHOMS [®] -32PT DSC in the TC	M.4-67
Table M.4-17	Vacuum Drying Fuel Cladding Maximum Temperatures.....	M.4-68
Table M.4-18	DSC Basket Assembly Maximum Component Temperatures During Vacuum Drying at 33 hours ⁽²⁾	M.4-69
Table M.5-1	PWR Fuel Assembly Design Characteristics ⁽³⁾	M.5-62
Table M.5-2	Burnable Poison Rod Assembly Weight Data	M.5-63
Table M.5-3	Dose Rates Due to the 32 PWR Fuel Assemblies with BPRAs	M.5-64
Table M.5-4	Summary of HSM Dose Rates	M.5-65
Table M.5-5	Summary of Onsite TC Dose Rates (Maximum ⁽¹⁾).....	M.5-66
Table M.5-6	PWR Fuel Assembly Materials Weights.....	M.5-67
Table M.5-7	Elemental Composition of LWR Fuel-Assembly Structural Materials.....	M.5-68
Table M.5-8	Flux Correct Factors By Assembly Region.....	M.5-69
Table M.5-9	Gamma Source Term for 41 GWd/MTU, 3.1 wt. % U-235 and 5-Year Cooled Fuel	M.5-70
Table M.5-10	Gamma Source Term for 30 GWd/MTU, 2.5 wt. % U-235 and 8-Year Cooled Fuel	M.5-71
Table M.5-11	Gamma Source Term for 45 GWd/MTU, 3.3 wt. % U-235 and 23-Year Cooled Fuel	M.5-72
Table M.5-12	Design-Basis BPRA Source Terms.....	M.5-73
Table M.5-13	Inner/Outer Heat Load Zone Region Volumes	M.5-74
Table M.5-14	Total Neutron Source Summary.....	M.5-75
Table M.5-15	Source Term Peaking Summary.....	M.5-76
Table M.5-16	Shielding Material Densities	M.5-77
Table M.5-17	Neutron Source for 45 GWd/MTU 3.3 wt. % U-235 16 Year Cooled Fuel.....	M.5-79
Table M.5-18	Gamma Source Term for 45 GWd/MTU, 3.3 wt. % U-235 and 16-Year Cooled Fuel	M.5-80
Table M.5-19	Explicit Model Material Densities	M.5-81
Table M.5-20	Smeared Model Material Densities	M.5-82
Table M.5-21	Stainless Steel, Aluminum and Air Material Densities.....	M.5-83
Table M.5-22	MCNP Explicit and Smeared Model Results	M.5-84

LIST OF TABLES
(Continued)

		<u>Page</u>
Table M.5-23	HSM Accident Dose Rates.....	M.5-85
Table M.5-24	3-D vs 2-D Comparison for 32PT-S100/32PT-L100 DSC Configuration	M.5-86
Table M.5-25	Comparison of Calculated Versus Measured Dose Rates for DSC 45.....	M.5-87
Table M.5-26	Comparison of Calculated Versus Measured Dose Rates for DSC 46.....	M.5-88
Table M.5-27	ANISN Material Densities	M.5-89
Table M.5-28	1.2 kW Fuel in the HSM	M.5-90
Table M.5-29	1.2 kW Fuel in the Transfer Cask.....	M.5-91
Table M.5-30	0.87 kW Fuel in the HSM	M.5-92
Table M.5-31	0.87 kW Fuel in the Transfer Cask.....	M.5-93
Table M.5-32	0.7 kW Fuel in the HSM	M.5-94
Table M.5-33	0.7 kW Fuel in the Transfer Cask.....	M.5-95
Table M.5-34	0.63 kW Fuel in the HSM	M.5-96
Table M.5-35	0.63 kW Fuel in the Transfer Cask.....	M.5-97
Table M.5-36	0.6 kW Fuel in the HSM	M.5-98
Table M.5-37	0.6 kW Fuel in the Transfer Cask.....	M.5-99
Table M.6-1	Maximum Initial Enrichment For Each Configuration	M.6-30
Table M.6-2	Authorized Contents for NUHOMS [®] -32PT System	M.6-31
Table M.6-3	Parameters For PWR Assemblies ⁽³⁾	M.6-32
Table M.6-4	Poison Rod Assembly (PRA) Description	M.6-33
Table M.6-5	Material Property Data	M.6-34
Table M.6-6	Most Reactive Fuel Type	M.6-35
Table M.6-7	Transition Rail Material Evaluation Results	M.6-36
Table M.6-8	Fuel Clad OD Evaluation Results	M.6-37
Table M.6-9	Poison/Aluminum and Aluminum Plate Thickness Evaluation Results	M.6-38
Table M.6-10	Basket Grid Structure Plate/Tube Thickness Evaluation Results	M.6-39
Table M.6-11	Fuel Compartment Width Evaluation Results.....	M.6-40
Table M.6-12	Assembly-to-Assembly Pitch Evaluation.....	M.6-41
Table M.6-13	WE 17x17 Class Assembly without BPRAs Results (20 Poison Plate).....	M.6-42
Table M.6-14	WE 17x17 Class Assembly with BPRAs Results (20 Poison Plate).....	M.6-43
Table M.6-15	B&W 15x15 Class Assembly without BPRAs Results (20 Poison Plate)	M.6-44
Table M.6-16	B&W 15x15 Class Assembly with BPRAs Results (20 Poison Plate)	M.6-45
Table M.6-17	CE 15x15 Class Assembly without BPRAs Results (20 Poison Plate).....	M.6-46
Table M.6-18	WE 15x15 Class Assembly without BPRAs Results (20 Poison Plate).....	M.6-47
Table M.6-19	CE 14x14 Class Assembly without BPRAs Results (20 Poison Plate).....	M.6-48
Table M.6-20	WE 14x14 Class Assembly without BPRAs Results (20 Poison Plate).....	M.6-49
Table M.6-21	Criticality Results	M.6-50
Table M.6-22	Benchmarking Results.....	M.6-51
Table M.6-23	USL-1 Results	M.6-55
Table M.6-24	USL Determination for Criticality Analysis	M.6-56
Table M.6-25	Enrichment Data for Loading Pattern 1	M.6-56a
Table M.6-26	Results for the Exxon/ANF 15x15 Fuel Assembly	M.6-56b
Table M.6-27	Results for the WE 17x17 Class Fuel Assembly without BPRAs (16 Poison Plates)	M.6-56d

LIST OF TABLES
(Continued)

		<u>Page</u>
Table M.6-28	Results for the WE 17x17 Class Fuel Assembly with BPRAs (16 Poison Plates)	M.6-56e
Table M.6-29	Results for the WE 17x17 Class Fuel Assembly without BPRAs (24 Poison Plates)	M.6-56f
Table M.6-30	Results for the WE 17x17 Class Fuel Assembly with BPRAs (24 Poison Plates)	M.6-56g
Table M.6-31	Results for the B&W 15x15 Class Fuel Assembly without BPRAs (16 Poison Plates)	M.6-56h
Table M.6-32	Results for the B&W 15x15 Class Fuel Assembly with BPRAs (16 Poison Plates)	M.6-56i
Table M.6-33	Results for the B&W 15x15 Class Fuel Assembly without BPRAs (24 Poison Plates)	M.6-56j
Table M.6-34	Results for the B&W 15x15 Class Fuel Assembly with BPRAs (24 Poison Plates)	M.6-56k
Table M.6-35	Results for the CE 15x15 Class Fuel Assembly without BPRAs (16 Poison Plates)	M.6-56l
Table M.6-36	Results for the WE 15x15 Class Fuel Assembly without BPRAs (16 Poison Plates)	M.6-56m
Table M.6-37	Results for the WE 15x15 Class Fuel Assembly without BPRAs (24 Poison Plates)	M.6-56n
Table M.6-38	Results for the CE 14x14 Class Fuel Assembly without BPRAs (16 Poison Plates)	M.6-56o
Table M.6-39	Results for the CE 14x14 Class Fuel Assembly without BPRAs (24 Poison Plates)	M.6-56p
Table M.6-40	Results for the WE 14x14 Class Fuel Assembly without BPRAs (16 Poison Plates)	M.6-56q
Table M.10-1	Occupational Exposure Summary (32PT-S125/32PT-L125 DSC configuration)	M.10-8
Table M.10-2	Occupational Exposure Summary (32PT-S100/32PT-L100 DSC configuration)	M.10-9
Table M.10-3	Total Annual Exposure	M.10-10
Table M.10-4	HSM Gamma-Ray Spectrum Calculation Results	M.10-11
Table M.10-5	HSM Neutron Spectrum Calculations	M.10-12
Table M.10-6	Summary of ISFSI Surface Activities	M.10-13
Table M.10-7	MCNP Front Detector Dose Rates for 2x10 Array	M.10-14
Table M.10-8	MCNP Back Detector Dose Rates for the Two 1x10 Arrays	M.10-15
Table M.10-9	MCNP Side Detector Dose Rates	M.10-16
Table M.11-1	Comparison of Total Dose Rates for HSM with and without Adjacent HSM Shielding Effects	M.11-13
Table M.11-2	TC Bounding Accident Dose Rate Results	M.11-14

LIST OF FIGURES

		<u>Page</u>
Figure M.1-1	NUHOMS®-32PT DSC Components	M.1-11
Figure M.1-2	Poison Rod Assemblies (PRAs)	M.1-12
Figure M.2-1	Heat Load Zoning Configuration 1	M.2-37
Figure M.2-2	Heat Load Zoning Configuration 2	M.2-38
Figure M.2-3	Heat Load Zoning Configuration 3	M.2-39
Figure M.2-4	Required PRA Locations for Configurations with Four PRAs (Basket Type B)	M.2-40
Figure M.2-5	Required PRA Locations for Configurations with Eight PRAs (Basket Type C)	M.2-41
Figure M.2-6	Required PRA Locations for Configurations with Sixteen PRAs (Basket Type D)	M.2-42
Figure M.3.1-1	32PT-DSC Pressure and Confinement Boundaries	M.3.1-9
Figure M.3.4-1	Potential Versus pH Diagram for Aluminum-Water System	M.3.4-15
Figure M.3.4-2	32PT Basket with Steel Transition Rails, Temperatures and Stress Intensities, -40°F in Cask	M.3.4-16
Figure M.3.4-3	32PT Basket with Steel Transition Rails, Temperatures and Stress Intensities, 117°F in Cask	M.3.4-17
Figure M.3.4-4	32PT Basket with Aluminum Transition Rails, Temperatures and Stress Intensities, -40°F in Cask	M.3.4-18
Figure M.3.4-5	32PT Basket with Aluminum Transition Rails, Temperatures and Stress Intensities, 117°F in Cask	M.3.4-19
Figure M.3.6-1	32PT Basket Model with Steel Transition Rails	M.3.6-22
Figure M.3.6-2	32PT Basket Model with Steel Transition Rails	M.3.6-23
Figure M.3.6-3	32PT Basket Model with Aluminum Transition Rails (1-Piece R90)	M.3.6-24
Figure M.3.6-4	32PT Basket Model with Aluminum Transition Rails (1-Piece R90)	M.3.6-26
Figure M.3.6-5	Location and Numbering of Stress Cuts for 32PT Basket Analyses	M.3.6-28
Figure M.3.6-6	Deadweight Stress Intensity, 32PT Basket with Steel Transition Rails (Support Rails at ±18.5°)	M.3.6-29
Figure M.3.6-7	Deadweight + Thermal Stress Intensity, 32PT Basket with Steel Transition Rails (Support Rails at ±18.5°)	M.3.6-30
Figure M.3.6-8	Deadweight Stress Intensity, 32PT Basket with Steel Transition Rails (Support Rails at ±30°)	M.3.6-31
Figure M.3.6-9	Deadweight + Thermal Stress Intensity, 32PT Basket with Steel Transition Rails (Support Rails at □□°)	M.3.6-32
Figure M.3.6-10	Deadweight Stress Intensity, 32PT Basket with Aluminum Transition Rails (1- Piece R90) (Support Rails at ±18.5°)	M.3.6-33
Figure M.3.6-11	Deadweight + Thermal Stress Intensity, 32PT Basket with Aluminum Transition Rails (1-Piece R90) (Support Rails at ±18.5°)	M.3.6-35
Figure M.3.6-12	Deadweight Stress Intensity, 32PT Basket with Aluminum Transition Rails (1-Piece R90) (Support Rails at ±30°)	M.3.6-37
Figure M.3.6-13	Deadweight +Thermal Stress Intensity, 32PT Basket with Aluminum Transition Rails (1-Piece R90) (Support Rails at ±30°)	M.3.6-39
Figure M.3.7-1	DSC Lift-Off Evaluation	M.3.7-29

LIST OF FIGURES
(Continued)

		<u>Page</u>
Figure M.3.7-2	0° Side Drop Stress Intensity, 32PT Basket with Steel Transition Rails (Support Rails at ±18.5°).....	M.3.7-30
Figure M.3.7-3	0° Side Drop Stress Intensity, 32PT Basket with Aluminum Transition Rails (1-Piece R90) (Support Rails at ±18.5°).....	M.3.7-31
Figure M.3.7-4	45° Side Drop Stress Intensity, 32PT Basket with Steel Transition Rails (Support Rails at ±18.5°).....	M.3.7-33
Figure M.3.7-5	45° Side Drop Stress Intensity, 32PT Basket with Aluminum Transition Rails (1-Piece R90) (Support Rails at ±18.5°).....	M.3.7-34
Figure M.3.7-6	Displaced Shape at 113g, LS-DYNA Confirmatory Stability Analysis for 0° Side Drop with Steel Transition Rails (Support Rails at ±18.5°).....	M.3.7-36
Figure M.3.7-7	Displacement Time History, LS-DYNA Confirmatory Stability Analysis for 0° Side Drop with Steel Transition Rails.....	M.3.7-37
Figure M.3.7-8	Displaced Shape at 124g, LS-DYNA Confirmatory Stability Analysis for 180° Side Drop with Steel Transition Rails.....	M.3.7-38
Figure M.3.7-9	Displacement Time History, LS-DYNA Confirmatory Stability Analysis for 180° Side Drop with Steel Transition Rails.....	M.3.7-39
Figure M.3.7-10	LS-DYNA 32PT Basket Model with Aluminum Transition Rails (3-Piece R90).....	M.3.7-40
Figure M.3.7-11	LS-DYNA 32PT Basket Model with Aluminum Transition Rails (3-Piece R90) – Detailed View.....	M.3.7-41
Figure M.3.7-12	32PT Basket with Aluminum Transition Rails Temperature Distribution, 100°F in Cask.....	M.3.7-42
Figure M.4-1	Heat Load Zoning Configuration 1, Maximum Decay Heat for Various Assemblies.....	M.4-70
Figure M.4-2	Heat Load Zoning Configuration 2, Maximum Decay Heat for Various Assemblies.....	M.4-71
Figure M.4-3	Heat Load Zoning Configuration 3, Maximum Decay Heat for Various Assemblies.....	M.4-72
Figure M.4-4	Axial Heat Profile for PWR Fuel.....	M.4-73
Figure M.4-5	32PT-DSC Thermal ANSYS Model, Isometric View.....	M.4-74
Figure M.4-6	32PT DSC Thermal ANSYS Model, Cross-Section View.....	M.4-75
Figure M.4-7	Thermal Model of DSC in HSM.....	M.4-76
Figure M.4-8	Thermal Model of TC.....	M.4-77
Figure M.4-9	Results for 100°F Storage Case With Heat Load Zoning Configuration 3.....	M.4-78
Figure M.4-10	Results for 100°F Transfer Case With Heat Load Zoning Configuration 3.....	M.4-79
Figure M.4-11	Results for 117°F Storage Case With Heat Load Zoning Configuration 3.....	M.4-80
Figure M.4-12	Results for 117°F Transfer Case With Heat Load Zoning Configuration 3.....	M.4-81
Figure M.4-13	Results for Blocked Vent Case With Heat Load Zoning Configuration 3 at 40 Hours.....	M.4-82
Figure M.4-14	NUHOMS®-32PT DSC and TC Temperature Response to 15 Minute Fire Accident Conditions.....	M.4-83

LIST OF FIGURES
(Continued)

		<u>Page</u>
Figure M.4-15	Time-History Profile of the Maximum Fuel Cladding Temperature during Blocked Vent Case, Configuration #3	M.4-84
Figure M.4-16	Maximum Fuel Temperature during Vacuum Drying with Heat Load Zoning Configuration 3	M.4-85
Figure M.4-17	Temperature Distribution from Bottom to Top of DSC at Cross-Section with Highest Temperatures, 70°F HSM Storage Case (Configuration 3).....	M.4-86
Figure M.4-18	Finite Element Model of B&W 15x15 Fuel Assembly.....	M.4-87
Figure M.4-19	Fuel Axial Effective Conductivity	M.4-88
Figure M.4-20	Fuel Transverse Effective Conductivity in Helium.....	M.4-89
Figure M.4-21	Fuel Transverse Effective Conductivity in Vacuum	M.4-90
Figure M.4-22	Alternate Basket Poison/Aluminum Configuration	M.4-91
Figure M.4-23	Finite Element Models of Alternate Basket Configurations	M.4-92
Figure M.5-1	Explicit MCNP Model – Radial View	M.5-100
Figure M.5-2	Explicit and Smearred MCNP Model – Axial View	M.5-101
Figure M.5-3	Smearred MCNP Model – Radial View	M.5-102
Figure M.5-4	HSM Roof Model Geometry (32PT-S125/32PT-L125 DSC Configuration)	M.5-103
Figure M.5-5	HSM Floor Model Geometry (32PT-S125/32PT-L125 DSC Configuration)	M.5-104
Figure M.5-6	HSM Side Model Geometry (32PT-S125/32PT-L125 DSC Configuration)	M.5-105
Figure M.5-7	HSM Top Model Geometry (32PT-S125/32PT-L125 and 32PT-S100/32PT-L100 DSC Configuration).....	M.5-106
Figure M.5-8	HSM Roof Model Geometry (32PT-S100/32PT-L100 DSC Configuration)	M.5-107
Figure M.5-9	HSM Front Wall Dose Rate Distribution (32PT-S125/32PT-L125 DSC Configuration)	M.5-108
Figure M.5-10	Geometry for Front Wall Average Dose Rate Calculation	M.5-109
Figure M.5-11	HSM Back Wall Dose Rate Distribution (32PT-S125/32PT-L125 DSC Configuration)	M.5-110
Figure M.5-12	HSM Roof Dose Rate Distribution Perpendicular to DSC Axis(32PT-S125/32PT-L125 DSC Configuration).....	M.5-111
Figure M.5-13	HSM Roof Dose Rate Distribution Parallel to DSC Axis (32PT-S125/32PT-L125 DSC Configuration).....	M.5-112
Figure M.5-14	Surface Average Calculation Geometry	M.5-113
Figure M.5-15	HSM Front Wall Dose Rate Distribution (32PT-S100/32PT-L100 DSC Configuration)	M.5-114
Figure M.5-16	HSM Back Wall Dose Rate Distribution (32PT-S100/32PT-L100 DSC Configuration)	M.5-115
Figure M.5-17	HSM Roof Dose Rate Distribution Perpendicular to DSC Axis (32PT-S100/32PT-L100 DSC Configuration).....	M.5-116

LIST OF FIGURES
(Continued)

		<u>Page</u>
Figure M.5-18	HSM Roof Dose Rate Distribution Parallel to DSC Axis (32PT-S100/32PT-L100 DSC Configuration).....	M.5-117
Figure M.5-19	Cask Model Geometry (32PT-S125/32PT-L125 DSC Configuration).....	M.5-118
Figure M.5-20	Dose Rate Distribution Along Cask Side During Onsite Transfer (32PT-S125/32PT-L125 DSC Configuration)	M.5-119
Figure M.5-21	Cask Top-End Dose Rates During Decontamination (32PT-S125/32PT-L125 DSC Configuration)	M.5-120
Figure M.5-22	Cask Top-End Dose Rates During Inner Cover Welding (32PT-S125/32PT-L125 DSC Configuration).....	M.5-121
Figure M.5-23	Cask Top-End Dose Rates During Outer Cover Welding (32PT-S125/32PT-L125 DSC Configuration)	M.5-122
Figure M.5-24	Cask Model Geometry (32PT-S100/32PT-L100 DSC Configuration).....	M.5-123
Figure M.5-25	Dose Rate Distribution Along Cask Side During Onsite Transfer (32PT-S100/32PT-L100 DSC Configuration)	M.5-124
Figure M.5-26	Cask Top-End Dose Rates During Decontamination (32PT-S100/32PT-L100 DSC Configuration)	M.5-125
Figure M.5-27	Cask Top-End Dose Rates During Inner Cover Welding (32PT-S100/32PT-L100 DSC Configuration).....	M.5-126
Figure M.5-28	Cask Top-End Dose Rates during Outer Cover Welding (32PT-S100/32PT-L100 DSC Configuration).....	M.5-127
Figure M.5-29	MCNP Model – Cut Alone Axial Centerline of the DSC (32PT-S100/32PT-L100 DSC Configuration).....	M.5-128
Figure M.5-30	MCNP Model – Cut through the Centerline of the DSC (32PT-S100/32PT-L100 DSC Configuration).....	M.5-129
Figure M.5-31	ANISN HSM Model.....	M.5-130
Figure M.5-32	ANISN TC Model	M.5-131
Figure M.6-1	Configuration with 20 Poison Plates (Analyzed as Base Type A/B/C/D Basket).....	M.6-57
Figure M.6-2	Required PRA Locations for Configurations with Four PRAs (Type B Basket).....	M.6-58
Figure M.6-3	Required PRA Locations for Configurations with Eight PRAs (Type C Basket).....	M.6-59
Figure M.6-4	Required PRA Locations for Configurations with Sixteen PRAs (Type D Basket).....	M.6-60
Figure M.6-5	KENO V.a units and Radial Cross Sections of the Model.....	M.6-61
Figure M.6-6	WE 17x17 Class Assembly	M.6-79
Figure M.6-7	CE 16x16 Class Assembly	M.6-80
Figure M.6-8	B&W 15x15 Class Assembly.....	M.6-81
Figure M.6-9	CE 15x15 Class Assembly	M.6-82
Figure M.6-10	WE 15x15 Class Assembly	M.6-83
Figure M.6-11	CE 14x14 Class Assembly	M.6-84
Figure M.6-12	WE 14x14 Class Assembly	M.6-85

LIST OF FIGURES
(Continued)

		<u>Page</u>
Figure M.6-13	Configuration with 16 Poison Plates (Analyzed as Alternate Type A Basket).....	M.6-86
Figure M.6-14	Configuration with 24 Poison Plates (Analyzed as Alternate Type A/B/C/D Basket)	M.6-87
Figure M.6-15	CE 15x15 Class Fuel Assembly – 16 poison plates	M.6-88
Figure M.6-16	WE 17x17 Class Fuel Assembly – with BPRAs and 8 PRAs – 24 poison plates'	M.6-89
Figure M.6-17	Exxon 15x15 Fuel Assembly with Radial Variation in Enrichment (Loading Pattern 1).....	M.6-90
Figure M.6-18	Exxon 15x15 CE Fuel Assembly with Radial Variation in Enrichment (Loading Pattern 2).....	M.6-91
Figure M.8-1	NUHOMS® System Loading Operations Flow Chart.....	M.8-12
Figure M.8-2	NUHOMS® System Retrieval Operations Flow Chart.....	M.8-21
Figure M.10-1	Annual Exposure from the ISFSI as a Function of Distance	M.10-17
Figure M.11-1	TC Bounding Accident Dose Rate Distribution.....	M.11-15

M.1 General Discussion

This Appendix M to the NUHOMS[®] Final Safety Analysis Report (FSAR) addresses the Important to Safety aspects of storing spent fuel in the NUHOMS[®]-32PT system. The NUHOMS[®]-32PT system consists of a NUHOMS[®]-32PT Dry Shielded Canister (DSC) stored in a Model 80 or Model 102 NUHOMS[®] Horizontal Storage Module (HSM) and transferred in a OS197 or OS197H Transfer Cask (TC). There is no change to the HSM or the TC as described in the NUHOMS[®] FSAR.

The format of this Appendix follows the guidance provided in NRC Regulatory Guide 3.61 [1.1]. The analysis presented in this Appendix shows that the NUHOMS[®]-32PT system meets all the requirements of 10CFR72 [1.1]. A separate analysis will be submitted to address the safety related aspects of transporting spent fuel in the NUHOMS[®]-32PT DSC in accordance with 10CFR71 [1.3].

The NUHOMS[®]-32PT system provides confinement, shielding, criticality control and passive heat removal independent of any other facility structures or components. The NUHOMS[®]-32PT DSC also maintains structural integrity of the fuel during storage.

Note: References to sections or chapters within this Appendix are identified with a prefix M (e.g., Section M.2.3 or Chapter M.2). References to sections or chapters of the FSAR outside of this Appendix (main body of the FSAR) are identified with the applicable FSAR section or chapter number (e.g., Section 2.3 or Chapter 2).

M.1.1 Introduction

The NUHOMS[®] System provides a modular canister based spent fuel storage and transport system. The system includes DSCs, HSMs, and the TC.

This Appendix M provides the supporting safety analysis for the addition of the 32PT DSC system. Only those features that are being revised or added to the NUHOMS[®] System are addressed and evaluated in this Appendix. The HSM and TC designs remain unchanged. The NUHOMS[®]-32PT DSC is similar to the existing 24P DSCs with the following exceptions:

- The basket has a capability to store 32, rather than 24, Pressurized Water Reactor (PWR) fuel assemblies.
- The canister shell thickness is reduced from 0.625 inches to 0.5 inches.
- The canister has been upgraded to provide a leak tight confinement.
- The basket represents a new design.
- The canister shell length and the thickness of the top and bottom end closure assemblies have been modified to accommodate the new basket design and the revised payload.

The NUHOMS[®]-32PT DSC system is designed to store intact standard PWR fuel assemblies with or without Burnable Poison Rod Assemblies (BPRAs). The NUHOMS[®]-32PT DSC system is designed for a maximum heat load of 24 kW/canister and a maximum of 1.2 kW/assembly when heat load zoning is considered. The fuel which may be stored in the NUHOMS[®]-32PT DSC is presented in Section M.2.

M.1.2 General Description of the NUHOMS®-32PT DSC

M.1.2.1 NUHOMS®-32PT DSC Characteristics

Each NUHOMS®-32PT DSC consists of a fuel basket and a canister body (shell, canister inner bottom and top cover plates and shield plugs). A sketch of the 32PT DSC components is shown in Figure M.1-1. A set of reference drawings is presented in Section M.1.5.

As shown in Table M.1-1, the 32PT DSC system consists of four design configurations or Types as follows:

- 32PT-S100, Short Canister (186.2 inch length)
- 32PT-L100, Long Canister (192.2 inch length)
- 32PT-S125, Short Canister (186.2 inch length)
- 32PT-L125, Long Canister (192.2 inch length)

These four design configurations allow flexibility to accommodate the payload fuel types described in Section M.2, with and without BPRAs. Dimensions and estimated weights of the NUHOMS®-32PT DSC are shown in Table M.1-1.

The thickness for the individual plate components of the top and bottom end cover plates has been increased to accommodate the higher internal pressure, while the top and bottom end shield plug thickness has been reduced relative to the 24P DSC configuration. The NUHOMS®-32PT DSC shell thickness is 0.50 inches instead of 0.625 inches as used for the NUHOMS®-24P or -52B DSC designs. The materials used to fabricate the DSC are shown in the Parts List on Drawings NUH-32PT-1001-SAR, -1002-SAR, -1003-SAR, -1004-SAR, and -1006-SAR.

The confinement vessel for the NUHOMS®-32PT DSC consists of a shell which is a welded stainless steel cylinder with an integrally-welded, stainless steel bottom closure assembly; and a stainless steel top closure assembly, which includes the vent and drain system.

There are no penetrations through the confinement vessel. The draining and venting systems are covered by the seal welded outer top closure plate and vent and siphon port plugs. To preclude air in-leakage, the canister cavity is inerted and pressurized above atmospheric pressure with helium. The NUHOMS®-32PT DSCs are designed and tested to meet the leak tight criteria of ANSI N14.5-1997.

The basket structure consists of a grid assembly of welded stainless steel plates or tubes that make up a grid of 32 fuel compartments. Each fuel compartment accommodates aluminum and/or neutron absorbing plates (which are made of either borated aluminum or metal matrix composites such as Boralyn®, Metamic® or equivalent) that provide the necessary criticality control and heat conduction paths from the fuel assemblies to the canister shell. The space between the fuel compartment grid assembly and the perimeter of the DSC shell is bridged by transition rail structures. The transition rails are solid aluminum segments that support the fuel

compartment grid assembly and transfer mechanical loads to the DSC shell. They also provide the thermal conduction path from the basket assembly to the canister shell wall, making it efficient in rejecting heat from its payload. This method of construction forms a robust structure of compartment assemblies which provides for storage of 32 fuel assemblies. The nominal clear dimension of each fuel compartment opening is 8.7 in. x 8.7 in., which provides clearance around the fuel assemblies.

During dry storage of the spent fuel in the NUHOMS[®]-32PT system, no active systems are required for the removal and dissipation of the decay heat from the fuel. The NUHOMS[®]-32PT DSC is designed to transfer the decay heat from the fuel to the basket, from the basket to the canister body and ultimately to the ambient via the HSM or TC.

Each canister is identified by a Mark Number as follows: WWW32PT-XXX-YYY-ZZZ, where: XXX is the canister type designation (S100/L100/S125/L125), YYY is the basket type designation (A/B/C/D) and WWW and ZZZ are designated by TN. Each canister is also marked with the patent number.

M.1.2.2 Operational Features

M.1.2.2.1 General Features

The NUHOMS[®]-32PT DSCs are designed to safely store 32 intact standard PWR fuel assemblies with or without BPRAs. The NUHOMS[®]-32PT DSC is designed to maintain the fuel cladding temperature below allowable limits during storage, short-term accident conditions, short-term off-normal conditions and fuel transfer operations.

The criticality control features of the NUHOMS[®]-32PT DSC are designed to maintain the neutron multiplication factor k-effective less than the upper subcritical limit equal to 0.95 minus benchmarking bias and modeling bias under all conditions.

M.1.2.2.2 Sequence of Operations

The sequence of operations to be performed in loading fuel into the NUHOMS[®]-32PT DSCs is presented in Chapter M.8.

M.1.2.2.3 Identification of Subjects for Safety and Reliability Analysis

M.1.2.2.3.1 Criticality Prevention

Criticality is controlled by geometry, soluble boron in spent fuel pool and by utilizing fixed neutron poison material in the fuel basket. If required, depending on fuel assembly design and initial enrichment, Poison Rod Assemblies (PRAs), as shown in Figure M.1-2 are also used for criticality control. The 32PT basket may contain 0, 4, 8 or 16 PRAs and is called a Type A, Type B, Type C, or Type D, respectively. These features are only necessary during the loading and unloading operations that occur in the loading pool (underwater). However, the PRAs are left in place following the completion of the DSC draining and drying operations which are discussed in M.8.1.3. During storage, with the DSC cavity dry and sealed from the environment, criticality control measures within the installation are not necessary because of the low reactivity of the

fuel in the dry NUHOMS[®]-32PT DSC and the assurance that no water can enter the DSC cavity during storage.

M.1.2.2.3.2 Chemical Safety

There are no chemical safety hazards associated with operations of the NUHOMS[®]-32PT system.

M.1.2.2.3.3 Operation Shutdown Modes

The NUHOMS[®]-32PT DSC system is a totally passive system so that consideration of operation shutdown modes is unnecessary.

M.1.2.2.3.4 Instrumentation

No change.

M.1.2.2.3.5 Maintenance Techniques

No change.

M.1.2.3 Cask Contents

The NUHOMS[®]-32PT DSC system is designed to store 32 intact standard PWR fuel assemblies with or without BPRAs. Each NUHOMS[®]-32PT DSC is designed for a maximum heat load of 24 kW/canister and 1.2 kW/assembly if zoning for heat load is used. The fuel that may be stored in the NUHOMS[®]-32PT DSC is presented in Chapter M.2.

Chapter M.5 provides the shielding analysis. Chapter M.6 covers the criticality safety of the NUHOMS[®]-32PT DSC system and its contents, listing material densities, moderator ratios, and geometric configurations.

M.1.3 Identification of Agents and Contractors

Transnuclear, Inc. (TN) provides the design, analysis, licensing support and quality assurance for the NUHOMS[®]-32PT system. Fabrication of the NUHOMS[®]-32PT system cask is done by one or more qualified fabricators under TN's quality assurance program described in Chapter M.13. This program is written to satisfy the requirements of 10 CFR 72, Subpart G and covers control of design, procurement, fabrication, inspection, testing, operations and corrective action. Experienced TN operations personnel provide training to utility personnel prior to first use of the NUHOMS[®]-32PT system and prepare generic operating procedures.

Managerial and administrative controls, which are used to ensure safe operation of the casks, are provided by the host utility. NUHOMS[®]-32PT system operations and maintenance are performed by utility personnel. Decommissioning activities will be performed by utility personnel in accordance with site procedures.

TN provides specialized services for the nuclear fuel cycle that support transportation, storage and handling of spent nuclear fuel, radioactive waste and other radioactive materials. TN is the holder of Certificate of Compliance 1004.

M.1.4 Generic Cask Arrays

No change.

M.1.5 Supplemental Data

The following Transnuclear drawings are enclosed:

1. NUHOMS[®]-32PT Transportable Storage Canister for PWR Fuel, Main Assembly, Drawing NUH-32PT-1001NP-SAR.
2. NUHOMS[®]-32PT Transportable Storage Canister for PWR Fuel, Shell Assembly, Drawing NUH-32PT-1002NP-SAR.
3. NUHOMS[®]-32PT Transportable Storage Canister for PWR Fuel, Basket Assembly Option 1, Drawing NUH-32PT-1003NP-SAR.
4. NUHOMS[®]-32PT Transportable Storage Canister for PWR Fuel, Basket Assembly Option 2, Drawing NUH-32PT-1004NP-SAR.
5. NUHOMS[®]-32PT Transportable Storage Canister for PWR Fuel, Aluminum Transition Rails, Drawing NUH-32PT-1006NP-SAR.

Figure Withheld Under 10 CFR 2.390

PARTS LIST			
REV		A	
QTY		1	
DESC	TRANSNUCLEAR		
REV		A	
QTY		1	
DESC	SAFETY ANALYSIS REPORT NUHOMS® 32PT TRANSPORTABLE STORAGE CANISTER FOR PWR FUEL MAIN ASSEMBLY		
REV		REV	REV
1	MLM-32PT-1000P-SAR	1	1 OF 3

Figure Withheld Under 10 CFR 2.390

FILE NO.	A		
PROJECT NO.	TRANSNUCLEAR		
DATE	SAFETY ANALYSIS REPORT		
DESCRIPTION	NUHOMS® 32FT TRANSPORTABLE STORAGE CANISTER FOR PWR FUEL MAIN ASSEMBLY		
FILE NO.	REV.	DATE	BY
MUN-32PT-100IMP-SAR	NONE	7 OF 1	2
2	1	1	

Figure Withheld Under 10 CFR 2.390

C D E F G H I J K L M N O P Q R S T U V W X Y Z AA AB AC AD AE AF AG AH AI AJ AK AL AM AN AO AP AQ AR AS AT AU AV AW AX AY AZ BA BB BC BD BE BF BG BH BI BJ BK BL BM BN BO BP BQ BR BS BT BU BV BW BX BY BZ CA CB CC CD CE CF CG CH CI CJ CK CL CM CN CO CP CQ CR CS CT CU CV CW CX CY CZ DA DB DC DD DE DF DG DH DI DJ DK DL DM DN DO DP DQ DR DS DT DU DV DW DX DY DZ EA EB EC ED EE EF EG EH EI EJ EK EL EM EN EO EP EQ ER ES ET EU EV EW EX EY EZ FA FB FC FD FE FF FG FH FI FJ FK FL FM FN FO FP FQ FR FS FT FU FV FW FX FY FZ GA GB GC GD GE GF GG GH GI GJ GK GL GM GN GO GP GQ GR GS GT GU GV GW GX GY GZ HA HB HC HD HE HF HG HH HI HJ HK HL HM HN HO HP HQ HR HS HT HU HV HW HX HY HZ IA IB IC ID IE IF IG IH II IJ IK IL IM IN IO IP IQ IR IS IT IU IV IW IX IY IZ JA JB JC JD JE JF JG JH JI JJ JK JL JM JN JO JP JQ JR JS JT JU JV JW JX JY JZ KA KB KC KD KE KF KG KH KI KJ KK KL KM KN KO KP KQ KR KS KT KU KV KW KX KY KZ LA LB LC LD LE LF LG LH LI LJ LK LL LM LN LO LP LQ LR LS LT LU LV LW LX LY LZ MA MB MC MD ME MF MG MH MI MJ MK ML MM MN MO MP MQ MR MS MT MU MV MW MX MY MZ NA NB NC ND NE NF NG NH NI NJ NK NL NM NN NO NP NQ NR NS NT NU NV NW NX NY NZ OA OB OC OD OE OF OG OH OI OJ OK OL OM ON OO OP OQ OR OS OT OU OV OW OX OY OZ PA PB PC PD PE PF PG PH PI PJ PK PL PM PN PO PP PQ PR PS PT PU PV PW PX PY PZ QA QB QC QD QE QF QG QH QI QJ QK QL QM QN QO QP QQ QR QS QT QU QV QW QX QY QZ RA RB RC RD RE RF RG RH RI RJ RK RL RM RN RO RP RQ RR RS RT RU RV RW RX RY RZ SA SB SC SD SE SF SG SH SI SJ SK SL SM SN SO SP SQ SR SS ST SU SV SW SX SY SZ TA TB TC TD TE TF TG TH TI TJ TK TL TM TN TO TP TQ TR TS TT TU TV TW TX TY TZ UA UB UC UD UE UF UG UH UI UJ UK UL UM UN UO UP UQ UR US UT UU UV UW UX UY UZ VA VB VC VD VE VF VG VH VI VJ VK VL VM VN VO VP VQ VR VS VT VU VV VW VX VY VZ WA WB WC WD WE WF WG WH WI WJ WK WL WM WN WO WP WQ WR WS WT WU WV WW WX WY WZ XA XB XC XD XE XF XG XH XI XJ XK XL XM XN XO XP XQ XR XS XT XU XV XW XX XY XZ YA YB YC YD YE YF YG YH YI YJ YK YL YM YN YO YP YQ YR YS YT YU YV YW YX YZ ZA ZB ZC ZD ZE ZF ZG ZH ZI ZJ ZK ZL ZM ZN ZO ZP ZQ ZR ZS ZT ZU ZV ZW ZX ZY ZZ					
	A				
	TRANSNUCLEAR				
	SAFETY ANALYSIS REPORT NUHOMS® 32FT TRANSPORTABLE STORAGE CANISTER FOR PWR FUEL MAIN ASSEMBLY				
REV	NO	REV	REV	REV	
2	1	1	1	2	

Figure Withheld Under 10 CFR 2.390


FORM 800			
DATE	REVISED		
1980	1980		
1	1		
2	2		
			
SAFETY ANALYSIS REPORT			
NUHOMS-32PT TRANSPORTABLE STORAGE CANISTER FOR PWR FUEL SHELL ASSEMBLY			
FILE NO	REV	PAGE	NO. OF
NUH-32PT-10020P-SAR	NONE	1 OF 2	2
2	1	1	2

Figure Withheld Under 10 CFR 2.390


JOB # REV. DATE		PAGE	SAFETY ANALYSIS REPORT			
			NUHOMS® 32PT TRANSPORTABLE STORAGE CANISTER FOR PWR FUEL SHELL ASSEMBLY			
1	NUM-32PT-1002NP-SAR	1	1	2	2	
		2	1	1		

Figure Withheld Under 10 CFR 2.390

REVISION		DATE		BY	
PARTS LIST					
DATE C.D.		A TRANSNUCLEAR			
E.					
REVISION C.D.					
1 SHEET	ALL	SAFETY ANALYSIS REPORT			
1	1	NUHOMS® 32PT TRANSPORTABLE STORAGE CANISTER FOR PWR FUEL BASKET ASSEMBLY - (PLATE OPTIONS)			
DATE	NUM	REV	NO	OF	SHEETS
	MUN-32PT-1003NP-SAR	NONE	1	0	2

2 1 1

Figure Withheld Under 10 CFR 2.390

REVISIONS DATE BY		TRANSNUCLEAR		
				SAFETY ANALYSIS REPORT
	NUHOMS® 32FT TRANSPORTABLE STORAGE CANISTER FOR PWR FUEL BASKET ASSEMBLY - (PLATE OPTIONS)			
	NO. 0003	REV. 1	DATE	10/1/82
REV. 1		REV. 1		
REV. 2		REV. 2		
REV. 3		REV. 3		
REV. 4		REV. 4		
REV. 5		REV. 5		
REV. 6		REV. 6		
REV. 7		REV. 7		
REV. 8		REV. 8		
REV. 9		REV. 9		
REV. 10		REV. 10		
REV. 11		REV. 11		
REV. 12		REV. 12		
REV. 13		REV. 13		
REV. 14		REV. 14		
REV. 15		REV. 15		
REV. 16		REV. 16		
REV. 17		REV. 17		
REV. 18		REV. 18		
REV. 19		REV. 19		
REV. 20		REV. 20		
REV. 21		REV. 21		
REV. 22		REV. 22		
REV. 23		REV. 23		
REV. 24		REV. 24		
REV. 25		REV. 25		
REV. 26		REV. 26		
REV. 27		REV. 27		
REV. 28		REV. 28		
REV. 29		REV. 29		
REV. 30		REV. 30		
REV. 31		REV. 31		
REV. 32		REV. 32		
REV. 33		REV. 33		
REV. 34		REV. 34		
REV. 35		REV. 35		
REV. 36		REV. 36		
REV. 37		REV. 37		
REV. 38		REV. 38		
REV. 39		REV. 39		
REV. 40		REV. 40		
REV. 41		REV. 41		
REV. 42		REV. 42		
REV. 43		REV. 43		
REV. 44		REV. 44		
REV. 45		REV. 45		
REV. 46		REV. 46		
REV. 47		REV. 47		
REV. 48		REV. 48		
REV. 49		REV. 49		
REV. 50		REV. 50		
REV. 51		REV. 51		
REV. 52		REV. 52		
REV. 53		REV. 53		
REV. 54		REV. 54		
REV. 55		REV. 55		
REV. 56		REV. 56		
REV. 57		REV. 57		
REV. 58		REV. 58		
REV. 59		REV. 59		
REV. 60		REV. 60		
REV. 61		REV. 61		
REV. 62		REV. 62		
REV. 63		REV. 63		
REV. 64		REV. 64		
REV. 65		REV. 65		
REV. 66		REV. 66		
REV. 67		REV. 67		
REV. 68		REV. 68		
REV. 69		REV. 69		
REV. 70		REV. 70		
REV. 71		REV. 71		
REV. 72		REV. 72		
REV. 73		REV. 73		
REV. 74		REV. 74		
REV. 75		REV. 75		
REV. 76		REV. 76		
REV. 77		REV. 77		
REV. 78		REV. 78		
REV. 79		REV. 79		
REV. 80		REV. 80		
REV. 81		REV. 81		
REV. 82		REV. 82		
REV. 83		REV. 83		
REV. 84		REV. 84		
REV. 85		REV. 85		
REV. 86		REV. 86		
REV. 87		REV. 87		
REV. 88		REV. 88		
REV. 89		REV. 89		
REV. 90		REV. 90		
REV. 91		REV. 91		
REV. 92		REV. 92		
REV. 93		REV. 93		
REV. 94		REV. 94		
REV. 95		REV. 95		
REV. 96		REV. 96		
REV. 97		REV. 97		
REV. 98		REV. 98		
REV. 99		REV. 99		
REV. 100		REV. 100		

2 1 1

Figure Withheld Under 10 CFR 2.390

A	TRANSNUCLEAR
NUHOMS® 32FT TRANSPORTABLE STORAGE CANISTER FOR PWR FUEL BASKET ASSEMBLY - (PLATE OPTIONS)	A
MEM-32FT-1003MP-SAR	REV 3.0 2

2 1 1

Figure Withheld Under 10 CFR 2.390

DATE Rev	A	TRANSNUCLEAR
REVISED Date		NUHOMS® 32FT TRANSPORTABLE STORAGE CANISTER FOR PWR FUEL BASKET ASSEMBLY - (PLATE OPTIONS)
NO. OF REV.	2	NO. OF REV. 2
		NO. OF REV. 1
		NO. OF REV. 1

Figure Withheld Under 10 CFR 2.390

REV	A	TRANSNUCLEAR	SAFETY ANALYSIS REPORT	
			NUHOMS [®] 32PT TRANSPORTABLE	
			STORAGE CANISTER FOR FWD FUEL	
			BASKET ASSEMBLY - (TUBE OPTIONS)	
REV	3	NUM-32PT-100HP-BA8	NONE	1 0 2
		2	1	1


Figure Withheld Under 10 CFR 2.390

20	A TRANSNUCLEAR	A
10		
0		
0		
10	SAFETY ANALYSIS REPORT	
0	NUHOMS® 32PT TRANSPORTABLE	
0	STORAGE CANISTER FOR PWR FUEL	
0	BASKET ASSEMBLY - (TUBE OPTIONS)	
0	FIG. 10	DATE
	NUM-33PT-100489-SAR	NONE 12 80 2
2	1	1

Figure Withheld Under 10 CFR 2.390

REV. DATE ISSUED BY CODE REV. DATE BY	A		
	TRANSNUCLEAR		
	SAFETY ANALYSIS REPORT NUHOMS [®] 32PT TRANSPORTABLE STORAGE CANISTER FOR PWR FUEL BASKET ASSEMBLY - (TUBE OPTIONS)		
	MIN-32PT-100-SEP-5AR	REV. 1 2	
2	1	1	A

Figure Withheld Under 10 CFR 2.390

DATE 1/2/81	 TRANSNUCLEAR	ALL	SAFETY ANALYSIS REPORT	
PROJECT L-1			NUHOMS® 32PT TRANSPORTABLE STORAGE CANISTER FOR PWR FUEL ALUMINUM TRANSITION RAILS	
DESIGN L-1	FILE NO. NUM-32PT-1000RP-SAR	REV. NONE	FIG. NO. 1 OF 1	PAGE NO. 2
	2	1	1	

M.1.6 References

- 1.1 U.S. Nuclear Regulatory Commission, Regulatory Guide 3.61, Standard Format and Content for a Topical Safety Analysis Report for a Spent Fuel Dry Storage Cask, February, 1989.
- 1.2 10CFR72, Rules and Regulations, Title 10, Chapter 1, Code of Federal Regulations - Energy, U.S. Nuclear Regulatory Commission, Washington, D.C., "Licensing Requirements for the Independent Storage of Spent Nuclear Fuel and High-Level Radioactive Waste."
- 1.3 10CFR71, Rules and Regulations, Title 10, Chapter 1, Code of Federal Regulations - Energy, U.S. Nuclear Regulatory Commission, Washington, D.C., "Packaging and Transportation of Radioactive Material."

**Table M.1-1
Nominal Dimensions and Weight of the NUHOMS®-32PT DSC**

	32PT DSC Design Configuration			
	32PT-S100	32PT-S125	32PT-L100	32PT-L125
Canister Length (in.)	186.2	186.2	192.2	192.2
Outside Diameter (in)	67.19	67.19	67.19	67.19
Cavity Length (in.)	169.6	167.1	175.6	173.1
Cavity Diameter (in)	66.19	66.19	66.19	66.19
Nominal DSC Loaded Weight, Dry (kips)	88.2 ⁽¹⁾	90.3 ⁽¹⁾	89.2 ⁽¹⁾	91.3 ⁽¹⁾
	98.3 ⁽²⁾	100.4 ⁽²⁾	99.3 ⁽²⁾	101.4 ⁽²⁾

Notes:

1. Based on fuel weight of 1,365 lbs. per assembly. This is the limit for any 32PT DSC for which the maximum lift weight of the loaded transfer cask is to remain under 100 tons.
2. Based on fuel weight of 1,682 lbs per assembly.

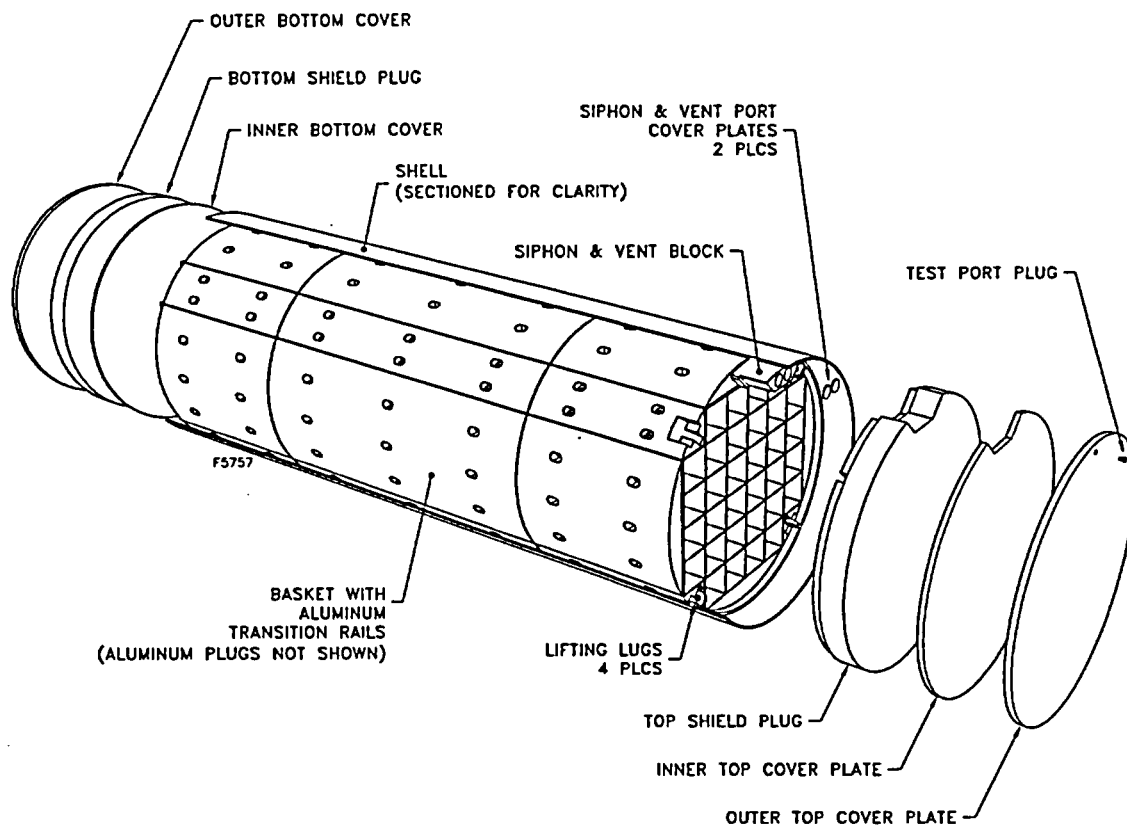
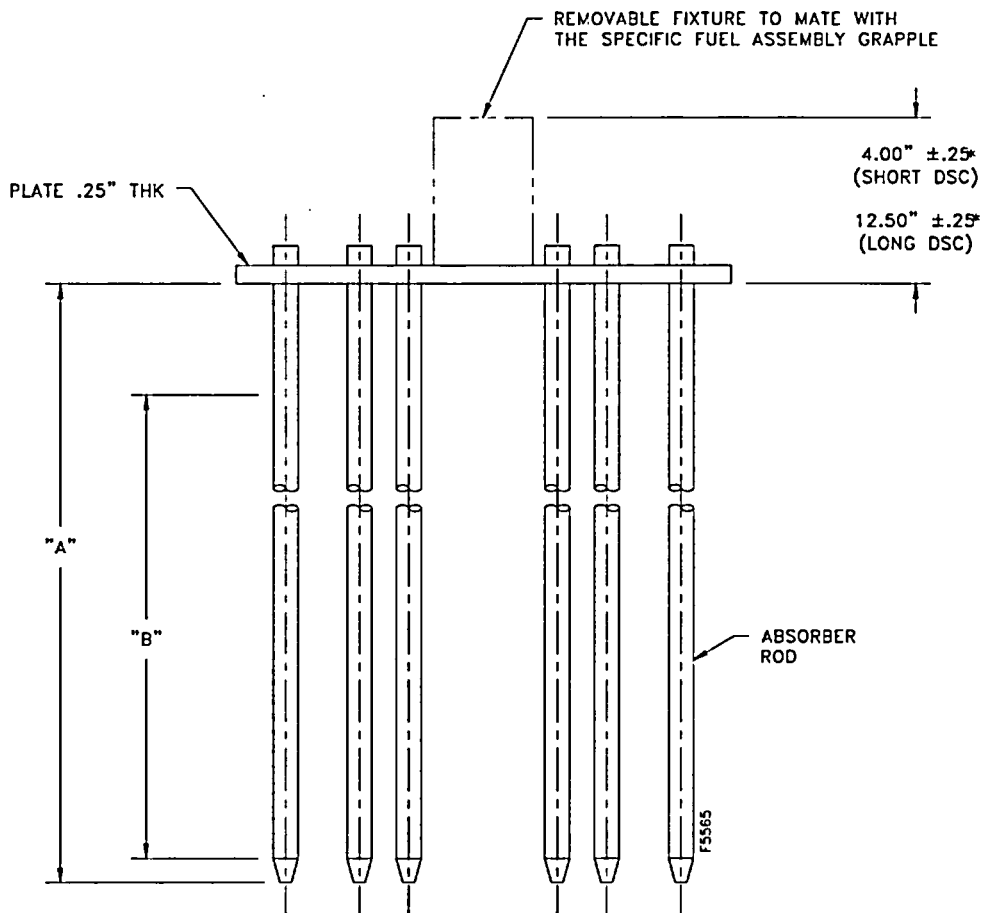


Figure M.1-1
NUHOMS®-32PT DSC Components



* THESE DIMENSIONS ARE FOR USE WITH WESTINGHOUSE 17x17 FUEL ASSEMBLIES. DIMENSIONS WILL VARY AS REQUIRED BY FUEL ASSEMBLY TYPE.

DIMENSION	FUEL ASSEMBLY TYPE				
	WE 17x17	B&W 15x15	WE 15x15	CE 14x14	WE 14x14
ABSORBER ROD OD NOMINAL (in)	.362	.438	.450	.975	.432
MINIMUM ABSORBER ROD DIMENSION "A" (IN)	156	160	156	143	156
MINIMUM B ₄ C PELETS STACK HEIGHT, "B" (IN)	151	151	150	129	150
CLAD THICKNESS NOMINAL (in)	.018	.022	.023	.049	.022
No. OF RODS	24	16	20	5	16
MATERIAL	304 SST	304 SST	304 SST	304 SST	304 SST

**Figure M.1-2
Poison Rod Assemblies (PRAs)**

M.2 Principal Design Criteria

This section provides the principal design criteria for the NUHOMS[®]-32PT system. The NUHOMS[®]-32PT Dry Shielded Canister (DSC) is handled, transferred and stored in the same manner as the existing NUHOMS[®]-24P DSC. There is no change to the NUHOMS[®] OS197 or the NUHOMS[®] OS197H Transfer Cask (TC), or the standard NUHOMS[®] Horizontal Storage Module (HSM). Only those principal design criteria that have changed from the existing FSAR, Chapter 3, are described in this chapter. Section M.2.1 presents a general description of the spent fuel to be stored. Section M.2.2 provides the design criteria for environmental conditions and natural phenomena. This section contains an assessment of the local damage due to the design basis environmental conditions and natural phenomena and the general loadings and design parameters used for analysis in subsequent chapters. Section M.2.3 provides a description of the systems that have been designated as important to safety. Section M.2.4 discusses decommissioning considerations. Section M.2.5 summarizes the NUHOMS[®]-32PT DSC design criteria.

M.2.1 Spent Fuel To Be Stored

There are four design configurations for the NUHOMS[®]-32PT DSC, two "short" canister configurations (the 32PT-S100 and 32PT-S125), and two "long" canister configurations (the 32PT-L100 and 32PT-L125). The main difference between the -S100/-L100 and -S125/-L125 configuration designs are the thicknesses of shield plugs and DSC cover plates. The basket layout for these two configurations is identical except for the length of the components. Each of the DSC configurations is designed to store 32 intact standard PWR fuel assemblies. The 32PT-L100 and 32PT-L125 are also designed to store 32 intact standard PWR fuel assemblies with or without BPRAs. The NUHOMS[®]-32PT DSCs can store intact PWR fuel assemblies and BPRAs with the characteristics described in Table M.2-1. The NUHOMS[®]-32PT DSC may store PWR fuel assemblies arranged in any of three alternate heat zoning configurations with a maximum decay heat of 1.2kW per assembly and a maximum heat load of 24 kW per canister. The heat load zoning configurations are shown in Figure M.2-1 through Figure M.2-3. The NUHOMS[®]-32PT DSC is inerted and backfilled with helium at the time of loading. The maximum fuel assembly weight with a BPRA is 1682 lbs. which is the same as the NUHOMS[®]-24P DSC design.

The maximum fuel cladding temperature limit of 400°C (752°F) is applicable to normal conditions of storage and all short term operations from spent fuel pool to ISFSI pad including vacuum drying and helium backfilling of the NUHOMS[®]-32PT DSC per Interim Staff Guidance (ISG) No. 11, Revision 2 [2.7]. In addition, ISG-11 does not permit thermal cycling of the fuel cladding with temperature differences greater than 65°C (117°F) during DSC drying, backfilling and transfer operations.

The maximum fuel cladding temperature limit of 570°C (1058°F) is applicable to accidents or off-normal thermal transients [2.7].

Calculations were performed to determine the fuel assembly type which was most limiting for each of the analyses including shielding, criticality, heat load and confinement. These evaluations are performed in Chapter M.5, M.6, M.4 and M.7. The fuel assembly types considered are listed in Table M.2-2. It was determined that the B&W 15x15 is the enveloping fuel design for the shielding source term calculation because of its total assembly weight and highest initial heavy metal loading. For criticality safety, the B&W 15x15 assembly is the most reactive assembly type for a given enrichment. This assembly is used to determine the most reactive configuration in the DSC. Using this most reactive configuration, criticality analysis for all other fuel assembly classes is performed to determine the maximum enrichment allowed as a function of number of Poison Rod Assemblies (PRAs). For thermal analysis, the WE 14x14 fuel assembly is limiting, since it results in the lowest fuel conductivity. The confinement analyses is based on B&W 15x15 fuel assembly, since it results in the smaller free volume inside the DSC cavity more than a 14x14 fuel assembly.

All four NUHOMS[®]-32PT DSC design configurations have the same minimum boron content for the poison neutron plates. The minimum boron-10 content for the poison plates is 0.0070

g/cm². The criticality analysis is based on 90% credit or 0.0063 g/cm² of B10. The use of 90% credit is allowed because poison material coupons are to be tested via neutron transmission plus statistical analysis of the neutron transmission results. A basket may contain 0, 4, 8, or 16 PRAs and is designated a Type A, Type B, Type C or Type D basket, respectively.

For calculating the maximum internal pressure in the NUHOMS[®]-32PT DSC, it is assumed that 1% of the fuel rods are damaged for normal conditions, up to 10% of the fuel rods are damaged for off normal conditions, and 100% of the fuel rods will be damaged following a design basis accident event. A minimum of 100% of the fill gas and 30% of the fission gases (e.g., H-3, Kr and Xe) within the ruptured fuel rods are assumed to be available for release into the DSC cavity, consistent with NUREG-1536 [2.1].

The maximum design basis internal pressures for the NUHOMS[®]-32PT DSC are 15, 20 and 105 psig for normal, off-normal and accident conditions of storage, respectively.

M.2.1.1 General Operating Functions

No change.

M.2.2 Design Criteria for Environmental Conditions and Natural Phenomena

The NUHOMS[®]-32PT DSC is handled and stored in the same manner as the existing NUHOMS[®]-24P System. The environmental conditions and natural phenomena are the same as described in the existing FSAR, Chapter 3. Updated criteria are given in the applicable section. Table M.2-20 summarizes the design criteria for the 32PT DSC. This table also summarizes the applicable codes and standards utilized for design. Design criteria for the NUHOMS[®] HSM and TC remain the same as shown in Table 3.2-1 of the FSAR.

M.2.2.1 Tornado Wind and Tornado Missiles

No change.

M.2.2.2 Water Level (Flood) Design

No change.

M.2.2.3 Seismic Design

No change.

M.2.2.4 Snow and Ice Loading

No change.

M.2.2.5 Combined Load Criteria

The NUHOMS[®]-32PT system is subjected to the same loads as the existing NUHOMS[®]-24P or -52B System. The criteria applicable to the HSM and the TC are the same as those found in the existing FSAR, Chapter 3. The criteria applicable to the NUHOMS[®]-32PT DSC are found in the following subsections.

M.2.2.5.1 NUHOMS[®]-32PT DSC Structural Design Criteria

The NUHOMS[®]-32PT DSC is designed using the ASME Boiler and Pressure Vessel Code [2.2] criteria given in the existing FSAR, Chapter 3, except as noted in the following sections. A summary of the NUHOMS[®]-32PT DSC load combinations is presented in Table M.2-15.

M.2.2.5.1.1 NUHOMS[®]-32PT DSC Shell Stress Limits

The stress limits for the NUHOMS[®]-32PT DSC shell are taken from the ASME Boiler and Pressure Vessel Code, Section III, Subsection NB, Article NB-3200 [2.2] for normal condition loads (Level A) and NB-3225, Appendix F for accident condition loads (Level D). The stress limits for Level B and Level C are taken from ASME, Section III, Subsection NB, Paragraph NB-3223 and 3224.

Stress criteria for Level A through Level D service loading conditions are given in Table M.2-16. Local yielding is permitted at the point of contact where the Level D load is applied. If elastic stress limits cannot be met, the plastic system analysis approach and acceptance criteria of Appendix F of ASME Section III are used.

The allowable stress intensity value, S_m , as defined by the Code is based on the temperature calculated for each service load condition or a bounding temperature.

M.2.2.5.1.2 NUHOMS[®]-32PT DSC Basket Stress Limits

The basket fuel support grid wall thickness is established to meet heat transfer, nuclear criticality, and structural requirements. The basket structure provides sufficient rigidity to maintain a subcritical configuration under the applied loads.

No credit is taken for neutron poison plates in any of the stress or stability analyses.

Normal Conditions

Normal Condition Stress Criteria for Steel Elements

As summarized in Table M.2-17, the normal condition stress criteria for the fuel support structure, and the R90 transition rail cover plates is based on Subsection NG [2.2] of the ASME Code, Section III.

Normal Condition Stress Criteria for Aluminum Transition Rails

The solid aluminum transition rail bodies (R90 and R45) perform their function (support of the fuel grid) by remaining in place. The loads on the rail bodies are primarily bearing from the fuel grid (transmitted through the cover plate on the R90 rails). "Failure" of the transition rail would require that the rail no longer provide support to the fuel grid. Since the solid aluminum rail bodies are constrained between the DSC shell and the fuel support grid, this cannot occur.

Therefore, for deadweight and handling condition loads, stress in the aluminum bodies will be compared to the allowable bearing stress, equal to S_y , from NG-3227.1(a). Values of S_y are taken from Table M.3.3-4 for annealed 6061 aluminum material at temperature (as described in Section M.3.3, these yield stresses are lower bound values).

Normal Condition Stability Criteria

Stability criteria are addressed in two parts:

- A. Under axial loads, the DSC shell and transfer/transport cask provide overall/global stability to the 32PT basket structure. Thus, only local stability effects are specifically addressed. For local (panel) stability under axial loads, the allowable stress in the fuel support grid and transition rail panels are taken as the smallest of the following three values:
 - The normal condition (Level A) primary membrane stress allowable, P_m ,

- Two-thirds of the material yield stress at temperature, $2/3 S_y$,
- The critical buckling value determined using Table 35, Case 1a of [2.3] for a rectangular plate under equal uniform compression on two opposite edges, with all edges simply supported.

$$\sigma_{CR} = K \frac{E}{1-\nu^2} \left(\frac{t}{b} \right)^2$$

- B. Under lateral loads, stability of the basket structure is demonstrated using hand calculations to evaluate the fuel support grid "ligaments" as columns using the stability criteria of NF-3322.1(c)(2) for stainless steel compression members.

Accident Conditions

Accident Condition Stress Criteria for Steel Elements

As summarized in Table M.2-17 the accident condition stress criteria for the fuel support structure is based on Appendix F of the ASME Code, Section III. Criteria are provided for both linear elastic and elastic-plastic stress analyses.

Accident Condition Criteria for Aluminum Transition Rails

For accident condition loading (i.e., the postulated drops), the solid transition rail bodies must support the fuel support grid such that stresses and displacements in the fuel grid are acceptable. Since, the solid rail bodies are captured between the fuel grid and the DSC shell, large displacements of the rails are prevented. Thus, no additional checks (of the solid aluminum) are required for accident/drop loading. Qualification of the fuel grid (and R90 transition rail cover plate) will demonstrate that the rails perform their intended function.

Accident Condition Stability Criteria

Similar to the normal condition evaluations, stability criteria are addressed in two parts:

- A. Accident condition axial stresses in the fuel support grid panels are calculated and compared to the lesser of:
1. The accident condition (Level D) primary membrane stress allowable, P_m ,
 2. 90% of the material yield stress at temperature, $.9S_y$,
 3. The critical buckling value determined using Table 35, Case 1a of [2.3] for a rectangular plate under equal uniform compression on two opposite edges, with all edges simply supported.

$$\sigma_{CR} = K \frac{E}{1-\nu^2} \left(\frac{t}{b} \right)^2$$

- B. Under lateral loads, stability of the basket structure is demonstrated using detailed finite element models and the Collapse Load criteria from F-1341.3. These criteria establish the allowable load as 90% of the Limit Analysis Collapse Load where the Limit Analysis Collapse Load is the maximum load determined using elastic-perfectly plastic material properties with a yield stress equal to the lesser of $2.3S_m$ or $0.7S_u$.

In addition, supplementary hand calculations were performed using the criteria of F-1334.3(b) for members under axial compression. Further confirmatory finite element analyses were performed using the LS-DYNA computer code.

M.2.3 Safety Protection Systems

M.2.3.1 General

The NUHOMS[®]-32PT DSC is designed to provide storage of spent fuel for at least 40 years. The DSC cavity is inerted and backfilled with helium and the internal pressure is always above atmospheric during the storage period as a precaution against in-leakage of air, which could be harmful to the fuel. Since the confinement vessel consists of a steel cylinder with an integrally-welded bottom closure, and a seal welded top closure that is verified to be leak tight after loading, the DSC cavity gas cannot escape.

Only those features that are not addressed in the existing FSAR, Chapter 3, or have been revised, are addressed in this Section. Those features include the thermal and nucleonic performance of the poison plates, and their acceptance. Components of the NUHOMS[®]-32PT DSC that are "Important to Safety" and "Not Important to Safety" are listed in Table M.2-18.

M.2.3.2 Protection By Multiple Confinement Barriers and Systems

The NUHOMS[®]-32PT DSC provides a leak tight confinement of the spent fuel. Although similar to the existing NUHOMS[®]-24P DSC, sealing of the NUHOMS[®]-32PT DSC involves leak testing in accordance with ANSI N14.5 [2.4] after loading and sealing the canister, as described in Section M.9.

M.2.3.3 Protection By Equipment and Instrumentation Selection

No change.

M.2.3.4 Nuclear Criticality Safety

M.2.3.4.1 Control Methods for Prevention of Criticality

The design criterion for criticality is that an upper subcritical limit (USL) of 0.95 minus benchmarking bias and modeling bias will be maintained for all postulated arrangements of fuel within the DSC. The intact fuel assemblies are assumed to stay within their basket compartment based on the DSC and basket geometry.

The control method used to prevent criticality is incorporation of poison material in the basket material, soluble boron in the pool and favorable geometry. The quantity and distribution of boron in the poison material is controlled by specific manufacturing and acceptance criteria of the poison plates and PRAs. The acceptance criteria of the plates and PRAs is described in Section M.9.

The basket has been designed to assure an ample margin of safety against criticality under the conditions of fresh fuel in a DSC flooded with borated pool water. The method of criticality control is in accordance with the requirements of 10CFR72.124.

The criticality analyses are described in Section M.6.

M.2.3.4.2 Error Contingency Criteria

Provision for error contingency is built into the criterion used in Section M.2.3.4.1 above. The criterion used in the criticality analysis is common practice for licensing submittals. Because conservative assumptions are made in modeling, it is not necessary to introduce additional contingency for error.

M.2.3.4.3 Verification Analysis-Benchmarking

The verification analysis-benchmarking used in the criticality safety analysis is described in Section M.6.

M.2.3.5 Radiological Protection

No change.

M.2.3.6 Fire and Explosion Protection

No change.

M.2.4 Decommissioning Considerations

No change.

M.2.5 Summary of NUHOMS®-32PT DSC Design Criteria

The additional principal design criteria for the NUHOMS®-32PT DSC are presented in Table M.2-19. The NUHOMS®-32PT DSC is designed to store 32 intact standard PWR fuel assemblies with or without BPRAs with assembly average burnup, initial enrichment and cooling time as described in Table M.2-1. The maximum total heat generation rate of the stored fuel is limited to 1.2 kW per fuel assembly and 24 kW per NUHOMS®-32PT DSC in order to keep the maximum fuel cladding temperature below the limit [2.7] necessary to ensure cladding integrity. The fuel cladding integrity is assured by the NUHOMS®-32PT DSC and basket design which limits fuel cladding temperature and maintains a nonoxidizing environment in the cask cavity as described in Section M.4.

The NUHOMS®-32PT DSC (shell and closure) is designed and fabricated as a Class 1 component in accordance with the rules of the ASME Boiler and Pressure Vessel Code, Section III, Subsection NB, and the alternative provisions to the ASME Code as described in Table M.3.1-1.

The NUHOMS®-32PT DSC is designed to maintain a subcritical configuration during loading, handling, storage and accident conditions. A combination of fixed neutron absorbers, soluble boron in the pool and favorable geometry are employed to maintain the upper subcritical limit of 0.9411. The fixed neutron absorbers are in the form of borated metallic plates and PRAs which are inserted in the guide tubes of certain assemblies in the basket. The basket is designed and fabricated in accordance with the rules of the ASME Boiler and Pressure Vessel Code, Section III, Subsection NG, Article NG-3200 and the alternative provisions to the ASME Code as described in Table M.3.1-1.

The NUHOMS®-32PT DSC design, fabrication and testing are covered by TN's Quality Assurance Program, which conforms to the criteria in Subpart G of 10CFR72.

The NUHOMS®-32PT DSC is designed to withstand the effects of severe environmental conditions and natural phenomena such as earthquakes, tornadoes, lightning and floods. Section M.11 describes the NUHOMS®-32PT DSC behavior under these accident conditions.

M.2.6 References

- 2.1 NUREG-1536, "Standard Review Plan for Dry Cask Storage Systems," 1997.
- 2.2 American Society of Mechanical Engineers, ASME Boiler And Pressure Vessel Code, Section III, Division 1 - Subsections NB, NG and NF, 1998 edition including 2000 Addenda.
- 2.3 Young, W.C., "Roark's Formulas for Stress and Strain," 6th Edition, McGraw-Hill Book Company, New York, 1989.
- 2.4 ANSI N14.5-1997, "Leakage Tests on Packages for Shipment," February 1998.
- 2.5 Deleted.
- 2.6 Deleted.
- 2.7 Interim Staff Guidance No. 11, Revision 2, "Cladding Considerations for the Transportation and storage of Spent Fuel", dated July 30, 2002.

**Table M.2-1
Intact PWR Fuel Assembly Characteristics**

<u>PHYSICAL PARAMETERS:</u>	
Fuel Class	B&W 15x15, WE 17x17, CE 15x15, WE 15x15, CE 14x14 and WE 14x14 assemblies that are enveloped by the fuel assembly design characteristics listed in Table M.2-2.
Fuel Cladding Material	Zircaloy
Fuel Damage	Cladding damage in excess of pinhole leaks or hairline cracks is not authorized to be stored as "Intact PWR Fuel."
Burnable Poison Rod Assemblies (BPRAs)	Standard BPRA designs for the B&W 15x15 and Westinghouse 17x17 class assemblies as listed in Appendix J of the FSAR.
Maximum Assembly plus BPRA Weight	-1365 lbs for 32PT-S100 & 32PT-L100 DSC System -1682 lbs for 32PT-S125 & 32PT-L125 DSC System
BPRA Damage	BPRAs with cladding failures are acceptable for loading.
<u>THERMAL/RADIOLOGICAL PARAMETERS:</u>	
Fuel Burnup and Cooling Time without BPRAs	Per Table M.2-5, Table M.2-6, Table M.2-7, Table M.2-8, Table M.2-9; and Figure M.2-1 or Figure M.2-2 or Figure M.2-3.
Fuel Burnup and Cooling Time with BPRAs	Per Table M.2-10, Table M.2-11, Table M.2-12, Table M.2-13, Table M.2-14; and Figure M.2-1 or Figure M.2-2 or Figure M.2-3.
Initial Enrichment	Per Table M.2-3; and Figure M.2-4 or Figure M.2-5 or Figure M.2-6, as applicable.
B&W 15x15 BPRA Burnup and Cooling Time	BPRA Burnup shall not exceed that of a BPRA irradiated in fuel assemblies with a total Burnup of 36,000 MWd/MTU. -Minimum Cooling Time 5 years
WE 17x17 BPRA Burnup and Cooling Time	BPRA Burnup shall not exceed that of a BPRA irradiated in fuel assemblies with a total Burnup of 36,000 MWd/MTU. -Minimum Cooling Time 10 years

**Table M.2-2
PWR Fuel Assembly Design Characteristics**

Assembly Class	B&W 15x15	WE 17x17	CE 15x15	WE 15x15	CE 14x14	WE 14x14
DSC Configuration	Max Unirradiated Length (in)					
32PT-S100/32PT-L100	165.75	165.75	165.75	165.75	165.75	165.75
32PT-S125/32PT-L125	171.71 ⁽¹⁾	171.71 ⁽¹⁾	171.71	171.71	171.71	171.71
Fissile Material	UO ₂	UO ₂	UO ₂	UO ₂	UO ₂	UO ₂
Maximum MTU/Assembly ⁽²⁾	0.475	0.475	0.475	0.475	0.475	0.475
Maximum Number of Fuel Rods	208	264	216	204	176	179
Maximum Number of Guide/ Instrument Tubes	17	25	9	21	5	17

⁽¹⁾ Maximum Assembly + BPRA Length (unirradiated)

⁽²⁾ The maximum MTU/assembly is based on the shielding analysis. The listed value is higher than the actual.

**Table M.2-3
Initial Enrichment and Number of PRAs for Various Fuel Assembly Types**

Assembly Class	Assembly Type	Maximum Initial Enrichment, wt. % U-235			
		0 PRAs Type A Basket	4 PRAs Type B Basket	8 PRAs Type C Basket	16 PRAs Type D Basket
WE 17x17 ⁽¹⁾	Westinghouse 17x17 LOPAR/Std	3.40	4.00	4.50	5.00
	Westinghouse 17x17 OFA/Vantage 5				
B&W 15x15 ⁽¹⁾	B&W 15x15 Mark B	3.30	3.90	NA	5.00
CE 15x15	CE 15x15 Palisades	3.40	Not Evaluated	Not Evaluated	Not Evaluated
	Exxon/ANF 15x15 CE				
WE 15x15	Westinghouse 15x15 Std/ZC	3.40	4.00	4.60	5.00
	Exxon/ANF 15x15 WE				
CE 14x14	CE 14x14 Std/Generic	3.80	4.60	5.00	Not Evaluated
	CE 14x14 Fort Calhoun				
WE 14x14	Westinghouse 14x14 ZCA/ZCB	4.00	5.00	Not Evaluated	Not Evaluated
	Westinghouse 14x14 OFA				
	Exxon/ANF 14x14 WE				

(1) With or without BPRAs. BPRAs shall not be stored in basket locations where a PRA is requested.

**Table M.2-4
Poison Rod Assembly (PRA) Description**

Assembly Class	Minimum Number of Rods/PRA	Modeled B₄C Content per Rod (g/cm) (75% Credit)	Minimum B₄C Content per Rod (g/cm)
WE 17x17	24	0.59	0.79
B&W 15x15	16	0.72	0.96
WE 15x15	20	0.72	0.96
CE 14x14	5	3.14	4.19
WE 14x14	16	0.72	0.96

Table M.2-5
PWR Fuel Qualification Table for 1.2 kW per Assembly for the NUHOMS®-32PT DSC (Fuel w/o BPRAs)
 (Minimum required years of cooling time after reactor core discharge)

BU (GWd/ MTU)	Initial Enrichment wt % U-235																														
	2.0	2.1	2.2	2.3	2.4	2.5	2.6	2.7	2.8	2.9	3.0	3.1	3.2	3.3	3.4	3.5	3.6	3.7	3.8	3.9	4.0	4.1	4.2	4.3	4.4	4.5	4.6	4.7	4.8	4.9	5.0
10	5	5	5	5	5	5	5	5	5	5	5	5	5	5	5	5	5	5	5	5	5	5	5	5	5	5	5	5	5	5	5
15	5	5	5	5	5	5	5	5	5	5	5	5	5	5	5	5	5	5	5	5	5	5	5	5	5	5	5	5	5	5	5
20	5	5	5	5	5	5	5	5	5	5	5	5	5	5	5	5	5	5	5	5	5	5	5	5	5	5	5	5	5	5	5
25	5	5	5	5	5	5	5	5	5	5	5	5	5	5	5	5	5	5	5	5	5	5	5	5	5	5	5	5	5	5	5
28	5	5	5	5	5	5	5	5	5	5	5	5	5	5	5	5	5	5	5	5	5	5	5	5	5	5	5	5	5	5	5
30	5	5	5	5	5	5	5	5	5	5	5	5	5	5	5	5	5	5	5	5	5	5	5	5	5	5	5	5	5	5	5
32	5	5	5	5	5	5	5	5	5	5	5	5	5	5	5	5	5	5	5	5	5	5	5	5	5	5	5	5	5	5	5
34	5	5	5	5	5	5	5	5	5	5	5	5	5	5	5	5	5	5	5	5	5	5	5	5	5	5	5	5	5	5	5
36	5	5	5	5	5	5	5	5	5	5	5	5	5	5	5	5	5	5	5	5	5	5	5	5	5	5	5	5	5	5	5
38	5	5	5	5	5	5	5	5	5	5	5	5	5	5	5	5	5	5	5	5	5	5	5	5	5	5	5	5	5	5	5
39	5	5	5	5	5	5	5	5	5	5	5	5	5	5	5	5	5	5	5	5	5	5	5	5	5	5	5	5	5	5	5
40	5	5	5	5	5	5	5	5	5	5	5	5	5	5	5	5	5	5	5	5	5	5	5	5	5	5	5	5	5	5	5
41	5	5	5	5	5	5	5	5	5	5	5	5	5	5	5	5	5	5	5	5	5	5	5	5	5	5	5	5	5	5	5
42	5	5	5	5	5	5	5	5	5	5	5	5	5	5	5	5	5	5	5	5	5	5	5	5	5	5	5	5	5	5	5
43	5	5	5	5	5	5	5	5	5	5	5	5	5	5	5	5	5	5	5	5	5	5	5	5	5	5	5	5	5	5	5
44	5	5	5	5	5	5	5	5	5	5	5	5	5	5	5	5	5	5	5	5	5	5	5	5	5	5	5	5	5	5	5
45	5	5	5	5	5	5	5	5	5	5	5	5	5	5	5	5	5	5	5	5	5	5	5	5	5	5	5	5	5	5	5

- Use burnup and enrichment to lookup minimum cooling time in years. Licensee is responsible for ensuring that uncertainties in fuel enrichment and burnup are correctly accounted for during fuel qualification.
- Round burnup UP to next higher entry, round enrichments DOWN to next lower entry.
- Fuel with an initial enrichment less than 2.0 and greater than 5.0 wt.% U-235 is unacceptable for storage.
- Fuel with a burnup greater than 45 GWd/MTU is unacceptable for storage
- Fuel with a burnup less than 10 GWd/MTU is acceptable for storage after 5-years cooling
- Example: An assembly with an initial enrichment of 3.75 wt. % U-235 and a burnup of 41.5 GWd/MTU is acceptable for storage after a six-year cooling time as defined by 3.7 wt. % U-235 (rounding down) and 42 GWd/MTU (rounding up) on the qualification table.

Table M.2-6
PWR Fuel Qualification Table for 0.87 kW per Assembly for the NUHOMS®-32PT DSC (Fuel w/o BPRAs)
 (Minimum required years of cooling time after reactor core discharge)

BU (GWd/ MTU)	Initial Enrichment wt % U-235																														
	2.0	2.1	2.2	2.3	2.4	2.5	2.6	2.7	2.8	2.9	3.0	3.1	3.2	3.3	3.4	3.5	3.6	3.7	3.8	3.9	4.0	4.1	4.2	4.3	4.4	4.5	4.6	4.7	4.8	4.9	5.0
10	5	5	5	5	5	5	5	5	5	5	5	5	5	5	5	5	5	5	5	5	5	5	5	5	5	5	5	5	5	5	5
15	5	5	5	5	5	5	5	5	5	5	5	5	5	5	5	5	5	5	5	5	5	5	5	5	5	5	5	5	5	5	5
20	5	5	5	5	5	5	5	5	5	5	5	5	5	5	5	5	5	5	5	5	5	5	5	5	5	5	5	5	5	5	5
25	5	5	5	5	5	5	5	5	5	5	5	5	5	5	5	5	5	5	5	5	5	5	5	5	5	5	5	5	5	5	5
28	5	5	5	5	5	5	5	5	5	5	5	5	5	5	5	5	5	5	5	5	5	5	5	5	5	5	5	5	5	5	5
30	5	5	5	5	5	5	5	5	5	5	5	5	5	5	5	5	5	5	5	5	5	5	5	5	5	5	5	5	5	5	5
32	5	5	5	5	5	5	6	6	5	5	5	5	5	5	5	5	5	5	5	5	5	5	5	5	5	5	5	5	5	5	5
34	5	5	5	5	5	5	6	6	6	6	6	6	6	6	6	6	6	6	6	6	6	6	6	6	6	6	6	6	6	6	6
36	5	5	5	5	5	5	6	6	6	6	6	6	6	6	6	6	6	6	6	6	6	6	6	6	6	6	6	6	6	6	6
38	5	5	5	5	5	5	6	6	6	6	6	6	6	6	6	6	6	6	6	6	6	6	6	6	6	6	6	6	6	6	6
39	5	5	5	5	5	5	6	6	6	6	6	6	6	6	6	6	6	6	6	6	6	6	6	6	6	6	6	6	6	6	6
40	5	5	5	5	5	5	6	6	6	6	6	6	6	6	6	6	6	6	6	6	6	6	6	6	6	6	6	6	6	6	6
41	5	5	5	5	5	5	6	6	6	6	6	6	6	6	6	6	6	6	6	6	6	6	6	6	6	6	6	6	6	6	6
42	5	5	5	5	5	5	6	6	6	6	6	6	6	6	6	6	6	6	6	6	6	6	6	6	6	6	6	6	6	6	6
43	5	5	5	5	5	5	6	6	6	6	6	6	6	6	6	6	6	6	6	6	6	6	6	6	6	6	6	6	6	6	6
44	5	5	5	5	5	5	6	6	6	6	6	6	6	6	6	6	6	6	6	6	6	6	6	6	6	6	6	6	6	6	6
45	5	5	5	5	5	5	6	6	6	6	6	6	6	6	6	6	6	6	6	6	6	6	6	6	6	6	6	6	6	6	6

- Use burnup and enrichment to lookup minimum cooling time in years. Licensee is responsible for ensuring that uncertainties in fuel enrichment and burnup are correctly accounted for during fuel qualification.
- Round burnup UP to next higher entry, round enrichments DOWN to next lower entry.
- Fuel with an initial enrichment less than 2.0 and greater than 5.0 wt.% U-235 is unacceptable for storage.
- Fuel with a burnup greater than 45 GWd/MTU is unacceptable for storage
- Fuel with a burnup less than 10 GWd/MTU is acceptable for storage after 5-years cooling.
- Example: An assembly with an initial enrichment of 3.75 wt. % U-235 and a burnup of 41.5 GWd/MTU is acceptable for storage after a eight-year cooling time as defined by 3.7 wt. % U-235 (rounding down) and 42 GWd/MTU (rounding up) on the qualification table.

Table M.2-7
PWR Fuel Qualification Table for 0.7 kW per Assembly for the NUHOMS®-32PT DSC (Fuel w/o BPRAs)
 (Minimum required years of cooling time after reactor core discharge)

BU (Gwd/ MTU)	Initial Enrichment wt % U-235																																
	2.0	2.1	2.2	2.3	2.4	2.5	2.6	2.7	2.8	2.9	3.0	3.1	3.2	3.3	3.4	3.5	3.6	3.7	3.8	3.9	4.0	4.1	4.2	4.3	4.4	4.5	4.6	4.7	4.8	4.9	5.0		
10	5	5	5	5	5	5	5	5	5	5	5	5	5	5	5	5	5	5	5	5	5	5	5	5	5	5	5	5	5	5			
15	5	5	5	5	5	5	5	5	5	5	5	5	5	5	5	5	5	5	5	5	5	5	5	5	5	5	5	5	5	5	5		
20	5	5	5	5	5	5	5	5	5	5	5	5	5	5	5	5	5	5	5	5	5	5	5	5	5	5	5	5	5	5	5		
25	5	5	5	5	5	5	5	5	5	5	5	5	5	5	5	5	5	5	5	5	5	5	5	5	5	5	5	5	5	5	5		
28				6	6	6	6	6	6	6	6	6	6	6	6	6	6	6	6	6	6	5	5	5	5	5	5	5	5	5	5		
30						6	6	6	6	6	6	6	6	6	6	6	6	6	6	6	6	6	6	6	6	6	6	6	6	6	6		
32							7	7	7	7	7	7	7	7	7	7	7	7	7	7	7	7	7	7	7	7	7	7	7	7	7		
34								8	8	8	8	8	8	8	8	8	8	8	8	8	8	8	8	8	8	8	8	8	8	8	8		
36									9	9	9	9	9	9	9	9	9	9	9	9	9	9	9	9	9	9	9	9	9	9	9		
38											10	10	10	10	10	10	10	10	10	10	10	10	10	10	10	10	10	10	10	10	10		
39												11	11	11	11	11	11	11	11	11	11	11	11	11	11	11	11	11	11	11	11		
40				Not Analyzed											11	11	11	11	11	11	11	11	11	11	11	11	11	11	11	11	11	11	11
41													12	12	12	12	12	12	12	12	12	12	12	12	12	12	12	12	12	12	12		
42													13	13	13	13	13	13	13	13	13	13	13	13	13	13	13	13	13	13	13		
43														14	14	14	14	14	14	14	14	14	14	14	14	14	14	14	14	14	14		
44															15	15	15	15	15	15	15	15	15	15	15	15	15	15	15	15	15		
45																16	16	16	16	16	16	16	16	16	16	16	16	16	16	16	16		

- Use burnup and enrichment to lookup minimum cooling time in years. Licensee is responsible for ensuring that uncertainties in fuel enrichment and burnup are correctly accounted for during fuel qualification.
- Round burnup UP to next higher entry, round enrichments DOWN to next lower entry.
- Fuel with an initial enrichment less than 2.0 and greater than 5.0 wt.% U-235 is unacceptable for storage.
- Fuel with a burnup greater than 45 GWd/MTU is unacceptable for storage
- Fuel with a burnup less than 10 GWd/MTU is acceptable for storage after 5-years cooling.
- Example: An assembly with an initial enrichment of 3.75 wt. % U-235 and a burnup of 41.5 GWd/MTU is acceptable for storage after a thirteen-year cooling time as defined by 3.7 wt. % U-235 (rounding down) and 42 GWd/MTU (rounding up) on the qualification table.

Table M.2-8
PWR Fuel Qualification Table for 0.63 kW per Assembly for the NUHOMS®-32PT DSC (Fuel w/o BPRAs)
 (Minimum required years of cooling time after reactor core discharge)

BU (Gwd/ MTU)	Initial Enrichment wt % U-235																														
	2.0	2.1	2.2	2.3	2.4	2.5	2.6	2.7	2.8	2.9	3.0	3.1	3.2	3.3	3.4	3.5	3.6	3.7	3.8	3.9	4.0	4.1	4.2	4.3	4.4	4.5	4.6	4.7	4.8	4.9	5.0
10	5	5	5	5	5	5	5	5	5	5	5	5	5	5	5	5	5	5	5	5	5	5	5	5	5	5	5	5	5	5	5
15	5	5	5	5	5	5	5	5	5	5	5	5	5	5	5	5	5	5	5	5	5	5	5	5	5	5	5	5	5	5	5
20	5	5	5	5	5	5	5	5	5	5	5	5	5	5	5	5	5	5	5	5	5	5	5	5	5	5	5	5	5	5	5
25		6	6	6	6	6	6	6	6	6	5	5	5	5	5	5	5	5	5	5	5	5	5	5	5	5	5	5	5	5	5
28				7	7	7	6	6	6	6	6	6	6	6	6	6	6	6	6	6	6	6	6	6	6	6	6	6	6	6	6
30						7	7	7	7	7	7	7	7	7	7	7	7	7	7	7	7	7	7	7	7	7	7	7	7	7	7
32							8	8	8	8	8	8	8	8	8	8	8	8	8	8	8	8	8	8	8	8	8	8	8	8	8
34								9	9	9	9	9	9	9	9	9	9	9	9	9	9	9	9	9	9	9	9	9	9	9	9
36									11	11	11	11	11	10	10	10	10	10	10	10	10	10	10	10	10	10	10	10	10	10	10
38										13	12	12	12	12	12	12	12	12	12	12	12	12	12	12	12	12	12	12	12	11	11
39											14	13	13	13	13	13	13	13	13	13	13	13	13	13	13	13	13	13	12	12	
40												15	15	14	14	14	14	14	14	14	14	14	14	14	14	14	14	14	13	13	
41												16	16	16	16	15	15	15	15	15	15	15	15	15	15	15	15	15	15	15	
42												17	17	17	17	17	17	16	16	16	16	16	16	16	16	16	16	16	16	16	
43													18	18	18	18	18	18	18	18	18	18	17	17	17	17	17	17	17	17	
44														20	19	19	19	19	19	19	19	19	19	19	19	19	18	18	18	18	
45															21	21	21	21	20	20	20	20	20	20	20	20	20	20	20	19	19

- Use burnup and enrichment to lookup minimum cooling time in years. Licensee is responsible for ensuring that uncertainties in fuel enrichment and burnup are correctly accounted for during fuel qualification.
- Round burnup UP to next higher entry, round enrichments DOWN to next lower entry.
- Fuel with an initial enrichment less than 2.0 and greater than 5.0 wt.% U-235 is unacceptable for storage.
- Fuel with a burnup greater than 45 GWd/MTU is unacceptable for storage
- Fuel with a burnup less than 10 GWd/MTU is acceptable for storage after 5-years cooling.
- Example: An assembly with an initial enrichment of 3.75 wt. % U-235 and a burnup of 41.5 GWd/MTU is acceptable for storage after a sixteen-year cooling time as defined by 3.7 wt. % U-235 (rounding down) and 42 GWd/MTU (rounding up) on the qualification table.

Table M.2-9
PWR Fuel Qualification Table for 0.6 kW per Assembly for the NUHOMS®-32PT DSC (Fuel w/o BPRAs)
 (Minimum required years of cooling time after reactor core discharge)

BU (GWd/ MTU)	Initial Enrichment wt % U-235																																
	2.0	2.1	2.2	2.3	2.4	2.5	2.6	2.7	2.8	2.9	3.0	3.1	3.2	3.3	3.4	3.5	3.6	3.7	3.8	3.9	4.0	4.1	4.2	4.3	4.4	4.5	4.6	4.7	4.8	4.9	5.0		
10	5	5	5	5	5	5	5	5	5	5	5	5	5	5	5	5	5	5	5	5	5	5	5	5	5	5	5	5	5	5			
15	5	5	5	5	5	5	5	5	5	5	5	5	5	5	5	5	5	5	5	5	5	5	5	5	5	5	5	5	5	5	5		
20	5	5	5	5	5	5	5	5	5	5	5	5	5	5	5	5	5	5	5	5	5	5	5	5	5	5	5	5	5	5	5		
25		6	6	6	6	6	6	6	6	6	6	6	6	6	6	6	6	6	6	6	6	6	6	6	6	6	6	6	5	5	5	5	
28				7	7	7	7	7	7	7	7	7	7	7	7	7	7	7	7	7	7	7	7	6	6	6	6	6	6	6	6	6	
30						8	8	8	8	8	8	8	8	8	8	7	7	7	7	7	7	7	7	7	7	7	7	7	7	7	7	7	
32							9	9	9	9	9	9	9	9	9	9	8	8	8	8	8	8	8	8	8	8	8	8	8	8	8	8	
34								10	10	10	10	10	10	10	10	10	10	10	10	10	10	10	10	10	10	10	10	9	9	9	9	9	
36									12	12	12	12	12	12	12	12	12	11	11	11	11	11	11	11	11	11	11	11	11	11	11	11	
38										14	14	14	14	14	14	14	14	14	14	14	13	13	13	13	13	13	13	13	13	13	13	13	
39											15	15	15	15	15	15	15	15	15	15	15	15	15	14	14	14	14	14	14	14	14	14	
40				Not Analyzed												17	16	16	16	16	16	16	16	16	16	16	16	16	15	15	15	15	15
41																18	18	18	18	18	17	17	17	17	17	17	17	17	17	17	17	16	
42																19	19	19	19	19	19	19	19	19	18	18	18	18	18	18	18	18	
43																	21	20	20	20	20	20	20	20	20	20	20	20	20	20	20	20	
44																		22	22	22	22	21	21	21	21	21	21	21	21	21	21	20	20
45																			23	23	23	23	23	23	23	23	22	22	22	22	22	22	22

- Use burnup and enrichment to lookup minimum cooling time in years. Licensee is responsible for ensuring that uncertainties in fuel enrichment and burnup are correctly accounted for during fuel qualification.
- Round burnup UP to next higher entry, round enrichments DOWN to next lower entry.
- Fuel with an initial enrichment less than 2.0 and greater than 5.0 wt.% U-235 is unacceptable for storage.
- Fuel with a burnup greater than 45 GWd/MTU is unacceptable for storage
- Fuel with a burnup less than 10 GWd/MTU is acceptable for storage after 5-years cooling.
- Example: An assembly with an initial enrichment of 3.75 wt. % U-235 and a burnup of 41.5 GWd/MTU is acceptable for storage after a nineteen-year cooling time as defined by 3.7 wt. % U-235 (rounding down) and 42 GWd/MTU (rounding up) on the qualification table.

Table M.2-10
PWR Fuel Qualification Table for 1.2 kW per Assembly for the NUHOMS®-32PT DSC (Fuel w/ BPRAs)
 (Minimum required years of cooling time after reactor core discharge)

BU (GWd/ MTU)	Initial Enrichment wt % U-235																														
	2.0	2.1	2.2	2.3	2.4	2.5	2.6	2.7	2.8	2.9	3.0	3.1	3.2	3.3	3.4	3.5	3.6	3.7	3.8	3.9	4.0	4.1	4.2	4.3	4.4	4.5	4.6	4.7	4.8	4.9	5.0
10	5	5	5	5	5	5	5	5	5	5	5	5	5	5	5	5	5	5	5	5	5	5	5	5	5	5	5	5	5	5	5
15	5	5	5	5	5	5	5	5	5	5	5	5	5	5	5	5	5	5	5	5	5	5	5	5	5	5	5	5	5	5	5
20	5	5	5	5	5	5	5	5	5	5	5	5	5	5	5	5	5	5	5	5	5	5	5	5	5	5	5	5	5	5	5
25		5	5	5	5	5	5	5	5	5	5	5	5	5	5	5	5	5	5	5	5	5	5	5	5	5	5	5	5	5	5
28			5	5	5	5	5	5	5	5	5	5	5	5	5	5	5	5	5	5	5	5	5	5	5	5	5	5	5	5	5
30					5	5	5	5	5	5	5	5	5	5	5	5	5	5	5	5	5	5	5	5	5	5	5	5	5	5	5
32						5	5	5	5	5	5	5	5	5	5	5	5	5	5	5	5	5	5	5	5	5	5	5	5	5	5
34							5	5	5	5	5	5	5	5	5	5	5	5	5	5	5	5	5	5	5	5	5	5	5	5	5
36								5	5	5	5	5	5	5	5	5	5	5	5	5	5	5	5	5	5	5	5	5	5	5	5
38									5	5	5	5	5	5	5	5	5	5	5	5	5	5	5	5	5	5	5	5	5	5	5
39										5	5	5	5	5	5	5	5	5	5	5	5	5	5	5	5	5	5	5	5	5	5
40											5	5	5	5	5	5	5	5	5	5	5	5	5	5	5	5	5	5	5	5	5
41												6	6	5	5	5	5	5	5	5	5	5	5	5	5	5	5	5	5	5	5
42													6	6	6	6	6	6	6	5	5	5	5	5	5	5	5	5	5	5	5
43														6	6	6	6	6	6	6	6	6	6	6	6	6	6	6	6	6	6
44															6	6	6	6	6	6	6	6	6	6	6	6	6	6	6	6	6
45																6	6	6	6	6	6	6	6	6	6	6	6	6	6	6	6

- Use burnup and enrichment to lookup minimum cooling time in years. Licensee is responsible for ensuring that uncertainties in fuel enrichment and burnup are correctly accounted for during fuel qualification.
- Round burnup UP to next higher entry, round enrichments DOWN to next lower entry.
- Fuel with an initial enrichment less than 2.0 and greater than 5.0 wt.% U-235 is unacceptable for storage.
- Fuel with a burnup greater than 45 GWd/MTU is unacceptable for storage
- Fuel with a burnup less than 10 GWd/MTU is acceptable for storage after 5-years cooling
- Example: An assembly with an initial enrichment of 3.75 wt. % U-235 and a burnup of 41.5 GWd/MTU is acceptable for storage after a six-year cooling time as defined by 3.7 wt. % U-235 (rounding down) and 42 GWd/MTU (rounding up) on the qualification table.

Table M.2-11
PWR Fuel Qualification Table for 0.87 kW per Assembly for the NUHOMS®-32PT DSC (Fuel w/ BPRAs)
 (Minimum required years of cooling time after reactor core discharge)

BU (GWd/ MTU)	Initial Enrichment wt % U-235																														
	2.0	2.1	2.2	2.3	2.4	2.5	2.6	2.7	2.8	2.9	3.0	3.1	3.2	3.3	3.4	3.5	3.6	3.7	3.8	3.9	4.0	4.1	4.2	4.3	4.4	4.5	4.6	4.7	4.8	4.9	5.0
10	5	5	5	5	5	5	5	5	5	5	5	5	5	5	5	5	5	5	5	5	5	5	5	5	5	5	5	5	5	5	5
15	5	5	5	5	5	5	5	5	5	5	5	5	5	5	5	5	5	5	5	5	5	5	5	5	5	5	5	5	5	5	5
20	5	5	5	5	5	5	5	5	5	5	5	5	5	5	5	5	5	5	5	5	5	5	5	5	5	5	5	5	5	5	5
25	5	5	5	5	5	5	5	5	5	5	5	5	5	5	5	5	5	5	5	5	5	5	5	5	5	5	5	5	5	5	5
28	5	5	5	5	5	5	5	5	5	5	5	5	5	5	5	5	5	5	5	5	5	5	5	5	5	5	5	5	5	5	5
30	5	5	5	5	5	5	5	5	5	5	5	5	5	5	5	5	5	5	5	5	5	5	5	5	5	5	5	5	5	5	5
32	6	6	6	6	6	6	6	6	6	6	6	6	6	6	6	6	6	6	6	6	6	6	6	6	6	6	6	6	6	6	6
434	6	6	6	6	6	6	6	6	6	6	6	6	6	6	6	6	6	6	6	6	6	6	6	6	6	6	6	6	6	6	6
36	7	7	7	7	7	7	7	7	7	7	7	7	7	7	7	7	7	7	7	7	7	7	7	7	7	7	7	7	7	7	7
38	7	7	7	7	7	7	7	7	7	7	7	7	7	7	7	7	7	7	7	7	7	7	7	7	7	7	7	7	7	7	7
39	7	7	7	7	7	7	7	7	7	7	7	7	7	7	7	7	7	7	7	7	7	7	7	7	7	7	7	7	7	7	7
40	8	8	8	8	8	8	8	8	8	8	8	8	8	8	8	8	8	8	8	8	8	8	8	8	8	8	8	8	8	8	8
41	8	8	8	8	8	8	8	8	8	8	8	8	8	8	8	8	8	8	8	8	8	8	8	8	8	8	8	8	8	8	8
42	9	9	9	9	9	9	9	9	9	9	9	9	9	9	9	9	9	9	9	9	9	9	9	9	9	9	9	9	9	9	9
43	9	9	9	9	9	9	9	9	9	9	9	9	9	9	9	9	9	9	9	9	9	9	9	9	9	9	9	9	9	9	9
44	9	9	9	9	9	9	9	9	9	9	9	9	9	9	9	9	9	9	9	9	9	9	9	9	9	9	9	9	9	9	9
45	10	10	10	10	10	10	10	10	10	10	10	10	10	10	10	10	10	10	10	10	10	10	10	10	10	10	10	10	10	10	10

- Use burnup and enrichment to lookup minimum cooling time in years. Licensee is responsible for ensuring that uncertainties in fuel enrichment and burnup are correctly accounted for during fuel qualification.
- Round burnup UP to next higher entry, round enrichments DOWN to next lower entry.
- Fuel with an initial enrichment less than 2.0 and greater than 5.0 wt.% U-235 is unacceptable for storage.
- Fuel with a burnup greater than 45 GWd/MTU is unacceptable for storage
- Fuel with a burnup less than 10 GWd/MTU is acceptable for storage after 5-years cooling.
- Example: An assembly with an initial enrichment of 3.75 wt. % U-235 and a burnup of 41.5 GWd/MTU is acceptable for storage after a eight-year cooling time as defined by 3.7 wt. % U-235 (rounding down) and 42 GWd/MTU (rounding up) on the qualification table.

Table M.2-12
PWR Fuel Qualification Table for 0.7 kW per Assembly for the NUHOMS®-32PT DSC (Fuel w/ BPRAs)
 (Minimum required years of cooling time after reactor core discharge)

BU (GWd/ MTU)	Initial Enrichment wt % U-235																																	
	2.0	2.1	2.2	2.3	2.4	2.5	2.6	2.7	2.8	2.9	3.0	3.1	3.2	3.3	3.4	3.5	3.6	3.7	3.8	3.9	4.0	4.1	4.2	4.3	4.4	4.5	4.6	4.7	4.8	4.9	5.0			
10	5	5	5	5	5	5	5	5	5	5	5	5	5	5	5	5	5	5	5	5	5	5	5	5	5	5	5	5	5	5	5			
15	5	5	5	5	5	5	5	5	5	5	5	5	5	5	5	5	5	5	5	5	5	5	5	5	5	5	5	5	5	5	5	5		
20	5	5	5	5	5	5	5	5	5	5	5	5	5	5	5	5	5	5	5	5	5	5	5	5	5	5	5	5	5	5	5	5		
25	5	5	5	5	5	5	5	5	5	5	5	5	5	5	5	5	5	5	5	5	5	5	5	5	5	5	5	5	5	5	5	5		
28				6	6	6	6	6	6	6	6	6	6	6	6	6	6	6	6	6	6	6	6	6	6	6	6	6	6	6	6	6		
30						6	6	6	6	6	6	6	6	6	6	6	6	6	6	6	6	6	6	6	6	6	6	6	6	6	6	6	6	
32							7	7	7	7	7	7	7	7	7	7	7	7	7	7	7	7	7	7	7	7	7	7	7	7	7	7	7	
34								8	8	8	8	8	8	8	8	8	8	8	8	8	8	7	7	7	7	7	7	7	7	7	7	7	7	
36									9	9	9	9	9	9	9	9	9	9	9	8	8	8	8	8	8	8	8	8	8	8	8	8	8	8
38										10	10	10	10	10	10	10	10	10	10	10	10	10	10	9	9	9	9	9	9	9	9	9	9	9
39											11	11	11	11	11	11	11	11	11	11	11	11	11	11	11	11	11	11	11	11	11	11	11	11
40				Not Analyzed									12	11	11	11	11	11	11	11	11	11	11	11	11	11	11	11	11	11	11	11	11	11
41												13	13	12	12	12	12	12	12	12	12	12	12	12	12	12	12	12	12	12	12	12	12	
42												14	14	13	13	13	13	13	13	13	13	13	13	13	13	13	13	13	13	13	13	13	13	
43													15	14	14	14	14	14	14	14	14	14	14	14	14	14	14	14	14	14	14	14	14	
44														16	15	15	15	15	15	15	15	15	15	15	15	15	15	15	15	15	15	15	15	
45															17	17	16	16	16	16	16	16	16	16	16	16	16	16	16	16	16	16	16	

- Use burnup and enrichment to lookup minimum cooling time in years. Licensee is responsible for ensuring that uncertainties in fuel enrichment and burnup are correctly accounted for during fuel qualification.
- Round burnup UP to next higher entry, round enrichments DOWN to next lower entry.
- Fuel with an initial enrichment less than 2.0 and greater than 5.0 wt.% U-235 is unacceptable for storage.
- Fuel with a burnup greater than 45 GWd/MTU is unacceptable for storage
- Fuel with a burnup less than 10 GWd/MTU is acceptable for storage after 5-years cooling.
- Example: An assembly with an initial enrichment of 3.75 wt. % U-235 and a burnup of 41.5 GWd/MTU is acceptable for storage after a thirteen-year cooling time as defined by 3.7 wt. % U-235 (rounding down) and 42 GWd/MTU (rounding up) on the qualification table.

Table M.2-13
PWR Fuel Qualification Table for 0.63 kW per Assembly for the NUHOMS®-32PT DSC (Fuel w/ BPRAs)
 (Minimum required years of cooling time after reactor core discharge)

BU (Gwd/ MTU)	Initial Enrichment wt % U-235																															
	2.0	2.1	2.2	2.3	2.4	2.5	2.6	2.7	2.8	2.9	3.0	3.1	3.2	3.3	3.4	3.5	3.6	3.7	3.8	3.9	4.0	4.1	4.2	4.3	4.4	4.5	4.6	4.7	4.8	4.9	5.0	
10	5	5	5	5	5	5	5	5	5	5	5	5	5	5	5	5	5	5	5	5	5	5	5	5	5	5	5	5	5	5		
15	5	5	5	5	5	5	5	5	5	5	5	5	5	5	5	5	5	5	5	5	5	5	5	5	5	5	5	5	5	5	5	
20	5	5	5	5	5	5	5	5	5	5	5	5	5	5	5	5	5	5	5	5	5	5	5	5	5	5	5	5	5	5	5	
25	6	6	6	6	6	6	6	6	6	6	6	6	6	6	6	6	6	6	6	6	6	6	6	6	6	6	6	6	6	6	6	
28	7	7	7	7	7	7	7	7	7	6	6	6	6	6	6	6	6	6	6	6	6	6	6	6	6	6	6	6	6	6	6	
30	7	7	7	7	7	7	7	7	7	7	7	7	7	7	7	7	7	7	7	7	7	7	7	7	7	7	7	7	7	7	7	
32	8	8	8	8	8	8	8	8	8	8	8	8	8	8	8	8	8	8	8	8	8	8	8	8	8	8	8	8	8	8	8	
34	10	10	9	9	9	9	9	9	9	9	9	9	9	9	9	9	9	9	9	9	9	9	9	9	9	9	9	9	9	9	9	
36	11	11	11	11	11	11	11	11	11	11	11	11	11	11	11	11	11	11	11	10	10	10	10	10	10	10	10	10	10	10	10	
38	13	13	13	13	13	13	13	13	13	13	13	13	13	13	13	13	12	12	12	12	12	12	12	12	12	12	12	12	12	12	12	
39	14	14	14	14	14	14	14	14	14	14	14	14	14	14	14	14	13	13	13	13	13	13	13	13	13	13	13	13	13	13	13	
40	Not Analyzed					15	15	15	15	15	15	15	15	15	15	15	15	14	14	14	14	14	14	14	14	14	14	14	14	14	14	
41	Not Analyzed					16	16	16	16	16	16	16	16	16	16	16	16	16	16	16	16	16	16	15	15	15	15	15	15	15	15	15
42	Not Analyzed					18	18	17	17	17	17	17	17	17	17	17	17	17	17	17	17	17	17	17	17	16	16	16	16	16	16	16
43	Not Analyzed					19	19	19	19	19	19	19	19	19	19	19	19	18	18	18	18	18	18	18	18	18	18	18	18	18	17	17
44	Not Analyzed					20	20	20	20	20	20	20	20	20	20	20	20	20	20	20	20	20	19	19	19	19	19	19	19	19	19	19
45	Not Analyzed					22	21	21	21	21	21	21	21	21	21	21	21	21	21	21	21	21	21	21	21	20	20	20	20	20	20	20

- Use burnup and enrichment to lookup minimum cooling time in years. Licensee is responsible for ensuring that uncertainties in fuel enrichment and burnup are correctly accounted for during fuel qualification.
- Round burnup UP to next higher entry, round enrichments DOWN to next lower entry.
- Fuel with an initial enrichment less than 2.0 and greater than 5.0 wt.% U-235 is unacceptable for storage.
- Fuel with a burnup greater than 45 GWd/MTU is unacceptable for storage
- Fuel with a burnup less than 10 GWd/MTU is acceptable for storage after 5-years cooling.
- Example: An assembly with an initial enrichment of 3.75 wt. % U-235 and a burnup of 41.5 GWd/MTU is acceptable for storage after a seventeen-year cooling time as defined by 3.7 wt. % U-235 (rounding down) and 42 GWd/MTU (rounding up) on the qualification table.

Table M.2-14
PWR Fuel Qualification Table for 0.6 kW per Assembly for the NUHOMS®-32PT DSC (Fuel w/ BPRAs)
 (Minimum required years of cooling time after reactor core discharge)

BU (Gwd/ MTU)	Initial Enrichment wt % U-235																														
	2.0	2.1	2.2	2.3	2.4	2.5	2.6	2.7	2.8	2.9	3.0	3.1	3.2	3.3	3.4	3.5	3.6	3.7	3.8	3.9	4.0	4.1	4.2	4.3	4.4	4.5	4.6	4.7	4.8	4.9	5.0
10	5	5	5	5	5	5	5	5	5	5	5	5	5	5	5	5	5	5	5	5	5	5	5	5	5	5	5	5	5	5	
15	5	5	5	5	5	5	5	5	5	5	5	5	5	5	5	5	5	5	5	5	5	5	5	5	5	5	5	5	5	5	5
20	5	5	5	5	5	5	5	5	5	5	5	5	5	5	5	5	5	5	5	5	5	5	5	5	5	5	5	5	5	5	5
25		6	6	6	6	6	6	6	6	6	6	6	6	6	6	6	6	6	6	6	6	6	6	6	6	6	6	6	6	6	6
28				7	7	7	7	7	7	7	7	7	7	7	7	7	7	7	7	7	7	7	7	7	7	7	7	7	7	7	6
30						8	8	8	8	8	8	8	8	8	8	8	8	8	8	8	8	8	7	7	7	7	7	7	7	7	7
32							9	9	9	9	9	9	9	9	9	9	9	9	9	9	9	9	9	9	9	9	8	8	8	8	8
34								11	11	11	10	10	10	10	10	10	10	10	10	10	10	10	10	10	10	10	10	10	10	10	10
36									12	12	12	12	12	12	12	12	12	12	12	12	12	12	12	12	12	12	12	11	11	11	11
38										15	15	14	14	14	14	14	14	14	14	14	14	14	14	14	14	14	14	14	14	14	13
39											16	16	16	16	16	15	15	15	15	15	15	15	15	15	15	15	15	15	15	15	15
40												17	17	17	17	17	17	17	17	16	16	16	16	16	16	16	16	16	16	16	16
41													19	18	18	18	18	18	18	18	18	18	18	17	17	17	17	17	17	17	17
42													20	20	20	20	19	19	19	19	19	19	19	19	19	19	19	19	19	19	19
43														21	21	21	21	21	21	21	20	20	20	20	20	20	20	20	20	20	20
44															23	22	22	22	22	22	22	22	22	22	22	21	21	21	21	21	21
45																24	24	24	24	24	23	23	23	23	23	23	23	23	23	23	22

- Use burnup and enrichment to lookup minimum cooling time in years. Licensee is responsible for ensuring that uncertainties in fuel enrichment and burnup are correctly accounted for during fuel qualification.
- Round burnup UP to next higher entry, round enrichments DOWN to next lower entry.
- Fuel with an initial enrichment less than 2.0 and greater than 5.0 wt.% U-235 is unacceptable for storage.
- Fuel with a burnup greater than 45 GWd/MTU is unacceptable for storage
- Fuel with a burnup less than 10 GWd/MTU is acceptable for storage after 5-years cooling.
- Example: An assembly with an initial enrichment of 3.75 wt. % U-235 and a burnup of 41.5 GWd/MTU is acceptable for storage after a nineteen-year cooling time as defined by 3.7 wt. % U-235 (rounding down) and 42 GWd/MTU (rounding up) on the qualification table.

**Table M.2-15
Summary of 32PT-DSC Load Combinations**

Load Case	Horizontal DW		Vertical DW		Internal Pressure	External Pressure	Thermal Condition	Lifting Loads	Other Loads	Service Level
	DSC	Fuel	DSC	Fuel						
Non-Operational Load Cases										
NO-1 Fab. Leak Testing	--	--	--	--	--	14.7 psi	70°F	--	155 kip axial	Test
NO-2 Fab. Leak Testing	--	--	--	--	18 psi				155 kip axial	Test
NO-3 DSC Uprighting	x	--	--	--	--	--	70°F	x	--	B
NO-4 DSC Vertical Lift	--	--	x	--	--	--	70°F	x	--	B
Fuel Loading Load Cases										
FL-1 DSC/Cask Filling	--	--	Cask	--	--	Hydrostatic	100°F Cask	x	x	A
FL-2 DSC/Cask Filling	--	--	Cask	--	Hydrostatic	Hydrostatic	100°F Cask	x	x	A
FL-3 DSC/Cask Xfer	--	--	Cask	--	Hydrostatic	Hydrostatic	100°F Cask	--	--	A
FL-4 Fuel Loading	--	--	Cask	x	Hydrostatic	Hydrostatic	100°F Cask	--	--	A
FL-5 Xfer to Decon	--	--	Cask	x	Hydrostatic	Hydrostatic	100°F Cask	--	--	A
FL-6 Inner Cover plate Welding	--	--	Cask	x	Hydrostatic	Hydrostatic	100°F Cask	--	--	A
FL-7 Fuel Deck Seismic Loading	--	--	Cask	x	Hydrostatic	Hydrostatic	100°F Cask	--	Note 10	D
Draining/Drying Load Cases										
DD-1 DSC Blowdown	--	--	Cask	x	Hydrostatic+ 20 psi	Hydrostatic	100°F Cask	--	--	B
DD-2 Vacuum Drying	--	--	Cask	x	0 psia	Hydrostatic+ 14.7psi	100°F Cask	--	--	B
DD-3 Helium Backfill	--	--	Cask	x	18 psi	Hydrostatic	100°F Cask	--	--	B
DD-4 Final Helium Backfill	--	--	Cask	x	3.5 psi	Hydrostatic	100°F Cask	--	--	B
DD-5 Outer Cover Plate Weld	--	--	Cask	x	3.5 psi	Hydrostatic	100°F Cask	--	--	B
Transfer Trailer Loading										
TL-1 Vertical Xfer to Trailer	--	--	Cask	x	15 psi	--	0°F Cask	--	--	A
TL-2 Vertical Xfer to Trailer	--	--	Cask	x	15 psi	--	100°F Cask	--	--	A
TL-3 Laydown	Cask	X	--	--	15 psi	--	0°F Cask	--	--	A
TL-4 Laydown	Cask	X	--	--	15 psi	--	100°F Cask	--	--	A

Table M.2-15
Summary of 32PT-DSC Load Combinations
(continued)

Load Case	Horizontal DW		Vertical DW		Internal Pressure	External Pressure	Thermal Condition	Handling Loads	Other Loads	Service Level
	DSC	Fuel	DSC	Fuel						
Transfer To/From ISFSI										
TR-1 Axial Load – Cold	Cask	X	--	--	15.0 psi	--	0°F Cask	1g Axial	--	A
TR-2 Transverse Load - Cold	Cask	X	--	--	15.0 psi	--	0°F Cask	1g Transverse	--	A
TR-3 Vertical Load – Cold	Cask	X	--	--	15.0 psi	--	0°F Cask	1g Vertical	--	A
TR-4 Oblique Load – Cold	Cask	X	--	--	15.0 psi	--	0°F Cask	½ g Axial + ½ g Trans + ½ g Vert.	--	A
TR-5 Axial Load – Hot	Cask	X	--	--	15.0 psi	--	100°F Cask	1g Axial	--	A
TR-6 Transverse Load - Hot	Cask	X	--	--	15.0 psi	--	100°F Cask	1g Trans.	--	A
TR-7 Vertical Load – Hot	Cask	X	--	--	15.0 psi	--	100°F Cask	1g Vertical	--	A
TR-8 Oblique Load – Hot	Cask	X	--	--	15.0 psi	--	100°F Cask	½ g Axial + ½ g Trans + ½ g Vert.	--	A
TR-9 25g Corner Drop	Note 1	Note 1	Note 1	Note 1	20 psi	--	100°F ⁽²⁾ Cask		25g Corner Drop	D
TR-10 75g Side Drop	Note 1	Note 1	--	--	20 psi	--	100°F ⁽²⁾ Cask		75g Side Drop	D
TR-11 Top or Bottom End Drops	Note 12									
HSM LOADING										
LD-1 Normal Loading - Cold	Cask	X	--	--	15.0 psi	--	0°F Cask	+80 Kip	--	A
LD-2 Normal Loading – Hot	Cask	X	--	--	15.0 psi	--	100° F Cask	+80 Kip	--	A
LD-3 Normal Loading – Hot	Cask	X	--	--	15.0 psi	--	117° F w/shade ⁽⁵⁾	+80 Kip	--	A
LD-4 Off-Normal Loading – Cold	Cask	X	--	--	20.0 psi	--	0° F Cask	+80 Kip	--	B
LD-5 Off-Normal Loading - Hot	Cask	X	--	--	20.0 psi	--	100° F Cask	+80 Kip	--	B
LD-6 Off-Normal Loading – Hot	Cask	X	--	--	20.0 psi	--	117° F w/shade ⁽⁵⁾	+80 Kip	--	B
LD-7 Accident Loading	Cask	X	--	--	20.0 psi	--	117° F w/shade ⁽⁵⁾	+80 Kip	--	C/D

Table M.2-15
Summary of 32PT-DSC Load Combinations
(continued)

Load Case	Horizontal DW		Vertical DW		Internal Pressure	External Pressure	Thermal Condition	Handling Loads	Other Loads	Service Level
	DSC	Fuel	DSC	Fuel						
HSM STORAGE										
HSM-1 Off-Normal	HSM	X	--	--	15.0 psi	--	-40° F HSM	--	--	B
HSM-2 Normal Storage	HSM	X	--	--	15.0 psi	--	0° F HSM	--	--	A
HSM-3 Off-Normal	HSM	X	--	--	15.0 psi	--	117° F HSM	--	--	B
HSM-4 Off-Normal Temp. + Failed Fuel	HSM	X	--	--	20.0 psi	--	117° F HSM	--	--	C
HSM-5 Blocked Vent Storage	HSM	X	--	--	105.0 psi	--	117° F HSM/BV ⁽⁴⁾	--	--	D
HSM-6 B.V. + Failed Fuel Storage	HSM	X	--	--	105.0 psi	--	117° F HSM/BV ⁽⁴⁾	--	--	D
HSM-7 Earthquake Loading – Cold	HSM	X	--	--	15.0 psi	--	0° F HSM	--	EQ	C
HSM-8 Earthquake Loading – Hot	HSM	X	--	--	15.0 psi	--	100° F HSM	--	EQ	C
HSM-9 Flood Load (50' H ₂ O) – Cold	HSM	X	--	--	0 psi	22 psi	0° F HSM	--	Flood ⁽³⁾	C
HSM-10 Flood Load (50' H ₂ O) – Hot	HSM	X	--	--	0 psi	22 psi	100° F HSM	--	Flood ⁽³⁾	C

HSM Unloading	Horizontal DW		Vertical DW		Internal Pressure	External Pressure	Thermal Condition	Handling Loads	Other Loads	Service Level
	DSC	Fuel	DSC	Fuel						
UL-1 Normal Unloading – Cold	HSM	X	--	--	15.0 psi	--	0° F HSM	-60 Kip	--	A
UL-2 Normal Unloading – Hot	HSM	X	--	--	15.0 psi	--	100° F HSM	-60 Kip	--	A
UL-3 Normal Unloading – Hot	HSM	X	--	--	15.0 psi	--	117° F HSM	-60 Kip	--	A
UL-4 Off-Normal Unloading – Cold	HSM	X	--	--	20.0 psi	--	0° F HSM	-60 Kip	--	B
UL-5 Off-Normal Unloading – Hot	HSM	X	--	--	20.0 psi	--	100° F HSM	-60 Kip	--	B
UL-6 Off-Normal Unloading – Hot	HSM	X	--	--	20.0 psi	--	117° F HSM	-60 Kip	--	B
UL-7 Off-Normal Unloading – Hot	HSM	X	--	--	20.0 psi	--	100° F HSM	-80 Kip	--	C
UL-8 Accident Unloading – Hot	HSM	X	--	--	105.0 psi	--	100° F HSM	-80 Kip	--	D

HSM Unloading / Reflood	Horizontal DW		Vertical DW		Internal Pressure ⁽¹³⁾	External Pressure	Thermal Condition	Handling Loads	Other Loads	Service Level
	DSC	Fuel	DSC	Fuel						
RF-1 32PT-DSC Reflood	--	--	Cask	X	105.0 psi (max)	Hydrostatic	100° F Cask	--	--	D

Table M.2-15
Summary of 32PT-DSC Load Combinations

Summary of 32PT-DSC Load Combinations Notes:

1. Drop acceleration includes gravity effects.
2. For Level D events, stress allowables are based considering the maximum temperature of the component (Thermal stresses are not limited for level D events and maximum temperatures give minimum allowables) or the actual temperature distribution (basket).
3. Flood load is an external pressure equivalent to 50 feet (164m) of water.
4. BV = HSM Vents are blocked.
5. At temperature over 100° F (38°C) a sunshade is required over the TC. Temperatures for these cases are enveloped by the 100° F (without sunshade) case.
6. Not used.
7. Not used.
8. Not used.
9. Not used.
10. Fuel deck seismic loads are assumed enveloped by handling loads.
11. Not used.
12. The 75g top end drop and bottom end drop are not credible events, therefore these drop analyses are not required. However, consideration of 60g end drops and the 75g side drop conservatively envelop the effects of a 25g corner drop.
13. Reflood pressure is limited to 20psi. For analysis purposes a 105psi pressure is considered.

Table M.2-16
Summary of Stress Criteria for Subsection NB Pressure Boundary Components
(e.g., Shells and Cover Plates)

Service Level	Stress Category
Level A ⁽¹⁾⁽²⁾	$P_m \leq 1.0S_m$ $P_L \leq 1.5S_m$ $P_m \text{ (or } P_L) + P_b \leq 1.5S_m$ $P_m \text{ (or } P_L) + P_b + Q \leq 3.0S_m$
Level B ⁽¹⁾⁽³⁾	$P_m \leq 1.0S_m$ $P_L \leq 1.5S_m$ $P_m \text{ (or } P_L) + P_b \leq 1.5S_m$ $P_m \text{ (or } P_L) + P_b + Q \leq 3.0S_m$
Level C ⁽⁴⁾	$P_m \leq \max(1.2S_m, 1.0S_y)$ $P_L \leq \max(1.8S_m, 1.5S_y)$ $P_m \text{ (or } P_L) + P_b \leq \max(1.8S_m, 1.5S_y)$ $P_m \text{ (or } P_L) + P_b + Q \leq \text{note 4}$ $F_p \leq 1.5S_y$ $\sigma_1 + \sigma_2 + \sigma_3 \leq 4.0S_m$
Carbon Steel Components (e.g., Shield Plugs)	
Level D ⁽⁴⁾ Elastic Analysis	$P_m \leq 0.7S_u$ $P_m \text{ (or } P_L) + P_b \leq 1.0S_u$
Level D ⁽⁴⁾ Plastic Analysis	$P_m \leq 0.7S_u$ $P_m \text{ (or } P_L) + P_b \leq 0.9S_u$
Austenitic Steel Components (e.g., Shell)	
Level D ⁽⁴⁾ Elastic Analysis	$P_m \leq \min(2.4S_m, 0.7S_u)$ $P_m \text{ (or } P_L) + P_b \leq \min(3.6S_m, 1.0S_u)$
Level D ⁽⁴⁾ Plastic Analysis	$P_m \leq \max(0.7S_u, S_y + (S_u - S_y)/3)$ $P_m \text{ (or } P_L) + P_b \leq 0.9S_u$

Notes:

1. The secondary stress limit may be exceeded provided the criteria of NB-3228.5 are satisfied.
2. There are no specific limits on primary stresses for Level A events. However, the stresses due to primary loads during normal service must be computed and combined with the effects of other loadings in satisfying other limits. See NB-3222.1.
3. The 10% increase in allowables from NB-3223(a) may be applicable for load combinations for which the pressure exceeds the design pressure.
4. Evaluation of secondary stresses not required for Level C and D events.

Table M.2-17
Summary of Stress Criteria for Subsection NG Components

Service Level	Stress Category (5)
Level A/B ⁽¹⁾	$P_m \leq 1.0S_m$ $P_m + P_b \leq 1.5S_m$ $P_m + P_b + Q \leq 3.0S_m$ (note 4)
Level C ⁽²⁾⁽³⁾ Elastic Analysis	$P_m \leq 1.5S_m$ $P_m + P_b \leq 2.25S_m$
Level D ⁽²⁾⁽⁶⁾ Elastic Analysis	$P_m \leq \min(2.4S_m, 0.7S_u)$ $P_m + P_b \leq \min(3.6S_m, 1.0S_u)$
Level D ⁽²⁾⁽⁶⁾ Plastic Analysis	$P_m \leq \max(0.7S_u, S_y + 1/3(S_u - S_y))$ $P_m + P_b \leq 0.9S_u$

Notes:

1. There are no pressure loads on the basket, therefore the 10% increase permitted by NG-3223(a) for pressures exceeding the design pressure does not apply.
2. Evaluation of secondary stresses not required for Level C and D events.
3. Criteria listed are for elastic analyses, other analysis methods permitted by NG-3224.1 are acceptable if performed in accordance with the appropriate paragraph of NG-3224.1.
4. This limit may be exceeded provided the requirements of NG-3228.3 are satisfied, see NG-3222.2 and NG-3228.3.
5. As appropriate, the special stress limits of NG-3227 are applicable.
6. Level D criteria are taken from ASME Code, Section III, Appendix F. Acceptable criteria for stability are from Section III of the ASME Code Appendix F.

Table M.2-18
Classification of NUHOMS®-32PT DSC Components

IMPORTANT TO SAFETY	NOT IMPORTANT TO SAFETY
Canister Assembly Canister shell Bottom shield plug Inner bottom cover Outer bottom cover Grapple ring and support Top shield plug Inner top cover plate Outer top cover plate Siphon/vent port cover plate Siphon vent block Support ring Test port plug Weld filler metal Storage Basket Assembly Poison plate Basket plate Weld stud, washer, hex nut Basket rails Weld filler metal	Siphon tube Quick connect coupling Male connector Alignment key Canister lifting lug Electroless nickel coating

Table M.2-19
Additional Design Criteria for NUHOMS®-32PT DSC

The Gross Weight (rounded) of the NUHOMS®-32PT DSC:

32PT-S100	88,200 ⁽¹⁾ lbs. / 98,300 ⁽²⁾ lbs.
32PT-S125	90,300 ⁽¹⁾ lbs. / 100,400 ⁽²⁾ lbs.
32PT-L100	89,200 ⁽¹⁾ lbs. / 99,300 ⁽²⁾ lbs.
32PT-L125	91,300 ⁽¹⁾ lbs. / 101,400 ⁽²⁾ lbs.
Payload Capacity:	up to 32 intact PWR assemblies (acceptable assemblies listed in Table M.2-2) and up to 16 BPRAs
Spent Fuel Characteristics:	See Table M.2-1 through Table M.2-3.

- (1) Based on fuel weight of 1365 lbs. per assembly.
- (2) Based on fuel weight of 1682 lbs. per assembly.

Table M.2-20
Summary of NUHOMS®-32PT Component Design Loadings⁽¹⁾

Component	Design Load Type	FSAR Section Reference	Design Parameters	Applicable Codes
32PT-DSC:	---	---	---	ASME Code, 1998 Edition with 2000 Addenda, Section III, Subsection NB and Appendix F (Shell) and Subsections NG, NF and Appendix F (Basket) with exceptions noted in Table M.3.1-2.
	Flood	M.2.2.2	Maximum water height: 50 ft.	10CFR72.122(b)
	Seismic	M.2.2.3	Horizontal ground acc: 0.25g Vertical ground acc.: 0.17g	NRC Reg. Guides 1.60 & 1.61
	Dead Load	M.3.6.1.2 M.3.6.1.3	Maximum enveloping weight of loaded 32PT DSCs: 101,400 lbs.	ANSI 57.9-1984
	Normal and Off-Normal Pressure	M.3.6.1.2 M.3.6.1.3	Enveloping internal pressure of ≤15 psig (Normal) and < 20 psig (Off-Normal)	10CFR72.122(h)
	Test Pressure	M.3.6.1.2	Enveloping internal pressure of 18 psig applied w/o DSC outer top cover plate	10CFR72.122(h)
	Normal and Off-Normal Operating Temperature	M.3.6.1.2 M.3.6.1.3 M.3.6.2.2 M.4.4 M.4.5	DSC with spent fuel rejecting 24 kW (PWR) decay heat. Ambient air temperature -40°F to 117°F	ANSI 57.9-1984
	Normal Handling Loads	M.3.6.1.2 M.3.6.1.3	1. Hydraulic ram load of 80,000 lb.(DSC HSM insertion) 60,000 lb (DSC HSM extraction) 2. Transfer (to/from ISFSI) Loads of: 2a. +/-1.0g axial 2b. +/-1.0g transverse 2c. +/-1.0g vertical 2d. +/-0.5g axial +/-0.5g transverse +/-0.5g vertical	ANSI 57.9-1984
	Off-Normal Handling Loads	M.3.6.1.2	Hydraulic ram load of: 80,000 lb (DSC HSM insertion) 80,000 lb (DSC HSM extraction)	ANSI-57.9-1984

Table M.2-20
Summary of NUHOMS®-32PT Component Design Loadings(1)
(Continued)

Component	Design Load Type	FSAR Section Reference	Design Parameters	Applicable Codes
	Accidental Cask Drop Loads	M.3.7.5	Equivalent static deceleration of 75g for horizontal side drops, and 25g oblique corner drop	10CFR72.122(b)
	Accident Internal Pressure	M.4	Enveloping internal pressure of ≤ 105 psig based on 100% fuel cladding rupture and fill gas release, 30% fission gas release, and ambient air temperature of 117°F	10CFR72.122(h)

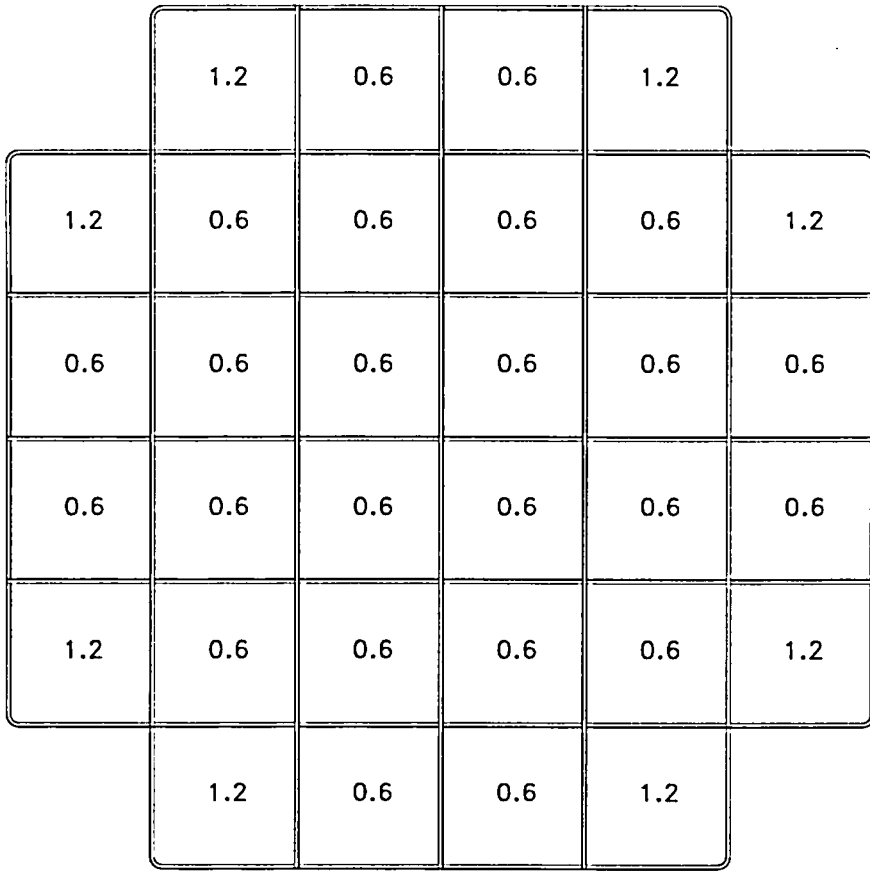
Note:

- (1) The design criteria for the HSM (including the DSC Steel Support Structure) and the TC remain unchanged from the FSAR (FSAR Table 3.2-1). These components have been evaluated for the effect of the higher weight of the 32PT-DSC.

	0.87	0.87	0.87	0.87	
0.87	0.63	0.63	0.63	0.63	0.87
0.87	0.63	0.63	0.63	0.63	0.87
0.87	0.63	0.63	0.63	0.63	0.87
0.87	0.63	0.63	0.63	0.63	0.87
	0.87	0.87	0.87	0.87	

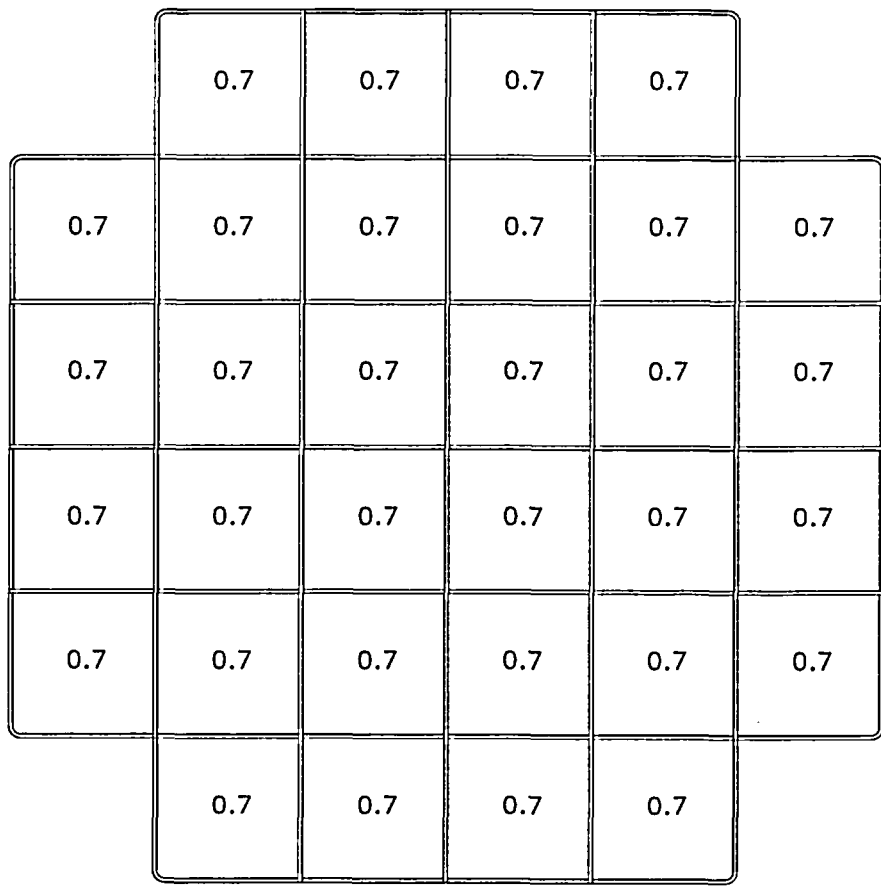
F5483

**Figure M.2-1
Heat Load Zoning Configuration 1**



F5485

**Figure M.2-2
Heat Load Zoning Configuration 2**



F5484

**Figure M.2-3
Heat Load Zoning Configuration 3**

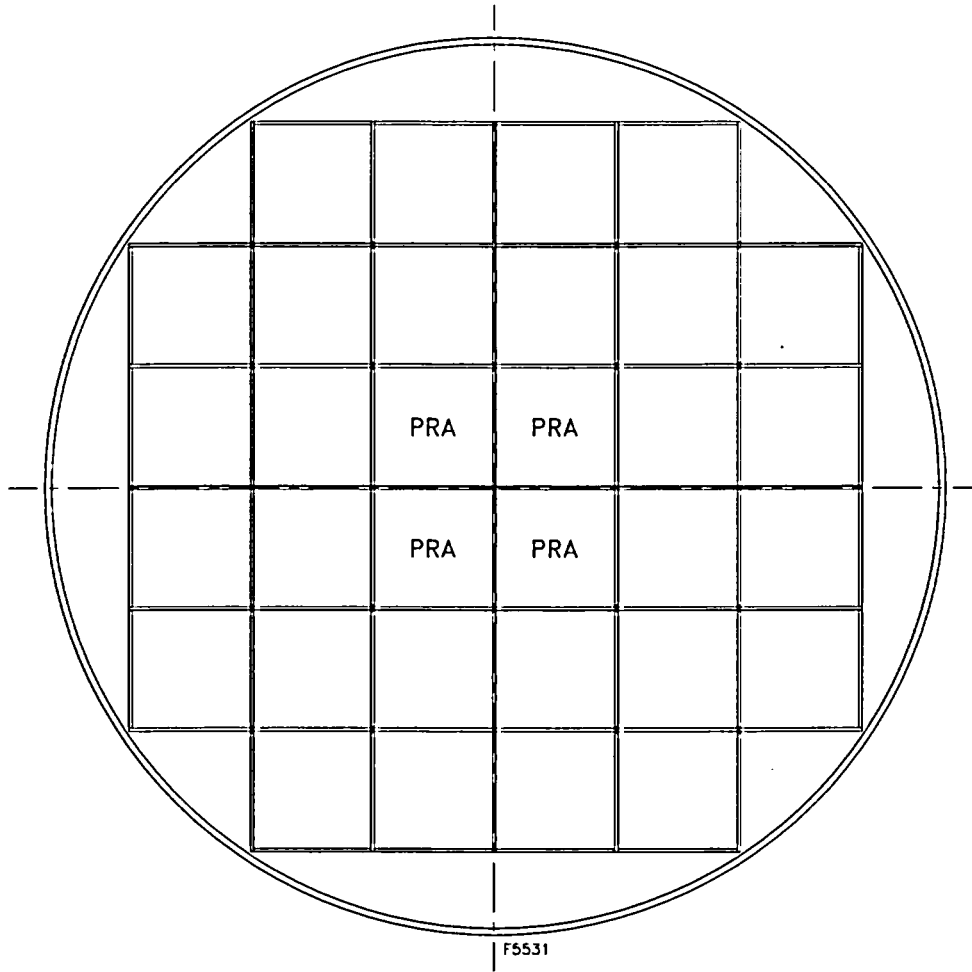
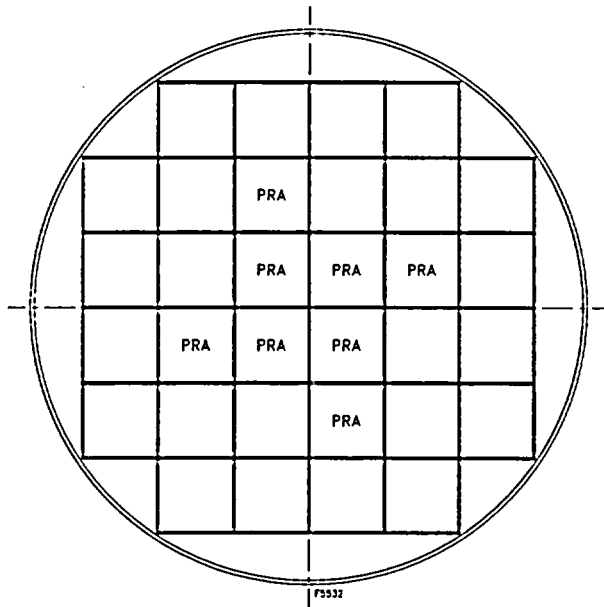


Figure M.2-4
Required PRA Locations for Configurations with Four PRAs
(Basket Type B)



OR

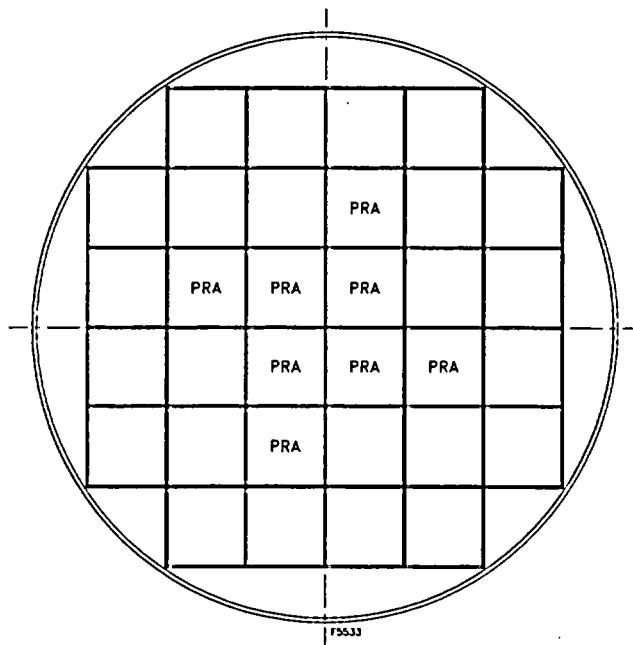


Figure M.2-5
Required PRA Locations for Configurations with Eight PRAs
(Basket Type C)

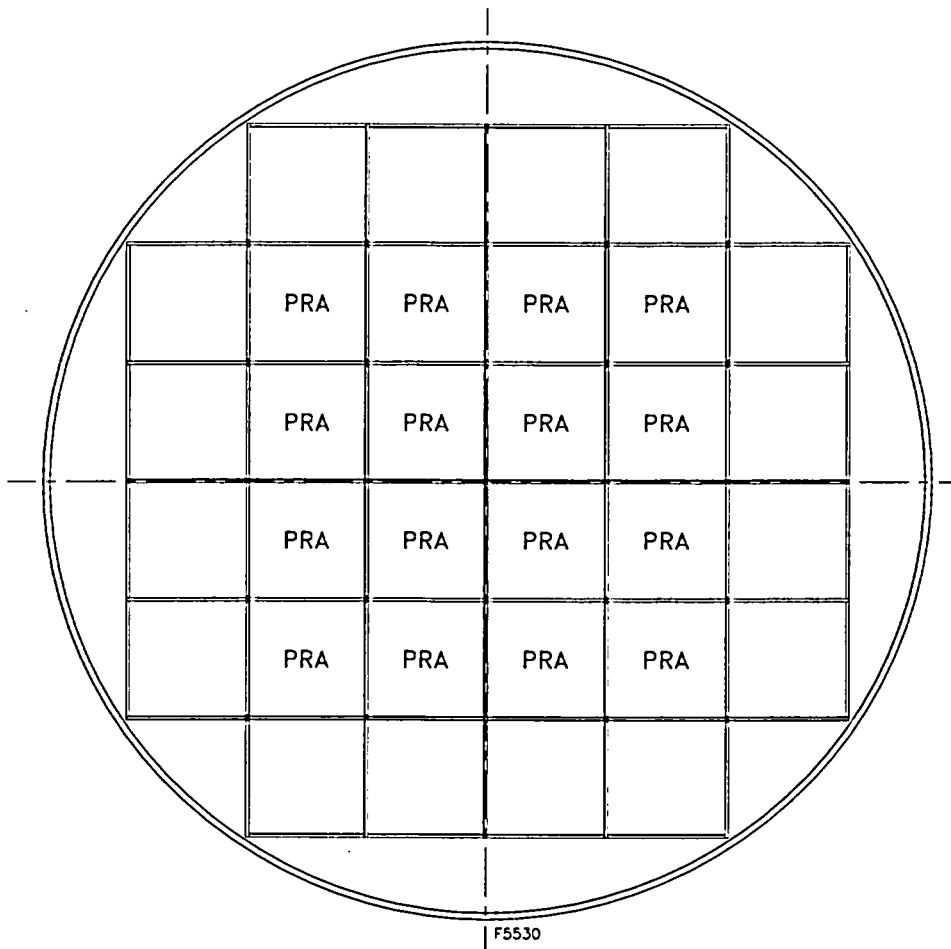


Figure M.2-6
Required PRA Locations for Configurations with Sixteen PRAs
(Basket Type D)

M.3 Structural Evaluation

M.3.1 Structural Design

M.3.1.1 Discussion

This section describes the structural evaluation of the NUHOMS[®]-32PT system. The NUHOMS[®]-32PT system consists of the NUHOMS[®] HSM, the OS197 and OS197H TCs, and the 32PT DSC basket and shell assemblies. No changes have been made to the HSM or the OS197 or OS197H TCs to accommodate the 32PT DSC. Where the new components have an effect on the structural evaluations presented in the FSAR, the changes are included in this section. Sections that do not effect the evaluations presented in the FSAR include a statement that there is no change to the FSAR. In addition, a complete evaluation of the 32PT DSC shell and basket components has been performed and is summarized in this section.

The 32PT DSC shell assembly is shown on drawings NUH-32PT-1001-SAR and NUH-32PT-1002-SAR. These drawings are provided in Section M.1.5. The NUHOMS[®]-32PT DSC shell assembly is the same as the NUHOMS[®]-24P DSC with the following exceptions:

- The nominal DSC shell thickness has been reduced to 0.5 inch thick from 0.625 inch thick.
- The nominal thickness of the outer top cover plate has been increased from 1.25 inches to 1.50 inches.
- The nominal thickness of the inner top cover plate has been increased from 0.75 inches to 1.25 inches.
- The nominal thickness of the inner bottom cover plate has been increased from 0.75 inches to 1.75 inches and has been designed for the internal pressure loads without credit taken for the structural support of the bottom shield plug and outer bottom cover plate.
- The nominal thickness of the top shield plug has been reduced from 8.25 inches to 6.25 inches for the 32PT-S100 and 32PT-L100 and to 7.5 inches for the 32PT-S125 and 32PT-L125.
- The nominal thickness of the bottom shield plug has been reduced from 6.25 inches to 4.00 inches for the 32PT-S100 and 32PT-L100 and to 5.25 inches for the 32PT-S125 and 32PT-L125.
- An optional configuration has been added for the inner bottom cover plate that allows the use of a forging to provide the same structural function as the plate design. The forging may be a single piece comprising the full thickness of the bottom end components.
- A test port has been added to the top cover plate to allow testing of the inner top cover plate welds and vent and siphon port cover plate welds to a leak tight criteria.

The NUHOMS[®]-32PT basket is a welded assembly of stainless steel plates or tubes that make up a fuel support assembly grid designed to accommodate up to 32 PWR fuel assemblies. The basket structure consists of the fuel support structure, the transition rails, aluminum heat transfer material, and neutron absorbing material.

The 32PT basket assembly is shown on drawings NUH-32PT-1003-SAR, -1004-SAR and -1006-SAR. These drawings are provided in Section M.1.5.

- The fuel support structure is fabricated from high strength (Type XM-19) stainless steel and contains 32 square fuel compartments in a box arrangement.
- The transition rails provide the transition between the "rectangular" fuel support grid and the cylindrical internal diameter of the DSC shell. There are two sizes of transition rails. The large rails are referred to as the R90 transition rails. The smaller transition rails are referred to as the R45 transition rails.

The thermal analysis results for the basket components are presented in Chapter M.4. These thermal analysis results correspond to the basket configuration with solid aluminum transition rails, shown in drawing NUH-32PT-1006-SAR. The stress evaluations documented in Chapter M.3 are generally based on bounding temperatures/thermal profiles that correspond to a welded stainless steel transition rail configuration which is not approved for use with a NUHOMS[®]-32PT basket. A detailed reconciliation of the Chapter M.4 thermal results with those used in Chapter M.3 was performed. The discussion below is a summary of this reconciliation. In cases where the Chapter M.4 maximum temperatures/thermal profiles are used, it is so noted.

Blocked Vent: Maximum temperatures and temperature gradients corresponding to the thermal analysis results documented in Chapter M.4 are lower for all basket components than the temperatures and temperature gradients used in the stress analysis. Therefore, the Chapter M.4 thermal results have no impact on the stress evaluations documented in this chapter for the blocked vent condition.

Vacuum Drying: The maximum temperatures corresponding to the thermal analysis results documented in Chapter M.4 are lower for all basket components than the maximum temperatures used in the stress analysis. The temperature gradients for the solid aluminum rail components are also lower. Therefore, the Chapter M. 4 thermal results have no impact on the stress evaluations of the solid aluminum rail components. The temperature gradient across the XM-19 steel grid component increases, causing an increase in the stress of about 1.0 ksi. The maximum thermal stress intensity in the grid component is small (4.33 ksi, from Table M.3.4-2). Considering that the only other load for this condition is deadweight (0.06 ksi, from Table M.3.6-5), the margin to allowable (84.6 ksi, from Table M.3.3-3, at 800°F) remains very large ($4.33+1.1+0.06=5.39$ ksi versus 84.6 ksi). Therefore, the impact of the revised thermal results is negligible.

Storage and Transfer Conditions: The maximum temperatures corresponding to the thermal analysis results documented in Chapter M.4 are lower for all basket components than the maximum temperatures used in the stress analysis. The temperature gradients for the solid aluminum rail components are also lower. Therefore, the Chapter M.4 thermal results have no

impact on the stress evaluations of the solid aluminum rail components. The temperature gradient across the XM-19 steel grid component increases, causing a maximum (envelope of all transfer/storage cases) stress increase of 1.55 ksi. The maximum thermal stress intensity in the grid component is small (4.95 ksi, from Table M.3.4-2). The controlling stress intensity (which includes the thermal stress) for the grid component is 18.3 ksi (from Table M.3.6-6). Considering the incremental stress, the revised stress intensity is 19.85 ksi versus 84.6 ksi allowable. Therefore, considering the large margin available, the impact of the Chapter M.4 thermal results is negligible.

Accident Transfer Case (117°F ambient, loss of sunshade, loss of neutron shield): The maximum temperature for the accident transfer case has increased. As shown in Table M.4-14, the maximum temperature for the steel grid is 852°F. The structural evaluation used allowable for the steel grid at 800°F. An exception to the material temperature limits of ASME Section II, Part D for the XM-19 grid plate material is added to Table M.3.1-2. This is a post-drop accident condition, where the only primary loads on the basket are due to deadweight and the expected reduction in material strength is small (less than 1 ksi by extrapolation, from Table M.3.3-3). Therefore, this case is not a concern considering that the deadweight stress is small.

The shell assembly temperatures used in the structural analysis are bounded by the thermal results documented in M.4 and, thus, there is no impact on the shell assembly. The calculated pressures due to the increased temperatures for the postulated post-drop accident transfer case (117°F ambient, loss of sunshade, loss of neutron shield) bound the pressures used in the structural evaluations.

Therefore, the thermal analysis results presented in Chapter M.4 have negligible impact on the DSC structural analysis results as presented in this Chapter.

Two fabrication designs are evaluated for the transition rails:

- **Single Piece Solid Aluminum Rails:** The transition rails are solid sections of 6061 aluminum alloy. The large (R90) rails include an XM-19 "cover plate" between the fuel support grid and the aluminum body. The structural evaluation of the rails uses properties for annealed aluminum (no credit is taken for enhanced properties obtained by heat treatment).
- **Multi-Piece Solid Aluminum Rails:** Optionally, the large (R90) transition rails may be made from 3 equal width sections of 6061 aluminum alloy. XM-19 cover plate is not changed. Analysis properties are the same as used for the solid rails.

The fuel support grid structure contains aluminum alloy 1100 plates as heat transfer material and, neutron absorbing plates. No credit is taken for the structural capacity of the aluminum heat transfer plates or neutron absorbing materials in the structural evaluation of the support grid structure.

The connections between the transition rails and fuel support structure are not required to maintain structural capacity of the basket assembly. These connections are primarily to simplify fabrication and are designed to allow free thermal expansion of the connected parts.

The basket structure is open at each end such that longitudinal fuel assembly loads are applied directly to the DSC/cask body and not to the basket structure. The fuel assemblies are laterally supported by the XM-19 fuel support structure. The basket is laterally supported by the basket transition rails and the DSC inner shell.

Inside the TC, the DSC rests on two 3" wide rails ("cask rails"), attached to the inside of the TC at $\pm 18.5^\circ$ from the bottom centerline of the DSC. In the HSM, the DSC is supported by rails located at $\pm 30^\circ$ from the bottom centerline of the DSC.

The nominal open dimension of each fuel compartment cell is 8.70 in. x 8.70 in. which provides clearance around the fuel assemblies. The overall basket length is less than the DSC cavity length to allow for thermal expansion and tolerances.

M.3.1.2 Design Criteria

Design criteria for the DSC shell and basket are provided in Section M.2.2.

M.3.1.2.1 DSC Shell Assembly Confinement Boundary

The primary confinement boundary consists of the DSC shell, the inner top cover plate, the inner bottom cover plate, the siphon vent block, the siphon/vent port cover plates, and the associated welds. Figure M.3.1-1 provides a graphic representation of the 32PT-DSC confinement boundary. The outer top cover plate forms the redundant confinement boundary.

The welds made during fabrication of the 32PT-DSC that affect the confinement boundary of the DSC include the inner bottom cover plate to shell weld and the circumferential and longitudinal seam welds applied to the shell. These welds are inspected (radiographic or ultrasonic inspection, and liquid penetrant inspection) according to the requirements of Subsection NB of the ASME Code.

The top inner cover plate and associated welds, the welds applied to the vent and siphon port covers, and the closure welds applied to the vent & siphon block, define the primary confinement boundary at the top end of the 32PT-DSC. These welds are in accordance with the alternative ASME Code Section III requirements of ASME Code Case N-595-2. These welds are applied using a multiple-layer technique and are liquid penetrant (PT) examined in accordance with Code Case N-595-2 [3.1] and Section III NB-5000.

During fabrication, leak tests of the 32PT-DSC shell assembly are performed in accordance with ANSI N14.5-1997 [3.13] to demonstrate that the shell is leaktight (1×10^{-7} std. cm^3/sec). The DSC inner top cover closure welds, including the vent and siphon pressure boundary welds, are also leak tested after fuel loading to demonstrate that the ANSI N14.5 leaktight criteria is met following installation of the outer cover plate root pass weld.

The basis for the allowable stresses for the confinement boundary is ASME Code Section III, Division I, Subsection NB Article NB-3200 [3.1] for normal (Level A) condition loads, off-normal (Level B) condition loads and off-normal/accident (Level C) condition loads, and Appendix F for accident (Level D) condition loads. See Section M.2.2 for additional design criteria.

M.3.1.2.2 DSC Basket

The basket is designed to meet heat transfer, nuclear criticality, and structural requirements. The basket structure provides sufficient rigidity to maintain a subcritical configuration under the applied loads. The Type XM-19 stainless steel members in the NUHOMS[®]-32PT basket are the primary structural components. The aluminum heat transfer plates and neutron poison plates are the primary heat conductors, and provide the necessary criticality control. The transition rails provide support to the fuel compartment grid for mechanical loads and also transfer heat from the fuel compartments to the DSC shell.

The stress analyses of the basket do not take credit for the neutron absorbing/heat transfer plate material.

The basket structural design criteria is provided in Section M.2.2. The basis for the allowable stresses for the stainless steel components in the basket assembly is Section III, Division 1, Subsection NG of the ASME Code [3.1]:

- Normal conditions are evaluated using criteria from NG-3200.
- Accident conditions are classified as Level D events and are evaluated using stress and stability criteria from Section III, Appendix F of the ASME Code [3.1].

M.3.1.2.3 Alternatives to the ASME Code for the 32PT DSC

The primary confinement boundary of the NUHOMS[®]-32PT DSC consists of the DSC shell, the inner top cover plate, the inner bottom cover plate, the siphon vent block, and the siphon/vent port cover plate. Even though the ASME B&PV code is not strictly applicable to the DSC, it is TN's intent to follow Section III, Subsection NB of the Code as closely as possible for design and construction of the confinement vessel. The DSC may, however, be fabricated by other than N-stamp holders and materials may be supplied by other than ASME Certificate Holders. Thus the requirements of NCA are not imposed. TN's quality assurance requirements, which are based on 10CFR72 Subpart G and NQA-1 are imposed in lieu of the requirements of NCA-3800. The SAR is prepared in place of the ASME design and stress reports. Surveillances are performed by TN and utility personnel rather than by an Authorized Nuclear Inspector (ANI).

The basket is designed, fabricated and inspected in accordance with the ASME Code Subsection NG. The following alternative provisions to the ASME Code Section III requirements are taken:

The poison rod assemblies, poison plates, and aluminum heat transfer plates are not considered for structural integrity. Therefore, these materials are not required to be Code materials. The quality assurance requirements of NQA-1 is imposed in lieu of NCA-3800. The basket is not Code stamped. Therefore, the requirements of NCA are not imposed. Fabrication and inspection surveillances are performed by TN and utility personnel rather than by an ANI.

A complete list of the alternatives to the ASME Code and corresponding justification for the NUHOMS[®]-32PT DSC and basket is provided in Table M.3.1-1 and Table M.3.1-2.

**Table M.3.1-1
 Alternatives to the ASME Code for the NUHOMS®-32PT DSC Confinement Boundary**

Reference ASME Code Section/Article	Code Requirement	Alternatives, Justification & Compensatory Measures
NCA	All	Not compliant with NCA. TN Quality Assurance requirements, which are based on 10CFR72 Subpart G, are used in lieu of NCA-4000. Fabrication oversight is performed by TN and utility personnel in lieu of an Authorized Nuclear Inspector.
NB-1100	Requirements for Code Stamping of Components	The NUHOMS®-32PT DSC shell is designed & fabricated in accordance with the requirements of ASME Code, Section III, Subsection NB and the alternative provisions described in this table. However, Code Stamping is not required. As Code Stamping is not required, the fabricator is not required to hold an ASME "N" or "NPT" stamp, or to be ASME Certified.
NB-2130	Material must be supplied by ASME approved material suppliers.	All materials designated as ASME on the SAR drawings are obtained from ASME approved Material Organization with ASME CMTR's. Material is certified to meet all ASME Code criteria but is not eligible for certification or Code Stamping if a non-ASME fabricator is used. As the fabricator is not required to be ASME certified, material certification to NB-2130 is not possible. Material traceability & certification are maintained in accordance with TN's NRC approved QA program.
NB-4121	Material Certification by Certificate Holder	
NB-4243 and NB-5230	Category C weld joints in vessels and similar weld joints in other components shall be full penetration joints. These welds shall be examined by UT or RT and either PT or MT	<p>The joints between the top outer and inner cover plates and containment shell are designed and fabricated per ASME Code Case N-595-2, which provides alternative requirements for the design and examination of spent fuel canister closures. This includes the inner top cover plate weld around the vent & siphon block and the vent and siphon block welds to the shell. The closure welds are partial penetration welds and the root and final layer are subject to PT examination (in lieu of volumetric examination) in accordance with the provisions of ASME Code Case N-595-2.</p> <p>The 32PT closure system employs austenitic stainless steel shell, lid materials, and welds. Because austenitic stainless steels are not subject to brittle failure at the operating temperatures of the DSC, crack propagation is not a concern. Thus, multi-level PT examination provides reasonable assurance that flaws of interest will be identified. The PT examination is done by qualified personnel, in accordance with Section V and the acceptance standards of Section III, Subsection NB-5000.</p> <p>This alternative does not apply to other shell confinement welds, i.e., the longitudinal and circumferential welds applied to the DSC shell, and the inner bottom cover plate-to-shell weld which comply with NB-4243 and NB-5230.</p>

Table M.3.1-1
Alternatives to the ASME Code for the NUHOMS®-32PT DSC Confinement Boundary
(Concluded)

Reference ASME Code Section/Article	Code Requirement	Alternatives, Exception, Justification & Compensatory Measures
NB-6100 and 6200	All pressure retaining components and completed systems shall be pressure tested. The preferred method shall be hydrostatic test.	The NUHOMS®-32PT DSC is pressure tested in accordance with ASME Code Case N-595-2. The shield plug support ring and the vent and siphon block are not pressure tested due to the manufacturing sequence. The support ring is not a pressure-retaining item and the vent and siphon block weld is helium leak tested after fuel is loaded to the same criteria as the inner top closure plate-to-shell weld (ANSI N14.5-1997 leaktight criteria).
NB-7000	Overpressure Protection	No overpressure protection is provided for the NUHOMS®-32PT DSC . The function of the NUHOMS®-32PT DSC is to contain radioactive materials under normal, off-normal and hypothetical accident conditions postulated to occur during transportation and storage. The NUHOMS®-32PT DSC is designed to withstand the maximum possible internal pressure considering 100% fuel rod failure at maximum accident temperature. The NUHOMS®-32PT DSC is pressure tested in accordance with ASME Code Case N-595-2.
NB-8000	Requirements for nameplates, stamping & reports per NCA-8000	The NUHOMS®-32PT DSC nameplate provides the information required by 10CFR71, 49CFR173 and 10CFR72 as appropriate. Code stamping is not required for the NUHOMS®-32PT DSC. In lieu of code stamping, QA data packages are prepared in accordance with the requirements of 10CFR71, 10CFR72 and TN's approved QA program.

Table M.3.1-2
Alternatives to the ASME Code Exceptions for the NUHOMS®-32PT DSC Basket Assembly

Reference ASME Code Section/Article	Code Requirement	Alternatives, Exception, Justification & Compensatory Measures
NG-1100	Requirements for Code Stamping of Components	The NUHOMS®-32PT DSC baskets are designed & fabricated in accordance with the ASME Code, Section III, Subsection NG as described in the SAR, but Code Stamping is not required. As Code Stamping is not required, the fabricator is not required to hold an ASME N or NPT stamp or be ASME Certified.
NG-2000	Use of ASME Material	The poison material and aluminum plates are not used for structural analysis, but to provide criticality control and heat transfer. They are not ASME Code Class 1 material. Material properties in the ASME Code for Type 6061 aluminum are limited to 400°F to preclude the potential for annealing out the hardening properties. Annealed properties (as published by the Aluminum Association and the American Society of Metals) are conservatively assumed for the solid aluminum rails for use above the Code temperature limits.
NG-2130	Material must be supplied by ASME approved material suppliers.	All materials designated as ASME on the SAR drawings are obtained from ASME approved Material Organization with ASME CMTR's. Material is certified to meet all ASME Code criteria, but is not eligible for certification or Code Stamping if a non-ASME fabricator is used. As the fabricator is not required to be ASME certified, material certification to NG-2130 is not possible. Material traceability & certification are maintained in accordance with TN's NRC approved QA program.
NG-4121	Material Certification by Certificate Holder	
NG-8000	Requirements for nameplates, stamping & reports per NCA-8000	The NUHOMS®-32PT DSC nameplate provides the information required by 10CFR71, 49CFR173 and 10CFR72 as appropriate. Code stamping is not required for the NUHOMS®-32PT DSC. In lieu of Code stamping, QA Data packages are prepared in accordance with the requirements of 10CFR71, 10CFR72 and TN's approved QA program.
NCA	All	Not compliant with NCA as no Code stamp is used. TN Quality Assurance requirements, which are based on 10CFR72 Subpart G, are used in lieu of NCA-4000. Fabrication oversight is performed by TN and utility personnel in lieu of an Authorized Nuclear Inspector.
NG-3000/ Section II, Part D, Table 2A	Maximum temperature limit for XM-19 plate material is 800°F	Not compliant with ASME Section II Part D Table 2A material temperature limit for XM-19 steel for the postulated transfer accident case (117°F, loss of sunshade, loss of neutron shield). This is a post-drop accident scenario, where the calculated maximum steady state temperature is 852°F, the expected reduction in material strength is small (less than 1 ksi by extrapolation), and the only primary stresses in the basket grid are deadweight stresses. The recovery actions following the postulated drop accident are as described in Section 8.2.5 of the FSAR.

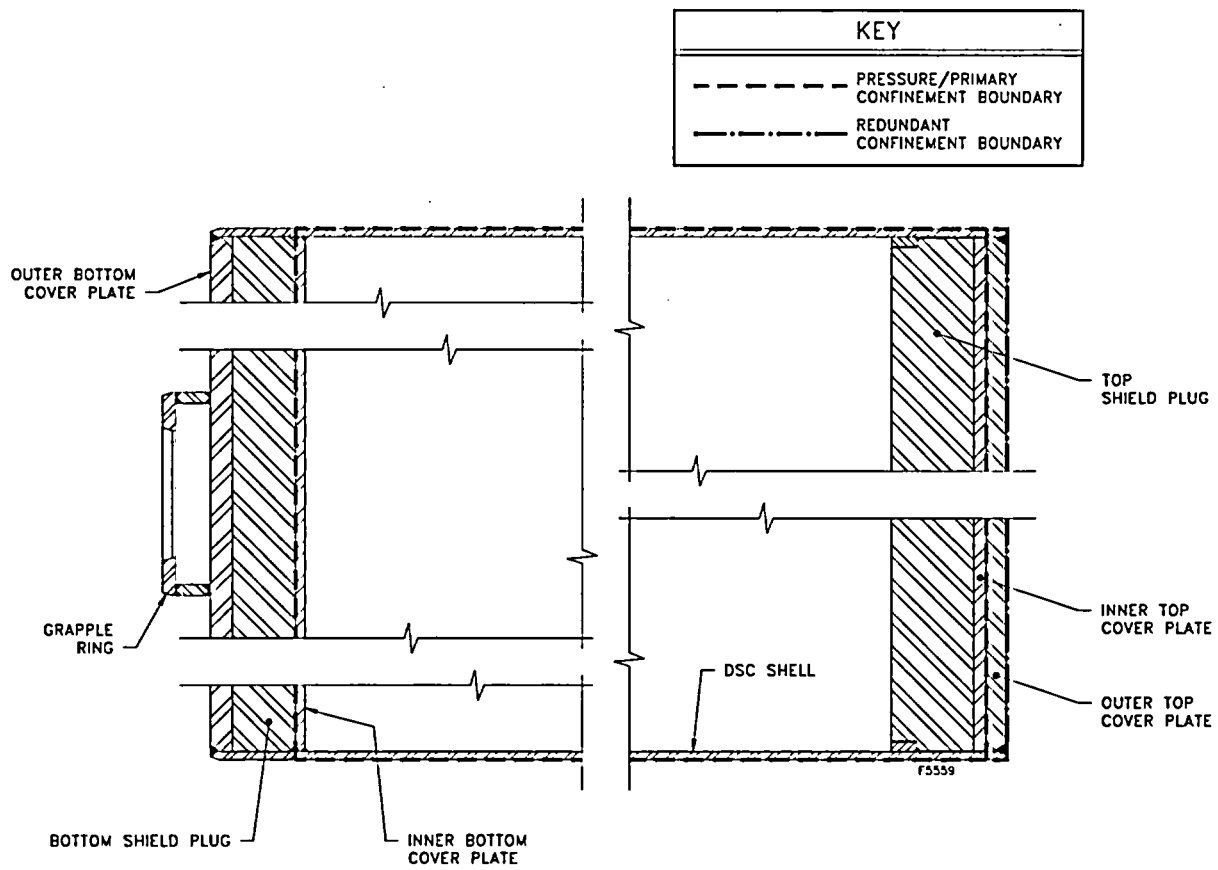


Figure M.3.1-1
32PT-DSC Pressure and Confinement Boundaries

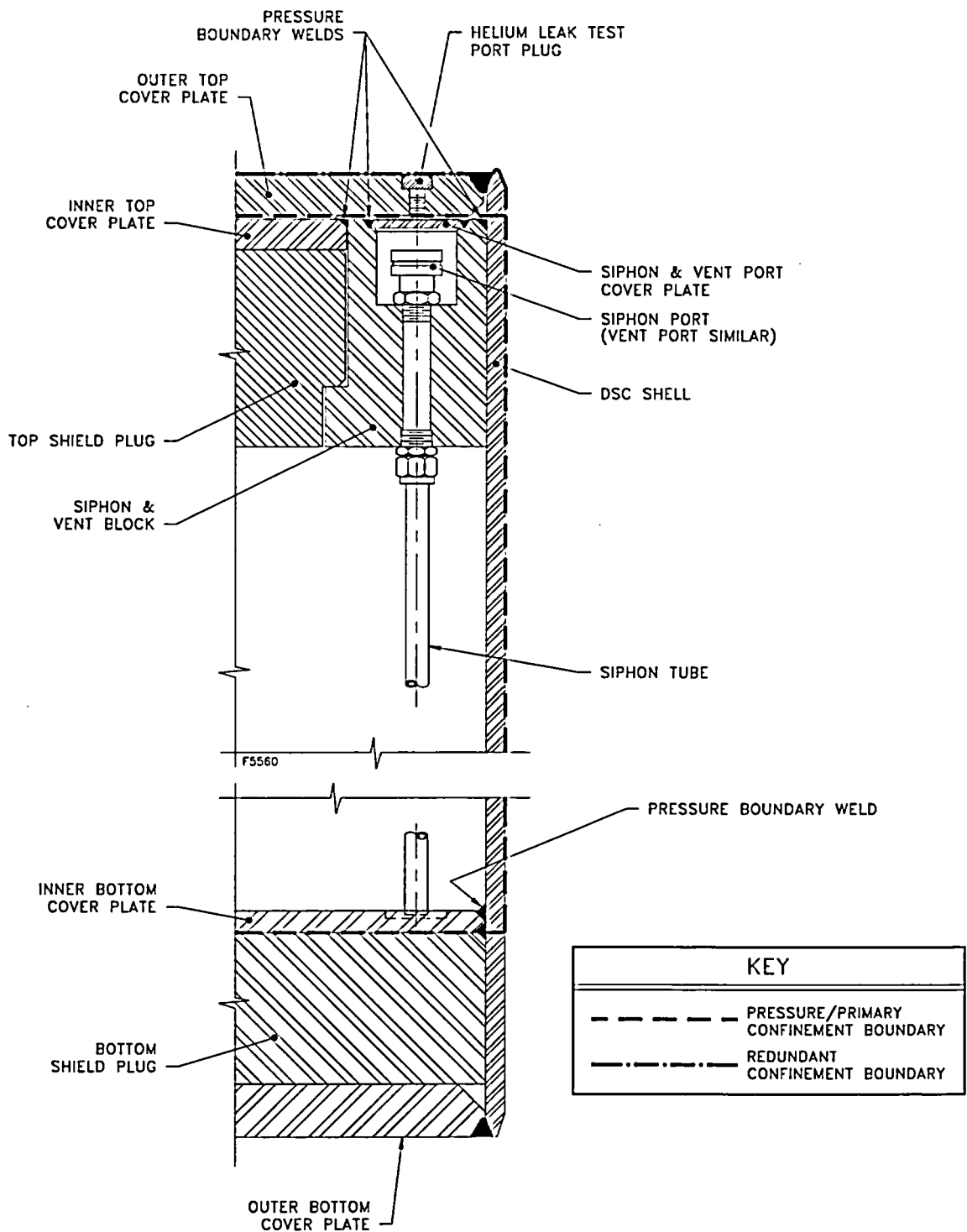


Figure M.3.1-1
32PT-DSC Pressure and Confinement Boundaries
(Concluded)

M.3.2 Weights and Centers of Gravity

Table M.3.2-1 shows the weights of the various components of the NUHOMS[®]-32PT system including basket, DSC, standard HSM and OS197 and OS197H TC. The dead weights of the components are determined based on nominal dimensions.

**Table M.3.2-1
Summary of the NUHOMS[®]-32PT System Component Nominal Weights**

Component Description	CALCULATED WEIGHT (kips)			
	32PT-S100	32PT-S125	32PT-L100	32PT-L125
DSC Shell Assembly ⁽¹⁾	13.06	14.28	13.24	14.46
DSC Top Shield Plug Assembly ⁽²⁾	8.71	9.93	8.71	9.93
DSC Internal Basket Assembly	22.74	22.40	23.55	23.21
Total Empty Weight	44.52	46.62	45.51	47.61
32 PWR Spent Fuel Assemblies	≤ 43.68 ⁽³⁾ ≤ 53.82 ⁽⁴⁾	≤ 43.68 ⁽³⁾ ≤ 53.82 ⁽⁴⁾	≤ 43.68 ⁽³⁾ ≤ 53.82 ⁽⁴⁾	≤ 43.68 ⁽³⁾ ≤ 53.82 ⁽⁴⁾
Total Loaded DSC Weight (Dry)	88.20⁽³⁾ 98.34⁽⁴⁾	90.30⁽³⁾ 100.44⁽⁴⁾	89.19⁽³⁾ 99.33⁽⁴⁾	91.29⁽³⁾ 101.43⁽⁴⁾
Water in Loaded DSC	6.81 ⁽⁵⁾ 13.61 ⁽⁷⁾	5.38 ⁽⁵⁾ 10.75 ⁽⁷⁾	6.40 ⁽⁶⁾ 14.23 ⁽⁷⁾	5.12 ⁽⁶⁾ 11.37 ⁽⁷⁾
Total Loaded DSC Weight (Wet)	95.0⁽⁸⁾ 111.9⁽⁹⁾	95.7⁽⁸⁾ 111.2⁽⁹⁾	95.6⁽⁸⁾ 113.6⁽⁹⁾	96.4⁽⁸⁾ 112.8⁽⁹⁾
Cask Spacer	1.10	1.10	0.79	0.79
OS197 (OS197H) TC Empty Weight ⁽¹⁰⁾	106.67 111.25	106.67 111.25	106.67 111.25	106.67 111.25
Total Loaded TC Weight	196.0⁽⁸⁾ 210.7⁽⁹⁾	198.1⁽⁸⁾ 212.8⁽⁹⁾	196.6⁽⁸⁾ 211.4⁽⁹⁾	198.7⁽⁸⁾ 213.5⁽⁹⁾
HSM Single Module Weight Maximum (Empty)	263.0	263.0	263.0	263.0
HSM Single Module Weight Maximum (Loaded)	351.2	363.4	352.1	364.4

Notes:

1. Excludes top cover plates and shield plug.
2. Includes top cover plates and shield plug.
3. Based on a fuel weight of 1,365 lbs per assembly. This is a limit for any 32PT DSCs for which the maximum lift weight of the loaded TC is to remain under 100 tons.
4. Based on B&W 15x15 fuel (with control components) weight of 1,682 lbs per assembly.
5. Based on DSC water volume reduced to 50% of capacity to ensure that the maximum lift weight of the loaded TC is under 100 tons.
6. Based on DSC water volume reduced to 45% of capacity to ensure that the maximum lift weight of the loaded TC is under 100 tons.
7. Based on 100% water volume in DSC.
8. Based on fuel assembly weight of 1,365 lbs and 50% water reduction in DSC.
9. Based on fuel assembly weight of 1,682 lbs. and 100% water in DSC.
10. Includes cask top cover plate. The first figure is when the neutron shield is not filled with demineralized water to ensure that the maximum lift weight of the loaded cask is under 100 tons. The second figure is when the neutron shield is filled with demineralized water.

M.3.3 Mechanical Properties of Materials

M.3.3.1 Material Properties

The DSC shell and inner and outer top and bottom cover plates are fabricated from Type 304 stainless steel. The properties for the material are from ASME Code Section II Part D [3.2] and are listed in Table M.3.3-1.

The top and bottom shield plugs are fabricated from A36 carbon steel. The properties from ASME Code Section II Part D [3.2], as listed in Table M.3.3-2, are applied to this material.

The fuel support grid in the 32PT basket is fabricated with Type XM-19 high strength stainless steel. The properties of this material are from ASME Code Section II, Part D [3.2] and are listed in Table M.3.3-3.

The aluminum transition rails use solid sections (e.g., machined plates) of Type 6061 aluminum. The large (R90) rails include a 1/4" thick XM-19 plate (same material and thickness as the fuel support structure) while the small (R45) transition rails are solid aluminum parts with no cover plates. Analysis properties are taken from [3.3] for annealed aluminum. Use of properties for annealed material ensures that no credit is taken for enhanced properties obtained by heat treatment. The selection of properties for annealed material is based on the possibility that the maximum temperature in the rails may exceed the temperatures for which strength properties are provided (for aluminum) in the ASME Code (see Table M.3.3-4). This is acceptable for the following reasons:

1. The transition rails are not pressure boundary parts. Loading on the rails is primarily bearing and the transition rails are "captured" between the fuel support structure and the DSC shell. Deformation of the transition rails (to conform to the inside diameter of the DSC shell) will distribute the applied loads and will not adversely impact the basket structure.
2. For applications where the aluminum properties result from heat treatment, it is necessary to limit the maximum temperature to values below which the effects of the heat treatment are maintained. Heat treatment provides significant differences in strength properties at low temperatures. However, as temperature increases, the effect(s) of heat treatment on strength properties decreases. The strength properties used in the design of the 32PT are based on annealed aluminum. Thus, changes in strength which may occur under exposure to temperatures exceeding 400°F have no adverse impact on the properties used in the design.

For the stress analyses of the 32PT basket, properties for the aluminum rails are taken directly from Table M.3.3-5. For elastic-plastic analyses, the plastic slope of the aluminum is taken as 0.01E. This approximates elastic-perfectly plastic properties while providing a small stiffness to enhance analytical stability.

Table M.3.3-6 provides additional material properties.

M.3.3.2 Materials Durability

The materials used in the fabrication of the NUHOMS®-32PT system are shown in Table M.3.3-1 through Table M.3.3-5. Essentially all of the materials meet the appropriate requirements of the ASME Code, ACI Code, and appropriate ASTM Standards. The durability of the shell assembly and basket assembly stainless steel components is well beyond the design life of the applicable components. The aluminum material used in the basket is only relied upon for its thermal conductivity and bearing strength properties. The poison material selected for criticality control of the NUHOMS®-32PT system has been tested and is currently in use for similar applications. Additionally, the NUHOMS®-32PT basket assembly resides in an inert helium gas environment for the majority of the design life. The materials used in the NUHOMS®-32PT system will maintain the required properties for the design life of the system.

**Table M.3.3-1
ASME Code Materials Data For SA-240 Type 304 Stainless Steel**

Materials Data, SA-240 Type 304 (18Cr-8Ni) Stainless Steel

Temp. (°F)	E (ksi)	S _m (ksi)	S _y (ksi)	S _u (ksi)	α _{AVG} (x 10 ⁻⁶ °F ⁻¹)
-100	29,100	--	--	--	--
-20	--	20.0	30.0	75.0	--
70	28,300	--	--	--	8.5
100	--	20.0	30.0	75.0	8.6
200	27,600	20.0	25.0	71.0	8.9
300	27,000	20.0	22.4	66.2	9.2
400	26,500	18.7	20.7	64.0	9.5
500	25,800	17.5	19.4	63.4	9.7
600	25,300	16.4	18.4	63.4	9.8
650	--	16.2	18.0	63.4	9.9
700	24,800	16.0	17.6	63.4	10.0
750	--	15.6	17.2	63.3	10.0
800	24,100	15.2	16.9	62.8	10.1
Reference Section II-D	Table TM-1 Group G	Table 2A	Table Y-1	Table U	18Cr-8Ni TE-1, Group 3

**Table M.3.3-2
Materials Data For ASTM A36 Steel**

(Properties are taken from ASME Code Section II for SA-36 Steel. The ASME material specification is identical to the ASTM A36 Steel specification.)

Temp. (°F)	E (ksi)	S _m (ksi)	S _y (ksi)	S _u (ksi)	α _{AVG} (x 10 ⁻⁶ °F ⁻¹)
-100	30,200	--	--	--	--
-20	--	19.3	36.0	58.0	--
70	29,500	19.3	36.0	58.0	--
100	--	19.3	36.0	58.0	6.5
200	28,800	19.3	33.0	58.0	6.7
300	28,300	19.3	31.8	58.0	6.9
400	27,700	19.3	30.8	58.0	7.1
500	27,300	19.3	29.3	58.0	7.3
600	26,700	17.7	27.6	58.0	7.4
650	--	17.4	26.7	58.0	7.5
700	25,500	17.3	25.8	58.0	7.6
750	--	--	--	--	7.7
800	24,200	--	--	--	7.8

**Table M.3.3-3
ASME Code Materials Data For SA-240 Type XM-19 Stainless Steel**

Materials Data, SA-240 Type XM-19 (22Cr-13Ni-5Mn)

Temp. (°F)	E (ksi)	S _m (ksi)	S _y (ksi)	S _u (ksi)	α _{AVG} (x 10 ⁻⁶ °F ⁻¹)
-100	29,100	--	--	--	--
-20	--	33.3	55.0	100.0	--
70	28,300	--	--	--	8.2
100	--	33.3	55.0	100.0	8.2
200	27,600	33.2	47.1	99.4	8.5
300	27,000	31.4	43.3	94.2	8.8
400	26,500	30.2	40.7	91.1	8.9
500	25,800	29.7	38.8	89.1	9.1
600	25,300	29.2	37.4	87.7	9.2
650	--	29.0	36.8	87.0	9.2
700	24,800	28.8	36.3	86.4	9.3
750	--	28.5	35.8	85.6	9.3
800	24,100	28.2	35.3	84.8	9.4
Reference Section II-D	Table TM-1 Group G	Table 2A	Table Y-1	Table U	22Cr-13Ni-5Mn TE-1, Group 4

**Table M.3.3-4
ASME Code Properties for 6061 Aluminum**

ASME Code Properties for 6061 Aluminum (Plate)

Temperature (°F)	Yield Strength (ksi)		E (ksi)	α ($\times 10^{-6} \text{ } ^\circ\text{F}^{-1}$)
	A96061-T451	A96061-T651		
75	16.0	35.0	10,000	12.1
100	16.0	35.0	--	12.4
150	15.7	34.6	--	12.7
200	15.5	33.7	9,600	13.0
250	15.3	32.4	--	13.1
300	15.3	27.4	9,200	13.3
350	15.3	20.0	--	13.4
400	11.6	13.3	8,700	13.6
450	--	--	--	13.8
500	--	--	8,100	13.9
550	--	--	--	14.1
600	--	--	--	14.2
Reference	Table Y-1 .250" - 3.00"	Table Y-1 .250" - 6.00"	Table TM-2 A96061	Table TE-2

**Table M.3.3-5
Analysis Properties for Aluminum Transition Rails**

6061-O Aluminum (Annealed)

Temperature (°F)	S _u , 6061-O (ksi)	S _y , 6061-O (ksi)	E (ksi)
75	18.0	8.0	9,900
212	18.0	8.0	9,500
300	15.0	8.0	9,100
350	12.0	8.0	8,900
400	10.0	7.5	8,600
450	8.5	6.0	8,300
500	7.0	5.5	7,900
600	5.0	4.2	6,800
700	3.6	3.0	5,500
800	2.8	2.2	--
900	2.2	1.6	--
1000	1.6	1.2	--

Note: Data from "Properties of Aluminum Alloys", ASM International/The Aluminum Association, 1999

**Table M.3.3-6
Additional Material Properties**

Material Property	Value	Reference
Aluminum Density (1100 and 6061)	0.098 lb/in ³	Section II, Part D, Table NF-2
Aluminum Melting Point (Alloy 1100)	1190°F - 1215°F	Section II, Part D, Table NF-2
Aluminum Melting Point (Alloy 6061)	1080°F - 1205°F	Section II, Part D, Table NF-2
Neutron Absorber Density	0.098 lb/in ³	Taken as equal to the density of pure aluminum
Steel Density	$\frac{493 \text{ lb}}{1728 \text{ in}^3} = .285 \frac{\text{lb}}{\text{in}^3}$	

M.3.4 General Standards for Casks

M.3.4.1 Chemical and Galvanic Reactions

The materials of the 32PT DSC and basket have been reviewed to determine whether chemical, galvanic or other reactions among the materials, contents and environment might occur during any phase of loading, unloading, handling or storage. This review is summarized below:

The 32PT DSC is exposed to the following environments:

- During loading and unloading, the DSC is placed inside of the OS197 or OS197H TC. The annulus between the cask and DSC is filled with demineralized water and an inflatable seal is used to cover the annulus between the DSC and cask. The exterior of the DSC will not be exposed to pool water.
- The space between the top of the DSC and inside of the TC is sealed to prevent contamination. For PWR plants the pool water is borated. This affects the interior surfaces of the DSC, the shield plug, and the basket. The TC and DSC are kept in the spent fuel pool for a short period of time, typically about 6 hours to load or unload fuel, and 2 hours to lift the loaded TC/DSC out of the spent fuel pool.
- During storage, the interior of the DSC is exposed to an inert helium environment. The helium environment does not support the occurrence of chemical or galvanic reactions because both moisture and oxygen must be present for a reaction to occur. The DSC is thoroughly dried before storage by a vacuum drying process. It is then backfilled with helium, thus stopping corrosion. Since the DSC is vacuum dried, galvanic corrosion is also precluded as no water is present at the point of contact between dissimilar metals.
- During storage, the exterior of the DSC is protected by the concrete NUHOMS[®] HSM. The HSM is vented, so the exterior of the DSC is exposed to the atmosphere. The DSC shell and cover plates are fabricated from austenitic stainless steel and are resistant to corrosion.

The NUHOMS[®]-32PT DSC materials are shown in the Parts List on Drawings NUH-32PT-1001 through NUH-32PT-1006 provided in Section M.1.5. The DSC shell material is SA-240 Type 304 Stainless Steel. The top and bottom shield plug material is A36 carbon steel. The top shield plug is coated with a corrosion resistant electroless nickel coating.

The basket grid structure is composed of either plate or tube assemblies made from XM-19 stainless steel. Within the grid structure are plates of Type 1100 aluminum and neutron absorbing materials composed of either enriched borated aluminum alloy or Boralyn[®] plates. These plates are attached to the grid structure using corrosion resistant fasteners. Poison Rod Assemblies (PRAs) are also used with some fuel assembly loading options.

The transition rails provide the transition between the fuel compartment grid structure and the DSC shell. The transition rails are made of alloy Type 6061 aluminum. The transition rails are bolted to the grid structure.

Potential sources of chemical or galvanic reactions are the interaction between the aluminum, aluminum-based neutron poison and stainless steel within the basket and the pool water. Additionally, an interaction exists with the stainless steel top and bottom plates and the top shield plug.

Typical water chemistry in a PWR Spent Fuel pool is as follows:

pH (77°F)	4.5 - 9.0
Chloride, max	0.15 ppm
Fluoride, max	0.1 ppm
Dissolved Air, max	Saturated
Lithium, max	2.5 ppm
Boric Acid	2100 - 2600 ppm
Pool Temperature Range	40 - 120°F

A. Behavior of Aluminum in Borated Water

Aluminum is used for many applications in spent fuel pools. In order to understand the corrosion resistance of aluminum within the normal operating conditions of spent fuel storage pools, a discussion of each of the types of corrosion is addressed separately. None of these corrosion mechanisms is expected to occur in the short time period that the cask is submerged in the spent fuel pool.

General Corrosion

General corrosion is a uniform attack of the metal over the entire surfaces exposed to the corrosive media. The severity of general corrosion of aluminum depends upon the chemical nature and temperature of the electrolyte and can range from superficial etching and staining to dissolution of the metal. Figure M.3.4-1 shows a potential-pH diagram for aluminum in high purity water at 77°F and 140°F. The potential for aluminum coupled with stainless steel and the limits of pH for PWR pools are shown in the diagram to be well within the passivation domain at both temperatures. The passivated surface of aluminum (hydrated oxide of aluminum) affords protection against corrosion in the domain shown because the coating is insoluble, non-porous and adherent to the surface of the aluminum. The protective surface formed on the aluminum is known to be stable up to 275°F and in a pH range of 4.5 to 8.5.

The water aluminum reactions are self limiting because the surface of the aluminum becomes passive by the formation of a protective and impervious coating making further reaction impossible until the coating is removed by mechanical or chemical means.

The ability of aluminum to resist corrosion from boron ions is evident from the wide usage of aluminum in the handling of borax and in the manufacture of boric acid. Aluminum storage racks with Boral plates (aluminum 1100 exterior layer) in contact with 800 ppm borated water showed only small amounts of pitting after 17 years in the pool at the Yankee Rowe Power Plant. These racks maintained their structural integrity.

During immersion in the spent fuel pool, the 32PT-DSC basket temperatures are close to the water temperature, which is typically near 80°F, and the pH range is typically 4.0 to 6.5. Based on the above discussion, general corrosion is not expected on the aluminum after the protective coating has been formed.

Galvanic Corrosion

Galvanic corrosion is a type of corrosion which could cause degradation of dissimilar metals exposed to a corrosive environment for a long period of time.

Galvanic corrosion is associated with the current of a galvanic cell consisting of two dissimilar conductors in an electrolyte. The two dissimilar conductors of interest in this discussion are aluminum and stainless steel in borated water. There is little galvanic corrosion in borated water since the water conductivity is very low. There is also less galvanic current flow between the aluminum-stainless steel couple than the potential difference on stainless steel which is known as polarization. It is because of this polarization characteristic that stainless steel is compatible with aluminum in all but severe marine, or high chloride, environmental conditions [3.4].

Pitting Corrosion

Pitting corrosion is the forming of small sharp cavities in a metal surface. The first step in the development of corrosion pits is a local destruction of the protective oxide film. Pitting will not occur on commercially pure aluminum when the water is kept sufficiently pure, even when the aluminum is in electrical contact with stainless steel. Pitting and other forms of localized corrosion occur under conditions like those that cause stress corrosion, and are subject to an induction time which is similarly affected by temperature and the concentration of oxygen and chlorides. As with stress corrosion, at the low temperatures and low chloride concentrations of a spent fuel pool, the induction time for initiation of localized corrosion will be greater than the time that the DSC internal components are exposed to the aqueous environment.

Crevice Corrosion

Crevice corrosion is the corrosion of a metal that is caused by the concentration of dissolved salts, metal ions, oxygen or other gases in crevices or pockets remote from the principal fluid stream, with a resultant build-up of differential galvanic cells that ultimately cause pitting. Crevice corrosion could occur in the basket grid assembly plates around the stainless steel welds. However, due to the short time in the spent fuel pool, this type of corrosion is expected to be insignificant.

Intergranular Corrosion

Intergranular corrosion is corrosion occurring preferentially at grain boundaries or closely adjacent regions without appreciable attack of the grains or crystals of the metal itself. Intergranular corrosion does not occur with commercially pure aluminum and other common work hardened aluminum alloys.

Stress Corrosion

Stress corrosion is failure of the metal by cracking under the combined action of corrosion and stresses approaching the yield stress of the metal. During spent fuel pool operations, the 32PT-DSC is upright and there is negligible load on the basket assembly. The stresses on the basket are small, well below the yield stress of the basket materials.

B. Behavior of Austenitic Stainless Steel in Borated Water

The fuel compartments are made from XM-19 stainless steel and the transition rails that support the fuel compartments are made from solid aluminum. Stainless steel does not exhibit general corrosion when immersed in borated water. Galvanic attack can occur between the aluminum in contact with the stainless steel in the water. However, the attack is mitigated by the passivity of the aluminum and the stainless steel in the short time the pool water is in the DSC. Also the low conductivity of the pool water tends to minimize galvanic reactions.

Stress corrosion cracking in the Type XM-19 stainless steel welds of the basket is also not expected to occur, since the baskets are not highly stressed during normal operations. There may be some residual fabrication stresses as a result of welding of the stainless steel plates together.

Of the corrosive agents that could initiate stress corrosion cracking in the stainless steel basket welds, only the combination of chloride ions with dissolved oxygen occurs in spent fuel pool water. Although stress corrosion cracking can take place at very low chloride concentrations and at low temperatures such as those in spent fuel pools (less than 10 ppb and 160°F, respectively), the effect of low chloride concentration and low temperature greatly increases the induction time. That is, the time period during which the corrodent is breaking down the passive oxide film on the stainless steel surface is increased. Below 60°C (140°F), stress corrosion cracking of austenitic stainless steel does not occur at all. At 100°C (212 °F), chloride concentration on the order of 15% is required to initiate stress corrosion cracking [3.5]. At 288 °C (550 °F), with tensile stress at 100% of yield in PWR water that contains 100 ppm O₂, time to crack is about 40 days in sensitized 304 stainless steel [3.6]. Thus, the combination of low chlorides, low temperature and short time of exposure to the corrosive environment eliminates the possibility of stress corrosion cracking in the basket and DSC welds.

C. Behavior of Aluminum Based Neutron Poison in Borated Water

To investigate the use of borated aluminum in a spent fuel pool, tests were performed by Eagle Picher to evaluate its dimensional stability, corrosion resistance and neutron capture ability. These studies showed that borated aluminum performed well in a spent fuel pool environment.

The 1100 series aluminum component is a ductile metal having a high resistance to corrosion. Its corrosion resistance is provided by the buildup of a protective oxide film on the metal surface when exposed to a water or moisture environment. As stated above, for aluminum, once a stable film develops, the corrosion process is arrested at the surface of the metal. The film remains stable over a pH range of 4.5 to 8.5.

Tests were performed by Eagle Picher which concluded that borated aluminum exhibits a strong corrosion resistance at room temperature in either reactor grade deionized water or in 2000 ppm

borated water. The behavior is only slightly different than 1100 series aluminum, hence, satisfactory long-term usage in these environments is expected. Neutron irradiation up to 10^{17} n/cm² level did not cause any measurable dimensional changes or any other damage to the material.

At high temperature, the borated aluminum still exhibits high corrosion resistance in the pure water environment. However, at temperatures of 80°C, in 2000 ppm borated water, local pitting corrosion has been observed. At 100°C and room temperature, the pitting attack was less than at 80°C. In all cases, passivation occurs limiting the pit depth.

From tests on pure aluminum, it was found that borated aluminum was more resistant to uniform corrosion attack than pure aluminum. Local pitting corrosion, can occur over time, causing localized damage to the borated aluminum.

There are no chemical, galvanic or other reactions that could reduce the areal density of boron in the 32PT-DSC neutron poison plates.

D. Electroless Nickel Plated Carbon Steel

The carbon steel top shield plug of the DSC is plated with electroless nickel. This coating is identical to the coating used on the NUHOMS[®]-52B DSC. It has been evaluated for potential galvanic reactions in Transnuclear West's response to NRC Bulletin 96-04 [3.7]. In PWR pools, the reported corrosion rates are insignificant and are expected to result in a negligible rate of reaction for the NUHOMS[®] PWR systems.

Lubricants and Cleaning Agents

Lubricants and cleaning agents used on the NUHOMS[®]-32PT DSC should be selected for compatibility with the spent fuel pool water chemistry and the DSC materials. Never-seez or Neolube (or equivalent) is used to coat the threads and bolt shoulders of the closure bolts. The lubricant should be selected for its ability to maintain lubricity under long term storage conditions.

The DSC is cleaned in accordance with approved procedures to remove cleaning residues prior to shipment to the storage site. The basket is also cleaned prior to installation in the DSC. The cleaning agents and lubricants have no significant affect on the DSC materials and their safety related functions.

Hydrogen Generation

During the initial passivation state, small amounts of hydrogen gas may be generated in the 32PT DSC. The passivation stage may occur prior to submersion of the TC into the spent fuel pool. Any amounts of hydrogen generated in the DSC will be insignificant and will not result in a flammable gas mixture within the DSC.

The small amount of hydrogen which may be generated during DSC operations does not result in a safety hazard. In order for concentrations of hydrogen in the cask to reach flammability

levels, most of the DSC would have to be filled with water for the hydrogen generation to occur, and the lid would have to be in place with both the vent and drain ports closed. This does not occur during DSC loading or unloading operations.

An estimate of the maximum hydrogen concentration can be made, ignoring the effects of radiolysis, recombination, and solution of hydrogen in water. Testing was conducted by Transnuclear [3.9] to determine the rate of hydrogen generation for aluminum metal matrix composite in intermittent contact with 304 stainless steel. The samples represent the neutron poison plates paired with the basket compartment tubes. The test specimens were submerged in deionized water for 12 hours at 70 °F to represent the period of initial submersion and fuel loading, followed by 12 hours at 150 °F to represent the period after the fuel is loaded, until the water is drained. The hydrogen generated during each period was removed from the water and the test vessel and measured. Since the test was performed in deionized water, and the 32PT DSC will be used in borated water, the test results over-predict the hydrogen generation rates.

The test results were:

Aluminum MMC/SS304	12 hours @ 70°F		12 hours @ 150°F	
	cm ³ hr ⁻¹ dm ⁻²	ft ³ hr ⁻¹ ft ⁻²	cm ³ hr ⁻¹ dm ⁻²	ft ³ hr ⁻¹ ft ⁻²
	0.517	1.696E-4	0.489	1.604E-4

During the welding cycle, the most limiting case for hydrogen concentration is the 32PT-L100 DSC because it has the most aluminum surfaces. The total surface area of all aluminum components including the neutron absorber plates is 3495 ft². After 750 gallons of water has been drained, 1868 ft² of aluminum remains submerged. This surface area, combined with the test data at 150°F above result in a hydrogen generation rate of

$$(1.60 \times 10^{-4} \text{ ft}^3/\text{ft}^2\text{hr})(1868 \text{ ft}^2) = 0.30 \text{ ft}^3/\text{hr}$$

The minimum free volume of the DSC is 99.6 ft³, which is equivalent to the 750 gallons of water drained from the DSC cavity. The following assumptions are made to arrive at a conservative estimate of hydrogen concentration:

- All generated hydrogen is released instantly to the plenum between the water and the shield plug, that is, no dissolved hydrogen is pumped out with the water, and no released hydrogen escapes through the open vent port, and
- The welding and backfilling process takes 8 hours to complete.

Under these assumptions, the hydrogen concentration in the space between the water and the shield plug is a function of the time water is in the DSC prior to backfilling with helium. The hydrogen concentration is $(0.30 \text{ ft}^3 \text{ H}_2/\text{hr}) \cdot (8 \text{ hr}) / (99.6 \text{ ft}^3) = 2.39\%$. Monitoring of the hydrogen concentration before and during welding operations is performed to ensure that the hydrogen concentration does not exceed 2.4%, which is well below the ignitable limit of 4%. If the hydrogen concentration exceeds 2.4%, welding operations are suspended and the DSC is purged with an inert gas. In an inert atmosphere, hydrogen will not be generated.

Effect of Galvanic Reactions on the Performance of the System

There are no significant reactions that could reduce the overall integrity of the DSC or its contents during storage. The DSC and fuel cladding thermal properties are provided in Section M.4. The emissivity of the fuel compartment is 0.46, which is typical for non-polished stainless steel surfaces. If the stainless steel is oxidized, this value would increase, improving heat transfer. The fuel rod emissivity value used is 0.80, which is a typical value for oxidized Zircaloy. Therefore, the passivation reactions would not reduce the thermal properties of the component cask materials or the fuel cladding.

There are no reactions that would cause binding of the mechanical surfaces or the fuel to basket compartment boxes due to galvanic or chemical reactions.

There is no significant degradation of any safety components caused directly by the effects of the reactions or by the effects of the reactions combined with the effects of long term exposure of the materials to neutron or gamma radiation, high temperatures, or other possible conditions.

M.3.4.2 Positive Closure

Positive closure is provided by the OS197 and OS197H TCs. No change.

M.3.4.3 Lifting Devices

The evaluations for the OS197 and OS197H TC trunnions are based on critical lift weights (with water in the DSC) of 208,500 lbs and 250,000 lbs, respectively. The maximum critical lift weight with a NUHOMS[®]-32PT DSC is approximately 224,000 lbs. Therefore, the OS197H cask is acceptable with any NUHOMS[®]-32PT DSC and the OS197 cask is acceptable with a NUHOMS[®]-32PT DSC where the total critical lift weight is not more than 208,500 lbs (with water drained from the DSC cavity, if needed, to meet the weight limit).

M.3.4.4 Heat and Cold

M.3.4.4.1 Summary of Pressures and Temperatures

Temperatures and pressures for the 32PT DSC and basket are calculated in Section M.4. Section M.4.4 provides the thermal evaluation of normal conditions. Section M.4.5 provides the thermal evaluation for off-normal conditions. Section M.4.6 provides the thermal evaluation of accident conditions. Section M.4.7 provides the thermal evaluation during vacuum drying operations. Section M.4 provides the calculated temperatures for the various components during storage, transfer and vacuum drying operations respectively.

Section M.4.4.4 also provides the maximum pressures during normal, off-normal and accident conditions which are used in the evaluations presented later in this Appendix.

M.3.4.4.2 Differential Thermal Expansion

To minimize thermal stress, clearance is provided between the poison plates and inside of the fuel cells, between the basket outer diameter and DSC cavity inside diameter, and in the axial

direction between the DSC cavity and all basket parts. Additionally, the connections between the transition rails and the fuel support grid and between the aluminum heat transfer plate material and the fuel support grid are made to permit relative axial growth.

- In the axial direction, required clearances are determined using hand calculations.
- In the “radial” direction, clearance between the fuel cells and the neutron absorbing and heat transfer plate materials, is evaluated using hand calculations.
- In the “radial” direction, clearance between the basket assembly (fuel support grid and transition rails) was included in the ANSYS thermal stress analyses described in Section M.3.4.4.3. The normal condition stress analyses are described in M.3.6 and the accident condition analyses are described in M.3.7. Thus, stresses due to any thermal interferences are included in the stress results.

As noted above, hand calculations are used to evaluate thermal expansion in the axial direction and between the fuel cells and the poison/heat transfer material. Sample calculations and results for the hand calculations are described below. Results from the ANSYS thermal stress evaluations are described in Section M.3.4.4.3.

Basket assembly temperatures for normal conditions are listed in Tables M.4-3 to M.4-5; off-normal temperatures are listed in Tables M.4-9 through M.4-11.

The thermal analyses of the basket for the handling/transfer conditions are described in Section M.4. As described there, thermal analyses are performed to determine the temperature distributions in the 32PT DSC for the following cases:

- Vacuum Drying
- Blocked Vent Storage
- On-Site Transfer at -40°F ambient
- On-Site Transfer at 0°F ambient
- On-Site Transfer at 100°F ambient
- On-Site Transfer at 117°F ambient
- HSM Storage at -40°F ambient
- HSM Storage at 0°F ambient
- HSM Storage at 70°F ambient
- HSM Storage at 100°F ambient
- HSM Storage at 117°F ambient

Based on the temperature distributions for the cases listed above, hand calculations are used to evaluate the effects of differential thermal expansion for the vacuum drying and -40°F storage cases. These cases are selected since they maximize the temperature differentials, and differential expansion, in the DSC and basket assembly.

The following calculations show the evaluation of relative radial growth between the fuel support grid and the heat transfer/neutron absorbing material. For these parts, the relative growth is evaluated between parts that are immediately adjacent to each other (i.e., between the

heat transfer/neutron absorbing material at the center of the basket and the XM-19 at the center of the basket), Thus the temperatures of the two materials are equal.

Radial Expansion

In the radial direction, the thermal expansion values for the fuel support grid and the heat transfer materials are evaluated at the maximum allowable material temperature of 800°F. This maximizes the relative expansion between the parts:

$$\begin{aligned}\Delta L_{\text{GRID}} &= \alpha_{\text{XM19}} L_{\text{GRID}} \Delta T \\ &= (9.40 \times 10^{-6} \text{ } ^\circ\text{F}^{-1}) (8.825 \text{ in}) (800^\circ\text{F} - 70^\circ\text{F}) \\ &= .061 \text{ in}\end{aligned}$$

$$\begin{aligned}\Delta L_{\text{AL}_N} &= \alpha_{1100} L_{\text{GRID}} \Delta T \\ &= (14.8 \times 10^{-6} \text{ } ^\circ\text{F}^{-1}) (8.56 \text{ in}) (800^\circ\text{F} - 70^\circ\text{F}) \\ &= .092 \text{ in}\end{aligned}$$

Comparing the relative expansion of the heat transfer/neutron absorbing material and the Type XM-19 fuel grid to the design clearance:

$$\begin{aligned}\text{Design Clearance} &= (8.825 \text{ in}) - (8.56 \text{ in}) \\ &= 0.265 \text{ in}\end{aligned}$$

$$\begin{aligned}\text{Relative Growth} &= \Delta L_{\text{AL}_N} - \Delta L_{\text{GRID}} \\ &= .092 \text{ in} - .061 \text{ in} \\ &= .031 \text{ in}\end{aligned}$$

The clearance is much larger than the differential growth. Thus there is no stress due to differential "radial" expansion between the heat transfer/neutron absorbing material(s) and the Type XM-19 fuel grid.

Axial Expansion

For the vacuum drying condition, axial thermal expansion of the basket components is calculated below using thermal results documented in Chapter M.4.

Component	T _{max} (°F)	T _{min} (°F)	α _{avg} (°F)	L	ΔL
Fuel Grid (XM-19)	656	—	9.2 x 10 ⁻⁶	174.7 in	0.942 in
"	—	314	8.8 x 10 ⁻⁶	174.7 in	0.375 in
"	Average Expansion:				0.658 in
Heat Transfer Material / Neutron Absorber	656	—	14.4 x 10 ⁻⁶	174.7 in	1.474 in
16061 (Al.) T. Rails	352	—	13.4 x 10 ⁻⁶	174.7 in	0.660 in
"	—	306	13.3 x 10 ⁻⁶	174.7 in	0.548 in
DSC Cavity	—	215	8.9 x 10 ⁻⁶	174.7 in	0.225 in

Relative expansion is determined by comparing values calculated above. For example, the "worst case" required clearances between the end of the DSC cavity and the structural parts of the basket assembly can be determined by comparing the cavity expansion to the expansion of the basket assembly calculated using the maximum component temperatures:

Relative Axial Thermal Growth (Vacuum Drying)	Component Growth	Cavity Growth	Required Clearance ⁽¹⁾
Fuel Grid to Cavity	0.942 in	0.225 in	0.72 in
6061 Transition Rails to Cavity	0.660 in	0.225 in	0.44 in

Notes: 1. Required Clearance is the room temperature clearance between the top of the listed component and the bottom of the top shield plug and is determined by subtracting the cavity expansion from the component expansion.

The differential axial growth between the Aluminum Alloy 1100 heat transfer material (and neutron absorbing material) and the fuel support grid is determined using similar methods. An average value of axial expansion is used since the overall growth of the fuel support grid will be related to the average grid temperature. A maximum value of aluminum expansion is used.

Relative Axial Thermal Growth (Vacuum Drying)	Fuel Support Grid Axial Growth	1100 Alloy Growth	Required Clearance ⁽¹⁾
Fuel Grid to Aluminum Heat Transfer Material (Alloy 1100)	$\Delta L = \frac{0.94 \text{ in} + 0.38 \text{ in}}{2}$ $= 0.66 \text{ in}$	1.47 in	0.81 in

Notes: 1. Required Clearance is the room temperature clearance between the neutron absorbing sheets and Alloy 1100 aluminum heat transfer material and the stop plates attached to the fuel grid.

M.3.4.4.3 Thermal Stress Calculations

The thermal stress calculations for the various system components other than the basket are provided in Sections 3.6 and 3.7 for normal, off-normal and accident conditions. The thermal stress calculations for the 32PT basket are presented below.

Thermal stresses are considered separately and in combination with other loads on the basket assembly. Only the separate thermal stresses are presented here. Thermal stresses in combination with other loads are addressed in the appropriate sections.

As noted in M.3.4.4.2, clearances are provided such that there is free thermal expansion in the axial direction.

Thermal stresses in the basket assembly are evaluated using the ANSYS [3.11] finite element model described in M.3.6.1.3. As described in M.3.6.1.3.1, the ANSYS model includes the fuel support grid, R90 transition rails, R45 transition rails, the DSC shell, and the cask ID and cask rails. For the evaluation of thermal stresses only (i.e., thermal stresses without deadweight or other loads), the cask ID and cask rails are removed from the solution by eliminating the contact elements between the shell OD and the cask ID with cask rails. For the evaluation of thermal loads combined with other loads (e.g., thermal plus deadweight), all contact elements are active and the effects of the cask and cask rails are included.

As listed below, a total of 30 thermal stress analyses were performed.

Condition / Ambient Temperature		Heat Load Zoning Configurations (see Figures M.1-1, M.1-2 and M.1-3)		
		1	2	3
Vacuum Drying		X	X	
Blocked Vent Storage		X		
On-Site Transfer	-40°F ambient	X	X	X
	0°F ambient	X	X	X
	100°F ambient	X	X	X
	117°F ambient	X	X	X
HSM Storage	-40°F ambient	X	X	X
	0°F ambient	X	X	X
	70°F ambient	X	X	X
	100°F ambient	X	X	X
	117°F ambient	X	X	X

Maximum thermal stresses (ANSYS nodal stress intensities) are summarized in Table M.3.4-2. These results apply directly to the single-piece solid R90 rail configuration and are conservative for the multi-piece R90 option (since decreasing stiffness reduces thermal stresses). As shown by the table, thermal stresses in the 32PT basket are low. Based on these results, the temperature distribution corresponding to 117°F ambient temperature, DSC in the TC, with heat load zoning configuration 1 was selected for combination with other loads.

Selection of a high temperature case ensures the application of lower allowable stresses (since allowable stresses decrease with temperature), and reduced structural stiffness (since stability is directly related to E and S_y).

Results of the thermal stress analysis are shown in Figure M.3.4-4 and Figure M.3.4-5. These figures show the applied temperature distribution and resulting thermal stresses for cold (-40°F in cask) and hot (117°F in cask) conditions.

Table M.3.4-1
Summary of Thermal Stress Results - 32PT Basket with Steel Transition Rails

DELETED

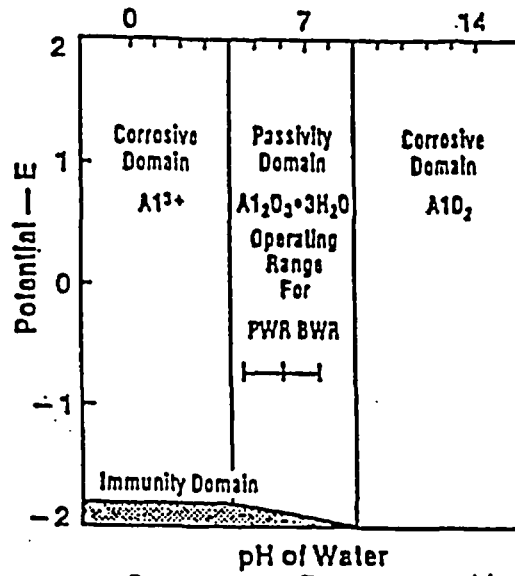
**Table M.3.4-2
Summary of Thermal Stress Results - 32PT Basket with Aluminum Transition Rails**

Operating Condition	Maximum Stress Intensities (ksi)			
	Fuel Grid	R90 Transition Rail (XM-19 Cover Plate)	R90 Transition Rail (Aluminum)	R45 Transition Rail (Aluminum)
Vacuum Drying	4.33	2.55	.55	1.40
Blocked Vent Storage	4.25	2.75	.60	1.40
On-Site Transfer & Storage ⁽¹⁾	4.95	2.50	.60	1.50

Note: 1. Includes all cases except for vacuum drying and blocked vent storage.

POTENTIAL VERSUS pH DIAGRAM FOR ALUMINUM-WATER SYSTEM

At 25°C (77°F):



At 60°C (140°F):

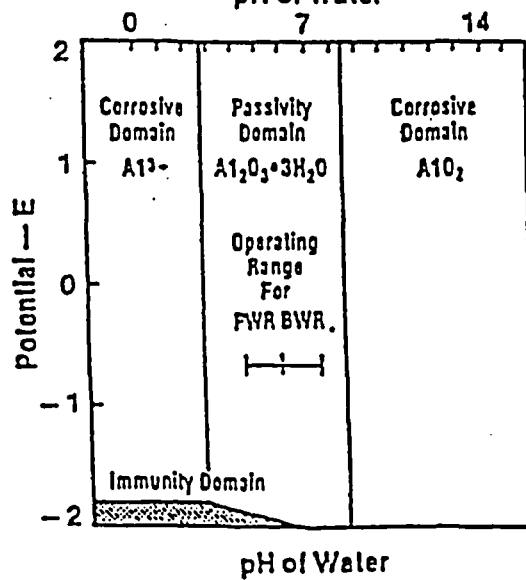


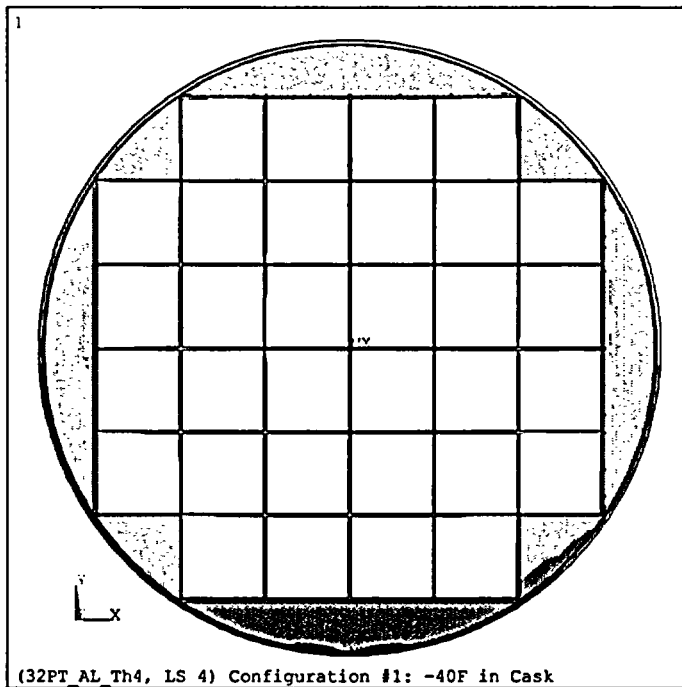
Figure M.3.4-1
Potential Versus pH Diagram for Aluminum-Water System

DELETED

**Figure M.3.4-2
32PT Basket with Steel Transition Rails,
Temperatures and Stress Intensities, -40°F in Cask**

DELETED

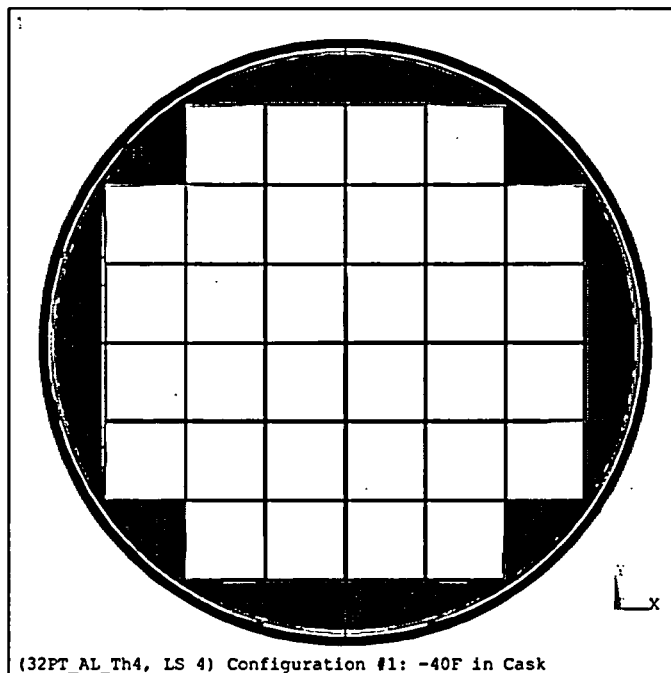
**Figure M.3.4-3
32PT Basket with Steel Transition Rails,
Temperatures and Stress Intensities, 117°F in Cask**



ANSYS 5.6.2
 MAY 25 2001
 10:02:02
 PLOT NO. 22
 NODAL SOLUTION
 STEP=4
 SUB =38
 TIME=4
 BFETEMP (AVG)
 DMX =.161296
 SMN =289
 SMX =641.757

■	289
■	328.195
■	367.391
■	406.586
■	445.781
■	484.976
■	524.172
■	563.367
■	602.562
■	641.757

(32PT AL Th4, LS 4) Configuration #1: -40F in Cask

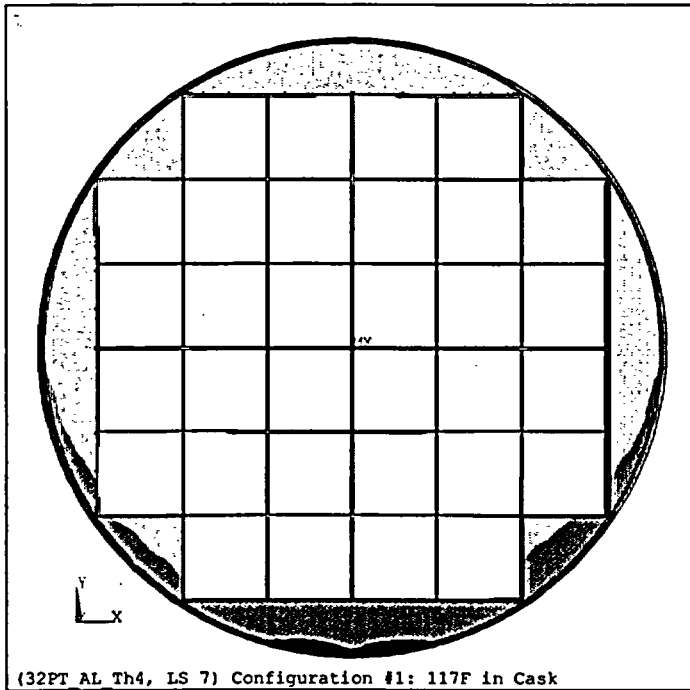


ANSYS 5.6.2
 JUN 27 2001
 11:12:30
 PLOT NO. 1
 NODAL SOLUTION
 STEP=4
 SUB =38
 TIME=4
 SINT (AVG)
 DMX =.161296
 SMX =4361

■	0
■	484.543
■	969.085
■	1454
■	1938
■	2423
■	2907
■	3392
■	3876
■	4361

(32PT AL Th4, LS 4) Configuration #1: -40F in Cask

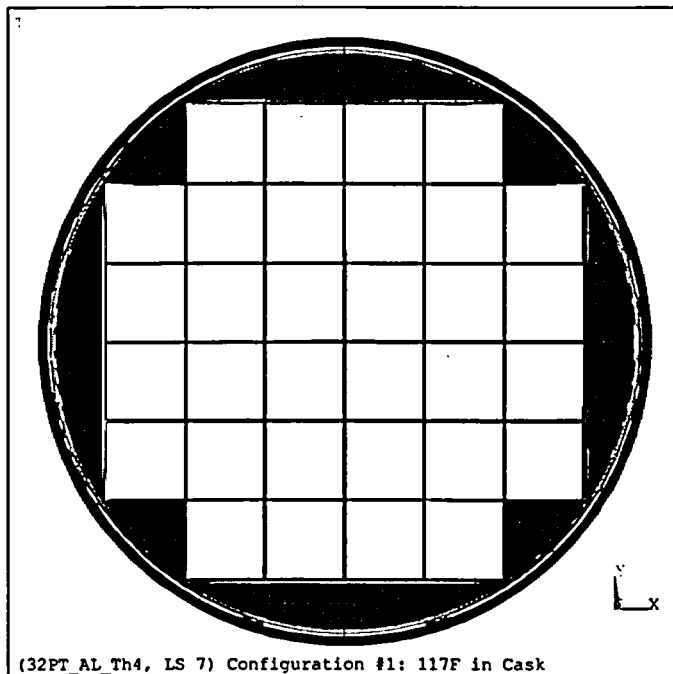
Figure M.3.4-4
32PT Basket with Aluminum Transition Rails,
Temperatures and Stress Intensities, -40°F in Cask



ANSYS 5.6.2
MAY 25 2001
10:02:36
PLOT NO. 43
NODAL SOLUTION
STEP=7
SUB =17
TIME=7
BFTEMP (AVG)
DMX =.198265
SMN =391
SMX =709.879

391
426.431
461.862
497.293
532.724
568.155
603.586
639.017
674.448
709.879

(32PT AL Th4, LS 7) Configuration #1: 117F in Cask



ANSYS 5.6.2
JUN 27 2001
11:14:04
PLOT NO. 2
NODAL SOLUTION
STEP=7
SUB =17
TIME=7
SINT (AVG)
DMX =.198265
SMX =4156

0
461.79
923.58
1385
1847
2309
2771
3233
3694
4156

(32PT AL Th4, LS 7) Configuration #1: 117F in Cask

Figure M.3.4-5
32PT Basket with Aluminum Transition Rails,
Temperatures and Stress Intensities, 117°F in Cask

M.3.5 Fuel Rods

No change to the evaluation presented in the FSAR.

M.3.6 Structural Analysis (Normal and Off-Normal Operations)

In accordance with NRC Regulatory Guide 3.48 [3.12], the design events identified by ANSI/ANS 57.9-1984, [3.14] form the basis for the accident analyses performed for the standardized NUHOMS[®] System. Four categories of design events are defined. Design event Types I and II cover normal and off-normal events and are addressed in Section 8.1. Design event Types III and IV cover a range of postulated accident events and are addressed in Section 8.2. The purpose of this section of the Appendix is to present the structural analyses for normal and off-normal operating conditions for the NUHOMS[®]-32PT system using a format similar to the one used in Section 8.1 for analyzing the NUHOMS[®]-24P systems.

M.3.6.1 Normal Operation Structural Analysis

Table M.3.6-1 shows the normal operating loads for which the NUHOMS[®] safety-related components are designed. The table also lists the individual NUHOMS[®] components which are affected by each loading. The magnitude and characteristics of each load are described in Section M.3.6.1.1.

The method of analysis and the analytical results for each load are described in Sections M.3.6.1.2 through M.3.6.1.9.

M.3.6.1.1 Normal Operating Loads

The normal operating loads for the NUHOMS[®] System components are:

- Dead Weight Loads
- Design Basis Internal and External Pressure Loads
- Design Basis Thermal Loads
- Operational Handling Loads
- Design Basis Live Loads

These loads are described in detail in the following paragraphs.

A. Dead Weight Loads

Table M.3.2-1 shows the weights of various components of the NUHOMS[®]-32PT system. The dead weight of the component materials is determined based on nominal component dimensions.

B. Design Basis Internal and External Pressure

The maximum internal pressures of the NUHOMS[®]-32PT DSC for the storage and transfer mode are presented in Section M.4.

C. Design Basis Thermal Loads

The normal condition temperature distributions for the 32PT-DSC are presented in Section M.4. Stress analysis for normal thermal loads for the DSC shell assembly are provided in Section M.3.6.1.2C and in Section M.3.4.4 for the basket assembly.

D. Operational Handling Loads

There are two categories of handling loads: (1) inertial loads associated with on-site handling and transporting the DSC between the fuel handling/loading area and the HSM, and (2) loads associated with loading the DSC into, and unloading the DSC from, the HSM. These handling loads are described in Section 8.1.1.1C.

Based on the surface finish and the contact angle of the DSC support rails inside the HSM (described in Chapter 4), a bounding coefficient of friction is conservatively assumed to be 0.25. Therefore, the nominal ram load required to slide the DSC under normal operating conditions is approximately 29,400 lbs., calculated as follows:

$$P = \frac{0.25W}{\cos\theta} = 0.29W = 0.29 (101,400 \text{ lbs.}) \approx 29,400 \text{ lbs.}$$

Where:

P = Push/Pull Load,

W = Loaded DSC Weight \approx 101,400 lbs. (See Table M.3.2-1), and

θ = 30 degrees, Angle of the Canister Support Rail.

However, the DSC bottom cover plate and grapple ring assembly are designed to withstand a normal operating insertion force equal to 80,000 pounds and a normal operating extraction force equal to 60,000 pounds. To insure retrievability for a postulated jammed DSC condition, the ram is sized with a capacity for a load of 80,000 pounds, as described in Section 8.1.2. These loads bound the friction force postulated to be developed between the sliding surfaces of the DSC and TC during worst case off-normal conditions.

E. Design Basis Live Loads

As discussed in Section 3.2.4, a live load of 200 pounds per square foot is conservatively selected to envelope all postulated live loads acting on the HSM, including the effects of snow and ice. Live loads which may act on the TC are negligible, as discussed in Section 3.2.4.

M.3.6.1.2 Dry Shielded Canister Analysis

The standardized NUHOMS[®]-32PT DSC shell assembly is analyzed for the normal, off-normal and postulated accident load conditions using two basic ANSYS [3.11] finite element models: a top-end half-length model of the DSC shell assembly and a bottom-end half-length model of the

DSC shell assembly. Typical models of the top and bottom halves of the DSC shell assembly are shown in Figures 8.1-14a and 8.1-14b.

These models are used to evaluate stresses in the NUHOMS[®]-32PT DSC due to:

- Dead Weight
- Design Basis Normal Operating Internal and External Pressure Loads
- Normal Operating Thermal Loads
- Normal Operation Handling Loads

The methodology used to evaluate the effects of these normal loads is addressed in the following paragraphs. Table M.3.6-2 summarizes the resulting stresses for normal operating loads.

Dead load analyses of the DSC are performed for both vertical and horizontal positions of the DSC. In the vertical position, the DSC shell supports its own empty weight and the entire weight of the top end components. When inside the TC, the weight of the fuel and the bottom end components is transferred to the TC by bearing through the inner bottom cover plate, shield plug and outer bottom cover plate. When in the horizontal position, the DSC is in the TC or in the HSM. In this position, the DSC shell assembly end components and the internal basket assembly bear against the DSC shell. The DSC shell assembly is supported by two rails located at $\pm 18.5^\circ$ when in the TC and at $\pm 30^\circ$ when in the HSM. This is shown schematically in Figure 8.1-13.

A. DSC Dead Load Analysis

Dead load stresses are obtained from static analyses performed using the ANSYS finite element models described above. Both, the top-end half and bottom-end half models are analyzed for a 1g load, using the appropriate finite element model and boundary conditions, for horizontal and vertical configurations. For the horizontal dead load analyses, the DSC is conservatively assumed to be supported on one rail. In addition, the fuel-loaded portions of the basket assembly bear on the inner surface of the DSC shell. DSC shell stresses in the region of the basket assembly resulting from the bearing load and from local deformations at the cask rails are evaluated using the ANSYS model described in Section M.3.6.1.3. The DSC shell assembly components are evaluated for primary membrane and membrane plus bending stress and for primary plus secondary stress range. Enveloping maximum stress intensities are summarized in Table M.3.6-2 for the NUHOMS[®]-32PT DSC.

B. DSC Normal Operating Design Basis Pressure Analysis

The NUHOMS[®]-32PT DSC shell assembly analytical models shown in Figure 8.1-14a and Figure 8.1-14b are used for the normal operating design pressure analyses. The calculated maximum internal pressures for the NUHOMS[®]-32PT DSC are shown in Section M.4. The design internal pressure of 20 psig is used. The resulting maximum stress intensities are reported in Table M.3.6-2.

C. DSC Normal Operating Thermal Stress Analysis

The thermal analysis of the DSC for the various conditions, as presented in Section M.4.0, provide temperature distributions for the DSC shell, along with maximum and minimum DSC component temperatures. These temperature distributions are imposed onto the DSC shell assembly ANSYS stress analysis models shown in Figure 8.1-14a and Figure 8.1-14b for thermal stress evaluation. Corresponding component temperatures are used to determine material properties and allowable stress values used in the stress analyses. DSC shell assembly materials are all Type 304 stainless steel with the exception of the shield plugs, which are made of A36 carbon steel. However, because these dissimilar materials are not mechanically fastened, allowing free differential thermal growth, the thermal stresses in the DSC shell components are due entirely to thermal gradients. The results of the thermal analysis show that for the range of normal operating ambient temperature conditions, the thermal gradients are primarily along the axial and tangential directions of the DSC and that no significant thermal gradients exist through the wall of the DSC. Stresses resulting from thermal gradients are classified as secondary stresses and are evaluated for Service Level A and B conditions. Maximum stress intensities resulting from the thermal stress analyses are summarized in Table M.3.6-2 for the NUHOMS®-32PT DSC.

D. DSC Operational Handling Load Analysis

To load the DSC into the HSM, the DSC is pushed out of the TC using a hydraulic ram. The applied force from the hydraulic ram, specified in Section M.3.6.1.1D, is applied to the center of the DSC outer bottom cover plate at the center of the grapple ring assembly. The ANSYS finite element model shown in Figure 8.1-14b is used to calculate the stresses in the DSC shell assembly. In the analysis, the ram load is applied to the cover plate in the form of two arcs, assuming that the load is concentrated at the barrel diameter of the ram, excluding the cutouts for extension of the grapple arms.

To unload the HSM, the DSC is pulled using grapples which fit into the grapple ring. For analysis of grapple pull loading, the 180° ANSYS finite element model of the bottom half DSC assembly is refined in the area of the grapple assembly and outer cover plate, as shown in Figure 8.1-15.

The controlling stresses from these analyses are tabulated in Table M.3.6-2.

E. Evaluation of the Results

The maximum calculated DSC shell stresses induced by normal operating load conditions are shown in Table M.3.6-2. The calculated stresses for each load case are combined in accordance with the load combinations presented in Table M.2-15. The resulting stresses for the controlling load combinations are reported in Section M.3.7.10 along with the ASME Code allowable stresses.

M.3.6.1.3 NUHOMS®-32PT Basket Structural Analysis

Stresses in the basket assembly are determined using a combination of hand calculations and a two dimensional (planar) ANSYS finite element model. The following loads are addressed:

- Dead Weight
- Thermal Stresses
- Handling/Transfer Loads
- Side Drops
- Seismic Loads

Thermal loads for the basket are addressed in Section M.3.4.4. The side drop loads are Level D loads and are addressed in Section M.3.7. The seismic loads are Level C loads, but are enveloped by the on-site handling loads as described in Section M.3.6.1.3.2.

M.3.6.1.3.1 ANSYS Finite Element Model Analysis

ANSYS is used for structural analysis of the 32PT basket for all normal and off-normal conditions.

A. ANSYS Finite Element Model Description

The ANSYS models of the 32PT basket assembly use Plane42 (2-D Structural Solid) elements to represent a unit length of the 32PT basket. A minimum of three (3) elements are used through the thickness of all parts except the cask shell and cask rails. The cask shell and cask rails, which are extremely rigid relative to the other parts of the structure, are included as "ground" and are fixed around their entire circumference. Therefore, the cask shell is modeled with only one through thickness element. Table M.3.6-3 lists the structural parts included in the model.

The geometry of the basket model is shown in Figures M.3.6-3, M.3.6-3A, M.3.6-4 and M.3.6-4A for the 32PT DSC with aluminum transition rails.

ANSYS contact elements, Contac48, 2-D Point-to-Surface Contact, are used between the separate parts of the structure. Since the components are modeled with actual thicknesses, the initial gap dimensions are determined by the geometry of the contacting surfaces. Contact elements are included between the following interfacing components:

- Fuel support grid to transition rails,
- Transition rails to DSC shell ID,
- DSC shell OD to cask ID and cask rail, and
- Between segments of the 3-piece R90 rails (as applicable).

Springs elements are provided between the fuel support grid and the transition rails. These springs, which act in parallel to the contact elements, are defined with non-linear stiffnesses such that low stiffness is active for motion of the rails away from the grid, allowing the transition rails to separate from the grid and a higher stiffness which is active for compression between the two structures.

Inertial loads are applied to the structure by including the appropriate weight density of the materials and applying accelerations. Fuel loads are applied using pressure loads on the fuel grid elements. Thermal effects are included by applying temperatures corresponding to the 117°F in cask temperature distribution, to each node in the model (see M.3.4.4.3).

For all stress analyses, 1g (deadweight) loads are applied and stresses determined. These deadweight stresses are classified as primary membrane and membrane plus bending stresses. Additional load steps are then used to apply temperatures corresponding to the 117°F ambient temperature condition. The thermal plus deadweight stresses are classified as primary plus secondary. Tables of the temperature-dependent material properties (e.g., S_y versus temperature) are included in the ANSYS model, such that the appropriate properties are applied at each point in the structure.

For each cell of the fuel support structure, stresses were linearized at the 12 locations shown in Figure M.3.6-5 using the ANSYS LPATH, and PRSECT commands. Maximum values are reported in this Appendix.

B. Material Properties

The material properties used in the ANSYS stress analyses for normal conditions are summarized in Table M.3.6-4. As listed in this table, linear elastic properties are used for the normal condition analyses. With the exception of the solid aluminum transition rails, properties for all materials are directly from the ASME Code. Properties for the aluminum rails are described in Section M.3.3.

M.3.6.1.3.2 Normal Condition Loading

Postulated loads on the 32PT basket structure for non-accident conditions are described in the following sections. The loads and load combinations for the 32PT basket structure are simplified by consideration that the basket is unaffected by either pressure loads or HSM insertion/retrieval loads.

A. Thermal

The analysis of the 32PT basket for thermal loads is described in Section M.3.4.4. As shown in Section M.3.4.4, thermal stresses are small.

B. Vertical Deadweight

Deadweight load conditions include: (1) vertical deadweight during fuel loading operations, (2) horizontal deadweight in the TC with support through the cask rails at $\pm 18.5^\circ$, and (3) horizontal deadweight in the HSM with support through the HSM rails at $\pm 30^\circ$.

Under axial loads, the fuel assemblies and fuel compartment are supported by the bottom of the cask. Thus, the fuel assemblies react directly against the bottom of the canister/cask and do not load the basket structure. Stresses under axial loading are from self weight of the basket structure. Maximum axial compressive stresses occur at the supported end of the basket.

Vertical deadweight was evaluated using hand calculations and by comparing the calculated axial compression stresses to stability allowables developed considering both stability criteria and the general membrane criteria (P_m) from Subsection NG (see M.2.2.5.1.2). Calculated stresses for the vertical deadweight condition also applied to the vacuum drying case.

Calculated stresses are listed in Table M.3.6-5 along with the appropriate compressive allowables. As shown by the table, stresses for this load condition are small.

C. Horizontal Deadweight

Horizontal deadweight cases were evaluated using the ANSYS model described in M.3.6.1.3.1. As appropriate the elements representing the support rails were located at either $\pm 18.5^\circ$ or $\pm 30^\circ$ from bottom center for support by the TC or HSM, respectively. Separate analyses were performed for the 32PT fuel grid supported by the solid 1-piece or 3-piece R90 transition rails. Thus, the following four (4) analysis cases were evaluated:

1. 32PT DSC with solid 1-piece R90 transition rails supported at $\pm 18.5^\circ$ (Figure M.3.6-10 and M.3.6-11)
2. 32PT DSC with solid 3-piece R90 transition rails supported at $\pm 18.5^\circ$ (Figure M.3.6-10A and M.3.6-11A)
3. 32PT DSC with solid 1-piece R90 transition rails supported at $\pm 30^\circ$ (Figure M.3.6-12 and M.3.6-13)
4. 32PT DSC with solid 3-piece R90 transition rails supported at $\pm 30^\circ$ (Figure M.3.6-12A and M.3.6-13A)

Primary plus secondary stresses were evaluated by combining deadweight stresses with the thermal stresses resulting from the 117°F in cask temperature distribution. Maximum stresses are summarized in Table M.3.6-5 along with a comparison to Level A allowables from Subsection NG.

D. Vacuum Drying

As described above, the axial compression stresses under the vacuum drying condition are equal to the axial compression stresses under vertical deadweight.

As described in M.3.4.4.3, maximum stresses from the vacuum drying temperature distribution are listed in Tables M.3.4-1 and M.3.4-2. These thermal stresses are classified as secondary by the Code and, as shown by the tables, these stresses are small.

E. Handling/On-Site Transfer Loads

These cases include the loads associated with loading (and unloading) the 32PT DSC into an HSM and the inertial loads associated with on-site handling. The insertion/retrieval loads do not directly impact the 32PT basket assembly and do not require additional consideration. The inertia loads to be considered are:

- DW + 1g Axial
- DW + 1g Transverse.
- DW + 1g Vertical
- DW + 0.5g Axial + 0.5 Transverse + 0.5 Vertical

These loads are enveloped by a 2g resultant acceleration applied in the most critical orientation.

The 2.0g resultant axial load is evaluated using hand calculations and the same methodology used for the vertical deadweight analyses. Maximum compressive stresses resulting from this load case are listed in Table M.3.6-6 along with a comparison to the axial stability criteria described in M.2.2.5.1.2.

Loads transverse to the axis of the DSC are evaluated using the ANSYS models described in M.3.6.1.3.1. Loads are enveloped by selection of maximum stresses from the analysis load cases listed in Table M.3.6-7. Table M.3.6-7 lists the on-site handling analyses performed for the 32PT basket considering the basket transition rail configuration and DSC support conditions in the OS197, OS197H and HSM. Enveloping 32PT basket stresses are summarized in Table M.3.6-6 along with a comparison to Service Level A allowables.

F. Evaluation of Results

ANSYS plots showing typical analysis results for the 32PT basket are provided in Figure M.3.6-10, Figure M.3.6-11, Figure M.3.6-12 and Figure M.3.6-13 for baskets with solid aluminum 1-piece R90 aluminum transition rails and Figure M.3.6-10A, Figure M.3.6-11A, Figure M.3.6-12A and Figure M.3.6-13A for baskets with solid aluminum 3-piece R90 transition rails. These figures and summary tables in the previous sections show that the basket stress criteria is met.

Welds in the fuel support structure are sized to maintain full moment capacity of the plates across all welded connections.

Within the basket grid structure are plates of Type 1100 aluminum and neutron absorbing materials composed of either enriched borated aluminum alloy or Boralyn[®] plates which perform heat transfer and criticality functions. As shown in Section M.4, the maximum short term basket temperature is 791°F, which is well below the melting point of the aluminum plates (approximately 1200°F). As discussed in Section M.3.4, adequate clearance is provided for thermal expansion so that thermal stresses in the aluminum plates are negligible. The bounding normal or off-normal axial stress in the plates is 0.04 ksi, due to the 2g handling load, which is well below the yield stress value of 1.3 ksi (Type 1100 aluminum at 791°F). This ensures that the plates remain in position to perform their heat transfer and criticality functions. Under inertia loading in the transverse direction, the aluminum plates are supported along their length by either the grid structure or the fuel assemblies. Deflection of the aluminum plates in the transverse direction is limited by the gap between the grid structure and the fuel assembly and does not significantly affect the heat transfer function of the plates. The effect of this gap is bounded by the criticality evaluation.

M.3.6.1.4 DSC Support Structure Analysis

The DSC support structure is shown in Figures 4.2-6 and 4.2-7.

As presented in Section 8.1.1.4, the various components of the DSC support structure are subjected to normal operating loads including dead weight, thermal, and operational handling loads which are greater than or equal to the corresponding loads for the 32PT DSC. Therefore, the limiting DSC support structure components are acceptable.

M.3.6.1.5 HSM Design Analysis

The HSM loads evaluated in Section 8.1.1.5 bound the corresponding loads for the 32PT system. Therefore, there is no change to the structural evaluation of the HSM.

M.3.6.1.6 HSM Door Analyses

As discussed in Section M.3.6.1.5 there is no change to the structural evaluation of the HSM.

M.3.6.1.7 HSM Heat Shield Analysis

As discussed in Section M.3.6.1.5 there is no change to the structural evaluation of the HSM.

M.3.6.1.8 HSM Axial Retainer for DSC

As discussed in Section M.3.6.1.5 there is no change to the structural evaluation of the HSM.

M.3.6.1.9 On-Site TC Analysis

The on-site TC is evaluated for normal operating condition loads including:

- Dead Weight Load

- Thermal Loads
- Handling Loads
- Live Loads.

Section 8.1.1.9 provides the evaluation of the TCs for the normal operating loads. Thermal loads and live loads for the OS197 and OS197H TCs with the 32PT DSC are equivalent to or less than those evaluated in Section 8.1.1.9. The evaluations for the OS197 and OS197H casks are based on DSC maximum allowable wet payloads of 102,410 lbs. and 126,000 lbs., and maximum allowable DSC dry payload weights of 97,250 lbs. and 116,000 lbs., respectively. The maximum total cask payload with a dry-loaded NUHOMS[®]-32PT DSC is approximately 102,000 lbs., and wet loaded 32PT DSC is approximately 114,000 lbs. Therefore, the OS197H cask is acceptable with any NUHOMS[®]-32PT DSC and the OS197 cask is acceptable with a NUHOMS[®]-32PT DSC where the total cask wet payload is not more than 102,410 lbs. and the total cask dry payload is not more than 97,250 lbs. Water may be drained from the DSC cavity to meet the weight limit.

M.3.6.2 Off-Normal Load Structural Analysis

Table M.3.6-8 shows the off-normal operating loads for which the NUHOMS[®] safety-related components are designed. This section describes the design basis off-normal events for the NUHOMS[®] System and presents analyses which demonstrate the adequacy of the design safety features of a NUHOMS[®] System with the 32PT DSC.

For an operating NUHOMS[®] System, off-normal events could occur during fuel loading, cask handling, trailer towing, canister transfer and other operational events. Two off-normal events are defined which bound the range of off-normal conditions. The limiting off-normal events are defined as a jammed DSC during loading or unloading from the HSM and the extreme ambient temperatures of -40°F (winter) and +117°F (summer). These events envelope the range of expected off-normal structural loads and temperatures acting on the DSC, TC, and HSM. These off-normal events are described in Section 8.1.2.

M.3.6.2.1 Jammed DSC During Transfer

The interfacing dimensions of the top end of the TC and the HSM access opening sleeve are specified so that docking of the TC with the HSM is not possible should gross misalignments between the TC and HSM exist. Furthermore, beveled lead-ins are provided on the ends of the TC, DSC, and DSC support rails to minimize the possibility of a jammed DSC during transfer. Nevertheless, it is postulated that if the TC is not accurately aligned with respect to the HSM, the DSC binds or becomes jammed during transfer operations.

The interfacing dimensions and design features of the HSM access opening, DSC Support Structure and the OS197 and OS197H TCs, as described in Section 8.1.2, remain unchanged. The insertion and extraction forces applied on the NUHOMS[®]-32PT during loading and unloading operations are the same as those specified for the NUHOMS[®]-24P system. The discussion in Section 8.1.2B applies to the 32PT DSC. However, the NUHOMS[®]-32PT DSC

shell thickness is 0.5 inches (compared to 0.625 inches for the NUHOMS[®]-24P DSC shell) and the outside radius is 33.595 inches. Hence, the NUHOMS[®]-32PT DSC shell stresses, based on a force of 80 kips and a moment arm of 33.595 inches are calculated below.

Axial Sticking of the DSC

$$S_{mx} = \frac{M}{S} \quad (\text{From Equation 8.1-9, Section 8.1.2.1})$$

Where:

$$M = 80 \times 33.595 = 2690 \text{ in.-kip, Bending moment}$$

$$S = 1734 \text{ in.}^3, \text{ DSC section modulus}$$

Therefore:

$$S_{mx} = 1.55 \text{ ksi}$$

This magnitude of stress is negligible when compared to the allowable membrane stress of 17.5 ksi and is bounded by stresses for other handling loads as shown Table M.3.6-2.

There is no change to the structural evaluation of the HSM.

Binding of the DSC

As discussed in Section 8.1.2C, if axial alignment within system operating specifications is not achieved, it may be possible to pinch the DSC shell as shown in Figure 8.1-32. From Section 8.1.2C, the pinching force is taken as the product of the maximum ram loading of 80,000 pounds and the sine of a 1 degree angle, or 1,400 pounds.

The 1,400 pound load is conservatively assumed to be applied as a point load at a location away from the ends of the cask or DSC. The resulting maximum stresses are given by Table 31, Case 9a of Roark [3.10] as:

Membrane stress:

$$\sigma = \frac{0.4P}{t^2}$$

Bending stress:

$$\sigma' = \frac{2.4P}{t^2}$$

Therefore, the maximum membrane plus bending stress is:

$$\sigma + \sigma' = \frac{2.8P}{t^2}$$

For the DSC shell, $t = 0.500$ inch. Substituting for t and using a value of P equal to 1,400 pounds, the maximum extreme fiber stresses in the DSC shell are 15.7 ksi. This local stress is conservative in that small deformations create a larger contact area, i.e., not a point load, and the stress is actually lower than calculated. In addition, the deformations are limited by the gap

between the shell and basket. As such, this stress is considered a secondary stress and is enveloped by the handling stresses shown in Table M.3.6-2.

The tangential component of ram loading under the assumed condition is less than the 80,000 lbs force of the jammed condition, axial sticking, calculated above and as such is not considered further.

In both scenarios for a jammed DSC, the stress in the DSC shell is demonstrated to be much less than the ASME Code allowable stress and below the yield value of the material. Therefore, permanent deformation of the DSC shell does not occur. There is no potential for breach of the DSC containment pressure boundary and, therefore, no potential for release of radioactive material.

There is no change to the structural evaluation of the OS197 and OS197H TC as shown in the FSAR.

There is no change to the required corrective actions, as described in the FSAR, for the jammed DSC conditions.

M.3.6.2.2 Off-Normal Thermal Loads Analysis

As described in Section 8.1.2, the NUHOMS[®] System is designed for use at all reactor sites within the continental United States. Therefore, off-normal ambient temperatures of -40°F (extreme winter) and 117°F (extreme summer) are conservatively chosen. In addition, even though these extreme temperatures would likely occur for a short period of time, it is conservatively assumed that these temperatures occur for a sufficient duration to produce steady

state temperature distributions in each of the affected NUHOMS[®] components. Each licensee should verify that this range of ambient temperatures envelopes the design basis ambient temperatures for the ISFSI site. The NUHOMS[®] System components affected by the postulated extreme ambient temperatures are the TC and DSC during transfer from the plant's fuel/reactor building to the ISFSI site, and the HSM during storage of a DSC.

Section M.4 provides the off-normal thermal analyses for storage and transfer mode for the NUHOMS[®]-32PT DSC. Maximum DSC shell assembly thermal stress analysis results for the normal and off-normal conditions are summarized in Table M.3.6-2. Basket assembly thermal results are summarized in Section M.3.4.4. The resulting stress intensities for the NUHOMS[®]-32PT are acceptable.

**Table M.3.6-1
NUHOMS® Normal Operating Loading Identification**

Load Type	AFFECTED COMPONENT				
	DSC Shell Assembly	DSC Basket	DSC Support Structure	Reinforced Concrete HSM	On-site TC
Dead Weight	X	X	X	X	X
Internal/External Pressure	X				
Normal Thermal	X	X	X	X	X
Normal Handling	X	X	X	X	X
Live Loads				X	X

Table M.3.6-2
Maximum NUHOMS®-32PT DSC Shell Assembly Stresses for Normal and Off-Normal Loads

DSC Components	Stress Type	Maximum Stress Intensity (ksi) ⁽¹⁾			
		Dead Weight	Internal Pressure ⁽⁶⁾	Thermal ⁽²⁾	Handling ⁽⁴⁾
DSC Shell	Primary Membrane	2.65	8.90	N/A	4.10
	Membrane + Bending	6.00	9.18	N/A	6.00
	Primary + Secondary	7.00	16.29	41.75	55.63
Inner Top Cover Plate	Primary Membrane	0.58	0.74	N/A	1.68
	Membrane + Bending	1.67	16.76	N/A	1.84
	Primary + Secondary ⁽⁵⁾	1.63	16.76	24.52	1.85
Outer Top Cover Plate	Primary Membrane	1.11	2.65	N/A	1.11
	Membrane + Bending	1.63	7.43	N/A	1.63
	Primary + Secondary ⁽⁵⁾	1.17	7.22	23.69	1.17

See end of table for notes.

Table M.3.6-2
Maximum NUHOMS®-32PT DSC Shell Assembly Stresses for Normal and Off-Normal
Loads
(concluded)

DSC Components	Stress Type	Maximum Stress Intensity (ksi) ⁽¹⁾			
		Dead Weight	Internal Pressure ⁽⁶⁾	Thermal ⁽²⁾	Handling ⁽⁴⁾
Inner Bottom Cover Plate ⁽⁹⁾	Primary Membrane	0.71	0.56	N/A	3.22
	Membrane + Bending	0.84	1.48	N/A	4.80
	Primary + Secondary ⁽⁵⁾	0.83	1.51	36.41	49.26 ⁽⁸⁾
Outer Bottom Cover Plate	Primary Membrane	0.74	0.83	N/A	5.27
	Membrane + Bending	1.31	1.47	N/A	22.72
	Primary + Secondary ⁽⁵⁾	1.18	1.15	30.81	39.97 ⁽⁸⁾

- (1) Values shown are maximum irrespective of location.
(2) Envelope of Normal and Off-Normal ambient temperature conditions.
(3) Not used.
(4) Maximum of deadweight, 1g axial, 60 kips pull or 80 kips push (except as noted).
(5) Per Note 2 of Table NB3217-1, the stress at the intersection between a shell and a flat head may be classified as secondary (Q) if the bending moment at the edge is not required to maintain the bending stresses in the middle of the head within acceptable limits. Thus, the primary plus secondary stresses were computed in a finite element model that assumed moment transferring connections, whereas the primary membrane plus bending stresses were computed assuming pinned connections. All thermal stresses are classified as secondary.
(6) Due to the off-normal 20 psig internal pressure condition.
(7) Results are for the combination of deadweight, 15 psi internal pressure, the 1g vertical transfer load and thermal.
(8) Results are for the combination of deadweight, 20 psi internal pressure, the 80 kip ram push load and thermal.
(9) These stresses may also be applied to the single bottom and forging, when used.

Table M.3.6-3
NUHOMS® -32PT Basket Model Components, Element Types and Materials

Structural Component	ANSYS Element Type	Material
Fuel Support Structure	Plane42	Type XM-19 Stainless Steel
DSC Shell	Plane42	Type 304 Stainless Steel
R45 Transition Rails	Plane42	6061 Aluminum
R90 Transition Rails	Plane42	6061 Aluminum w/XM-19 Cover Plate
Cask Shell & Cask Rails	Plane42	Type 304 (Elastic)
DSC/Cask Shell Springs	Combin39	N/A

**Table M.3.6-4
Material Properties Used in Normal Condition 32PT Basket Analyses**

Component	Material	Normal Condition Stress Analysis Material Properties ⁽²⁾	Evaluation Temperature ⁽¹⁾
Fuel Support Grid	1/4" Thick, Type XM-19 Stainless Steel	Elastic (Code Properties)	800°F (All conditions)
Solid Aluminum Transition Rails, R90 Cover Plates	1/4" Thick, Type XM-19 Stainless Steel	Elastic (Code Properties)	610°F/600°F (Vacuum Drying/Other)
Solid Aluminum Transition Rails, Aluminum Bodies	6061 Aluminum Alloy	Elastic ⁽³⁾	500°F/450°F (Blocked Vent / Other)

- Notes:
1. For the steel components, stress checks were performed at the enveloping temperatures listed. For the aluminum transition rails, stress checks were performed at temperatures corresponding to the maximum stress point. Temperatures listed are for the maximum stress points of the most highly loaded rail (the large R90 transition rail at the "bottom" of the basket).
 2. ASME Code properties for Type XM-19 and Type 304 Stainless Steels from Tables M.3.3-3 and M.3.3-2, respectively.
 3. Properties for 6061 Aluminum from Table M.3.3-5.

**Table M.3.6-5
Summary of Results for 32PT Basket Assembly Deadweight Analyses**

Vertical Deadweight

Component	Stress (Axial Compression)			Notes ⁽¹⁾
	Calculated	Allowable	Ratio	
Fuel Support Grid	.06 ksi	23.7 ksi	< .01	XM-19, 800°F
Aluminum Transition Rails	.02 ksi	4.2 ksi	< .01	6061 Al., ≈600°F

Notes: 1. For vacuum drying, the maximum transition rail temperature is less than 610°F. It occurs in the R90 rails and is localized at the point closest to the basket center, the average temperature is less than 600°F.

Horizontal Deadweight

Component	Stress Category	Stress Intensity		Stress Ratio	Notes
		Calculated	Allowable		
1-Piece R90 Transition Rails					
Fuel Support Grid	P _m	.57 ksi	28.2 ksi	.02	XM-19, 800°F
	P _m + P _b	2.72 ksi	42.3 ksi	.06	
	P _m + P _b + Q	7.41 ksi	84.6 ksi	.09	
Transition Rail Cover Plates	P _m	.30 ksi	28.2 ksi	.01	XM-19, 800°F
	P _m + P _b	2.50 ksi	42.3 ksi	.06	
	P _m + P _b + Q	2.50 ksi	84.6 ksi	.03	
6061 Aluminum Transition Rails	Maximum Stress	1.32 ksi	6.0 ksi	.22	Al. 6061, 450°F
3-Piece R90 Transition Rails					
Fuel Support Grid	P _m	.70 ksi	28.2 ksi	.02	XM-19, 800°F
	P _m + P _b	4.73 ksi	42.3 ksi	.11	
	P _m + P _b + Q	8.07 ksi	84.6 ksi	.10	
Transition Rail Cover Plates	P _m	.41 ksi	28.2 ksi	.01	XM-19, 800°F
	P _m + P _b	5.32 ksi	42.3 ksi	.13	
	P _m + P _b + Q	5.32 ksi	84.6 ksi	.06	
6061 Aluminum Transition Rails	Maximum Stress	1.72 ksi	6.0 ksi	.29	Al. 6061, 450°F

Table M.3.6-6
Summary of Results for 32PT Basket Assembly On-Site Handling (2.0g Loads)

Vertical Handling/Seismic

Component	Stress (Axial Compression)			Notes
	Calculated	Allowable	Ratio	
Fuel Support Grid	.11 ksi	23.7 ksi	< .01	XM-19, 800°F
Aluminum Transition Rails	.04 ksi	4.2 ksi	.01	6061 Al., 600°F

Horizontal/45° Handling/Seismic

Component	Stress	Stress Intensity		Stress	Notes
	Category	Calculated	Allowable	Ratio	
1-Piece R90 Transition Rails					
Fuel Support Grid	P_m	2.68 ksi	28.2 ksi	.10	XM-19, 800°F
	$P_m + P_b$	18.3 ksi	42.3 ksi	.43	
	$P_m + P_b + Q$	18.3 ksi	84.6 ksi	.22	
Transition Rail Cover Plates	P_m	2.19 ksi	28.2 ksi	.08	XM-19, 800°F
	$P_m + P_b$	11.1 ksi	42.3 ksi	.26	
	$P_m + P_b + Q$	11.1 ksi	84.6 ksi	.13	
6061 Aluminum Transition Rails	Maximum Stress	4.64 ksi	6.0 ksi	0.77	Al. 6061, 450°F
3-Piece R90 Transition Rails					
Fuel Support Grid	P_m	1.52ksi	28.2 ksi	.05	XM-19, 800°F
	$P_m + P_b$	20.7 ksi	42.3 ksi	.49	
	$P_m + P_b + Q$	20.7 ksi	84.6 ksi	.24	
Transition Rail Cover Plates	P_m	1.05 ksi	28.2 ksi	.04	XM-19, 800°F
	$P_m + P_b$	10.1 ksi	42.3 ksi	.24	
	$P_m + P_b + Q$	10.1 ksi	84.6 ksi	.12	
6061 Aluminum Transition Rails	Maximum stress	2.06 ksi	6.0 ksi	.56	Al. 6061, 450°F

Note: 1. For the steel components, stress checks were performed at the enveloping temperatures listed. For the aluminum transition rails, stress checks were performed at temperatures corresponding to the maximum stress point. Temperatures listed are for the maximum stress points of the most highly loaded rail (the large R90 transition rail at the "bottom" of the basket).

**Table M.3.6-7
32PT Basket Analyses Used to Determine On-Site Handling Loads**

Case	Resultant Load	Basket Assembly Configuration	Support Conditions
1	2g resultant load in the "vertical" orientation	32PT Basket Assembly with 1-piece R90 aluminum transition rails	HSM (Support Rails at ± 30)
2	2g resultant load in the "vertical" orientation	32PT Basket Assembly with 1-piece R90 aluminum transition rails	OS197 (Support Rails at $\pm 18.5^\circ$)
3	2g resultant load oriented 45° from bottom center	32PT Basket Assembly with 1-piece R90 aluminum transition rails	OS197 (Support Rails at $\pm 18.5^\circ$)
4	2.5g resultant load in the "vertical" orientation	32PT Basket Assembly with 3-piece R90 aluminum transition rails	HSM (Support Rails at ± 30)
5	2.5g resultant load in the "vertical" orientation	32PT Basket Assembly with 3-piece R90 aluminum transition rails	OS197 (Support Rails at $\pm 18.5^\circ$)
6	2.0g g resultant load oriented 45° from bottom center	32PT Basket Assembly with 3-piece R90 aluminum transition rails	OS197 (Support Rails at $\pm 18.5^\circ$)

**Table M.3.6-8
NUHOMS® Off-Normal Operating Loading Identification**

Load Type	AFFECTED COMPONENT				
	DSC Shell Assembly	DSC Basket	DSC Support Structure	Reinforced Concrete HSM	On-site TC
Dead Weight	X	X	X	X	X
Internal/External Pressure	X				
Off-Normal Thermal	X	X	X	X	X
Off-Normal Handling	X	X	X	X	X

DELETED

Figure M.3.6-1
32PT Basket Model with Steel Transition Rails

DELETED

**Figure M.3.6-2
32PT Basket Model with Steel Transition Rails**

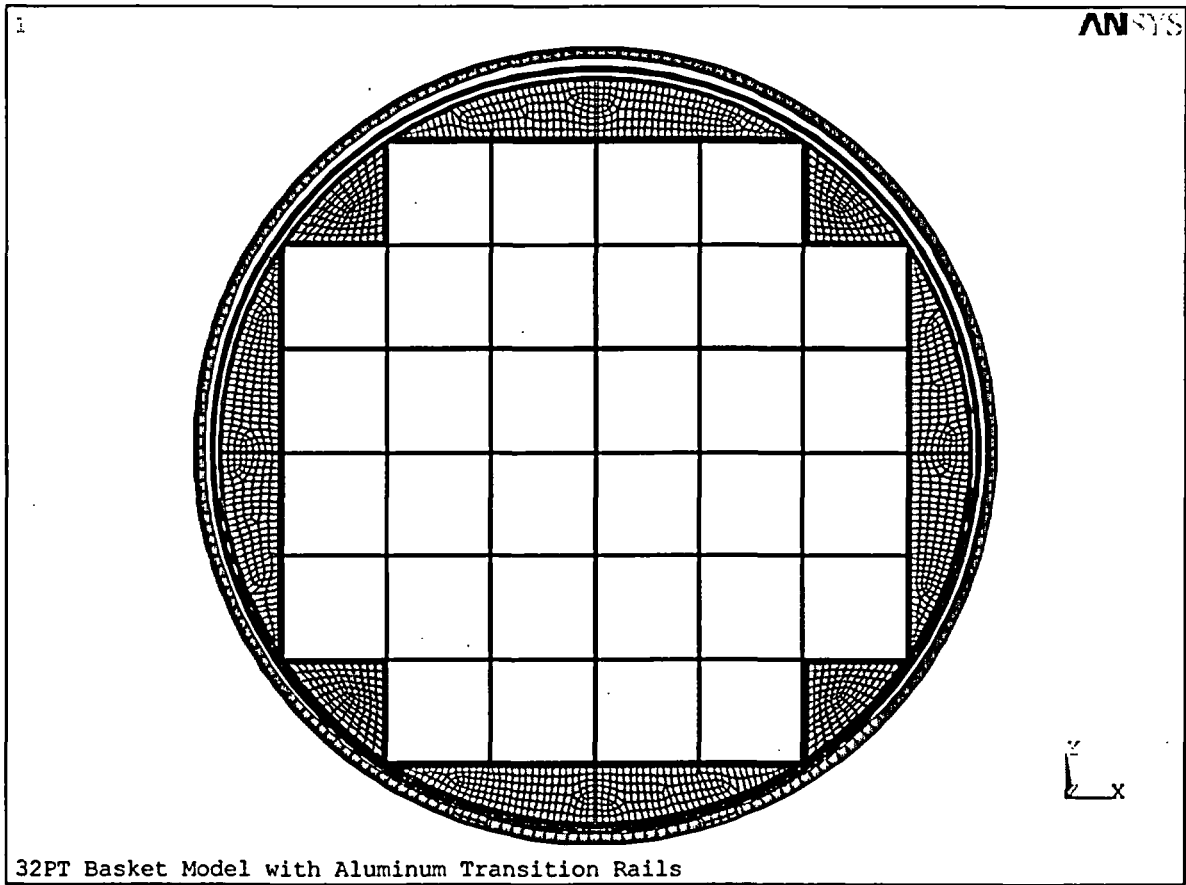


Figure M.3.6-3
32PT Basket Model with Aluminum Transition Rails (1-Piece R90)

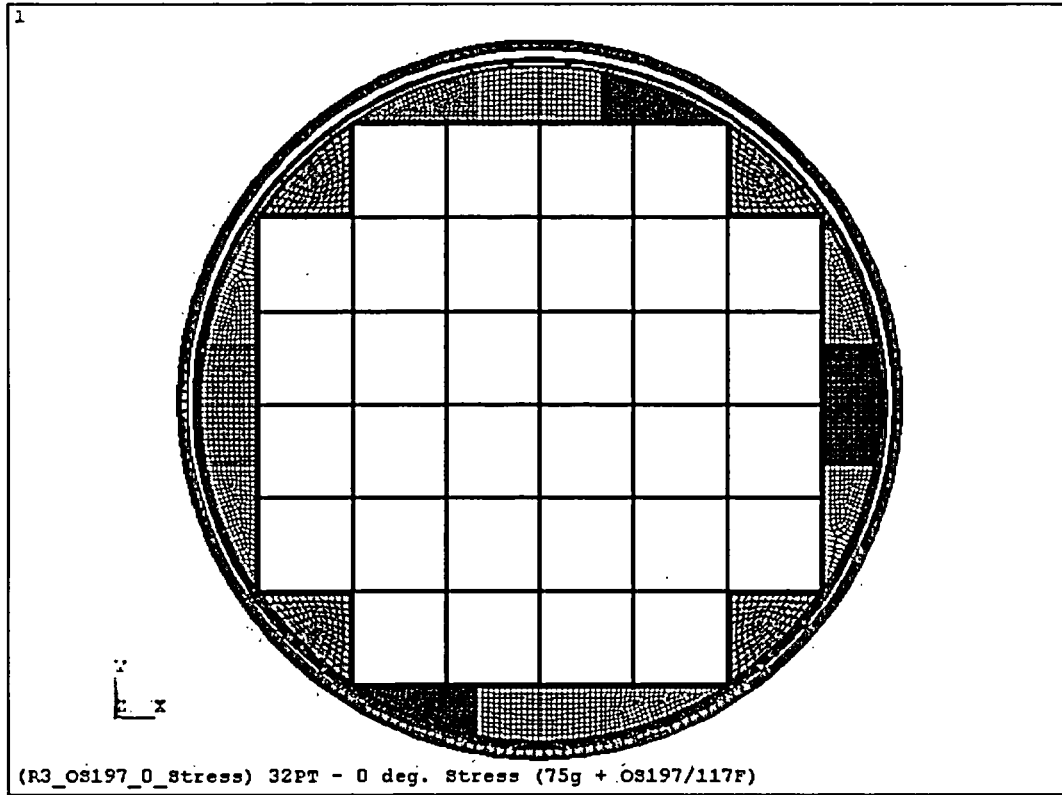


Figure M.3.6-3A
32PT Basket Model with Aluminum Transition Rails (3-Piece R90)

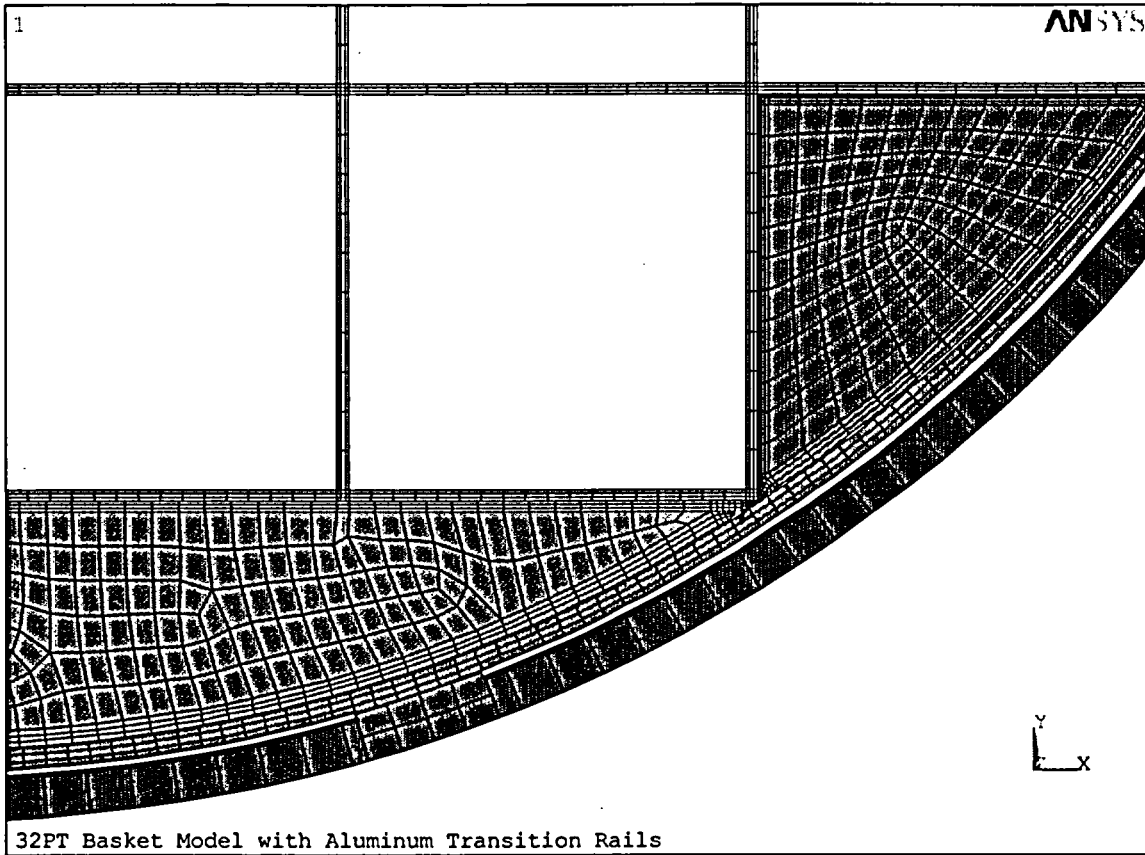


Figure M.3.6-4
32PT Basket Model with Aluminum Transition Rails (1-Piece R90)

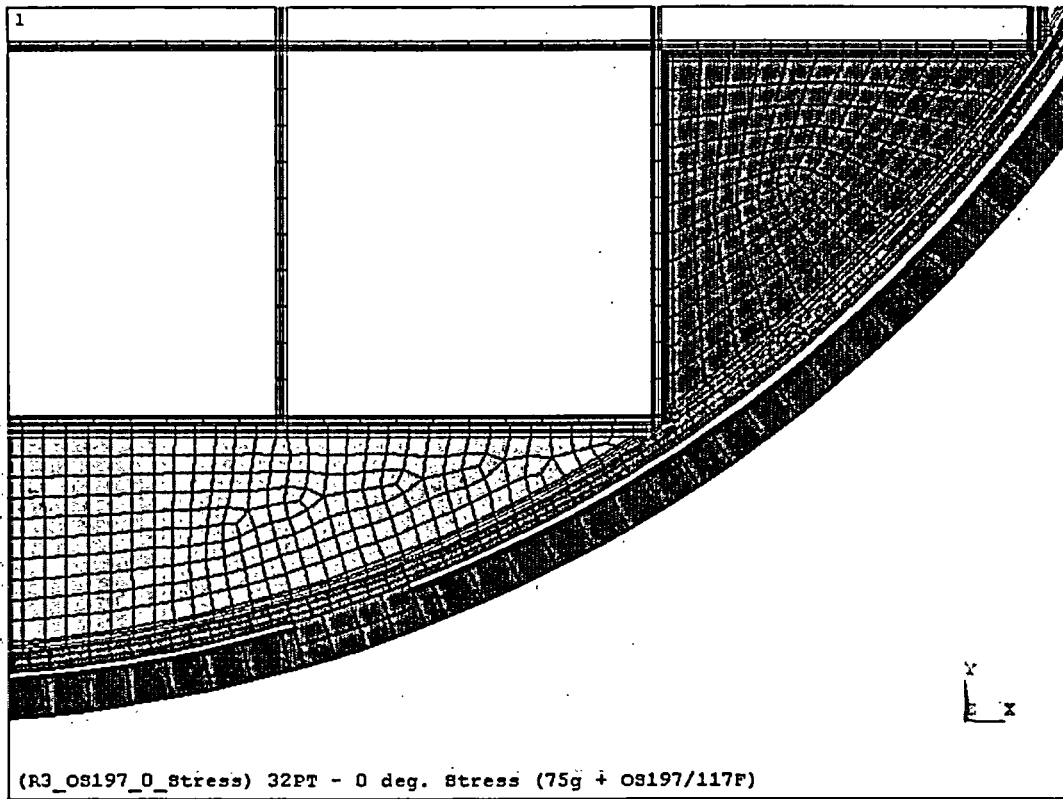


Figure M.3.6-4A
32PT Basket Model with Aluminum Transition Rails (3-Piece R90)

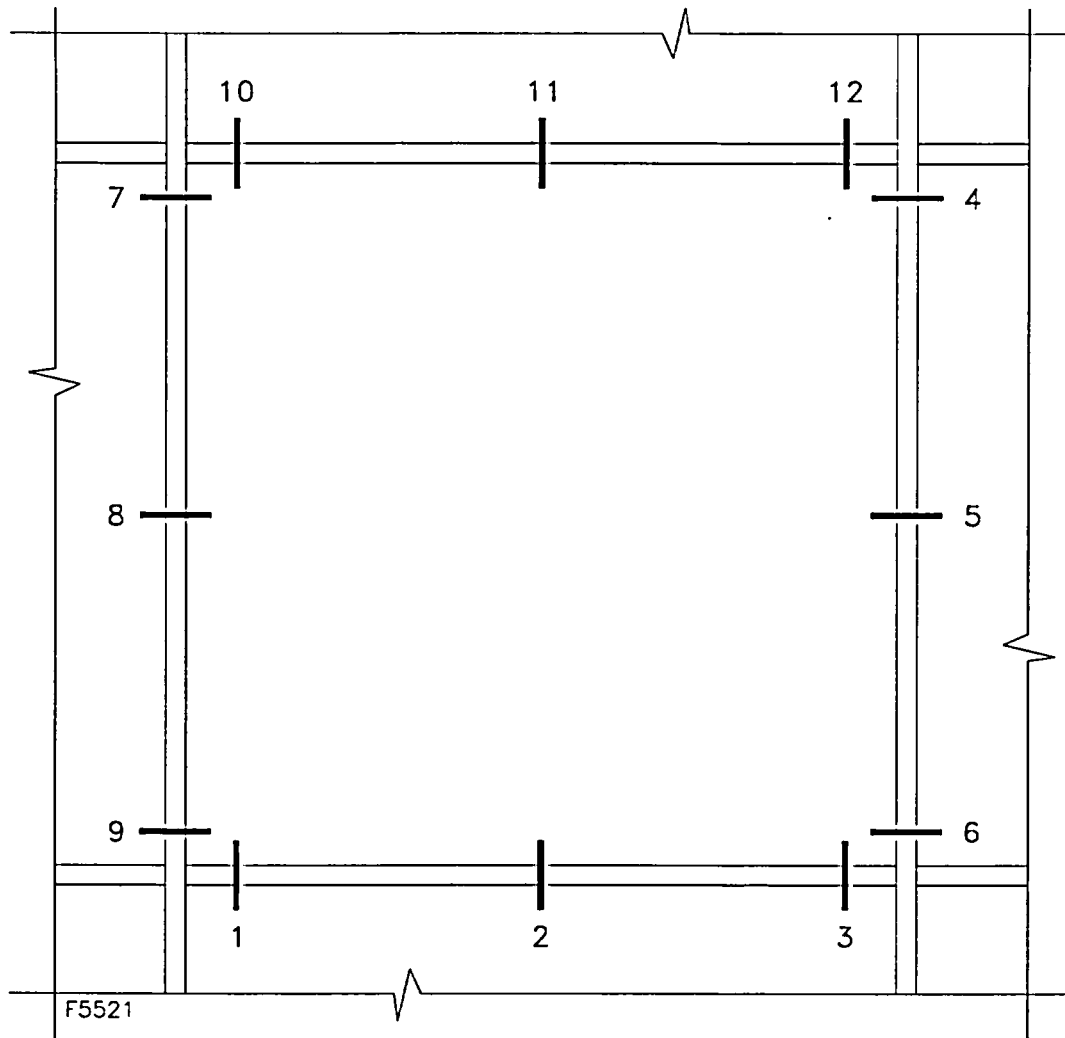


Figure M.3.6-5
Location and Numbering of Stress Cuts for 32PT Basket Analyses

DELETED

Figure M.3.6-6
Deadweight Stress Intensity, 32PT Basket with Steel Transition Rails
(Support Rails at $\pm 18.5^\circ$)

DELETED

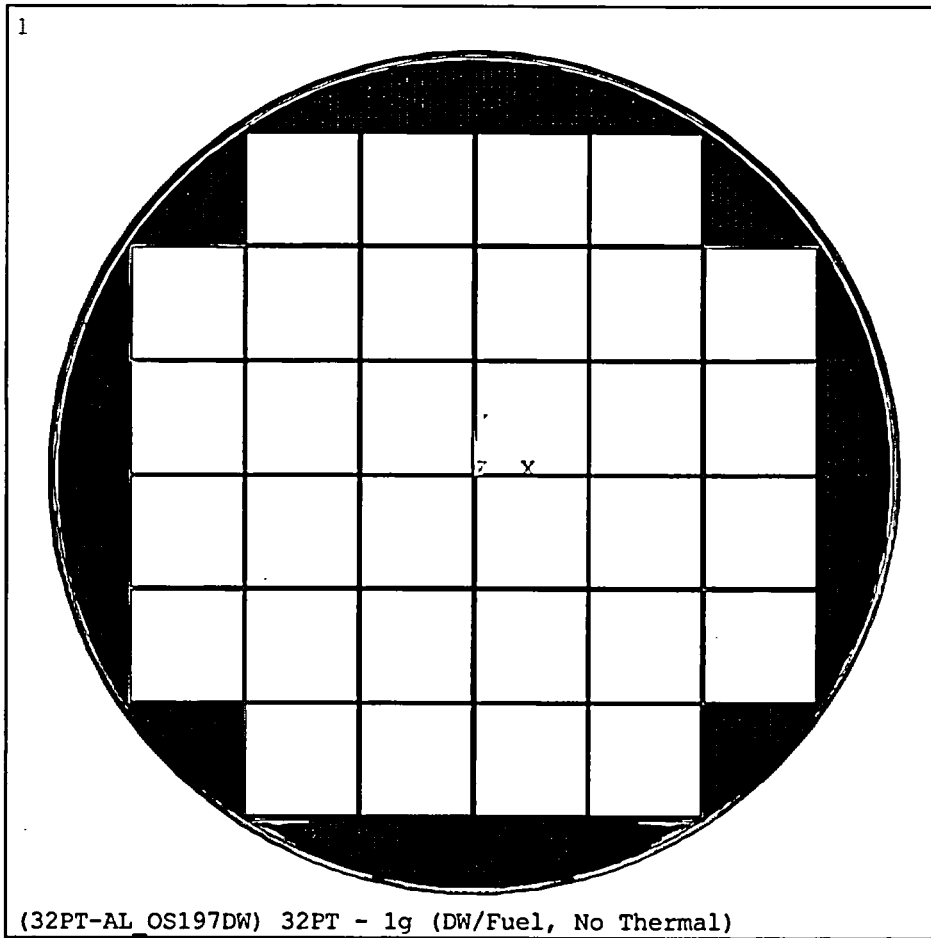
Figure M.3.6-7
Deadweight + Thermal Stress Intensity, 32PT Basket with Steel Transition Rails
(Support Rails at $\pm 18.5^\circ$)

DELETED

Figure M.3.6-8
Deadweight Stress Intensity, 32PT Basket with Steel Transition Rails
(Support Rails at $\pm 30^\circ$)

DELETED

Figure M.3.6-9
Deadweight + Thermal Stress Intensity, 32PT Basket with Steel Transition Rails
(Support Rails at $\pm 30^\circ$)



ANSYS 5.6.2
 JUN 6 2001
 17:34:08
 PLOT NO. 1
 NODAL SOLUTION
 STEP=3
 SUB =6
 TIME=.75
 SINT (AVG)
 DMX =.141006
 SMN =.013127
 SMX =4380
 .013127
 486.638
 973.263
 1460
 1947
 2433
 2920
 3406
 3893
 4380

Figure M.3.6-10
Deadweight Stress Intensity, 32PT Basket with Aluminum Transition Rails (1- Piece R90)
(Support Rails at $\pm 18.5^\circ$)

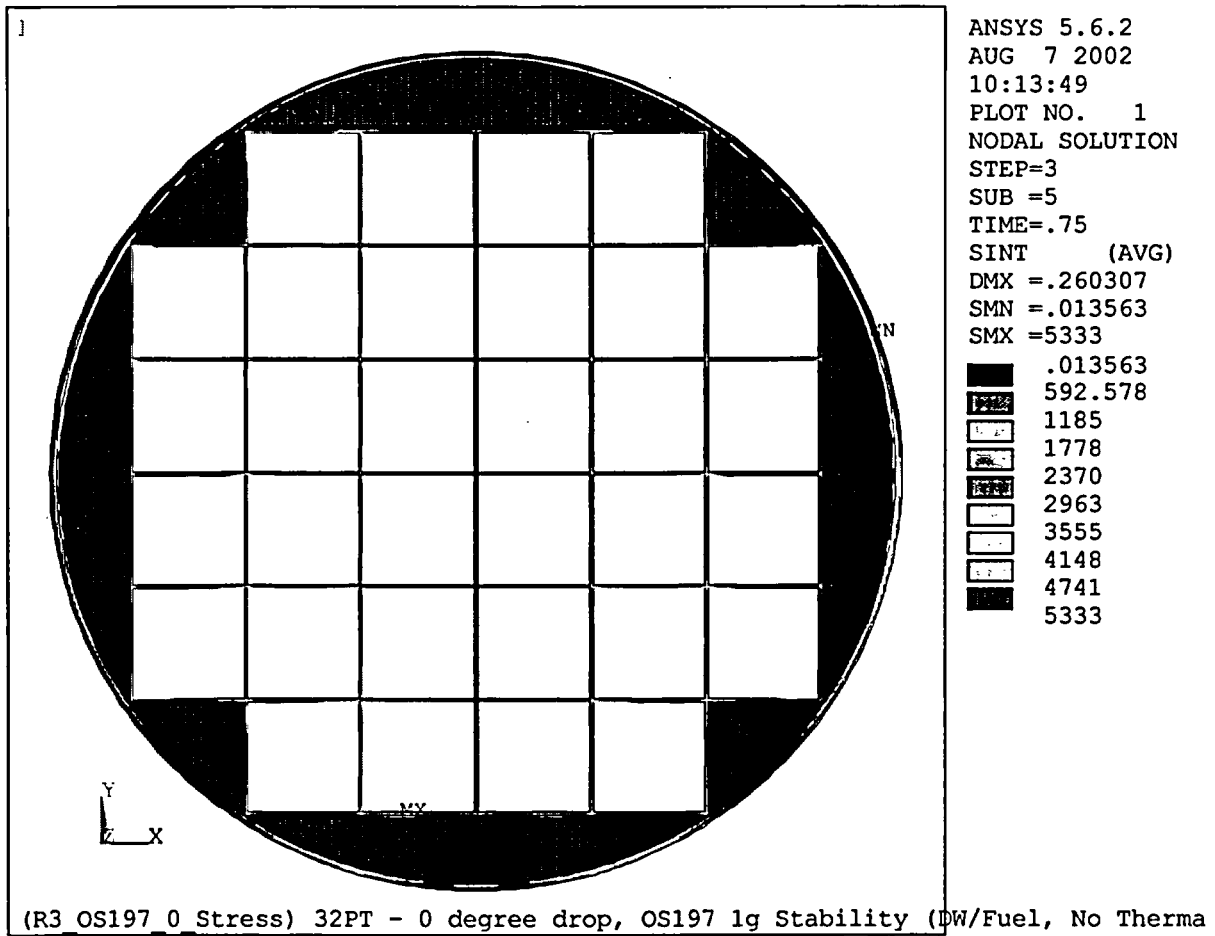
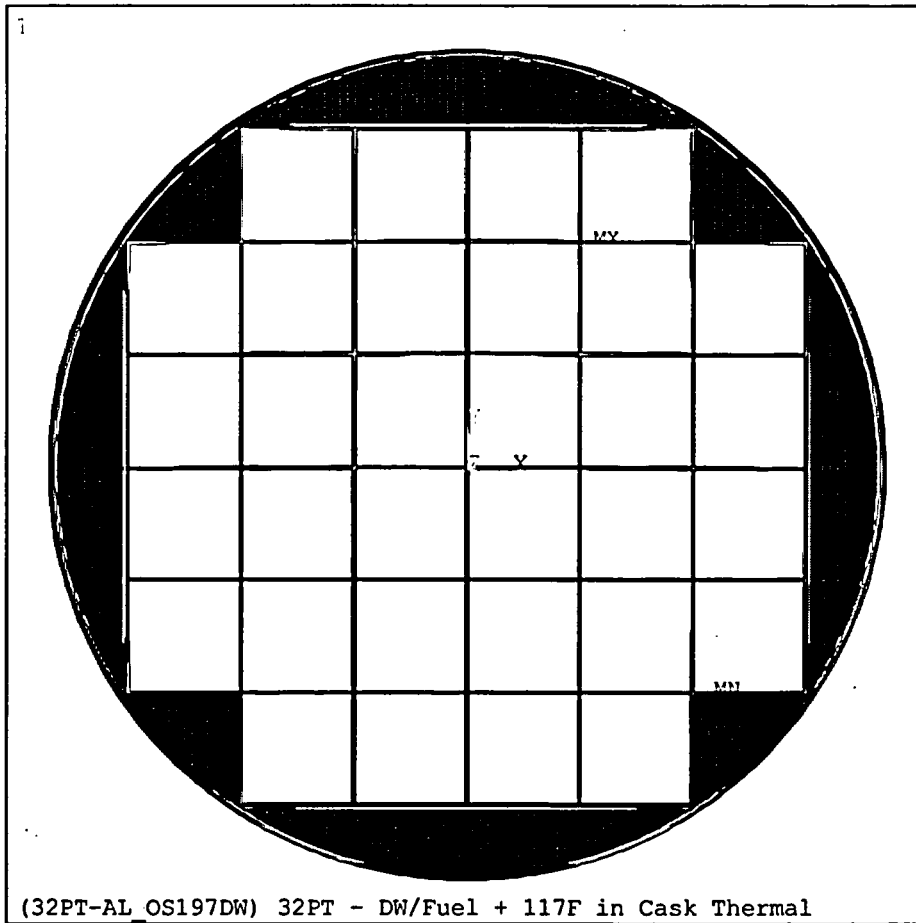
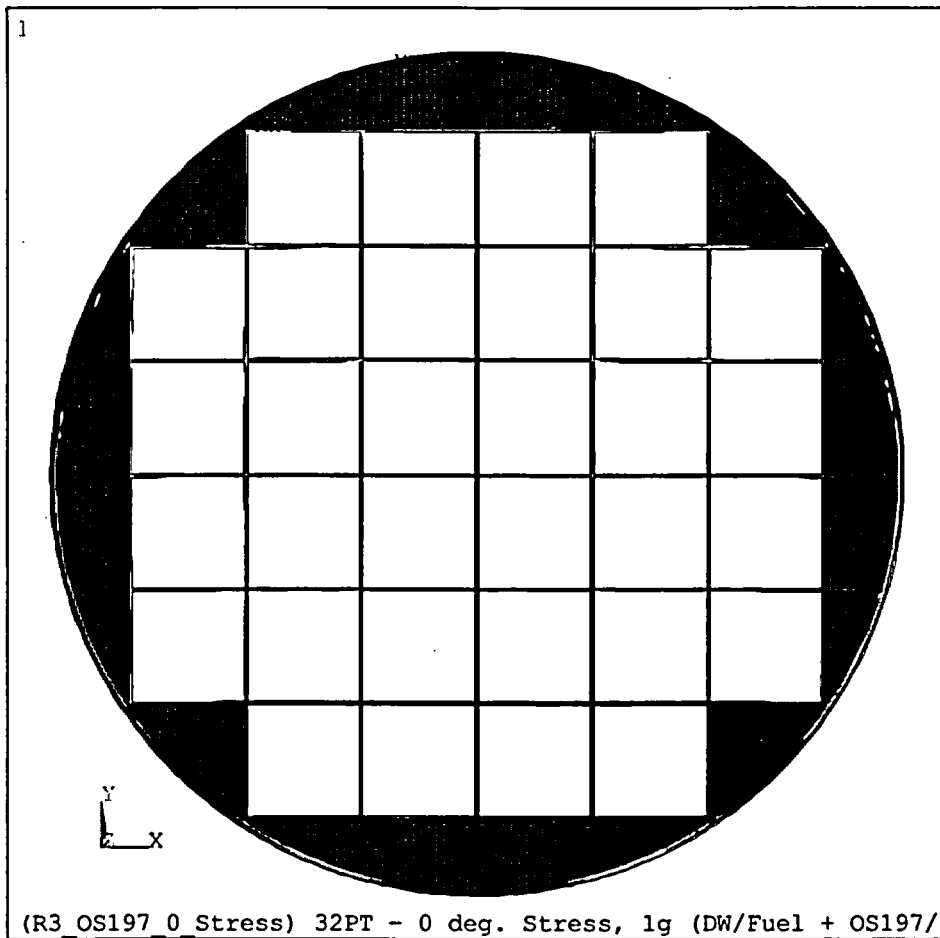


Figure M.3.6-10A
Deadweight Stress Intensity, 32PT Basket with Aluminum Transition Rails (3-Piece R90)
(Support Rails at $\pm 18.5^\circ$)



ANSYS 5.6.2
 JUN 6 2001
 17:35:01
 PLOT NO. 11
 NODAL SOLUTION
 STEP=5
 SUB =8
 TIME=1
 SINT (AVG)
 DMX =.335374
 SMN =2.901
 SMX =6401
 2.901
 713.85
 1425
 2136
 2847
 3558
 4269
 4980
 5690
 6401

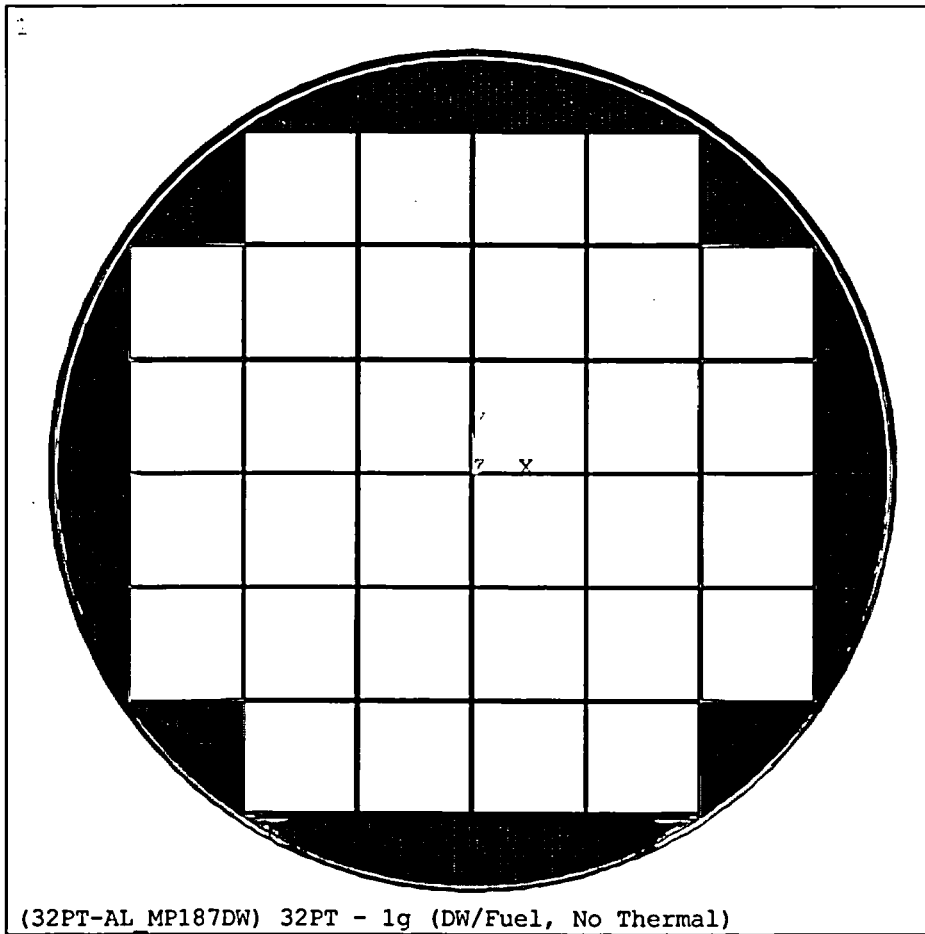
Figure M.3.6-11
 Deadweight + Thermal Stress Intensity, 32PT Basket with Aluminum Transition Rails
 (1-Piece R90) (Support Rails at $\pm 18.5^\circ$)



ANSYS 5.6.2
 AUG 7 2002
 10:14:52
 PLOT NO. 32
 NODAL SOLUTION
 STEP=5
 SUB =9
 TIME=1
 SINT (AVG)
 DMX =.339962
 SMN =.717265
 SMX =7522

■	.717265
■	836.456
■	1672
■	2508
■	3344
■	4179
■	5015
■	5851
■	6687
■	7522

Figure M.3.6-11A
Deadweight + Thermal Stress Intensity, 32PT Basket with Aluminum Transition Rails
(3-Piece R90) (Support Rails at ±18.5°)



ANSYS 5.6.2
 JUN 6 2001
 17:31:05
 PLOT NO. 1
 NODAL SOLUTION
 STEP=3
 SUB =6
 TIME=.75
 SINT (AVG)
 DMX =.066957
 SMN =.013436
 SMX =4477

■	.013436
■	497.459
■	994.905
■	1492
■	1990
■	2487
■	2985
■	3482
■	3980
■	4477

Figure M.3.6-12
Deadweight Stress Intensity, 32PT Basket with Aluminum Transition Rails
(1-Piece R90) (Support Rails at $\pm 30^\circ$)

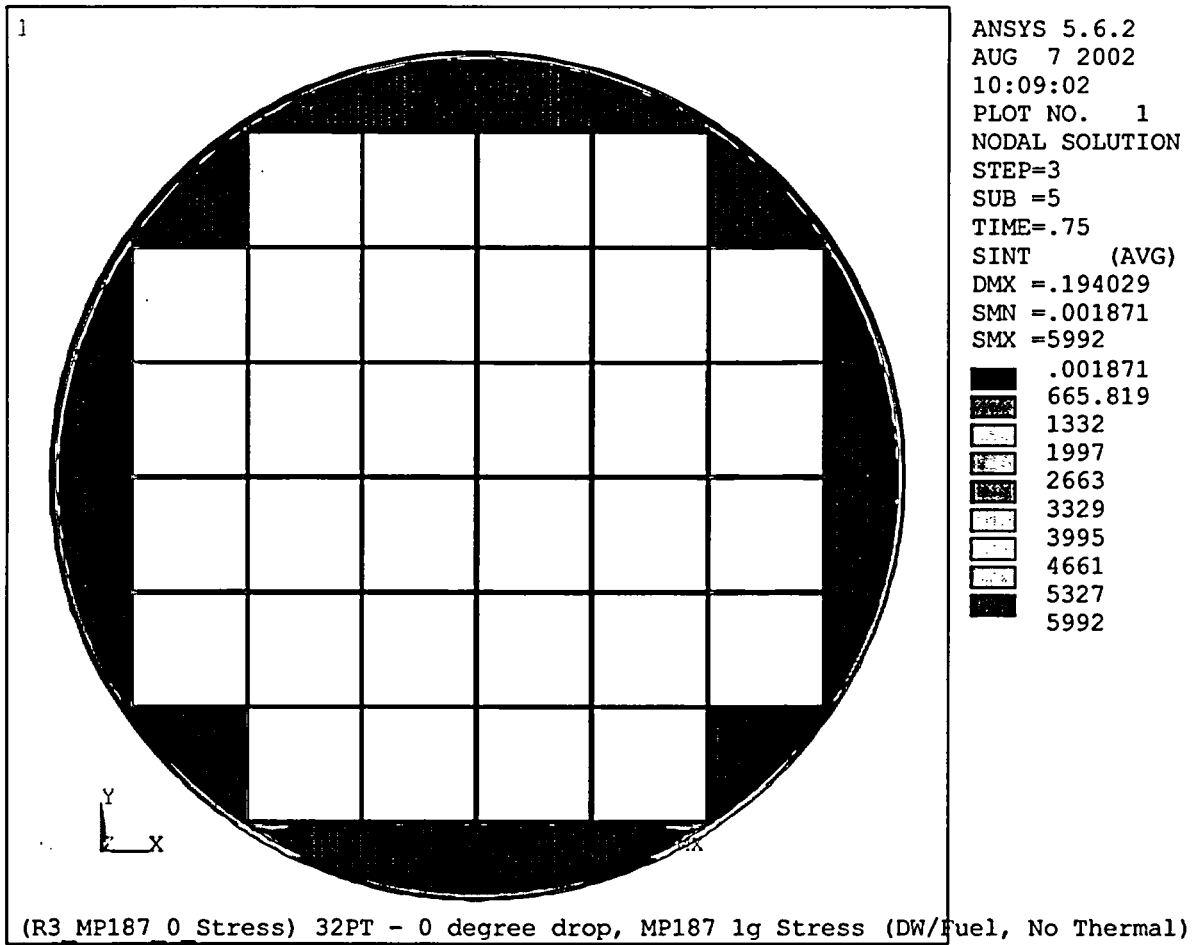
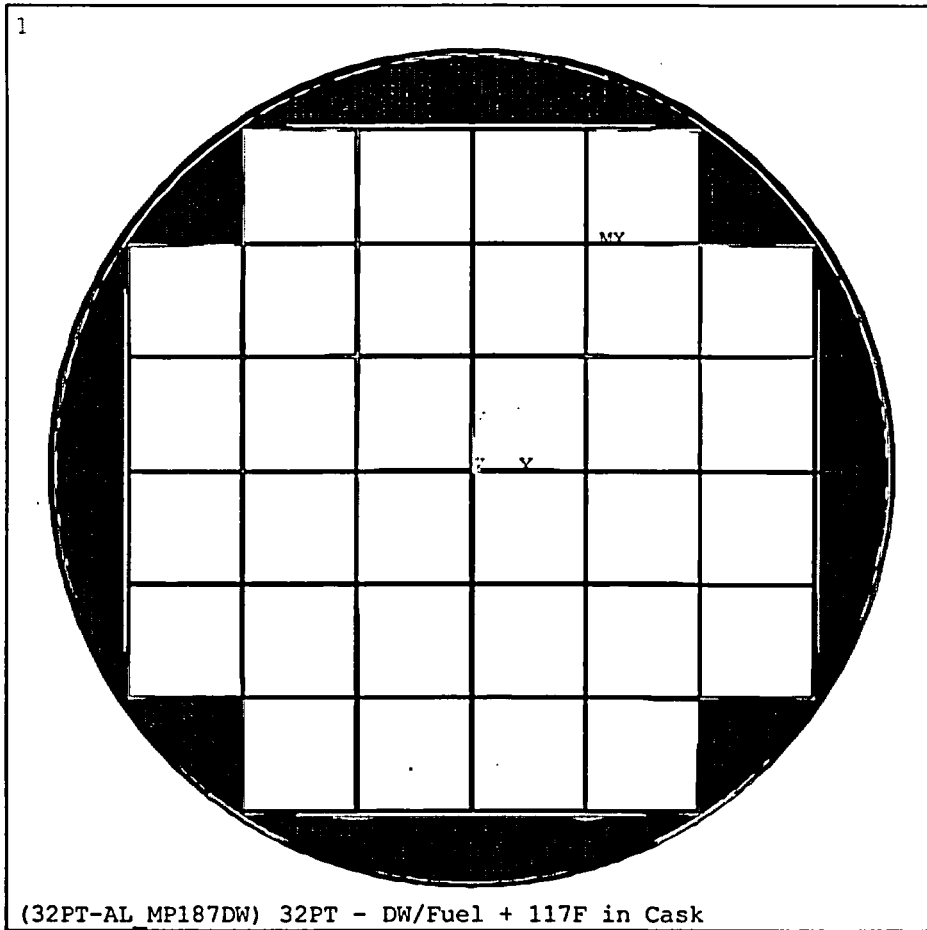


Figure M.3.6-12A
Deadweight Stress Intensity, 32PT Basket with Aluminum Transition Rails (3-Piece R90)
(Support Rails at $\pm 30^\circ$)



ANSYS 5.6.2
 JUN 6 2001
 17:31:59
 PLOT NO. 11
 NODAL SOLUTION
 STEP=6
 SUB =8
 TIME=1
 SINT (AVG)
 DMX =.339001
 SMN =3.013
 SMX =6016

■	3.013
■	671.168
■	1339
■	2007
■	2676
■	3344
■	4012
■	4680
■	5348
■	6016

Figure M.3.6-13
Deadweight +Thermal Stress Intensity, 32PT Basket with Aluminum Transition Rails
(1-Piece R90) (Support Rails at $\pm 30^\circ$)

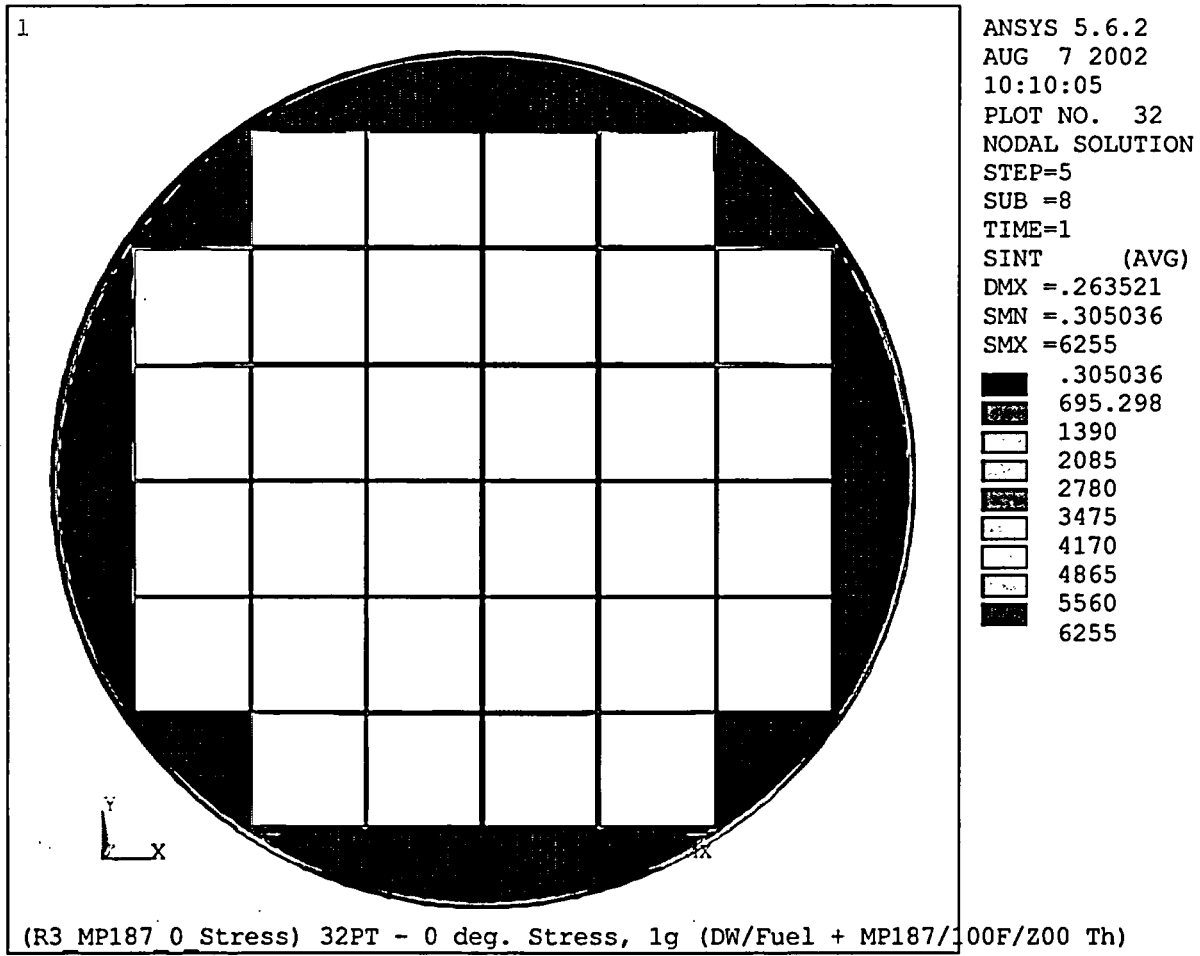


Figure M.3.6-13A
Deadweight+ Thermal Stress Intensity, 32PT Basket with Aluminum Rails (3-Piece R90)
(Support Rails at $\pm 30^\circ$)

M.3.7 Structural Analysis (Accidents)

The design basis accident events specified by ANSI/ANS 57.9-1984, and other credible accidents postulated to affect the normal safe operation of the standardized NUHOMS[®] System are addressed in this section. Analyses are provided for a range of hypothetical accidents, including those with the potential to result in an annual dose greater than 25 mrem outside the owner controlled area in accordance with 10CFR72. The postulated accidents considered in the analysis of the 32PT DSC and the associated NUHOMS[®] components affected by each accident condition are the same as those shown in Table 8.2-1.

In the following sections, each accident condition is analyzed to demonstrate that the requirements of 10CFR72.122 are met and that adequate safety margins exist for the standardized NUHOMS[®] System design. The resulting accident condition stresses in the NUHOMS[®] System components are evaluated and compared with the applicable code limits set forth in Section 3.2. Where appropriate, these accident condition stresses are combined with those of normal operating loads in accordance with the load combination definitions in Tables 3.2-5, 3.2-6, and 3.2-7. Load combination results for the HSM, DSC, and TC and the evaluation for fatigue effects are presented in Section M.3.7.10.

The postulated accident conditions addressed in this section include:

- Reduced HSM air inlet and outlet shielding (M.3.7.1),
- Tornado winds and tornado generated missiles (M.3.7.2),
- Design basis earthquake (M.3.7.3),
- Design basis flood (M.3.7.4),
- Accidental TC drop with loss of neutron shield (M.3.7.5),
- Lightning effects (M.3.7.6),
- Debris blockage of HSM air inlet and outlet opening (M.3.7.7),
- Postulated DSC leakage (M.3.7.8), and
- Pressurization due to fuel cladding failure within the DSC (M.3.7.9).

M.3.7.1 Reduced HSM Air Inlet and Outlet Shielding

This postulated accident is the partial loss of shielding for the HSM air inlet and outlet vents provided by the adjacent HSM. All other components of the NUHOMS[®] System are assumed to be functioning normally.

There are no structural consequences that affect the safe operation of the NUHOMS[®] System resulting from the separation of the HSMs. The thermal effects of this accident results from the

blockage of HSM air inlet and outlet openings on the HSM side walls in contact with each other. This would block the ventilation air flow provided to the HSMs in contact from these inlet and outlet openings. The increase in spacing between the HSM on the opposite side from 6 inches to 12 inches will reduce the ventilation air flow resistance through the air inlet and outlet openings on these side walls, which will partially compensate the ventilation reduction from the blocked side. However, the effect on the DSC, HSM and fuel temperatures is bounded by the complete blockage of air inlet and outlet openings described in Section M.3.7.7.

M.3.7.2 Tornado Winds/Tornado Missile

The applicable design parameters for the design basis tornado (DBT) are specified in Section 3.2.1. The determination of the tornado wind and tornado missile loads acting on the HSM are detailed in Section 3.2.2. The end modules of an array utilize shield walls to resist tornado wind and missile loads. For this conservative generic analysis, the tornado loads are assumed to act on a single free-standing HSM (with two end shield walls and a rear shield wall). This case conservatively envelopes the effects of wind on an HSM array. The TC is also designed for the tornado wind and tornado missile loads defined in Section 3.2.2. Thus, the requirements of 10CFR72.122 are met.

For DBT wind and missile effects, the HSM is more stable when loaded with a heavier DSC since the overturning moment is not a function of the DSC weight while the resisting moment increases with the increased payload. The DSC weight does not have any effect on HSM sliding stability, since the weight terms on either side of the sliding equation presented in Section 8.2.2 cancel out. Since the weight of the NUHOMS[®]-32PT DSC is bounded by the DSC weights used in Section 8.2.2, there is no change to the structural evaluation of the HSM for DBT winds and missile effects.

M.3.7.3 Earthquake

As discussed in Section 3.2.3 and as shown in Figure 8.2-2, the peak horizontal ground acceleration of 0.25g and the peak vertical ground acceleration of 0.17g are utilized for the design basis seismic analysis of the NUHOMS[®] components. Based on NRC Reg. Guide 1.61 [3.15], a damping value of three percent is used for the DSC seismic analysis. Similarly, a damping value of seven percent for DSC support steel and concrete is utilized for the HSM. An evaluation of the frequency content of the loaded HSM is performed to determine the dynamic amplification factors associated with the design basis seismic response spectra for the NUHOMS[®] HSM and DSC. Since the weight of the NUHOMS[®]-32PT DSC is bounded by the DSC weights used in Section 8, there is no change to the seismic response of the HSM.

M.3.7.3.1 DSC Seismic Evaluation

The maximum calculated seismic accelerations for the DSC inside the HSM are 0.40g horizontally and 0.17g vertically. An analysis using these seismic loads shows that the DSC will not lift off the support rails inside the HSM. The resulting stresses in the DSC shell due to vertical and horizontal seismic loads are also determined and included in the appropriate load combinations. The seismic evaluation of the DSC is described in the paragraphs that follow.

The DSC basket and support structure are also subjected to the calculated DSC seismic reaction loads as discussed in Sections M.3.7.3.2 and M.3.7.3.4, respectively.

M.3.7.3.1.1 DSC Natural Frequency Calculation

Two natural frequencies, each associated with a distinct mode of vibration of the DSC are evaluated. These two modes are the DSC shell cross-sectional ovaling mode and the mode with the DSC shell bending as a beam.

M.3.7.3.1.1.1 DSC Shell Ovaling Mode

The natural frequency for the DSC shell ovaling mode is determined from the Blevins [3.16] correlation as follows.

$$f = \frac{\lambda_i}{2\pi R} \sqrt{\frac{E}{\mu(1-\nu^2)}} \quad (\text{Blevins, Table 12-1, Case 3})$$

where: $R = 33.34$ in, DSC mean radius,

$E = 26.5 \times 10^6$ psi, Young's Modulus,

$\nu = 0.3$, Poisson's ratio,

$$\lambda_i = \lambda_i = 0.289 \frac{t}{R} \frac{i(i^2-1)}{\sqrt{1+i^2}},$$

$t = 0.5$ in., Thickness of DSC shell, and

$\mu = 0.288$ /g lb/in³, Steel mass density.

The lowest natural frequency corresponds to the case when $i = 2$.

Hence: $\lambda_2 = 0.0116$ sec.

Substituting gives: $f = 10.9$ Hertz

The resulting spectral accelerations in the horizontal and vertical directions for this DSC ovaling frequency are less than 1.0g and 0.68g, respectively.

M.3.7.3.1.1.2 DSC Beam Bending Mode

The DSC shell is conservatively assumed to be simply supported at the two ends of the DSC. The beam bending mode natural frequency of the DSC was calculated from the Blevins correlation:

$$f_i = \frac{\lambda_i^2}{2\pi L^2} \sqrt{\frac{EI}{m}} \quad (\text{Blevins, Table 8.1, Case 5})$$

where: $E = 26.5E6$ psi, Young's Modulus,
 $I = 58,400$ in.⁴, DSC moment of inertia,
 $L = 192.55$ in., Total length of DSC,
 $m = 101,130/192.55 = 525/g$ lb/in, and
 $\lambda = i\pi$; for lowest natural frequency, $i = 1$.

Substituting yields: $f_1 = 45.1$ Hertz.

The DSC spectral accelerations at this frequency correspond to the zero period acceleration. These seismic accelerations are bounded by those of the ovaling mode frequency that are used in the subsequent stress analysis of the DSC shell.

M.3.7.3.1.2 DSC Seismic Stress Analysis

With the DSC conservatively assumed to be resting on a single support rail inside the HSM, the stresses induced in the DSC shell are calculated due to the 1.0g horizontal and 0.68g vertical seismic accelerations, and increased by a factor of 1.5 to account for the effects of possible multimode excitation. Thus, the DSC shell is qualified to seismic accelerations of 1.5g horizontal and 1.0g vertical. The DSC shell stresses obtained from the analyses of vertical and horizontal seismic loads are summed absolutely. See Table M.3.7-9 for the Level C seismic stress evaluation of the NUHOMS[®]-32PT DSC. The seismic load combination includes deadweight + pressure + 1.5g horizontal and 1g vertical (load combinations HSM-7 and HSM-8 as shown in Table M.2-15).

As stated, in Section 4.2.3.2, an axial retainer is included in the design of the DSC support system inside the HSM to prevent sliding of the DSC in the axial direction during a postulated seismic event. The stresses induced in the DSC shell and bottom cover plate due to the restraining action of this retainer for a horizontal seismic load, applied along the axis of the DSC, are included in the seismic response evaluation of the DSC shell assembly.

The stability of the DSC against lifting off one of the support rails during a seismic event is evaluated by performing a rigid body analysis, using the 0.40g horizontal and 0.17g vertical input accelerations. The factor of 1.5 used in the DSC analysis to account for multimode behavior need not be included in the seismic accelerations for this analysis, as the potential for lift off is due to rigid body motion, and no frequency content effects are associated with this action. The horizontal equivalent static acceleration of 0.40g is applied laterally to the center of gravity of the DSC. The point of rigid body rotation of the DSC is assumed to be the center of the support rail, as shown in Figure M.3.7-1. The applied moment acting on the DSC is calculated by summing the overturning moments. The stabilizing moment, acting to oppose the applied moment, is calculated by subtracting the effects of the upward vertical seismic acceleration of 0.17g from the total weight of the DSC and summing moments at the support rail. Since the stabilizing moment calculated below is greater than that of the applied moment, the DSC will not lift off the DSC support structure inside the HSM.

Referring to Figure M.3.7-1, the factor of safety associated with DSC lift-off is calculated as follows:

$$M_{am} = yF_H,$$

and $M_{sm} = (F_{v1} - F_{v2})x.$

where: M_{am} = the applied seismic moment, and

$$M_{sm} = \text{the stabilizing moment}$$

All other variables are defined in Figure M.3.7-1.

Substituting yields: $M_{am} = 1177.1 \text{ K-in.}$

and $M_{sm} = 1410.2 \text{ K-in.}$

Thus, the factor of safety (SF) against DSC lift off from the DSC support rails inside the HSM obtained from this bounding analysis is:

$$SF = \frac{M_{sm}}{M_{am}} = 1.20$$

M.3.7.3.2 Basket Seismic Evaluation

Seismic loads on the 32PT basket are enveloped by the 2.0g loads used for the on-site handling evaluation described in Section M.3.6. Therefore, based on the following considerations, specific qualification/evaluation for seismic loads is not required for the 32PT basket assembly:

- seismic loads are enveloped by the on-site handling loads evaluated in Section M.3.6.1.3.2(E).
- the handling load evaluation is performed using Service Level A allowables, while seismic loads are classified as Service Level C loads.

Therefore, the qualification for on-site handling in Section M.3.6.1.3.2(E) also demonstrates qualification for seismic loading and no additional evaluation is required.

M.3.7.3.3 HSM Seismic Evaluation

The weight of the NUHOMS[®]-32PT DSC is bounded by the DSC weight used in Section 8.2.3.2(B). Therefore, there is no change to the HSM seismic evaluation.

M.3.7.3.4 DSC Support Structure Seismic Evaluation

The weight of the NUHOMS[®]-32PT DSC is bounded by the DSC weight used in Section 8.2.3.2(C). Therefore, there is no change to the DSC support structure seismic evaluation.

M.3.7.3.5 DSC Axial Retainer Seismic Evaluation

The weight of the NUHOMS®-32PT DSC is bounded by the DSC weight used in Section 8.2.3.2(C). Therefore, there is no change to the DSC Axial Retainer seismic evaluation.

M.3.7.3.6 TC Seismic Evaluation

The effects of a seismic event occurring when a loaded NUHOMS®-24P DSC is resting inside the TC are described in Section 8.2.3.2(D). The stabilizing moment to prevent overturning of the cask/trailer assembly due to the 0.25g horizontal and 0.17g vertical seismic ground accelerations is calculated and compared to the dead weight stabilizing moment. The results of this analysis show that there is a factor of safety of at least 2.0 against overturning that ensures that the cask/trailer assembly has sufficient margin for the design basis seismic loading. Since the weight of the NUHOMS®-32PT DSC is bounded by the DSC weights used in Section 8.2.3, and the TC was evaluated using peak spectrum amplification factors (See Section 8.2.3.2D) this factor of safety against overturning due to seismic remains bounding for the NUHOMS®-32PT DSC.

M.3.7.4 Flood

Since the source of flooding is site specific, the exact source, or quantity of flood water, should be established by the licensee. However, for this generic evaluation of the 32PT DSC and HSM, bounding flooding conditions are specified that envelop those that are postulated for most plant sites. As described in Section 3.2, the design basis flooding load is specified as a 50 foot static head of water and a maximum flow velocity of 15 feet per second. Each licensee should confirm that this represents a bounding design basis for their specific ISFSI site.

M.3.7.4.1 HSM Flooding Analysis

For flooding effects, the HSM is more stable when loaded with a heavier DSC since the overturning moment is not a function of the DSC weight while the resisting moment increases with the increased payload. Since the weight of the NUHOMS®-32PT DSC is bounded by the DSC weights used in Section 8.2.4, there is no change to the HSM flooding analysis.

M.3.7.4.2 DSC Flooding Analyses

The DSC is evaluated for the design basis fifty foot hydrostatic head of water producing external pressure on the DSC shell and outer cover plates. To conservatively determine design margin which exists for this condition, the maximum allowable external pressure on the DSC shell is calculated for Service Level A stresses using the methodology presented in NB-3133.3 of the ASME Code [3.1]. The resulting allowable pressure of 39.7 psi is 1.8 times the maximum external pressure of 21.7 psi due to the postulated fifty foot flood height. This demonstrates stability of the DSC under the worst case external pressure due to flooding.

The DSC shell stresses for the postulated flood condition are determined using the ANSYS analytical model shown in Figure 8.1-14a and Figure 8.1-14b. The 21.7 psig external pressure is applied to the model as a uniform pressure on the outer surfaces of the top cover plate, DSC shell and bottom cover plate. The maximum DSC shell primary membrane plus bending stress

intensity for the 21.7 psi external pressure is 3.00 ksi which is considerably less than the Service Level C allowable primary membrane plus bending stress of 32.6 ksi. The maximum primary membrane plus bending stress in the flat heads of the DSC occurs in the inner bottom cover plate. The maximum primary membrane plus bending stress in the inner bottom cover plate is 1.54 ksi. This value is considerably less than the ASME Service Level C allowable of 32.6 ksi for primary membrane plus bending. These stresses are combined using the load combinations shown in Table M.2-15.

M.3.7.5 Accidental Cask Drop

This section addresses the structural integrity of the standardized NUHOMS[®] on-site TC, the DSC and its internal basket assembly when subjected to postulated cask drop accident conditions.

Cask drop evaluations include the following:

- DSC Shell Assembly (M.3.7.5.2),
- Basket Assembly (M.3.7.5.3),
- On-Site TC (M.3.7.5.4), and
- Loss of the TC Neutron Shield (M.3.7.5.5).

The DSC shell assembly, TC, and loss of TC neutron shield evaluations are based on the approaches and results presented in Section 8.2. The 32PT DSC basket assembly cask drop evaluation is presented in more detail since the 32PT basket assembly is a new design.

A short discussion of the effect of the NUHOMS[®]-32PT DSC on the transfer operation, accident scenario and load definition is presented in Section M.3.7.5.1.

M.3.7.5.1 General Discussion

Cask Handling and Transfer Operation

Various TC drop scenarios have been evaluated in Section 8.2.5. The NUHOMS[®]-32PT DSC is heavier than the NUHOMS[®]-24P DSC. Therefore, the expected g loads for the postulated drop accidents would be lower. However, for conservatism, the g loads used for the NUHOMS[®]-24P analyses in Section 8.2.5 are also used for the NUHOMS[®]-32PT DSC analyses.

Cask Drop Accident Scenarios

In spite of the incredible nature of any scenario that could lead to a drop accident for the TC, a conservative range of drop scenarios are developed and evaluated. These bounding scenarios assure that the integrity of the DSC and spent fuel cladding is not compromised. Analyses of these scenarios demonstrate that the TC will maintain the structural integrity of the DSC pressure containment boundary. Therefore, there is no potential for a release of radioactive materials to the environment due to a cask drop. The range of drop scenarios conservatively selected for design are:

1. A horizontal side drop from a height of 80 inches.
2. A vertical end drop from a height of 80 inches onto the top or bottom of the TC (two cases). Vertical end drops for the NUHOMS[®] DSC are non-mechanistic. However, 60g vertical end drop analyses are performed as a means of enveloping the 25g corner drop (in conjunction with the 75g horizontal drop).
3. An oblique corner drop from a height of 80 inches at an angle of 30° to the horizontal, onto the top or bottom corner of the TC. This case is not specifically evaluated. The side drop and end drop cases envelope the corner drop.

Cask Drop Accident Load Definitions

Same as Section 8.2.5.1(C).

Cask Drop Surface Conditions

Same as 8.2.5.1(D).

M.3.7.5.2 DSC Shell Assembly Drop Evaluation

The shell assembly consists of the DSC shell, the shield plugs, and the top and bottom inner and outer cover plates. The shell assembly drop evaluation is presented in three parts:

1. DSC shell assembly horizontal drop analysis,
2. DSC shell assembly vertical drop analysis, and
3. DSC shell stability analysis.

M.3.7.5.2.1 DSC Shell Assembly Horizontal Drop Analysis

The DSC shell assembly is analyzed for the postulated horizontal side drop using the ANSYS 3-D models of the DSC shell assembly discussed in Section M.3.6.1.2. Half-symmetry (180°) models of the top end and bottom end sections of the DSC shell assembly are developed based on the models for the end drops shown in Figure 8.1-14a and Figure 8.1-14b. Each model includes one-half of the height of the cylindrical shell. Each of the DSC shell assembly components is modeled using ANSYS solid 3-D elements. The full weight of the DSC is conservatively assumed to drop directly onto a single TC rail. Elastic-plastic analyses are performed and stresses are determined for each DSC shell assembly component. The NUHOMS[®]-32PT DSC shell stresses in the region of the basket assembly are also analyzed for the postulated horizontal side drop conditions. This analysis and results are presented in Section M.3.7.5.3.1.

M.3.7.5.2.2 DSC Shell Assembly Vertical Drop Analysis

For this drop accident case, the TC is assumed to be oriented vertically and dropped onto a uniform surface. The vertical cask drop evaluation conservatively assumes that the TC could be dropped onto either the top or bottom surfaces. No credit is taken for the energy absorbing

capacity of the cask top or bottom cover plate assemblies during the drop. Therefore, the DSC is analyzed as though it is dropped on to an unyielding surface. The principal components of the DSC and internals affected by the vertical drop are the DSC shell, the inner and outer top cover plates, the shield plugs, and the inner and outer bottom cover plates.

M.3.7.5.2.3 DSC Shell Assembly Stress Analysis

The ANSYS analytical models of the DSC shell assembly as described in Section M.3.6.1.2 and shown in Figure 8.1-14a and Figure 8.1-14b are used to determine the vertical end drop accident stresses in the DSC shell, the inner cover plates, the outer cover plates, and the shield plugs. The models consist of 90° quarter symmetry models and include one-half of the height of the cylindrical shell. To capture the maximum stress state in the DSC assembly components, each model was analyzed for end drop loading on the opposite end (i.e., the bottom end model was analyzed for top end drop, and the top end model was analyzed for bottom end drop). In these drop orientations, the end plates are supported at the perimeter by the shell. For the top and bottom end drops, the nodal locations on the impacted end are restrained in the vertical direction. An equivalent static linear elastic analysis is conservatively used for the vertical end drop analyses. Inertia loadings based on forces associated with the 75g deceleration are statically applied to the models. Analyses show that the stresses in the DSC cover plates and shield plugs are low. These low stresses occur because for the bottom end drop, the inner and outer top cover plates are supported by the top shield plug. During a top end drop, the outer top cover plate is assumed to be supported by the unyielding impacted surface and is subjected to a uniform bearing load imposed by the DSC internals. The same is true for the DSC bottom outer cover plate and shield plug for the bottom end drop. The highest stresses occur in the DSC shell and bottom inner cover plate. The maximum stresses in the inner bottom cover plate result from the top end vertical drop condition, in which the inner bottom cover plate is supported only at the edges. The maximum DSC shell membrane stresses, which occur near the top end of the DSC shell area, result from the accelerated weight of the DSC shell and the bottom end (for top end drop case) or top end (for the bottom end drop case) assemblies.

A summary of the calculated stresses for the main components of the DSC and associated welds is provided in Table M.3.7-1.

M.3.7.5.2.4 DSC Shell Stability Analysis

The stability of the DSC shell for a postulated vertical drop impact is also evaluated. For Level D conditions, the allowable axial stress in the DSC shell is based on Appendix F of the ASME Code. The maximum axial stress in the DSC shell obtained from the 75g end drop analyses is 11.08 ksi. The allowable axial stress is 11.14 ksi. Therefore, buckling of the DSC shell for a 75g vertical deceleration load does not occur.

M.3.7.5.3 Basket Assembly Drop Evaluation

As discussed in previous chapters, the structural components of the basket assembly include the fuel support grid and the transition rails.

The DSC resides in the TC for all drop conditions. Horizontally, the DSC is supported in the TC by two cask rails that are integral to the cask wall. The effect of these cask rails are included in the horizontal drop evaluations.

Vertical drops are non-mechanistic for the 32PT horizontal storage system, therefore, as noted in Section M.3.7.5.1, no end drops are postulated. However, to provide an enveloping load for the postulated 25g corner drop, a 60g end drop is evaluated. For this drop, the end of the DSC/basket assembly is supported by the ends of the TC.

The stress evaluation of the 32PT DSC basket assembly is presented in three parts:

1. Basket assembly horizontal drop stress analyses, including evaluation of the fuel support grid and the transition rails: The ANSYS model described in Section M.3.6.1.3 is used for all stress analyses except for the 45° drop evaluation of the basket assembly with 3-piece R90 transition rails, where the LS-DYNA model described in Section M.3.7.12 is used.
2. Basket assembly horizontal drop stability analyses including the fuel support grid and the transition rails: The ANSYS model described in Section M.3.6.1.3 is used for all stability analyses except for the 45° drop evaluation of the basket assembly with 3-piece R90 transition rails, where the LS-DYNA model described in Section M.3.7.12 is used. The criteria of the ASME B&PV Code, Appendix F-1341.3 is used.
3. Basket assembly vertical drop analysis which includes a stress evaluation of the fuel support grid and transition rails using hand calculations as described in Section M.3.6.1.3 for vertical deadweight. The stress criteria used for the vertical drop analysis also provide assurance of structural stability.

Within the basket grid structure are plates of Type 1100 aluminum and neutron absorbing materials composed of either enriched borated aluminum alloy or Boralyn[®] plates which perform heat transfer and criticality functions and are not included in the finite element models. The hand-calculated bounding accident condition axial stress in the plates is 1.0 ksi, due to the 60g end drop, which is below the yield stress value of 1.5 ksi (Type 1100 aluminum at 720°F). This ensures that the plates remain in position to perform their heat transfer and criticality functions. For the 75g side drop loading, the aluminum plates are supported in the transverse direction along their length by either the grid structure or the fuel assemblies. Deflection of the aluminum plates in the transverse direction is limited by the gap between the grid structure and the fuel assembly and does not significantly affect the heat transfer function of the plates. The effect of this gap is bounded by the criticality evaluation.

M.3.7.5.3.1 Basket Assembly Horizontal Drop Analysis

M.3.7.5.3.1.1 Basket and Basket Rail Stress Analysis

The ANSYS and LS-DYNA models described in Section M.3.6.1.3 and in Section M.3.7.12, respectively, are used to perform stress analyses of the 32PT basket assembly for horizontal drop loads. The finite element models include the fuel support grid, transition rails, DSC shell, and

the effects of the TC rails. Contact elements between the parts of the structure are active for all the stress analyses.

Loads

Inertia loads corresponding to the drop accelerations are applied to the structure by including the appropriate weight density of the materials and applying accelerations. Fuel loads are applied using pressure loads (or nodal forces) on the fuel grid elements. As previously described, thermal effects are included by applying temperatures (corresponding to the 117°F ambient temperature condition, DSC in the TC case) to each node in the model. This includes thermal effects in the model and applies the temperature dependent material properties at different model locations.

Side drop orientations were selected to maximize both axial compression and bending stresses in the basket structure. Zero degree (0°) drop orientations were selected to maximize axial compression while an orientation of 45° (from vertical) was selected to maximize bending loads. Drops onto the TC rails were selected to maximize load concentrations. Table M.3.7-2 lists the stress analyses configurations performed for the postulated side drop.

Material Properties

The material properties used in the accident condition stress analyses are listed in Table M.3.7-3 for the 32PT basket structural components. The evaluations were performed using bilinear elastic-plastic material properties. For the steel components, the plastic slope was taken as 5% of the elastic modulus ($E_{tan} = 0.05E$) and Code values of yield stresses were used. For the aluminum transition rails, yield stresses were taken from Table M.3.3-5, and a lower bound plastic slope of 0.01E was used.

Results

Fuel grid stresses are linearized at the locations shown in Figure M.3.6-5. Enveloping stresses in each basket component are listed in Table M.3.7-4 for the postulated 75g side drop. The stresses are the maximum values in each component from the analyses listed in Table M.3.7-2. Table M.3.7-4 includes a comparison of the calculated stresses to Service Level D stress allowables for elastic-plastic analyses based on the stress criteria from Table M.2-17 and materials data from Table M.3.3-1 and Table M.3.3-3. As shown, all stress ratios are less than 1.0. Results are illustrated in Figure M.3.7-3 and Figure M.3.7-5 for the 1-piece R90 rail configuration and Figure M.3.7-3A and Figure M.3.7-5A for the 3-piece R90 rail configuration.

M.3.7.5.3.2 Basket Assembly Part71 End Drop Analysis

As noted in Section M.3.7.5.1, end drops are non-mechanistic for the 32PT system. End drop results are included to demonstrate margin for the postulated 25g corner drop.

Under axial loading, the fuel assemblies and basket assembly are supported by the bottom of the DSC/cask. The fuel assemblies react directly against the bottom or top end of the DSC/cask and do not load the basket structure. Stresses under axial loading result only from the self weight/inertia of the basket structure. In addition, since any connections between the fuel

support grid and transition rails are slotted (to allow for thermal expansion preventing thermal stresses), each part of the basket structure is loaded only by its own weight/inertia.

Compressive axial stresses are maximum at the "supported" end of the basket structure. Stresses are calculated using hand calculations and are summarized, and compared to the acceptance criteria, in Table M.3.7-5. As shown by the table, all stresses are well below the allowable values.

M.3.7.5.3.3 Basket Assembly Stability Analysis

Stability under axial loading is demonstrated by the results described in Section M.3.7.5.3.2 above. To demonstrate stability of the 32PT basket structure under side loading, a series of stability analyses were performed. As listed in Table M.3.7-3, the stability evaluations were performed using the criteria of ASME B&PV Code, Appendix F-1341.3 which establishes the allowable load as 90% of the Limit Analysis Collapse Load where the Limit Analysis Collapse Load is the maximum load determined using elastic-perfectly plastic material properties with a yield stress equal to the lesser of $2.3S_m$ or $0.7S_u$.

- For the basket configuration with 1-piece R90 transition rails, the stability analyses were performed using the ANSYS models described in Section M.3.6.1.3
- For the basket configuration with 3-piece R90 transition rails, stability analyses for 0° and 180° drop orientations were performed using the ANSYS models described in Section M.3.6.1.3. For the 45° drop orientation, the stability analysis was performed using the LS-DYNA model described in M.3.7.12.

The stability analyses performed for the 32PT basket assembly are listed in Table M.3.7-6. The results of the stability analyses are summarized in Table M.3.7-7. These analyses demonstrate stability of the structural components of the basket structure with ample margin for 75g loading.

LS-DYNA was also used to perform confirmatory stability analyses. The LS-DYNA confirmatory analyses used the same material properties and assumptions as the ANSYS analyses. Results of these analyses are listed in Table M.3.7-7A along with the ANSYS results. These confirmatory analyses are performed using the welded steel rail configuration and are included here for comparison purposes only. Displaced shape plots from the 0° and 180° analyses are included as Figure M.3.7-6 and Figure M.3.7-8, respectively. The plots show the geometry just past the stability load. Also included are displacement "time history" (load [time] vs. displacement) plots for the node locations indicated in the geometry plots (See Figure M.3.7-7 and Figure M.3.7-9). These "time history" plots clearly show the stability point of the structure.

M.3.7.5.3.3.1 Fuel Support Structure Stability Evaluation Using Hand Calculations

A confirmatory stability analyses for the fuel grid structure was performed using hand calculations, the column stability criteria of ASME B&PV Code, Appendix F-1334.3(b), and ASME Code yield stress values as listed in Table M.3-3. The criteria were developed for a material temperature of 600°F , which corresponds to the maximum temperature at the most highly loaded ligaments at the periphery of the fuel support grid.

The "bottom" span of the "center" ligament is selected as the critical location. The compressive load in this ligament is determined as follows:

- A load of 11.0 lb/in was applied to each fuel cell. This represents an enveloping load.
- The loads from the four (4) cells along the bottom edge of the basket are transferred directly into the transition rails without loading the "columns" of the fuel grid.
- The subject ligament is assumed to carry half the load in the central cells above the bottom row. Thus, there are 10 cells above the ligament, and 1/2 the load is carried by the subject ligament while the remaining load is carried by the adjacent columns. Therefore, the load from 5 fuel cells is applied to the subject ligament.

The self weight/inertia of the basket assembly was neglected.

The load on the subject ligament is:

$$P = (75g)(11.0 \text{ lb/in})(5 \text{ cells})(1.0 \text{ in})$$

$$= 4.13 \text{ kip/ligament}$$

The stress is:

$$f_s = \frac{(4.13 \text{ kip/ligament})}{0.25 \text{ in}} = 16.5 \text{ ksi}$$

The allowable under the side drop load is determined using the following equations from ASME B&PV Code, Appendix F-1334.3(b):

$$F_s = S_y \left(\frac{(1 - \lambda^2/4)}{1.11 + 0.5\lambda + .17\lambda^2 - 0.28\lambda^3} \right)$$

$$\text{where: } \lambda = \left(\frac{KI}{r} \right) \left(\frac{1}{\pi} \right) \left(\frac{S_y}{E} \right)^{1/2}$$

$$r = \frac{t}{(12)^{1/2}}$$

$$L = \text{cell height of } 8.825''$$

The allowable axial compression stress, F_s , is 19.0 ksi and the ratio of calculated to allowable stresses is:

$$\frac{16.5 \text{ ksi}}{19.0 \text{ ksi}} = 0.87$$

M.3.7.5.3.2 Results of Basket Stability Analysis

The results of the analyses indicate the structural capacity of the NUHOMS[®]-32PT basket assembly is higher than the postulated 75g side drop impact load. Thus, the 32PT basket assembly is stable under the postulated side drop loads.

M.3.7.5.4 On-site TC Horizontal and Vertical Drop Evaluation

An analysis has been performed in Section 8.2.5.2 to evaluate the OS197 and OS197H TCs for postulated horizontal and vertical drop accidents with a static equivalent deceleration of 75g's. The evaluations for the OS197 and OS197H casks are based on payload weights of 97,250 lbs and 116,000 lbs, respectively. The maximum total cask payload weight with a dry-loaded NUHOMS[®]-32PT DSC is approximately 102,000 lbs. Therefore, the OS197H cask is acceptable with any NUHOMS[®]-32PT DSC and the OS197 cask is acceptable with a NUHOMS[®]-32PT DSC where the total cask payload weight is not more than 97,250 lbs.

M.3.7.5.5 Loss of Neutron Shield

No impact on the structural evaluation.

M.3.7.6 Lightning

No impact on the structural evaluation.

M.3.7.7 Blockage of Air Inlet and Outlet Openings

This accident conservatively postulates the complete blockage of the HSM ventilation air inlet and outlet openings on the HSM side walls.

Since the NUHOMS[®] HSMs are located outdoors, there is a remote probability that the ventilation air inlet and outlet vent openings could become blocked by debris. The NUHOMS[®] design features such as the perimeter security fence and the redundant protected location of the air inlet and outlet vent openings reduces the probability of occurrence of such an accident. Nevertheless, for this conservative generic analysis, such an accident is postulated to occur and is analyzed.

The structural consequences due to the weight of the debris blocking the air inlet and outlet vent openings are negligible and are bounded by the HSM loads induced for a postulated tornado (Section 8.2.2) or earthquake (Section 8.2.3).

The thermal effects of this accident for the NUHOMS[®]-32PT DSC are described in Section M.4.0.

M.3.7.8 DSC Leakage

The 32PT DSC is leak tested to meet the leaktight (1×10^{-7} std. cm³/sec) of ANSI N145-1997 [3.13]. The analyses of the 32PT demonstrate that the pressure boundary is not breached since it meets the applicable stress limits for normal, off-normal and postulated accident conditions.

M.3.7.9 Accident Pressurization of DSC

The NUHOMS[®] 32PT DSC is evaluated and designed for the maximum accident pressures calculated in Section M.4.0. The pressure boundary stresses due to this pressure load are bounded by the results presented in Table M.3.7-10. Therefore, the 32PT-DSC is acceptable for this postulated accident condition.

M.3.7.10 Load Combinations

The load categories associated with normal operating conditions, off-normal conditions and postulated accident conditions are described and analyzed in previous sections. The load combination results for the NUHOMS[®] components important to safety are presented in this section. Fatigue effects on the TC and the DSC are also addressed in this section.

M.3.7.10.1 DSC Load Combination Evaluation

As described in Section 3.2, the stress intensities in the DSC at various critical locations for the appropriate normal operating condition loads are combined with the stress intensities experienced by the DSC during postulated accident conditions. It is assumed that only one postulated accident event occurs at any one time. The DSC load combinations summarized in Table 3.2-6 are expanded in Table M.2-15 for the 32PT DSC. Since the postulated cask drop accidents are by far the most critical, the load combinations for these events envelope all other accident event combinations. Table M.3.7-8 through Table M.3.7-10 tabulate the maximum stress intensity for each component of the DSC calculated for the enveloping normal operating, off-normal, and accident load combinations. For comparison, the appropriate ASME Code allowables are also presented in these tables.

M.3.7.10.2 DSC Fatigue Evaluation

Although the normal and off-normal internal pressures for the NUHOMS[®]-32PT DSC are higher relative to the NUHOMS[®]-24P DSC, the range of pressure fluctuations due to seasonal temperature changes are essentially the same as those evaluated for the NUHOMS[®]-24P DSC. Similarly, the normal and off-normal temperature fluctuations for the NUHOMS[®]-32PT DSC due to seasonal fluctuations are essentially the same as those calculated for the NUHOMS[®]-24P DSC. Therefore, the fatigue evaluation presented in Section 8.2.10.2 for the 24P DSC remains applicable to the NUHOMS[®]-32PT DSC.

M.3.7.10.3 TC Load Combination Evaluation

There is no change to the TC load combination evaluations. The evaluations performed in Sections 8.1 and 8.2 for the OS197 and OS197H casks are based on payloads of 97,250 lbs and 116,000 lbs, respectively. The maximum total cask payload with a dry-loaded NUHOMS[®]-32PT DSC is approximately 102,000 lbs. Therefore, the OS197H cask is acceptable with any NUHOMS[®]-32PT DSC and the OS197 cask is acceptable with a NUHOMS[®]-32PT DSC where the total cask payload is not more than 97,250 lbs.

M.3.7.10.4 TC Fatigue Evaluation

No change.

M.3.7.10.5 HSM Load Combination Evaluation

Since the weight of the NUHOMS[®]-32PT DSC is bounded by the DSC weights used in Sections 8.1 and 8.2, there is no change to the HSM load combination evaluation.

M.3.7.10.6 Thermal Cycling of the HSM

No change.

M.3.7.10.7 DSC Support Structure Load Combination Evaluation

See Section M.3.7.10.5 above.

M.3.7.11 Evaluation of Poison Rod Assemblies

The Poison Rod Assemblies (PRA) consist of Type 304 stainless steel tubes filled with Boron carbide pellets or Boron powder that are inserted into the fuel assemblies through the guide tubes. They each contain up to 24 rods depending on the type of fuel assembly and are held together at the top end with a support plate as shown schematically in Figure M.1-2.

The PRAs are near the fuel rods, so their temperature is conservatively assumed to be the same temperature as the fuel cladding. Table M.4-13 reports that the maximum fuel cladding temperature during the postulated accidental blocked vent condition remains below 800°F. Table M.4-16 reports that the maximum fuel cladding temperature during vacuum drying is 810°F, which is acceptable because vacuum drying is a short term event.

In the vertical direction, the PRAs are supported by the support plate at the top end of the fuel assembly. The most limiting vertical load occurs during the postulated 60g end drop (See Section M.3.7.5.1) where the PRAs are supported by the support plate. All longitudinal loading is due solely to the inertia of each tube and contents. The PRAs are continuously supported by the guide tubes, thus elastic stability is not limiting. The PRAs are an open system and are thus not pressurized, so there is no hoop component of stress. Using the geometry of the PRA cladding shown in Figure M.1-2, the maximum fuel assembly length is 171.71 inches (see Table M.2-2). Assuming that the PRA contents have a density of 2.5 lb/in³, the maximum longitudinal stress (and stress intensity) in the PRA cladding is approximately 5.9 ksi. This stress intensity is well below the Type 304 Service Level D membrane allowable stress of 36.5 ksi at 800° F (See Tables M.3-2 and M.2-16).

In the horizontal direction, the PRAs are supported by the guide tubes during all normal, off-normal and postulated accident conditions; therefore, there are no limiting stresses associated with horizontal deadweight, transfer handling (with a horizontal load component), and the postulated side drop.

M.3.7.12 LS-DYNA Finite Element Model Analysis

An LS-DYNA (Version 960) model is used to evaluate stresses in the basket assembly with 3-piece R90 transition rails under 45° loading. LS-DYNA is used because its contact algorithm is a lot more robust than the one in ANSYS and, therefore, is better able to solve problems that include a large number of parts in contact with each other such as is the case for the 3-piece R90 transition rail configuration. The LS-DYNA model includes contact between all parts of the DSC, transfer cask, and basket, including the following:

- Fuel support grid to the four (4) R90 transition rail cover plates
- Fuel support grid to the four (4) R45 transition rails
- Each R90 transition rail cover plates to the three (3) parts of the adjacent 3-piece R90 transition rails
- The corners/ends of the R90 transition rail cover plates and the DSC Shell
- The DSC shell and the four R45 transition rails and the 12 pieces of the 3-piece R90 transition rail
- Between all adjacent sections of the 3-piece R90 transition rails
- The DSC shell and the Cask and Cask Rails.

The LS-DYNA model is based on the ANSYS model of the basket with the 3-piece R90 transition rails configuration. As noted above, contact was defined (modeled) between all parts that are in contact to each other. No connections were modeled between the transition rails, fuel grid, and/or R90 transition rails cover plates.

The LS-DYNA model uses plane stress elements to represent a unit length of the 32PT basket. The fuel support grid is modeled with four (4) elements through the thickness. A minimum of three (3) elements are used through the thickness of all other parts except the cask shell and the cask rails. The cask shell and cask rails are extremely rigid relative to the other parts of the structure and are modeled as rigid bodies and are fixed around their entire circumference. Therefore, the cask shell is modeled with only one through thickness element.

The geometry of the LS-DYNA basket model is shown in Figure M.3.7-10 and Figure M.3.7-11.

Inertial loads are applied to the structure by including the appropriate weight density of the materials and applying accelerations. Fuel loads are applied as forces to the nodes on the surfaces of the fuel grid elements. Thermal effects are included by applying temperatures corresponding to the 100°F in cask temperature distribution (fuel configuration 1) documented in Chapter M.4 and shown in Figure M.3.7-12.

**Table M.3.7-1
Maximum NUHOMS®-32PT DSC Stresses for Drop Accident Loads**

DSC Components	Stress Type	Calculated Stress (ksi) ⁽¹⁾	
		Vertical ⁽³⁾	Horizontal
DSC Shell	Primary Membrane	14.54	36.47
	Membrane + Bending	39.64	55.83
Inner Top Cover Plate	Primary Membrane	2.41	25.08
	Membrane + Bending	5.87	39.19
Outer Top Cover Plate	Primary Membrane	2.22	34.46
	Membrane + Bending	5.12	55.25
Inner Bottom Cover Plate ⁽⁴⁾	Primary Membrane	7.61	21.84
	Membrane + Bending	25.27	55.17
Outer Bottom Cover Plate	Primary Membrane	1.69	31.91
	Membrane + Bending	3.67	49.85
Inner Top Cover Plate Weld ⁽²⁾	Primary	2.18	22.81
Outer Top Cover Plate Weld ⁽²⁾	Primary	0.68	11.53

Notes:

- (1) Values shown are maximums irrespective of location.
- (2) Stress values are the envelope of drop loads with and without 20psig internal pressure.
- (3) The vertical end drops are non-mechanistic for the NUHOMS® 32PT DSC. They are performed as a means of demonstrating qualification of the 25g corner drop. The analyses reported here are conservatively based on 75g deceleration.
- (4) These stresses may also be applied to the single bottom end forging, when used.

Table M.3.7-2
List of Drop Condition ANSYS Stress Analyses of the 32PT Basket Assembly

Case	Load	DSC Configuration	Support Conditions	Analysis Code
1	75g Side Drop at 0°	32PT DSC with 1-piece aluminum transition rails	OS197 (Support Rails at ± 18.5°)	ANSYS
2	75g Side Drop at 45° from bottom center	32PT DSC with 1-piece aluminum transition rails	OS197 (Support Rails at ± 18.5°)	ANSYS
3	75g Side Drop at 180°	32PT with 1-Piece Aluminum Transition Rails	OS197 (Cask Rails Not Impacted)	ANSYS
4	75g Side Drop at 0°	32PT with 3-Piece R90 Aluminum Transition Rails	OS197 (±18.5°)	ANSYS
5	75g Side Drop at 45°	32PT with 3-Piece R90 Aluminum Transition Rails	OS197 (±18.5°)	LS-DYNA
6	75g Side Drop at 180°	32PT with 3-Piece R90 Aluminum Transition Rails	OS197 (Cask Rails Not Impacted)	ANSYS

Note: See Table M.3.7-6 for additional stability analyses performed for the 75g side drop load.

Table M.3.7-3
Summary of Material Properties for Drop Accident Analyses of the 32PT Basket Assembly

Component	Material	Drop Condition Analysis Material Properties		Evaluation Temperature
		Stress Analyses ⁽¹⁾	Stability Analyses ^(1,2)	
Fuel Support Grid	1/4" Thick, Type XM-19 Stainless Steel	Bilinear Elastic-Plastic $S_y = \text{Code } S_y \text{ (Table M.3.3-3)}$ $E_{tan} = .05E_{Code} \text{ (Table M.3.3-3)}$	Bilinear Elastic-Perfectly Plastic (F-1341.3): $S_y = \min(2.3S_m, 0.7S_u)$ $E_{tan} = 0$	800°F
Solid Aluminum Transition Rails, R90 Cover Plates	1/4" Thick, Type XM-19 Stainless Steel	Bilinear Elastic-Plastic $S_y = \text{Code } S_y \text{ (Table M.3.3-3)}$ $E_{tan} = .05E_{Code} \text{ (Table M.3.3-3)}$	Bilinear Elastic-Perfectly Plastic (F-1341.3): $S_y = \min(2.3S_m, 0.7S_u)$ $E_{tan} = 0$	600°
Solid Aluminum Transition Rails, Aluminum Bodies	6061 Aluminum Alloy	Bilinear Elastic-Plastic $S_y = \text{(Table M.3.3-5)}$ $E_{tan} = .01E \text{ (Table 3.3-5)}$	Bilinear Elastic-Plastic $S_y = \text{(Table M.3.3-5)}$ $E_{tan} = .01E \text{ (Table M.3.3-5)}$	Note 3

- Notes:**
1. Prior to application of drop loads, the structure was initialized to the temperatures corresponding to the 117°F in cask case.
 2. For the steel components, stress checks were performed at the enveloping temperatures listed. For the aluminum transition rails, stress checks were performed at temperatures corresponding to the maximum stress point. Temperatures listed are for the maximum stress points of the most highly loaded rail (the large 90° transition rail at the "bottom" of the basket).
 3. For accident condition loading, the transition rails support the fuel support grid such that stresses and displacements in the fuel grid are acceptable. Since the transition rails are entrapped between the fuel grid and the DSC shell, no additional checks (of the aluminum) are required for accident/drop loading. Qualification of the fuel grid (and R90 cover plate) demonstrate that the rails perform their intended function.

**Table M.3.7-4
32PT Basket, Enveloping Stress Results - 75g Side Drops**

Component	Stress Category	Stress Intensity		Stress Ratio	Notes
		Calculated	Allowable		
Basket with 1-Piece R90 Transition Rails					
Fuel Support Grid	P_m	26.2 ksi	59.4 ksi	.44	XM-19, 800°F ⁽²⁾
	$P_m + P_b$	73.9 ksi	76.3 ksi	.97	
Transition Rail Cover Plates	P_m	7.63 ksi	59.4 ksi	0.13	XM-19, 800°F ⁽²⁾
	$P_m + P_b$	64.4 ksi	76.3 ksi	.84	
Basket with 3-Piece R90 Transition Rails					
Fuel Support Grid	P_m	27.0	60.4	0.45	XM-19, 705°F ⁽³⁾
	$P_m + P_b$	76.2	77.7	0.98	

- Note:**
1. Although all the listed values include thermal effects, evaluation of secondary stress not required for Level D events.
 2. Allowable stress based on an enveloping temperature of 800°F.
 3. Allowable stress based on maximum basket temperature (see Figure M.3.7-12).

**Table M.3.7-5
32PT Basket, Enveloping Stress Results - 60g Part 71 End Drop**

Component	Stress (Axial (Compression))			Notes
	Calculated	Allowable	Ratio	
Fuel Support Grid	3.30 ksi	31.8 ksi	.10	XM-19, 800°F
Aluminum Transition Rails	1.03 ksi	4.20 ksi	.25	6061 Al., 600°F

**Table M.3.7-6
Drop Condition Stability Analyses for the 32PT Basket Assembly**

Case	Load	DSC Configuration	Support Conditions	Analysis Code
1	Side Drop at 0°	32PT DSC with aluminum transition rails	OS197 (Support Rails at ± 18.5°)	ANSYS
2	Side Drop at 45° from bottom center	32PT DSC with aluminum transition rails	OS197 (Support Rails at ± 18.5°)	LS-DYNA
3	Side Drop at 180° from Bottom center	32PT DSC with aluminum transition rails	OS197 n/a (cask rails not impacted)	ANSYS

Table M.3.7-7
Summary of 32PT Basket Stability Analysis -- Side Drops

Drop Orientation ⁽¹⁾	Stability Analyses	
	3-Piece Aluminum Transition Rails	1-Piece Aluminum Transition Rails
0° (OS197)	83.6g	107.6g
45° (OS197)	81.0g	90.7g
180°	112g	88.4g

Notes: 1. The OS197 cask rails are at $\pm 18.5^\circ$ from bottom center.
The 180° drops do not impact cask rails.

Table M.3.7-7A
Summary of 32PT Analysis Confirmatory Stability Analysis⁽¹⁾

Drop Orientation	ANSYS	LS-DYNA
0°	98.0g	98.6g
180°	99.9g	110.4g

Notes: 1. The confirmatory analyses were performed for the Type 304-SS transition rails configuration.

Table M.3.7-8
NUHOMS®-32PT DSC Enveloping Load Combination Results for Normal and Off-Normal
Loads
(ASME Service Levels A and B)

DSC Components	Stress Type	Controlling Load Combination ⁽¹⁾	Stress (ksi)	
			Calculated	Allowable ⁽²⁾
DSC Shell	Primary Membrane	DD-1	9.09	17.5
	Membrane + Bending	TR-8	21.24	26.3
	Primary + Secondary	TR-3	55.63	60.0
Inner Bottom Cover Plate ⁽⁷⁾	Primary Membrane	LD-5	4.49	17.5
	Membrane + Bending	NO-1	23.07	40.5
	Primary + Secondary	LD-4	49.26	54.3
Outer Bottom Cover Plate	Primary Membrane	UL-5, UL-6	6.83	18.7
	Membrane + Bending	UL-5, UL-6	25.53	28.1
	Primary + Secondary	LD-4	39.97	54.3
Inner Top Cover Plate	Primary Membrane	TR-5	2.65	17.5
	Membrane + Bending	DD-1	16.83	26.3
	Primary + Secondary	DD-1	30.45	52.5
Outer Top Cover Plate	Primary Membrane	TR-7	4.21	17.5
	Membrane + Bending	TR-7	8.83	26.3
	Primary + Secondary	TR-7	27.38	52.5

See Table M.3.7-11 for notes.

Table M.3.7-9
NUHOMS®-32PT DSC Enveloping Load Combination Results
for Accident Loads
(ASME Service Level C)

DSC Components	Stress Type	Controlling Load Combination ⁽¹⁾	Stress (ksi)	
			Calculated	Allowable ⁽²⁾
DSC Shell	Primary Membrane	HSM-8	17.79	21.7
	Membrane + Bending	HSM-8	30.58	32.6
Inner Bottom Cover Plate ⁽⁷⁾	Primary Membrane	HSM-8	5.58	22.4
	Membrane + Bending	HSM-8	7.01	33.7
Outer Bottom Cover Plate	Primary Membrane	UL-7	8.59	22.4
	Membrane + Bending	UL-7	33.06	35.0
Inner Top Cover Plate	Primary Membrane	HSM-8	5.07	21.7
	Membrane + Bending	HSM-8	14.95	32.6
Outer Top Cover Plate	Primary Membrane	HSM-8	10.23	21.7
	Membrane + Bending	HSM-8	19.06	32.6

See Table M.3.7-11 for notes.

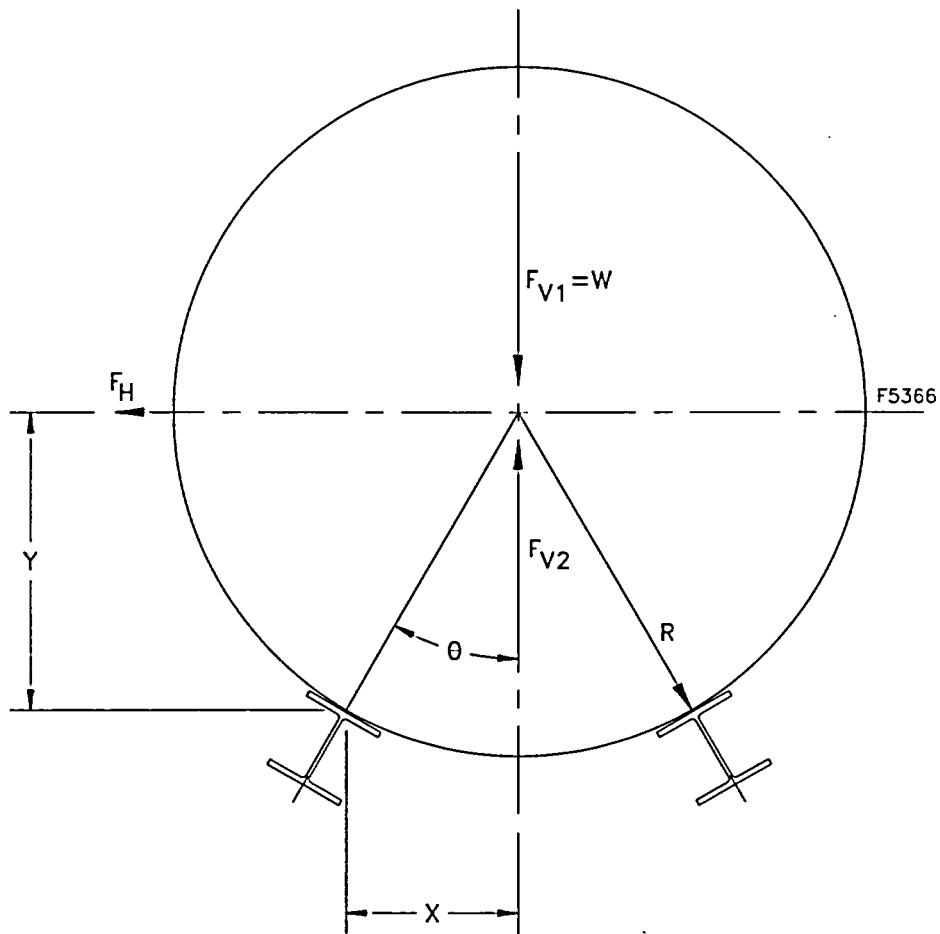
Table M.3.7-10
NUHOMS®-32PT DSC Enveloping Load Combination Results
for Accident Loads
(ASME Service Level D)⁽³⁾

DSC Components	Stress Type	Controlling Load Combination ⁽¹⁾	Stress (ksi)	
			Calculated	Allowable ⁽²⁾
DSC Shell	Primary Membrane	TR-10	36.47	44.4
	Membrane + Bending	TR-10	55.83	61.0 ⁽⁴⁾
Inner Bottom Cover Plate ⁽⁷⁾	Primary Membrane	TR-10	38.36	44.4
	Membrane + Bending	TR-10	56.65	59.6 ⁽⁵⁾
Outer Bottom Cover Plate	Primary Membrane	TR-10	32.74	44.4
	Membrane + Bending	TR-10	51.31	57.1
Inner Top Cover Plate	Primary Membrane	TR-10	25.08	44.4
	Membrane + Bending	TR-10	46.30	57.1
Outer Top Cover Plate	Primary Membrane	TR-10	36.85	44.4
	Membrane + Bending	TR-10	55.86	58.6 ⁽⁶⁾

See Table M.3.7-11 for notes.

Table M.3.7-11
DSC Enveloping Load Combination Table Notes

- (1) See Table M.2-15 for load combination nomenclature.
- (2) See Table M.2-16 and M.2-17 for allowable stress criteria. Material properties were obtained from Section M.3.3 at a design temperature of 500° F or as noted.
- (3) In accordance with the ASME Code, thermal stresses need not be included in Service Level D load combinations.
- (4) The maximum side drop membrane + bending stress is highly localized near the cask rail, at the outer bottom cover plate. The maximum temperature in this region is less than 266°F.
- (5) The maximum side drop membrane + bending stress is highly localized over the cask rail. The maximum temperature in this region is less than 300°F.
- (6) The maximum side drop membrane + bending stress is highly localized over the cask rail. The maximum temperature in this region is less than 350°F.
- (7) These stresses may also be applied to the single bottom end forging, when used.



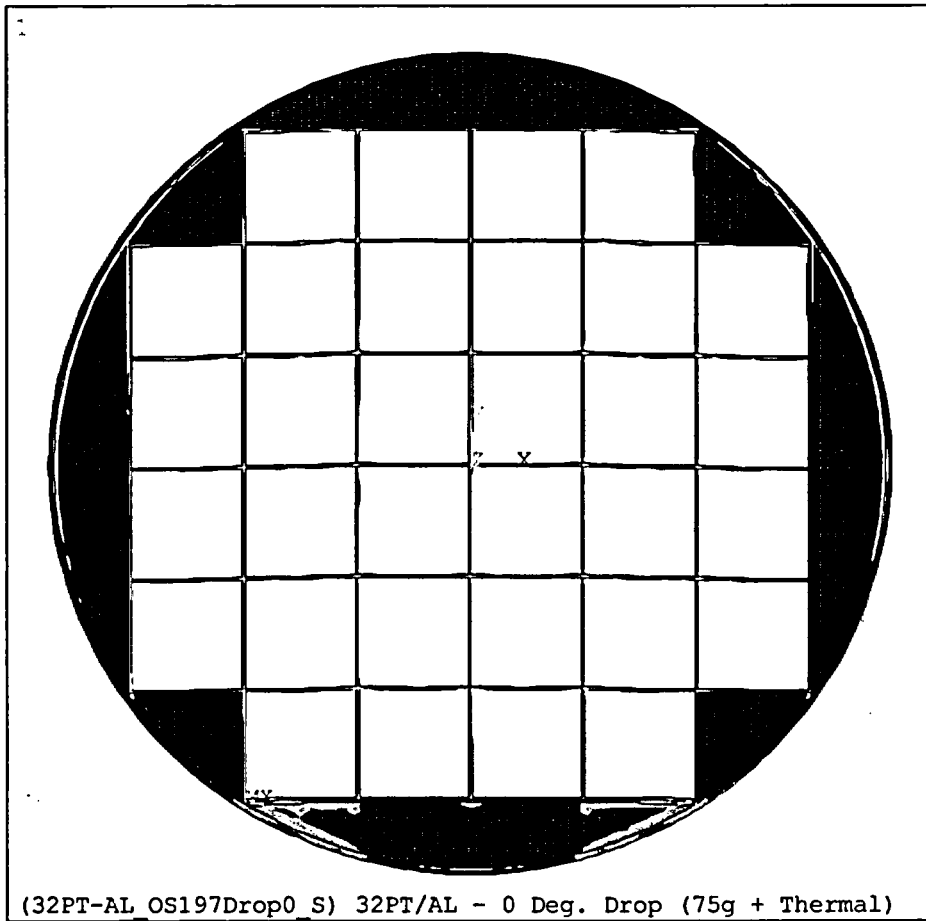
WHERE:

- $R = 33.595$ in., DSC outer radius
- $\theta = 30^\circ$
- $X = R \sin \theta = 16.8$ in.
- $Y = R \cos \theta = 29.1$ in.
- $F_{V1} = W =$ weight of DSC
- $F_{V2} = W(0.17g) =$ upward vertical seismic load
- $F_H = W(0.40g) =$ horizontal seismic load

Figure M.3.7-1
DSC Lift-Off Evaluation

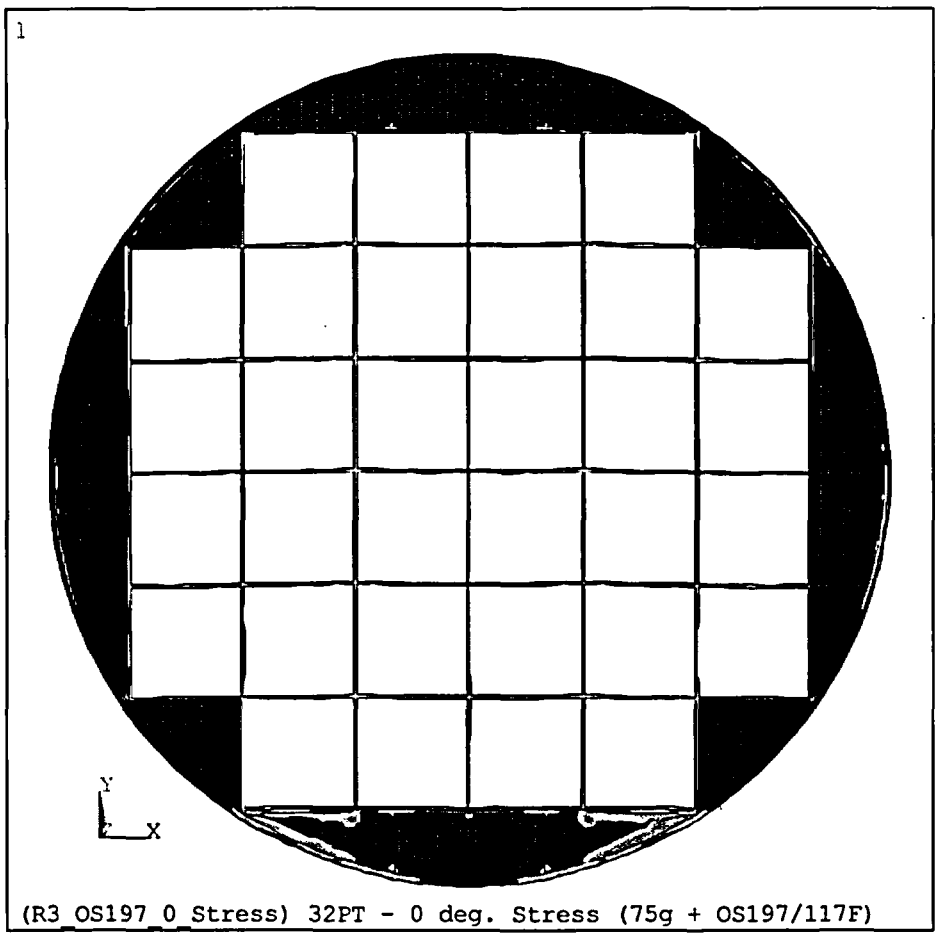
DELETED

Figure M.3.7-2
0° Side Drop Stress Intensity, 32PT Basket with Steel Transition Rails
(Support Rails at $\pm 18.5^\circ$)



ANSYS 5.6.2
MAY 31 2001
14:15:57
PLOT NO. 1
NODAL SOLUTION
TIME=75
SINT (AVG)
DMX =.488641
SMN =5.648
SMX =49711
5.648
5528
11051
16574
22097
27620
33143
38665
44188
49711

Figure M.3.7-3
0° Side Drop Stress Intensity, 32PT Basket with Aluminum Transition Rails (1-Piece R90)
(Support Rails at ±18.5°)



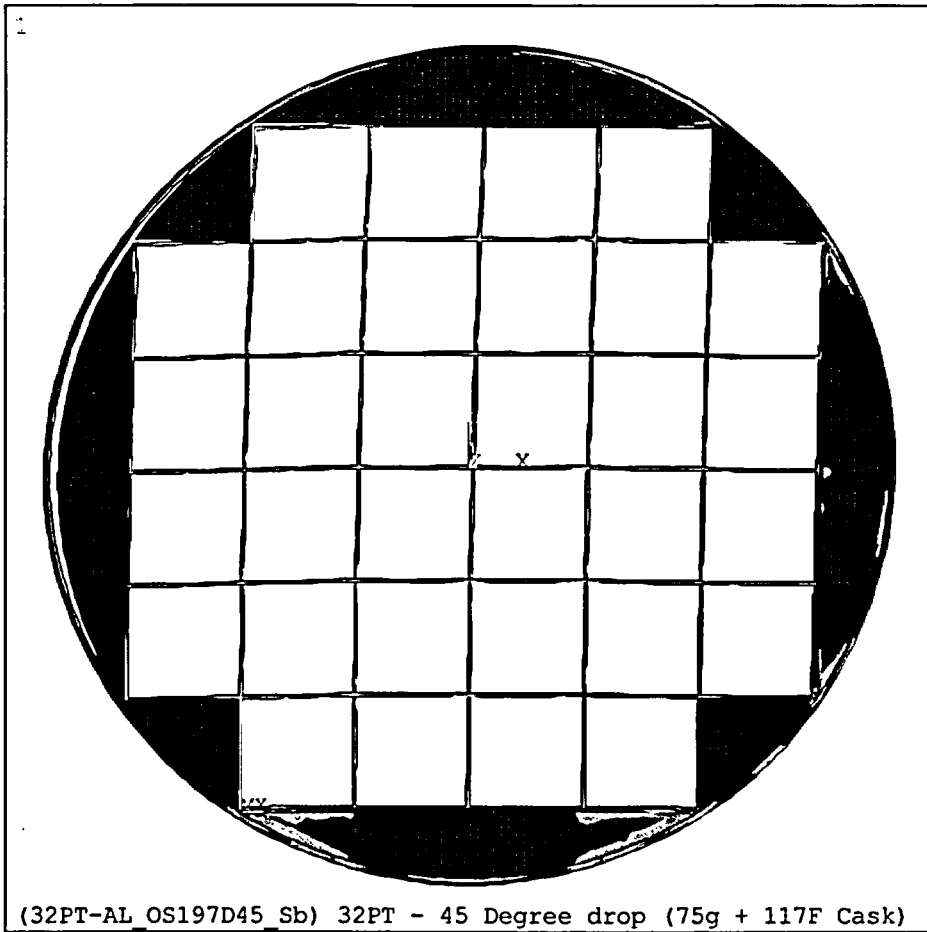
ANSYS 5.6.2
 AUG 7 2002
 10:15:54
 PLOT NO. 63
 NODAL SOLUTION
 STEP=36
 SUB =7
 TIME=75
 SINT (AVG)
 DMX =.471324
 SMN =5.79
 SMX =48410

■	5.79
■	5384
■	10762
■	16141
■	21519
■	26897
■	32275
■	37654
■	43032
■	48410

Figure M.3.7-3A
0° Side Drop Stress Intensity, 32PT Basket with Aluminum Transition Rails (3-Piece R90)
(Support Rails at ± 18.5°)

DELETED

Figure M.3.7-4
45° Side Drop Stress Intensity, 32PT Basket with Steel Transition Rails
(Support Rails at $\pm 18.5^\circ$)

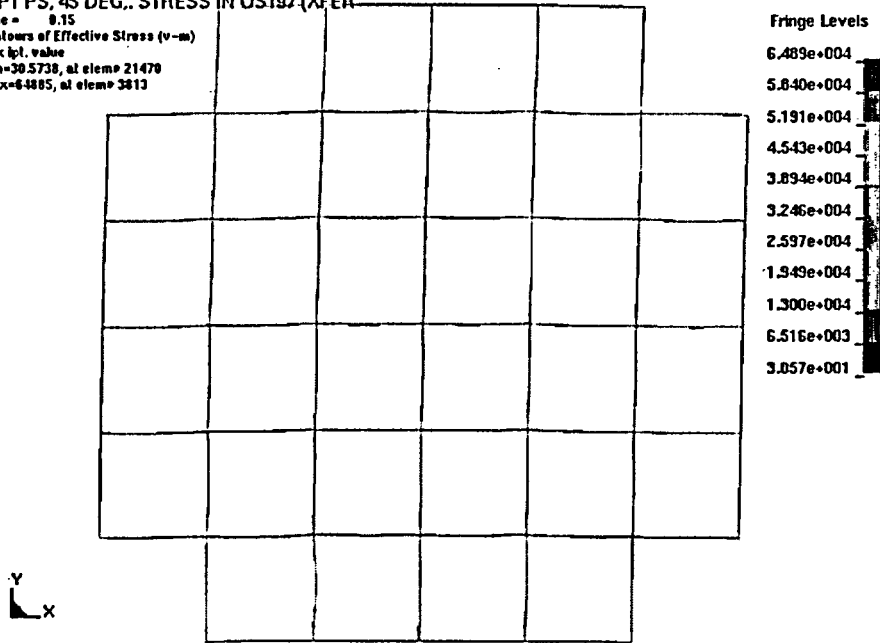


ANSYS 5.6.2
 JUN 7 2001
 13:58:44
 PLOT NO. 31
 NODAL SOLUTION
 STEP=37
 SUB =5
 TIME=75
 SINT (AVG)
 DMX =1.467
 SMN =28.178
 SMX =48002

■	28.178
■	5359
■	10689
■	16019
■	21350
■	26680
■	32011
■	37341
■	42672
■	48002

Figure M.3.7-5
45° Side Drop Stress Intensity, 32PT Basket with Aluminum Transition Rails (1-Piece R90)
(Support Rails at ±18.5°)

32PT PS, 45 DEG., STRESS IN OS197 (XFER)
 Time = 8.15
 Colours of Effective Stress (v-m)
 max lpl. value
 min=305738, at elem= 21470
 max=64865, at elem= 3813



32PT PS, 45 DEG., STRESS IN OS197 (XFER)
 Time = 8.15
 Colours of Effective Stress (v-m)
 max lpl. value
 min=4.95684, at elem= 75830
 max=18467.9, at elem= 60802

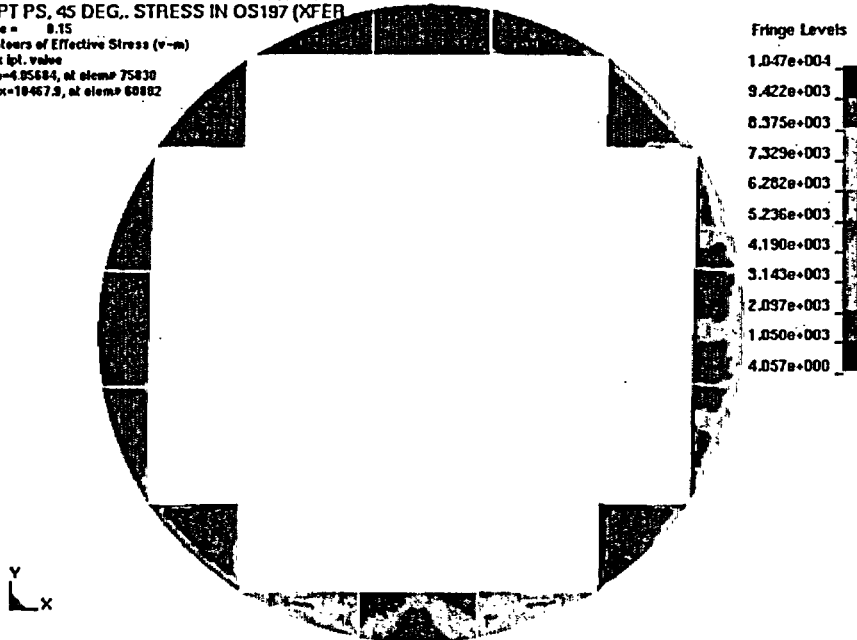


Figure M.3.7-5A
 45° Side Drop Von Misses Effective Stresses, 32PT Basket with Aluminum Transition Rails
 (3-Piece R90) (Support Rails at ± 18.5°)

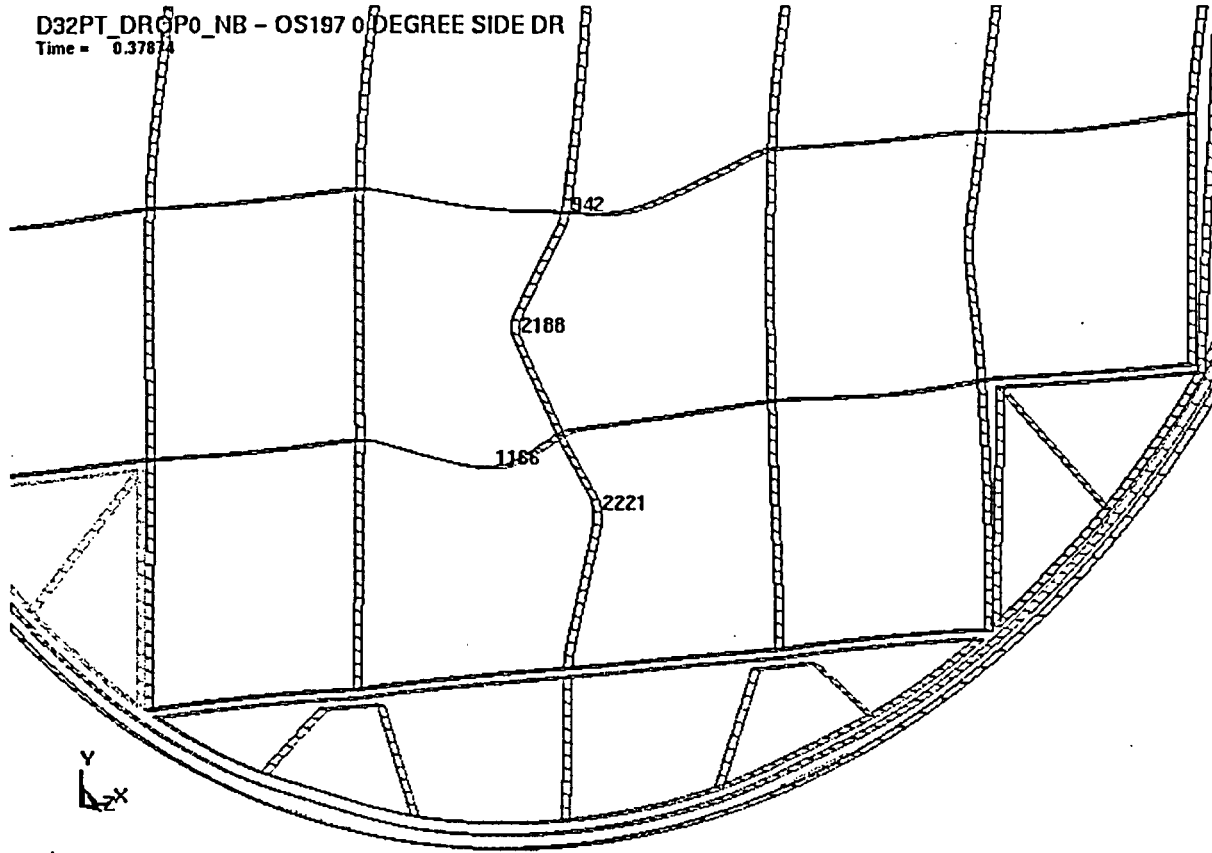
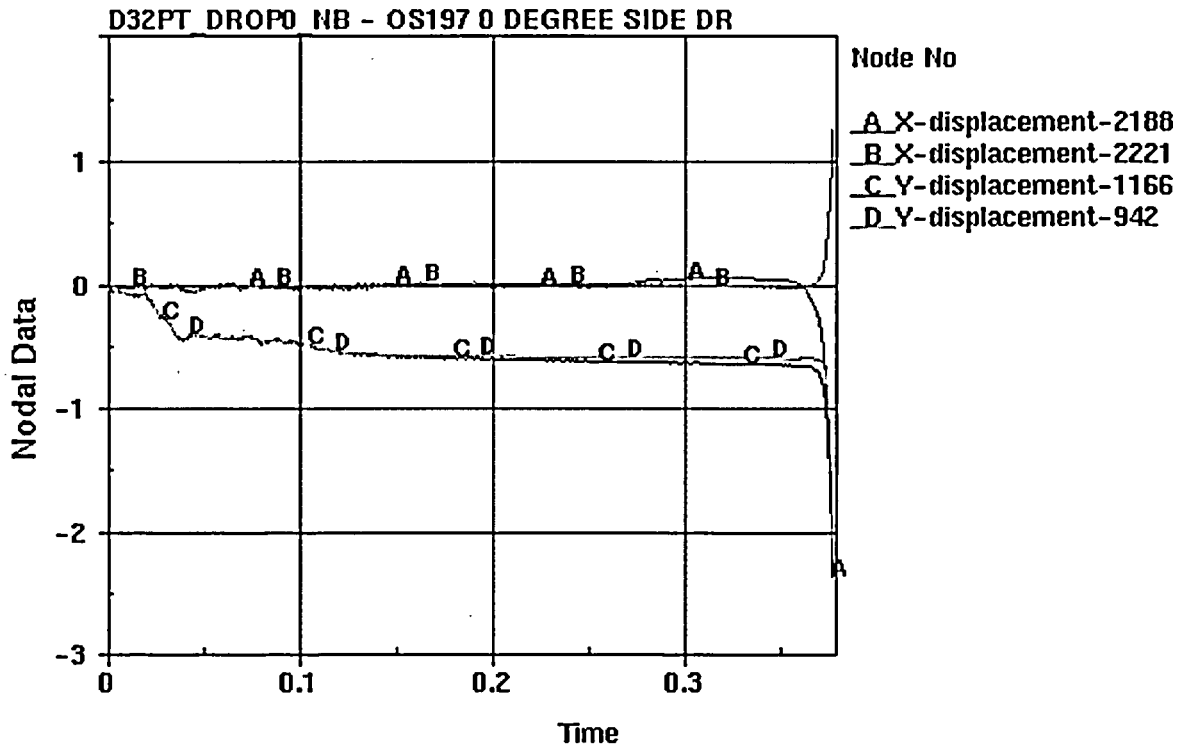


Figure M.3.7-6
Displaced Shape at 113g, LS-DYNA Confirmatory Stability Analysis for 0° Side Drop
with Steel Transition Rails
(Support Rails at ±18.5°)

(See displacement time history on following page)



Time	g-load
0.10 sec.	1. g
0.15 sec.	26. g
0.20 sec.	50. g
0.25 sec.	75. g
0.30 sec.	90. g
0.35 sec.	105. g
0.40 sec.	120. g
0.45 sec.	135. g

Figure M.3.7-7
Displacement Time History, LS-DYNA Confirmatory Stability Analysis for 0° Side Drop
with Steel Transition Rails

(See previous page for displaced shape and node locations)

D32PT_DROP180NB - OS197 180 DEGREE SIDE
Time = 0.414

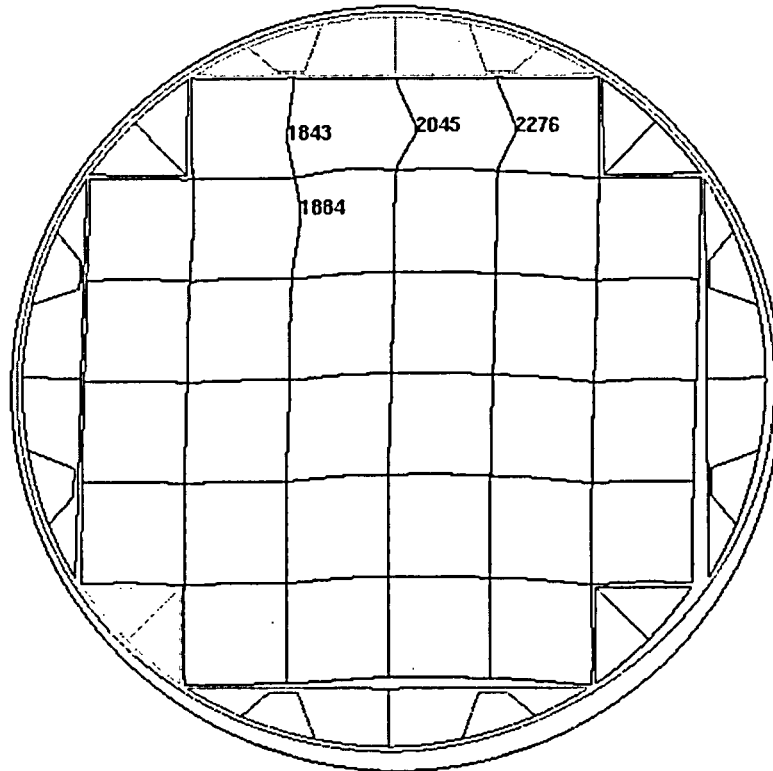
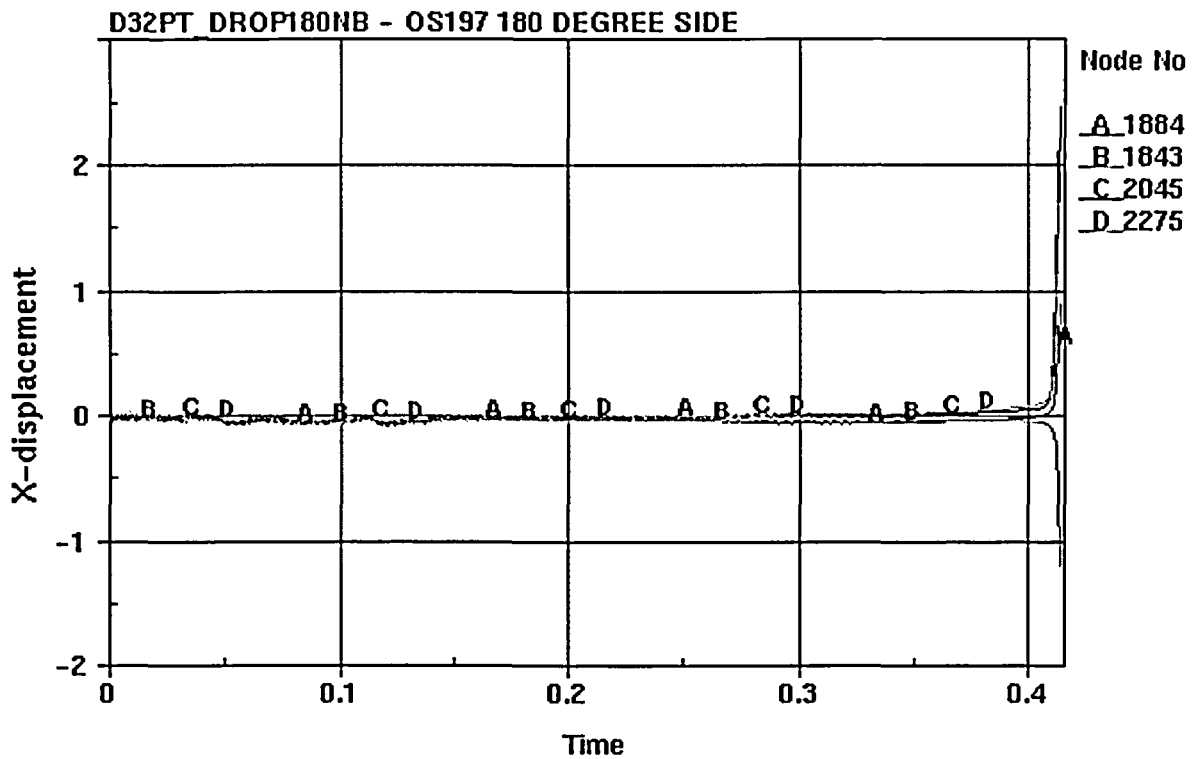


Figure M.3.7-8
Displaced Shape at 124g, LS-DYNA Confirmatory Stability Analysis for 180° Side Drop
with Steel Transition Rails
(No Cask Rails at 180°)
(See displacement time history on following page)



Time	g-load
0.10 sec.	1. g
0.15 sec.	26. g
0.20 sec.	50. g
0.25 sec.	75. g
0.30 sec.	90. g
0.35 sec.	105. g
0.40 sec.	120. g
0.45 sec.	135. g

Figure M.3.7-9
Displacement Time History, LS-DYNA Confirmatory Stability Analysis for 180° Side Drop
with Steel Transition Rails

(See previous page for displaced shape and node locations)

32PT PS, 45 DEG., STRESS IN OS197 (XFER)
Time = 0

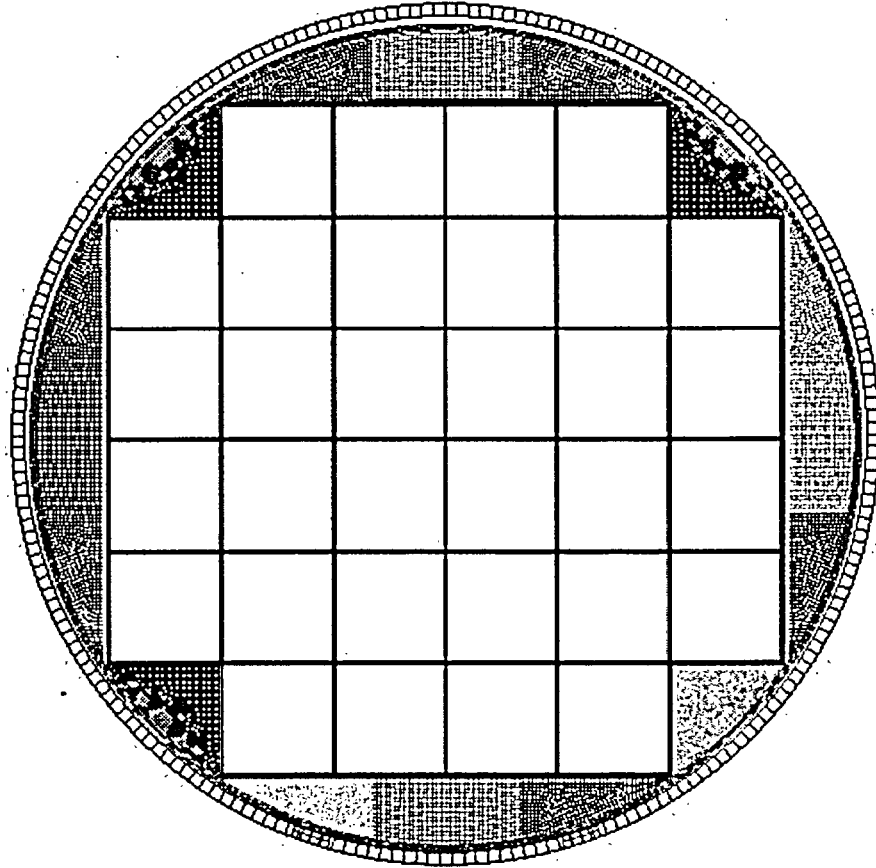


Figure M.3.7-10
LS-DYNA 32PT Basket Model with Aluminum Transition Rails (3-Piece R90)

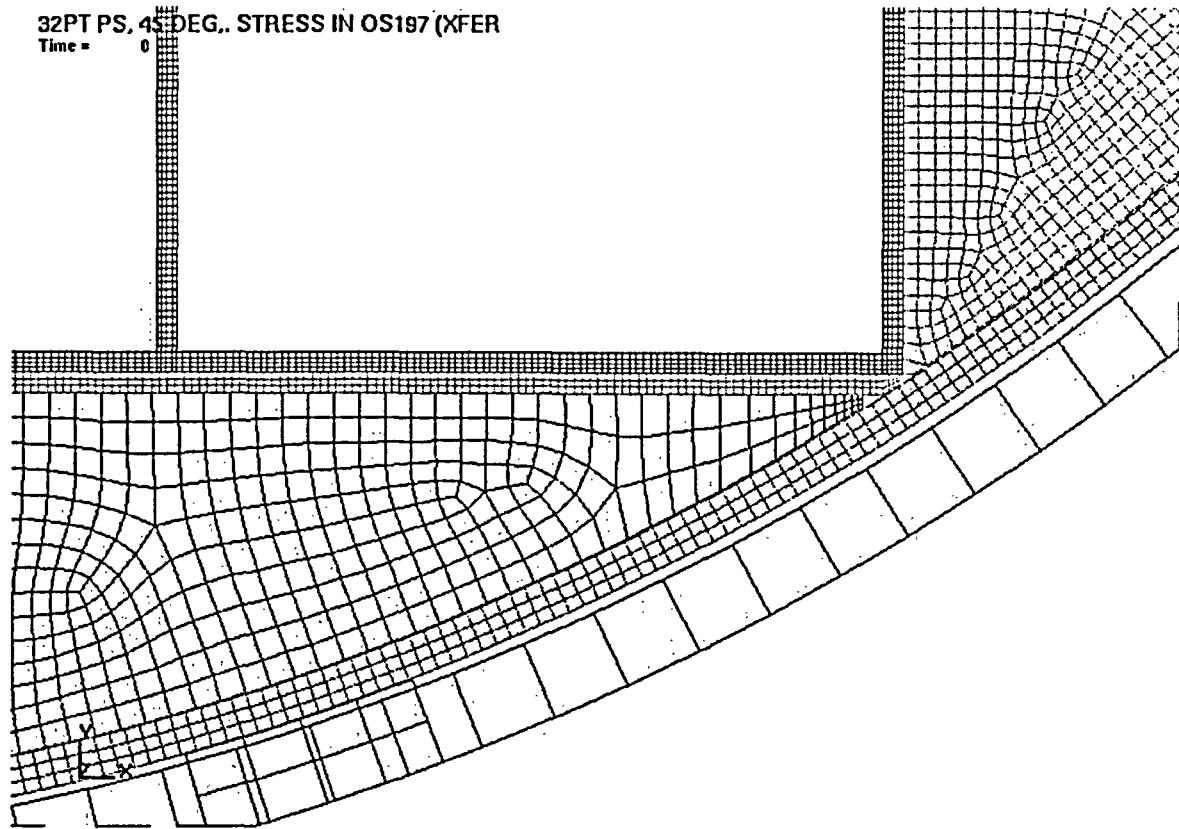


Figure M.3.7-11
LS-DYNA 32PT Basket Model with Aluminum Transition Rails (3-Piece R90) –
Detailed View

32PT PS, 45 DEG., STRESS IN OS197 (XFER)

Time = 0.15
Contours of Temperature
min=367, at node# 40002
max=704.8, at node# 9817

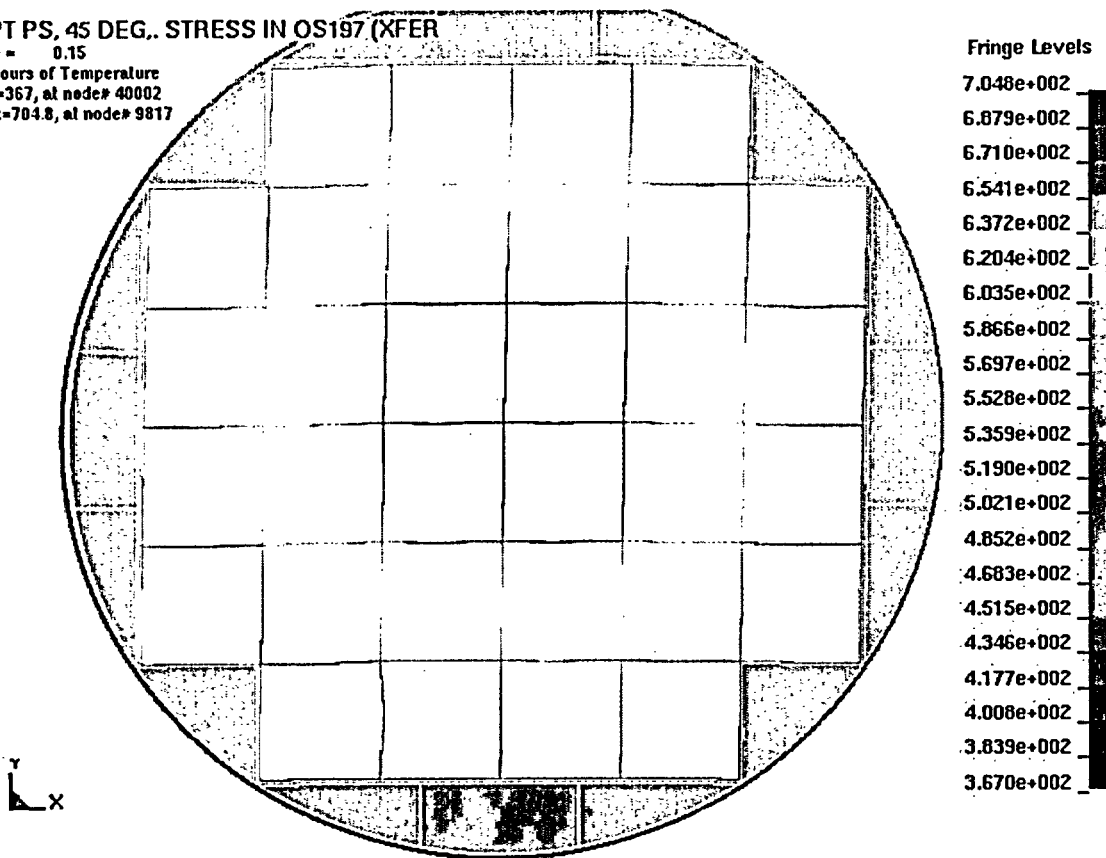


Figure M.3.7-12
32PT Basket with Aluminum Transition Rails Temperature Distribution,
100°F in Cask

M.3.8 References

- 3.1 American Society of Mechanical Engineers, ASME Boiler and Pressure Vessel Code, Section III, Subsections NB, NF, NG, and Appendices 1998, with 2000 Addenda including Code Case N-595-2.
- 3.2 American Society of Mechanical Engineers, ASME Boiler and Pressure Vessel Code, Section II, Part D, 1998 with 2000 Addenda.
- 3.3 Kaufman, J.G., ed., "Properties of Aluminum Alloys: Tensile, Creep, and Fatigue Data and High and Low Temperatures", The Aluminum Association (Washington, D.C.) and ASM International (Metals Park, Ohio), 1999.
- 3.4 Pacific Northwest Laboratory Annual Report – FY 1979, "Spent Fuel and Fuel Pool Component Integrity," May 1980.
- 3.5 G. Wranglen, "An Introduction to Corrosion and Protection of Metals," Chapman and Hall, 1985, pp. 109-112.
- 3.6 A.J. McEvily, Jr., ed., "Atlas of Stress Corrosion and Corrosion Fatigue Curves," ASM Int'l, 1995, p. 185.
- 3.7 TN West Document No. 31-B9604.97-003, dated December 19, 1997; Addendum to TN West Document No. 31-B9604.0102, Rev. 2, "An Assessment of Chemical, Galvanic and Other Reactions in NUHOMS® Spent Fuel Storage and Transportation Casks."
- 3.8 Baratta, et al. "Evaluation of Dimensional Stability and Corrosion Resistance of Borated Aluminum," Final Report submitted to Eagle-Pitcher Industries, Inc. by the Nuclear Engineering Department, Pennsylvania State University.
- 3.9 "Hydrogen Generation Analysis Report for TN-68 Cask Materials," Test Report No. 61123-99N, Rev. 0, Oct 23, 1998, National Technical Systems.
- 3.10 W.C. Young, "Roark's Formulas for Stress and Strain," Sixth Edition, McGraw-Hill, New York, N.Y., 1989.
- 3.11 ANSYS Engineering Analysis System, Users Manual for ANSYS Rev. 5.6, Swanson Analysis Systems, Inc., Houston, PA, 1998.
- 3.12 U.S. Nuclear Regulatory Commission (U.S. NRC), "Standard Format and Content for the Safety Analysis Report for an Independent Spent Fuel Storage Installation (Dry Storage)," Regulatory Guide 3.48 (Task FP-029-4), (October 1981).
- 3.13 ANSI N14.5-1997, "Leakage Tests on Packages for Shipment," February 1998.

- 3.14 American National Standard, "Design Criteria for an Independent Spent Fuel Storage Installation (Dry Storage Type)," ANSI/ANS 57.9-1984, American Nuclear Society, La Grange Park, Illinois (1984).
- 3.15 U.S. Atomic Energy Commission, "Damping Values for Seismic Design of Nuclear Power Plants," Regulatory Guide 1.61, (October 1973).
- 3.16 R. D. Blevins, "Formulas for Natural Frequency and Mode Shape," Van Nostrand Reinhold Co., New York, N.Y., (1979).

M.4 Thermal Evaluation

M.4.1 Discussion

The NUHOMS[®]-32PT system is designed to passively reject decay heat during storage and transfer for normal, off-normal and accident conditions while maintaining temperatures and pressures within specified regulatory limits. Objectives of the thermal analyses performed for this evaluation include: (1) determination of maximum and minimum temperatures with respect to material limits to ensure components perform their intended safety functions, (2) determination of temperature distributions for the NUHOMS[®]-32PT DSC components to support the calculation of thermal stresses for the structural components, (3) determination of maximum internal pressures for the normal, off-normal and accident conditions, (4) determination of the maximum fuel cladding temperature, and (5) confirmation that this temperature will remain sufficiently low to prevent unacceptable degradation of the fuel during storage.

The methodology used to calculate the effective fuel conductivity and to predict the fuel and basket temperature distribution in the NUHOMS[®]-32PT DSC has been benchmarked [4.25] against experimental data obtained for the TN-24 cask [4.26]. The results of the benchmarking study show that with the cask in a horizontal configuration, the TN methodology predicted fuel cladding temperatures which are 77°F higher than the test data.

In the specific case of the TN-24 cask, with the cask backfilled with helium and in a horizontal configuration, the maximum fuel cladding temperature noted in the PNL Test Report [4.26] was 419°F. The use of TN-24 test data is appropriate for validating the thermal model which is intended for use at higher temperature levels based on the following justification:

- For a thermal model that captures the basic thermo physical processes (i.e., conduction, convection, and radiation) present, the primary areas of uncertainty will be the modeling of the geometry and the thermal properties used for each component. Once the correct geometry and thermal properties are captured, the effect of higher temperature levels on the fundamental heat transfer processes involved is well understood and documented. Thus, simply changing the temperature level for a simulation will not necessarily increase the uncertainty level for the thermal model.
- Changes to the thermal conductivity of the metallic components with temperature are well understood and documented for temperature levels well in excess of 700°F. As such, the effect is easily captured through the use of temperature dependant properties.
- Radiation heat transfer is a function of view factor, surface area, and emissivity. View factors and surface area do not change with increased temperature level. As such, a thermal model that incorporates radiation exchange and which has been validated at a lower temperature is typically conservative (i.e., yield higher temperatures) for application at a higher temperature level.

- Any impact on temperatures due to the potential changes in the thermal parameters between the TN-24 temperature regime and the NUHOMS[®]-32PT DSC temperature regime is fully bounded by the conservatism demonstrated in the results of the benchmark analysis.

Therefore, a thermal model that has been properly constructed and predicts conservatively high temperatures in comparison with the TN-24 test data can be fully expected to yield accurate results at the higher temperature levels similar of the NUHOMS[®]-32PT DSC design.

Several thermal design criteria are established for the thermal analysis of the 32PT DSC basket as discussed below.

- Maximum temperatures of the confinement structural components must not adversely affect the confinement function,
- Maximum fuel cladding temperature limit of 400°C (752°F) is applicable to normal conditions of storage and all short term operations including vacuum drying and helium backfilling of the 32PT DSC per Interim Staff Guidance (ISG) No. 11, Revision 2 [4.24]. In addition, ISG-11 does not permit thermal cycling of the fuel cladding with temperature differences greater than 65°C (117°F) during drying and backfilling operations,
- Maximum fuel cladding temperature limit of 570°C (1058°F) is applicable to accidents or off-normal thermal transients [4.24],
- The maximum DSC cavity internal pressures during normal, off-normal and accident conditions must be below the design pressures of 15 psig, 20 psig and 105 psig, respectively, and
- Figure M.4-1, Figure M.4-2, and Figure M.4-3 show the heat load zoning configurations used in the NUHOMS[®]-32PT DSC design. The maximum total heat load per DSC is 24 kW or 22.4 kW depending on the specific heat load zoning configuration.

The analyses consider the effect of the decay heat flux varying axially along a fuel assembly. The axial heat flux profile for a PWR fuel assembly is shown in Figure M.4-4 and is based on [4.3].

A description of the detailed analyses performed for normal storage and transfer conditions is provided in Section M.4.4, off-normal conditions in Section M.4.5, accident conditions in Section M.4.6, and loading/unloading conditions in Section M.4.7. The thermal evaluation concludes that with a design basis heat load of up to 24 kW per DSC, all design criteria are satisfied.

The effective thermal conductivity of the fuel assemblies used in the 32PT DSC thermal analysis is based on the conservative assumption of radiation and conduction heat transfer only where any convection heat transfer is neglected. In addition, the fuel assembly with the lowest effective thermal conductivity at the maximum heat load, WE 14x14, is selected as the basis for the thermal analysis. Section M.4.8 presents the calculations that determined WE 14x14 to be the fuel assembly with the lowest effective thermal conductivity in a helium or vacuum environment.

The thermal analysis model conservatively neglects convection heat transfer in the basket regions.

The basket design used for the NUHOMS[®]-32PT DSC is similar to the basket design of the TN-32 cask [Docket 72-1021]. Both designs use a tube and support rail type of basket which is significantly different than the spacer disc and guide sleeve type of basket design used for the NUHOMS[®]-24P DSCs.

M.4.2 Summary of Thermal Properties of Materials

The analyses use interpolated values where appropriate for intermediate temperatures. The interpolation assumes a linear relationship between the reported values. The use of linear interpolation between temperature values in the tables for determining intermediate value of property is justified by the near-linear behavior as a function of temperature for the range of interest.

The emissivity of stainless steel is 0.587 [4.7]. For additional conservatism an emissivity of 0.46 for stainless steel is used for the basket steel plates in the analysis. The emissivity values assumed in the analysis for the aluminum sheets (Type 1100) and aluminum based neutron poison plates is 0.85 which is achieved by either anodizing or other processes. The emissivity of the oxidized Zircaloy surface is 0.8 [4.14]. Emissivity for the aluminum rail material (Type 6061) is not required for the analysis because radiation between the rails and the DSC shell is conservatively neglected in the analysis. For the two alternate basket configuration shown in Figure M.4-22, a minimum emissivity value of 0.8 is assumed for the neutron poison plates.

The tables below provide the thermal properties of materials used in the analysis of the NUHOMS®-32PT DSC.

1. PWR Fuel with Helium Backfill

The effective thermal conductivity is the lowest calculated value for the various PWR fuel assembly types that may be stored in this DSC and corresponds to the WE 14x14 PWR assembly. Section M.4.8 presents the calculations that determined WE 14x14 to be the fuel assembly with the lowest effective thermal conductivity in both helium and vacuum environment.

Temperature (°F)	K (Btu/min-in-°F)	ρ (lb _m /in ³)	T (°F)	C _p (Btu/lb _m -°F)
Fuel in Helium, Transverse [Section M.4.8]				
138	2.894E-04	0.1166	80	0.0592
233	3.317E-04		260	0.0654
328	3.968E-04		692	0.0725
423	4.744E-04		1502	0.0778
519	5.668E-04			
616	6.715E-04			
714	7.879E-04			
812	9.208E-04			

Temperature (°F)	K (Btu/min-in-°F)	ρ (lb _m /in ³)	T (°F)	C _p (Btu/lb _m -°F)
Fuel in Helium, Axial [Section M.4.8]				
200	7.949E-04	0.1166	See values above	
300	8.387E-04			
400	8.824E-04			
500	9.189E-04			
600	9.554E-04			
800	1.036E-03			

2. PWR Fuel in Vacuum

Temperature (°F)	K (Btu/min-in-°F)	ρ (lb _m /in ³)	T (°F)	C _p (Btu/lb _m -°F)
Fuel in a Vacuum [Section M.4.8]				
215	9.484E-05	0.1166	80	0.0592
288	1.246E-04		260	0.0654
367	1.633E-04		692	0.0725
452	2.119E-04		1502	0.0778
540	2.701E-04			
632	3.373E-04			
726	4.125E-04			
822	4.949E-04			

3. Zircaloy

Temperature (°F)	K (Btu/min-in-°F) [4.14]	ρ (lb _m /in ³) [4.28]	C _p (Btu/lb _m -°F) [4.14]	
200	0.0109	0.237	80	0.067
300	0.0115		260	0.072
400	0.0121		692	0.079
500	0.0126		1502	0.090
600	0.0131		-	
800	0.0142			

4. UO₂ Fuel Pellet

Temperature (°F)	K (Btu/min-in-°F) [4.14]	ρ (lb _m /in ³) [4.28]	C _p (Btu/lb _m -°F) [4.14]	
200	5.537E-3	0.396	32	0.056
300	5.038E-3		212	0.063
400	4.622E-3		392	0.068
500	4.270E-3		752	0.072
600	3.968E-3		2192	0.079
700	3.707E-3			
800	3.478E-3			

5. SA-240, Type 304 Stainless Steel [4.4]

Temperature (°F)	K (Btu/min-in-°F)	ρ (lbm/in ³)	C_p (Btu/lb _m -°F)
70	0.0119	0.284	0.116
100	0.0121		0.117
150	0.0125		0.119
200	0.0129		0.121
250	0.0133		0.124
300	0.0136		0.125
350	0.0140		0.127
400	0.0144		0.128
500	0.0151		-
600	0.0157		-
700	0.0164		-
800	0.0169		-

6. SA-240 Type XM-19 (22Cr-13Ni-5Mn) [4.4]

Temperature (°F)	K (Btu/min-in-°F)	ρ (lb _m /in ³)	C_p (Btu/lb _m -°F)
70	8.89e-3	0.284	0.113
100	9.17e-3		0.116
150	9.58e-3		0.119
200	9.86e-3		0.120
300	0.0107		0.125
400	0.0114		0.127
500	0.0122		0.130
600	0.0129		0.133
700	0.0138		0.135
800	0.0144		0.137
900	0.0150		0.137

7. Aluminum, Type 1100 [4.4]

Temperature (°F)	K (Btu/min-in-°F)	ρ (lb _m /in ³)	C _p (Btu/lb _m -°F)
70	0.185	0.098	0.214
100	0.183		0.216
150	0.181		0.219
200	0.178		0.222
250	0.177		0.224
300	0.175		0.227
350	0.174		0.229
400	0.173		0.232
774	0.173(*)		0.232*

* For aluminum Type 1100 and aluminum based neutron poison material, the calculated maximum temperatures do not exceed 774°F during blocked vent conditions. The assumption of constant conductivity value at 400°F for temperatures up to 774°F is justified since, for pure aluminum, the conductivity change is approximately 2% for range of 400°F – 774°F [4.19]. Therefore, this small change would have a negligible impact on thermal results.

8. Aluminum, Type 6061 (used for transition rails only) [4.4]

Temperature (°F)	K (Btu/min-in-°F)	ρ (lb _m /in ³)	C _p (Btu/lb _m -°F)
70	0.133	0.098	0.213
100	0.135		0.215
150	0.136		0.218
200	0.138		0.221
250	0.139		0.223
300	0.140		0.226
350	0.141		0.228
400	0.142		0.230
633	0.142(*)		0.230(*)

(*) Assumed values.

9. Aluminum Based Neutron Poison (from Section M.4.3)

Temperature (°F)	K (Btu/min-in-°F)	ρ (lb _m /in ³)**	C _p (Btu/lb _m -°F)**
68	0.120	0.098	0.214
212	0.144		0.222
482	0.148		0.232
572	0.148		0.232
774	0.148(*)		0.232(*)

(*) Assumed values.

(**) Assumed to be the same as aluminum.

10. Air [4.5]

Temperature (°F)	K (Btu/min-in-°F)	ρ (lb _m /in ³)	C _p (Btu/lb _m -°F)
71	2.075E-5	4.323e-5	0.240
107	2.199E-5	4.051e-5	0.241
206	2.528E-5	3.443e-5	0.242
314	2.869E-5	2.963e-5	0.243
404	3.139E-5	2.656e-5	0.245
512	3.447E-5	2.361e-5	0.248
602	3.693E-5	2.159e-5	0.251
692	3.929E-5	1.991e-5	0.253
764	4.114E-5	1.875e-5	0.256
800	4.203E-5	1.823e-5	0.257

11. Helium [4.6]

Temperature (°F)	K (Btu/min-in-°F)	ρ (lb _m /in ³)	C _p (Btu/lb _m -°F)
200	1.361E-4	4.81e-6	1.240
300	1.493E-4	4.18e-6	
400	1.635E-4	3.69e-6	
500	1.793E-4	3.31e-6	
600	1.949E-4	2.99e-6	
700	2.094E-4	2.74e-6	
800	2.232E-4	2.52e-6	

M.4.3 Specifications for Components

The thermal conductivity of the neutron poison plates must be verified by testing. The neutron poison plates must have the following minimum thermal conductivity.

Temperature (°F)	Thermal Conductivity (Btu/min-in-°F)
68	0.120
212	0.144
482	0.148
572	0.148
774	0.148

M.4.4 Thermal Evaluation for Normal Conditions of Storage (NCS) and Transfer (NCT)

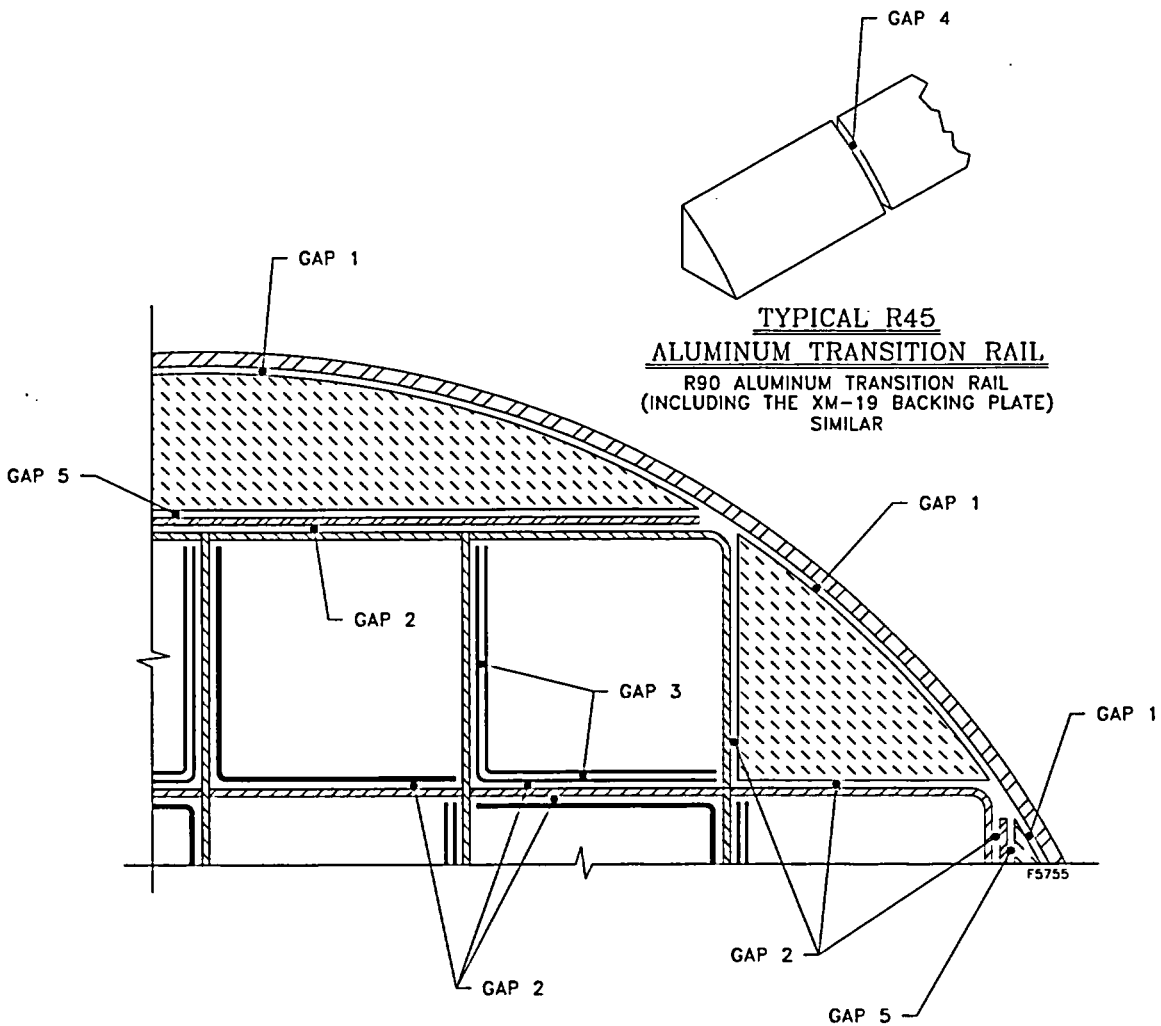
M.4.4.1 NUHOMS[®]-32PT DSC Thermal Models

The NUHOMS[®]-32PT DSC finite element models are developed using the ANSYS computer code [4.9]. ANSYS is a comprehensive thermal, structural and fluid flow analysis package. It is a finite element analysis code capable of solving steady state and transient thermal analysis problems in one, two or three dimensions. Heat transfer via a combination of conduction, radiation and convection can be modeled by ANSYS. Solid entities are modeled by SOLID70 Elements for 3-D models and PLANE55 elements for 2-D models.

M.4.4.1.1 NUHOMS[®]-32PT DSC Basket and Payload Model

The three-dimensional model (Figure M.4-5) represents the NUHOMS[®]-32PT DSC with all aluminum transition rails, and includes the geometry and material properties of the basket components, the basket rails, and DSC shell. The cross-section view is shown in Figure M.4-6. Each component of the basket (XM-19 grid, poison plates, aluminum plates, and aluminum transition rails) is modeled individually with SOLID70 elements. The gaps between adjacent basket components are also represented with SOLID70 elements with helium or air conductivity as appropriate. The material properties from Section M.4.2 are used for the fuel region. Within the model, heat is transferred via conduction through fuel regions, the poison plates, steel of the basket and the gas gaps between the poison plate and steel members. Generally, good surface contact is expected between adjacent components within the basket structure. However, to bound the heat conductance uncertainty between adjacent components owing to imperfect contact between the neutron poison material, aluminum and the basket grid structure, uniform gaps along the entire surfaces are assumed. This is a conservative assumption because, although there will be imperfect contact between the adjacent plates, they will be in contact with each other at most of the locations. Therefore, thermal resistance to heat flow from the fuel assembly out to the DSC surface is lower with the actual imperfect contact as compared with the modeled uniform gaps along the entire surfaces. The gaps used in the thermal analysis of the 32PT DSC are summarized in the table below and shown in the figure below.

Gap Number	Gap Location	Gap Size, Inches
1	DSC Shell and Transition Rails	0.08
2	Basket grid structural plates and adjacent rails, or aluminum or composite material poison plates	0.0075
3	Aluminum and composite material poison plates	0.00375
4	Between any two pieces of aluminum rails in axial direction	0.125
5	Aluminum block and XM-19 plate for R-90 rail	0.0075



All heat transfer across the gaps is by gaseous conduction. Other modes of heat transfer i.e. radiation and convection across the gaps are conservatively neglected. Heat is transferred through the basket support rails via conduction.

Each aluminum rail may be fabricated as a single piece or in separate segments (3 maximum). Rails consisting of three segments are assumed for thermal analyses. An axial gap of 0.125 in. is considered between any two pieces of aluminum rail. The elements representing the XM-19 grid structure include an adjustment to the conductivity to account for gaps between the basket components.

The 3-D model is extended to approximately half the length of the DSC cavity, or 83.8 in. to model the bottom half of the canister. A symmetry boundary is applied on the axial top of the model. The heat generations are applied over the active fuel, starting from 8.625 in. from the bottom of the fuel regions and extending all the way to the top of the model. The placement of the active fuel and the model size results in slight overprediction of temperatures since the symmetry boundary at $(167/2 - 8.625) = 74.875$ in. from the beginning of active fuel is located well beyond half of the active fuel, or $141.8/2 = 70.9$ in., where peak temperatures would be expected. Active length of B&W 15x15 assembly is shorter than that of WE 14x14 assembly. Therefore using the active length of B&W assembly results in higher heat generating rates in the model, which is conservative. In addition, active fuel of WE 14x14 assembly begins about 4" from the bottom of fuel assembly. Shifting the active fuel length to 8.625" from the bottom, shifts the active fuel length away from regions of dropping DSC shell temperature in the model. This is conservative, since being away from the regions of dropping DSC shell temperatures causes higher fuel cladding temperature. Longer DSC cavity configurations (32PT-L100 and 32PT-L125) provide larger radial surface areas for heat dissipation and are therefore bounded by the shorter cavity (32PT-S100 and 32PT-S125) DSC configurations.

A basket model with alternate poison plate configuration has been developed with the following changes.

1. The emissivity of the anodized poison plate has a minimum value of 0.8, which will cause a reduction in the transverse fuel effective thermal conductivities.
2. The R90 aluminum transition rails are split into three sections in the radial direction.
3. The intermittent weld with 8 in. sections of weld out of every 10 inches of basket length is explicitly modeled. Figure M.4-23 shows the gap in the rail and the intermittent weld as modeled.
4. All the poison plate/aluminum plates "chevrons" have been rotated so that they have an "L" or reversed "L" orientation. There are two types of poison plate configurations developed. One is a 16 poison plate and the second is a 24 poison plate configuration as shown in Figure M.4-22.

The analysis performed for the basket with alternate poison plate configuration concludes that the resultant maximum component temperatures and DSC internal pressures are all bounded by the basket with original poison plate configuration.

M.4.4.1.2 Mesh Sensitivity Study

The 32PT DSC model described above is based on a 14x14 mesh for the cross section of each fuel assembly. A sensitivity study was performed with fuel mesh sizes of 12x12 and 16x16. The results show that convergence is achieved with a 14x14 mesh and the maximum fuel cladding

temperature change is less than 1°F with a 16x16 mesh. Hence the 14x14 mesh size model is mesh insensitive.

M.4.4.1.3 Boundary Conditions for the DSC Basket Model

For the DSC shell near the end (where the shield plug is located), a linear decrease in the temperature to the end is assumed. The temperatures at the end of the cylindrical shell are assumed to be 90% (based on degrees Rankine) of the temperature in the active fuel region. This assumption is reasonable for the normal and off-normal storage and transfer cases because the heat generating region is 8.675" from the bottom cover plate. The DSC shell temperature drop from the active fuel region to the bottom cover plate is expected to be exponential because the metal on the end of the fuel assembly should thermally behave as a fin. An exponential drop would result in lower temperatures and thus more axial heat transfer. Therefore, the linear decrease is considered reasonable.

To determine the sensitivity of the 32PT DSC thermal model to the variation in the assumed boundary conditions at the axial periphery of the model (the cold end of the DSC), two alternate configurations are evaluated. Alternate No. 1 assumes the same DSC shell temperature profile as described above, but extended it to the entire DSC length. No change was made to the manner in which the DSC end was modeled (a linear temperature distribution between T_{top} , T_{side} and T_{bottom} was modeled). Alternate No. 2 is similar to Alternate No. 1 but applied adiabatic boundary condition at the DSC end. The results show that the variations in the boundary conditions (at the cold end of the DSC) have a negligible impact on the heat transfer within the hottest region of the DSC and on the maximum fuel cladding temperature.

M.4.4.1.4 Heat Generation for the DSC Basket Model

Heat generation is calculated based on the dimensions of the fuel and basket. The heat is assumed to be distributed evenly radially through the 8.7 in. square nominal fuel cell opening. Axial variations are accounted for in ANSYS by using the peaking factors in Figure M.4-4 along the active length of the PWR fuel assembly. Heat generation rates with the corresponding peaking factors are applied according to the decay heat load zoning configurations 1 through 3 given in Figure M.4-1, Figure M.4-2, and Figure M.4-3.

The equation below shows a typical calculation for peak heat generation (for 1.2 kW heat load) based on these peaking factors.

$$\ddot{q} = \frac{1.2kW \cdot 1.108 \cdot 3414 \frac{Btu}{hr} \cdot \frac{1hr}{60min}}{(8.7in)^2 \cdot 141.8in} = 7.049e-3 \frac{Btu}{min \cdot in^3}$$

A peaking factor is applied to the base heat generation rate based on axial location of each element within 12 zones of the active fuel region (a half-length model). The volumetric heat generation multiplied by the average peaking factor of each zone is then used in the ANSYS models.

An example of the ANSYS input file routine, which applies the decay heat load for outer fuel assemblies is shown in Section M.4.11.1.

The normal conditions of storage are used for the determination of the maximum fuel cladding temperature, basket component temperatures, NUHOMS[®]-32PT DSC internal pressure and thermal stresses. The 10CFR Part 71.71(c) insolation averaged over a 24-hour period is used as steady state boundary condition.

M.4.4.1.5 Thermal Model of DSC in Horizontal Storage Module

The methodology used to calculate the HSM concrete and DSC shell temperatures with 32PT DSC is the same as that used for the NUHOMS[®]-24P DSC design described in FSAR Section 8.1.3. The axial location of the cross-section is the mid-section of the HSM, which also corresponds to the mid-section of the DSC at the approximate center of the active fuel.

There are two inlet and two outlet vents at each of the two sidewalls of the HSM. The location of these vents is designed such that it results in nearly uniform natural circulation flow patterns around the heat-generating region of a fuel assembly. The methodology given in Section 8.1.3 is used to calculate bulk air temperatures within the HSM. Note that bulk air temperatures are based on the conservative assumption of 100% of the heat removal from the DSC surface by convection ignoring any heat removal by radiation to the heat shield and concrete. These conservative assumptions provide reasonable assurance that the selected cross-section of the HSM/DSC results in hottest temperatures.

To determine the temperature distribution on the surface of the DSC during storage, a two-dimensional ANSYS model of the cross section of the HSM with loaded DSC is used to represent the NUHOMS[®]-32PT system (Figure M.4-7). Solid entities are modeled in ANSYS by PLANE55 two-dimensional thermal elements. Radiation within the HSM is modeled in ANSYS by MATRIX50 super elements.

The decay heat from the payload is modeled as a uniform heat flux on the inner surface of the DSC shell. Heat from the DSC surface dissipates via natural convection to the air within the HSM and via radiation to the HSM heat shield and walls. Heat dissipates from the HSM heat shield via radiation to walls and then via conduction through the walls of the HSM, via convection to the HSM air and via convection and radiation from the HSM outer surfaces to the ambient environment.

There are two length configurations for the NUHOMS[®]-32PT DSC: Short (186.2 inches long) and Long (192.2 inches). The NUHOMS[®] HSM can accommodate DSCs with lengths from 186.05 to 195.92 inches. The shorter HSM and shorter 32PT DSC is used to calculate the maximum HSM concrete temperatures. This configuration is conservative in calculating HSM concrete temperatures because it has higher thermal resistance to the air flow compared to the configuration with the longer HSM and longer 32PT DSC.

M.4.4.1.6 Transfer Cask (TC) Thermal Model

To determine the temperature distribution on the surface of the DSC during transfer operations, a two-dimensional model of the cross-section of the TC with a loaded 32PT DSC was created using ANSYS.

The 32PT DSC is qualified for transfer in the OS197/OS197H transfer cask. The geometry of the transfer cask used in the thermal analysis is identical for both OS197 and OS197H casks.

The ANSYS model shown in Figure M.4-8 represents a two-dimensional slice of the OS197 cask at the axial centerline. The following dimensions from Appendix E are used for the model:

- The inner diameter of the inner liner is 68",
- The thickness of the inner liner is 0.5" and it is made of stainless steel (SA-240, Type 304),
- The thickness of the lead is 3.56",
- The air gap between lead and structural shell is assumed to be 0.03125",
- The thickness of the structural shell portion is 1.5". This shell is made of stainless steel (SA-240, type 304) material,
- The neutron shield is water, with 24 stainless steel stiffeners which connect the structural shell to the neutron shield panel. Each stiffener consists 0.12" thick plate and is made up of two side plates 4.25" long oriented at 45° that connect the structural shell to the neutron shield panel, and, a top side 1.00" long welded to the neutron shield panel. The thickness of the neutron shield region is 3". The stiffener material is SA-240, type 304,
- The neutron shield panel is constructed of SA-240, Type 304 material and is 0.1875" thick, and
- DSC shell thickness is 0.5".

The material properties are taken from Section 8.1 with the exception of the calculation of the effective conductivity of water within the neutron shield, which is calculated in Section M.4.9.

The neutron shield region of the cask model is broken into 24 angular segments 7.5 degrees each. For each angular segment, the bounding k_{eff} value (as calculated in Section M.4.9) is applied to the ANSYS model.

Radiation is modeled by overlaying surface elements and using the /AUX12 processor to compute view factors to the environment with SURF151 elements in ANSYS. The emissivity of the outer surface is 0.587 for unfinished steel [4.7]. An absorptivity of the outer surface is 0.587. Radiation is also modeled between the DSC shell surface and the cask inner surface with unfinished steel emissivities of 0.587 [4.7] using the /AUX12 processor in ANSYS.

The DSC shell is offset in the model to provide a realistic approximation of the horizontal orientation gap thicknesses at the top and bottom of the DSC. The DSC-cask air gap thicknesses

are assumed to be 0.702" at the top and 0.108" at the bottom based on a nominal cask inner diameter of 68" and a nominal shell outer diameter of 67.19". The DSC rests on two cask rails that are located 18.5° from vertical downward below the DSC. A thickness of 0.12" is used for the cask rails. The gap at the bottom closes from 0.12" to 0.105".

Insolation is applied to the top half of the model. The insolation considered is 123 Btu/hr-ft², which is consistent with the maximum insolation used for storage in the HSM. The absorptivity of 0.587 was applied to the outer cask surface.

The convection to the ambient is conservatively based on the average film temperature for convection coefficient evaluation in the ANSYS model.

The heat is applied to the model as a heat flux on the inner surface of the DSC using SURF151 elements in ANSYS. The heat transfer through the ends of the DSC is conservatively neglected in calculating the heat flux. The heat flux is calculated based on DSC shell length as:

$$\ddot{q} = \frac{24kW \cdot 3414 \frac{\text{Btu/hr}}{\text{kW}}}{60 \frac{\text{min}}{\text{hr}} \cdot (\pi \cdot 66 \text{ in} \cdot 186.2 \text{ in})} = 0.0354 \frac{\text{Btu}}{\text{min} \cdot \text{in}^2}$$

A second set of cases with 22.4 kW total heat load (and 0.0330 BTU/min.in²) was run in order to support heat load zoning configuration #3.

An example of ANSYS input file routine that overlays surface effect elements on the top outside surface of the cask is included in Section M.4.11.2.

M.4.4.1.7 Boundary Conditions, Storage

Normal Conditions of Storage analyses of the NUHOMS[®]-32PT DSC within the HSM are carried out for the following ambient conditions:

- Maximum normal ambient temperature of 100°F with insolation,
- Minimum normal ambient temperature of 0°F without insolation, and
- Long-term average maximum ambient temperature of 70°F, with insolation.

The HSM thermal model described in Section M.4.4.1.5 provides the surface temperatures of the DSC shell. These temperatures are applied as boundary conditions to the DSC shell in the basket and payload models in Section M.4.4.1.1 which calculate the temperature distribution in the basket components and fuel.

M.4.4.1.8 Boundary Conditions, Transfer

In accordance with Section 8.1, analyses of the NUHOMS[®]-32PT DSC within the TC are performed for the following ambient conditions:

- Maximum normal ambient temperature of 100°F with insolation, and
- Minimum normal ambient temperature of 0°F without insolation.

The maximum calculated DSC temperatures using the TC thermal model described in Section M.4.4.1.6, are conservatively applied to the exterior surface of the DSC in the DSC/Basket/Payload finite element model in Section M.4.4.1.1.

M.4.4.2 Maximum Temperatures

M.4.4.2.1 Fuel Cladding

M.4.4.2.1.1 Long-Term Storage Temperatures

The maximum fuel cladding temperatures for long-term storage with 70°F ambient condition are evaluated for each of the three decay heat load zoning configurations and compared with the corresponding fuel cladding temperature limit for long-term storage in Table M.4-1.

The conservatisms in the cladding temperature limit method and conservative assumptions included in the calculation of maximum cladding temperatures are described below:

- 1) Credit for any convection in the DSC basket cavity is not taken.
- 2) Conservative gaps are assumed between basket component plates even though adjacent basket components are connected to each other by mechanical fasteners.
- 3) Credit for any radiation in the gaps between the adjacent basket components is not taken.

Based on these conservatisms, there is a higher margin in the calculated maximum cladding temperatures than those shown in Table M.4-1. Thus, there is reasonable assurance that the cladding will maintain its integrity during storage conditions.

M.4.4.2.1.2 Short-Term Event Temperatures

The short-term events are defined in Section M.4.1 for storage and transfer. The results are reported for heat load zoning configuration 1, 2, and 3 which yield the highest fuel cladding temperatures. The maximum fuel cladding temperatures for short-term normal conditions of storage and transfer are given in Table M.4-2.

M.4.4.2.1.3 DSC Basket Material Temperatures

The maximum and minimum temperatures of the basket assembly components for normal conditions of storage and transfer for heat load zoning configurations 1, 2 and 3 are listed in Table M.4-3, Table M.4-4, and Table M.4-5, respectively. The minimum component temperatures reported in these tables represent the minimum temperature for those components at the hottest radial cross section, not the minimum component temperature in the entire basket. The maximum basket temperature distributions for configuration 3 during normal conditions of

storage and transfer are presented in Figure M.4-9 and Figure M.4-10, respectively. The temperature distribution from the bottom to the top of the DSC at the hottest cross-section is shown in Figure M.4-17 for 70°F ambient storage case.

M.4.4.3 Minimum Temperatures

Under the minimum temperature condition of 0°F ambient, the resulting DSC component temperatures will approach 0°F if no credit is taken for the decay heat load. Since the DSC materials, including confinement structures, continue to function at this temperature, the minimum temperature condition has no adverse effect on the performance of the NUHOMS®-32PT DSC.

M.4.4.4 Maximum Internal Pressures

M.4.4.4.1 Pressure Calculation

This section describes the pressure calculations used to determine maximum internal pressures during storage and transfer within the NUHOMS®-32PT DSC and basket when loaded with a payload of worst case B&W 15x15 fuel assemblies with a maximum burnup of 45 GWd/MTU. The limiting fuel assembly type considered in this evaluation is the B&W 15 x 15 assembly. The fission gasses produced by the WE 17x17 are slightly higher than those from the B&W 15x15, but the B&W 15x15 fuel assembly has the highest heavy metal and fuel assembly weight and therefore displaces the most free volume relative to all the other assembly types considered in Chapter M.2.

The calculations include the DSC free volume, the quantities of DSC backfill gas, fuel rod fill gas, and fission products and the average DSC cavity gas temperature. The 32PT-S100, 32PT-S125, 32PT-L100 and 32PT-L125 canister configurations are considered. The 32PT-L100 and 32PT-L125 DSC internal pressure evaluations also include the contribution due to BPRAs. The internal pressures are then calculated using:

$$P = \frac{nRT}{V}$$

where:

- n = Total number of moles of gases,
- R = Universal gas constant,
- T = Gas temperature (°R),
- V = Gas volume, and
- P = Internal pressure.

M.4.4.4.2 Free Volume

M.4.4.4.2.1 DSC Cavity

The DSC Cavity free volumes are shown below:

Canister Type	32PT-S100	32PT-S125	32PT-L100	32PT-L125
Cavity Volume (in ³)	583,580	574,977	604,225	595,623
Basket Volume (in ³)	176,312	173,689	182,613	180,008
Fuel Volume (in ³)	181,126	181,126	185,518	185,518
Free Volume (in ³)	226,141	220,163	236,095	230,097

M.4.4.4.3 Quantity of Helium Fill Gas in DSC

The DSC free volume is assumed to be filled with 3.5 psig (18.2 psia) of helium. The maximum temperatures from the 70°F ambient storage case are used to estimate the number of moles of helium backfill.

The average long-term helium fill temperature for the worst case payload, 449°F (909°R) is used. Using the ideal gas law, the quantity of helium in each DSC is calculated and the results are presented in Table M.4-6.

M.4.4.4.4 Quantity of Fill Gas in Fuel Rod

The volume of the helium fill gas in a B&W 15x15 fuel pin at cold, unirradiated conditions is 1.326 in³, and there are 208 fuel pins in an assembly. The maximum fill pressure is 415 psig (429.7 psia) and the fill temperature is assumed to be room temperature (70°F or 530°R). The quantity of fuel rod fill gas in 32 fuel assemblies is:

$$n_{he} = \frac{(429.7 \text{ psia})(6894.8 \text{ Pa/psi})(32 \cdot 208 \cdot 1.326 \text{ in}^3)(1.6387 \times 10^{-5} \text{ m}^3 / \text{in}^3)}{(8.314 \text{ J/mol} \cdot \text{K})(530^\circ \text{R})(5/9 \text{ K}/^\circ \text{R})}$$
$$n_{he} = 175.0 \text{ g} - \text{moles}$$

Based on NUREG 1536 [4.10], the maximum fraction of the fuel pins that are assumed to rupture and release their fill and fission gas for normal, off-normal and accident events is 1, 10 and 100%, respectively. 100% of the fill gas in each ruptured rod is assumed to be released. The amount of helium fill gas released for each of these conditions is summarized below.

Case	Percentage of Rods Ruptured	Moles of Helium Fill Gas Released
Normal	1	1.75
Off-Normal	10	17.50
Accident	100	175.0

M.4.4.4.5 Quantity of Fission Product Gases in Fuel Rod

The B&W 15x15 fuel assembly used in the pressure calculations is assumed to be burned to 45,000 MWd/MTU, which is the highest burnup proposed for the NUHOMS[®]-32PT configuration. The maximum burnup creates a bounding case for the amount of fission gases produced in the fuel rod during reactor operation. The amounts of tritium, krypton-85 and xenon-131m at STP for each assembly are summarized below.

Isotope	Volume (liters/assy)	Volume (in ³ /assy)
Tritium (H ³)	0.26	16
Kr ⁸⁵	60.4	3,686
Xe ^{131m}	547	33,380
Total	607.7	37,081

The total fission gas volume for a fuel assembly is equal to 607.7 liters (37,081 in³). The total amount of fission gas products produced is calculated using 32°F as:

$$n_{fg} = \frac{(32)(14.7)(6894.8 \text{ Pa / psi})(37,081 \text{ in}^3)(1.6387 \times 10^{-5} \text{ m}^3 / \text{in}^3)}{(8.314 \text{ J / mol} \cdot \text{K})(460^\circ \text{R} + 32^\circ \text{F})(5/9 \text{ K} / ^\circ \text{R})}$$

$$n_{fg} = 867 \text{ g} - \text{moles}$$

The amount of fission gas released into the DSC cavity for normal, off-normal and accident condition cases assuming a 30% gas release from the fuel pellets and a 1%, 10%, and 100% rod rupture percentage, respectively, is summarized below.

Case	Percentage of Rods Ruptured	Moles of Fission Gas Released
Normal	1	2.6
Off-Normal	10	26.0
Accident	100	260

M.4.4.4.6 Quantity of Gas in Control Components (BPRAs)

The 32PT-L100 and 32PT-L125 DSC configurations may include BPRAs. In the NUHOMS[®]-32PT DSC, a maximum of 16 BPRAs per DSC are allowed. These BPRAs have an initial helium fill of 14.7 psia, and if 100% of the boron is consumed, and 30% released into the DSC, a total of 53.8 *(16/24) = 35.9 g-moles of gas could be released to the DSC assuming 100% cladding rupture (the 53.8 g-moles is based on 24 BPRAs in the 24P DSC; from Appendix J, Section J.4).

The percentage of BPRA rods ruptured during normal, off-normal and accident conditions is assumed to be 1%, 10% and 100%, respectively, similar to the assumptions for the fuel rod

rupturing. The maximum amount of gas released to the DSC cavity from the BPRAs for normal, off-normal and accident conditions is given below.

Case	Percentage of Rods Ruptured	Moles of Fission Gas Released per DSC from BPRAs
Normal	1	0.359
Off-Normal	10	3.59
Accident	100	35.9

The maximum average helium temperature for normal conditions of storage and transfer occurs when the 32PT DSC is in the TC with an ambient temperature of 100°F and maximum insolation. This case bounds the 100°F ambient case in the HSM. In addition the maximum pressure will occur with the 45,000 MWd/MTU burnup fuel so that lesser burnups will be enveloped by this calculation. The average helium temperature is 545°F (1005°R), however 550°F (1,010°R) is conservatively used. The maximum normal operating condition pressures are summarized in Table M.4-7.

M.4.4.5 Maximum Thermal Stresses

The maximum thermal stresses during normal conditions of storage and transfer are calculated in Section M.3.

M.4.4.6 Evaluation of Cask Performance for Normal Conditions

The NUHOMS[®]-32PT DSC shell and basket are evaluated for the calculated temperatures and pressures in Section M.3. The maximum fuel cladding temperatures are well below the allowable long-term fuel temperature limits and the short-term limit of 752°F (400°C). The maximum DSC internal pressure remains below 15.0 psig during normal conditions of storage and transfer. Based on the thermal analysis, it is concluded that the NUHOMS[®]-32PT DSC design meets all applicable normal condition thermal requirements.

M.4.5 Thermal Evaluation for Off-Normal Conditions

The NUHOMS[®]-32PT system components are evaluated for the extreme ambient temperatures of -40°F (winter) and 117°F (summer). Should these extreme temperatures ever occur, they would be expected to last for a very short duration of time. Nevertheless, these ambient temperatures are conservatively assumed to occur for a significant duration to result in a steady-state temperature distribution in the NUHOMS[®]-32PT system components.

The 117°F off-normal ambient temperature is considered extreme in a given 24-hour period. It is reasonable to consider a 24-hour average given the large thermal mass of the canister, HSM and transfer casks. The temperature of the fuel is not expected to vary with temperature cycles over 24-hour periods.

In order to calculate a conservative 24-hour average temperature given a maximum temperature, a minimum daily range must be specified. From Table 1 in Chapter 24 of [4.20], the minimum mean daily temperature range in the contiguous United States with a maximum summer ambient above 110°F is 27°F in Needles, California. For the 117°F ambient condition, [4.20] is used to derive a daily average for the steady-state condition with a mean range of 27°F. The mean range is defined as the difference between the average daily maximum and the average daily minimum during the warmest month of the year. The use of a mean range is appropriate since the HSM and DSC would take several days to heat up to steady-state conditions in such a scenario.

Reference [4.20] gives a method for calculating the temperature variations in a day, given a daily range in Chapter 26, Table 3. Percentages ranging between 0 and 100% of the mean range are given as a function of hour in the day. The temperature variation is calculated using this methodology for a maximum temperature of 117°F with daily range of 27°F. A sample calculation shows the expected temperature at 8 o'clock in the morning:

$$T_{amb} = 117 - 0.84 \cdot 27 = 94.3^{\circ}F$$

The remaining calculated temperatures are presented in the table below.

Ambient Temperature Variation on 117°F Ambient Day.		
Time, hour	% Daily Range	T, °F
1	87	93.5
2	92	92.2
3	96	91.1
4	99	90.3
5	100	90.0
6	98	90.5
7	93	91.9
8	84	94.3
9	71	97.8
10	56	101.9
11	39	106.5
12	23	110.8
13	11	114.0
14	3	116.2
15	0	117.0
16	3	116.2
17	10	114.3
18	21	111.3
19	34	107.8
20	47	104.3
21	58	101.3
22	68	98.6
23	76	96.5
24	82	94.9

The corresponding average is 101.8°F. 107°F was used as the ambient air temperature in the steady-state analyses to be conservative for the maximum off-normal condition.

M.4.5.1 Off-Normal Maximum/Minimum Temperatures during Storage

The thermal performance of the NUHOMS®-32PT DSC within the HSM under the extreme minimum ambient temperatures of -40°F with no insolation and 117°F with maximum insolation are evaluated with heat load zoning configurations 1, 2 and 3.

M.4.5.1.1 Boundary Conditions, Storage

Off-normal conditions of storage analyses of the NUHOMS®-32PT DSC within the HSM includes:

- Maximum off-normal ambient temperature of 117°F with insolation, and
- Minimum off-normal ambient temperature of -40° F without insolation.

The HSM thermal model described above provide the surface temperatures that are applied to the DSC, basket and payload model.

M.4.5.2 Off-Normal Maximum/Minimum Temperatures during Transfer

The thermal performance of the NUHOMS[®]-32PT DSC during transfer under the extreme minimum ambient temperature of 0°F with no insolation and 117°F with maximum insolation, and decay heat load configurations 1, 2 and 3 are examined. For transfer operations when ambient temperatures exceed 100°F up to 117°F, a solar shield is used.

M.4.5.2.1 Boundary Conditions, Transfer

In accordance with Section M.4.4.1.6, analyses of a 32PT DSC within the TC are performed for the following ambient conditions:

- Maximum normal ambient temperature of 117°F with solar shield in place, and
- Minimum off-normal extreme ambient temperature of 0°F without insolation.

These analyses determine maximum DSC surface temperatures. The maximum calculated DSC temperatures are applied to the exterior surface of the DSC in the DSC/basket/payload finite element model.

M.4.5.3 Off-Normal Maximum and Minimum Temperatures During Storage/Transfer

According to the NUHOMS[®] CoC 1004, Technical Specification 1.2.4, "TC/DSC Transfer Operations at High Ambient Temperatures" for transfer operations, when ambient temperatures exceed 100°F up to 125°F, a solar shield shall be used to provide protection against direct solar radiation.

The thermal performance of the DSC during transfer operations when the DSC is in the transfer cask without the sunshade at an ambient temperature of 100°F is limiting and bounds the maximum off-normal 117°F transfer case with sunshade. This is demonstrated by results provided in Table M.4-8 and Table M.4-2.

A comparison of the thermal analysis results for 32PT-DSC during transfer operations for the cases of 100°F ambient temperature without sunshade and 117°F ambient temperature with sunshade shows that the maximum fuel cladding temperatures are 720°F (Table M.4-2) and 715°F (Table M.4-8), respectively.

M.4.5.3.1 Fuel Cladding

The results are reported in Table M.4-8 for heat load zoning configurations 1, 2 and 3 which yield the highest fuel cladding temperatures.

M.4.5.3.2 DSC Basket Materials

The maximum and minimum temperatures of the basket assembly for off-normal conditions of storage and transfer for heat load zoning configurations 1, 2 and 3 are listed in Table M.4-9, Table M.4-10, and Table M.4-11, respectively. The minimum temperatures reported for each component are not the minimum absolute component temperature in the entire basket. The minimum component temperatures reported in these tables represent the minimum temperature for those components at the hottest radial cross section. The bounding basket temperature distributions for heat load zoning configuration 3 off-normal conditions of storage and transfer are presented in Figure M.4-11 and Figure M.4-12, respectively.

M.4.5.4 Off-Normal Maximum Internal Pressure During Storage/Transfer

The off-normal condition maximum pressure calculation also considers the DSC in the TC at 100°F ambient. This case bounds the case in which the DSC is in the HSM with 117°F ambient and the 117°F TC case with the sunshade in place. The average helium temperature is 545°F (1005°R), however, 550°F (1010°R) is conservatively used. Per NUREG 1536, the percentage of fuel rods ruptured for off-normal cases is 10%.

A summary of the maximum off-normal operating pressures for the various 32PT DSC configurations are presented in Table M.4-12.

M.4.5.5 Maximum Thermal Stresses

The maximum thermal stresses during off-normal conditions of storage and transfer for the NUHOMS®-32PT DSC are calculated in Section M.3.

M.4.5.6 Evaluation of Cask Performance for Off-Normal Conditions

The NUHOMS®-32PT DSC shell and basket are evaluated for calculated temperatures and pressures in Section M.3. The maximum fuel cladding temperatures are well below the allowable fuel temperature limit of 752°F (400°C) for transfer and 1058°F (570°C) for storage conditions. The maximum DSC internal pressures remain below 20.0 psig during off-normal conditions of storage and transfer. The pressures and temperatures associated with off-normal conditions in the NUHOMS®-32PT DSC design meet all applicable off-normal thermal requirements.

M.4.6 Thermal Evaluation for Accident Conditions

Since the NUHOMS[®] HSMs are located outdoors, there is a remote possibility that the ventilation air inlet and outlet openings could become blocked by debris from such unlikely events as floods and tornadoes. The NUHOMS[®] HSM system design features such as the perimeter security fence and redundant protected location of the air inlet and outlet openings reduces the probability of occurrence of such an accident. Nevertheless, for this conservative generic analysis, such an accident is postulated to occur and is analyzed.

During transfer under maximum ambient temperature and insolation, the loss of the sun shield and the liquid neutron shield in the TC represents the controlling transfer case.

It is determined in Section 3.3.6 that the HSM and DSC contain no flammable material and the concrete and steel used for their fabrication can withstand any credible fire accident condition. Fire parameters are dependent on the amount and type of fuel within the transporter and the fire accident condition shall be addressed within site-specific applications. Licensees are required to verify that loadings resulting from potential fires and explosions are acceptable in accordance with 10CFR72.212(b)(2). The hypothetical fire evaluation for the NUHOMS[®]-32PT system is included in Section M.4.6.3.

M.4.6.1 Blocked Vent Accident Evaluation

For the postulated blocked vent accident condition, the HSM ventilation inlet and outlet openings are assumed to be completely blocked for a 40-hour period concurrent with the extreme off-normal ambient condition of 117°F with insolation.

For conservatism, a transient thermal analysis is performed using the 3-D model developed in Section M.4.4.1, for heat load zoning configurations 1, 2, and 3. Heat load zoning configuration 3 envelopes the temperature results for heat load zoning configurations 1 and 2. When the inlet and outlet vents are blocked, the air surrounding the DSC in the HSM cavity is contained (trapped) in the HSM cavity. The temperature difference between the hot DSC surface and the surrounding cooler heat shield and concrete surfaces in the HSM cavity will result in closed cavity convection. This closed cavity convection in the HSM cavity is accounted for by calculating an effective conductivity of air. The HSM cavity is modeled as a combination of few separate enclosures as described below:

Enclosure 1 includes the HSM cavity within 0° to 90° sector limited by DSC shell surface, vertical and top horizontal heat shield surfaces. Enclosure 2 includes the HSM cavity within -90° to 0° sector limited by DSC shell, vertical heat shield and space under the bottom line of DSC shell surfaces. Enclosure 3 includes bottom of Enclosure 2 and inside surfaces of HSM side wall and floor. Enclosure 4 includes horizontal space limited by concrete roof surface and top horizontal heat shield surface. Enclosure 5 is vertical space limited by inside surface of concrete side wall and vertical heat shield. To be conservative, the closed cavity convection in Enclosure 3 is neglected and Enclosure 2 was assumed to be the average of Enclosure 1 and 3 $(9.09 + 1)/2 = 5.045$.

For zones of closed cavity convection to adjust a thermal conductivity of air k_{air} to account convection an empirical generalized formula was applied [4.12]:

$$\frac{k_{eff\ air}}{k_{air}} = C \cdot Ra^n \cdot \left(\frac{L}{\delta}\right)^m$$

where Ra - Raleigh number, L, δ - length and width of an enclosure, C, n, m - constants, to be defined by flow circumstances (Ra) and geometry (L/ δ).

Iterative process is used to determine the mean temperatures used in air property calculations. The results are given below:

Enclosure in HSM Cavity	δ , in	L, in	\bar{T}_{hot} , °F	\bar{T}_{cold} , °F	Gr_{δ}	Pr	C	n	m	$k_{eff\ air}/k_{air}$
1	9.95	63	561	428	8.91e+6	0.68	0.4	0.2	0	9.09
4	2	40	432	319	1.55e+5	0.683	0.11	0.29	0	3.149
5	3	72	393	271	7.15e+5	0.685	0.197	0.25	-0.111	3.662

These effective conductivities are used in the ANSYS model to determine the transient DSC shell temperatures during blocked vent accident. These DSC shell temperatures are then used as boundary conditions to calculate the basket and fuel cladding temperatures during blocked vent transient.

The calculated temperature distribution within the hottest cross section is shown in Figure M.4-13 and the time history plot is shown in Figure M.4-15. Summaries of the calculated NUHOMS[®]-32PT DSC cladding and component temperatures are listed in Table M.4-13 and Table M.4-14, respectively.

M.4.6.2 Transfer Accident Evaluation

The postulated transfer accident event consists of transfer in the TC in a 117°F ambient environment with loss of the solar shield and the liquid neutron shielding. Heat load zoning configurations 1, 2 and 3 were evaluated. Heat load zoning configuration 1 bounded the results of configurations 2 and 3. The results for heat load zoning configuration 1 are shown in Table M.4-13.

M.4.6.3 Hypothetical Fire Accident Evaluation

For the postulated worst case fire accident, a 300 gallon diesel fire is simulated for a NUHOMS[®]-32PT DSC with a decay heat load of 24 kW during transfer in the TC. This bounds fire scenarios associated with loading operations and storage within the HSM due to the large thermal mass of the HSM and the HSM vent configuration which provides protection for the DSC and payload.

Steady-state, off-normal conditions are assumed prior to the fire, which consist of a 117°F ambient condition without solar shield in place on the TC but water filled neutron shield. The fire has a temperature of 1,475°F, and an emittance of 0.9 and a duration of 15 minutes based on the 300 gallon diesel fuel source and complete engulfment of the TC for the duration of the fire. The gap between lead shielding and structural shell of the transfer cask is conservatively closed for the duration of the fire in the model. Subsequent to the fire, the TC is subjected to 117°F ambient conditions with maximum insolation. Note that these hypothetical fire parameters are very conservative.

The fire transient analysis presented is based on very conservative assumptions. It is assumed that liquid neutron shield (water) is present throughout the 15-minute fire transient even though it is expected to be lost and replaced with air very early in the fire transient. This assumption maximizes the heat input from the fire to the canister because of the high conductivity of water compared to air. To maximize the canister temperature during the post-fire transient, it is assumed that water in neutron shield cavity is lost at the beginning of post-fire transient and replaced by air as the heat flow is now from canister to the ambient. The gap between lead shielding and structural shell of the transfer cask is kept open for the post fire transient.

The gaps included in the thermal model of the 32PT DSC basket are summarized in Section M.4.4.1.1. These gaps are not removed for calculating the cladding temperatures during accident conditions. The canister shell temperatures change by a negligibly small amount ($<2^{\circ}\text{F}$) during fire transient. This change is small during fire transient as the canister is protected due to the large thermal mass of the transfer cask. This shows that heat input from the fire to the canister is not significant. Since the canister shell temperature is almost unchanged, the cladding temperatures during 15-minute fire transient also are almost unchanged. Therefore, the assumption of not removing the gaps during fire transient has negligible impact on the cladding temperatures.

The calculated temperature response of selected components in the TC and DSC during the first 2,000 minutes of the fire accident is shown in Figure M.4-14. A summary of the calculated maximum fire transient temperatures for these components is listed in Table M.4-16. The calculated maximum fire transient DSC surface temperature is 545°F, which is less than the transfer accident case maximum DSC temperature of 591°F calculated in Section M.4.6.2. Therefore, the NUHOMS[®]-32PT DSC temperatures and pressures calculated for the transfer accident case bound the hypothetical fire accident case.

M.4.6.4 Fuel Cladding and Basket Materials

The short-term events are defined in Section M.4.1 for storage and transfer conditions. The blocked vent results are reported for 40 hours. The transfer accident case results are reported at steady state conditions. The results are reported for heat load zoning configuration 3 for blocked vent transient and heat load zoning configuration 1 for transfer accident in Table M.4-13. The maximum and minimum temperatures of the basket assembly are listed in Table M.4-14. The minimum temperatures reported for each component are not the minimum absolute component temperature in the entire basket. The minimum component temperatures reported in this table represents the minimum temperature for those components at the hottest radial cross-section.

M.4.6.5 Maximum Internal Pressures

The maximum accident pressure condition for the DSC occurs during the transfer accident case with the loss of the sun shield and liquid neutron shielding in the TC under extreme ambient temperature conditions of 117°F and maximum insolation. For this transfer accident condition, the average helium temperature is 703°F (1,163°R). In accordance with NUREG 1536, 100% of the fuel pins are assumed to rupture during this event. During the blocked vent case, the average gas temperature is 623°F. However, since no DSC drop events can occur in conjunction with a blocked vent event, the maximum fraction of fuel pins that can be ruptured is limited.

A summary of the maximum accident operating pressures for the various 32PT DSC configurations are presented in Table M.4-15.

M.4.6.6 Evaluation of Cask Performance During Accident Conditions

The temperatures in the NUHOMS[®] HSM and TC are bounded by the existing analyses because of the same heat load for the NUHOMS[®]-24P DSC design. The NUHOMS[®]-32PT DSC shell and basket are evaluated for calculated pressures and temperatures in Section M.3.

The maximum fuel cladding temperature of 863°F is below the short-term limit of 1058°F (570°C). The accident pressure in the NUHOMS[®]-32PT DSC of 101.7 psig remains below the accident design pressure of 105 psig. It is concluded that the NUHOMS[®]-32PT system maintains confinement during the postulated accident condition.

M.4.7 Thermal Evaluation for Loading/Unloading Conditions

All fuel transfer operations occur when the NUHOMS[®]-32PT DSC and TC are in the spent fuel pool. The fuel is always submerged in free-flowing pool water permitting heat dissipation. After fuel loading is complete, the cask and DSC are removed from the pool and the DSC is drained, dried, backfilled with helium and sealed.

M.4.7.1 Maximum Fuel Cladding Temperatures During Vacuum Drying

The loading condition evaluated for the NUHOMS[®]-32PT DSC is the heatup of the DSC before its cavity is backfilled with helium. This typically occurs during the performance of the vacuum drying operation of the DSC cavity with the Cask in the vertical configuration inside the fuel handling building, and the annulus between the Cask and the DSC full of water.

The vacuum drying of the DSC generally does not reduce the pressure sufficiently to reduce the thermal conductivity of the water vapor and air in the DSC cavity [4.22] and [4.23]. Therefore, air is assumed during vacuum drying operations. Radiation in the gaps within the basket and rail components is conservatively neglected. Analyses are performed to determine the transient heat-up during the vacuum drying condition.

A transient thermal analysis is performed using the three-dimensional model developed in Section M.4.4.1, decay heat loads for heat load zoning configuration 1, 2, and 3 and a maximum DSC temperature of 215°F. The initial temperature of the DSC, basket and fuel is assumed to be 215°F, based on the boiling temperature of the fill water. Table M.4-17 and Table M.4-18 provide the maximum calculated temperatures for the fuel cladding and basket components, respectively, for all three configurations. Figure M.4-16 provides the maximum fuel cladding temperatures during the vacuum drying transient. The maximum cladding temperature reached during vacuum drying after 33 hours is 678°F, which is below the limit of 752°F [4.24].

M.4.7.2 Evaluation of Thermal Cycling of Fuel Cladding During Vacuum Drying, Helium Backfilling and Transfer Operations

ISG-11 also states that thermal cycling is to be minimized and imposes a limit of 65°C (118°F) on thermal cycling (reduction in fuel clad temperature from previous peak temperature). The basis for the limit is that as the cladding temperature is reduced more than 65°C the concentration of hydrogen available for hydride reorientation becomes significant.

After completion of vacuum drying step, the DSC is backfilled with helium, with the Cask in the same configuration as described above and the annulus between the Cask and DSC filled with water. This case results in the lowest steady state fuel cladding temperature of 578°F during the DSC drying/backfilling operations. Thus, the maximum temperature difference for the fuel cladding during this drying and backfilling operations is $(678 - 578) = 100^\circ\text{F}$. This temperature difference meets the thermal cycling criteria specified by ISG-11 [4.24].

It is expected that with a lower DSC decay heat load, the vacuum drying operation may require a longer time duration to meet the limit of Technical Specification 1.2.2. An additional evaluation

is performed to determine the sensitivity of the thermal cycling analysis of fuel cladding temperatures when loading a DSC with a payload of up to 8.4 kW decay heat load. The Cask configuration for drying, backfilling and transfer operations is identical to that described above except for the DSC heat load. Figure M.4-16 provides the maximum fuel cladding temperatures during the vacuum drying transient for this case. The maximum cladding temperature reached during vacuum drying after 38 hours is 592°F, which is well below the limit of 752°F [4.24]. This 8.4 kW case results in the lowest steady state fuel cladding temperature of 492°F during the helium backfilling operations. Thus, the maximum temperature difference for the fuel cladding during this drying and backfilling operations is $(592-492) = 100^\circ\text{F}$. The results demonstrate that with a vacuum drying time limit of 38 hours for a DSC with up to 8.4 kW heat load, the design meets the ISG-11 [4.24] maximum fuel cladding temperature limit of 752°F as well as the maximum fuel cladding temperature difference limit of 117°F.

M.4.7.3 Reflooding Evaluation

For unloading operations, the DSC will be filled with the spent fuel pool water through the siphon port. During this filling operation, the DSC vent port is maintained open with effluents routed to the plant's off-gas monitoring system. The NUHOMS®-32PT DSC operating procedures recommend that the DSC cavity atmosphere be sampled first before introducing any reflood water in the DSC cavity.

When the pool water is added to a DSC cavity containing hot fuel and basket components, some of the water will flash to steam causing internal cavity pressure to rise. This steam pressure is released through the vent port. The procedures also specify that the flow rate of the reflood water be controlled such that the internal pressure in the DSC cavity does not exceed 20 psig. This is assured by monitoring the maximum internal pressure in the DSC cavity during the reflood event. The reflood for the DSC is considered as a Service Level D event and the design pressure of the DSC is 105 psig. Therefore, there is sufficient margin in the DSC internal pressure during the reflooding event to assure that the DSC will not be over pressurized.

The maximum fuel cladding temperature during reflooding event is significantly less than the vacuum drying condition owing to the presence of water/steam in the DSC cavity. The analysis presented in Section M.4.7.2 shows that the maximum cladding temperature during vacuum drying after 33 hours is 678°F. Hence, the peak cladding temperature during the reflooding operation will be less than 678°F.

To evaluate the effects of the thermal loads on the fuel cladding during reflooding operations, a conservative assumption of high maximum fuel rod temperature of 750°F and a low quench water temperature of 50°F are used.

The material properties, corresponding to a temperature of 750°F, are used in the evaluation:

Modulus of Elasticity, E (psi) = 11.1×10^6 [from Figure 4 of 4.13]

Coefficient of thermal expansion, α , (in/in/°F) = 3.73×10^{-6} [4.14]

Poisson's Ratio, ν , = 0.38 [4.15]

Yield Stress (irradiated), S_y , = 50,500 psi [4.13]

The fuel cladding is evaluated as a hollow cylinder with an outer surface temperature of T (50°F), and the inner surface temperature of T+ΔT (750°F) using [4.16] equations. The maximum thermal stress in the fuel cladding due to the temperature gradient during reflooding is calculated as follows:

The maximum circumferential stress at the outer surface is given by:

$$\sigma_t = \frac{\Delta T * \alpha * E}{2(1 - \nu) \log_e(c/b)} * \left(1 - \frac{2 * b^2}{(c^2 - b^2)} * \log_e c/b\right)$$

The maximum circumferential stress at the inner surface is given by:

$$\sigma_t = \frac{\Delta T * \alpha * E}{2(1 - \nu) \log_e(c/b)} * \left(1 - \frac{2 * c^2}{(c^2 - b^2)} * \log_e c/b\right)$$

The maximum stresses are calculated as 22,420 psi (outer surface) and 24,325 psi (inner surface). Based on the results of the thermal stress analysis, these stresses in the cladding during reflood is much less than the yield stress of 50,500 psi [4.13]. Therefore, cladding integrity is maintained during reflood operations.

Therefore, no cladding damage is expected due to the reflood event. This is also substantiated by the operating experience gained with the loading and unloading of transportation packages like IF-300 [4.11] which show that fuel cladding integrity is maintained during these operations and fuel handling and retrieval is not impacted.

M.4.8 Determination of Minimum Effective Fuel Conductivity

In order to determine the bounding effective thermal conductivity of a fuel assembly for use in the thermal analysis of the NUHOMS[®]-32PT DSC, the fuel assembly with the lowest thermal conductivity at the design basis heat load is selected.

This section presents the methodology for the determination of axial and transverse effective thermal conductivity of spent fuel and the determination of the bounding fuel effective thermal conductivity. In addition, the methodology for calculation of effective specific heat and effective density of the fuel is also presented.

M.4.8.1 Determination of Bounding Effective Fuel Thermal Conductivity

M.4.8.1.1 Fuel Assemblies Evaluated

The fuel assemblies that are considered for storage in the NUHOMS[®]-32PT DSC are listed in Section M.2. The design data for each of the fuel assemblies are presented in Section M.2.

M.4.8.1.2 Summary of Thermal Properties of Materials

The thermal conductivity and specific heat values of Zircaloy, UO₂ pellets, and Helium are presented in Section M.4.2. The emissivity of Zircaloy is also presented in Section M.4.2.

M.4.8.1.3 Calculation of Fuel Axial Effective Thermal Conductivity

The axial fuel conductivity is assumed to be limited to the cladding conductivity weighted by its fractional area as required in NUREG 1536 [4.10].

$$K_{axl} = (K_{zirc})(A_{zirc}/A_{eff}) \quad (1)$$

K_{zirc} = Conductivity of Zircaloy 4

A_{eff} = (8.70") x (8.70") = 75.69 in²

A_{zirc} = Cross section area of Zircaloy cladding in the fuel assembly

Equation (1) is used to calculate axial effective conductivity for the fuel assembly types listed in Section M.2. The results are plotted in Figure M.4-19.

M.4.8.1.4 Calculation of Fuel Transverse Effective Thermal Conductivity

The transverse fuel effective conductivity is determined by creating a two-dimensional finite element model of the fuel assembly centered within a fuel compartment. The outer surfaces, representing the fuel compartment walls, are held at a constant temperature, and heat generating boundary condition is applied to the fuel pellets within the model. A maximum fuel assembly temperature is then determined. The isotropic effective thermal conductivity of a heat generating square, such as the fuel assembly, can be calculated as described in [4.27].

$$K_{\text{eff}} = 0.29468 \times \frac{Q'''}{a^2 (T_c - T_o)} \quad (2)$$

where:

Q''' = heat load per unit volume of fuel assembly (Btu/hr-in³),
 a = half width of fuel compartment opening = 8.7 / 2 = 4.35",
 T_c = Maximum Temperature of Fuel Assembly (°F),
 T_o = Compartment Wall Temperature (°F).

with

$$Q''' = \frac{Q}{4a^2 L_a} \quad (3)$$

where:

Q = decay heat load per assembly = 24 kW/32 = 0.75 kW/assembly, and
 L_a = active fuel length

In determining the temperature dependent effective fuel conductivities, an average temperature, equal to $(T_c + T_o)/2$, is used for the fuel temperature.

2-D finite element models of each fuel assembly representing a quarter of the fuel assembly were modeled within ANSYS [4.9]. Plane 55 elements were used to model components such as the fuel pellets, fuel cladding, and the helium back fill gas. The gap between the fuel cladding and the fuel pellets is also included in the model.

Heat generated in the fuel pellets dissipates by conduction and radiation to the fuel compartment walls. Convection is not considered in the model. Radiation between the fuel rods, guide tubes, and basket walls was simulated using the radiation super-element processor (/AUX12). LINK32 elements were used for modeling of radiating surfaces in creating the radiation super-element and were unselected prior to the solution of the model. The compartment walls are not modeled as a solid entity. Only the LINK32 elements aligned with the outermost nodes of the model (not on symmetry lines) are given the emissivity of the compartment walls.

Emissivity of stainless steel was applied to the LINK elements on one compartment wall. The link elements on the other compartment wall were given the emissivity of 0.85 (aluminum with anodized or other processes). To eliminate the radiation heat transfer across the symmetry lines, the link elements on symmetry lines were given a very low emissivity (0.001). Although the symmetry boundaries result in the aluminum surfaces being not adjacent, as it would be in the actual compartment, the impact is negligible.

Since a quarter of fuel assembly is modeled in each case, the reaction solution after solving the 2D model is equal to the heat generated per unit length of the active fuel divided by four.

$$Q_{\text{react}} = \frac{Q}{4L_a} \quad (4)$$

Substitution of equations (3) and (4) in equation (2) gives:

$$K_{\text{eff}} = 0.29468 \times \frac{Q_{\text{react}}}{(T_c - T_o)} \quad (5)$$

Equation (5) is used to calculate the transverse effective fuel conductivity for each fuel assembly model.

The heat generating boundary conditions for each assembly is calculated as shown in equation 6.

$$dhl = \frac{Q/N}{n \left(\frac{\pi}{4} d_p^2 \right) L_a} \quad (6)$$

- dhl = Heat generating boundary condition (Btu/min-in-°F)
- Q = Total decay heat load = 24 kW = 1364.9 Btu/min
- N = Number of assemblies = 32
- n = Number of fuel rods
- d_p = Pellet outer diameter
- L_a = Active fuel length

The models were run with a series of isothermal boundary conditions applied to the nodes representing the fuel compartment walls. The symmetry lines going through the center of the fuel assembly are kept at the adiabatic boundary conditions.

A finite element model for B&W 15x15 fuel assembly is shown in Figure M.4-18.

M.4.8.1.5 Results and Conclusion

Figure M.4-19 shows the calculated axial effective conductivities. As Figure M.4-19 shows, WE 14x14 has the minimum (bounding) axial conductivity. Backfill gas property does not have any effect on the axial effective fuel conductivity. Therefore, identical axial effective fuel conductivity values can be used for helium and vacuum conditions.

The calculated bounding axial effective conductivities are listed in the following table:

Temperature °F	k-axial (Btu/min-in-°F)
200	7.949E-04
300	8.387E-04
400	8.824E-04
500	9.189E-04
600	9.554E-04
800	1.036E-03

The calculated transverse conductivities are presented in Figure M.4-20 and Figure M.4-21 for helium and vacuum conditions, respectively. As shown in Figure M.4-20 and Figure M.4-21,

WE 14x14 assembly has the (bounding) minimum transverse conductivity. The bounding transverse effective conductivity values are listed in the following table:

Temperature °F	k-transverse in Helium (Btu/min-in-°F)	Temperature °F	k-transverse in Vacuum (Btu/min-in-°F)
138	2.894E-04	215	9.484E-05
233	3.317E-04	288	1.246E-04
328	3.968E-04	367	1.633E-04
423	4.744E-04	452	2.119E-04
519	5.668E-04	540	2.701E-04
616	6.715E-04	632	3.373E-04
714	7.879E-04	726	4.125E-04
812	9.208E-04	822	4.949E-04

M.4.8.2 Calculation of Fuel Effective Specific Heat and Density

This section presents the calculation of the fuel effective specific heat and density used in the transient thermal analyses.

Volume average density and weight average specific heat are calculated to determine the effective density and specific heat for the fuel assembly.

The equations to determine the fuel effective density ρ_{eff} and specific heat $C_{p,eff}$ are shown below.

$$\rho_{eff} = \frac{\sum \rho_i V_i}{V_{assembly}} = \frac{\rho_{UO_2} V_{UO_2} + \rho_{Zr_4} V_{Zr_4}}{4a^2 L_a}$$

$$C_{p,eff} = \frac{\sum \rho_i V_i C_{p,i}}{\sum \rho_i V_i} = \frac{\rho_{UO_2} V_{UO_2} C_{p,UO_2} + \rho_{Zr_4} V_{Zr_4} C_{p,Zr_4}}{\rho_{UO_2} V_{UO_2} + \rho_{Zr_4} V_{Zr_4}}$$

where:

$\rho_i, C_{p,i}, V_i$ = density, specific heat, and volume of component,
 L_a = active fuel length, and
 a = half of compartment width.

The properties of Zircalloy-4 and UO₂ are provided in Section M.4.2

The calculated values of fuel effective specific heat and fuel effective density are summarized below:

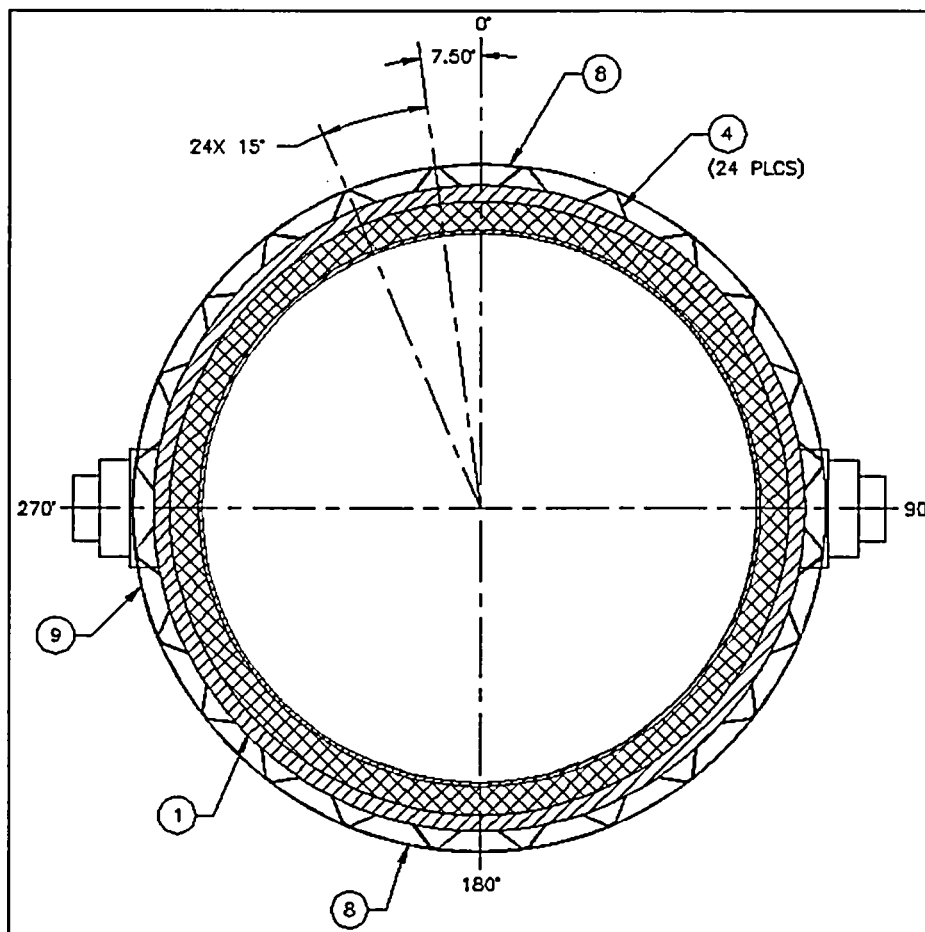
Temperature °F	Fuel Effective Specific Heat (Btu/lbm-F)
80	0.0592
260	0.0654
692	0.0725
1502	0.0778

Fuel Effective Density (lbm/in3)	0.1166
-------------------------------------	--------

M.4.9 Derivation of Effective Thermal Conductivity of Water Within the Neutron Shield of the OS197/OS197H Transfer Cask

This Section presents the derivation of effective thermal conductivity of water within the liquid neutron shield of the OS197/OS197H Transfer Cask.

The neutron shield of the OS197/OS197H transfer cask is a water filled jacket surrounding the cask's structural shell. Support ribs are used to support the 3/16" stainless steel panels that make up the outer skin of the neutron shield. The layout of the twenty-four (24) support ribs (i.e., Item 4) within the neutron shield is illustrated in the following figure.



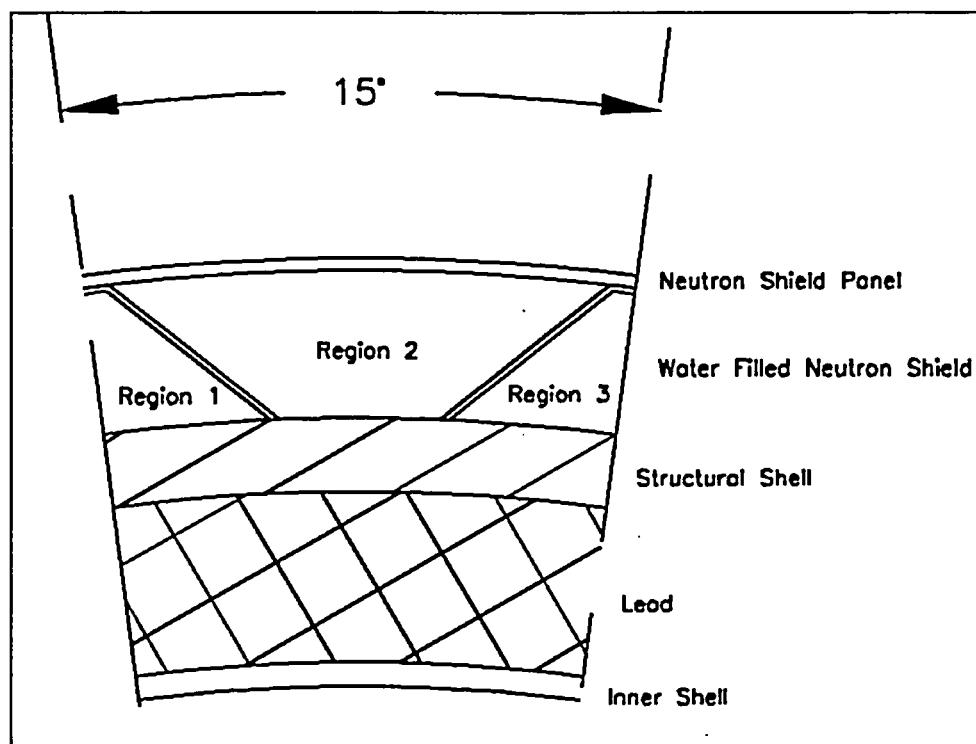
Cross-Section Through OS197/OS197H Cask

The presence of the support ribs act to divide up the void volume within the neutron shield into multiple enclosed regions. Heat transfer through the neutron shield is a combination of conduction and convection. Given the relatively large changes in the density of water with temperature, treating the water regions as a solid conductor material is grossly conservative from

a heat transfer point of view. Accordingly, a methodology based on established heat transfer principles is applied to determine the effective thermal conductivity within water-filled neutron shield for a transfer cask in a horizontal configuration.

No credit is taken for any flow through the drainage holes that exist in the ribs. Instead, credit is only taken for the convection that does occur as separate flow patterns within each region of the neutron shield.

A 15° segment of the cask circumference considered for the purposes of this analysis is presented in the following figure.



Modeling Layout of a 15° Segment of Cask Circumference

The symmetry planes that lie on either side of the modeled segment bisect the “hat” section of adjacent ribs. This modeling arrangement was selected for computational ease. Region 1 represents the enclosed region under one support rib, while Region 3 represents an identical region under the adjoining support rib. Region 2 represents the enclosed region between adjacent support ribs.

Each of these regions can be represented as enclosures with opposing parallel plates that are maintained at different temperatures. Heat transfer within such enclosures has been extensively studied and the presence of convective flow conclusively established for Rayleigh numbers (based on the separation distance between the parallel plates) in excess of 1000.

The Nusselt number, Nu_v , for a vertical enclosure is determined from Equations 126 to 129, page 6-53 of [4.22] for fluids with $Pr \approx 0.7$ and from Equations 130 and 131 for fluids with $Pr \geq 1.4$. Since the Pr of the water in the neutron shielding at the water temperatures expected under the transfer operation is approximately 1.4, Equations 126 to 129 are the appropriate set of equations to be used in calculating the Nusselt number. Equations 126 to 129 from [4.22] are as follows:

$$Nu_v = [Nu_{cl}, Nu_l, Nu_t]_{\max}$$

where:

$$Nu_{cl} = \left[1 + \left\{ \frac{0.0104 Ra^{0.293}}{1 + (6310/Ra)^{1.36}} \right\}^3 \right]^{0.3333}$$

$$Nu_l = 0.242 \left(\frac{Ra * L}{H} \right)^{0.273}$$

$$Nu_t = 0.0606 (Ra)^{0.3333}$$

$$Ra = \frac{g * \beta * (T_{hot} - T_{cold}) * L^3 * \mu * C_p}{\nu^2 \kappa}$$

where:

g = gravitational acceleration

β = coefficient of thermal expansion

T_{hot} = temperature of structural shell

T_{cold} = temperature of neutron shield skin

μ = dynamic viscosity

C_p = specific heat

L = width of the cavity

ν = kinematic viscosity

k = thermal conductance

For a horizontal cavity where the hot wall lies below the cold wall, the Nusselt number, Nu_h , is determined from Equations 114 to 117, page 6-46 of [4.22]. These equations are:

$$Nu_h = 1 + \left[1 - \frac{1708}{Ra} \right]^* \left[k_1 + 2 \left(\frac{Ra^{1/3}}{k_2} \right)^{1 - \ln \left(\frac{Ra^{1/3}}{k_2} \right)} \right] + \left[\left(\frac{Ra}{5830} \right)^{1/3} - 1 \right]^*$$

where:

$$k_1 = \frac{1.44}{1 + 0.018/Pr + 0.00136/Pr^2}$$

$$k_2 = 75 \exp(1.5 Pr^{-0.5})$$

The brackets with a dot []^{*} indicate that only positive terms are retained, otherwise the value within the brackets is to be set to zero.

The above equations can be used to estimate the Nusselt number at the top (i.e., circumferential position = 0 degrees) and the side (i.e., circumferential position = 90 degrees) of the cask. For other positions on the cask, scaling laws provided by Equations 134 to 139, page 6-58 of [4.22] are to be used.

For angles of $90^\circ < \Theta \leq 180^\circ$ (i.e., the bottom of the cask), the recommended scaling law is:

$$Nu_\Theta = 1 + (Nu_v - 1) * \sin \Theta$$

As seen, this equation will yield a Nusselt number = 1 (i.e., conduction only) for the bottom of the cask.

For angles of $45^\circ < \Theta < 90^\circ$, the recommended scaling law for an enclosure with $H/L \cong 2$ is:

$$Nu_\Theta = Nu_v (Ra * \sin \Theta)$$

While for angles of $0^\circ < \Theta < 45^\circ$, the recommended scaling law for an enclosure with $H/L \cong 2$ is:

$$Nu_\Theta = Nu_h * \left[\frac{Nu_v (Ra * \sin 45^\circ)}{Nu_h} \right]^{\frac{\Theta}{45}}$$

For the purposes of this calculation, H is assumed to be 7" and L is set equal to 3" or the thickness of the neutron shield. The choice of H=7 is based on the mean distance between the legs of the ribs. However, as seen from [4.22] the use of smaller values of H yields higher Nusselt numbers. Thus, the use of 7" yields conservative values of the Nusselt number.

To arrive at an effective thermal conductivity across the neutron shield, the thermal resistances for the heat transfer paths through Regions 1, 2, and 3 of the shield, as well as the heat conducted along the steel support ribs are computed and then summed assuming they represent parallel paths. The effective thermal conductivity across the neutron shield, k_{eff} , is then determined via:

$$\frac{1}{\frac{1}{R_{Region 1}} + \frac{1}{R_{Region 2}} + \frac{1}{R_{Region 3}} + \frac{1}{R_{Ribs}}} = \frac{\ln\left(\frac{r_2}{r_1}\right)}{2 * \pi * Z * k_{effective}}$$

where:

k_{eff} = Effective thermal conductivity across the neutron shield,

$R_{\text{Region } i}$ = Thermal Resistance of Region I,

r_2 = inside radius of neutron shield shell = 42.56",

r_1 = outside radius of structural shell = 39.56", and

Z = axial length of model section of the cask.

Since the Rayleigh number is a function of the temperature difference and the mean temperature within the neutron shield, an iterative process is used to arrive at a value for both temperature difference and the mean temperature that is required to balance the flow of heat across the neutron shield, assuming a decay heat loading of 24 kW.

The computed thermal resistances for each of the assumed thermal paths through the water-filled neutron shield, together with the computed effective thermal conductivity, are presented in the following table:

K_{eff} for OS197 Cask Neutron Shield (Water Filled) vs. Circumferential Position

Angle	Nu (Ra)	R Region 1	R Region 2	R Region 3	R Support Ribs	Total R	k effective, Btu/min-in-F
0	36.36	1.853	1.907	1.853	58.556	0.617	0.019
30	33.07	2.037	2.097	2.037	58.556	0.678	0.017
60	33.34	2.021	2.080	2.021	58.556	0.672	0.017
90	34.67	1.943	2.000	1.943	58.556	0.647	0.018
120	30.16	2.234	2.300	2.234	58.556	0.742	0.016
150	17.84	3.777	3.889	3.777	58.556	1.244	0.009
180	1.00	67.371	69.353	67.371	58.556	16.344	0.001

As expected, the presence of the convection within the shield will enhance the apparent thermal conductivity by a factor of 10 to 20 over that computed assuming the water acts as a solid material.

The computed thermal resistances for an air-filled neutron shield are presented in the following table:

K_{eff} for OS197 Cask Neutron Shield (Air Filled) vs. Circumferential Position

Angle	Nu (Ra)	R Region 1	R Region 2	R Region 3	R Support Ribs	Total R	k effective, Btu/min-in-F
0	6.98	187.650	193.169	187.650	58.556	30.239	0.000385
30	7.29	179.736	185.022	179.736	58.556	29.615	0.000393
60	7.88	166.434	171.329	166.434	58.556	28.500	0.000408
90	8.19	160.025	164.732	160.025	58.556	27.931	0.000417
120	7.23	181.356	186.690	181.356	58.556	29.745	0.000391
150	4.60	285.226	293.615	285.226	58.556	36.163	0.000322
180	1.00	1310.670	1349.219	1310.670	58.556	51.278	0.000227

As seen from the table, the lower Rayleigh numbers associated with an air filled neutron shield results in the presence of convection within the shield enhancing the apparent thermal conductivity by only a factor of approximately 2 over that computed assuming the air acts as a solid material.

The effective conductivity values interpolated from these tables are applied to the 24 segments (7.5 degrees each) along the neutron shield region of the transfer cask model described in Section M.4.4.1.5.

For each segment, the lowest k_{eff} value along the segment was applied.

M.4.9.1 Validation of the Methodology Used to Determine K_{eff} for OS197 Cask Neutron Shield

To validate the methodology used in Section M.4.9, a confirmatory analysis [4.29] using a computational fluid dynamics (CFD) methodology is performed. This confirmatory analysis calculates the effective thermal conductivity across the neutron shield structure of the OS197 Cask due to the combination of conduction through the support angles, and conduction/convection through the water filled regions of the neutron shield. The 100°F ambient temperature case is selected for this validation because it has the least margin to the cladding temperature as documented in Table M.4-2.

The confirmatory analysis uses a CFD methodology to directly calculate the prototypical flow regime within the OS197 neutron shield at various circumferential positions around the cask when the cask is horizontal, at steady-state conditions in 100°F ambient air, and with an internal decay heat loading of 24 kW. The CFD model results are used to calculate the effective thermal conductivity values across the neutron shield structure (water and support angles combined) at cask circumferential positions of 0, 30, 60, 90, 120, 150, and 180 degrees in order to match the cask angular configuration presented in Section M.4.9. The comparison is documented in the table below:

OS197 Neutron Shield Effective Thermal Conductivity Comparison

Angle ⁽¹⁾	K _{eff} with CFD method [4.29] (Btu/min-in-°F)	K _{eff} from Section M.4.9 (Btu/min-in-°F)
0°	1.1520E-02	1.8900E-02
30°	1.0848E-02	1.7200E-02
60°	1.0933E-02	1.7300E-02
90°	1.0708E-02	1.8000E-02
120°	8.8687E-03	1.5700E-02
150°	8.6958E-03	9.4000E-03
180°	7.4030E-03	7.0000E-04

(1) The angle is measured from top at 0° to bottom at 180°.

M.4.9.1.1 Comparison of Δt Across Neutron Shield and DSC Shell Temperatures

The effective conductivities of the neutron shield structure (water and support angles combined) calculated by the CFD method are then used in the ANSYS model of Section M.4.4.1.6 to determine the Δt across the neutron shield and the temperature of the NUHOMS[®]-32PT DSC shell. All the other input parameters from Section M.4.4.1.6 remain unchanged.

A comparison of the temperature difference across the neutron shield at the top, side, and bottom locations is provided in the following table.

Comparison of Δt across the OS197 Neutron Shield

Location ⁽¹⁾	With K _{eff} from CFD method [4.29] (°F)	With K _{eff} from Section M.4.9 (°F)	Difference (°F)
Top	7	5	2
Side	8	5	3
Bottom	12	76	-64

(1) The top, side and bottom correspond to 0°, 90°, and 180° respectively.

The above comparison shows that the CFD computed temperature difference across the neutron shield for the top and the side have increased slightly, while the temperature difference at the bottom has decreased significantly by 64°F.

A similar comparison of the DSC shell temperatures at the top, side, and bottom locations resulting from substituting the K_{eff} values from the CFD method in the ANSYS model of Section M.4.4.1.6 are provided in the following table.

DSC Shell Temperature Comparison

Location ⁽¹⁾	With K_{eff} from CFD method [4.29] (°F)	With K_{eff} from Section M.4.9 (°F)	Difference (°F)
Top	447	445	2
Side	425	424	1
Bottom	354	367	-13

(1) The top, side and bottom correspond to 0°, 90°, and 180° respectively.

The above comparison shows that the DSC shell temperatures for the top and the side have increased slightly, while the DSC shell temperature at the bottom has decreased significantly by 13°F when the CFD calculated K_{eff} values are used.

M.4.9.1.2 Comparison of Fuel Cladding Temperatures

These revised DSC shell temperatures are then used in the ANSYS model of Section M.4.4.1.1 to calculate the fuel cladding temperatures. All the other input parameters from Section M.4.4.1.1 remain unchanged. The calculated maximum cladding temperature is compared with the results from Table M.4-2 to determine the validity of the effective conductivity values calculated in Section M.4.9.

Fuel Cladding Temperature Comparison

Case	Fuel Cladding Temperature with CFD K_{eff} (°F)	Fuel Cladding Temperature with Section M.4.9 K_{eff} (°F)
100°F ambient, DSC in TC	718.4	720

The above comparison shows that the fuel cladding temperature has decreased slightly when the CFD calculated K_{eff} values are used.

M.4.9.1.3 Conclusion

The neutron shield effective thermal conductivity computed using the CFD methodology [4.29] results in a 2°F increase in the computed temperature difference across the neutron shield at the top of the cask when compared to the Section M.4.9 values, a 3°F increase at the side of the cask, and a 64°F decrease in the temperature difference at the bottom of the cask.

The net effect of these changes in the computed difference across the neutron shield is a 6°F decrease in the maximum temperature of the transfer cask component. The overall effects of these neutron shield effective thermal conductivity differences on the DSC shell temperatures and the maximum fuel cladding temperature are also small, and considered to be negligible. Therefore, the effective thermal conductivities calculated in Section M.4.9 are valid for calculating the cask, DSC shell and fuel cladding temperatures.

M.4.10 References

- 4.1 Deleted.
- 4.2 Deleted.
- 4.3 Report, "Topical Report on Actinide-Only Burnup Credit for PWR Spent Nuclear Fuel Packages," Office of Civilian Radioactive Waste Management, DOE/RW-0472, Revision 2, September, 1998.
- 4.4 ASME Boiler and Pressure Vessel Code, Section II, Part D, Properties, 1998, including 2000 addenda.
- 4.5 Roshenow, W. M., J. P. Hartnett, and Y. I. Cho, *Handbook of Heat Transfer*, 3rd Edition, 1998.
- 4.6 Bolz, R. E., G. L. Tuve, *CRC Handbook of Tables for Applied Engineering Science*, 2nd Edition, 1973. Transfer, McGraw Hill, 1989.
- 4.7 Bucholz, J. A., *Scoping Design Analysis for Optimized Shipping Casks Containing 1-, 2-, 3-, 5-, 7-, or 10-Year old PWR Spent Fuel*, Oak Ridge National Laboratory, January, 1983, ORNL/CSD/TM-149.
- 4.8 Deleted.
- 4.9 ANSYS, Inc., ANSYS Engineering Analysis System User's Manual for ANSYS Revision 5.6, Houston, PA.
- 4.10 NRC NUREG-1536, *Standard Review Plan for Dry Cask Storage Systems*, January 1997.
- 4.11 Consolidated Safety Analysis Report for IF-300 Shipping Cask, CoC 9001.
- 4.12 J.P. Holman, *Heat Transfer*, McGraw Hill, 1989.
- 4.13 Chun, Ramsey; Witte, Monika; Schwartz, Martin, "Dynamic Impact Effects on Spent Fuel Assemblies," Lawrence Livermore National Laboratory, Report UCID-21246, October, 1987.
- 4.14 NUREG/CR-0497, "MATPRO-Version 11: "A Handbook of Materials Properties for Use in the Analysis of Light Water Reactor, Fuel Rod Behavior," EG&G, Inc. February, 1979.
- 4.15 Glasstone, S., Seasonske, A., "Nuclear Reactor Engineering," Third Edition, 1981.
- 4.16 Young, W.C., "Roark's Formulas for Stress and Strain," Sixth Edition, McGraw Hill.
- 4.17 Deleted.

- 4.18 Deleted.
- 4.19 Aluminum. Volume 1, Properties, Physical Metallurgy and Phase Diagrams, edited by Kent R. Van Horn, American Society for Metals, Metals Park, Ohio, 1967.
- 4.20 ASHRAE Handbook, 1981 Fundamentals, 4th Printing, 1983.
- 4.21 Deleted.
- 4.22 Rohsenow, Hartnett, "Handbook of Heat Transfer Fundamentals, " 2nd Edition, 1985.
- 4.23 Roth, A., "Vacuum Technology," 2nd Edition, 1982.
- 4.24 Interim Staff Guidance No. 11, Revision 2, "Cladding Considerations for the Transportation and Storage of Spent Fuel," July 30, 2002.
- 4.25 Calculation, "TN-24P Benchmarking Analysis Using ANSYS," Calculation No. NUH32PT.0408, Revision 0.
- 4.26 J. M. Creer, et al, "The TN-24 PWR Spent Fuel Storage Cask: Testing and Analyses," PNL Report, Report No. PNL-6054, 1987.
- 4.27 SAND90-2806, Sanders, T. L., et al., "A Method for Determining the Spent Fuel Contribution to Transport Cask Containment Requirements," TTC-1019, UC-820, November 1992.
- 4.28 Oak Ridge National Laboratory, RSIC Computer Code Collection, "SCALE, A Modular Code System for Performing Standardized Computer Analysis for Licensing Evaluation for Workstations and Personal Computers", NUREG/CR-0200, Rev. 6, ORNL/NUREG/CSD-2/V3/R6.
- 4.29 TN Calculation, Confirmatory Analysis of the Effective Thermal Conductivity Calculation within the Neutron Shield of the OS197 Transfer Cask Using a CFD Method, Calculation NUH32PT.0413, Revision 1.

M.4.11 Example Input Files

M.4.11.1 Example ANSYS Input File for Applying Heat Generation

```
/com apply heat generation to fuel regions
/com select elements to apply heat generation
csys,0
cmsel,s,f_outer ! select fuel elements
nsle,s,allc
nsl,r,loc,z,act_end,0
esln,r,0
esel,u,type,,7
bfedele,all,hgen

/com read in z coordinates of burnup curve and values

*dim,z_fuel,,12
*dim,h_gen,,12
z_fuel(1)=act_end
h_gen(1)=0
z_fuel(2)= act_end +0.0278*act_fuel
h_gen(2)=0.652*heat_gen
z_fuel(3)= act_end +0.0833*act_fuel
h_gen(3)=0.967*heat_gen
z_fuel(4)= act_end +0.1389*act_fuel
h_gen(4)=1.074*heat_gen
z_fuel(5)= act_end +0.1944*act_fuel
h_gen(5)=1.103*heat_gen
z_fuel(6)= act_end +0.25*act_fuel
h_gen(6)=1.108*heat_gen
z_fuel(7)= act_end +0.3056*act_fuel
h_gen(7)=1.106*heat_gen
z_fuel(8)= act_end +0.3611*act_fuel
h_gen(8)=1.102*heat_gen
z_fuel(9)= act_end +0.4167*act_fuel
h_gen(9)=1.097*heat_gen
z_fuel(10)= act_end +0.4722*act_fuel
h_gen(10)=1.094*heat_gen
z_fuel(11)= act_end +0.5278*act_fuel
h_gen(11)=1.094*heat_gen
z_fuel(12)= act_end +0.5833*act_fuel
h_gen(12)=1.095*heat_gen

*get,emin,elem,0,num,min ! get the minimum element #
*get,emax,elem,0,num,max ! get the maximum element #
eln=0
*do,cnt,emin,emax,1
  *get,elnn,elem,eln,nxth ! get next higher element number than eln
  and store in elnn
  eln=elnn
  *get,ei,elem,eln,node,1 ! get nodes which are attached to eln
  nzi=nz(ei)
  *get,ej,elem,eln,node,2 ! get nodes which are attached to eln
  nzj=nz(ej)
  *get,ek,elem,eln,node,3 ! get nodes which are attached to eln
```

```

nzk=nz(ek)
*get,el,elem,eln,node,4      ! get nodes which are attached to eln
nzl=nz(el)
*get,em,elem,eln,node,5      ! get nodes which are attached to eln
nzm=nz(em)
*get,en,elem,eln,node,6      ! get nodes which are attached to eln
nzn=nz(en)
*get,eo,elem,eln,node,7      ! get nodes which are attached to eln
nzo=nz(eo)
*get,ep,elem,eln,node,8      ! get nodes which are attached to eln
nzp=nz(ep)
n_z=(nzi+nzj+nzk+nzl+nzm+nzn+nzo+nzp)/8      ! find average z
*do,i,1,12,1
  *if,n_z,ge,z_fuel(i),then
    *if,n_z,lt,z_fuel(i+1),then
      z_diff=z_fuel(I+1)-z_fuel(I)
      gen_diff=h_gen(I+1)-h_gen(I)
      gen=(n_z-z_fuel(i))/(z_diff)*(gen_diff)+h_gen(i)
      bfe,eln,hgen,,gen
    *endif
  *endif
*enddo
*if,eln,eq,emax,exit
*enddo

```

M.4.11.2 Example ANSYS Input File for Solar Heat Flux Application

```
/com create radiation elements on outer surface of cask
```

```
type,9  
real,9  
mat,10
```

```
/com define space node  
k,300,0,50,0  
n,10000,0,50,0
```

```
esel,s,type,,1  
esel,a,type,,2  
esel,a,type,,3  
esel,a,type,,4  
esel,a,type,,5
```

```
nsle,s,all
```

```
esurf,10000
```

```
esel,s,type,,9  
nsle,s,all  
csys,1  
nsel,r,loc,x,0,shell_od/2  
nsel,a,node,,10000  
esln,r,1  
edele,all  
csys,0
```

```
/com create surface elements for insolation
```

```
alls  
csys,1  
esel,s,type,,5  
esel,a,type,,1  
cmsel,s,a_nsp  
cmsel,a,a_ns3  
esla,r  
type,6  
esurf
```

```
csys,1  
esel,s,type,,6  
nsle,s,all  
x1=cask_ir+inner_t+lead_t+struct_t  
nsel,r,loc,x,x1-gy2,x1+gy2  
esln,r,1  
edele,all
```

```
/com delete elements on bottom half  
esel,s,type,,6  
nsle,s,all  
x1=cask_ir+inner_t+lead_t+struct_t+ns3_t+nsp_t
```

```
nselect,r,loc,x,x1-gy2,x1+gy2
csys,0
nselect,r,loc,y,-100,0
esln,r,1
edelete,all
```

```
csys,0
```

The ANSYS input file routine to apply insolation to the top outside surface of the cask is as follows:

```
/com 3rd load step, 100 deg F
```

```
/com load parameters
```

```
T_amb=100.
```

```
Insol=123/144/60
```

```
.  
.
.
```

```
/com isolate insolation elements
```

```
csys,22
```

```
eset,s,type,,6
```

```
nsle,s,all
```

```
nselect,r,loc,x,cask_ir+inner_t+lead_t+struct_t+ns3_t+nsp_t
```

```
esln,r,1
```

```
sfedelete,all,all,hflux
```

```
sfe,all,1,hflux,,insol
```

```
csys,0
```

```
alls
```

```
eset,u,type,,7
```

```
nsle,s,all
```

```
lswrite,3
```

Table M.4-1
Fuel Cladding Long-Term Storage Temperatures

Configuration No.	Maximum Temperature (°F)	Limit (°F)
1	634	752
2	619	
3	638	

**Table M.4-2
Fuel Cladding Short-Term Normal Condition Maximum Temperatures**

Operating Condition	Configuration 1 (°F)	Configuration 2 (°F)	Configuration 3 (°F)	Limit (°F)
0°F Storage	585	570	589	752
100°F Storage	655	640	658	
0°F Transfer	675	661	675	
100°F Transfer	720	705	720	

Table M.4-3
DSC Basket Assembly Maximum Normal Operating Component Temperatures;
Configuration 1

Configuration	T_{grid,max} (°F)	T_{grid,min} (°F)	T_{rail,max} (°F)	T_{rail,min} (°F)	T_{Al,max} ⁽¹⁾ (°F)	T_{DSCshell} ⁽²⁾ (°F)
DSC in HSM, 0°F	565	233	304	230	565	277
DSC in HSM, 100°F	638	316	395	312	638	374
DSC horizontal in cask, 0°F	659	344	418	340	659	390
DSC horizontal in cask, 100°F	705	405	471	402	705	445

- (1) Includes aluminum and poison plates.
(2) Maximum temperature is at top of shell.

Table M.4-4
DSC Basket Assembly Maximum Normal Operating Component Temperatures;
Configuration 2

Configuration	T _{grid,max} (°F)	T _{grid,min} (°F)	T _{rail,max} (°F)	T _{rail,min} (°F)	T _{Al,max} ⁽¹⁾ (°F)	T _{DSC shell} ⁽²⁾ (°F)
DSC in HSM, 0°F	550	233	306	229	549	277
DSC in HSM, 100°F	623	316	397	311	623	374
DSC horizontal in cask, 0°F	644	342	420	339	644	390
DSC horizontal in cask, 100°F	691	406	473	401	691	445

- (1) Includes aluminum and poison plates.
- (2) Maximum temperature is at top of shell.

Table M.4-5
DSC Basket Assembly Maximum Normal Operating Component Temperatures;
Configuration 3

Configuration	T _{grid,max} (°F)	T _{grid,min} (°F)	T _{rall,max} (°F)	T _{rall,min} (°F)	T _{Al,max} ⁽¹⁾ (°F)	T _{DSC shell} ⁽²⁾ (°F)
DSC in HSM, 0°F	567	220	289	218	567	264
DSC in HSM, 100°F	639	304	381	301	639	361
DSC horizontal in cask, 0°F	657	327	400	323	657	374
DSC horizontal in cask, 100°F	704	390	456	387	704	431

- (1) Includes aluminum and poison plates.
(2) Maximum temperature is at top of shell.

Table M.4-6
32PT DSC Initial Helium Fill Molar Quantities

DSC Configuration	Helium Fill (g-moles)
S100	110.8
S125	107.8
L100	115.6
L125	112.7

**Table M.4-7
32PT DSC Maximum Normal Operating Condition Pressures**

DSC Configuration	DSC Cavity Free Volume (in³)	Helium Fill (g-moles)	Plenum Helium (g-moles)	BPRA Gas (g-moles)	Fission Products (g-moles)	Total Gas (g-moles)	Pressure (psig)	DSC Design Pressure (psig)
S100	226,141	110.74	1.75	0.00	2.60	115.11	6.31	15
S125	220,162	107.83	1.75	0.00	2.60	112.18	6.34	15
L100	236,094	115.62	1.75	0.359	2.60	120.34	6.35	15
L125	230,097	112.68	1.75	0.359	2.60	117.41	6.37	15

**Table M.4-8
Off-Normal Event Fuel Cladding Maximum Temperatures**

Operating Condition	Configuration 1 (°F)	Configuration 2 (°F)	Configuration 3 (°F)	Limit (°F)
-40°F Storage	558	542	562	1,058
117°F Storage	660	646	663	
117°F Transfer ⁽¹⁾	715	700	715	752

(1) Sunshade is used for ambient temperatures >100°F and ≤117°F.

**Table M.4-9
Off-Normal Event DSC Basket Assembly Maximum Component Temperatures;
Configuration 1**

Configuration	T _{grid,max} (°F)	T _{grid,min} (°F)	T _{rail,max} (°F)	T _{rail,min} (°F)	T _{Al,max} ⁽¹⁾ (°F)	T _{DSC shell} ⁽²⁾ (°F)
DSC in HSM, -40°F	536	200	266	197	536	237
DSC in HSM, 117°F	643	322	402	318	643	382
DSC horizontal in cask, -40°F(3)	-	-	-	-	-	-
DSC horizontal in cask with shade, 117°F	700	404	463	401	700	433

- (1) Includes aluminum and poison plates.
- (2) Maximum temperature is at top of shell.
- (3) Not evaluated for cask with liquid neutron shield (OS197/OS197H). Per Technical Specification 1.2.13 transfer operations outside the fuel handling building at basket temperatures (assumed conservatively equal to ambient temperature) below 0°F are not permitted.

Table M.4-10
Off-Normal Event DSC Basket Assembly Maximum Component Temperatures;
Configuration 2

Configuration	T _{grid,max} (°F)	T _{grid,min} (°F)	T _{rail,max} (°F)	T _{rail,min} (°F)	T _{Al,max} ⁽¹⁾ (°F)	T _{DSC shell} ⁽²⁾ (°F)
DSC in HSM, -40°F	520	200	268	196	520	237
DSC in HSM, 117°F	629	322	404	317	628	382
DSC horizontal in cask, -40°F ⁽³⁾	-	-	-	-	-	-
DSC horizontal in cask with shade, 117°F	686	405	464	400	686	433

- (1) Includes aluminum and poison plates.
- (2) Maximum temperature is at top of shell.
- (3) Not evaluated for cask with liquid neutron shield (OS197/OS197H). Per Technical Specification 1.2.13 transfer operations outside the fuel handling building at basket temperatures (assumed conservatively equal to ambient temperature) below 0°F are not permitted.

**Table M.4-11
Off-Normal Event DSC Basket Assembly Maximum Component Temperatures;
Configuration 3**

Configuration	T _{grid,max} (°F)	T _{grid,min} (°F)	T _{rail,max} (°F)	T _{rail,min} (°F)	T _{Al,max} ⁽¹⁾ (°F)	T _{DSC shell} ⁽²⁾ (°F)
DSC in HSM, -40°F	538	187	252	185	538	224
DSC in HSM, 117°F	645	310	388	307	644	368
DSC horizontal in cask, -40°F ⁽³⁾	-	-	-	-	-	-
DSC horizontal in cask with shade, 117°F	699	389	447	386	698	418

(1) Includes aluminum and poison plates.

(2) Maximum temperature is at top of shell.

(3) Not evaluated for cask with liquid neutron shield (OS197/OS197H). Per Technical Specification 1.2.13 transfer operations outside the fuel handling building at basket temperatures (assumed conservatively equal to ambient temperature) below 0°F are not permitted..

Table M.4-12
32PT DSC Maximum Off-Normal Operating Condition Pressures

	DSC Cavity Free Volume (in3)	Helium Fill (g-moles)	Plenum Helium (g-moles)	BPRA Gas (g-moles)	Fission Products (g-moles)	Total Gas (g-moles)	Pressure (psig)	DSC Design Pressure (psig)
S100	226,142	110.76	17.50	0.00	26.02	154.28	13.36	20
S125	220,163	107.83	17.50	0.00	26.02	151.35	13.57	20
L100	236,095	115.63	17.50	3.59	26.02	162.74	13.66	20
L125	230,097	112.68	17.50	3.59	26.02	159.81	13.87	20

Table M.4-13
Accident Fuel Cladding Maximum Temperatures

Operating Condition	Temperature (°F)	Limit (°F)
DSC in HSM blocked vent at 40 hours, 117°F – Configuration 3	788	1,058
Post accident transfer 117°F (loss of sunshade, loss of neutron shield) – Configuration 1	863	1,058

Table M.4-14
DSC Basket Assembly Maximum Accident Condition Component Temperatures;

Configuration	$T_{grid,max}$ (°F)	$T_{grid,min}$ (°F)	$T_{rail,max}$ (°F)	$T_{rail,min}$ (°F)	$T_{Al,max}^{(1)}$ (°F)	$T_{DSC\ shell}^{(2)}$ (°F)
DSC in HSM blocked vent at 40 hours, 117°F – Configuration 3	774	479	582	476	774	574
Post accident transfer 117°F (loss of sunshade, loss of neutron shield) – Configuration 1	852	611	631	609	852	600

- (1) Includes aluminum and poison plates.
- (2) Maximum temperature is at top of shell.

**Table M.4-15
32PT DSC Maximum Accident Condition Pressures**

	DSC Cavity Free Volume (in3)	Helium Fill (g-moles)	Plenum Helium (g-moles)	BPRA Gas (g-moles)	Fission Products (g-moles)	Total Gas (g-moles)	Pressure (psig)	DSC Design Pressure (psig)
S100	226,142	110.76	175.04	0.00	260.17	545.95	95.96	105
S125	220,163	107.83	175.04	0.00	260.17	543.03	98.25	105
L100	236,095	115.63	175.04	35.9	260.17	586.74	99.40	105
L125	230,097	112.69	175.04	35.9	260.17	583.80	101.68	105

Table M.4-16
Maximum Component Temperatures for the Hypothetical Fire Accident Case for the
NUHOMS®-32PT DSC in the TC

Component	Maximum Temperature (°F)	Allowable Range (°F)
DSC Shell	545	*
Cask Lead Shielding	485	621

* The components perform their intended safety function within the operating range.

Table M.4-17
Vacuum Drying Fuel Cladding Maximum Temperatures

Operating Condition	Configuration 1 (°F)	Configuration 2 (°F)	Configuration 3 (°F)	Limit (°F)
Vacuum Drying, 33 hours	663	645	678	752

Table M.4-18
DSC Basket Assembly Maximum Component Temperatures During Vacuum Drying at 33
hours⁽²⁾

Condition/Configuration	T _{grid,max} (°F)	T _{grid,min} (°F)	T _{rail,max} (°F)	T _{rail,min} (°F)	T _{Al,max} (°F) ⁽¹⁾
Vacuum Drying/Configuration 1	645	324	345	314	644
Vacuum Drying/Configuration 2	626	326	352	314	626
Vacuum Drying/Configuration 3	656	314	335	306	656

(1) Includes aluminum and poison plates.

(2) Temperatures correspond to 35 hours into vacuum drying which is conservative for 33 hour case.

	0.87	0.87	0.87	0.87	
0.87	0.63	0.63	0.63	0.63	0.87
0.87	0.63	0.63	0.63	0.63	0.87
0.87	0.63	0.63	0.63	0.63	0.87
0.87	0.63	0.63	0.63	0.63	0.87
	0.87	0.87	0.87	0.87	

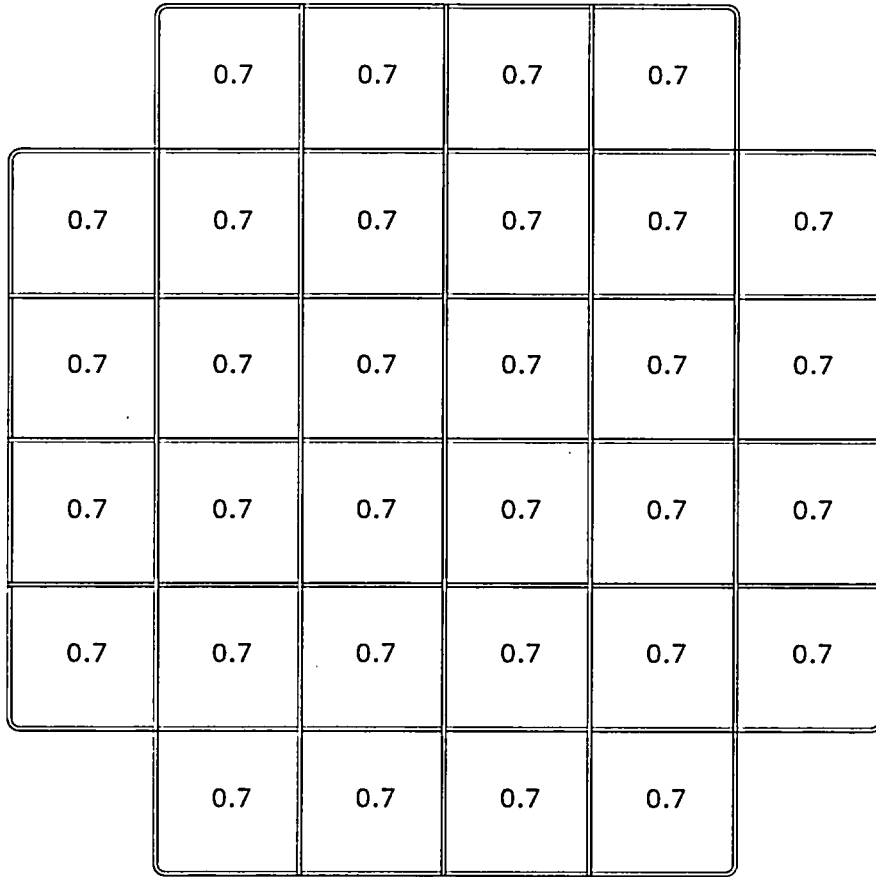
F5483

Figure M.4-1
Heat Load Zoning Configuration 1, Maximum Decay Heat for Various Assemblies

	1.2	0.6	0.6	1.2	
1.2	0.6	0.6	0.6	0.6	1.2
0.6	0.6	0.6	0.6	0.6	0.6
0.6	0.6	0.6	0.6	0.6	0.6
1.2	0.6	0.6	0.6	0.6	1.2
	1.2	0.6	0.6	1.2	

F5485

Figure M.4-2
Heat Load Zoning Configuration 2, Maximum Decay Heat for Various Assemblies



F5484

Figure M.4-3
Heat Load Zoning Configuration 3, Maximum Decay Heat for Various Assemblies



Figure M.4-4
Axial Heat Profile for PWR Fuel

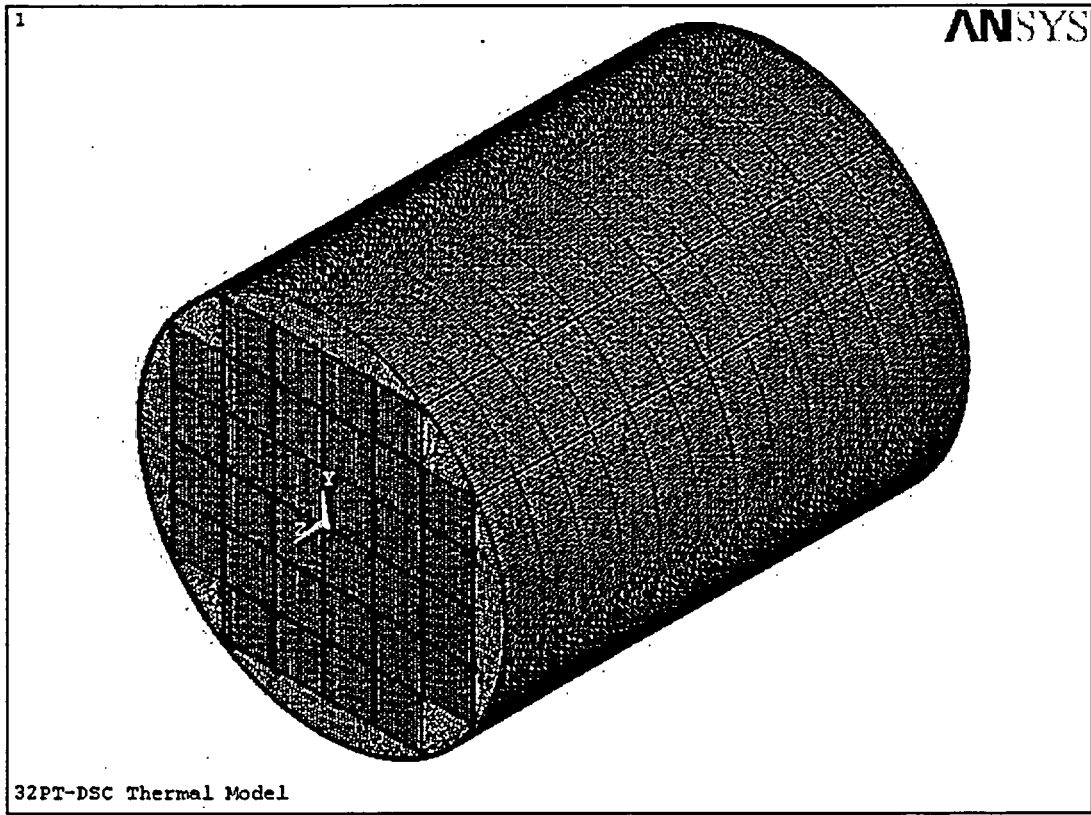


Figure M.4-5
32PT-DSC Thermal ANSYS Model, Isometric View

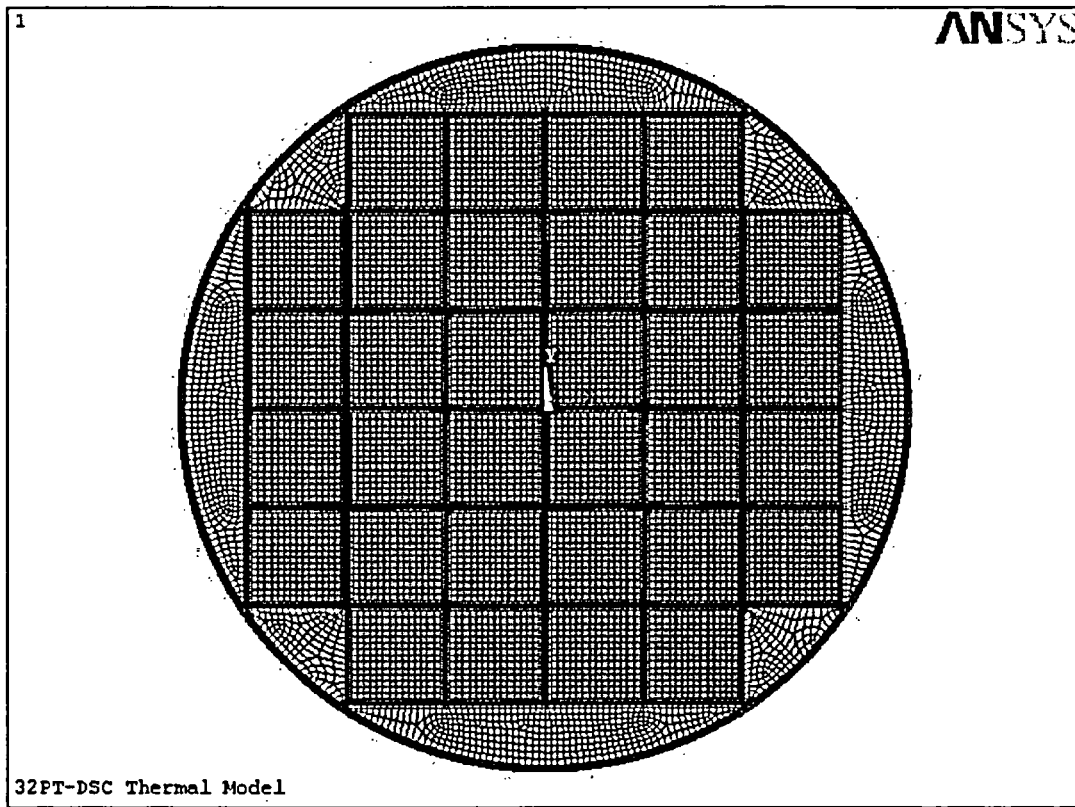


Figure M.4-6
32PT DSC Thermal ANSYS Model, Cross-Section View

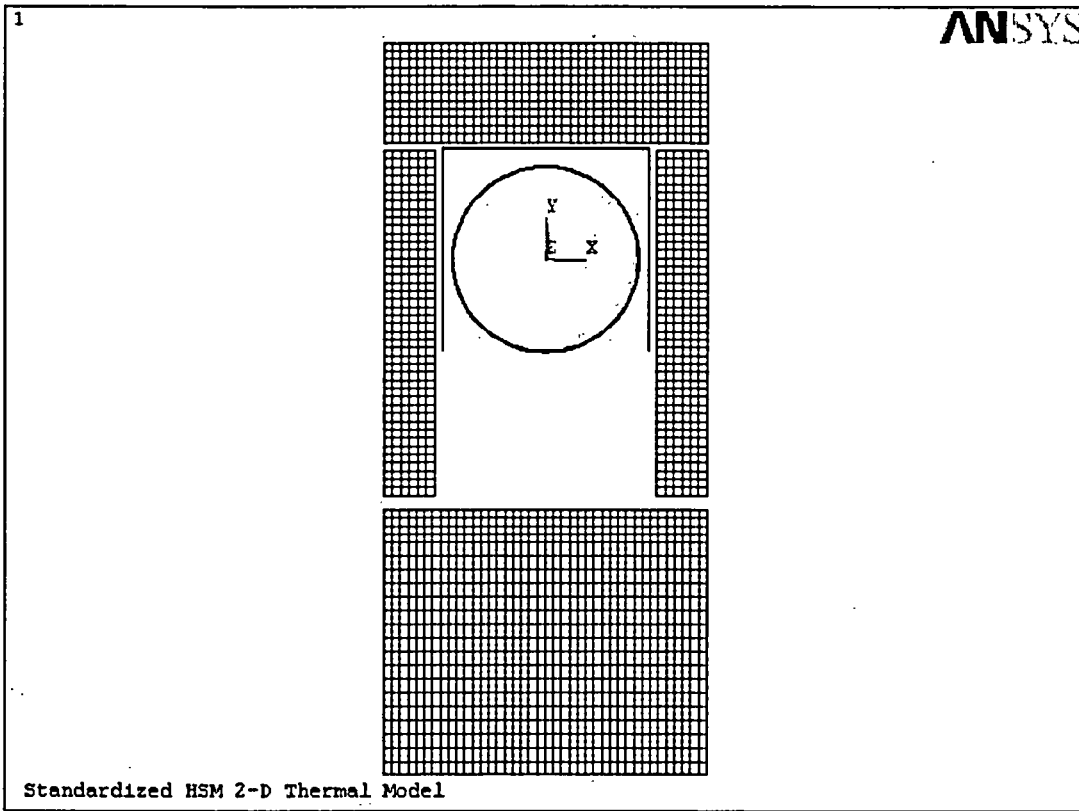


Figure M.4-7
Thermal Model of DSC in HSM

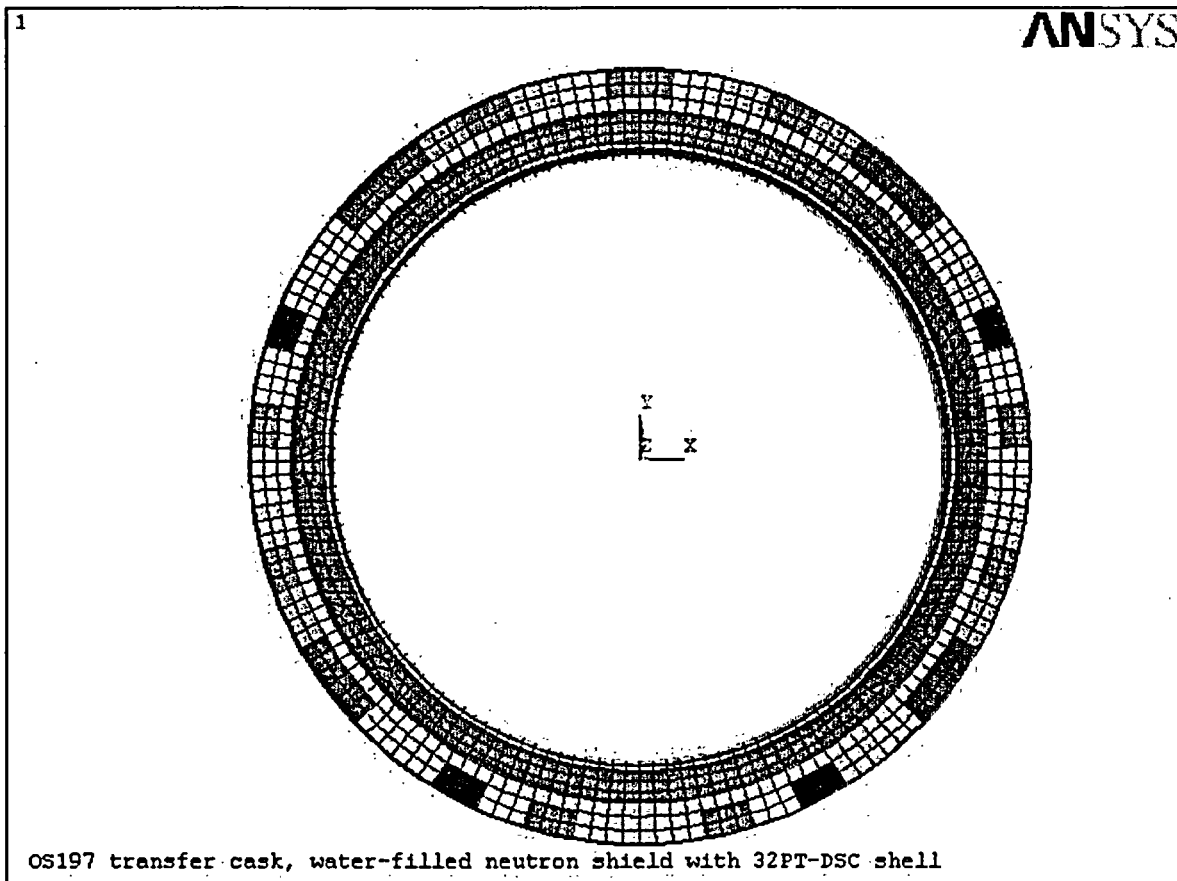
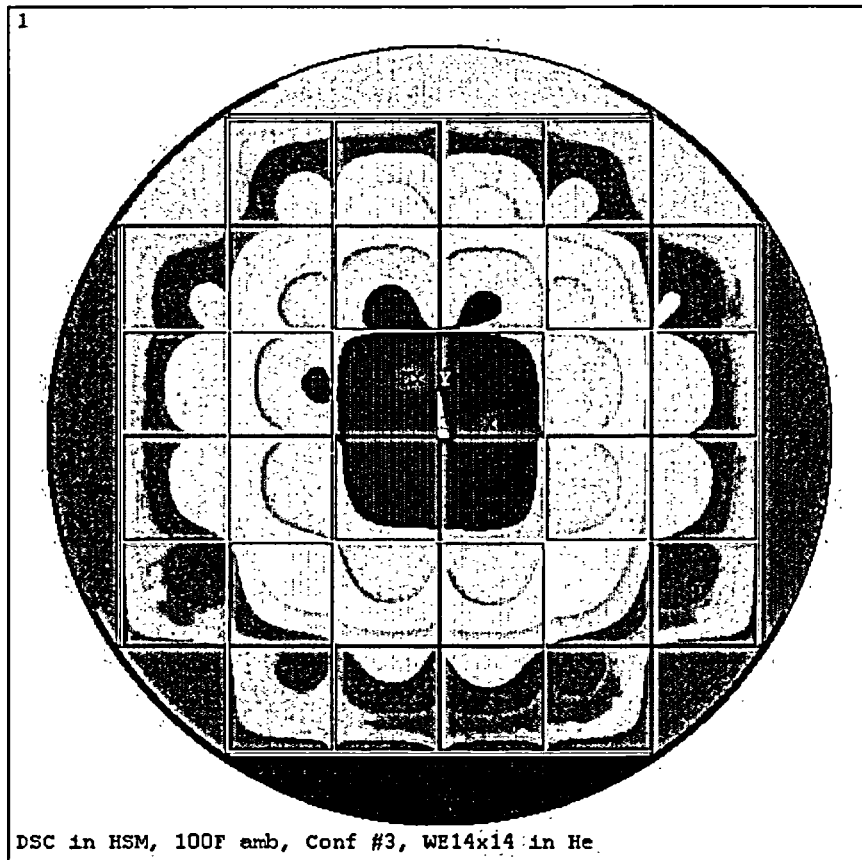


Figure M.4-8
Thermal Model of TC



ANSYS 5.6.2
 JAN 21 2003
 10:28:58
 NODAL SOLUTION
 STEP=1
 SUB =1
 TIME=1
 TEMP
 SMN =264
 SMX =658.224
 264
 307.803
 351.605
 395.408
 439.211
 483.013
 526.816
 570.619
 614.421
 658.224

Figure M.4-9
Results for 100°F Storage Case With Heat Load Zoning Configuration 3

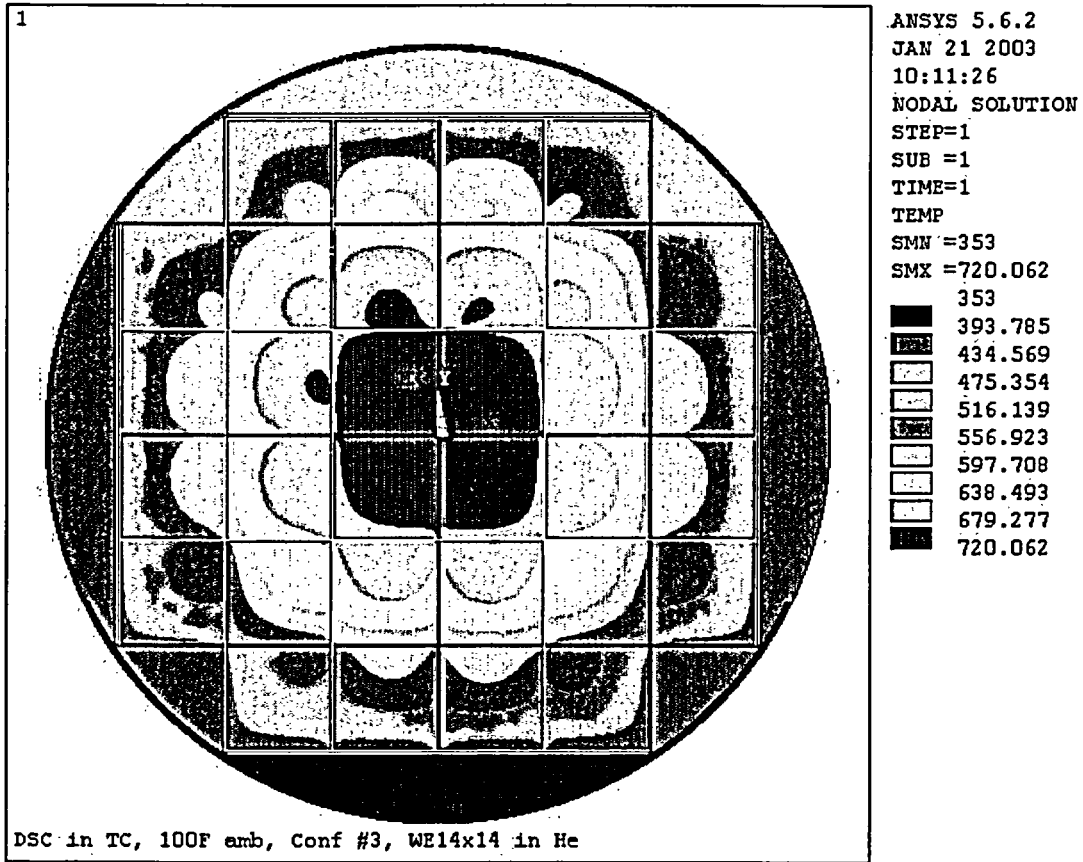
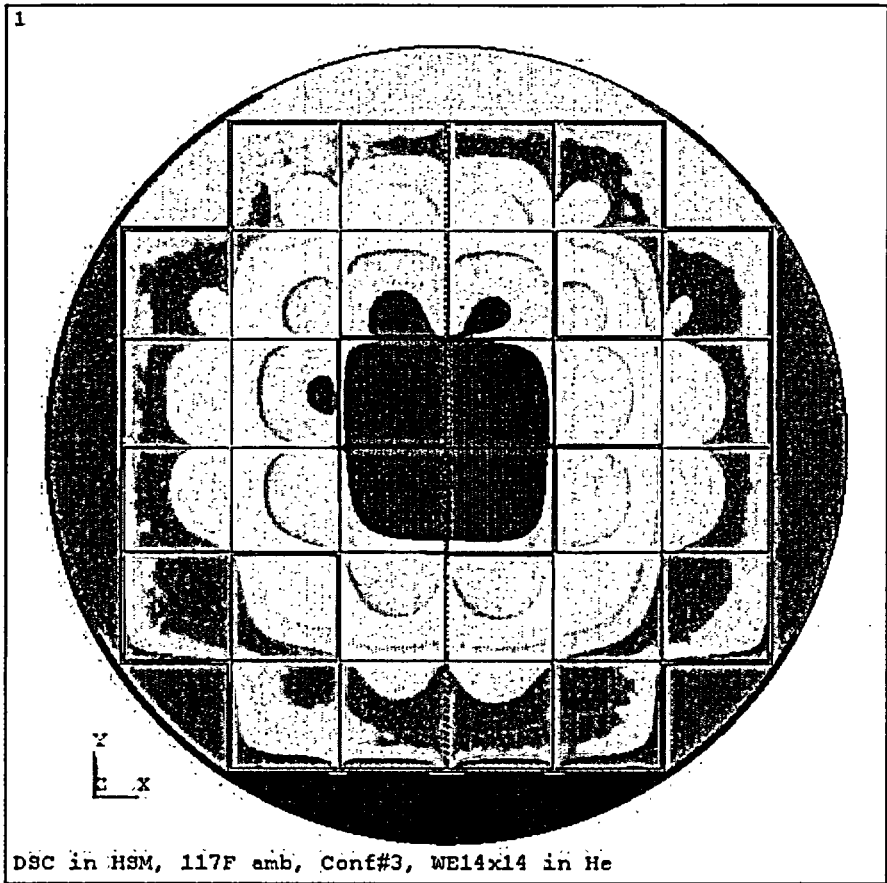


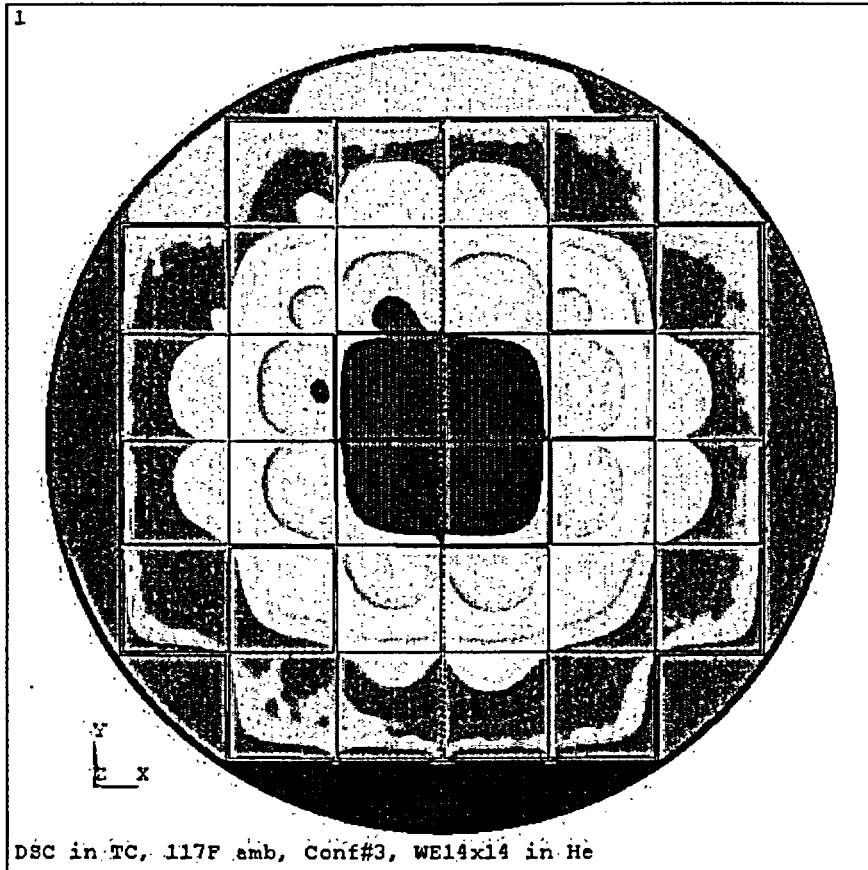
Figure M.4-10
Results for 100°F Transfer Case With Heat Load Zoning Configuration 3



ANSYS 5.6.2
 JAN 14 2003
 10:48:01
 NODAL SOLUTION
 STEP=1
 SUB =1
 TIME=1
 TEMP
 TEPIC=98.764
 SMN =270
 SMX =663.413

ZV =1
 DIST=36.955
 Z-BUFFER
 270
 313.713
 357.425
 401.138
 444.85
 488.563
 532.275
 575.988
 619.7
 663.413

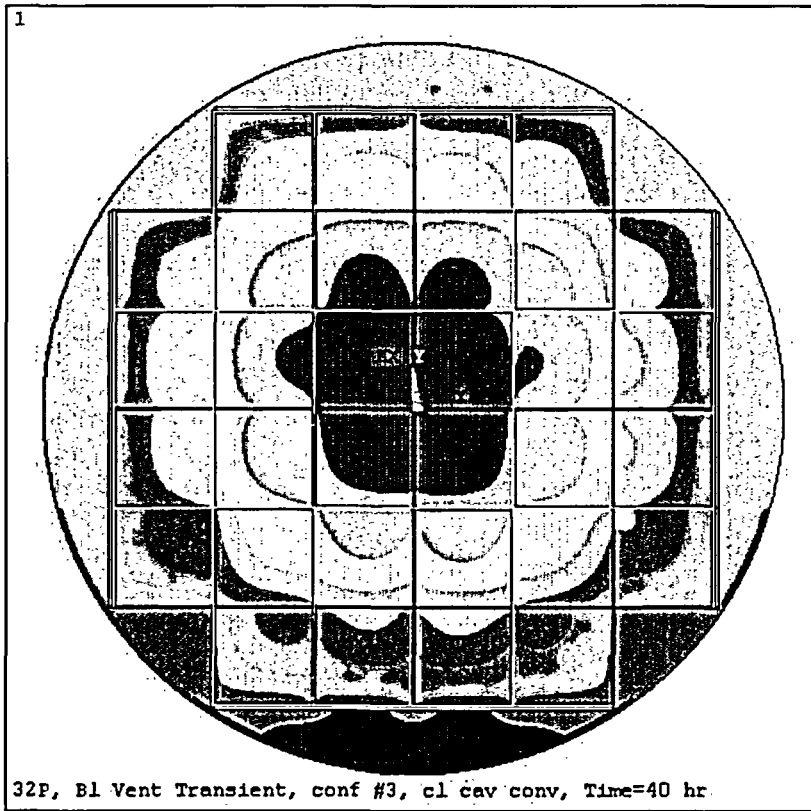
Figure M.4-11
Results for 117°F Storage Case With Heat Load Zoning Configuration 3



ANSYS 5.6.2
 JAN 14 2003
 11:22:25
 NODAL SOLUTION
 STEP=1
 SUB =1
 TIME=1
 TEMP
 TEPC=98.746
 SMN =354
 SMX =714.857

ZV =1
 DIST=36.955
 2-BUFFER
 354
 394.095
 434.19
 474.286
 514.381
 554.476
 594.571
 634.667
 674.762
 714.857

Figure M.4-12
Results for 117°F Transfer Case With Heat Load Zoning Configuration 3



ANSYS 5.6.2
 JAN 17 2003
 10:01:35
 NODAL SOLUTION
 STEP=11
 SUB =1
 TIME=2400
 TEMP
 SMN =440
 SMX =787.677

■	440
■	478.631
■	517.262
■	555.892
■	594.523
■	633.154
■	671.785
■	710.415
■	749.046
■	787.677

Figure M.4-13
Results for Blocked Vent Case With Heat Load Zoning Configuration 3 at 40 Hours

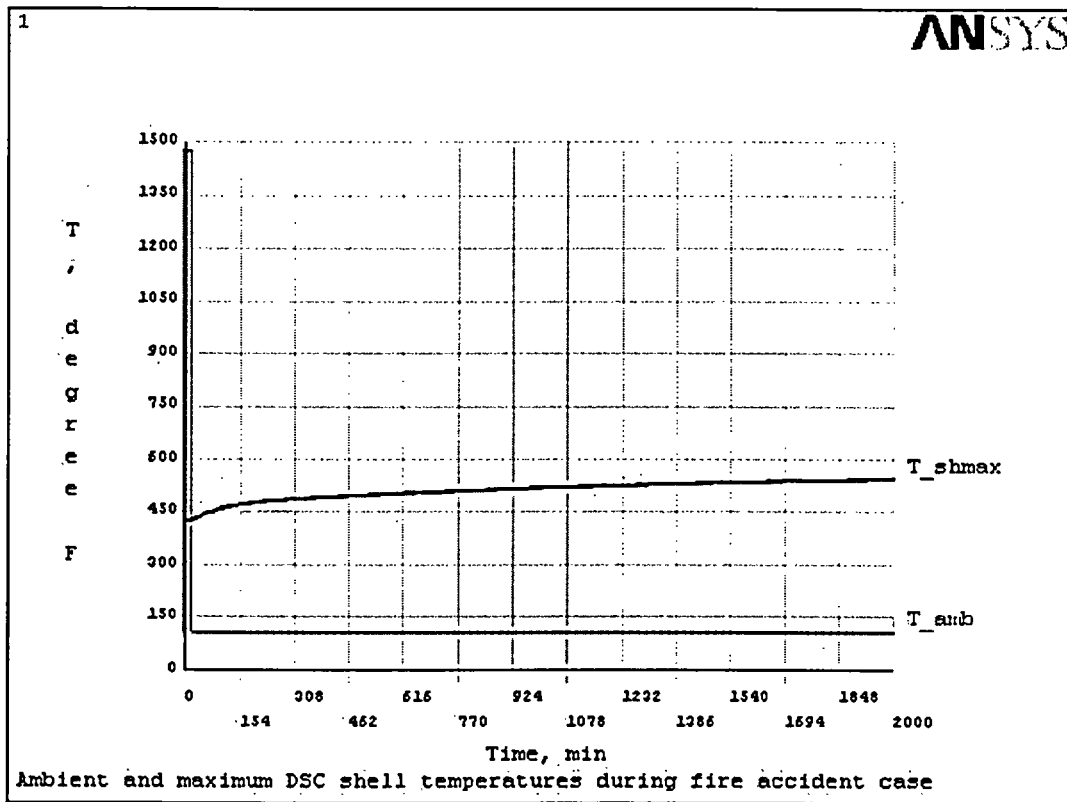


Figure M.4-14
 NUHOMS[®]-32PT DSC and TC Temperature Response to
 15 Minute Fire Accident Conditions

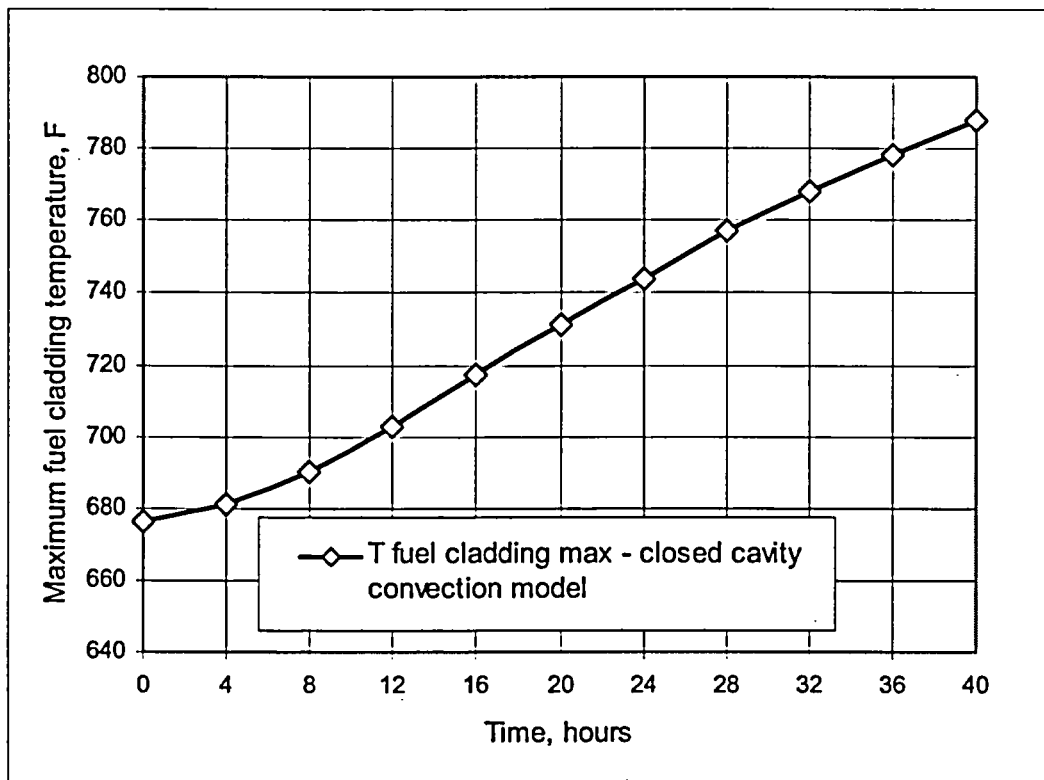


Figure M.4-15
Time-History Profile of the Maximum Fuel Cladding Temperature during Blocked Vent
Case, Configuration #3

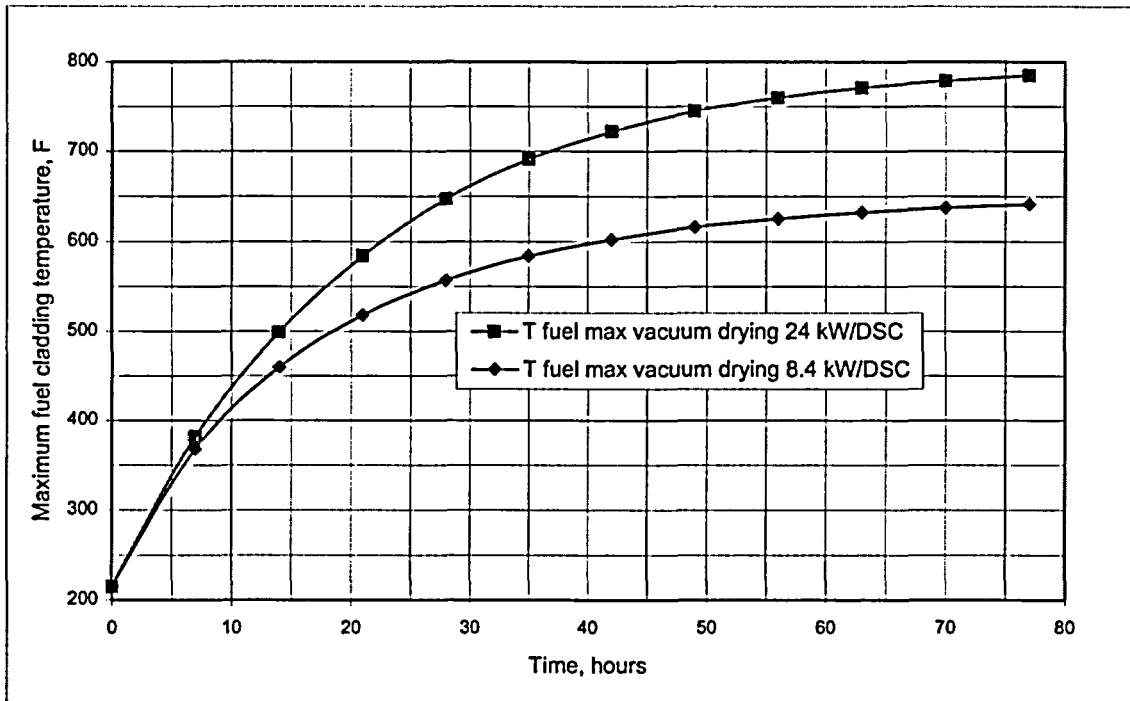


Figure M.4-16
Maximum Fuel Temperature during Vacuum Drying
with Heat Load Zoning Configuration 3

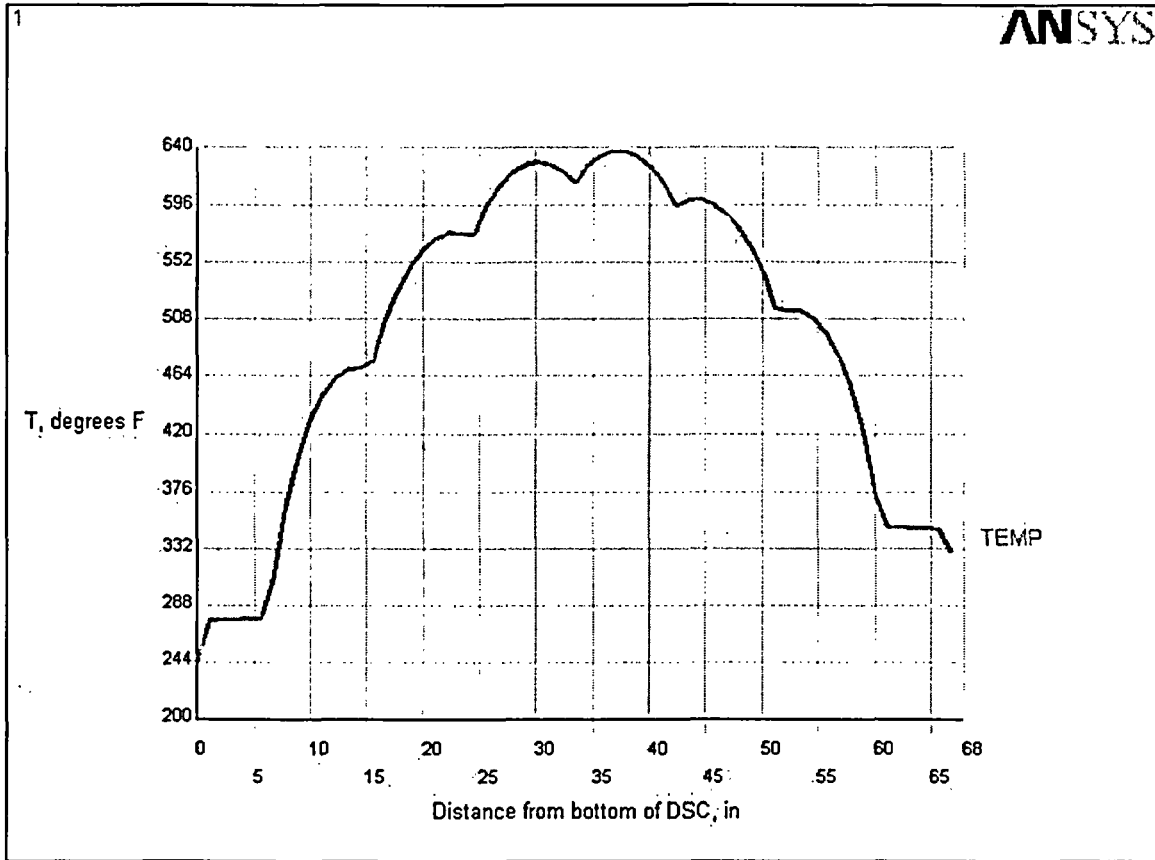


Figure M.4-17
Temperature Distribution from Bottom to Top of DSC at Cross-Section with Highest
Temperatures, 70°F HSM Storage Case (Configuration 3)

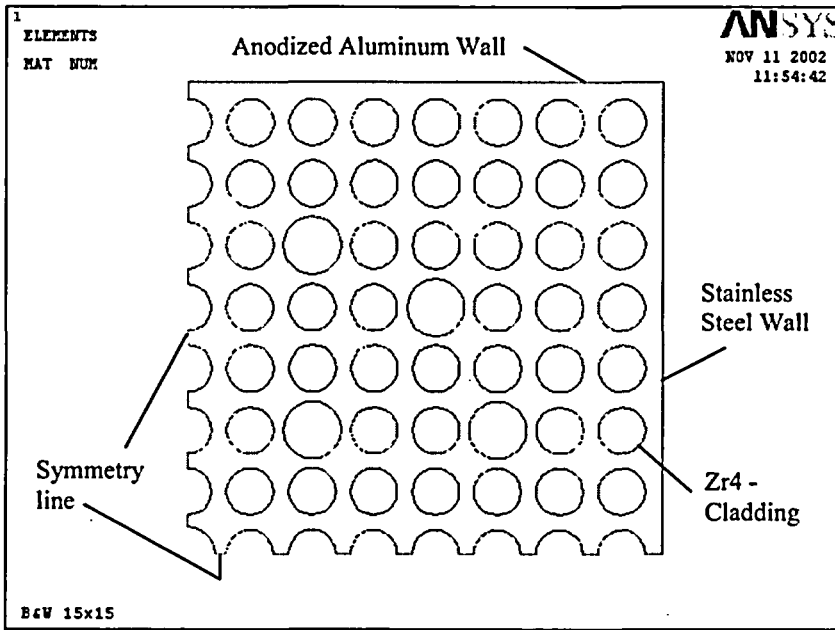
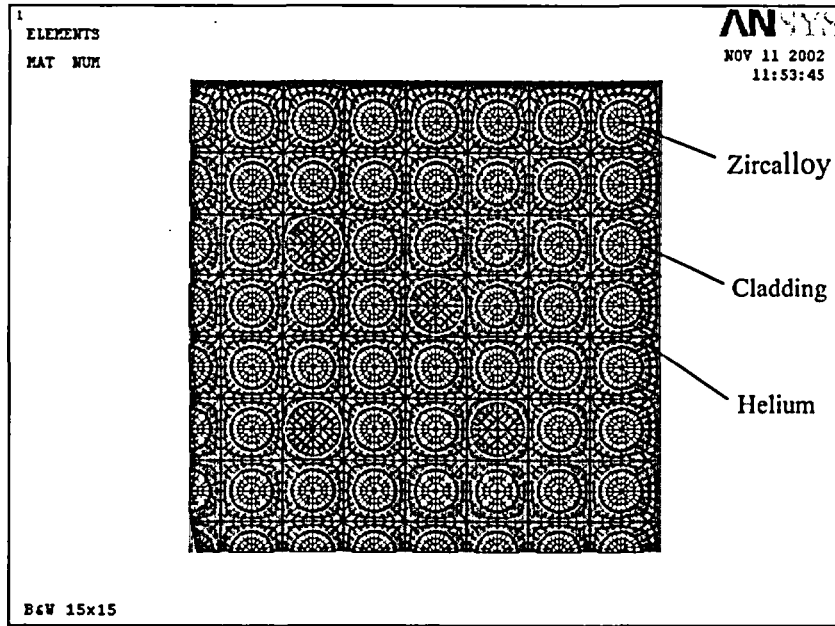
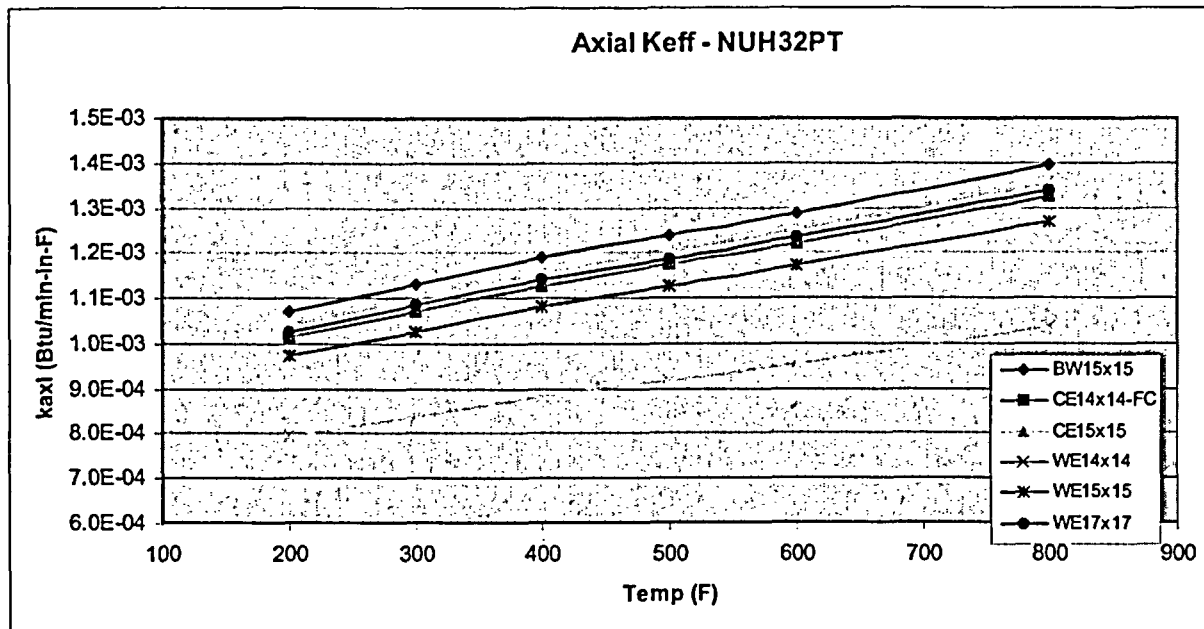


Figure M.4-18
Finite Element Model of B&W 15x15 Fuel Assembly



**Figure M.4-19
Fuel Axial Effective Conductivity**

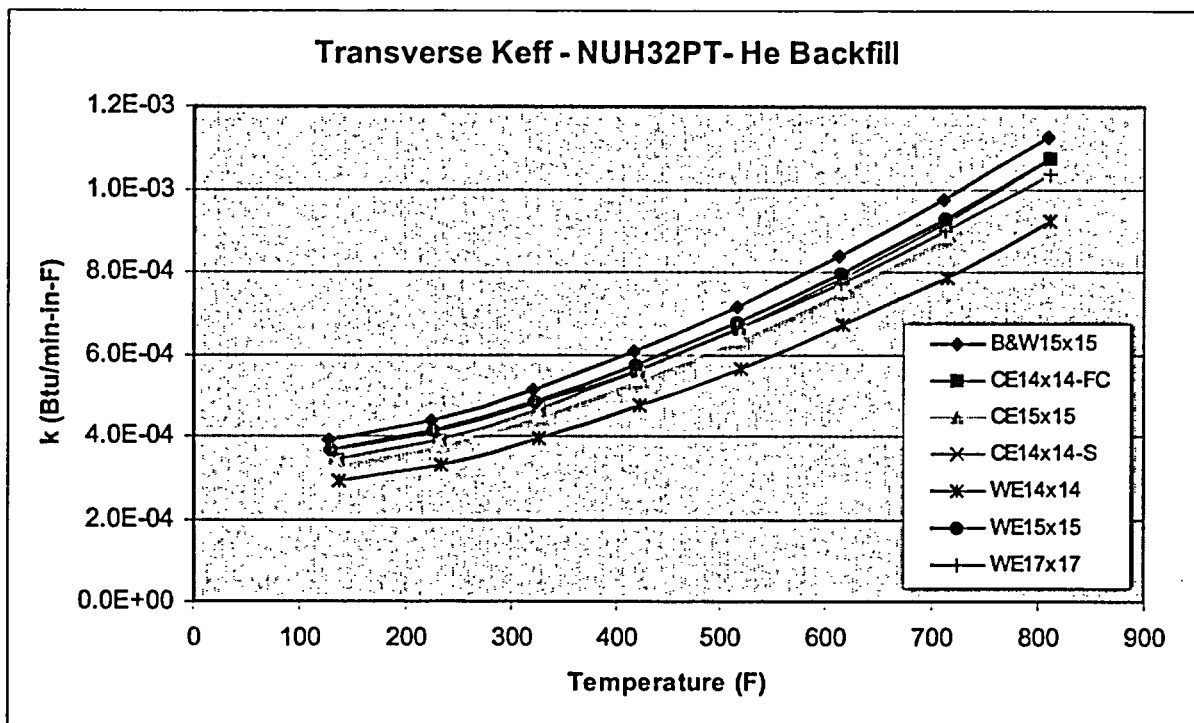


Figure M.4-20
Fuel Transverse Effective Conductivity in Helium

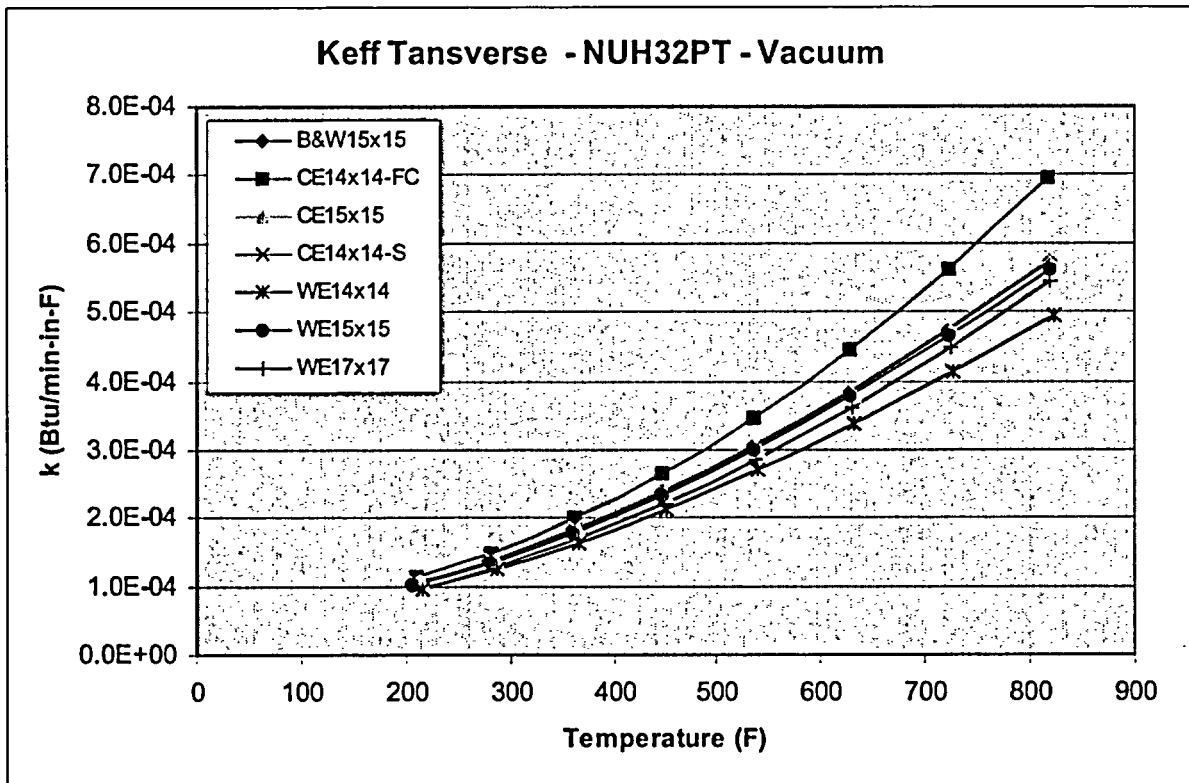
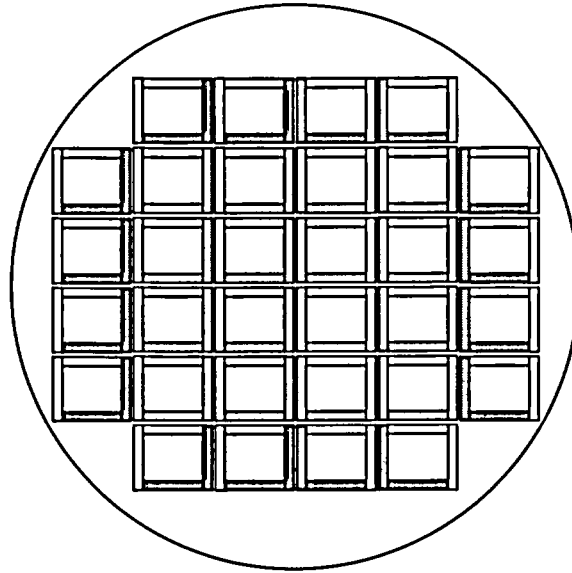


Figure M.4-21
Fuel Transverse Effective Conductivity in Vacuum

16 Poison Plate Configuration



24 Poison Plate Configuration

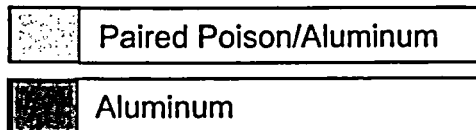
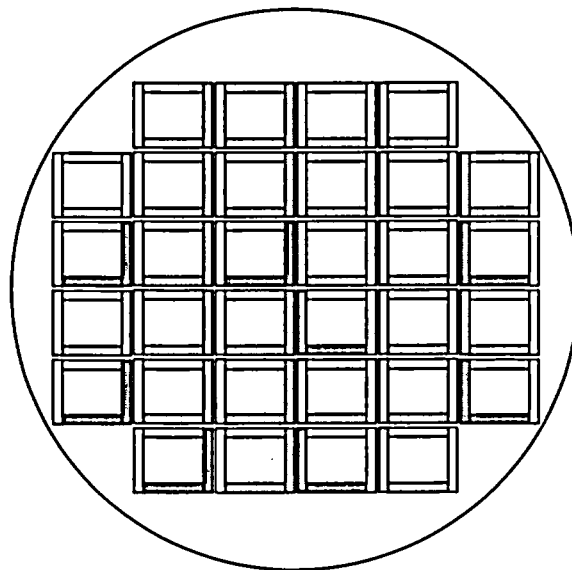


Figure M.4-22
Alternate Basket Poison/Aluminum Configuration

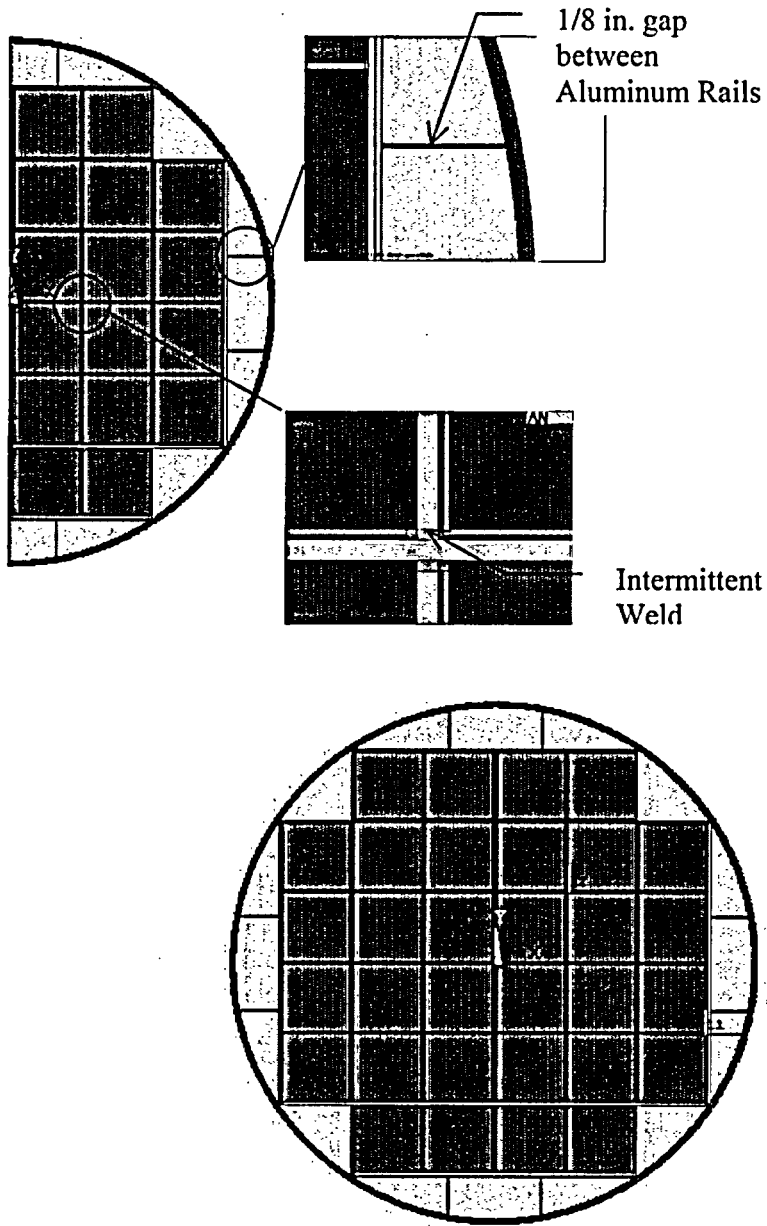


Figure M.4-23
Finite Element Models of Alternate Basket Configurations

M.5 Shielding Evaluation

The radiation shielding evaluation for the Standardized NUHOMS[®] System (during loading, transfer and storage) for the 24P and 52B canisters is discussed in Sections 3.3.5, 7.0 and 8.0. The following radiation shielding evaluation specifically addresses the dose rates due to design-basis PWR fuel and Burnable Poison Rod Assemblies (BPRAs) loaded in a NUHOMS[®]-32PT DSC. The shielding analysis is carried out for the four DSC configurations of the NUHOMS[®]-32PT system described in Section M.2.1. The basket layout for these configurations is identical except for the length of the DSC components. For shielding purposes, the only difference between the 32PT-S100/32PT-L100 and 32PT-S125/32PT-L125 versions is the thickness of the shield plug designs. The 32PT-S100/32PT-L100 versions have somewhat thinner shield plugs than the 32PT-S125/32PT-L125 versions. Each of the configurations is designed to store up to 32 intact standard PWR fuel assemblies. The 32PT-L100 and 32PT-L125 are also designed to store up to 32 intact standard PWR fuel assemblies with or without BPRAs. Therefore, for shielding purposes, the two long-cavity versions bound the short-cavity versions because of the additional gamma source due to the BPRAs. Therefore, the shielding evaluation presented herein is performed only for the 32PT-L100 and 32PT-L125 with fuel plus BPRAs. To assure that this evaluation is conservative, the fuel source terms are not adjusted to account for the additional decay required to accommodate the BPRAs.

The design-basis PWR fuel source terms are derived from the bounding fuel, B&W 15x15 Mark B assembly design as described in Section M.5.2

The NUHOMS[®]-32PT DSCs can store intact PWR fuel assemblies and BPRAs with the characteristics described in Table M.2-1. The NUHOMS[®]-32PT DSC may store PWR fuel assemblies arranged in any of three alternate heat zoning configurations with a maximum decay heat of 1.2 kW per assembly and a maximum heat load of 24 kW per canister. The heat load configurations are shown in Figure M.2-1, Figure M.2-2 and Figure M.2-3. Note that while the B&W, CE, and Westinghouse fuel designs are specifically listed, storing reload fuel designed by other manufacturers is also allowed provided an analysis is performed to demonstrate that the limiting features listed in Table M.2-1 bound the specific manufacturers replacement fuel. The limiting features are burnup, initial enrichment, cooling time, fissile material type, number of fuel rods, number of guide tube/instrument tube holes, cobalt impurities in the hardware and initial heavy metal.

The design-basis fuel source terms for this evaluation are defined as the source terms from fuel with the burnup/initial enrichment/cooling time combination given in Table M.2-5 through Table M.2-9 (without BPRAs) and located in the basket as shown in Figure M.2-1, Figure M.2-2 or Figure M.2-3, that gives the maximum dose rate on the surface of the HSM and/or OS197/OS197H Transfer Cask (TC). This approach is consistent with the method used to generate the fuel qualification tables for the Standardized NUHOMS[®]-24P and -52B canister designs as described in Section 7.2.3.

The Heat Load Zoning Configuration 2 (Figure M.2-2) is the configuration that produces the highest dose rates on the surfaces of the HSM and TCs. These bounding gamma and neutron source terms are then used in the radiation shielding models to conservatively calculate dose rates on and around the NUHOMS[®]-32PT system. In order to model Heat Load Zoning Configuration 2, all sixteen assemblies in the outer ring of the DSC are modeled with source

terms consistent with 1.2 kW. Therefore, the source terms result in fairly conservative dose rates because the shielding analysis is based on a 28.8 kW heat load compared to the 24 kW heat load limit.

The bounding burnup, minimum initial enrichment and cooling time combinations used in this analysis are as follows:

- 30 GWd/MTU, 2.5 wt. % U-235, 8-year cooled – Inner sixteen assemblies in the HSM models,
- 41 GWd/MTU, 3.1 wt. % U-235, 5-year cooled – Outer sixteen assemblies in the HSM and TC models, and
- 45 GWd/MTU, 3.3 wt. % U-235, 23-year cooled - Inner sixteen assemblies in the TC models.

The design-basis source terms for the authorized BPRAs are taken from Appendix J. The design-basis source terms cover three BPRAs designs: (1) B&W 15x15 Burnable Absorber Assemblies with up to 2 cycles burnup and 5-year cooled, (2) WE 17x17 Pyrex Burnable Absorber, 2-24 Rodlets with up to 2 cycles burnup and 10-year cooled, and (3) WE 17x17 WABA Burnable Absorber, 3-24 Rodlets with up to 2 cycles burnup and 10-year cooled. The properties used to calculate the design-basis source terms for the authorized BPRAs are reproduced in Table M.5-2.

The methodology, assumptions, and criteria used in this evaluation are summarized in the following subsections.

M.5.1 Discussion and Results

The maximum dose rates due to 32 design-basis PWR fuel assemblies with BPRAs in the NUHOMS[®]-32PT DSC loaded into the Standardized NUHOMS[®]-HSM are summarized in Table M.5-3 for both the 32PT-S100/32PT-L100 and 32PT-S125/32PT-L125 design configurations. Table M.5-4 provides maximum and surface average dose rates on the HSM loaded with the NUHOMS[®]-32PT DSC for both the 32PT-S100/32PT-L100 and 32PT-S125/32PT-L125 design configurations. Table M.5-5 provides a summary of the dose rates on and around the TC for canister transfer for 32PT-S100/32PT-L100 and 32PT-S125/32PT-L125 configurations. The dose rates in these tables are for the bounding Configuration 2.

A basket with two alternate poison plate configurations is also considered. One is a 16 poison plate and the second is a 24 poison plate configuration. Since the total weight of the material in the basket is the same as the original poison plate configuration, the results calculated here are also applicable to baskets with these alternate poison plate configurations.

A discussion of the method used to determine the design-basis fuel and BPRA source terms is included in Section M.5.2. The model specification and shielding material densities are given in Section M.5.3. The method used to determine the dose rates due to 32 design-basis fuel assemblies with BPRAs in the NUHOMS[®]-32PT DSC design configurations is provided in Section M.5.4. Thermal and radiological source terms are calculated with the SAS2H/ORIGEN-S modules of SCALE 4.4 [5.1] for the fuel. The shielding evaluation is performed with the DORT [5.2] code with the CASK-81 cross section library [5.3]. Sample input files used for calculating neutron and gamma source terms and dose rates are included in Section M.5.5.1.

M.5.2 Source Specification

Thermal and radiological source terms are calculated with the SAS2H/ORIGEN-S modules of SCALE 4.4 [5.1] for the fuel. The SAS2H/ORIGEN-S results are used to develop the fuel qualification tables listed in Table M.2-5 through Table M.2-14 and the design-basis fuel source terms suitable for use in the shielding calculations. The thermal and radiological source terms for the BPRAs are taken from Appendix J.

The B&W 15x15 assembly is the bounding fuel assembly design for shielding purposes because it has the highest initial heavy metal loading as compared to the 14x14, other 15x15, and 17x17 fuel assemblies which are also authorized contents of the NUHOMS[®]-32PT DSC. In addition, the maximum Co59 content of the hardware regions for each assembly type is less than that of the B&W 15x15 Mark B fuel assembly. The neutron flux during reactor operation is peaked in the in-core region of the fuel assembly and drops off rapidly outside the in-core region. Much of the fuel assembly hardware is outside of the in-core region of the fuel assembly. To account for this reduction in neutron flux, the fuel assembly is divided into four exposure "regions." The four axial regions used in the source term calculation are: the bottom (nozzle) region, the in-core region, the (gas) plenum region, and the top (nozzle) region. The B&W 15x15 fuel assembly masses for each irradiation region are listed in Table M.5-6. The light elements that make up the various materials for the various fuel assembly materials are taken from reference [5.4] and are listed in Table M.5-7. The design-basis heavy metal weight is 0.475 MTU. These masses are irradiated in the appropriate fuel assembly region in the SAS2H/ORIGEN-S models. To account for the reduction in neutron flux outside the In-Core regions neutron flux (fluence) correction factors are applied to light element composition for each region. The neutron flux correction factors are given in Table M.5-8.

The fuel qualification tables are generated based on the decay heat limits for the various heat load zoning configurations shown in Figure M.2-1, Figure M.2-2 and Figure M.2-3. SAS2H is used to calculate the minimum required cooling time as a function of assembly initial enrichment and burnup for each decay heat limit. The total decay heat includes the contribution from the fuel as well as the hardware in the entire assembly. The fuel qualification table for fuel plus BPRAs also includes 8 watts per BPRA to account for the design-basis decay heat from the BPRAs. Because the decay heat generally increases slightly with decreasing enrichment for a given burnup, it is conservative to assume that the required cooling time for a higher enrichment assembly is the same as that for a lower enrichment assembly with the same burnup. The required cooling time for initial enrichments that fall between any two SAS2H runs are assumed to be that of the lower enrichment case results.

The design-basis source terms are defined as the burnup/initial enrichment/cooling time combination given in the fuel qualification tables that result in the maximum dose rate on the surface of the HSM and OS197/OS197H TC. The initial enrichment and burnups used for generating the design basis source terms are assembly averages. The 1-D discrete ordinates code ANISN [5.5] and the CASK-81 22 neutron, 18 gamma-ray energy group, coupled cross-section library [5.3] is used to determine these design-basis source terms. Finding the burnup/initial enrichment/cooling time combinations from the fuel qualification tables and decay heat load zoning configurations that produce the maximum dose rate on the HSM roof determine the design-basis source term for the HSM shielding calculations. Similarly the design-basis source terms for the OS197/OS197H TC are determined by finding the maximum surface dose rates on

the side of the cask. This approach, described in detail in Section M.5.2.4, is consistent with the method used to determine the fuel qualification tables for the Standardized NUHOMS[®] canister designs described in Section 7.2.3. The radiological source terms generated in the SAS2H/ORIGEN-2 runs are used in the ANISN evaluations to calculate the surface dose rates. The ANISN models are similar to the appropriate DORT models for the locations of interest. Heat load configuration 2 (Figure M.2-2) produced the bounding total surface dose rate for both the HSM and TC. The HSM design-basis source terms for the outer ring of assemblies (modeled as sixteen assemblies) are from fuel with 41 GWd/MTU burnup, an initial enrichment of 3.1 wt. % U-235 and 5-years cooling. The HSM design-basis source terms for the inner sixteen assemblies are from fuel with 30 GWd/MTU burnup, and initial enrichment of 2.5 wt. % U-235 and 8-years cooling. Note that using this approach in modeling the outer ring of sixteen assemblies with the 1.2 kW source terms for all of the shielding analyses results in fairly conservative dose rates because the shielding analysis is in reality based on a 28.8 kW heat load. The TC design-basis source terms for the outer ring of assemblies (conservatively modeled as sixteen assemblies) are from fuel with 41 GWd/MTU burnup, an initial enrichment of 3.1 wt. % U-235 and 5-years cooling. The TC design-basis source terms for the inner sixteen assemblies are from fuel with 45 GWd/MTU burnup, and initial enrichment of 3.3 wt. % U-235 and 23-years cooling.

A sample SAS2H/ORIGEN-S input file for the In-Core Region for the 41 GWd/MTU, 3.1 wt. % U-235 and 5-years cooling case is listed and commented in Section M.5.5.1.

M.5.2.1 Gamma Source

Four SAS2H/ORIGEN-S runs are required for each burnup/initial enrichment/cooling time combination to determine gamma source terms for the four regions of interest for each fuel assembly; the bottom, in-core, plenum and top regions. The only difference between the runs is in Block #10 "Light Elements" of the SAS2H input and the 81\$\$ card in the ORIGEN-S input. Each run includes the appropriate Light Elements for the region being evaluated and the 81\$\$ card is adjusted to have ORIGEN-S output the total gamma source for the in-core region and only the light element source for the plenum and top nozzle regions.

The design-basis source terms for the authorized BPRAs designs are taken from Appendix J of the FSAR. The design-basis source terms from Appendix J of the FSAR cover three BPRAs designs 1) B&W 15x15 Burnable Absorber Assemblies with up to 2 cycles burnup and 5-year cooled, 2) WE 17x17 Pyrex Burnable Absorber, 2-24 Rodlets with up to 2 cycles burnup and 10-year cooled, and 3) WE 17x17 WABA Burnable Absorber, 3-24 Rodlets with up to 2 cycles burnup and 10-year cooled.

The SAS2H/ORIGEN-S gamma ray source is output in the CASK-81 energy group structure.

Gamma source terms for the in-core region include contributions from actinides, fission products, and activation product. The bottom, plenum and top nozzle regions include the contribution from the activation products in the specified region only. These results for the 41 GWd/MTU, 3.1 wt. % U-235 and 5-years cooling case are shown in Table M.5-9. The results for the 30 GWd/MTU, 2.5 wt. % U-235 and 8-years cooling case are shown in Table M.5-10. Finally, the results for the 45 GWd/MTU, 3.3 wt. % U-235 and 23-years cooling case are shown in Table M.5-11.

As stated above the design-basis BPRA source terms are taken from Appendix J of the FSAR and are listed in Table M.5-12.

Gamma source terms for use in the shielding models are calculated by multiplying the assembly sources by the number of assemblies in the region of interest (16) and dividing by the appropriate inner/outer heat load region volume. The appropriate assembly region volumes for both the inner and outer heat load zones are listed in Table M.5-13.

M.5.2.2 Neutron Source Term

One SAS2H/ORIGEN-S run is required for each burnup/initial enrichment/cooling time combination to determine the total neutron source terms for the in-core regions. The results for each burnup/initial enrichment/cooling time combination of interest are summarized in Table M.5-14.

Neutron source terms for use in the shielding models are calculated by multiplying the assembly sources by the number of assemblies in the in-core region of interest (16) and dividing by the appropriate in-core inner/outer heat load region volume. The appropriate assembly region volumes for both the inner and outer heat load regions are listed in Table M.5-13.

M.5.2.3 Axial Peaking

Axial peaking factors for both neutron and gamma sources in PWR fuel are taken from Reference [5.6]. These peaking factors were derived from work performed by the Department of Energy in support of its Topical Report for burnup credit [5.7]. The neutron and gamma peaking factors are shown as a function of the core height in Table M.5-15. These factors are directly applied to each DORT interval in the fuel region. Neutron peaking factors in each zone are equal to the gamma factor raised to the fourth power to correctly account for the variation of neutron source with burnup. The axial source distribution defined in Table M.5-15 introduces some level of conservatism into this calculation because the length average peaking factor of 1.06 is greater than 1.

M.5.2.4 ANISN Evaluation for Bounding Source Terms

As discussed above, the fuel qualification tables are generated based on the decay heat limits for the various heat load zoning configurations shown in Figure M.2-1, Figure M.2-2 and Figure M.2-3. SAS2H is used to calculate the minimum required cooling time as a function of assembly initial enrichment and burnup for each decay heat limit. To determine which configuration and burnup, wt. % initial enrichment and cooling time combinations result in the bounding dose rates on the surface of the HSM and TC, the total source term, which includes the contribution from the fuel as well as the hardware in the entire assembly (including end fittings) is used to calculate its total ANISN dose rate on the HSM roof and TC radial using the ANISN code.

The BPRA contribution is fixed and is included in the design basis shielding evaluation as such and therefore is not included in this ANISN evaluation.

ANISN [5.5] determines the fluence of particles throughout one-dimensional geometric systems by solving the Boltzmann transport equation using the method of discrete ordinates. Particles

can be generated by either particle interaction with the transport medium or extraneous sources incident upon the system. Anisotropic cross-sections can be expressed in a Legendre expansion of arbitrary order.

The ANISN code implements the discrete ordinates method as its primary mode of operation. Balance equations are solved for the flow of particles moving in a set of discrete directions in each cell of a space mesh and in each group of a multigroup energy structure. Iterations are performed until all implicitness in the coupling of cells, directions, groups, and source regeneration is resolved.

ANISN coupled with the CASK-81 22 neutron, 18 gamma-ray energy group, coupled cross-section library [5.3] and the ANSI/ANS-6.1.1-1977 flux-to-dose conversion factors [5.10] is chosen to generate the ANISN dose rates used to determine the relative strength of the various source terms from fuel assemblies to determine the design basis source terms for the HSM and TC. These design basis source terms are used with DORT to calculate the bounding system dose rates. ANISN provides an efficient method to calculate the design basis source terms.

The surface dose rates are calculated using ANISN models to perform the evaluation for the fuel assembly parameters in the fuel qualification table. The ANISN model used to calculate the relative dose rates on the HSM surface is similar to the cut through the center of the DORT HSM roof model used for the shielding evaluation (for each configuration). The ANISN model used to generate the relative dose rates on the TC is similar to the cut through the center of the DORT TC side model used for the shielding evaluation. Figure M.5-31 and Figure M.5-32 provide sketches for the ANISN models of the HSM roof and TC centerline respectively. When modeling 0.63 kW or 0.60 kW source region in Region A (16 assemblies) of Figure M.5-31 and Figure M.5-32, the Region B does not include any source terms. Similarly, when modeling 0.87 kW or 1.2 kW source region in Region B (16 assemblies), of these figures, the Region A does not include any source terms. For modeling 0.7 kW source region, both Region A and Region B (32 total assemblies) include source terms corresponding to 0.7 kW. An example ANISN input file is included in Section M.5.5.5.

The material densities used in the ANISN models for the various model regions are listed in Table M.5-27. These material densities are very similar to those used for the DORT and MCNP analysis, but are simplified to reduce the size of the ANISN input decks. Only the important elements of a give material are included and the gram density of the material is maintained. The density of NS-3 is used instead of water in ANISN models. This has no impact on the results of ANISN evaluation because ANISN is only used to compare the relative strength of the source terms for each entry in the fuel qualification table.

The results of the ANISN runs are given in Table M.5-28 through Table M.5-37.

To determine the design basis source terms to be used in the HSM shielding calculations, the total roof surface dose rates for the configurations shown in Figure M.2-1, Figure M.2-2 and Figure M.2-3 are calculated using the results provided in Table M.5-28 through Table M.5-37. For Configuration 1, the maximum total roof dose rate is 35.0 plus 0.19 or 35.2 mrem/hr. For Configuration 2, the total roof dose rate is 46.87 plus 0.16 or 47.03 mrem/hr, while for Configuration 3, the total roof dose rate is 28.4 mrem/hr. Based on these results, Configuration 2 results in the maximum dose rates for the HSM with design basis source terms for the outer ring

of assemblies (conservatively modeled as sixteen assemblies) are from fuel with 41 GWd/MTU burnup, an initial enrichment of 3.1 wt. % U-235 and 5 years cooling. The design basis source terms for the inner sixteen assemblies are from fuel with 30 GWd/MTU burnup, and initial enrichment of 2.5 wt. % U-235 and 8 year cooling. Note that using this approach in modeling, the outer ring of sixteen assemblies with the 1.2 kW source terms, results in fairly conservative dose rates because the shielding analysis is in reality based on a 28.8 kW heat load.

Similarly, to determine the design basis source terms to be used in the Transfer Cask shielding calculations, the total side centerline surface dose rates for the configurations shown in Figure M.2-1, Figure M.2-2 and Figure M.2-3 are calculated using the results provided in Table M.5-28 through Table M.5-37. For Configuration 1, the total side dose rate is 404.86 plus 34.57 or 439.43 mrem/hr. For Configuration 2, the total side dose rate is 593.8 plus 32.08 or 625.88 mrem/hr, while for Configuration 3, the total roof dose rate is 331.4 mrem/hr. Based on these results, Configuration 2 results in the maximum dose rates for the TC with design basis source terms for the outer ring of assemblies (conservatively modeled as sixteen assemblies) are from fuel with 41 GWd/MTU burnup, an initial enrichment of 3.1 wt. % U-235 and 5 years cooling. The design basis source terms for the inner sixteen assemblies are from fuel with 45 GWd/MTU burnup, and initial enrichment of 3.3 wt. % U-235 and 23 year cooling.

M.5.3 Model Specification

M.5.3.1 Material Densities

With the exception of the DSC basket and fuel, all material densities are taken directly from the calculations used to support Section 7 of the FSAR.

The material weight given in Table M.5-6 for the fuel assembly and Table M.5-2 for the BPRAs are used to calculate material densities for in-core, plenum, top and bottom regions of the fuel assembly. The poison in the BPRAs is modeled as pure aluminum because it is a relatively light element with little shielding capability. In addition, while the source terms account for 32 BPRAs the material densities conservatively account for only 24 BPRAs. For the HSM axial dose rates and all of the TC calculations, only 20% of the steel plates used to form the fuel compartments is modeled in the shielding analysis. All other components of the basket such as the neutron poison material; aluminum plates, etc., have been conservatively neglected for all models. For the lateral HSM DORT shielding model only, the homogenized fuel regions also include all of the steel from the DSC basket inner fuel compartment. The zircaloy is modeled as Zr and the inconel, carbon steel and stainless steel are all modeled as Fe. This assumption has little effect on the dose rate results. The smeared active fuel region volume of the basket is the sum of the inner and outer heat load region volumes given in Table M.5-13.

In order to account for subcritical multiplication, an initial enrichment of ~4.9 wt. % U-235 is used to calculate the amount of U-235 in the shielding models. For an initial enrichment of ~4.9%, there are 23,044 grams of U-235 per assembly and 451,956 grams of U-238.

The material densities used in the various models are summarized in Table M.5-16.

M.5.4 Shielding Evaluation

Dose rate contributions from the bottom, in core, plenum and top regions, as appropriate, from 32 fuel assemblies with BPRAs are calculated with the DORT Code [5.2] at various location on and around the NUHOMS® -32PT DSCs, HSM, and OS197/OS197H TC.

The radiation shielding evaluation for the Standardized NUHOMS® System during loading, transfer and storage for the 24P and 52B canisters is discussed in Sections 3.3.5, 7.0 and 8.0 of the FSAR. The following shielding evaluation discussion specifically addresses the NUHOMS® -32PT-S100/32PT-L100 and 32PT-S125/32PT-L125 DSCs in an HSM and TC using the design-basis source terms determined in Section M.5.2.

M.5.4.1 Computer Programs

DORT [5.2] determines the fluence of particles throughout one-dimensional or two-dimensional geometric systems by solving the Boltzmann transport equation using either the method of discrete ordinates or a diffusion theory approximation. Particles can be generated by either particle interaction with the transport medium or extraneous sources incident upon the system. Anisotropic cross-sections can be expressed in a Legendre expansion of arbitrary order.

The DORT code implements the discrete ordinates method as its primary mode of operation. Balance equations are solved for the flow of particles moving in a set of discrete directions in each cell of a space mesh and in each group of a multigroup energy structure. Iterations are performed until all implicitness in the coupling of cells, directions, groups, and source regeneration is resolved.

DORT was chosen for this application because of its ability to solve two dimensional, cylindrical, deep penetration radiation transport problems similar to the NUHOMS® System.

M.5.4.2 Spatial Source Distribution

The source components are:

- The neutron sources due to the active fuel regions of the inner sixteen and outer sixteen fuel assemblies,
- The gamma source due to the active fuel regions of the inner sixteen and outer sixteen fuel assemblies,
- The gamma source due to the plenum regions of the inner sixteen and outer sixteen fuel assemblies,
- The gamma source due to the top regions of the inner sixteen and outer sixteen fuel assemblies,
- The gamma source due to the bottom region of the inner sixteen and outer sixteen fuel assemblies,

- The gamma source due to the 32 BPRAs in the active fuel region,
- The gamma source due to the 32 BPRAs in the plenum region, and
- The gamma source due to the 32 BPRAs in the top region.

The U-235 fission spectrum is input into the 1* array of the DORT input file to account for subcritical multiplication, increasing the neutron source in the active fuel region. Axial peaking is accounted for in the active fuel region by inputting a relative flux factor at each node in the 97* array. The flux factor data is discussed in Section M.5.2.3.

M.5.4.3 Cross Section Data

The cross-section data used in this analysis is taken from the CASK-81 22 neutron, 18 gamma-ray energy group, coupled cross-section library [5.3]. CASK-81 is an industry standard cross-section library compiled for performing calculations of spent fuel shipping casks and is distributed by ORNL/RSIC. The cross-section data allows coupled neutron/gamma-ray dose rate evaluation to be made that account for secondary gamma radiation (n, γ).

Microscopic P₃ cross-sections are taken from the CASK-81 library and mixed using the GIP-PC computer program distributed with DORT [5.2] to provide macroscopic cross-sections for the materials in the cask model.

An additional element and material, "fluxdosium," is included in the cross-section data and mixing table in the GIP input file. Fluxdosium is used to provide flux-to-dose rate conversion factors as described in Section M.5.4.4 for use in activity calculations. The presence of fluxdosium in the cross-section data does not affect the actual flux calculations.

M.5.4.4 Flux-to-Dose-Rate Conversion

The flux distribution calculated by the DORT code is converted to dose rates using the same flux-to-dose rate conversion factors as those used in the FSAR from ANSI/ANS-6.1.1-1977. The flux-to-dose rate conversion factors are entered into DORT through the cross section tables as material "fluxdosium".

The dose rate at each node in the DORT models is calculated using the activity calculation feature of DORT. The "cross-section" data for "fluxdosium" is specified for the activity calculations, which determine the gamma and neutron dose rate at each node.

M.5.4.5 Methodology

The methodologies used in this calculation are similar to those previously used to support NUHOMS[®] storage and transportation applications. The computer codes, basic modeling techniques, and analyses are based in large part on those used to support the Sacramento Municipal Utility Districts storage license at their Rancho Seco Nuclear Generating Station (TAC Number L10017, Materials License Number SNM-2510) and to support the certificate of compliance application for the NUHOMS[®]-61BT storage system [5.8]. The methodology used herein is summarized below.

1. Volumetric sources in the CASK-81 format are developed for all fuel regions using the source term data developed in Section M.5.2. Source regions include the active fuel region, bottom end fitting (including all materials below the active fuel region), plenum, and top end fitting (including all materials above the active fuel region). Sources for control components are added group-by-group to the fuel sources.
2. Suitable shielding material densities are calculated for the fuel, DSC, HSM, and TC.
3. The 2-D discrete ordinates code DORT [5.2] is used to calculate dose rates on and around the DSC, HSM, and TC. The DORT code is selected because of its ability to readily handle thick, multi-layered shields and account for streaming through both the HSM air vents and cask/DSC annulus. The simple NUHOMS[®] geometry lends itself to 2-D models (RZ models are used for the cask and both RZ and XY models are used for the HSM).

The discrete-ordinates code DORT is selected over monte-carlo methods for this calculation because it can quickly and reliably calculate dose rate distributions around the cask and HSM without the need to fine-tune biasing parameters for each case addressed. Additionally, the surface or volume crossing estimators typically used in monte-carlo calculations tend to average dose rates across an area or volume and may therefore underpredict the magnitude of radiation streaming. While DORT is subject to instabilities commonly referred to as "ray effects", these tend to result in conservative overpredictions of radiation streaming.

4. The DORT results are used to calculate offsite exposures.
5. DORT models are also generated to determine the effects of accident scenarios including HSM sliding and loss of cask neutron shield for the bounding Configuration 2.

M.5.4.6 Assumptions

The following general assumptions are used in the analyses.

Source Terms

- The primary neutron source in LWR spent fuel is the spontaneous fission of ²⁴⁴Cm. For the ranges of exposures, enrichments, and cooling times in the fuel qualification tables, ²⁴⁴Cm represents more than 85% of the total neutron source. The neutron spectrum is, therefore, relatively constant for the fuel parameters addressed herein. Surface gamma dose rates are calculated for the HSM and cask surfaces using the actual photon spectrum applicable for each case.
- The PWR heavy metal weight is assumed to be 0.475 MTU per assembly to bound existing PWR fuel designs.

Shielding Materials

- Source regions are homogenized (smeared) to simplify the shielding calculations.

- The HSM reinforcing bars (rebars) have been included in smeared regions in the HSM walls and roof. The rebar steel is included in three inch thick regions for each face of each HSM surface. This layered method of including the rebar in the shielding model is consistent with ANSI/ANS 6.4 Guidelines.

HSM Dose Rates

- The HSM design evaluated in this calculation dose not include the thicker door and steel vent liners described in Section 8.1.1.6.
- The DSC and fuel assemblies are positioned as close to the front door as possible to maximize the front wall dose rates.
- Cylindrical (RZ) models are used to calculate dose rates on the front and back walls. Planes of reflection are used to simulate adjacent HSMs. Although the actual HSM geometry is rectangular, the cylindrical models conservatively calculate dose rates along the centerline of each HSM surface.
- Cartesian (XY) models are used to calculate the peak dose rates on the roof and side walls. Additional cylindrical results are used to estimate the dose rate distribution along the DSC axis.
- In the cartesian models, the DSC and fuel are modeled as a square source region. The size of this region was selected to maintain the total source volume.
- Fully symmetric S16 quadrature is used for all cylindrical models. An upward biased, 210-direction quadrature set [5.9] is used for the cartesian models.
- Embedments in the HSM concrete are neglected.
- For the accident case, an HSM is assumed to slide against its neighbor, opening a 12-inch gap between HSMs.

Cask Dose Rates

- The cask and DSC are modeled in cylindrical coordinates.
- Three inches of supplemental neutron shielding and one inch of steel are placed on top of the DSC cover plates during welding.
- During the accident case, the water in the cask neutron shield is lost.

M.5.4.7 Source Region Homogenization

While it is acceptable to smear the materials from the NUHOMS[®]-32PT “egg crate” basket design into the assembly regions of the shielding models for dose rates in the radial direction of the canister, it is non-conservative to take full credit for the basket materials in the axial direction of the canister. MCNP is used to demonstrate that taking only 20% credit for the basket materials results in conservative dose rates in the axial directions.

Two MCNP models are used to perform this evaluation. The first model explicitly evaluates the basket design in full three-dimensional space. The second model replicates the homogenized (smeared) or two-dimensional model of the source regions with the fuel assembly and 20% credit for the basket material in the various assembly regions. A representative source, 45 GWd/MTU burnup, 3.3 wt. % U-235 initial enrichment and 16 year cooling time, is used for this evaluation.

M.5.4.7.1 Source Terms

SAS2H is used to generate the neutron and gamma source terms for 45 GWd/MTU 3.3 wt. % U-235 and 16 year cooled fuel. The models are identical to those used to generate the design basis source terms described in Section M.5.2 except the burnup, initial enrichment and cooling time is adjusted for a burnup of 45 GWd/MTU, an initial enrichment of 3.3 wt. % U-235 and a cooling time of 16 years.

The neutron source is given in Table M.5-17 and the gamma sources for the top, plenum and in-core regions are given in Table M.5-18.

M.5.4.7.2 Material Densities

Table M.5-19 and Table M.5-20 list the gram and atom densities for the fuel assembly materials used in the explicit and smeared MCNP models, respectively. Only the top half of the canister is modeled in MCNP with a reflective boundary condition at the center of the fuel region. The in-core, plenum and top regions of the fuel assembly are modeled along with the steel in the basket, the DSC shell and shield plugs. Portions of the aluminum in the transition rail region are also included in the models. The material densities for stainless steel, aluminum and air are given in Table M.5-21. This analysis is also valid for the alternate 32PT transition rail design that uses a solid aluminum insert in place of the transition rails as this region is external to the basket and only affects the side wall dose rates, not the top end dose rates which limit the amount of credit one can take for the basket. The poison plates and aluminum inside the fuel compartments are not modeled in either model. The canister shell, shield plugs and the aluminum in the transition region are modeled identically in both the explicit and smeared cases. For the explicit model, the basket is explicitly modeled as a series of 0.25" thick steel plates with the appropriate assembly region smeared inside the open square formed by the plates. For the smeared case, 20% of the steel from the basket structure and the appropriate assembly region are smeared into an equivalent right circular cylinder.

M.5.4.7.3 MCNP Models

Figure M.5-1 shows the radial cross section of the explicit MCNP models. Figure M.5-2 shows the axial layout of the assembly regions and shield plug in the explicit and smeared MCNP models. Finally, Figure M.5-3 shows the radial cross section of the smeared MCNP models. These models are used to calculate the average dose rates on the surface of the shield plug, on the surface of the canister shell next to the top region, next to the plenum region and next to in-core region. Eight MCNP runs, four each for the explicit and smeared models, are used to calculate these dose rates on the surfaces of the canister. The first run calculates the contribution from the in-core neutron source, the second determines the contribution from the in-core gamma source, the third from the plenum gamma source and finally the fourth from the top region.

M.5.4.7.4 MCNP Results

The results for each set of runs are given in Table M.5-22. Table M.5-22 also includes the ratio of the smeared to the explicit results demonstrating that smearing up to 20% of the basket into a 2-D model of the DSC gives slightly conservative results in both the axial and radial dose rates.

M.5.4.8 HSM Dose Rates for the 32PT-S125/32PT-L125 Configuration

Dose rates on and around an HSM containing a design-basis NUHOMS[®]-32PT-S125/32PT-L125 DSC are calculated using the DORT 2-D discrete-ordinates code. Five sets of HSM models are generated, four for normal conditions and one for accident conditions. These models are discussed and listed in the following sections.

M.5.4.8.1 HSM Roof Model

The HSM roof model is a cylindrical model representing a vertical plane through the DSC, HSM front and back walls, and HSM roof. This model is used to calculate dose rates on and around the upper half of the HSM. Note that a similar model (discussed in the next section as HSM floor model) is used to calculate dose rates around the lower half of the HSM.

The geometry of the roof model is shown in Figure M.5-4. Sources and materials are as defined above.

M.5.4.8.2 HSM Floor Model

The HSM floor model is similar to the roof model. It is used to calculate the dose rates on the front and back walls of the HSM below the centerline of the DSC. The geometry of the floor model is shown in Figure M.5-5. As with the roof model, two sets of six runs are made to represent the six source regions and to model an adjacent HSM.

M.5.4.8.3 HSM Side Model

The HSM side model is similar to the roof and floor models. It is used to calculate the dose rates near the front vent and on the end shield wall. The geometry of the side model is shown in Figure M.5-6. This model represents a horizontal plane that includes the DSC centerline. As such, the air vents through the side wall (located well above and below the DSC centerline) are not included in the model. This is not expected to significantly affect the accuracy of the calculation. Previous experience loading NUHOMS[®] HSMs indicates that the remaining conservatism in the shielding models, including applying bounding 2-D dose rates on 3-D surfaces, more than outweigh this modeling choice. The impact of this choice is further reduced because the vents are well away from the DSC and particles would have to scatter several times before reaching the front screen. As with the roof model, two sets of six runs are made to represent the six source regions and to model an adjacent HSM.

M.5.4.8.4 HSM Top Model

The HSM Top models represent a vertical plane that is perpendicular to the longitudinal axis of the DSC. This model is used to calculate the dose rate distribution on the HSM roof and end shield wall. This XY cartesian model is shown in Figure M.5-7. The source region is modeled

as a square 49.92 inches on a side in order to keep its volume (and hence the total source strength) the same as in the cylindrical models. The radial number densities are used in this model. Two sets of five runs are made to represent the five source regions (inner neutron, outer neutron in the $\pm Y$ directions, inner gamma, outer gamma in the $+ X$ direction, outer gamma in the $\pm Y$ directions) and to model an adjacent HSM. The presence of an adjacent HSM is approximated using a plane of reflection in the center of the air vent. This model applies to both the 32PT-S125/32PT-L125 and 32PT-S100/32PT-L100 DSC configurations.

M.5.4.8.5 HSM Accident

The postulated accident condition, consisting of an HSM sliding laterally 6-inches until it contacts its neighbor, results in increased dose rates on one of the affected HSM's air vents. Accordingly, the dose rates on the roof and front face of the HSM will increase because of this event.

The shielding models for the accident case are identical to the lateral and side models discussed above, except that the vent width is increased from 6 inches to 12 inches. Reflection in the air vent is assumed for both.

M.5.4.9 HSM Models for the 32PT-S100/32PT-L100 DSC Configuration

The 32PT-S100/32PT-L100 NUHOMS[®]-32PT DSCs are the same length and carry the same payload as the 32PT-S125/32PT-L125 DSCs configurations. The main differences are the thicknesses of the top and bottom shield plugs. Accordingly, the DORT models described in Section M.5.4.8 are modified to create models applicable to the 32PT-S100/32PT-L100 DSC configuration. All other dimensions and materials are the same. The 32PT-S100/32PT-L100 HSM roof model geometry is shown in Figure M.5-8.

M.5.4.10 Data Reduction and HSM Dose Rate Results for the 32PT-S125/32PT-L125 DSC Configuration

The dose rate distribution for each case is calculated by summing the neutron and gamma DORT results. Surface average dose rates for each HSM surface are calculated as discussed below.

M.5.4.10.1 Front Surface for the 32PT-S125/32PT-L125 DSC Configuration

The dose rates on the HSM front are calculated using the floor (reflection at rear), roof (reflection at rear), and side (reflection in vent) models. The dose rates along the vertical centerline of the HSM front wall, from the floor and roof models, are shown in Figure M.5-9 for the 32PT-S125/32PT-L125 DSC configuration. Also shown in Figure M.5-9 (for comparison) is the total dose rate from the side model.

Based on the information in Figure M.5-9, the average dose rate on the HSM front wall is conservatively estimated by using the surface average dose rate from the floor/top models in the center region of the HSM (18.4 mrem/hr gamma and 9.2 mrem/hr neutron) and the surface average dose rate from the side model in the areas adjacent to and including the vents (146.7 mrem/hr gamma and 2.3 mrem/hr neutron). This is shown in Figure M.5-10 and conservatively assumes that the peak front vent dose rate (at the same height as the DSC centerline) exists along

the entire height of the front vent. The resulting maximum and average dose rates on the HSM front wall are shown in Table M.5-4.

M.5.4.10.2 Back Surface for the 32PT-S125/32PT-L125 DSC Configuration

The dose rates on the HSM rear shield wall are calculated using the floor and roof models (no reflection, rear shield wall included). Note that the side model results are bounded by the floor/roof models on the rear shield wall. The dose rates along the vertical centerline of the HSM front wall, from the floor and roof models, are shown in Figure M.5-11 for the 32PT-S125/32PT-L125 DSC configuration. The surface average dose rate on the rear shield wall is conservatively estimated using the surface-average results from the floor and roof models (these results are taken on the DSC centerline). The rear shield wall maximum and average dose rates are shown in Table M.5-4.

M.5.4.10.3 Roof Surface for the 32PT-S125/32PT-L125 DSC Configuration

The HSM roof dose rates are calculated using the top and roof models. The top model provides the peak dose rates across the width of the HSM as shown in Figure M.5-12 (top model with adjacent HSM shown) for the 32PT-S125/32PT-L125 configuration. The roof model results, which are shown in Figure M.5-13 and are orthogonal to those in Figure M.5-12, are used to estimate an overall average on the HSM roof. The length-average dose rates from the top model (as shown in Figure M.5-12) are 73.7 mrem/hr and 1.36 mrem/hr for gammas and neutrons, respectively. Figure M.5-14 shows the geometry used in calculating surface area average dose rates. The resulting roof dose rates are listed in Table M.5-4.

M.5.4.10.4 End Shield Wall Surface for the 32PT-S125/32PT-L125 DSC Configuration

The HSM end shield wall dose rates are calculated using the top and side models. The top model provides the peak dose rates down the side of the end shield wall. The side model results, which are orthogonal to those in the top model, are used to estimate an overall average on the HSM end shield wall. The average dose calculation is performed in the same manner as was used on the HSM roof. The length-average dose rates from the lateral model are 2.5 mrem/hr and 0.088 mrem/hr for gammas and neutrons, respectively. Because the top model is a cross-section at the center of the DSC, these are the peak "average" dose rates along the DSC length. By multiplying these results by the ratio of average to centerline from the side model, an overall surface average dose rate can be estimated (refer to Figure M.5-14). The resulting end shield wall dose rates are listed in Table M.5-4.

M.5.4.10.5 HSM Accident Case for the 32PT-S125/32PT-L125 DSC Configuration

The accident dose rates are calculated using the models described in Section M.5.4.8.5. The resulting dose rates are tabulated in Table M.5-23 for the bounding Configuration 2.

M.5.4.11 HSM Dose Rates for the 32PT-S100/32PT-L100 DSC Configuration

The HSM dose rate results are summarized in Table M.5-4 for the 32PT-S100/32PT-L100 DSC configuration.

M.5.4.11.1 Front Surface for the 32PT-S100/32PT-L100 DSC Configuration

The dose rate results are shown in Table M.5-4 and Figure M.5-15.

M.5.4.11.2 Back Surface for the 32PT-S100/32PT-L100 DSC Configuration

The dose rate results are shown in Table M.5-4 and Figure M.5-16.

M.5.4.11.3 Roof Surface for the 32PT-S100/32PT-L100 DSC Configuration

The dose rate results are shown in Table M.5-4 and Figure M.5-17 and Figure M.5-18.

M.5.4.11.4 End Shield Wall Surface for the 32PT-S100/32PT-L100 DSC Configuration

The dose rate results are shown in Table M.5-4.

M.5.4.11.5 HSM Accident Case for the 32PT-S100/32PT-L100 DSC Configuration

The dose rate results are shown in Table M.5-23 for the bounding Configuration 2.

M.5.4.12 TC Dose Rates for the 32PT-S125/32PT-L125 DSC Configuration

The NUHOMS[®] OS197/OS197H cask containing a NUHOMS[®]-32PT 32PT-S125/32PT-L125 DSC is modeled in cylindrical coordinates using 29 material zones as shown in Figure M.5-19. The materials used in zones 18-26 shown in Figure M.5-19 are varied to model the various welding and decontamination cases.

All cask cases use the same DORT model, with only the materials assigned to each zone being varied. The onsite transfer case, listed and commented below, includes all cask and DSC covers (zones 18, 19, 21-26), air in the DSC cavity (air versus helium has no effect on the results), air in the cask/DSC annulus (zones 7 and 16), and water in the neutron shield cavity (zone 9). The decontamination model includes water only in the cask/DSC annulus (all the way to the top of the DSC - zones 7 and 16), no water in the DSC cavity or neutron shield, and both the DSC and cask top covers removed. In the welding models, the DSC cavity is empty and the annulus is drained 12 inches below the top of the DSC. The inner cover welding case includes the DSC inner top cover (zone 18) and supplemental shielding consisting of three inches of NS-3 (zones 19 and 20, some NS-3 neglected for simplicity) and one inch of steel (zone 21). The outer cover welding case is identical except that the DSC outer cover (zone 19) is installed as well (supplemental NS-3 in zones 20-22, steel in zone 23).

M.5.4.12.1 Transfer Operations for 32PT-S125/32PT-L125 DSC Configuration

The cask normal operation (onsite transfer) dose rate results for 32PT-S125/32PT-L125 DSC configuration are summarized in Table M.5-5 and Figure M.5-20. The results are applicable to most activities performed outside the plant reactor building. The relatively high dose rate on the cask bottom surface is due to the area with reduced shielding directly below the DSC grapple ring. The peak along the cask side near its top end is due to the presence of control components in the fuel assemblies.

M.5.4.12.2 Decontamination Operations for 32PT-S125/32PT-L125 DSC Configuration

The results from the cask decontamination models for 32PT-S125/32PT-L125 DSC configuration are shown in Figure M.5-21.

M.5.4.12.3 Inner Cover Welding for 32PT-S125/32PT-L125 DSC Configuration

The dose rates during inner cover welding for 32PT-S125/32PT-L125 DSC configuration are shown in Figure M.5-22.

M.5.4.12.4 Outer Cover Welding for 32PT-S125/32PT-L125 DSC Configuration

The dose rates during outer cover welding for 32PT-S125/32PT-L125 DSC configuration are shown in Figure M.5-23.

M.5.4.13 Cask Dose Rates for 32PT-S100/32PT-L100 DSC Configuration

The dose rates around the NUHOMS[®] TC with the 32PT-S100/32PT-L100 DSC configuration are calculated in the same manner as was used for the heavier 32PT-S125/32PT-L125 DSC configuration. Data reduction for each case is summarized in the following sections. The 32PT-S100/32PT-L100 DSC configuration geometry is shown in Figure M.5-24.

The shielding configurations are identical to those listed in Section M.5.4.12.1. However, some lifting operations of the 32PT-S100/32PT-L100 DSC configuration are performed without water in the cavity and neutron shield. For these operations, the accident case results will be used to estimate dose rates and occupational exposures for the bounding Configuration 2.

M.5.4.13.1 Transfer Operations for 32PT-S100/32PT-L100 DSC Configuration

The cask normal operation (onsite transfer) dose rate results are summarized in Table M.5-5 and Figure M.5-25. The results are applicable to most activities performed outside the plant reactor building. The relatively high dose rate on the cask bottom surface is due to the area with reduced shielding directly below the DSC grapple ring. The peak along the cask side near its top end is due to the presence of control components in the fuel assemblies.

M.5.4.13.2 Decontamination Operations for 32PT-S100/32PT-L100 DSC Configuration

The dose rates during the cask decontamination for 32PT-S100/32PT-L100 DSC configuration are shown in Figure M.5-26.

M.5.4.13.3 Inner Cover Welding 32PT-S100/32PT-L100 DSC Configuration

The dose rates during inner cover welding for 32PT-S100/32PT-L100 DSC configuration are shown in Figure M.5-27.

M.5.4.13.4 Outer Cover Welding 32PT-S100/32PT-L100 DSC Configuration

The dose rates during outer cover welding for 32PT-S100/32PT-L100 DSC configuration are shown in Figure M.5-28.

M.5.4.14 Supporting 3-D Analysis

The purpose of this section is to provide supportive three-dimensional shielding analysis of the NUHOMS[®]-32PT System to demonstrate that the 2-D DORT analysis described above bounds a three dimensional analysis of the HSM with the bounding 32PT canister and source terms. As demonstrated in Table M.5-3 and Table M.5-4, the bounding 32PT canister is the 32PT-S100/32PT-L100 DSC Design Configuration with eight (modeled as 16) 1.2 kW (41 GWd/MTU, 3.1 wt. % U-235, 5-year cooled fuel) fuel assemblies and 24 (modeled as 16) 0.6 kW (30 GWd/MTU, 2.5 wt. % U-235, 8-year cooled fuel) fuel assemblies with 32 design basis BPRAs. The source terms (Section M.5.2) and material densities (Section M.5.3.1) used in the MCNP models are the same as those used in the DORT models including the axial peaking factors described in Section M.5.2.3. Figure M.5-29 and Figure M.5-30 are MCNP generated cuts through the 3-D model of the canister and HSM. The figures show the shielding materials and thicknesses as modeled with MCNP. An example input deck is included in Section M.5.5.4.

To demonstrate that the 2-D DORT analysis bounds a 3-D analysis the peak neutron and gamma dose rates on the roof and front vents; roof surface average; and peak neutron and gamma dose rates on the HSM door are compared. The results are provided in Table M.5-24. As shown by the results reported in Table M.5-24, the 2-D DORT analysis bounds the 3-D MCNP analysis.

In addition, this 3-D shielding analysis with MCNP has been validated by comparison to actual measured dose rate data from installed NUHOMS[®] Systems.

The actual measured dose rate data is from surveys taken at which utilizes the NUHOMS[®]-24P storage system. The HSM Model 80 and B&W 15x15 mark B fuel assembly type are identical to that evaluated with the 32PT System. MCNP models are developed for the stored canister and the HSM. The MCNP models were used to calculate dose rates at locations around the HSM that correspond to the various survey locations for which the data is reported.

The results of these benchmark runs are shown in Table M.5-25 and Table M.5-26.

The results show that MCNP predicts conservatively higher total (neutron plus gamma) dose rates compared to the measured data. For those two points (neutron dose on the roof bird screens for DSC 45 and gamma dose rate on HSM door) where the measured data is higher than the calculated data, it should be noted that the magnitude of these dose rates is small. However, at these two locations the calculated total dose rate is still higher than the measured dose rates. Therefore, a ratio of 0.8 for calculated/measured dose rates for the aforementioned two points is regarded as a fairly accurate estimate. Some conservatism still exists in the methodology used to calculate the source terms, and this is why the calculated dose rates are, in general, higher than the measured dose rates.

M.5.5 Appendix

Section M.5.5.1 includes a sample SAS2H/ORIGEN-S code input file used for the NUHOMS[®]-32PT system. The DORT code models are described in Section M.5.4. Section M.5.5.2 includes a sample DORT code input file used for the HSM analysis. Section M.5.5.3 includes a sample DORT code input file used for the TC analysis.

M.5.5.1 Sample SAS2H/ORIGEN-S Input File

```
=SAS2H      PARM=(HALT03,SKIPSHIPDATA)
Worst Case B&W 15x15 (0.475 MTU) Design 3.10 Wt% U235, 41 GWd/MTU
Burnup
'---Composition block is needed by Material Information Processor---
'
'   Data Input Blocks #3 and #4
'
```

The first line invokes SAS2H module, requests to produce time dependent and cell weighted cross sections but do not calculate dose rates. The second line is the title card and the next four lines are comment cards. The next line specifies the name of the cross section library to be used and the cell type to be used to evaluate cross sections. The 44GROUPNDF5 library is a 44-group ENDF/B-V library developed for use in the analysis of fresh and spent fuel and radioactive waste systems. This library contains approximately 300 nuclides from ENDF/B-V. LATTICECELL specifies, as the name implies, a lumped fuel lattice for performing the cell calculations to generate the cell weighted cross sections and collapsed fluxes.

```
44GROUPNDF5      LATTICECELL
UO2  1 0.96 811 92235 3.10 92238 96.8581 92234 0.0276 92236 0.0143
END
```

UO₂ is a component name from the Standard Composition Library, 1 –indicates the mixture number (≤ 3 if pin cell, ≥ 4 if cask or larger unit cell mixture), next is a density multiplier, 811 is the fuel temperature in K. The next set of numbers is U isotope identifiers and their abundance. For example, 92235 3.21 indicates 3.21 wt. % U-235 etc. The following four cards specify the other materials used in the calculation. Finally, the “END COMP” card indicates to SAS2H that all of the materials required to be specified for this evaluation are entered. Note that when the density multiplier is set to zero, the next entry is the material atom density in atoms/barn-cm.

```
ZIRC4  2 1 620 END
H2O    3 0.711 580 END
BORON  3 DEN=515-6 1 580 END
CO-59  3 0 1.0-20 580 END
END COMP
.....
'   Data Input Block #5
'
SQUAREPITCH  1.44272 0.946658 1 3 1.0922 2 0.95758 0 END
.....
```

Block #5 specifies the unit cell geometry. SQUAREPITCH specifies a square pitch lattice of fuel, gap, clad and moderator.

The first numerical entry specifies the pitch of the lattice cell in cm. The next entry specifies the fuel pellet diameter in cm. The next two entries, 1 and 3, indicate for mixture numbers for the fuel and moderator. The next two entries are the clad OD, in cm, and the clad mixture number. The last two entries are the clad ID and gap mixture number.

```
' Data Input Block #6
```

```
,'  
MORE DATA SZF=0.9 END  
.....
```

Block #6 specifies optional parameters. MORE DATA specifies that at least one optional parameters will be entered. SZF is a mesh factor used by XSDRNPM module of SAS2H during the depletion analysis. The default is SZF=1. 0 < SZF >1 indicates the user wants a finer mesh.

```
' Data Input Block #7
```

```
,'  
NPIN/ASSM=208 FUELENGTH=349.86 NCYCLES=3 NLIB/CYC=1  
PRINTLEVEL=5 LIGHTEL=35  
.....
```

The first three items in block #7 are self-explanatory. FUELENGTH is the active length of the fuel rods, it is adjusted to be consistent with the basis for the calculation, which is 0.475 MTU. NLIB/CYC is the number of equally spaced libraries produced per irradiation cycle. PRINTLEVEL=5 specifies the type and extent of information to be included in the output file. LIGHTEL specifies the number of light elements to be included in block #10 below.

```
' Data Input Block #9 (#8 is not required for INPLLEVEL=0)
```

```
,'  
POWER=22.2318 BURN=292 DOWN=73 END  
POWER=22.2318 BURN=292 DOWN=73 BFRAC=0.95 END  
POWER=22.2318 BURN=292 DOWN=12054 BFRAC= 0.95 END
```

Block #9 specifies the burnup history for the fuel. POWER is an average power (megawatts) to be produced for the burnup time specified by BURN. BURN specifies the number of days in this irradiation period (days). DOWN is the downtime (days). For each cycle, BFRAC sets the average boron moderator concentration. BFRAC is multiplied by the boron number density in the moderator (mixture 3) to obtain the average boron for each cycle.

```
.....  
' Data Input Block #10
```

```
,'  
H 0.0015 Li 0.0005 B 0.0005 C 0.0585 N 0.0276 O 63.9772 F 0.0051  
Na 0.0071 Mg 0.0010 Al 0.0401 Si 0.0155 P 0.0166 S 0.0045 Cl 0.0025  
Ca 0.0010 Ti 0.0420 V 0.0038 Cr 1.0785 Mn 0.0129 Fe 1.1536 Co 0.0247  
Ni 2.5599 Cu 0.0077 Zn 0.0191 Zr 114.9867 Nb 0.2717 Mo 0.1516 Ag  
0.0000  
Cd 0.0119 In 0.0010 Sn 1.8809 Gd 0.0012 Hf 0.0092 W 0.0033 Pb 0.0005  
END  
END
```

Block #10 is a list of the chemical identification numbers for each element followed by the effective weight per assembly in kg.

.....
=ORIGENS

ORIGENS invokes the ORIGIN-S module following the completion of the SAS2H module. ORIGEN-S performs both nuclide generation and depletion calculations for specified reactor history. It also calculates the neutron, gamma and decay heat sources for the assembly. In this case, ORIGEN-S is only being used to pick up the burnup dependent material concentrations at the end of the last cycle (before the last decay) to calculate the requested neutron, gamma and thermal decay source terms for a series of specified decay times. The following cards indicate to ORIGEN-S where to find the appropriate material concentrations, the requested decay times, and the gamma group structure for the gamma source.

```
0$$ A8 26 A11 71 E 1$$ 1 1T
' DECAY 5 6 9 10 12 13 20 21 22 23 YEARS
3$$ 21 A3 1 A30 18 A33 18 T
T
56$$ 0 10 A13 -1 5 E T
60** 5.0 6.0 9.0 10.0 15.0 16.0 20.0 21.0 22.0 23.0
61** F1 65$$ A25 1 E
65$$ A10 1 A31 1 A52 1 E
81$$ 2 0 26 1 E 82$$ F2
83** 10+6 8+6 6.5+6 5+6 4+6 3+6 2.5+6 2+6 1.66+6 1.33+6
1+6 8+5 6+5 4+5 3+5 2+5 1+5 5+4 0
T
  5 Year Cooling In-Core Region
  6 Year Cooling In-Core Region
  9 Year Cooling In-Core Region
 10 Year Cooling In-Core Region
 15 Year Cooling In-Core Region
 16 Year Cooling In-Core Region
 20 Year Cooling In-Core Region
 21 Year Cooling In-Core Region
 22 Year Cooling In-Core Region
 23 Year Cooling In-Core Region
56$$ F0 6T
END
```

M.5.5.2 Sample HSM DORT Model (RZ Roof Neutron Model)

```
NUHOMS-32P HSM Roof RZ Model
/ (Rf)oof
/ (S)hort Cavity
/ (H)eavy - >100ton
/ (N)eutron (In-Core) Source
/ (W)all (Rear Shield)
/ Cylindrical Source Region
/ Standard HSM Dimensions
/ Design-basis PWR Source
/ S16 Quadrature, Symmetry Around Middle
61$$
/ ntlx ntfog ntsig ntbsi ntksi
```

```

      0      0      8      0      2
/      ntfc  ntibi  ntibo  ntnpr  ntdir
      0      0      0      0      0
/      ntdso
      0      e
62$$
/      iadj  isctm  izm    im     jm
      0      3     30    84    178
/      igm   iht    ihs    ihm    mixl
      40     3     4     43    0
/      mmesh  mtp    mtm    idfac  mm
      0     64    64    0     160
/      ingeom ibl    ibr    ibb    ibt
      1     1     0     0     0
/      isrmx  ifxmi  ifxmf  mode   ktype
      20    -1    50    2     0
/      iacc   kalf   igtype  inpfxm  inpsrm
      2     0     0     0     3
/      njntsr nintsr  njntfx  nintfx  iact
      0     0     0     0     2
/      ired   ipdb2  ifxprr  icsprt  idirf
      -1    0     1     1     0
/      jdirf  jdir1  nbuf   iepzbz  minblk
      0     0     0     0     0
/      maxblk isbt   msbt   msdm   ibfsc1
      1     1     1     1     2
/      intsc1 itmsc1  nofis  ifdb2z  iswp
      1     99    0     0     0
/      keyjn  keyin  nsigtp  norpos  normat
      0     0     0     0     0
      0 -1   f0     e

```

```

63**
/      tmax   xnf    eps    epp    epv
      0.0    0.0    0.0    5.0e-3 5.0e-3
/      epf    ekobj  evth   evchm  evmax
      1.0e-2 1.0    0.0    0.0    0.0
/      evkmx  evi    devdki  evdelk  sormin
      0.0    0.0    0.0    0.0    5.0
/      conacc conscl  conepts  wsoloi  wsolii
      5.0e-2 5.0e-3 0.01   0.0    -1.5
/      wsolcn orf    fsnacc  flxmin  smooth
      2.0    0.6    0.0    1.0e-30 0.0
/      epo    extrcv  theta
      0.0    0.2    0.9    e

```

```

t
t
/ S16 Symmetrical Quadrature
82*
0 -21082- 5 0 -14907- 5 0 +14907- 5 0 -42164- 5 0 -39441- 5 0 -
14907- 5
0 +14907- 5 0 +39441- 5 0 -55777- 5 0 -53748- 5 0 -39441- 5 0 -
14907- 5
0 +14907- 5 0 +39441- 5 0 +53748- 5 0 -66667- 5 0 -64979- 5 0 -
53748- 5
0 -39441- 5 0 -14907- 5 0 +14907- 5 0 +39441- 5 0 +53748- 5 0
+64979- 5

```

0 -76012- 5 0 -74536- 5 0 -64979- 5 0 -53748- 5 0 -39441- 5 0 -
 14907- 5
 0 +14907- 5 0 +39441- 5 0 +53748- 5 0 +64979- 5 0 +74536- 5 0 -
 84327- 5
 0 -82999- 5 0 -74536- 5 0 -64979- 5 0 -53748- 5 0 -39441- 5 0 -
 14907- 5
 0 +14907- 5 0 +39441- 5 0 +53748- 5 0 +64979- 5 0 +74536- 5 0
 +82999- 5
 0 -91894- 5 0 -90676- 5 0 -82999- 5 0 -74536- 5 0 -64979- 5 0 -
 53748- 5
 0 -39441- 5 0 -14907- 5 0 +14907- 5 0 +39441- 5 0 +53748- 5 0
 +64979- 5
 0 +74536- 5 0 +82999- 5 0 +90676- 5 0 -98883- 5 0 -97753- 5 0 -
 90676- 5
 0 -82999- 5 0 -74536- 5 0 -64979- 5 0 -53748- 5 0 -39441- 5 0 -
 14907- 5
 0 +14907- 5 0 +39441- 5 0 +53748- 5 0 +64979- 5 0 +74536- 5 0
 +82999- 5
 0 +90676- 5 0 +97753- 5 0 -21082- 5 0 -14907- 5 0 +14907- 5 0 -
 42164- 5
 0 -39441- 5 0 -14907- 5 0 +14907- 5 0 +39441- 5 0 -55777- 5 0 -
 53748- 5
 0 -39441- 5 0 -14907- 5 0 +14907- 5 0 +39441- 5 0 +53748- 5 0 -
 66667- 5
 0 -64979- 5 0 -53748- 5 0 -39441- 5 0 -14907- 5 0 +14907- 5 0
 +39441- 5
 0 +53748- 5 0 +64979- 5 0 -76012- 5 0 -74536- 5 0 -64979- 5 0 -
 53748- 5
 0 -39441- 5 0 -14907- 5 0 +14907- 5 0 +39441- 5 0 +53748- 5 0
 +64979- 5
 0 +74536- 5 0 -84327- 5 0 -82999- 5 0 -74536- 5 0 -64979- 5 0 -
 53748- 5
 0 -39441- 5 0 -14907- 5 0 +14907- 5 0 +39441- 5 0 +53748- 5 0
 +64979- 5
 0 +74536- 5 0 +82999- 5 0 -91894- 5 0 -90676- 5 0 -82999- 5 0 -
 74536- 5
 0 -64979- 5 0 -53748- 5 0 -39441- 5 0 -14907- 5 0 +14907- 5 0
 +39441- 5
 0 +53748- 5 0 +64979- 5 0 +74536- 5 0 +82999- 5 0 +90676- 5 0 -
 98883- 5
 0 -97753- 5 0 -90676- 5 0 -82999- 5 0 -74536- 5 0 -64979- 5 0 -
 53748- 5
 0 -39441- 5 0 -14907- 5 0 +14907- 5 0 +39441- 5 0 +53748- 5 0
 +64979- 5
 0 +74536- 5 0 +82999- 5 0 +90676- 5 0 +97753- 5
 83*
 3r-97753- 5 5r-90676- 5 7r-82999- 5 9r-74536- 5 11r-64979- 5 13r-
 53748- 5
 15r-39441- 5 17r-14907- 5 3r+97753- 5 5r+90676- 5 7r+82999- 5
 9r+74536- 5
 11r+64979- 5 13r+53748- 5 15r+39441- 5 17r+14907- 5
 81*
 0 + 0+ 0 2r+13586- 6 0 + 0+ 0 0 +97681- 7 2r+97681- 7 0
 +97681- 7
 0 + 0+ 0 0 +64738- 7 0 +50390- 7 2r+64738- 7 0 +50390- 7 0
 +64738- 7

```

0 + 0+ 0 0 +64634- 7 0 +71124- 7 0 +71124- 7 2r+64634- 7 0
+71124- 7
0 +71124- 7 0 +64634- 7 0 + 0+ 0 0 +64634- 7 0 +14381- 7 0
+36342- 7
0 +14381- 7 2r+64634- 7 0 +14381- 7 0 +36342- 7 0 +14381- 7 0
+64634- 7
0 + 0+ 0 0 +64738- 7 0 +71124- 7 0 +36342- 7 0 +36342- 7 0
+71124- 7
2r+64738- 7 0 +71124- 7 0 +36342- 7 0 +36342- 7 0 +71124- 7 0
+64738- 7
0 + 0+ 0 0 +97681- 7 0 +50390- 7 0 +71124- 7 0 +14381- 7 0
+71124- 7
0 +50390- 7 2r+97681- 7 0 +50390- 7 0 +71124- 7 0 +14381- 7 0
+71124- 7
0 +50390- 7 0 +97681- 7 0 + 0+ 0 0 +13586- 6 0 +97681- 7 0
+64738- 7
0 +64634- 7 0 +64634- 7 0 +64738- 7 0 +97681- 7 2r+13586- 6 0
+97681- 7
0 +64738- 7 0 +64634- 7 0 +64634- 7 0 +64738- 7 0 +97681- 7 0
+13586- 6
0 + 0+ 0 2r+13586- 6 0 + 0+ 0 0 +97681- 7 2r+97681- 7 0
+97681- 7
0 + 0+ 0 0 +64738- 7 0 +50390- 7 2r+64738- 7 0 +50390- 7 0
+64738- 7
0 + 0+ 0 0 +64634- 7 0 +71124- 7 0 +71124- 7 2r+64634- 7 0
+71124- 7
0 +71124- 7 0 +64634- 7 0 + 0+ 0 0 +64634- 7 0 +14381- 7 0
+36342- 7
0 +14381- 7 2r+64634- 7 0 +14381- 7 0 +36342- 7 0 +14381- 7 0
+64634- 7
0 + 0+ 0 0 +64738- 7 0 +71124- 7 0 +36342- 7 0 +36342- 7 0
+71124- 7
2r+64738- 7 0 +71124- 7 0 +36342- 7 0 +36342- 7 0 +71124- 7 0
+64738- 7
0 + 0+ 0 0 +97681- 7 0 +50390- 7 0 +71124- 7 0 +14381- 7 0
+71124- 7
0 +50390- 7 2r+97681- 7 0 +50390- 7 0 +71124- 7 0 +14381- 7 0
+71124- 7
0 +50390- 7 0 +97681- 7 0 + 0+ 0 0 +13586- 6 0 +97681- 7 0
+64738- 7
0 +64634- 7 0 +64634- 7 0 +64738- 7 0 +97681- 7 2r+13586- 6 0
+97681- 7
0 +64738- 7 0 +64634- 7 0 +64634- 7 0 +64738- 7 0 +97681- 7 0
+13586- 6

```

```

t
/ U-235 Fission Spectrum
1**

```

```

1.984e-04 1.064e-03 4.013e-03 1.559e-02 3.676e-02
5.035e-02 1.093e-01 9.024e-02 2.149e-02 1.190e-01
2.138e-01 1.928e-01 1.298e-01 1.549e-02 7.893e-05
5.740e-06 3.775e-07 5.453e-08 1.176e-08 1.832e-09
4.039e-10 1.166e-10 f0.0

```

```

/ Fine Mesh in the Z-direction

```

```

2**

```

```

/ Front Air

```

```

-281.68 -251.68 -226.68 -201.68 -176.68
-156.68 -136.68 -116.68 -97.68 -81.68

```



```

-73.68 -69.68 -67.68
/ HSM Intervals
2i-66.68 2i-62.87 2i-55.25 1i-47.96 7i-46.69
3i0.00 5i5.72 1i13.34 9i22.23 43.50
/ Active Fuel Intervals
47.11 50.73 57.95 65.18 72.41
79.64 86.87 94.10 101.32 108.55
115.78 123.01 130.24 137.47 151.92
166.38 180.84 195.29 209.75 224.21
238.66 253.12 267.58 282.03 296.49
310.95 318.17 325.40 332.63 339.86
347.09 354.32 361.54 368.77 376.00
383.23 390.46 397.69 401.30
/ HSM Intervals
4i404.91 4i427.09 1i442.91 13i446.91 2i466.60
2i469.14 2i472.95 2i485.78 5i493.40 2i508.64
3i516.26 15i523.88 3i569.60 577.22
/ Back Air
577.72 579.22 582.22 588.22 600.22
617.72 637.22 657.22 677.22 699.72
724.72 749.72 777.22
/ Fine Mesh in the R-direction
4**
/ DSC and HSM
6i0.00 7i50.59 1i71.54 1i71.86 1i82.09
2i83.11 1i85.33 4i87.96 1i100.66 1i106.05
3i106.68 27i114.30 3i190.50 198.12
/ Top Air
199.12 201.12 205.12 213.12 229.12
248.12 268.12 288.12 308.12 333.12
358.12 383.12 413.12
/ Material Zone by Mesh
/ left to right (rsmall to rlarge)
/ bottom to top (zsmall to zlarge)
8$$
71r1 13r2 12q84
33r3 38r1 13r2 2q84
31r4 36r22 4r25 13r2 2q84
31r4 36r5 4r25 13r2 2q84
31r6 36r5 4r25 13r2 1q84
26r7 41r5 4r25 13r2 7q84
21r8 3r9 2r7 41r5 4r25 13r2 3q84
21r8 3r9 2r7 41r23 4r25 13r2 5q84
21r8 3r9 11r7 4r24 28r5 4r25 13r2 1q84
15r10 2r20 2r21 2r11 3r9 11r7 4r24 28r5 4r25 13r2 9q84
15r12 2r20 2r21 2r11 3r9 11r7 4r24 28r5 4r25 13r2 39q84
15r13 2r20 2r21 2r11 3r9 11r7 4r24 28r5 4r25 13r2 4q84
15r30 2r20 2r21 2r11 3r9 11r7 4r24 28r5 4r25 13r2 4q84
21r17 3r9 11r7 4r24 28r5 4r25 13r2 1q84
21r14 3r9 11r7 4r24 28r5 4r25 13r2 13q84
21r15 3r9 11r7 4r24 28r5 4r25 13r2 2q84
21r16 3r9 11r7 4r24 28r5 4r25 13r2 2q84
35r7 4r24 28r5 4r25 13r2 2q84
67r26 4r25 13r2 2q84
67r5 4r25 13r2 5q84
67r27 4r25 13r2 2q84
67r28 4r25 13r2 3q84

```

```

67r5 4r25 13r2 15q84
67r29 4r25 13r2 3q84
71r19 13r2 12q84
/ Mixture by Material Zone
/ 1 = Fluxdosium      5 = Fuel Radial      9 = Fuel Axial
/ 13 = Top            17 = Plenum           21 = Bottom
/ 25 = Concrete       29 = Air              33 = Steel
/ 37 = Roof Concrete  41 = Front Concrete   45 = Side Concrete
/ 49 = Rear Concrete  53 = End Shield       57 = Back Shield
/ 61 = Aluminum
9$$ 29 29 33 25 25      33 29 33 33 21
      61 9 17 33 33      33 29 25 29 33
      29 41 41 37 37      49 49 57 57 13
/ Material for use in Activity Calculations
25$$ f-1
/ Position in Cross-Section Table for Activity Calcs
/ 1 = Total  2 = Neutron  3 = Gamma
26$$ 2 3
/ Activity Multiplication Factors
27** 1.0 1.0
/ Initial Iteration Limits by Energy Group
28$$ 22r7 f1 t
/ Source Multiplication in the R direction
96** 7r0.355 8r1.0 f0.0 t
/ Source Multiplication in the Z direction
97** 44r0.0
      10r0.0
      0.33 0.33 0.33 0.78 0.78
      0.78 1.57 1.57 1.57 1.57
      1.57 1.57 1.57 1.57 1.57
      1.57 1.57 1.57 1.57 1.57
      1.57 1.57 1.57 1.57 1.57
      1.57 1.57 1.57 1.57 1.46
      1.46 1.46 1.46 1.46 0.72
      0.72 0.72 0.24 0.24 0.24
      5r0.0
      5r0.0
      f0.0 t
/ Group Volumetric Sources
98**
      4.322e-1 2.454e+0 9.575e+0 3.786e+1 8.924e+1
      1.208e+2 2.563e+2 2.059e+2 4.831e+1 2.628e+2
      4.519e+2 3.842e+2 2.437e+2 2.786e+1 1.404e-1
      1.020e-2 6.712e-4 9.695e-5 2.090e-5 3.257e-6
      7.181e-7 2.074e-7
      f0.0
      t

```

M.5.5.3 Sample TC DORT Model (RZ Transfer Configuration)

```

NUHOMS-32P Cask Transfer RZ Model
/ (L)ong Cavity
/ (H)eavy Configuration (>100ton)
/ (N)eutron In-Core Source
/ (T)ransfer Configuration
/ Cylindrical Source Region
/ OS197 Cask Dimensions
/ Design-basis PWR Source
/ S16 Quadrature, Symmetry Around Middle
61$$
/      ntlx  ntfg  ntsig  ntbsi  ntksi
/      0     0     8     0     2
/      ntfc  ntibi  ntibo  ntnpr  ntldr
/      0     0     0     0     0
/      ntaso
/      0     e
62$$
/      iadj  isctm  izm    im     jm
/      0     3     29   103   191
/      igm   iht    ihs    ihm   mixl
/      40    3     4     43    0
/      mmesh  mtp    mtm    idfac  mm
/      0     68    68    0     160
/      ingeom  ibl    ibr    ibb    ibt
/      1     1     0     0     0
/      isrmx  ifxmi  ifxmf  mode  ktype
/      20    -1    50    2     0
/      iacc   kalf   igtype  inpfm  inpsrm
/      2     0     0     0     3
/      njntsr nintsr  njntfx  nintfx  iact
/      0     0     0     0     2
/      ired   ipdb2  ifxprr  icsprt  idirf
/      -1    0     1     1     0
/      jdirf  jdirl  nbuf   iepzbz  minblk
/      0     0     0     0     0
/      maxblk  isbt   msbt   msdm   ibfscl
/      1     1     1     1     2
/      intsc1  itmscl  nofis  ifdb2z  iswp
/      1     99    0     0     0
/      keyjn  keyin  nsigtp  norpos  normat
/      0     0     0     0     0
/      0 -1   f0     e
63**
/      tmax   xnf    eps    epp    epv
/      0.0    0.0    0.0    5.0e-3 5.0e-3
/      epf    ekobj  evth   evchm  evmax
/      1.0e-2 1.0    0.0    0.0    0.0
/      evkmx  evi    devdki  evdelk  sormin
/      0.0    0.0    0.0    0.0    5.0
/      conacc  conscl  conepts  wsoloi  wsolii
/      5.0e-2 5.0e-3 0.01    0.0    -1.5
/      wsolcn  orf    fsnacc  flxmin  smooth
/      2.0    0.6    0.0    1.0e-30 0.0

```

```

/      epo  extrcv  theta
      0.0   0.2   0.9   e
      t
      t
/ S16 Symmetrical Quadrature
82*
 0 -21082- 5 0 -14907- 5 0 +14907- 5 0 -42164- 5 0 -39441- 5 0 -
14907- 5
 0 +14907- 5 0 +39441- 5 0 -55777- 5 0 -53748- 5 0 -39441- 5 0 -
14907- 5
 0 +14907- 5 0 +39441- 5 0 +53748- 5 0 -66667- 5 0 -64979- 5 0 -
53748- 5
 0 -39441- 5 0 -14907- 5 0 +14907- 5 0 +39441- 5 0 +53748- 5 0
+64979- 5
 0 -76012- 5 0 -74536- 5 0 -64979- 5 0 -53748- 5 0 -39441- 5 0 -
14907- 5
 0 +14907- 5 0 +39441- 5 0 +53748- 5 0 +64979- 5 0 +74536- 5 0 -
84327- 5
 0 -82999- 5 0 -74536- 5 0 -64979- 5 0 -53748- 5 0 -39441- 5 0 -
14907- 5
 0 +14907- 5 0 +39441- 5 0 +53748- 5 0 +64979- 5 0 +74536- 5 0
+82999- 5
 0 -91894- 5 0 -90676- 5 0 -82999- 5 0 -74536- 5 0 -64979- 5 0 -
53748- 5
 0 -39441- 5 0 -14907- 5 0 +14907- 5 0 +39441- 5 0 +53748- 5 0
+64979- 5
 0 +74536- 5 0 +82999- 5 0 +90676- 5 0 -98883- 5 0 -97753- 5 0 -
90676- 5
 0 -82999- 5 0 -74536- 5 0 -64979- 5 0 -53748- 5 0 -39441- 5 0 -
14907- 5
 0 +14907- 5 0 +39441- 5 0 +53748- 5 0 +64979- 5 0 +74536- 5 0
+82999- 5
 0 +90676- 5 0 +97753- 5 0 -21082- 5 0 -14907- 5 0 +14907- 5 0 -
42164- 5
 0 -39441- 5 0 -14907- 5 0 +14907- 5 0 +39441- 5 0 -55777- 5 0 -
53748- 5
 0 -39441- 5 0 -14907- 5 0 +14907- 5 0 +39441- 5 0 +53748- 5 0 -
66667- 5
 0 -64979- 5 0 -53748- 5 0 -39441- 5 0 -14907- 5 0 +14907- 5 0
+39441- 5
 0 +53748- 5 0 +64979- 5 0 -76012- 5 0 -74536- 5 0 -64979- 5 0 -
53748- 5
 0 -39441- 5 0 -14907- 5 0 +14907- 5 0 +39441- 5 0 +53748- 5 0
+64979- 5
 0 +74536- 5 0 -84327- 5 0 -82999- 5 0 -74536- 5 0 -64979- 5 0 -
53748- 5
 0 -39441- 5 0 -14907- 5 0 +14907- 5 0 +39441- 5 0 +53748- 5 0
+64979- 5
 0 +74536- 5 0 +82999- 5 0 -91894- 5 0 -90676- 5 0 -82999- 5 0 -
74536- 5
 0 -64979- 5 0 -53748- 5 0 -39441- 5 0 -14907- 5 0 +14907- 5 0
+39441- 5
 0 +53748- 5 0 +64979- 5 0 +74536- 5 0 +82999- 5 0 +90676- 5 0 -
98883- 5
 0 -97753- 5 0 -90676- 5 0 -82999- 5 0 -74536- 5 0 -64979- 5 0 -
53748- 5

```

0 -39441- 5 0 -14907- 5 0 +14907- 5 0 +39441- 5 0 +53748- 5 0
+64979- 5
0 +74536- 5 0 +82999- 5 0 +90676- 5 0 +97753- 5
83*
3r-97753- 5 5r-90676- 5 7r-82999- 5 9r-74536- 5 11r-64979- 5 13r-
53748- 5
15r-39441- 5 17r-14907- 5 3r+97753- 5 5r+90676- 5 7r+82999- 5
9r+74536- 5
11r+64979- 5 13r+53748- 5 15r+39441- 5 17r+14907- 5
81*
0 + 0+ 0 2r+13586- 6 0 + 0+ 0 0 +97681- 7 2r+97681- 7 0
+97681- 7
0 + 0+ 0 0 +64738- 7 0 +50390- 7 2r+64738- 7 0 +50390- 7 0
+64738- 7
0 + 0+ 0 0 +64634- 7 0 +71124- 7 0 +71124- 7 2r+64634- 7 0
+71124- 7
0 +71124- 7 0 +64634- 7 0 + 0+ 0 0 +64634- 7 0 +14381- 7 0
+36342- 7
0 +14381- 7 2r+64634- 7 0 +14381- 7 0 +36342- 7 0 +14381- 7 0
+64634- 7
0 + 0+ 0 0 +64738- 7 0 +71124- 7 0 +36342- 7 0 +36342- 7 0
+71124- 7
2r+64738- 7 0 +71124- 7 0 +36342- 7 0 +36342- 7 0 +71124- 7 0
+64738- 7
0 + 0+ 0 0 +97681- 7 0 +50390- 7 0 +71124- 7 0 +14381- 7 0
+71124- 7
0 +50390- 7 2r+97681- 7 0 +50390- 7 0 +71124- 7 0 +14381- 7 0
+71124- 7
0 +50390- 7 0 +97681- 7 0 + 0+ 0 0 +13586- 6 0 +97681- 7 0
+64738- 7
0 +64634- 7 0 +64634- 7 0 +64738- 7 0 +97681- 7 2r+13586- 6 0
+97681- 7
0 +64738- 7 0 +64634- 7 0 +64634- 7 0 +64738- 7 0 +97681- 7 0
+13586- 6
0 + 0+ 0 2r+13586- 6 0 + 0+ 0 0 +97681- 7 2r+97681- 7 0
+97681- 7
0 + 0+ 0 0 +64738- 7 0 +50390- 7 2r+64738- 7 0 +50390- 7 0
+64738- 7
0 + 0+ 0 0 +64634- 7 0 +71124- 7 0 +71124- 7 2r+64634- 7 0
+71124- 7
0 +71124- 7 0 +64634- 7 0 + 0+ 0 0 +64634- 7 0 +14381- 7 0
+36342- 7
0 +14381- 7 2r+64634- 7 0 +14381- 7 0 +36342- 7 0 +14381- 7 0
+64634- 7
0 + 0+ 0 0 +64738- 7 0 +71124- 7 0 +36342- 7 0 +36342- 7 0
+71124- 7
2r+64738- 7 0 +71124- 7 0 +36342- 7 0 +36342- 7 0 +71124- 7 0
+64738- 7
0 + 0+ 0 0 +97681- 7 0 +50390- 7 0 +71124- 7 0 +14381- 7 0
+71124- 7
0 +50390- 7 2r+97681- 7 0 +50390- 7 0 +71124- 7 0 +14381- 7 0
+71124- 7
0 +50390- 7 0 +97681- 7 0 + 0+ 0 0 +13586- 6 0 +97681- 7 0
+64738- 7
0 +64634- 7 0 +64634- 7 0 +64738- 7 0 +97681- 7 2r+13586- 6 0
+97681- 7

0 +64738- 7 0 +64634- 7 0 +64634- 7 0 +64738- 7 0 +97681- 7 0
+13586- 6

t

/ U-235 Fission Spectrum

1**

1.984e-04 1.064e-03 4.013e-03 1.559e-02 3.676e-02
5.035e-02 1.093e-01 9.024e-02 2.149e-02 1.190e-01
2.138e-01 1.928e-01 1.298e-01 1.549e-02 7.893e-05
5.740e-06 3.775e-07 5.453e-08 1.176e-08 1.832e-09
4.039e-10 1.166e-10 f0.0

/ Fine Mesh in the Z-direction

2**

/ Bottom Air

-227.70 -197.70 -172.70 -147.70 -122.70
-102.70 -82.70 -62.70 -43.70 -27.70
-19.70 -15.70 -13.70

/ Cask Intervals

2i-12.70 1i-10.80 5i-10.16 5i-7.62 5i-5.08
1i0.00 1i5.08 1i6.10 1i7.37 1i9.19
11i10.16 9i31.42 52.69

/ Active Fuel Intervals

56.31 59.92 67.15 74.38 81.61
88.83 96.06 103.29 110.52 117.75
124.98 132.20 139.43 146.66 161.12
175.57 190.03 204.49 218.94 233.40
247.86 262.31 276.77 291.23 305.68
320.14 327.37 334.60 341.83 349.05
352.43 363.51 370.74 377.97 385.20
392.42 399.65 406.88 410.49

/ Cask Intervals

4i414.11 4i436.28 2i452.12 1i466.90 1i471.35
2i474.35 1i480.70 1i483.24 1i484.51 3i485.78
1i489.59 3i491.03 3i493.57 3i497.38 5i499.75
5i502.29 3i505.00 7i507.37 1i512.45 513.08

/ Top Air

514.08 516.08 520.08 528.08 544.08
563.08 583.08 603.08 623.08 648.08
673.08 698.08 728.08

/ Fine Mesh in the R-direction

4**

/ DSC and Cask

3i0.00 1i27.94 1i35.56 6i50.60 1i71.55
1i71.86 1i82.09 2i83.11 1i85.34 1i86.36
3i87.63 15i89.05 15i91.59 7i96.67 1i99.85
3i100.48 9i101.75 1i108.10 108.59

/ Side Air

109.59 111.59 115.59 123.59 139.59
158.59 178.59 198.59 218.59 243.59
268.59 293.59 323.59

/ Material Zone by Mesh

/ left to right (rsmall to rlarge)

/ bottom to top (zsmall to zlarge)

8\$\$

103r1 12q103
74r2 29r1 2q103
6r2 42r4 26r2 29r1 1q103
4r3 2r2 42r4 26r2 29r1 5q103

```

4r3  2r2  26r4  42r2  29r1  5q103
4r3  70r2  29r1  5q103
26r7  48r2  29r1  1q103
26r7  2r2  20r8  26r2  29r1  1q103
26r7  2r2  20r8  26r2  16r10  13r1  1q103
26r7  2r2  20r8  26r2  14r9  2r10  13r1  1q103
21r5  3r6  2r7  2r2  20r8  26r2  14r9  2r10  13r1  1q103
21r5  3r6  2r7  2r2  36r8  10r2  14r9  2r10  13r1  11q103
15r11 2r28  2r29  2r12  3r6  2r7  2r2  36r8  10r2  14r9  2r10
      13r1  9q103
15r13 2r28  2r29  2r12  3r6  2r7  2r2  36r8  10r2  14r9  2r10
      13r1  30q103
15r13 2r28  2r29  2r12  3r6  2r7  2r2  36r8  14r2  10r9  2r10
      13r1  8q103
15r14 2r28  2r29  2r12  3r6  2r7  2r2  36r8  14r2  10r9  2r10
      13r1  4q103
15r27 2r28  2r29  2r12  3r6  2r7  2r2  36r8  14r2  10r9  2r10
      13r1  4q103
21r15 3r6  2r7  2r2  36r8  14r2  10r9  2r10  13r1  2q103
21r15 3r6  2r16  2r2  36r8  14r2  10r9  2r10  13r1  1q103
21r17 3r6  2r16  2r2  36r8  14r2  10r9  2r10  13r1  1q103
21r17 3r6  2r16  2r2  36r8  10r2  14r9  2r10  13r1  2q103
21r17 3r6  2r16  2r2  20r8  26r2  14r9  2r10  13r1  1q103
21r17 3r6  2r16  2r2  20r8  26r2  16r10  13r1  1q103
21r17 3r6  2r16  2r2  20r8  26r2  29r1  1q103
21r17 3r6  2r16  48r2  29r1  3q103
21r17 3r6  4r16  46r2  29r1  1q103
21r18 3r6  4r16  46r2  29r1  3q103
21r19 3r6  4r16  46r2  29r1  3q103
21r20 7r16  46r2  29r1  3q103
21r21 7r24  46r2  29r1  5q103
21r22 53r24 29r1  5q103
21r23 53r24 29r1  3q103
72r25 2r26  29r1  7q103
74r26 29r1  1q103
103r1 12q103
/ Mixture by Material Zone
/ 1 = Fluxdosium      5 = Fuel Radial      9 = Fuel Axial
/ 13 = Top            17 = Plenum          21 = Bottom
/ 25 = NS-3          29 = Air             33 = Steel
/ 37 = Aluminum       41 = Water           45 = Lead
/ 49 = Wet Fuel Rad   53 = Wet Fuel Axial  57 = Wet Top
/ 61 = Wet Plenum     65 = Wet Bottom
9$$ 29 33 29 25 33      33 29 45 41 33
      21 37 9 17 29      29 33 33 33 29
      33 33 33 33 25      33 13 33 29
/ Material for use in Activity Calculations
25$$ f-1
/ Position in Cross-Section Table for Activity Calcs
/ 1 = Total  2 = Neutron  3 = Gamma
26$$ 2 3
/ Activity Multiplication Factors
27** 1.0 1.0
/ Initial Iteration Limits by Energy Group
28$$ 22r7 f1 t
/ Source Multiplication in the R direction
96** 8r0.671 7r1.0 f0.0 t

```

```

/ Source Multiplication in the Z direction
97** 58r0.0
      10r0.0
      0.33 0.33 0.33 0.78 0.78
      0.78 1.57 1.57 1.57 1.57
      1.57 1.57 1.57 1.57 1.57
      1.57 1.57 1.57 1.57 1.57
      1.57 1.57 1.57 1.57 1.57
      1.57 1.57 1.57 1.57 1.46
      1.46 1.46 1.46 1.46 0.72
      0.72 0.72 0.24 0.24 0.24
      5r0.0
      5r0.0
      f0.0 t
/ Group Volumetric Sources
98**
      4.322e-1 2.454e+0 9.575e+0 3.786e+1 8.924e+1
      1.208e+2 2.563e+2 2.059e+2 4.831e+1 2.628e+2
      4.519e+2 3.842e+2 2.437e+2 2.786e+1 1.404e-1
      1.020e-2 6.712e-4 9.695e-5 2.090e-5 3.257e-6
      7.181e-7 2.074e-7
      f0.0
      t

```

M.5.5.4 Sample MCNP Model

```

MCNP4 - Standard HSM with 32PT DSC. Fuel Regions Have two Radial Zones.
c Inner and Outer zones have 16 FAs.
c Weights for cells 300-335 were optimised fro tallies 54,64 and 74
c
c Roof bird screen dose rate distribution
c
c Cells
c *****
c *****
c
c density pz/c/y px py
c Bottom Nozzle Inner and Outer Zones
1 1 -1.39 -404 200 340 -345
2 1 -1.39 404 -405 200 340 -345
c In-core Inner and Outer Zone
3 2 -3.10 -404 200 345 -350
4 2 -3.10 404 -405 200 345 -350
c Fuel Plenum Inner and Outer Zones
5 3 -0.396 -404 200 350 -351
6 3 -0.396 404 -405 200 350 -351
c Top Nozzle Region Inner and Outer Zones
7 4 0.016421 -404 200 351 -355
8 4 0.016421 404 -405 200 351 -355
c ground
10 9 -1.701 99 -100 200 -250 300 -385
c
c
c air in front of HSM
15 5 -0.001097 100 -181 200 -250 300 -305
c
c air in back of HSM
20 5 -0.001097 100 -181 200 -250 381 -385

```


c 1 cm. thick air cell on HSM back for tallying purposes
21 5 -0.001097 100 -181 200 -250 380 -381
c
c air over HSM
25 5 -0.001097 181 -185 200 -250 300 -385
c
c tally cell (roof bird screen)
30 5 -0.001097 180 -181 240 -250 310 -375
c air on top of HSM (1 cm)
31 5 -0.001097 180 -181 338 -250 310 -380 #30
c
c
c base slab
75 8 -2.310 100 -110 200 -215 335 -370
c
c front wall
80 8 -2.310 100 -160 200 -215 315 -335 420
81 8 -2.310 100 -160 200 -215 310 -315 425
c front penetration - inner cavity (air)
83 5 -0.001097 -420 200 325 -335
#(200 -415 330 -335)
c door inner liner
87 6 -7.80 -420 200 315 -325
c Air Cell in front of the door
89 5 -0.001097 200 305 -320 -166
c door larger middle piece (front part, see cell 950)
93 8 -2.310 -425 200 310 -428
c door outer rect. piece
105 6 -7.80 200 320 -310 -166
c air around door rect piece
110 5 -0.001097 100 -181 200 -240 305 -310 166
c
c air in front of the vent space
c tally cell (front bird screen)
114 5 -0.001097 100 -181 240 -250 309 -310
c air in front of tally cell
115 5 -0.001097 100 -181 240 -250 305 -309
c
c back wall
120 8 -2.310 100 -160 200 -215 370 -375
c
c back shield wall
121 8 -2.310 100 -180 200 -250 375 -380
c
c roof slab (original templete)
c 122 8 -2.310 160 -180 200 -213 310 -375
c
c Part of the roof slab above HSM door
122 11 -2.680 160 -167 200 -213 310 -335
123 8 -2.310 167 -168 200 -213 310 -335
124 8 -2.310 168 -169 200 -213 310 -335
125 8 -2.310 169 -170 200 -213 310 -335
126 8 -2.310 170 -171 200 -213 310 -335
127 8 -2.310 171 -172 200 -213 310 -335
128 8 -2.310 172 -173 200 -213 310 -335
129 8 -2.310 173 -174 200 -213 310 -335
130 11 -2.680 174 -180 200 -213 310 -335
c Part of the roof slab above Bottom Nozzle Region of DSC
300 11 -2.680 160 -167 200 -213 335 -336
301 8 -2.310 167 -168 200 -213 335 -336
302 8 -2.310 168 -169 200 -213 335 -336
303 8 -2.310 169 -170 200 -213 335 -336
304 8 -2.310 170 -171 200 -213 335 -336

305	8	-2.310	171 -172	200 -213	335 -336	
306	8	-2.310	172 -173	200 -213	335 -336	
307	8	-2.310	173 -174	200 -213	335 -336	
308	11	-2.680	174 -180	200 -213	335 -336	
c	Part of the roof slab above In-core Region of DSC					
309	11	-2.680	160 -167	200 -213	336 -337	
310	8	-2.310	167 -168	200 -213	336 -337	
311	8	-2.310	168 -169	200 -213	336 -337	
312	8	-2.310	169 -170	200 -213	336 -337	
313	8	-2.310	170 -171	200 -213	336 -337	
314	8	-2.310	171 -172	200 -213	336 -337	
315	8	-2.310	172 -173	200 -213	336 -337	
316	8	-2.310	173 -174	200 -213	336 -337	
317	11	-2.680	174 -180	200 -213	336 -337	
c	Part of the roof slab above Plenum, Top Nozzle Regions of DSC					
318	11	-2.680	160 -167	200 -213	337 -360	
319	8	-2.310	167 -168	200 -213	337 -360	
320	8	-2.310	168 -169	200 -213	337 -360	
321	8	-2.310	169 -170	200 -213	337 -360	
322	8	-2.310	170 -171	200 -213	337 -360	
323	8	-2.310	171 -172	200 -213	337 -360	
324	8	-2.310	172 -173	200 -213	337 -360	
325	8	-2.310	173 -174	200 -213	337 -360	
326	11	-2.680	174 -180	200 -213	337 -360	
c	Part of the roof slab resting on HSM rear wall					
327	11	-2.680	160 -167	200 -213	360 -375	
328	8	-2.310	167 -168	200 -213	360 -375	
329	8	-2.310	168 -169	200 -213	360 -375	
330	8	-2.310	169 -170	200 -213	360 -375	
331	8	-2.310	170 -171	200 -213	360 -375	
332	8	-2.310	171 -172	200 -213	360 -375	
333	8	-2.310	172 -173	200 -213	360 -375	
334	8	-2.310	173 -174	200 -213	360 -375	
335	11	-2.680	174 -180	200 -213	360 -375	
c	Cells are created for tylling purposes, 1 cm. thick, 15 cm wide					
336	5	-0.001097	180 -181	200 -338	310 -335	\$ "Detector" # 1
337	5	-0.001097	180 -181	200 -338	335 -336	\$ "Detector" # 2
338	5	-0.001097	180 -181	200 -338	336 -337	\$ "Detector" # 3
339	5	-0.001097	180 -181	200 -338	337 -360	\$ "Detector" # 4
347	5	-0.001097	180 -181	200 -338	360 -375	\$ "Detector" # 5
348	5	-0.001097	180 -181	200 -338	375 -380	\$ "Detector" # 6
c	top portion of sidewall					
135	8	-2.310	167 -168	215 -230	310 -375	
136	8	-2.310	167 -168	230 -231	310 -375	
137	8	-2.310	167 -168	231 -232	310 -375	
138	8	-2.310	167 -168	232 -235	310 -375	
139	8	-2.310	167 -168	235 -236	310 -375	
140	11	-2.680	167 -168	236 -237	310 -375	
141	11	-2.680	167 -168	237 -240	310 -375	
c						
144	8	-2.310	168 -169	215 -230	310 -375	
145	8	-2.310	168 -169	230 -231	310 -375	
146	8	-2.310	168 -169	231 -232	310 -375	
147	8	-2.310	168 -169	232 -235	310 -375	
148	8	-2.310	168 -169	235 -236	310 -375	
150	11	-2.680	168 -169	236 -237	310 -375	
151	11	-2.680	168 -169	237 -240	310 -375	
c						
154	8	-2.310	169 -170	215 -230	310 -375	
155	8	-2.310	169 -170	230 -231	310 -375	
156	8	-2.310	169 -170	231 -232	310 -375	
157	8	-2.310	169 -170	232 -235	310 -375	

158	8	-2.310	169	-170	235	-236	310	-375
160	11	-2.680	169	-170	236	-237	310	-375
161	11	-2.680	169	-170	237	-240	310	-375
c								
164	8	-2.310	170	-171	215	-230	310	-375
165	8	-2.310	170	-171	230	-231	310	-375
166	8	-2.310	170	-171	231	-232	310	-375
167	8	-2.310	170	-171	232	-235	310	-375
168	8	-2.310	170	-171	235	-236	310	-375
170	11	-2.680	170	-171	236	-237	310	-375
171	11	-2.680	170	-171	237	-240	310	-375
c								
174	8	-2.310	171	-172	215	-230	310	-375
175	8	-2.310	171	-172	230	-231	310	-375
176	8	-2.310	171	-172	231	-232	310	-375
177	8	-2.310	171	-172	232	-235	310	-375
178	8	-2.310	171	-172	235	-236	310	-375
180	11	-2.680	171	-172	236	-237	310	-375
181	11	-2.680	171	-172	237	-240	310	-375
c								
184	8	-2.310	172	-173	215	-230	310	-375
185	8	-2.310	172	-173	230	-231	310	-375
186	8	-2.310	172	-173	231	-232	310	-375
187	8	-2.310	172	-173	232	-235	310	-375
188	8	-2.310	172	-173	235	-236	310	-375
190	11	-2.680	172	-173	236	-237	310	-375
191	11	-2.680	172	-173	237	-240	310	-375
c								
194	8	-2.310	173	-174	215	-230	310	-375
195	8	-2.310	173	-174	230	-231	310	-375
196	8	-2.310	173	-174	231	-232	310	-375
197	8	-2.310	173	-174	232	-235	310	-375
198	8	-2.310	173	-174	235	-236	310	-375
200	11	-2.680	173	-174	236	-237	310	-375
201	11	-2.680	173	-174	237	-240	310	-375
c								
204	11	-2.680	174	-180	215	-230	310	-375
205	11	-2.680	174	-180	230	-231	310	-375
206	11	-2.680	174	-180	231	-232	310	-375
207	11	-2.680	174	-180	232	-235	310	-375
208	11	-2.680	174	-180	235	-236	310	-375
210	11	-2.680	174	-180	236	-237	310	-375
211	11	-2.680	174	-180	237	-240	310	-375
c								
c roof subdivision next to top of sidewall								
214	11	-2.680	160	-165	214	-215	310	-375
215	11	-2.680	165	-167	214	-215	310	-375
216	8	-2.310	167	-168	214	-215	310	-375
217	8	-2.310	168	-169	214	-215	310	-375
218	8	-2.310	169	-170	214	-215	310	-375
219	8	-2.310	170	-171	214	-215	310	-375
220	8	-2.310	171	-172	214	-215	310	-375
221	8	-2.310	172	-173	214	-215	310	-375
222	8	-2.310	173	-174	214	-215	310	-375
223	11	-2.680	174	-180	214	-215	310	-375
c								
c roof subdivision next to top of sidewall								
224	11	-2.680	160	-165	213	-214	310	-375
225	11	-2.680	165	-167	213	-214	310	-375
226	8	-2.310	167	-168	213	-214	310	-375
227	8	-2.310	168	-169	213	-214	310	-375
228	8	-2.310	169	-170	213	-214	310	-375
229	8	-2.310	170	-171	213	-214	310	-375

230	8	-2.310	171 -172	213 -214	310 -375
231	8	-2.310	172 -173	213 -214	310 -375
232	8	-2.310	173 -174	213 -214	310 -375
233	11	-2.680	174 -180	213 -214	310 -375
c					
c sidewall (just above - vents)					
250	11	-2.680	160 -167	215 -230	310 -375
251	11	-2.680	160 -167	230 -231	310 -375
252	11	-2.680	160 -167	231 -232	310 -375
253	11	-2.680	160 -167	232 -235	310 -375
254	11	-2.680	160 -167	235 -236	310 -375
255	11	-2.680	160 -167	236 -237	310 -375
256	11	-2.680	160 -167	237 -240	310 -375
c					
c sidewall around the upper vents					
260	8	-2.310	150 -160	215 -230	310 -375
			# (150 -160	215 -230	510 -525)
			# (150 -160	215 -230	530 -545)
c					
261	8	-2.310	150 -160	230 -231	310 -375
			# (150 -160	230 -231	510 -525)
			# (150 -160	230 -231	530 -545)
c					
262	8	-2.310	150 -160	231 -232	310 -375
			# (150 -160	231 -232	510 -525)
			# (150 -160	231 -232	530 -545)
c					
263	8	-2.310	150 -160	232 -235	310 -375
			# (150 -160	232 -235	510 -525)
			# (150 -160	232 -235	530 -545)
c					
264	8	-2.310	150 -160	235 -236	310 -375
			# (150 -160	235 -236	510 -525)
			# (150 -160	235 -236	530 -545)
c					
265	8	-2.310	150 -160	236 -237	310 -375
			# (150 -160	236 -237	510 -525)
			# (150 -160	236 -237	530 -545)
c					
266	8	-2.310	150 -160	237 -240	310 -375
			# (150 -160	237 -240	510 -525)
			# (150 -160	237 -240	530 -545)
c					
c sidewall between upper and lower vents					
270	8	-2.310	120 -150	215 -230	310 -375
271	8	-2.310	120 -150	230 -231	310 -375
272	8	-2.310	120 -150	231 -232	310 -375
273	8	-2.310	120 -150	232 -235	310 -375
274	8	-2.310	120 -150	235 -236	310 -375
275	8	-2.310	120 -150	236 -237	310 -375
276	8	-2.310	120 -150	237 -240	310 -375
c					
c sidewall around the lower vents					
280	8	-2.310	105 -120	215 -230	310 -375
			# (105 -120	215 -230	510 -525)
			# (105 -120	215 -230	530 -545)
c					
281	8	-2.310	105 -120	230 -231	310 -375
			# (105 -120	230 -231	510 -525)
			# (105 -120	230 -231	530 -545)
c					
282	8	-2.310	105 -120	231 -232	310 -375
			# (105 -120	231 -232	510 -525)

```

# (105 -120 231 -232 530 -545)
c
283 8 -2.310 105 -120 232 -235 310 -375
# (105 -120 232 -235 510 -525)
# (105 -120 232 -235 530 -545)
c
284 8 -2.310 105 -120 235 -236 310 -375
# (105 -120 235 -236 510 -525)
# (105 -120 235 -236 530 -545)
c
285 8 -2.310 105 -120 236 -237 310 -375
# (105 -120 236 -237 510 -525)
# (105 -120 236 -237 530 -545)
c
286 8 -2.310 105 -120 237 -240 310 -375
# (105 -120 237 -240 510 -525)
# (105 -120 237 -240 530 -545)
c
c
c
c sidewall below lower vents
290 8 -2.310 100 -105 215 -230 310 -375
291 8 -2.310 100 -105 230 -231 310 -375
292 8 -2.310 100 -105 231 -232 310 -375
293 8 -2.310 100 -105 232 -235 310 -375
294 8 -2.310 100 -105 235 -236 310 -375
295 8 -2.310 100 -105 236 -237 310 -375
296 8 -2.310 100 -105 237 -240 310 -375
c
c
c vent air space down low
340 5 -0.001097 100 -701 240 -250 310 -375
341 5 -0.001097 701 -702 240 -250 310 -375
342 5 -0.001097 702 -703 240 -250 310 -375
343 5 -0.001097 703 -704 240 -250 310 -375
344 5 -0.001097 704 -705 240 -250 310 -375
345 5 -0.001097 705 -706 240 -250 310 -375
346 5 -0.001097 706 -165 240 -250 310 -375
c
c vent air space close to top
351 5 -0.001097 165 -167 240 -250 310 -375
352 5 -0.001097 167 -168 240 -250 310 -375
353 5 -0.001097 168 -169 240 -250 310 -375
354 5 -0.001097 169 -170 240 -250 310 -375
355 5 -0.001097 170 -171 240 -250 310 -375
356 5 -0.001097 171 -172 240 -250 310 -375
357 5 -0.001097 172 -173 240 -250 310 -375
358 5 -0.001097 173 -174 240 -250 310 -375
359 5 -0.001097 174 -180 240 -250 310 -375
c
c
c
c Vent geometry
c
c front lower vent
400 8 -2.310 105 -120 215 -230 510 -525
# (110 -115 215 -230 515 -520)
401 5 -0.001097 110 -115 215 -230 515 -520
c
402 8 -2.310 105 -120 230 -231 510 -525
# (110 -115 230 -231 515 -520)
403 5 -0.001097 110 -115 230 -231 515 -520
c

```

404	8	-2.310	105 -120	231 -232	510 -525
			# (110 -115	231 -232	515 -520)
405	5	-0.001097	110 -115	231 -232	515 -520
c					
406	8	-2.310	105 -120	232 -235	510 -525
			# (110 -115	232 -235	515 -520)
407	5	-0.001097	110 -115	232 -235	515 -520
c					
408	8	-2.310	105 -120	235 -236	510 -525
			# (110 -115	235 -236	515 -520)
409	5	-0.001097	110 -115	235 -236	515 -520
c					
410	8	-2.310	105 -120	236 -237	510 -525
			# (110 -115	236 -237	515 -520)
411	5	-0.001097	110 -115	236 -237	515 -520
c					
412	8	-2.310	105 -120	237 -240	510 -525
			# (110 -115	237 -240	515 -520)
413	5	-0.001097	110 -115	237 -240	515 -520
c					
c					
c					
c					
		front upper vent			
420	8	-2.310	150 -160	215 -230	510 -525
			# (155 -160	215 -230	515 -520)
421	5	-0.001097	155 -160	215 -230	515 -520
c					
422	8	-2.310	150 -160	230 -231	510 -525
			# (155 -160	230 -231	515 -520)
423	5	-0.001097	155 -160	230 -231	515 -520
c					
424	8	-2.310	150 -160	231 -232	510 -525
			# (155 -160	231 -232	515 -520)
425	5	-0.001097	155 -160	231 -232	515 -520
c					
426	8	-2.310	150 -160	232 -235	510 -525
			# (155 -160	232 -235	515 -520)
427	5	-0.001097	155 -160	232 -235	515 -520
c					
428	8	-2.310	150 -160	235 -236	510 -525
			# (155 -160	235 -236	515 -520)
429	5	-0.001097	155 -160	235 -236	515 -520
c					
430	8	-2.310	150 -160	236 -237	510 -525
			# (155 -160	236 -237	515 -520)
431	5	-0.001097	155 -160	236 -237	515 -520
c					
432	8	-2.310	150 -160	237 -240	510 -525
			# (155 -160	237 -240	515 -520)
433	5	-0.001097	155 -160	237 -240	515 -520
c					
c					
c					
c					
		back lower vent			
440	8	-2.310	105 -120	215 -230	530 -545
			# (110 -115	215 -230	535 -540)
441	5	-0.001097	110 -115	215 -230	535 -540
c					
442	8	-2.310	105 -120	230 -231	530 -545
			# (110 -115	230 -231	535 -540)
443	5	-0.001097	110 -115	230 -231	535 -540
c					
444	8	-2.310	105 -120	231 -232	530 -545

		# (110 -115	231 -232	535 -540)				
445	5	-0.001097	110 -115	231 -232	535 -540			
	c							
446	8	-2.310	105 -120	232 -235	530 -545			
			# (110 -115	232 -235	535 -540)			
447	5	-0.001097	110 -115	232 -235	535 -540			
	c							
448	8	-2.310	105 -120	235 -236	530 -545			
			# (110 -115	235 -236	535 -540)			
449	5	-0.001097	110 -115	235 -236	535 -540			
	c							
450	8	-2.310	105 -120	236 -237	530 -545			
			# (110 -115	236 -237	535 -540)			
451	5	-0.001097	110 -115	236 -237	535 -540			
	c							
452	8	-2.310	105 -120	237 -240	530 -545			
			# (110 -115	237 -240	535 -540)			
453	5	-0.001097	110 -115	237 -240	535 -540			
	c							
	c							
	c							
	c	back upper vent						
460	8	-2.310	150 -160	215 -230	530 -545			
			# (155 -160	215 -230	535 -540)			
461	5	-0.001097	155 -160	215 -230	535 -540			
	c							
462	8	-2.310	150 -160	230 -231	530 -545			
			# (155 -160	230 -231	535 -540)			
463	5	-0.001097	155 -160	230 -231	535 -540			
	c							
464	8	-2.310	150 -160	231 -232	530 -545			
			# (155 -160	231 -232	535 -540)			
465	5	-0.001097	155 -160	231 -232	535 -540			
	c							
466	8	-2.310	150 -160	232 -235	530 -545			
			# (155 -160	232 -235	535 -540)			
467	5	-0.001097	155 -160	232 -235	535 -540			
	c							
468	8	-2.310	150 -160	235 -236	530 -545			
			# (155 -160	235 -236	535 -540)			
469	5	-0.001097	155 -160	235 -236	535 -540			
	c							
470	8	-2.310	150 -160	236 -237	530 -545			
			# (155 -160	236 -237	535 -540)			
471	5	-0.001097	155 -160	236 -237	535 -540			
	c							
472	8	-2.310	150 -160	237 -240	530 -545			
			# (155 -160	237 -240	535 -540)			
473	5	-0.001097	155 -160	237 -240	535 -540			
	c							
	c	DSC						
	c							
	c	shell						
900	6	-7.80	410 -415	200	330 -365			
	c	radial air gap between fuel and shell						
905	5	-0.001097	406 -407	200	340 -360	#940 #941 #942 #943		
						#944 #945 #946 #947		
	c							
	c							
	c	shield plug/top closure lids (All iron)						
913	6	-7.80	-410	200	360 -429	\$ Top Shield Plug		
914	6	-7.80	-410	200	430 -361	\$ Top Shield Plug		
915	6	-7.80	-410	200	429 -430	\$ Top Shield Plug		

```

916 7 -7.82 -410 200 361 -362 $ Inner Top Cover Plate
917 7 -7.82 -410 200 362 -365 $ Outer Top Cover Plate
c air gap between top/plenum and top shield plug
920 5 -0.001097 -406 200 355 -360
c bottom shield plug/closure plates
910 6 -7.80 -410 200 426 -427 $ Bottom Shield Plug (Middle
part, see 948 and 949)
911 7 -7.82 -410 200 332 -340 $ Inner Bottom Cover Plate
912 7 -7.82 -410 200 330 -331 $ Outer Top Cover Plate
c DSC Spacer Disks. All 2 in. thick
940 5 -0.001097 200 406 -407 346 -347 $ Spacer Disk (SD) #1.
941 like 940 but trcl=1 $ Spacer Disk (SD) #2.
942 like 940 but trcl=2 $ Spacer Disk (SD) #3.
943 like 940 but trcl=3 $ Spacer Disk (SD) #4.
944 like 940 but trcl=4 $ Spacer Disk (SD) #5.
945 like 940 but trcl=5 $ Spacer Disk (SD) #6.
946 like 940 but trcl=6 $ Spacer Disk (SD) #7.
947 like 940 but trcl=7 $ Spacer Disk (SD) #8.
c
c air around DSC
960 5 -0.001097 110 -160 200 -215 335 -370
#(200 -415 335 -365)
c
c Splitted Bottom Shield Plug (similar to 910)
948 6 -7.80 -410 200 331 -426 $ Bottom Shield Plug (Front
part)
949 6 -7.80 -410 200 427 -332 $ Bottom Shield Plug (Rear
part)
c
950 6 -7.80 405 -406 200 340 -355 $ 0.125" thick Outer Basket
951 10 -2.699 407 -410 200 340 -360 $ 0.4" thick Aluminum
Transition Rails
c door larger middle piece (front part, see cell 93)
952 8 -2.310 -425 200 428 -315
c void
999 0 -200 : 250 : -99 : 185 : -300 : 385

c Surfaces
c *****
c *****
c
99 pz -30.48 $ underground
100 pz 0 $ ground
105 pz 26.67 $ lower vent liner/HSM base top
110 pz 30.48 $ lower vent liner
115 pz 43.18 $ lower vent liner
120 pz 46.99 $ lower vent liner
122 pz 153.035 $ door bottom edge
150 pz 353.695 $ upper vent liner
155 pz 357.505 $ upper vent liner
157 pz 365.125 $ door top edge
160 pz 365.76 $ upper vent liner/roof slab bottom
165 pz 369.57 $ upper vent liner
166 c/y 0 259.08 111.44 $ Outer Radius of Door Outer Steel Cover plate
c
167 pz 373.38 $ z-axis subdivision of the sidewall
c
168 pz 390 $ z-axis subdivision of the sidewall
169 pz 400 $ z-axis subdivision of the sidewall
170 pz 410 $ z-axis subdivision of the sidewall
171 pz 420 $ z-axis subdivision of the sidewall
172 pz 430 $ z-axis subdivision of the sidewall
173 pz 440 $ z-axis subdivision of the sidewall

```


174	pz	449.58	\$	z-axis subdivision of the sidewall
c				
180	pz	457.2	\$	HSM top surface
181	pz	458.2	\$	tally cell surface - bird screen
185	pz	762	\$	10 feet above HSM top surface
c				
c				tally segments surfaces
700	pz	45.82	\$	surfaces for segmenting the
701	pz	91.64	\$	front bird screen tally
702	pz	137.46		
703	pz	183.28		
704	pz	229.1		
705	pz	274.92		
706	pz	320.74		
707	pz	366.56		
708	pz	412.38		
c				
729	py	48.006	\$	surfaces for segmenting the
730	py	78.232	\$	roof bird screen tally
731	py	108.458		
732	py	138.684		
733	py	168.91		
734	py	199.136		
735	py	229.362		
736	py	259.588		
737	py	289.814		
738	py	320.04		
739	py	350.266		
740	py	380.492		
741	py	410.718		
742	py	440.944		
743	py	471.17		
744	py	501.396		
745	py	531.622		
746	py	561.848		
747	py	592.074		
c				
c				
*200	px	0.0	\$	HSM/DSC center - refl surf.
213	px	81.0	\$	roof subdivision
214	px	91.0	\$	roof subdivision
215	px	101.6	\$	sidewall - inner edge
220	px	106.045	\$	outer door piece - side edge
230	px	107	\$	sidewall subdivision
231	px	115	\$	sidewall subdivision
232	px	122	\$	sidewall subdivision
235	px	129	\$	sidewall subdivision
236	px	139.7	\$	sidewall subdivision
237	px	143	\$	sidewall subdivision
240	px	147.32	\$	sidewall - outer edge
*250	px	154.94	\$	vent center - reflective surf.
c				
c	300	py -774.192	\$	10 feet from outer door piece - front surf.
300	py	-100.192		
305	py	0.00	\$	
309	py	16.78	\$	tally cell surface - bird screen
310	py	17.78	\$	HSM front wall surf.
315	py	31.75	\$	middle door piece - transition surf.
316	py	50		
320	py	13.37	\$	outer door piece - front surf.
325	py	33.02	\$	door liner - inner surf.
330	py	80.645	\$	DSC bottom surf.
331	py	81.915	\$	RHS of Outer Bottom Cover Plate

```

332 py 97.785 $ LHS of Inner Bottom Cover Plate
335 py 93.98 $ door penetration - inner section
336 py 150.00 $ Used to split roof slab vertically near Bottom
Region of DSC
337 py 452.00 $ Used to split roof slab vertically near Top Region
of DSC
338 px 15.00 $ Used to create "detectors" on HSM roof
340 py 99.695 $ fuel bottom - bottom surf.
345 py 120.96 $ AFL - bottom surf.
346 py 109.22 $ LHS of Spacer Disk (SD) #1
347 py 114.30 $ RHS of Spacer Disk (SD) #1 (LHS+2 in.)
c
510 py 125.73 $ front vent liner outer edge
515 py 129.54 $ front vent liner inner edge
520 py 281.94 $ front vent liner outer edge
525 py 285.75 $ front vent liner outer edge
530 py 353.06 $ back vent liner outer edge
535 py 356.87 $ back vent liner inner edge
540 py 509.27 $ back vent liner inner edge
545 py 513.08 $ back vent liner outer edge
c
350 py 482.38 $ AFL - top surf
351 py 504.55 $ Plenum Surface
355 py 520.38 $ top/plenum - top surf.
360 py 545.97 $ shield lid - bottom surfaces
361 py 561.84 $ LHS of Inner Cover Plate Top
362 py 565.02 $ LHS of Outer Top Cover Plate
365 py 568.83 $ shield lid - top surface
370 py 591.82 $ HSM back wall - inner surf.
375 py 622.3 $ HSM back wall - outer surf.
380 py 683.26 $ HSM back shield wall - outer surf.
381 py 684.26 $ Bounds 1 cm. thick Air Cell on HSM Back
385 py 783.26
c 385 py 988.06 $ 10 feet from HSM back shield wall - outer
surf
c these surfaces added to keep subdivision of cells in important regions
601 py 60.9346 $ Could be used to replace old surface 320
602 py 63.4746 $ Is used to replace old surface 325
c
404 c/y 0 259.08 50.58 $ fuel - inner Radius
405 c/y 0 259.08 71.86 $ fuel - outer Radius
406 c/y 0 259.08 72.17 $ Bounds Outer Basket around Fuel
407 c/y 0 259.08 82.09 $ Bounds Radial Air Gap inside of DSC
410 c/y 0 259.08 83.10 $ can shell - inner R
415 c/y 0 259.08 85.33 $ can shell - outer R
420 c/y 0 259.08 87.9602 $ HSM front penetration - small radius
425 c/y 0 259.08 100.6602 $ HSM front penetration - large radius
c
426 py 87.205 $ For Splitting Bottom Shield Plug
427 py 92.495 $ For Splitting Bottom Shield Plug
428 py 24.50 $ For Splitting Front Door
429 py 551.97 $ For Splitting Top Shield Plug
430 py 556.97 $ For Splitting Top Shield Plug
c Added to segment tallies on HSM Door Surface (89.96 outer radius.)
526 c/y 0 259.08 15.00 $ Inner Splitting Cylinder
527 c/y 0 259.08 44.32 $ Middle Splitting Cylinder
528 c/y 0 259.08 73.64 $ Outer Splitting Cylinder
c
mode p
c
c Source
c *****

```

```

c *****
c
sdef cel=d7 x fcel d1 z fcel d4 y fcel d8 erg fcel d13
c *** Sample X ***
dsl q 1 2 2 3 3 2 4 3 5 2 6 3 7 2 8 3
si2 h 0.0 50.58
sp2 0 1
si3 h 0.0 71.86
sp3 0 1
c **** Sample Z ****
ds4 q 1 5 2 6 3 5 4 6 5 5 6 6 7 5 8 6
si5 h 208.50 309.66
sp5 0 1
si6 h 187.22 330.94
sp6 0 1
c *** Chose Source Regions ***
si7 l 1 1 2 3 4 5 6 7 8 $ Chose Source
Regions
sp7 d 1.792e-04 1.775e-03 3.076e-01 6.877e-01
1.996e-04 8.492e-04 3.320e-04 1.333e-03 $ Fraction of
Source in each Region
ds8 q 1 9 2 9 3 10 4 10 5 11 6 11 7 12 8 12 $ Sample within Fuel
Axial Zones
si9 h 99.695 120.96 $
Bottom Region Extents
sp9 0 1
si10 a 120.96 139.03 157.10 193.24 229.38 265.53
301.67 337.81 373.95 410.09 446.23 464.31 482.38
sp10 d 0.0 0.94 1.12 1.12 1.12 1.12
1.12 1.12 1.12 1.10 0.92 0.70 0.00 $ In-
Core Axial Extents
si11 h 482.38 504.55 $ Plenum Region
Extents
sp11 0 1
si12 h 504.55 520.38 $ Top Nozzle Region
Extents
sp12 0 1
dsl3 q 1 14 2 14 3 15 4 16 5 17 6 17 7 18 8 18 $ Energy
Distributions
c ****Sample Spectral Distribution within Bottom Nozzle****
si14 l 0.03 0.08 0.15 0.25 0.35 0.50
0.70 0.90 1.17 1.50 1.83 2.25
2.75 3.50 4.50 5.75 7.25 9.00
sp14 d 1.224e+13 1.523e+12 3.675e+11 1.826e+10 2.393e+10 1.517e+09
4.256e+10 3.443e+12 4.446e+14 1.255e+14 3.695e+04 2.979e+09
4.620e+06 5.551e-08 0.000e+00 0.000e+00 0.000e+00 0.000e+00 $
Bottom Nozzle
c ****Sample Spectral Distribution within 16 Inner Assemblies.In-Core
Region****
si15 l 0.03 0.08 0.15 0.25 0.35 0.50
0.70 0.90 1.17 1.50 1.83 2.25
2.75 3.50 4.50 5.75 7.25 9.00
sp15 d 1.603e+16 3.166e+15 2.308e+15 6.748e+14 4.494e+14 2.923e+15
2.138e+16 1.382e+15 2.048e+15 5.792e+14 2.734e+12 2.999e+12
1.492e+11 1.879e+10 7.582e+07 3.043e+07 5.968e+06 1.267e+06 $
In-core Region
c ****Sample Spectral Distribution within 16 Outer Assemblies.In-Core
Region****
si16 l 0.03 0.08 0.15 0.25 0.35 0.50
0.70 0.90 1.17 1.50 1.83 2.25
2.75 3.50 4.50 5.75 7.25 9.00
sp16 d 1.170e+10 2.405e+09 1.954e+09 5.540e+08 3.903e+08 4.604e+09
1.385e+10 1.960e+09 1.352e+09 4.113e+08 7.291e+06 1.640e+07

```

```

5.610e+05 7.001e+04 7.378e+01 2.961e+01 5.809e+00 1.233e+00 $
In-core Region
c *****Sample Spectral Distribution within Plenum Region*****
si17 1 0.03 0.08 0.15 0.25 0.35 0.50
      0.70 0.90 1.17 1.50 1.83 2.25
      2.75 3.50 4.50 5.75 7.25 9.00
sp17 d 1.331e+13 7.697e+11 5.565e+11 1.365e+11 8.586e+11 2.826e+12
      1.429e+12 2.988e+11 2.003e+14 6.076e+13 1.839e+04 1.368e+09
      2.468e+06 4.415e-08 0.000e+00 0.000e+00 0.000e+00 0.000e+00 $
Plenum Region
c *****Sample Spectral Distribution within Top Nozzle Region*****
si18 1 0.03 0.08 0.15 0.25 0.35 0.50
      0.70 0.90 1.17 1.50 1.83 2.25
      2.75 3.50 4.50 5.75 7.25 9.00
sp18 d 1.024e+13 1.199e+12 2.650e+11 1.783e+10 1.697e+10 1.968e+09
      1.625e+11 2.107e+12 3.275e+14 1.001e+14 2.568e+04 2.240e+09
      4.103e+06 3.842e-08 0.000e+00 0.000e+00 0.000e+00 0.000e+00 $
Top Nozzle
c Tallies
c *****
c *****
c Use these multipliers: fm:p 8.280e+16 fm:n 4.216e+09
c
f14:p 30
fc14 ***** roof bird screen *****
fs14 -729 -730 -731 -732 -733
      -734 -735 -736 -737 -738
      -739 -740 -741 -742 -743
      -744 -745 -746 -747 t
sd14 230.322 230.322 230.322 230.322 230.322
      230.322 230.322 230.322 230.322 230.322
      230.322 230.322 230.322 230.322 230.322
      4606.44
fm14 8.280e+16
f24:p 89
fc24 **Tally inside of 13.37 cm. thick Air Cell on Outer Surface of Door ****
fs24 -526 -527 -528 -420 t
sd24 4725.35 36527.20 72635.68 48599.93 98327.40 260815.55
fm24 8.280e+16
c
f34:p 21
fc34 **Tally inside of 1.0 cm. thick Air Cell on Rear Shield Wall ****
fs34 -526 -527 -528 -420 -166 t
sd34 353.4292 2732.0270 5432.7361 3634.9986 7354.3302
      51485.9870 70993.5080
fm34 8.280e+16
f44:p 336
fc44 **Roof "Detector" # 1 (cell 336) ****
fm44 8.280e+16
c
f54:p 337
fc54 **Roof "Detector" # 2 (cell 337) ****
fm54 8.280e+16
c
f64:p 338
fc64 **Roof "Detector" # 3 (cell 338) ****
fm64 8.280e+16
c
f74:p 339
fc74 **Roof "Detector" # 4 (cell 339) ****
fm74 8.280e+16
c

```

```

f84:p 347
fc84 **Roof "Detector" # 5 (cell 347) ****
fm84 8.280e+16
c
f94:p 348
fc94 **Roof "Detector" # 6 (cell 348) ****
fm94 8.280e+16
c
***Average Dose rate over the rest of the roof, not bird screen and
detectors 1-6)***
f104:p 31
fc104 **Average Dose Rate over the rest of roof (cell 31) ****
fm104 8.280e+16
f114:p (30 31 336 337 338 339 347 348)
fc114 **Average Dose Rate over roof including roof bird screen (F4) **
fs114 240 -335 -370 t
sd114 5070.9576 11225.784 73341.7888 13470.9408 103109.4712
fm114 8.280e+16
f2:p 181
fc2 **Average Dose Rate over roof except roof bird screens (F2) **
fm2 8.280e+16
fs2 240 -335 -370
sd2 6731.90424 28605.41904 73341.7888 28202.9408
c
****Mesh Tallies on the roof (comment these cards if using MCNP4C)***
tmesh
c *****Dose at the roof centreline*****
rmesh1:p dose 20 1 1 1.0
coral 0.0 15.00
corbl 17.78 2i 93.98 1i 150.00 9i 452.00 2i 545.97 1i 622.3 1i 683.26
corcl 457.3 458.0
rmesh11:p dose 20 1 1 1.0
cora11 15.0 3i 147.32 1i 154.94
corb11 17.78 2i 93.98 1i 150.00 9i 452.00 2i 545.97 1i 622.3 1i 683.26
corc11 457.3 458.0
endmd
c *****End of Mesh Tallies*****
de0 0.01 0.03 0.05 0.07 0.10 0.15
0.20 0.25 0.30 0.35 0.40 0.45
0.50 0.55 0.60 0.65 0.70 0.80
1.00 1.40 1.80 2.20 2.60 2.80
3.25 3.75 4.25 4.75 5.00 5.25
5.75 6.25 6.75 7.50 9.00 11.0
13.0 15.0
df0 3.96e-3 5.82e-4 2.90e-4 2.58e-4 2.83e-4 3.79e-4
5.01e-4 6.31e-4 7.59e-4 8.78e-4 9.85e-4 1.08e-3
1.17e-3 1.27e-3 1.36e-3 1.44e-3 1.52e-3 1.68e-3
1.98e-3 2.51e-3 2.99e-3 3.42e-3 3.82e-3 4.01e-3
4.41e-3 4.83e-3 5.23e-3 5.60e-3 5.80e-3 6.01e-3
6.37e-3 6.74e-3 7.11e-3 7.66e-3 8.77e-3 1.03e-2
1.18e-2 1.33e-2
c
wwg 14 4 0 150 350 500
wwge:p 0.05 0.1 0.4 0.6 1.0 2.0 3.0 100.00
c
wwp:p 5 3 5
wwe:p 0.05 0.1 0.4 0.6 1.0 2.0 3.0 100.00
wwnl:p 3.2655E-02 3.2655E-02 5.0000E-01 5.0000E-01 9.0384E-02 $ 5
9.0384E-02 9.0384E-02 9.0384E-02 3.4834E-01 2.8755E-04 $ 10
0.0000E+00 0.0000E+00 5.2837E-06 3.0719E-08 2.0335E-06 $ 15
7.6657E-02 9.6567E-02 0.0000E+00 0.0000E+00 0.0000E+00 $ 20
0.0000E+00 0.0000E+00 0.0000E+00 1.3248E-04 3.5966E-04 $ 25
3.7665E-04 0.0000E+00 4.3074E-04 0.000E+00 0.000E+00 $ 30

```

0.000E+00	0.000E+00	0.000E+00	0.000E+00	0.000E+00	\$ 35
0.000E+00	0.000E+00	0.000E+00	0.000E+00	0.000E+00	\$ 40
0.000E+00	0.000E+00	0.000E+00	0.000E+00	0.000E+00	\$ 45
0.000E+00	0.000E+00	0.000E+00	0.000E+00	0.000E+00	\$ 50
0.000E+00	0.000E+00	0.000E+00	0.000E+00	0.000E+00	\$ 55
0.000E+00	0.000E+00	0.000E+00	0.000E+00	0.000E+00	\$ 60
0.000E+00	0.000E+00	0.000E+00	0.000E+00	0.000E+00	\$ 65
0.000E+00	0.000E+00	0.000E+00	0.000E+00	0.000E+00	\$ 70
0.000E+00	0.000E+00	0.000E+00	0.000E+00	0.000E+00	\$ 75
0.000E+00	0.000E+00	0.000E+00	0.000E+00	8.7908E-04	\$ 80
4.2448E-04	1.4178E-04	6.0136E-05	1.9999E-05	7.7718E-06	\$ 85
3.0539E-06	4.1586E-04	2.1060E-04	7.2196E-05	3.1791E-05	\$ 90
1.4967E-05	5.7045E-06	2.0533E-06	8.5410E-04	1.0477E-04	\$ 95
3.6979E-05	1.4614E-05	6.8236E-06	3.4880E-06	1.3863E-06	\$ 100
2.2070E-04	1.5810E-04	1.8452E-05	7.2631E-06	3.0422E-06	\$ 105
1.6578E-06	7.7937E-07	0.0000E+00	9.6530E-05	2.6767E-05	\$ 110
3.9607E-06	1.2628E-06	7.1596E-07	4.2074E-07	0.0000E+00	\$ 115
0.0000E+00	4.8543E-05	5.9488E-06	7.0618E-07	2.6665E-07	\$ 120
2.1437E-07	0.0000E+00	0.0000E+00	8.4709E-04	5.5726E-05	\$ 125
1.4097E-06	1.6098E-07	1.0924E-07	0.0000E+00	0.0000E+00	\$ 130
0.0000E+00	0.0000E+00	2.9685E-06	1.0557E-06	9.4109E-08	\$ 135
3.6977E-03	4.1264E-03	2.4367E-03	5.8823E-03	2.4534E-03	\$ 140
7.7501E-03	0.0000E+00	0.0000E+00	0.0000E+00	0.0000E+00	\$ 145
5.9848E-03	2.3337E-02	2.8905E-02	2.7552E-02	2.6046E-02	\$ 150
0.0000E+00	0.0000E+00	0.0000E+00	0.0000E+00	0.0000E+00	\$ 155
1.5288E-03	6.2525E-04	2.1523E-04	8.3590E-05	2.9948E-05	\$ 160
1.1740E-05	2.9982E-06	1.9506E-03	1.0136E-03	3.3529E-04	\$ 165
1.3755E-04	5.6310E-05	2.3435E-05	6.4476E-06	1.1307E-02	\$ 170
7.1278E-03	2.4588E-03	9.7339E-04	3.7292E-04	1.3072E-04	\$ 175
4.7174E-05	0.0000E+00	0.0000E+00	0.0000E+00	0.0000E+00	\$ 180
0.0000E+00	0.0000E+00	2.2421E-05	0.0000E+00	0.0000E+00	\$ 185
0.0000E+00	0.0000E+00	0.0000E+00	0.0000E+00	0.0000E+00	\$ 190
1.2151E-04	2.6408E-05	2.7204E-05	2.1617E-05	1.1135E-05	\$ 195
6.1246E-06	9.3331E-06	4.0664E-07	2.4863E-07	1.7994E-07	\$ 200
1.4402E-07	1.1796E-07	1.0253E-07	8.6856E-08	7.4657E-08	\$ 205
5.5402E-08	0.0000E+00	5.7944E-04	0.0000E+00	4.4819E-04	\$ 210
0.0000E+00	2.9497E-04	0.0000E+00	2.0075E-04	0.0000E+00	\$ 215
1.6222E-04	1.8774E-03	1.2000E-04	5.2505E-03	7.5037E-05	\$ 220
2.5798E-03	2.3188E-04	1.8661E-03	1.3990E-04	6.7812E-04	\$ 225
7.9228E-05	4.7292E-04	6.1535E-05	1.6582E-04	4.0201E-05	\$ 230
5.0906E-05	2.5624E-05	1.3159E-05	1.2968E-05	0.0000E+00	\$ 235
0.0000E+00	0.0000E+00	0.0000E+00	0.0000E+00	0.0000E+00	\$ 240
0.0000E+00	0.0000E+00	0.0000E+00	0.0000E+00	0.0000E+00	\$ 245
0.0000E+00	0.0000E+00	0.0000E+00	2.3812E-03	2.8602E-04	\$ 250
1.5515E-03	1.8521E-04	6.1850E-04	1.0422E-04	2.6717E-04	\$ 255
6.2116E-05	1.8145E-04	3.9872E-05	4.8921E-05	1.9986E-05	\$ 260
1.1703E-05	1.4510E-05	1.3112E-02	1.3594E-02	0.0000E+00	\$ 265
0.0000E+00	0.0000E+00	0.0000E+00	0.0000E+00	1.8960E-02	\$ 270
0.0000E+00	0.0000E+00	0.0000E+00	1.3594E-02	1.3594E-02	\$ 275
1.3594E-02	1.3594E-02	1.3594E-02	1.3594E-02	1.3594E-02	\$ 280
1.3594E-02	7.5912E-03	0.0000E+00	0.0000E+00	1.3594E-02	\$ 285
1.3594E-02	0.0000E+00	-1.0000E+00			\$ 288
3.2655E-02	3.2655E-02	5.0000E-01	5.0000E-01	9.0384E-02	\$ 5
9.0384E-02	9.0384E-02	9.0384E-02	3.4834E-01	2.8755E-04	\$ 10
0.0000E+00	0.0000E+00	5.2837E-06	3.0719E-08	2.0335E-06	\$ 15
7.6657E-02	9.6567E-02	0.0000E+00	0.0000E+00	0.0000E+00	\$ 20
0.0000E+00	0.0000E+00	0.0000E+00	1.3248E-04	3.5966E-04	\$ 25
3.7665E-04	0.0000E+00	4.3074E-04	0.000E+00	0.000E+00	\$ 30
0.000E+00	0.000E+00	0.000E+00	0.000E+00	0.000E+00	\$ 35
0.000E+00	0.000E+00	0.000E+00	0.000E+00	0.000E+00	\$ 40
0.000E+00	0.000E+00	0.000E+00	0.000E+00	0.000E+00	\$ 45
0.000E+00	0.000E+00	0.000E+00	0.000E+00	0.000E+00	\$ 50
0.000E+00	0.000E+00	0.000E+00	0.000E+00	0.000E+00	\$ 55

wvn2:p

0.000E+00	0.000E+00	0.000E+00	0.000E+00	0.000E+00	\$ 60	
0.000E+00	0.000E+00	0.000E+00	0.000E+00	0.000E+00	\$ 65	
0.000E+00	0.000E+00	0.000E+00	0.000E+00	0.000E+00	\$ 70	
0.000E+00	0.000E+00	0.000E+00	0.0000E+00	0.0000E+00	\$ 75	
0.0000E+00	0.0000E+00	0.0000E+00	0.0000E+00	8.7908E-04	\$ 80	
4.2448E-04	1.4178E-04	6.0136E-05	1.9999E-05	7.7718E-06	\$ 85	
3.0539E-06	4.1586E-04	2.1060E-04	7.2196E-05	3.1791E-05	\$ 90	
1.4967E-05	5.7045E-06	2.0533E-06	8.5410E-04	1.0477E-04	\$ 95	
3.6979E-05	1.4614E-05	6.8236E-06	3.4880E-06	1.3863E-06	\$ 100	
2.2070E-04	1.5810E-04	1.8452E-05	7.2631E-06	3.0422E-06	\$ 105	
1.6578E-06	7.7937E-07	0.0000E+00	9.6530E-05	2.6767E-05	\$ 110	
3.9607E-06	1.2628E-06	7.1596E-07	4.2074E-07	0.0000E+00	\$ 115	
0.0000E+00	4.8543E-05	5.9488E-06	7.0618E-07	2.6665E-07	\$ 120	
2.1437E-07	0.0000E+00	0.0000E+00	8.4709E-04	5.5726E-05	\$ 125	
1.4097E-06	1.6098E-07	1.0924E-07	0.0000E+00	0.0000E+00	\$ 130	
0.0000E+00	0.0000E+00	2.9685E-06	1.0557E-06	9.4109E-08	\$ 135	
3.6977E-03	4.1264E-03	2.4367E-03	5.8823E-03	2.4534E-03	\$ 140	
7.7501E-03	0.0000E+00	0.0000E+00	0.0000E+00	0.0000E+00	\$ 145	
5.9848E-03	2.3337E-02	2.8905E-02	2.7552E-02	2.6046E-02	\$ 150	
0.0000E+00	0.0000E+00	0.0000E+00	0.0000E+00	0.0000E+00	\$ 155	
1.5288E-03	6.2525E-04	2.1523E-04	8.3590E-05	2.9948E-05	\$ 160	
1.1740E-05	2.9982E-06	1.9506E-03	1.0136E-03	3.3529E-04	\$ 165	
1.3755E-04	5.6310E-05	2.3435E-05	6.4476E-06	1.1307E-02	\$ 170	
7.1278E-03	2.4588E-03	9.7339E-04	3.7292E-04	1.3072E-04	\$ 175	
4.7174E-05	0.0000E+00	0.0000E+00	0.0000E+00	0.0000E+00	\$ 180	
0.0000E+00	0.0000E+00	2.2421E-05	0.0000E+00	0.0000E+00	\$ 185	
0.0000E+00	0.0000E+00	0.0000E+00	0.0000E+00	0.0000E+00	\$ 190	
1.2151E-04	2.6408E-05	2.7204E-05	2.1617E-05	1.1135E-05	\$ 195	
6.1246E-06	9.3331E-06	4.0664E-07	2.4863E-07	1.7994E-07	\$ 200	
1.4402E-07	1.1796E-07	1.0253E-07	8.6856E-08	7.4657E-08	\$ 205	
5.5402E-08	0.0000E+00	5.7944E-04	0.0000E+00	4.4819E-04	\$ 210	
0.0000E+00	2.9497E-04	0.0000E+00	2.0075E-04	0.0000E+00	\$ 215	
1.6222E-04	1.8774E-03	1.2000E-04	5.2505E-03	7.5037E-05	\$ 220	
2.5798E-03	2.3188E-04	1.8661E-03	1.3990E-04	6.7812E-04	\$ 225	
7.9228E-05	4.7292E-04	6.1535E-05	1.6582E-04	4.0201E-05	\$ 230	
5.0906E-05	2.5624E-05	1.3159E-05	1.2968E-05	0.0000E+00	\$ 235	
0.0000E+00	0.0000E+00	0.0000E+00	0.0000E+00	0.0000E+00	\$ 240	
0.0000E+00	0.0000E+00	0.0000E+00	0.0000E+00	0.0000E+00	\$ 245	
0.0000E+00	0.0000E+00	0.0000E+00	2.3812E-03	2.8602E-04	\$ 250	
1.5515E-03	1.8521E-04	6.1850E-04	1.0422E-04	2.6717E-04	\$ 255	
6.2116E-05	1.8145E-04	3.9872E-05	4.8921E-05	1.9986E-05	\$ 260	
1.1703E-05	1.4510E-05	1.3112E-02	1.3594E-02	0.0000E+00	\$ 265	
0.0000E+00	0.0000E+00	0.0000E+00	0.0000E+00	1.8960E-02	\$ 270	
0.0000E+00	0.0000E+00	0.0000E+00	1.3594E-02	1.3594E-02	\$ 275	
1.3594E-02	1.3594E-02	1.3594E-02	1.3594E-02	1.3594E-02	\$ 280	
1.3594E-02	7.5912E-03	0.0000E+00	0.0000E+00	1.3594E-02	\$ 285	
1.3594E-02	0.0000E+00	-1.0000E+00			\$ 288	
wnn3:p	3.2655E-02	3.2655E-02	5.0000E-01	5.0000E-01	9.0384E-02	\$ 5
	9.0384E-02	9.0384E-02	9.0384E-02	3.4834E-01	2.8755E-04	\$ 10
	0.0000E+00	0.0000E+00	5.2837E-06	3.0719E-08	2.0335E-06	\$ 15
	7.6657E-02	9.6567E-02	0.0000E+00	0.0000E+00	0.0000E+00	\$ 20
	0.0000E+00	0.0000E+00	0.0000E+00	1.3248E-04	3.5966E-04	\$ 25
	3.7665E-04	0.0000E+00	4.3074E-04	0.000E+00	9.364E+00	\$ 30
	6.656E-01	4.731E-02	3.363E-03	2.391E-04	1.699E-05	\$ 35
	1.208E-06	8.587E-08	0.000E+00	9.364E+00	6.656E-01	\$ 40
	4.731E-02	3.363E-03	2.391E-04	1.699E-05	1.208E-06	\$ 45
	8.587E-08	0.000E+00	9.364E+00	6.656E-01	4.731E-02	\$ 50
	3.363E-03	2.391E-04	1.699E-05	1.208E-06	8.587E-08	\$ 55
	0.000E+00	9.364E+00	6.656E-01	4.731E-02	3.363E-03	\$ 60
	2.391E-04	1.699E-05	1.208E-06	8.587E-08	0.000E+00	\$ 65
	9.364E+00	6.656E-01	4.731E-02	3.363E-03	2.391E-04	\$ 70
	1.699E-05	1.208E-06	8.587E-08	0.0000E+00	0.0000E+00	\$ 75
	0.0000E+00	0.0000E+00	0.0000E+00	0.0000E+00	8.7908E-04	\$ 80

4.2448E-04	1.4178E-04	6.0136E-05	1.9999E-05	7.7718E-06	\$ 85	
3.0539E-06	4.1586E-04	2.1060E-04	7.2196E-05	3.1791E-05	\$ 90	
1.4967E-05	5.7045E-06	2.0533E-06	8.5410E-04	1.0477E-04	\$ 95	
3.6979E-05	1.4614E-05	6.8236E-06	3.4880E-06	1.3863E-06	\$ 100	
2.2070E-04	1.5810E-04	1.8452E-05	7.2631E-06	3.0422E-06	\$ 105	
1.6578E-06	7.7937E-07	0.0000E+00	9.6530E-05	2.6767E-05	\$ 110	
3.9607E-06	1.2628E-06	7.1596E-07	4.2074E-07	0.0000E+00	\$ 115	
0.0000E+00	4.8543E-05	5.9488E-06	7.0618E-07	2.6665E-07	\$ 120	
2.1437E-07	0.0000E+00	0.0000E+00	8.4709E-04	5.5726E-05	\$ 125	
1.4097E-06	1.6098E-07	1.0924E-07	0.0000E+00	0.0000E+00	\$ 130	
0.0000E+00	0.0000E+00	2.9685E-06	1.0557E-06	9.4109E-08	\$ 135	
3.6977E-03	4.1264E-03	2.4367E-03	5.8823E-03	2.4534E-03	\$ 140	
7.7501E-03	0.0000E+00	0.0000E+00	0.0000E+00	0.0000E+00	\$ 145	
5.9848E-03	2.3337E-02	2.8905E-02	2.7552E-02	2.6046E-02	\$ 150	
0.0000E+00	0.0000E+00	0.0000E+00	0.0000E+00	0.0000E+00	\$ 155	
1.5288E-03	6.2525E-04	2.1523E-04	8.3590E-05	2.9948E-05	\$ 160	
1.1740E-05	2.9982E-06	1.9506E-03	1.0136E-03	3.3529E-04	\$ 165	
1.3755E-04	5.6310E-05	2.3435E-05	6.4476E-06	1.1307E-02	\$ 170	
7.1278E-03	2.4588E-03	9.7339E-04	3.7292E-04	1.3072E-04	\$ 175	
4.7174E-05	0.0000E+00	0.0000E+00	0.0000E+00	0.0000E+00	\$ 180	
0.0000E+00	0.0000E+00	2.2421E-05	0.0000E+00	0.0000E+00	\$ 185	
0.0000E+00	0.0000E+00	0.0000E+00	0.0000E+00	0.0000E+00	\$ 190	
1.2151E-04	2.6408E-05	2.7204E-05	2.1617E-05	1.1135E-05	\$ 195	
6.1246E-06	9.3331E-06	4.0664E-07	2.4863E-07	1.7994E-07	\$ 200	
1.4402E-07	1.1796E-07	1.0253E-07	8.6856E-08	7.4657E-08	\$ 205	
5.5402E-08	0.0000E+00	5.7944E-04	0.0000E+00	4.4819E-04	\$ 210	
0.0000E+00	2.9497E-04	0.0000E+00	2.0075E-04	0.0000E+00	\$ 215	
1.6222E-04	1.8774E-03	1.2000E-04	5.2505E-03	7.5037E-05	\$ 220	
2.5798E-03	2.3188E-04	1.8661E-03	1.3990E-04	6.7812E-04	\$ 225	
7.9228E-05	4.7292E-04	6.1535E-05	1.6582E-04	4.0201E-05	\$ 230	
5.0906E-05	2.5624E-05	1.3159E-05	1.2968E-05	0.0000E+00	\$ 235	
0.0000E+00	0.0000E+00	0.0000E+00	0.0000E+00	0.0000E+00	\$ 240	
0.0000E+00	0.0000E+00	0.0000E+00	0.0000E+00	0.0000E+00	\$ 245	
0.0000E+00	0.0000E+00	0.0000E+00	2.3812E-03	2.8602E-04	\$ 250	
1.5515E-03	1.8521E-04	6.1850E-04	1.0422E-04	2.6717E-04	\$ 255	
6.2116E-05	1.8145E-04	3.9872E-05	4.8921E-05	1.9986E-05	\$ 260	
1.1703E-05	1.4510E-05	1.3112E-02	1.3594E-02	0.0000E+00	\$ 265	
0.0000E+00	0.0000E+00	0.0000E+00	0.0000E+00	1.8960E-02	\$ 270	
0.0000E+00	0.0000E+00	0.0000E+00	1.3594E-02	1.3594E-02	\$ 275	
1.3594E-02	1.3594E-02	1.3594E-02	1.3594E-02	1.3594E-02	\$ 280	
1.3594E-02	7.5912E-03	0.0000E+00	0.0000E+00	1.3594E-02	\$ 285	
1.3594E-02	0.0000E+00	-1.0000E+00			\$ 288	
wnn4:p	3.2655E-02	3.2655E-02	5.0000E-01	5.0000E-01	9.0384E-02	\$ 5
	9.0384E-02	9.0384E-02	9.0384E-02	3.4834E-01	2.8755E-04	\$ 10
	0.0000E+00	0.0000E+00	5.2837E-06	3.0719E-08	2.0335E-06	\$ 15
	7.6657E-02	9.6567E-02	0.0000E+00	0.0000E+00	0.0000E+00	\$ 20
	0.0000E+00	0.0000E+00	0.0000E+00	1.3248E-04	3.5966E-04	\$ 25
	3.7665E-04	0.0000E+00	4.3074E-04	0.000E+00	1.768E+01	\$ 30
	2.373E+00	3.185E-01	4.275E-02	5.738E-03	7.702E-04	\$ 35
	1.034E-04	1.387E-05	0.000E+00	1.768E+01	2.373E+00	\$ 40
	3.185E-01	4.275E-02	5.738E-03	7.702E-04	1.034E-04	\$ 45
	1.387E-05	0.000E+00	1.768E+01	2.373E+00	3.185E-01	\$ 50
	4.275E-02	5.738E-03	7.702E-04	1.034E-04	1.387E-05	\$ 55
	0.000E+00	1.768E+01	2.373E+00	3.185E-01	4.275E-02	\$ 60
	5.738E-03	7.702E-04	1.034E-04	1.387E-05	0.000E+00	\$ 65
	1.768E+01	2.373E+00	3.185E-01	4.275E-02	5.738E-03	\$ 70
	7.702E-04	1.034E-04	1.387E-05	0.0000E+00	0.0000E+00	\$ 75
	0.0000E+00	0.0000E+00	0.0000E+00	0.0000E+00	8.7908E-04	\$ 80
	4.2448E-04	1.4178E-04	6.0136E-05	1.9999E-05	7.7718E-06	\$ 85
	3.0539E-06	4.1586E-04	2.1060E-04	7.2196E-05	3.1791E-05	\$ 90
	1.4967E-05	5.7045E-06	2.0533E-06	8.5410E-04	1.0477E-04	\$ 95
	3.6979E-05	1.4614E-05	6.8236E-06	3.4880E-06	1.3863E-06	\$ 100
	2.2070E-04	1.5810E-04	1.8452E-05	7.2631E-06	3.0422E-06	\$ 105

1.6578E-06	7.7937E-07	0.0000E+00	9.6530E-05	2.6767E-05	\$ 110	
3.9607E-06	1.2628E-06	7.1596E-07	4.2074E-07	0.0000E+00	\$ 115	
0.0000E+00	4.8543E-05	5.9488E-06	7.0618E-07	2.6665E-07	\$ 120	
2.1437E-07	0.0000E+00	0.0000E+00	8.4709E-04	5.5726E-05	\$ 125	
1.4097E-06	1.6098E-07	1.0924E-07	0.0000E+00	0.0000E+00	\$ 130	
0.0000E+00	0.0000E+00	2.9685E-06	1.0557E-06	9.4109E-08	\$ 135	
3.6977E-03	4.1264E-03	2.4367E-03	5.8823E-03	2.4534E-03	\$ 140	
7.7501E-03	0.0000E+00	0.0000E+00	0.0000E+00	0.0000E+00	\$ 145	
5.9848E-03	2.3337E-02	2.8905E-02	2.7552E-02	2.6046E-02	\$ 150	
0.0000E+00	0.0000E+00	0.0000E+00	0.0000E+00	0.0000E+00	\$ 155	
1.5288E-03	6.2525E-04	2.1523E-04	8.3590E-05	2.9948E-05	\$ 160	
1.1740E-05	2.9982E-06	1.9506E-03	1.0136E-03	3.3529E-04	\$ 165	
1.3755E-04	5.6310E-05	2.3435E-05	6.4476E-06	1.1307E-02	\$ 170	
7.1278E-03	2.4588E-03	9.7339E-04	3.7292E-04	1.3072E-04	\$ 175	
4.7174E-05	0.0000E+00	0.0000E+00	0.0000E+00	0.0000E+00	\$ 180	
0.0000E+00	0.0000E+00	2.2421E-05	0.0000E+00	0.0000E+00	\$ 185	
0.0000E+00	0.0000E+00	0.0000E+00	0.0000E+00	0.0000E+00	\$ 190	
1.2151E-04	2.6408E-05	2.7204E-05	2.1617E-05	1.1135E-05	\$ 195	
6.1246E-06	9.3331E-06	4.0664E-07	2.4863E-07	1.7994E-07	\$ 200	
1.4402E-07	1.1796E-07	1.0253E-07	8.6856E-08	7.4657E-08	\$ 205	
5.5402E-08	0.0000E+00	5.7944E-04	0.0000E+00	4.4819E-04	\$ 210	
0.0000E+00	2.9497E-04	0.0000E+00	2.0075E-04	0.0000E+00	\$ 215	
1.6222E-04	1.8774E-03	1.2000E-04	5.2505E-03	7.5037E-05	\$ 220	
2.5798E-03	2.3188E-04	1.8661E-03	1.3990E-04	6.7812E-04	\$ 225	
7.9228E-05	4.7292E-04	6.1535E-05	1.6582E-04	4.0201E-05	\$ 230	
5.0906E-05	2.5624E-05	1.3159E-05	1.2968E-05	0.0000E+00	\$ 235	
0.0000E+00	0.0000E+00	0.0000E+00	0.0000E+00	0.0000E+00	\$ 240	
0.0000E+00	0.0000E+00	0.0000E+00	0.0000E+00	0.0000E+00	\$ 245	
0.0000E+00	0.0000E+00	0.0000E+00	2.3812E-03	2.8602E-04	\$ 250	
1.5515E-03	1.8521E-04	6.1850E-04	1.0422E-04	2.6717E-04	\$ 255	
6.2116E-05	1.8145E-04	3.9872E-05	4.8921E-05	1.9986E-05	\$ 260	
1.1703E-05	1.4510E-05	1.3112E-02	1.3594E-02	0.0000E+00	\$ 265	
0.0000E+00	0.0000E+00	0.0000E+00	0.0000E+00	1.8960E-02	\$ 270	
0.0000E+00	0.0000E+00	0.0000E+00	1.3594E-02	1.3594E-02	\$ 275	
1.3594E-02	1.3594E-02	1.3594E-02	1.3594E-02	1.3594E-02	\$ 280	
1.3594E-02	7.5912E-03	0.0000E+00	0.0000E+00	1.3594E-02	\$ 285	
1.3594E-02	0.0000E+00	-1.0000E+00			\$ 288	
wnw5:p	3.2655E-02	3.2655E-02	5.0000E-01	5.0000E-01	9.0384E-02	\$ 5
	9.0384E-02	9.0384E-02	9.0384E-02	3.4834E-01	2.8755E-04	\$ 10
	0.0000E+00	0.0000E+00	5.2837E-06	3.0719E-08	2.0335E-06	\$ 15
	7.6657E-02	9.6567E-02	0.0000E+00	0.0000E+00	0.0000E+00	\$ 20
	0.0000E+00	0.0000E+00	0.0000E+00	1.3248E-04	3.5966E-04	\$ 25
	3.7665E-04	0.0000E+00	4.3074E-04	0.000E+00	0.000E+00	\$ 30
	0.000E+00	1.306E+00	2.806E-01	6.028E-02	1.295E-02	\$ 35
	2.782E-03	5.977E-04	0.000E+00	0.000E+00	0.000E+00	\$ 40
	1.306E+00	2.806E-01	6.028E-02	1.295E-02	2.782E-03	\$ 45
	5.977E-04	0.000E+00	0.000E+00	0.000E+00	1.306E+00	\$ 50
	2.806E-01	6.028E-02	1.295E-02	2.782E-03	5.977E-04	\$ 55
	0.000E+00	0.000E+00	0.000E+00	1.306E+00	2.806E-01	\$ 60
	6.028E-02	1.295E-02	2.782E-03	5.977E-04	0.000E+00	\$ 65
	0.000E+00	0.000E+00	1.306E+00	2.806E-01	6.028E-02	\$ 70
	1.295E-02	2.782E-03	5.977E-04	0.0000E+00	0.0000E+00	\$ 75
	0.0000E+00	0.0000E+00	0.0000E+00	0.0000E+00	8.7908E-04	\$ 80
	4.2448E-04	1.4178E-04	6.0136E-05	1.9999E-05	7.7718E-06	\$ 85
	3.0539E-06	4.1586E-04	2.1060E-04	7.2196E-05	3.1791E-05	\$ 90
	1.4967E-05	5.7045E-06	2.0533E-06	8.5410E-04	1.0477E-04	\$ 95
	3.6979E-05	1.4614E-05	6.8236E-06	3.4880E-06	1.3863E-06	\$ 100
	2.2070E-04	1.5810E-04	1.8452E-05	7.2631E-06	3.0422E-06	\$ 105
	1.6578E-06	7.7937E-07	0.0000E+00	9.6530E-05	2.6767E-05	\$ 110
	3.9607E-06	1.2628E-06	7.1596E-07	4.2074E-07	0.0000E+00	\$ 115
	0.0000E+00	4.8543E-05	5.9488E-06	7.0618E-07	2.6665E-07	\$ 120
	2.1437E-07	0.0000E+00	0.0000E+00	8.4709E-04	5.5726E-05	\$ 125
	1.4097E-06	1.6098E-07	1.0924E-07	0.0000E+00	0.0000E+00	\$ 130

0.0000E+00	0.0000E+00	2.9685E-06	1.0557E-06	9.4109E-08	\$ 135
3.6977E-03	4.1264E-03	2.4367E-03	5.8823E-03	2.4534E-03	\$ 140
7.7501E-03	0.0000E+00	0.0000E+00	0.0000E+00	0.0000E+00	\$ 145
5.9848E-03	2.3337E-02	2.8905E-02	2.7552E-02	2.6046E-02	\$ 150
0.0000E+00	0.0000E+00	0.0000E+00	0.0000E+00	0.0000E+00	\$ 155
1.5288E-03	6.2525E-04	2.1523E-04	8.3590E-05	2.9948E-05	\$ 160
1.1740E-05	2.9982E-06	1.9506E-03	1.0136E-03	3.3529E-04	\$ 165
1.3755E-04	5.6310E-05	2.3435E-05	6.4476E-06	1.1307E-02	\$ 170
7.1278E-03	2.4588E-03	9.7339E-04	3.7292E-04	1.3072E-04	\$ 175
4.7174E-05	0.0000E+00	0.0000E+00	0.0000E+00	0.0000E+00	\$ 180
0.0000E+00	0.0000E+00	2.2421E-05	0.0000E+00	0.0000E+00	\$ 185
0.0000E+00	0.0000E+00	0.0000E+00	0.0000E+00	0.0000E+00	\$ 190
1.2151E-04	2.6408E-05	2.7204E-05	2.1617E-05	1.1135E-05	\$ 195
6.1246E-06	9.3331E-06	4.0664E-07	2.4863E-07	1.7994E-07	\$ 200
1.4402E-07	1.1796E-07	1.0253E-07	8.6856E-08	7.4657E-08	\$ 205
5.5402E-08	0.0000E+00	5.7944E-04	0.0000E+00	4.4819E-04	\$ 210
0.0000E+00	2.9497E-04	0.0000E+00	2.0075E-04	0.0000E+00	\$ 215
1.6222E-04	1.8774E-03	1.2000E-04	5.2505E-03	7.5037E-05	\$ 220
2.5798E-03	2.3188E-04	1.8661E-03	1.3990E-04	6.7812E-04	\$ 225
7.9228E-05	4.7292E-04	6.1535E-05	1.6582E-04	4.0201E-05	\$ 230
5.0906E-05	2.5624E-05	1.3159E-05	1.2968E-05	0.0000E+00	\$ 235
0.0000E+00	0.0000E+00	0.0000E+00	0.0000E+00	0.0000E+00	\$ 240
0.0000E+00	0.0000E+00	0.0000E+00	0.0000E+00	0.0000E+00	\$ 245
0.0000E+00	0.0000E+00	0.0000E+00	2.3812E-03	2.8602E-04	\$ 250
1.5515E-03	1.8521E-04	6.1850E-04	1.0422E-04	2.6717E-04	\$ 255
6.2116E-05	1.8145E-04	3.9872E-05	4.8921E-05	1.9986E-05	\$ 260
1.1703E-05	1.4510E-05	1.3112E-02	1.3594E-02	0.0000E+00	\$ 265
0.0000E+00	0.0000E+00	0.0000E+00	0.0000E+00	1.8960E-02	\$ 270
0.0000E+00	0.0000E+00	0.0000E+00	1.3594E-02	1.3594E-02	\$ 275
1.3594E-02	1.3594E-02	1.3594E-02	1.3594E-02	1.3594E-02	\$ 280
1.3594E-02	7.5912E-03	0.0000E+00	0.0000E+00	1.3594E-02	\$ 285
1.3594E-02	0.0000E+00	-1.0000E+00			\$ 288
3.2655E-02	3.2655E-02	5.0000E-01	5.0000E-01	9.0384E-02	\$ 5
9.0384E-02	9.0384E-02	9.0384E-02	3.4834E-01	2.8755E-04	\$ 10
0.0000E+00	0.0000E+00	5.2837E-06	3.0719E-08	2.0335E-06	\$ 15
7.6657E-02	9.6567E-02	0.0000E+00	0.0000E+00	0.0000E+00	\$ 20
0.0000E+00	0.0000E+00	0.0000E+00	1.3248E-04	3.5966E-04	\$ 25
3.7665E-04	0.0000E+00	4.3074E-04	0.0000E+00	0.0000E+00	\$ 30
0.0000E+00	3.686E+00	1.119E+00	3.398E-01	1.031E-01	\$ 35
3.132E-02	9.507E-03	0.000E+00	0.000E+00	0.000E+00	\$ 40
3.686E+00	1.119E+00	3.398E-01	1.031E-01	3.132E-02	\$ 45
9.507E-03	0.000E+00	0.000E+00	0.000E+00	3.686E+00	\$ 50
1.119E+00	3.398E-01	1.031E-01	3.132E-02	9.507E-03	\$ 55
0.000E+00	0.000E+00	0.000E+00	3.686E+00	1.119E+00	\$ 60
3.398E-01	1.031E-01	3.132E-02	9.507E-03	0.000E+00	\$ 65
0.000E+00	0.000E+00	3.686E+00	1.119E+00	3.398E-01	\$ 70
1.031E-01	3.132E-02	9.507E-03	0.0000E+00	0.0000E+00	\$ 75
0.0000E+00	0.0000E+00	0.0000E+00	0.0000E+00	8.7908E-04	\$ 80
4.2448E-04	1.4178E-04	6.0136E-05	1.9999E-05	7.7718E-06	\$ 85
3.0539E-06	4.1586E-04	2.1060E-04	7.2196E-05	3.1791E-05	\$ 90
1.4967E-05	5.7045E-06	2.0533E-06	8.5410E-04	1.0477E-04	\$ 95
3.6979E-05	1.4614E-05	6.8236E-06	3.4880E-06	1.3863E-06	\$ 100
2.2070E-04	1.5810E-04	1.8452E-05	7.2631E-06	3.0422E-06	\$ 105
1.6578E-06	7.7937E-07	0.0000E+00	9.6530E-05	2.6767E-05	\$ 110
3.9607E-06	1.2628E-06	7.1596E-07	4.2074E-07	0.0000E+00	\$ 115
0.0000E+00	4.8543E-05	5.9488E-06	7.0618E-07	2.6665E-07	\$ 120
2.1437E-07	0.0000E+00	0.0000E+00	8.4709E-04	5.5726E-05	\$ 125
1.4097E-06	1.6098E-07	1.0924E-07	0.0000E+00	0.0000E+00	\$ 130
0.0000E+00	0.0000E+00	2.9685E-06	1.0557E-06	9.4109E-08	\$ 135
3.6977E-03	4.1264E-03	2.4367E-03	5.8823E-03	2.4534E-03	\$ 140
7.7501E-03	0.0000E+00	0.0000E+00	0.0000E+00	0.0000E+00	\$ 145
5.9848E-03	2.3337E-02	2.8905E-02	2.7552E-02	2.6046E-02	\$ 150
0.0000E+00	0.0000E+00	0.0000E+00	0.0000E+00	0.0000E+00	\$ 155

wnn6:p

1.5288E-03	6.2525E-04	2.1523E-04	8.3590E-05	2.9948E-05	\$ 160	
1.1740E-05	2.9982E-06	1.9506E-03	1.0136E-03	3.3529E-04	\$ 165	
1.3755E-04	5.6310E-05	2.3435E-05	6.4476E-06	1.1307E-02	\$ 170	
7.1278E-03	2.4588E-03	9.7339E-04	3.7292E-04	1.3072E-04	\$ 175	
4.7174E-05	0.0000E+00	0.0000E+00	0.0000E+00	0.0000E+00	\$ 180	
0.0000E+00	0.0000E+00	2.2421E-05	0.0000E+00	0.0000E+00	\$ 185	
0.0000E+00	0.0000E+00	0.0000E+00	0.0000E+00	0.0000E+00	\$ 190	
1.2151E-04	2.6408E-05	2.7204E-05	2.1617E-05	1.1135E-05	\$ 195	
6.1246E-06	9.3331E-06	4.0664E-07	2.4863E-07	1.7994E-07	\$ 200	
1.4402E-07	1.1796E-07	1.0253E-07	8.6856E-08	7.4657E-08	\$ 205	
5.5402E-08	0.0000E+00	5.7944E-04	0.0000E+00	4.4819E-04	\$ 210	
0.0000E+00	2.9497E-04	0.0000E+00	2.0075E-04	0.0000E+00	\$ 215	
1.6222E-04	1.8774E-03	1.2000E-04	5.2505E-03	7.5037E-05	\$ 220	
2.5798E-03	2.3188E-04	1.8661E-03	1.3990E-04	6.7812E-04	\$ 225	
7.9228E-05	4.7292E-04	6.1535E-05	1.6582E-04	4.0201E-05	\$ 230	
5.0906E-05	2.5624E-05	1.3159E-05	1.2968E-05	0.0000E+00	\$ 235	
0.0000E+00	0.0000E+00	0.0000E+00	0.0000E+00	0.0000E+00	\$ 240	
0.0000E+00	0.0000E+00	0.0000E+00	0.0000E+00	0.0000E+00	\$ 245	
0.0000E+00	0.0000E+00	0.0000E+00	2.3812E-03	2.8602E-04	\$ 250	
1.5515E-03	1.8521E-04	6.1850E-04	1.0422E-04	2.6717E-04	\$ 255	
6.2116E-05	1.8145E-04	3.9872E-05	4.8921E-05	1.9986E-05	\$ 260	
1.1703E-05	1.4510E-05	1.3112E-02	1.3594E-02	0.0000E+00	\$ 265	
0.0000E+00	0.0000E+00	0.0000E+00	0.0000E+00	1.8960E-02	\$ 270	
0.0000E+00	0.0000E+00	0.0000E+00	1.3594E-02	1.3594E-02	\$ 275	
1.3594E-02	1.3594E-02	1.3594E-02	1.3594E-02	1.3594E-02	\$ 280	
1.3594E-02	7.5912E-03	0.0000E+00	0.0000E+00	1.3594E-02	\$ 285	
1.3594E-02	0.0000E+00	-1.0000E+00			\$ 288	
wnn7:p	3.2655E-02	3.2655E-02	5.0000E-01	5.0000E-01	9.0384E-02	\$ 5
	9.0384E-02	9.0384E-02	9.0384E-02	3.4834E-01	2.8755E-04	\$ 10
	0.0000E+00	0.0000E+00	5.2837E-06	3.0719E-08	2.0335E-06	\$ 15
	7.6657E-02	9.6567E-02	0.0000E+00	0.0000E+00	0.0000E+00	\$ 20
	0.0000E+00	0.0000E+00	0.0000E+00	1.3248E-04	3.5966E-04	\$ 25
	3.7665E-04	0.0000E+00	4.3074E-04	0.0000E+00	0.0000E+00	\$ 30
	0.0000E+00	3.618E+00	4.020E+00	1.680E+00	7.022E-01	\$ 35
	2.935E-01	1.227E-01	0.000E+00	0.000E+00	0.000E+00	\$ 40
	3.618E+00	4.020E+00	1.680E+00	7.022E-01	2.935E-01	\$ 45
	1.227E-01	0.000E+00	0.000E+00	0.000E+00	3.618E+00	\$ 50
	4.020E+00	1.680E+00	7.022E-01	2.935E-01	1.227E-01	\$ 55
	0.000E+00	0.000E+00	0.000E+00	3.618E+00	4.020E+00	\$ 60
	1.680E+00	7.022E-01	2.935E-01	1.227E-01	0.000E+00	\$ 65
	0.000E+00	0.000E+00	3.618E+00	4.020E+00	1.680E+00	\$ 70
	7.022E-01	2.935E-01	1.227E-01	0.0000E+00	0.0000E+00	\$ 75
	0.0000E+00	0.0000E+00	0.0000E+00	0.0000E+00	8.7908E-04	\$ 80
	4.2448E-04	1.4178E-04	6.0136E-05	1.9999E-05	7.7718E-06	\$ 85
	3.0539E-06	4.1586E-04	2.1060E-04	7.2196E-05	3.1791E-05	\$ 90
	1.4967E-05	5.7045E-06	2.0533E-06	8.5410E-04	1.0477E-04	\$ 95
	3.6979E-05	1.4614E-05	6.8236E-06	3.4880E-06	1.3863E-06	\$ 100
	2.2070E-04	1.5810E-04	1.8452E-05	7.2631E-06	3.0422E-06	\$ 105
	1.6578E-06	7.7937E-07	0.0000E+00	9.6530E-05	2.6767E-05	\$ 110
	3.9607E-06	1.2628E-06	7.1596E-07	4.2074E-07	0.0000E+00	\$ 115
	0.0000E+00	4.8543E-05	5.9488E-06	7.0618E-07	2.6665E-07	\$ 120
	2.1437E-07	0.0000E+00	0.0000E+00	8.4709E-04	5.5726E-05	\$ 125
	1.4097E-06	1.6098E-07	1.0924E-07	0.0000E+00	0.0000E+00	\$ 130
	0.0000E+00	0.0000E+00	2.9685E-06	1.0557E-06	9.4109E-08	\$ 135
	3.6977E-03	4.1264E-03	2.4367E-03	5.8823E-03	2.4534E-03	\$ 140
	7.7501E-03	0.0000E+00	0.0000E+00	0.0000E+00	0.0000E+00	\$ 145
	5.9848E-03	2.3337E-02	2.8905E-02	2.7552E-02	2.6046E-02	\$ 150
	0.0000E+00	0.0000E+00	0.0000E+00	0.0000E+00	0.0000E+00	\$ 155
	1.5288E-03	6.2525E-04	2.1523E-04	8.3590E-05	2.9948E-05	\$ 160
	1.1740E-05	2.9982E-06	1.9506E-03	1.0136E-03	3.3529E-04	\$ 165
	1.3755E-04	5.6310E-05	2.3435E-05	6.4476E-06	1.1307E-02	\$ 170
	7.1278E-03	2.4588E-03	9.7339E-04	3.7292E-04	1.3072E-04	\$ 175
	4.7174E-05	0.0000E+00	0.0000E+00	0.0000E+00	0.0000E+00	\$ 180

wnn8:p

0.0000E+00	0.0000E+00	2.2421E-05	0.0000E+00	0.0000E+00	\$ 185
0.0000E+00	0.0000E+00	0.0000E+00	0.0000E+00	0.0000E+00	\$ 190
1.2151E-04	2.6408E-05	2.7204E-05	2.1617E-05	1.1135E-05	\$ 195
6.1246E-06	9.3331E-06	4.0664E-07	2.4863E-07	1.7994E-07	\$ 200
1.4402E-07	1.1796E-07	1.0253E-07	8.6856E-08	7.4657E-08	\$ 205
5.5402E-08	0.0000E+00	5.7944E-04	0.0000E+00	4.4819E-04	\$ 210
0.0000E+00	2.9497E-04	0.0000E+00	2.0075E-04	0.0000E+00	\$ 215
1.6222E-04	1.8774E-03	1.2000E-04	5.2505E-03	7.5037E-05	\$ 220
2.5798E-03	2.3188E-04	1.8661E-03	1.3990E-04	6.7812E-04	\$ 225
7.9228E-05	4.7292E-04	6.1535E-05	1.6582E-04	4.0201E-05	\$ 230
5.0906E-05	2.5624E-05	1.3159E-05	1.2968E-05	0.0000E+00	\$ 235
0.0000E+00	0.0000E+00	0.0000E+00	0.0000E+00	0.0000E+00	\$ 240
0.0000E+00	0.0000E+00	0.0000E+00	0.0000E+00	0.0000E+00	\$ 245
0.0000E+00	0.0000E+00	0.0000E+00	0.0000E+00	2.3812E-03	\$ 250
1.5515E-03	1.8521E-04	6.1850E-04	1.0422E-04	2.6717E-04	\$ 255
6.2116E-05	1.8145E-04	3.9872E-05	4.8921E-05	1.9986E-05	\$ 260
1.1703E-05	1.4510E-05	1.3112E-02	1.3594E-02	0.0000E+00	\$ 265
0.0000E+00	0.0000E+00	0.0000E+00	0.0000E+00	1.8960E-02	\$ 270
0.0000E+00	0.0000E+00	0.0000E+00	0.0000E+00	1.3594E-02	\$ 275
1.3594E-02	1.3594E-02	1.3594E-02	1.3594E-02	1.3594E-02	\$ 280
1.3594E-02	7.5912E-03	0.0000E+00	0.0000E+00	1.3594E-02	\$ 285
1.3594E-02	0.0000E+00	-1.0000E+00			\$ 288
3.2655E-02	3.2655E-02	5.0000E-01	5.0000E-01	9.0384E-02	\$ 5
9.0384E-02	9.0384E-02	9.0384E-02	3.4834E-01	2.8755E-04	\$ 10
0.0000E+00	0.0000E+00	5.2837E-06	3.0719E-08	2.0335E-06	\$ 15
7.6657E-02	9.6567E-02	0.0000E+00	0.0000E+00	0.0000E+00	\$ 20
0.0000E+00	0.0000E+00	0.0000E+00	1.3248E-04	3.5966E-04	\$ 25
3.7665E-04	0.0000E+00	4.3074E-04	0.000E+00	0.000E+00	\$ 30
0.000E+00	0.000E+00	0.000E+00	0.000E+00	0.000E+00	\$ 35
0.000E+00	0.000E+00	0.000E+00	0.000E+00	0.000E+00	\$ 40
0.000E+00	0.000E+00	0.000E+00	0.000E+00	0.000E+00	\$ 45
0.000E+00	0.000E+00	0.000E+00	0.000E+00	0.000E+00	\$ 50
0.000E+00	0.000E+00	0.000E+00	0.000E+00	0.000E+00	\$ 55
0.000E+00	0.000E+00	0.000E+00	0.000E+00	0.000E+00	\$ 60
0.000E+00	0.000E+00	0.000E+00	0.000E+00	0.000E+00	\$ 65
0.000E+00	0.000E+00	0.000E+00	0.000E+00	0.000E+00	\$ 70
0.000E+00	0.000E+00	0.000E+00	0.0000E+00	0.0000E+00	\$ 75
0.0000E+00	0.0000E+00	0.0000E+00	0.0000E+00	8.7908E-04	\$ 80
4.2448E-04	1.4178E-04	6.0136E-05	1.9999E-05	7.7718E-06	\$ 85
3.0539E-06	4.1586E-04	2.1060E-04	7.2196E-05	3.1791E-05	\$ 90
1.4967E-05	5.7045E-06	2.0533E-06	8.5410E-04	1.0477E-04	\$ 95
3.6979E-05	1.4614E-05	6.8236E-06	3.4880E-06	1.3863E-06	\$ 100
2.2070E-04	1.5810E-04	1.8452E-05	7.2631E-06	3.0422E-06	\$ 105
1.6578E-06	7.7937E-07	0.0000E+00	9.6530E-05	2.6767E-05	\$ 110
3.9607E-06	1.2628E-06	7.1596E-07	4.2074E-07	0.0000E+00	\$ 115
0.0000E+00	4.8543E-05	5.9488E-06	7.0618E-07	2.6665E-07	\$ 120
2.1437E-07	0.0000E+00	0.0000E+00	8.4709E-04	5.5726E-05	\$ 125
1.4097E-06	1.6098E-07	1.0924E-07	0.0000E+00	0.0000E+00	\$ 130
0.0000E+00	0.0000E+00	2.9685E-06	1.0557E-06	9.4109E-08	\$ 135
3.6977E-03	4.1264E-03	2.4367E-03	5.8823E-03	2.4534E-03	\$ 140
7.7501E-03	0.0000E+00	0.0000E+00	0.0000E+00	0.0000E+00	\$ 145
5.9848E-03	2.3337E-02	2.8905E-02	2.7552E-02	2.6046E-02	\$ 150
0.0000E+00	0.0000E+00	0.0000E+00	0.0000E+00	0.0000E+00	\$ 155
1.5288E-03	6.2525E-04	2.1523E-04	8.3590E-05	2.9948E-05	\$ 160
1.1740E-05	2.9982E-06	1.9506E-03	1.0136E-03	3.3529E-04	\$ 165
1.3755E-04	5.6310E-05	2.3435E-05	6.4476E-06	1.1307E-02	\$ 170
7.1278E-03	2.4588E-03	9.7339E-04	3.7292E-04	1.3072E-04	\$ 175
4.7174E-05	0.0000E+00	0.0000E+00	0.0000E+00	0.0000E+00	\$ 180
0.0000E+00	0.0000E+00	2.2421E-05	0.0000E+00	0.0000E+00	\$ 185
0.0000E+00	0.0000E+00	0.0000E+00	0.0000E+00	0.0000E+00	\$ 190
1.2151E-04	2.6408E-05	2.7204E-05	2.1617E-05	1.1135E-05	\$ 195
6.1246E-06	9.3331E-06	4.0664E-07	2.4863E-07	1.7994E-07	\$ 200
1.4402E-07	1.1796E-07	1.0253E-07	8.6856E-08	7.4657E-08	\$ 205

	5.5402E-08	0.0000E+00	5.7944E-04	0.0000E+00	4.4819E-04	\$ 210
	0.0000E+00	2.9497E-04	0.0000E+00	2.0075E-04	0.0000E+00	\$ 215
	1.6222E-04	1.8774E-03	1.2000E-04	5.2505E-03	7.5037E-05	\$ 220
	2.5798E-03	2.3188E-04	1.8661E-03	1.3990E-04	6.7812E-04	\$ 225
	7.9228E-05	4.7292E-04	6.1535E-05	1.6582E-04	4.0201E-05	\$ 230
	5.0906E-05	2.5624E-05	1.3159E-05	1.2968E-05	0.0000E+00	\$ 235
	0.0000E+00	0.0000E+00	0.0000E+00	0.0000E+00	0.0000E+00	\$ 240
	0.0000E+00	0.0000E+00	0.0000E+00	0.0000E+00	0.0000E+00	\$ 245
	0.0000E+00	0.0000E+00	0.0000E+00	2.3812E-03	2.8602E-04	\$ 250
	1.5515E-03	1.8521E-04	6.1850E-04	1.0422E-04	2.6717E-04	\$ 255
	6.2116E-05	1.8145E-04	3.9872E-05	4.8921E-05	1.9986E-05	\$ 260
	1.1703E-05	1.4510E-05	1.3112E-02	1.3594E-02	0.0000E+00	\$ 265
	0.0000E+00	0.0000E+00	0.0000E+00	0.0000E+00	1.8960E-02	\$ 270
	0.0000E+00	0.0000E+00	0.0000E+00	1.3594E-02	1.3594E-02	\$ 275
	1.3594E-02	1.3594E-02	1.3594E-02	1.3594E-02	1.3594E-02	\$ 280
	1.3594E-02	7.5912E-03	0.0000E+00	0.0000E+00	1.3594E-02	\$ 285
	1.3594E-02	0.0000E+00	-1.0000E+00			\$ 288
c	***transformations used to create SD #2 through SD # 8 from SD #1***					
tr1	0.0	65.02	0.0			
tr2	0.0	118.62	0.0			
tr3	0.0	172.21	0.0			
tr4	0.0	225.81	0.0			
tr5	0.0	279.40	0.0			
tr6	0.0	333.50	0.0			
tr7	0.0	385.32	0.0			
c	Materials					
c	*****					
c	*****					
c	**Bottom Nozzle Region**					
m1	13027.50	1.187E-05	\$	Al		
	22000.50	8.942E-06	\$	Ti		
	24000.50	1.436E-03	\$	Cr		
	26000.55	4.534E-03	\$	Fe		
	28000.50	1.008E-03	\$	Ni		
	40000.56	3.517E-05	\$	Zr		
	42000.50	1.672E-05	\$	Mo		
c	*****Dry Radial Dencities, atoms/(barn*cm)*****					
c	**In-Core Region*****					
m2	8016.50	8.495E-03	\$	O		
	40000.56	1.345E-03	\$	Zr		
	50000.35c	1.345E-03	\$	Sn		
	92235.50	1.627E-04	\$	U-235		
	92238.35c	4.066E-03	\$	U-238		
c	**Plenum Region***					
m3	24000.50	2.864E-06	\$	Cr		
	26000.55	1.007E-05	\$	Fe		
	28000.50	1.235E-06	\$	Ni		
	40000.56	1.643E-03	\$	Zr		
	50000.35c	1.643E-03	\$	Sn		
c	**Top Nozzle Region***					
m4	13027.50	2.210E-05	\$	Al		
	22000.50	1.664E-05	\$	Ti		
	24000.50	2.161E-03	\$	Cr		
	26000.55	6.641E-03	\$	Fe		
	28000.50	1.656E-03	\$	Ni		
	40000.56	6.547E-05	\$	Zr		
	42000.50	3.112E-05	\$	Mo		
m5	7014.50	0.790018501	\$	N		
	8016.50	0.209981499	\$	O	Air	
m6	26000.55	-1.0	\$	Fe	We call it Carbon Steel	
m7	24000.50	1.743e-2	\$	Cr		
	26000.55	6.128e-2	\$	Fe		
	28000.50	7.511e-3	\$	Ni	We call it SS304	

```

c      8. "base" concrete
m8    1001.50 7.770e-3      $ H
      8016.50 4.386e-2      $ O
      11023.51 1.048e-3     $ Na
      12000.50 1.487e-4     $ Mg
      13027.50 2.389e-3     $ Al
      14000.51 1.531e-2     $ Si
      19000.51 6.933e-4     $ K
      20000.51 2.916e-3     $ Ca
      26000.55 3.128e-4     $ Fe                $ "Base" Concrete

c
c      9. Soil
m9    1001.50 0.977      8016.50 3.48      13027.50 0.488
      14000.51 1.16

c      10. Aluminum
m10   13027.50 -1.00      $ Al                Aluminum
c      11. "roof" concrete
m11   1001.50 7.261e-3    $ H
      8016.50 4.099e-2    $ O
      11023.51 9.794e-4    $ Na
      12000.50 1.390e-4    $ Mg
      13027.50 2.233e-3    $ Al
      14000.51 1.431e-2    $ Si
      19000.51 6.479e-4    $ K
      20000.51 2.725e-3    $ Ca
      26000.55 5.847e-3    $ Fe                $ "Roof" Concrete

c
c      *****
cut:p j j 0 0 j
c      nps 147456000 ? 22528000
ctme 166000

```

M.5.5.5 Sample ANISN Model (HSM -1.2 kW - 3.3 wt%/45,000MWd/MTU 6-yr cooled)

PWR HSM Roof 3.3 wt%/45,000MWd/MTU 6-yr cooled(Outer)

' Fuel qualification

15\$\$

'	ID	ITH	ISCT	ISN	IGE
	32	0	3	8	2
'	IBL	IBR	IZM	IM	IEVT
	1	0	8	149	0
'	IGM	IHT	IHS	IHM	MS
	40	3	4	43	76
'	MCR	MTP	MT	IDFM	IPVT
	48	0	80	0	0
'	IQM	IPM	IPP	IIM	ID1
	1	0	0	40	0
'	ID2	ID3	ID4	ICM	IDAT1
	0	3	1	50	0
'	IDAT2	IFG	IFLU	IFN	IPRT
	0	0	0	1	1
'	IXTR				
	0				

16**

'	EV	EVM	EPS	BF	DY
	0.0	0.0	0.0001	1.420892	361.42
'	DZ	DFM1	XNF	PV	RYF
	0.0	0.0	0.0	0.0	0.5000
'	XLAL	EQL	XNPM	T	

0.0002 F0.0

T

14*

Cross Sections not listed for brevity.

T

17** 19R0.0 9R3.391E-01 121R0.0
 19R0.0 9R2.883E+00 121R0.0
 19R0.0 9R7.931E+00 121R0.0
 19R0.0 9R3.953E+01 121R0.0
 19R0.0 9R1.001E+02 121R0.0
 19R0.0 9R1.324E+02 121R0.0
 19R0.0 9R3.324E+02 121R0.0
 19R0.0 9R2.721E+02 121R0.0
 19R0.0 9R6.650E+01 121R0.0
 19R0.0 9R3.434E+02 121R0.0
 19R0.0 9R6.120E+02 121R0.0
 19R0.0 9R5.426E+02 121R0.0
 19R0.0 9R2.500E+02 121R0.0
 19R0.0 9R1.077E-02 121R0.0
 19R0.0 9R0.000E+00 121R0.0

7Q149

19R0.0 9R1.556E+00 121R0.0
 19R0.0 9R7.329E+00 121R0.0
 19R0.0 9R3.736E+01 121R0.0
 19R0.0 9R9.310E+01 121R0.0
 19R0.0 9R3.950E+04 121R0.0
 19R0.0 9R3.148E+05 121R0.0
 19R0.0 9R7.873E+06 121R0.0
 19R0.0 9R4.263E+06 121R0.0
 19R0.0 9R3.564E+08 121R0.0
 19R0.0 9R1.287E+09 121R0.0
 19R0.0 9R1.660E+09 121R0.0
 19R0.0 9R1.371E+10 121R0.0
 19R0.0 9R3.694E+09 121R0.0
 19R0.0 9R3.162E+08 121R0.0
 19R0.0 9R4.661E+08 121R0.0
 19R0.0 9R1.629E+09 121R0.0
 19R0.0 9R2.071E+09 121R0.0
 19R0.0 9R1.038E+10 121R0.0

T

3** 19R0.0 9R1.0 121R0.0 39Q149

T

1** F0.0

4** 18I0.0 8I50.586 2I71.540 6I71.8575 4I82.0928
 7I83.1088 9I85.3313 7I1106.68 1I198.12 13I199.39
 300.0

5** F1.0

6** .00 .0604938 .0453704 .0453704 .0604938 .0604938 .0453704
 .0453704 .0604938 0.0 .0453704 .0462962 .0453704
 .0453704 .0462962 .0453704 0.0 .0453704 .0453704
 .0453704 .0453704 0.0 .0604938 .0604938

7** -.9759000 -.9511897 -.7867958 -.5773503 -.2182179 .2182179
 .5773503 .7867958 .9511897 -.8164965 -.7867958 -.5773503
 -.2182179 .2182179 .5773503 .7867958 -.6172134 -.5773503
 -.2182179 .2182179 .5773503 -.3086067 -.2182179 .2182179

8\$\$ 28R1 3R2 7R3 5R4 8R5 10R6 72R7 16R8

9\$\$ 49 53 57 77 53 57 65 57

'	MAT	1, 4	= H
'	MAT	5, 8	= C
'	MAT	9, 12	= O
'	MAT	13, 16	= AL
'	MAT	17, 20	= SI
'	MAT	21, 24	= CA
'	MAT	25, 28	= FE
'	MAT	29, 32	= ZR
'	MAT	33, 36	= PB
'	MAT	37, 40	= U235
'	MAT	41, 44	= U238
'	MAT	45, 48	= FX
'			
'	MIXTURE	49, 52	= FUEL-RADIAL
'	MIXTURE	53, 56	= STEEL
'	MIXTURE	57, 60	= AIR
'	MIXTURE	61, 64	= LEAD
'	MIXTURE	65, 68	= CONCRETE
'	MIXTURE	69, 72	= BOT NOZZLE
'	MIXTURE	73, 76	= TOP NOZZLE
'	MIXTURE	77, 80	= ALUMINUM

10\$\$

'	FUEL-RADIAL				
	49	50	51	52	
	49	50	51	52	
	49	50	51	52	
	49	50	51	52	
	49	50	51	52	
'	STEEL-				
	53	54	55	56	
'	AIR-				
	57	58	59	60	
'	LEAD-				
	61	62	63	64	
'	CONCRETE				
	65	66	67	68	
	65	66	67	68	
	65	66	67	68	
	65	66	67	68	
	65	66	67	68	
	65	66	67	68	
'	BOT-NOZZLE				
	69	70	71	72	
	69	70	71	72	
'	TOP-NOZZLE				
	73	74	75	76	
	73	74	75	76	
'	ALUMINUM				
	77	78	79	80	

11\$\$

'	FUEL-RADIAL				
	9	10	11	12	
	25	26	27	28	
	29	30	31	32	
	37	38	39	40	
	41	42	43	44	


```

' STEEL-
  25 26 27 28
' AIR-
  9 10 11 12
' LEAD-
  33 34 35 36
' CONCRETE
  1 2 3 4
  9 10 11 12
  13 14 15 16
  17 18 19 20
  21 22 23 24
  25 26 27 28
' BOT-NOZZLE
  25 26 27 28
  29 30 31 32
' TOP-NOZZLE
  25 26 27 28
  29 30 31 32
' ALUMINUM
  13 14 15 16
12**
' FUEL-RADIAL
  4R1.326E-2
  4R5.047E-3
  4R4.251E-3
  4R3.252E-4
  4R6.299E-3
' STEEL
  4R8.487E-2
' AIR
  4R5.28E-6
' LEAD
  4R3.296E-2
' CONCRETE
  4R7.770E-3
  4R4.386E-2
  4R2.389E-3
  4R1.581E-2
  4R2.916E-3
  4R3.128E-4
' BOT-NOZZLE
  4R9.781E-3
  4R7.029E-4
' TOP-NOZZLE
  4R4.031E-3
  4R8.469E-4

```

' ALUMINUM

4R6.026E-2

19\$\$

F3

22\$\$

F-45

23\$\$

7 8 9

T

T

M.5.6 References

- 5.1 Oak Ridge National Laboratory, RSIC Computer Code Collection, "SCALE: A Modular Code System for Performing Standardized Computer Analysis for Licensing Evaluations for Workstations and Personal Computers," NUREG/CR-0200, Revision 6, ORNL/NUREG/CSD-2/V2/R6.
- 5.2 "DORT-PC - Two-Dimensional Discrete Ordinates Transport Code System," CCC-532, Oak Ridge National Laboratory, RSIC Computer Code Collection, Version 2.10.1, October 1991.
- 5.3 CASK-81 - 22 Neutron, 18 Gamma-Ray Group, P3, Cross Sections for Shipping Cask Analysis," DLC-23, Oak Ridge National Laboratory, RSIC Data Library Collection, June 1987.
- 5.4 Ludwig, S.B., and J.P. Renier, "Standard- and Extended-Burnup PWR and BWR Reactor Models for the ORIGEN2 Computer Code," ORNL/TM-11018 Oak Ridge National Laboratory, December 1989.
- 5.5 "ANISN-ORNL - One-Dimensional Discrete Ordinates Transport Code System with Anisotropic Scattering", CCC-254, Oak Ridge National Laboratory, RSIC Computer Code Collection, April 1991.
- 5.6 NUHOMS[®] MP187 Multi-Purpose Cask Transportation Safety Analysis Report," Revision 10, NRC Docket Number 71-9255.
- 5.7 "Topical Report on Actinide-Only Burnup Credit for PWR Spent Nuclear Fuel Packages", Rev. 0, Office of Civilian Radioactive Waste Management, DOE/RW-0472 Rev. 0, May 1995.
- 5.8 "Addition of 61BT DSC to Standardized NUHOMS[®] System," Amendment No. 3, NUHOMS[®] CoC 1004, TAC No. L23137.
- 5.9 Jenal, J. P., P. J. Erickson, W. A. Rhoades, D. B. Simpson, and M. L. Williams, "The Generation of a Computer Library for Discrete Ordinates Quadrature Sets," ORNL/TM-6023, Oak Ridge National Laboratory, October 1977.
- 5.10 "American National Standard Neutron and Gamma-Ray Flux-to-Dose Rate Factors," ANSI/ANS-6.1.1-1977, American Nuclear Society, LaGrange Park, Illinois, March 1977.

**Table M.5-1
PWR Fuel Assembly Design Characteristics⁽³⁾**

Assembly Class	B&W 15x15	WE 17x17	CE 15x15	WE 15x15	CE 14x14	WE 14x14
DSC Configuration	Max Unirradiated Length (in)					
32PT-S100	165.75	165.75	165.75	165.75	165.75	165.75
32PT-L100	171.71 ⁽¹⁾	171.71 ⁽¹⁾	171.71	171.71	171.71	171.71
32PT-S125	165.75	165.75	165.75	165.75	165.75	165.75
32PT-L125	171.71 ⁽¹⁾	171.71 ⁽¹⁾	171.71	171.71	171.71	171.71
Fissile Material	UO ₂	UO ₂	UO ₂	UO ₂	UO ₂	UO ₂
Maximum MTU/assembly ⁽²⁾	0.475	0.475	0.475	0.475	0.475	0.475
Maximum Number of Fuel Rods	208	264	216	204	176	179
Maximum Number of Guide/ Instrument Tubes	17	25	9	21	5	17

⁽¹⁾ Maximum Assembly + BPRA Length (unirradiated)

⁽²⁾ The maximum MTU/assembly is based on the shielding analysis. The listed value is higher than the actual.

⁽³⁾ Maximum Co-59 content in the Top End Fitting Region is 15.6 grams per assembly.

Maximum Co-59 content in the Plenum Region is 5.0 grams per assembly.

Maximum Co-59 content in the In-Core Region is 24.7 grams per assembly.

Maximum Co-59 content in the Bottom Region is 12.8 grams per assembly.

**Table M.5-2
Burnable Poison Rod Assembly Weight Data**

Component Name: B&W 15 X 15 Burnable Absorber Assembly

Burnup: 2 cycle, 5-year cooled

Region	SS304 (Kgs)	Inconel-750 (Kgs)	Poison (Kgs)	Zr-4 (Kgs)
Top	3.602	0.058	0	0
Plenum	1.068	0	0.724	1.197
Core	2.468	0	9.146	11.98

Component Name: WE 17 X 17 Pyrex Burnable Absorber, 2 - 24 Rodlets (Worst Case)

Burnup: 2 cycle, 10-year cooled

Region	SS304 (Kgs)	Inconel-718 (Kgs)	Poison (Kgs)	Zr-4 (Kgs)
Top	2.62	0.42	0	0
Plenum	2.85	0	0	0
Core	11.9	0	5.08	0

Component Name: WE 17 X 17 WABA Burnable Absorber, 3 - 24 Rodlets (Worst Case)

Burnup: 2 cycle, 10-year cooled

Region	SS304 (Kgs)	Inconel-718 (Kgs)	Poison (Kgs)	Zr-4 (Kgs)
Top	2.95	0	0	0
Plenum	2.76	0	0	2.61
Core	0	0	2.5	14.8

**Table M.5-3
Dose Rates Due to the 32 PWR Fuel Assemblies with BPRAs**

Dose Rate Location	Configuration 2 32PT-S100/32PT-L100 DSC Design Configuration			Configuration 2 32PT-S125/32PT-L125 DSC Design Configurations		
	Gamma (mrem/hr)	Neutron (mrem/hr)	Total ⁽¹⁾ (mrem/hr)	Gamma (mrem/hr)	Neutron (mrem/hr)	Total ⁽¹⁾ (mrem/hr)
HSM Roof (centerline)	38.6	0.6	39.2	38.6	0.6	39.2
HSM Roof Birdscreen	1201	16.9	1218	1201	16.9	1218
HSM End Shield Wall Surface	5.4	0.2	5.6	5.4	0.2	5.6
HSM Door Exterior Surface (centerline)	158	36.3	185	77.5	28.1	99.3
HSM Front Birdscreen	780	7.3	788	745	6.8	752
HSM Back Shield Wall	1.45	0.05	1.50	1.37	0.05	1.41
Centerline Top DSC Cover Plate w/3"ns3+1" steel Dry Welding	123	18.7	142	36.7	15.0	51.7
Outer Edge Centerline Top DSC (Peak Annulus)	3834	132	3966	1458	111	1569
Cask Surface (Radial) Contact Normal Condition	784	261	950	784	259	947
3 ft from Cask Surface (Radial) Normal Condition	293	98.3	391	293	97.8	390
Cask Surface (Radial) Contact Accident Condition	1070	3780	4640	1070	3770	4630
Cask Top Axial Surface	94.8	32.6	107	37.7	27.5	48.7
Cask Bottom Axial Surface	758 ⁽²⁾	957 ⁽²⁾	1707 ⁽²⁾	193 ⁽³⁾	770 ⁽³⁾	960 ⁽³⁾

Notes:

- ⁽¹⁾ Gamma and Neutron peaks do not always occur at same location therefore the total is not always the sum of the gamma plus neutron.
- ⁽²⁾ The peak bottom surface dose rate is directly below the grapple ring cut out in the bottom of the cask. The bottom average dose rates, including the grapple area, are 170 mrem/hr gamma, 115 mrem/hr neutron for a total average dose rate of 285 mrem/hr.
- ⁽³⁾ The peak bottom surface dose rate is directly below the grapple ring cut out in the bottom of the cask. The bottom average dose rates, including the grapple area, are 48.7 mrem/hr gamma, 92.3 mrem/hr neutron for a total average dose rate of 141 mrem/hr.

**Table M.5-4
Summary of HSM Dose Rates**

Surface	Dose Rate Component	Configuration 2 32PT-S100/32PT-L100 DSC Configuration		Configuration 2 32PT-S125/32PT-L125 DSC Configurations	
		Maximum Dose Rate (mrem/hr)	Surface Average Dose Rate (mrem/hr)	Maximum Dose Rate (mrem/hr)	Surface Average Dose Rate (mrem/hr)
Rear ⁽¹⁾	Gamma	1.45	0.48	1.37	0.45
	Neutron	0.05	0.02	0.05	0.02
Front	Gamma	780	86.4	745	56.2
	Neutron	7.3	9.1	6.8	7.2
Roof	Gamma	1201	54.5	1201	54.2
	Neutron	16.9	0.75	16.9	0.75
Side ⁽¹⁾	Gamma	5.4	1.7	5.4	1.7
	Neutron	0.2	0.05	0.2	0.05

⁽¹⁾ Includes 24 inch shield wall.

**Table M.5-5
Summary of Onsite TC Dose Rates (Maximum⁽¹⁾)**

	Configuration 2 32PT-S100/32PT-L100 DSC Configuration			Configuration 2 32PT-S125/32PT-L125 DSC Configuration		
	Cask Surface			Cask Surface		
	Side (mrem/hr)	Top (mrem/hr)	Bottom ⁽²⁾ (mrem/hr)	Side (mrem/hr)	Top (mrem/hr)	Bottom ⁽³⁾ (mrem/hr)
Neutron	2.61E+02	3.26E+01	9.57E+02	2.59E+02	2.75E+01	7.70E+02
Gamma	7.84E+02	9.48E+01	7.58E+02	7.84E+02	3.77E+01	1.93E+02
Total	9.50E+02	1.07E+02	1.71E+03	9.47E+02	4.87E+01	9.60E+02
	1-Meter from Cask Surface			1-Meter from Cask Surface		
	Side (mrem/hr)	Top (mrem/hr)	Bottom ⁽²⁾ (mrem/hr)	Side (mrem/hr)	Top (mrem/hr)	Bottom ⁽³⁾ (mrem/hr)
	Neutron	9.83E+01	1.13E+01	8.95E+01	9.78E+01	9.58E+00
Gamma	2.93E+02	1.69E+01	1.85E+02	2.93E+02	6.63E+00	4.92E+01
Total	3.91E+02	2.52E+01	2.74E+02	3.90E+02	1.45E+01	1.21E+02
	2-Meters from Cask Surface			2-Meters from Cask Surface		
	Side (mrem/hr)	Top (mrem/hr)	Bottom ⁽²⁾ (mrem/hr)	Side (mrem/hr)	Top (mrem/hr)	Bottom ⁽³⁾ (mrem/hr)
	Neutron	5.26E+01	4.47E+00	2.83E+01	5.24E+01	3.80E+00
Gamma	1.73E+02	8.87E+00	8.07E+01	1.73E+02	3.28E+00	2.15E+01
Total	2.26E+02	1.31E+01	1.09E+02	2.25E+02	6.82E+00	4.40E+01

⁽¹⁾ Gamma and Neutron peaks do not always occur at same location therefore the total is not always the sum of the gamma plus neutron.

⁽²⁾ This bottom surface dose rate is directly below the grapple ring cut out in the cask bottom. The bottom surface average dose rates are 115 neutron, 170 gamma or 285 total. These average dose rates include the area below grapple ring cutout in the cask.

⁽³⁾ This bottom surface dose rate is directly below the grapple ring cut out in the cask bottom. The bottom surface average dose rates are 92.3 neutron, 48.7 gamma or 141 total. These average dose rates include the area below grapple ring cutout in the cask.

**Table M.5-6
PWR Fuel Assembly Materials Weights**

Item	Material	Average Weight (Kg/assembly)
In-Core Region		
Cladding	Zircaloy-4	108.16
Guide Tubes	Zircaloy-4	8.0
Instrument Tubes	Zircaloy-4	0.64
Spacers	Inconel-718	4.9
Grid Supports	Zircaloy-4	0.64
Plenum Region		
Cladding	Zircaloy	8.8
Springs	Stainless Steel	0.02
Spacer	Inconel-718	1.04
Top Region		
Top Nozzle	Stainless Steel	7.48
End Plugs & Nuts	Stainless Steel	0.57
Springs Retainer	Stainless Steel	0.91
Hold-Down Springs	Inconel-718	1.80
Bottom Region		
Bottom Spacer	Inconel-718	1.30
Lower Nuts	Stainless Steel	0.15
Bottom Nozzle	Stainless Steel	8.16

Table M.5-7
Elemental Composition of LWR Fuel-Assembly Structural Materials

Element Atomic Number		Material Composition, grams per kg of material				
		Zircaloy-4	Inconel-718	Inconel X-750	Stainless Steel 304	UO ₂ Fuel
H	1	1.30E-02	-	-	-	-
Li	3	-	-	-	-	1.00E-03
B	5	3.30E-04	-	-	-	1.00E-03
C	6	1.20E-01	4.00E-01	3.99E-01	8.00E-01	8.94E-02
N	7	8.00E-02	1.30E+00	1.30E+00	1.30E+00	2.50E-02
O	8	9.50E-01	-	-	-	1.34E+02
F	9	-	-	-	-	1.07E-02
Na	11	-	-	-	-	1.50E-02
Mg	12	-	-	-	-	2.00E-03
Al	13	2.40E-02	5.99E+00	7.98E+00	-	1.67E-02
Si	14	-	2.00E+00	2.99E+00	1.00E+01	1.21E-02
P	15	-	-	-	4.50E-01	3.50E-02
S	16	3.50E-02	7.00E-02	7.00E-02	3.00E-01	-
Cl	17	-	-	-	-	5.30E-03
Ca	20	-	-	-	-	2.00E-03
Ti	22	2.00E-02	7.99E+00	2.49E+01	-	1.00E-03
V	23	2.00E-02	-	-	-	3.00E-03
Cr	24	1.25E+00	1.90E+02	1.50E+02	1.90E+02	4.00E-03
Mn	25	2.00E-02	2.00E+00	6.98E+00	2.00E+01	1.70E-03
Fe	26	2.25E+00	1.80E+02	6.78E+01	6.88E+02	1.80E-02
Co	27	1.00E-02	4.69E+00	6.49E+00	8.00E-01	1.00E-03
Ni	28	2.00E-02	5.20E+02	7.22E+02	8.92E+01	2.40E-02
Cu	29	2.00E-02	9.99E-01	4.99E-01	-	1.00E-03
Zn	30	-	-	-	-	4.03E-02
Zr	40	9.79E+02	-	-	-	-
Nb	41	-	5.55E+01	8.98E+00	-	-
Mo	42	-	3.00E+01	-	-	1.00E-02
Ag	47	-	-	-	-	1.00E-04
Cd	48	2.50E-04	-	-	-	2.50E-02
In	49	-	-	-	-	2.00E-03
Sn	50	1.60E+01	-	-	-	4.00E-03
Gd	64	-	-	-	-	2.50E-03
Hf	72	7.80E-02	-	-	-	-
W	74	2.00E-02	-	-	-	2.00E-03
Pb	82	-	-	-	-	1.00E-03
U	92	2.00E-04	-	-	-	1.00E+03

Table M.5-8
Flux Correct Factors By Assembly Region

Assembly Region	Flux Factor
Bottom	0.20
In-Core	1.00
Plenum	0.20
Top	0.10

Table M.5-9
Gamma Source Term for 41 GWd/MTU, 3.1 wt. % U-235 and 5-Year Cooled Fuel

CASK-81 Energy Group	E_{upper} (MeV)	E_{mean} (MeV)	Top Region $\gamma/s/assembly$	Plenum Region $\gamma/s/assembly$	Fuel Region $\gamma/s/assembly$	Bottom Region $\gamma/s/assembly$
23	10	9	0.000E+00	0.000E+00	2.240E+05	0.000E+00
24	8	7.25	0.000E+00	0.000E+00	1.055E+06	0.000E+00
25	6.5	5.75	0.000E+00	0.000E+00	5.378E+06	0.000E+00
26	5	4.5	0.000E+00	0.000E+00	1.340E+07	0.000E+00
27	4	3.5	1.201E-09	1.380E-09	1.271E+10	1.735E-09
28	3	2.75	8.880E+04	5.535E+04	1.019E+11	1.444E+05
29	2.5	2.25	5.727E+07	3.570E+07	2.979E+12	9.311E+07
30	2	1.83	7.069E+02	4.866E+02	1.324E+12	1.155E+03
31	1.66	1.495	2.413E+12	1.504E+12	6.474E+13	3.923E+12
32	1.33	1.165	8.545E+12	5.326E+12	2.219E+14	1.389E+13
33	1	0.9	5.889E+10	5.157E+09	3.559E+14	1.076E+11
34	0.8	0.7	9.223E+08	2.682E+10	2.515E+15	1.330E+09
35	0.6	0.5	2.916E+07	4.978E+10	8.362E+14	4.741E+07
36	0.4	0.35	4.601E+08	2.522E+09	7.088E+13	7.480E+08
37	0.3	0.25	3.511E+08	7.843E+08	1.006E+14	5.707E+08
38	0.2	0.15	7.064E+09	1.386E+10	3.548E+14	1.149E+10
39	0.1	0.075	2.928E+10	1.888E+10	4.367E+14	4.760E+10
40	0.05	0.025	2.352E+11	2.778E+11	2.123E+15	3.826E+11

Table M.5-10
Gamma Source Term for 30 GWd/MTU, 2.5 wt. % U-235 and 8-Year Cooled Fuel

CASK-81 Energy Group	E_{upper} (MeV)	E_{mean} (MeV)	Top Region γ/s/assembly	Plenum Region γ/s/assembly	Fuel Region γ/s/assembly	Bottom Region γ/s/assembly
23	10	9	0.000E+00	0.000E+00	7.919E+04	0.000E+00
24	8	7.25	0.000E+00	0.000E+00	3.730E+05	0.000E+00
25	6.5	5.75	0.000E+00	0.000E+00	1.902E+06	0.000E+00
26	5	4.5	0.000E+00	0.000E+00	4.739E+06	0.000E+00
27	4	3.5	3.457E-11	4.016E-11	1.174E+09	5.032E-11
28	3	2.75	4.744E+04	2.959E+04	9.325E+09	7.711E+04
29	2.5	2.25	3.059E+07	1.908E+07	1.873E+11	4.973E+07
30	2	1.83	1.652E-02	2.174E+01	1.709E+11	2.643E-02
31	1.66	1.495	1.289E+12	8.040E+11	2.625E+13	2.096E+12
32	1.33	1.165	4.565E+12	2.847E+12	1.044E+14	7.421E+12
33	1	0.9	4.583E+09	1.161E+09	8.634E+13	8.097E+09
34	0.8	0.7	7.120E+08	9.788E+09	1.336E+15	1.026E+09
35	0.6	0.5	1.553E+07	1.734E+10	1.827E+14	2.525E+07
36	0.4	0.35	2.458E+08	9.316E+08	2.809E+13	3.995E+08
37	0.3	0.25	1.877E+08	3.140E+08	4.217E+13	3.050E+08
38	0.2	0.15	3.775E+09	5.647E+09	1.442E+14	6.136E+09
39	0.1	0.075	1.564E+10	9.968E+09	1.977E+14	2.543E+10
40	0.05	0.025	1.247E+11	1.167E+11	1.001E+15	2.025E+11

Table M.5-11
Gamma Source Term for 45 GWd/MTU, 3.3 wt. % U-235 and 23-Year Cooled Fuel

CASK-81 Energy Group	E_{upper} (MeV)	E_{mean} (MeV)	Top Region $\gamma/s/assembly$	Plenum Region $\gamma/s/assembly$	Fuel Region $\gamma/s/assembly$	Bottom Region $\gamma/s/assembly$
23	10	9	0.000E+00	0.000E+00	1.492E+05	0.000E+00
24	8	7.25	0.000E+00	0.000E+00	7.026E+05	0.000E+00
25	6.5	5.75	0.000E+00	0.000E+00	3.582E+06	0.000E+00
26	5	4.5	0.000E+00	0.000E+00	8.926E+06	0.000E+00
27	4	3.5	1.507E-11	1.829E-11	2.651E+07	2.259E-11
28	3	2.75	8.942E+03	5.575E+03	2.528E+08	1.454E+04
29	2.5	2.25	5.767E+06	3.595E+06	3.396E+09	9.375E+06
30	2	1.83	4.318E-03	3.072E+01	6.492E+10	6.219E-03
31	1.66	1.495	2.430E+11	1.515E+11	4.859E+12	3.951E+11
32	1.33	1.165	8.605E+11	5.365E+11	2.974E+13	1.399E+12
33	1	0.9	9.882E+08	1.116E+09	1.220E+13	1.430E+09
34	0.8	0.7	9.861E+08	1.425E+09	1.236E+15	1.420E+09
35	0.6	0.5	2.928E+06	5.651E+08	2.120E+13	4.760E+06
36	0.4	0.35	4.640E+07	5.428E+07	2.529E+13	7.542E+07
37	0.3	0.25	3.584E+07	2.904E+07	3.769E+13	5.817E+07
38	0.2	0.15	7.152E+08	5.551E+08	1.231E+14	1.162E+09
39	0.1	0.075	2.960E+09	1.858E+09	1.922E+14	4.810E+09
40	0.05	0.025	2.555E+10	1.779E+10	9.237E+14	4.131E+10

**Table M.5-12
Design-Basis BPR Source Terms**

CASK-81 Energy Group	E_{upper} (MeV)	E_{mean} (MeV)	Top Region γ/s/BPRA	Plenum Region γ/s/BPRA	Fuel Region γ/s/BPRA
23	10	9	0.000E+00	0.000E+00	0.000E+00
24	8	7.25	0.000E+00	0.000E+00	0.000E+00
25	6.5	5.75	0.000E+00	0.000E+00	0.000E+00
26	5	4.5	0.000E+00	0.000E+00	0.000E+00
27	4	3.5	3.947E-15	6.520E-14	7.266E-18
28	3	2.75	3.942E+04	2.179E+04	5.495E+05
29	2.5	2.25	1.274E+07	7.040E+06	1.775E+08
30	2	1.83	9.577E+01	8.812E+01	9.153E-05
31	1.66	1.495	7.138E+11	3.946E+11	9.953E+12
32	1.33	1.165	1.690E+12	9.340E+11	2.356E+13
33	1	0.9	6.951E+09	4.180E+09	4.699E+09
34	0.8	0.7	4.155E+09	1.783E+10	2.835E+09
35	0.6	0.5	3.235E+07	3.854E+10	4.508E+08
36	0.4	0.35	7.014E+07	2.431E+10	9.776E+08
37	0.3	0.25	2.060E+08	3.482E+09	2.872E+09
38	0.2	0.15	1.217E+09	3.534E+09	1.697E+10
39	0.1	0.075	8.191E+09	5.176E+09	1.142E+11
40	0.05	0.025	8.484E+10	1.382E+11	1.170E+12

Table M.5-13
Inner/Outer Heat Load Zone Region Volumes

Assembly Region	Inner Heat Load Region (cm³)	Outer Heat Load Region (cm³)
Bottom	1.710x10 ⁵	1.710x10 ⁵
In-Core	2.905x10 ⁶	2.905x10 ⁶
Plenum	1.783x10 ⁵	1.783x10 ⁵
Top	1.272x10 ⁵	1.272x10 ⁵

Table M.5-14
Total Neutron Source Summary

CASK-81 Energy Group	E _{upper} (MeV)	E _{mean} (MeV)	Normalized Cm-244 Fission Source	Neutrons per second per assembly		
				41GWd/MTU 3.1 wt. % 5-year cooled	30 GWd/MTU 2.5 wt. % U-235 8-year cooled	45 GWd/MTU 3.3 wt. % U-235 23-year cooled
1	1.49E+01	1.36E+01	2.018E-04	7.848E+04	2.787E+04	5.263E+04
2	1.22E+01	1.11E+01	1.146E-03	4.457E+05	1.583E+05	2.989E+05
3	1.00E+01	9.09E+00	4.471E-03	1.739E+06	6.174E+05	1.166E+06
4	8.18E+00	7.27E+00	1.768E-02	6.876E+06	2.442E+06	4.611E+06
5	6.36E+00	5.66E+00	4.167E-02	1.621E+07	5.755E+06	1.087E+07
6	4.96E+00	4.51E+00	5.641E-02	2.194E+07	7.790E+06	1.471E+07
7	4.06E+00	3.54E+00	1.197E-01	4.655E+07	1.653E+07	3.122E+07
8	3.01E+00	2.74E+00	9.616E-02	3.740E+07	1.328E+07	2.508E+07
9	2.46E+00	2.41E+00	2.256E-02	8.774E+06	3.116E+06	5.884E+06
10	2.35E+00	2.09E+00	1.227E-01	4.772E+07	1.694E+07	3.200E+07
11	1.83E+00	1.47E+00	2.110E-01	8.206E+07	2.914E+07	5.503E+07
12	1.11E+00	8.30E-01	1.794E-01	6.977E+07	2.478E+07	4.679E+07
13	5.50E-01	3.31E-01	1.138E-01	4.426E+07	1.572E+07	2.968E+07
14	1.11E-01	5.72E-02	1.301E-02	5.060E+06	1.797E+06	3.393E+06
15	3.35E-03	1.97E-03	6.555E-05	2.549E+04	9.052E+03	1.710E+04
16	5.83E-04	3.42E-04	4.765E-06	1.853E+03	6.580E+02	1.243E+03
17	1.01E-04	6.50E-05	3.134E-07	1.219E+02	4.328E+01	8.173E+01
18	2.90E-05	1.96E-05	4.527E-08	1.761E+01	6.252E+00	1.181E+01
19	1.01E-05	6.58E-06	9.759E-09	3.795E+00	1.348E+00	2.545E+00
20	3.06E-06	2.09E-06	1.521E-09	5.915E-01	2.101E-01	3.967E-01
21	1.12E-06	7.67E-07	3.353E-10	1.304E-01	4.630E-02	8.745E-02
22	4.14E-07	2.12E-07	9.683E-11	3.766E-02	1.337E-02	2.525E-02
Total			1.000E+00	3.889E+08	1.381E+08	2.608E+08

Table M.5-15
Source Term Peaking Summary

Zone	Fraction of Core Height	Neutron Factor	Gamma Factor
1	0.00	0.33	0.76
2	0.05	0.78	0.94
3	0.10	1.57	1.12
4	0.20	1.57	1.12
5	0.30	1.57	1.12
6	0.40	1.57	1.12
7	0.50	1.57	1.12
8	0.60	1.57	1.12
9	0.70	1.57	1.12
10	0.80	1.46	1.10
11	0.90	0.72	0.92
12	0.95	0.24	0.70

**Table M.5-16
Shielding Material Densities**

Assembly Region Material Densities – Dry

Element	Atomic Number	Number Density (atoms/bn-cm)				
		Fuel Radial	Fuel Axial	Top End Fitting	Plenum	Bottom End Fitting
H	1					
C	6					
N	7					
O	8	1.326E-02	1.326E-02		2.825E-05	
Na	11					
Mg	12					
Al	13	4.714E-04	4.714E-04	3.026E-05	1.101E-03	1.626E-05
Si	14					
K	19					
Ca	20					
Cr	24	1.142E-03	3.699E-04	3.928E-03	5.718E-04	2.171E-03
Fe	26	3.857E-03	1.131E-03	1.252E-02	1.452E-03	6.961E-03
Ni	28	6.197E-04	2.986E-04	2.908E-03	7.411E-04	1.561E-03
Zr	40	4.251E-03	4.251E-03		5.723E-03	
Pb	82					
U-235	92	3.251E-04	3.251E-04			
U-238	92	6.298E-03	6.298E-03			

Assembly Region Material Densities – Wet (atoms/bn-cm)

Element	Atomic Number	Number Density (atoms/bn-cm)				
		Fuel Radial	Fuel Axial	Top End Fitting	Plenum	Bottom End Fitting
H	1	3.486E-02	3.486E-02	4.776E-02	3.430E-02	5.552E-02
C	6					
N	7					
O	8	3.069E-02	3.069E-02	2.388E-02	1.718E-02	2.775E-02
Na	11					
Mg	12					
Al	13	4.714E-04	4.714E-04	3.026E-05	1.101E-03	1.626E-05
Si	14					
K	19					
Ca	20					
Cr	24	1.142E-03	3.699E-04	3.928E-03	5.718E-04	2.171E-03
Fe	26	3.857E-03	1.131E-03	1.252E-02	1.452E-03	6.961E-03
Ni	28	6.197E-04	2.986E-04	2.908E-03	7.411E-04	1.561E-03
Zr	40	4.251E-03	4.251E-03		5.723E-03	
Pb	82					
U-235	92	3.251E-04	3.251E-04			
U-238	92	6.298E-03	6.298E-03			

Table M.5-16
Shielding Material Densities
(Continued)

Reinforced Concrete by HSM Region

Element	Atomic Number	Concrete Regions (atoms/bn-cm)					
		Roof Concrete	Front Concrete	Side Concrete	Rear Concrete	End Shield	Back Shield
H	1	7.261E-03	7.505E-03	7.389E-03	7.447E-03	7.277E-03	7.378E-03
C	6	0.000E+00	0.000E+00	0.000E+00	0.000E+00	0.000E+00	0.000E+00
N	7	0.000E+00	0.000E+00	0.000E+00	0.000E+00	0.000E+00	0.000E+00
O	8	4.099E-02	4.236E-02	4.171E-02	4.204E-02	4.108E-02	4.165E-02
Na	11	9.794E-04	1.012E-03	9.966E-04	1.004E-03	9.816E-04	9.951E-04
Mg	12	1.390E-04	1.436E-04	1.414E-04	1.425E-04	1.393E-04	1.412E-04
Al	13	2.233E-03	2.308E-03	2.272E-03	2.290E-03	2.238E-03	2.268E-03
Si	14	1.431E-02	1.479E-02	1.456E-02	1.467E-02	1.434E-02	1.454E-02
K	19	6.479E-04	6.697E-04	6.593E-04	6.645E-04	6.493E-04	6.583E-04
Ca	20	2.725E-03	2.817E-03	2.773E-03	2.795E-03	2.731E-03	2.769E-03
Fe	26	5.847E-03	3.195E-03	4.463E-03	3.829E-03	5.674E-03	4.579E-03

Other Shielding Materials

Element	Atomic Number	Number Density (atoms/bn-cm)						
		NS-3	Concrete	Water	Air	Lead	Steel	Aluminum
H	1	4.591E-02	7.770E-03	6.687E-02				
C	6	8.252E-03						
N	7				1.980E-05			
O	8	3.780E-02	4.386E-02	3.343E-02	5.280E-06			
Na	11		1.048E-03					
Mg	12		1.487E-04					
Al	13	7.028E-03	2.389E-03					6.026E-02
Si	14	1.268E-03	1.531E-02					
K	19		6.933E-04					
Ca	20	1.484E-03	2.916E-03					
Cr	24							
Fe	26	1.063E-04	3.128E-04				8.487E-02	
Ni	28							
Zr	40							
Pb	82					3.296E-02		
U-235	92							
U-238	92							

Table M.5-17
Neutron Source for 45 GWd/MTU 3.3 wt. % U-235 16 Year Cooled Fuel

CASK-81 Energy Group	E_{upper} (MeV)	E_{mean} (MeV)	n/s/assembly
1	1.49E+01	1.36E+01	6.815E+04
2	1.22E+01	1.11E+01	3.870E+05
3	1.00E+01	9.09E+00	1.510E+06
4	8.18E+00	7.27E+00	5.971E+06
5	6.36E+00	5.66E+00	1.407E+07
6	4.96E+00	4.51E+00	1.905E+07
7	4.06E+00	3.54E+00	4.042E+07
8	3.01E+00	2.74E+00	3.247E+07
9	2.46E+00	2.41E+00	7.619E+06
10	2.35E+00	2.09E+00	4.144E+07
11	1.83E+00	1.47E+00	7.125E+07
12	1.11E+00	8.30E-01	6.058E+07
13	5.50E-01	3.31E-01	3.843E+07
14	1.11E-01	5.72E-02	4.393E+06
15	3.35E-03	1.97E-03	2.214E+04
16	5.83E-04	3.42E-04	1.609E+03
17	1.01E-04	6.50E-05	1.058E+02
18	2.90E-05	1.96E-05	1.529E+01
19	1.01E-05	6.58E-06	3.296E+00
20	3.06E-06	2.09E-06	5.136E-01
21	1.12E-06	7.67E-07	1.132E-01
22	4.14E-07	2.12E-07	3.270E-02
Total			3.377E+08

Table M.5-18
Gamma Source Term for 45 GWd/MTU, 3.3 wt. % U-235 and 16-Year Cooled Fuel

CASK-81 Energy Group	E_{upper} (MeV)	E_{mean} (MeV)	Top Region $\gamma/s/assembly$	Plenum Region $\gamma/s/assembly$	Fuel Region $\gamma/s/assembly$
23	10	9	0.00E+00	0.00E+00	1.94E+05
24	8	7.25	0.00E+00	0.00E+00	9.13E+05
25	6.5	5.75	0.00E+00	0.00E+00	4.65E+06
26	5	4.5	0.00E+00	0.00E+00	1.16E+07
27	4	3.5	1.86E-11	2.25E-11	4.22E+07
28	3	2.75	2.25E+04	1.40E+04	3.29E+08
29	2.5	2.25	1.45E+07	9.03E+06	4.77E+09
30	2	1.83	5.13E-03	3.65E+01	7.85E+10
31	1.66	1.495	6.10E+11	3.80E+11	1.17E+13
32	1.33	1.165	2.16E+12	1.35E+12	6.17E+13
33	1	0.9	1.05E+09	1.15E+09	2.71E+13
34	0.8	0.7	9.88E+08	2.86E+09	1.48E+15
35	0.6	0.5	7.35E+06	3.34E+09	4.49E+13
36	0.4	0.35	1.16E+08	2.22E+08	3.02E+13
37	0.3	0.25	8.92E+07	9.37E+07	4.59E+13
38	0.2	0.15	1.79E+09	1.75E+09	1.53E+14
39	0.1	0.075	7.41E+09	4.67E+09	2.24E+14
40	0.05	0.025	6.07E+10	4.58E+10	1.11E+15

**Table M.5-19
Explicit Model Material Densities**

Region	In-Core		Plenum		Top	
Element	Gram Density g/cm ³	Atom Density atoms/bn-cm	Gram Density g/cm ³	Atom Density atoms/bn-cm	Gram Density g/cm ³	Atom Density atoms/bn-cm
O	0.3731	1.405E-02	0.0008	2.992E-05	0.0000	0.000E+00
Al	0.0002	5.219E-06	0.0006	1.366E-05	0.0014	3.205E-05
Ti	0.0002	3.078E-06	0.0008	1.014E-05	0.0019	2.409E-05
Cr	0.0063	7.286E-05	0.0202	2.336E-04	0.2723	3.154E-03
Fe	0.0067	7.257E-05	0.0210	2.268E-04	0.9034	9.743E-03
Ni	0.0177	1.816E-04	0.0611	6.273E-04	0.2543	2.609E-03
Zr	0.6819	4.502E-03	0.8328	5.499E-03	0.0000	0.000E+00
Mo	<0.0001	1.739E-07	0.0000	0.000E+00	0.0000	0.000E+00
U-235	0.1344	3.444E-04	0.0000	0.000E+00	0.0000	0.000E+00
U-238	2.6361	6.671E-03	0.0000	0.000E+00	0.0000	0.000E+00
Total	3.8567	2.590E-02	0.9373	6.640E-03	1.4334	1.556E-02

**Table M.5-20
Smearred Model Material Densities**

Region	In-Core		Plenum		Top	
Element	Gram Density g/cm ³	Atom Density atoms/bn-cm	Gram Density g/cm ³	Atom Density atoms/bn-cm	Gram Density g/cm ³	Atom Density atoms/bn-cm
O	0.3523	1.326E-02	0.0008	2.825E-05	0.0000	0.000E+00
Al	0.0002	4.927E-06	0.0006	1.290E-05	0.0014	3.026E-05
Ti	0.0002	2.906E-06	0.0008	9.577E-06	0.0018	2.274E-05
Cr	0.0226	2.618E-04	0.0357	4.136E-04	0.2737	3.171E-03
Fe	0.0696	7.502E-04	0.0831	8.958E-04	0.9162	9.881E-03
Ni	0.0245	2.517E-04	0.0655	6.725E-04	0.2479	2.544E-03
Zr	0.6438	4.251E-03	0.7863	5.192E-03	0.0000	0.000E+00
Mo	0.0000	1.642E-07	0.0000	0.000E+00	0.0000	0.000E+00
U-235	0.1269	3.251E-04	0.0000	0.000E+00	0.0000	0.000E+00
U-238	2.4888	6.298E-03	0.0000	0.000E+00	0.0000	0.000E+00
Total	3.7290	2.541E-02	0.9727	7.224E-03	1.4410	1.565E-02

Table M.5-21
Stainless Steel, Aluminum and Air Material Densities

For Use with Explicit vs Smear Model Only

Material	Stainless Steel		Aluminum		Air	
Element	Gram Density g/cm ³	Atom Density atom/bn-cm	Gram Density g/cm ³	Atom Density atom/bn-cm	Gram Density g/cm ³	Atom Density atom/bn-cm
N	0.0000	0.000E+00	0.0000	0.000E+00	0.0008	3.587E-05
O	0.0000	0.000E+00	0.0000	0.000E+00	0.0003	9.534E-06
Al	0.0000	0.000E+00	2.7000	6.026E-02	0.0000	0.000E+00
Cr	1.4920	1.728E-02	0.0000	0.000E+00	0.0000	0.000E+00
Fe	5.6320	6.073E-02	0.0000	0.000E+00	0.0000	0.000E+00
Ni	0.7258	7.447E-03	0.0000	0.000E+00	0.0000	0.000E+00
Total	7.8498	8.546E-02	2.7000	6.026E-02	0.0011	4.540E-05

**Table M.5-22
MCNP Explicit and Smeared Model Results**

Explicit Model (mrem/hr)								
Shell next to Fuel		Shell next to Plenum		Shell next to Top		Top of Shield Plug		Source
Cell 23	1 sigma	Cell 24	1 sigma	Cell 25	1 sigma	Cell 26	1 sigma	
4.55E+03	0.0027	2.03E+03	0.0119	1.42E+03	0.0171	1.23E+02	0.01	In-Core Neutron
3.25E+06	0.0238	1.23E+06	0.1189	1.58E+05	0.2697	4.53E+01	0.1764	In-Core Gamma
1.68E+04	0.0043	3.48E+05	0.0024	1.94E+05	0.004	1.35E+02	0.0044	Plenum Gamma
8.91E+03	0.0125	2.69E+05	0.0056	4.88E+05	0.0046	8.31E+02	0.0034	Top Gamma
3.28E+06		1.85E+06		8.41E+05		1.13E+03		Total
Smeared Model (mrem/hr)								
Shell next to Fuel		Shell next to Plenum		Shell next to Top		Top of Shield Plug		Source
Cell 23	1 sigma	Cell 24	1 sigma	Cell 25	1 sigma	Cell 26	1 sigma	
5.13E+03	0.0063	2.45E+03	0.0281	1.66E+03	0.0377	1.37E+02	0.0225	In-Core Neutron
4.10E+06	0.0216	1.38E+06	0.1074	3.53E+05	0.2109	6.70E+01	0.1300	In-Core Gamma
2.27E+04	0.0044	4.58E+05	0.0024	2.70E+05	0.0040	1.74E+02	0.0044	Plenum Gamma
1.40E+04	0.013	3.76E+05	0.0061	6.11E+05	0.0053	8.90E+02	0.0041	Top Gamma
4.14E+06		2.22E+06		1.24E+06		1.27E+03		Total
Ratio of Smeared to Explicit MCNP Results								
Shell next to Fuel		Shell next to Plenum		Shell next to Top		Top of Shield Plug		Source
1.13		1.21		1.17		1.11		
1.26		1.12		2.24		1.48		In-Core Gamma
1.35		1.32		1.39		1.29		Plenum Gamma
1.57		1.40		1.25		1.07		Top Gamma
1.26		1.20		1.47		1.12		Total

**Table M.5-23
HSM Accident Dose Rates**

HSM Roof Accident Dose Rates, mrem/hr (32PT-S125/32PT-L125 DSC Configuration)

	Neutron	Gamma	Total
Centerline	7.65E-01	4.23E+01	4.31E+01
Peak Vent	3.22E+01	2.43E+03	2.46E+03
Average	2.01E+00	1.81E+02	1.83E+02

HSM Front Accident Dose Rates, mrem/hr (32PT-S125/32PT-L125 DSC Configuration)

	Neutron	Gamma	Total
Peak Door	2.81E+01	7.75E+01	9.93E+01
Peak Vent	1.74E+01	1.85E+03	1.87E+03
Average	7.91E+00	1.75E+02	1.83E+02

HSM Roof Accident Dose Rates, mrem/hr (32PT-S100/32PT-L100 DSC Configuration)

	Neutron	Gamma	Total
Centerline	7.65E-01	4.23E+01	4.31E+01
Peak Vent	3.22E+01	2.43E+03	2.46E+03
Average	2.04E+00	1.82E+02	1.84E+02

HSM Front Accident Dose Rates, mrem/hr (32PT-S100/32PT-L100 DSC Configuration)

	Neutron	Gamma	Total
Peak Door	3.63E+01	1.58E+02	1.85E+02
Peak Vent	1.79E+01	1.89E+03	1.91E+03
Average	9.74E+00	2.07E+02	2.16E+02

Table M.5-24
3-D vs 2-D Comparison for 32PT-S100/32PT-L100 DSC Configuration

Location	Dose Rate Component	SAR Table with 2-D Results	2-D DORT Result	3-D MCNP Result	MCNP 1 σ error	Ratio 3-D/2-D
HSM Roof Birdscreen-Vent (mrem/hr)	Gamma	Table M.5-3	1201	1073	3.43%	0.89
	Neutron		16.9	9.96	2.55%	0.59
	Total		1218	1101	NA	0.90
Roof Surface Average Dose Rate (mrem/hr)	Gamma	Table M.5-4	54.5	49.2	2.10%	0.90
	Neutron		0.75	0.65	2.28%	0.87
HSM Front Birdscreen - Vent (mrem/hr)	Gamma	Table M.5-3	780	638.6	4.46%	0.82
	Neutron		7.3	5.34	3.16%	0.73
	Total		788	643.9	NA	0.82
HSM Door Exterior Surface (centerline)	Gamma	Table M.5-3	158	77.22	0.79%	0.49
	Neutron		36.3	34.4	3.98%	0.95
	Total		185	112	NA	0.61

Table M.5-25
Comparison of Calculated Versus Measured Dose Rates for DSC 45

Description	Maximum Measured Dose Rate, mrem/hr		Maximum Calculated with MCNP		Ratio, Calculated/Measured
			mrem/hr	MCNP 1 σ error, %	
In front of HSM Front Bird Screen	Neutron	0.6	1.43	2.4	2.4
	Gamma	30	281.98	6.8	9.4
	Total	30.6	283.42	6.8	9.3
Above HSM Roof Bird Screen	Neutron	3	2.53	1.6	0.8
	Gamma	130	661.46	2.0	5.1
	Total	133	663.99	2.0	5.0
On HSM Door	Neutron	3	7.36	1.1	2.5
	Gamma	7	13.17	2.1	1.9
	Total	10	20.53	1.4	2.1

**Table M.5-26
Comparison of Calculated Versus Measured Dose Rates for DSC 46**

Description	Maximum Measured Dose Rate, mrem/hr		Maximum Calculated with MCNP		Ratio, Calculated/ Measured
			mrem/hr	MCNP 1 σ error, %	
In front of HSM Front Bird Screen	Neutron	0.3	1.34	2.4	4.5
	Gamma	20	266.20	7.0	13.3
	Total	20.3	267.54	6.9	13.2
Above HSM Roof Bird Screen	Neutron	0.7	2.39	1.6	3.4
	Gamma	180	635.22	2.1	3.5
	Total	180.7	637.61	2.1	3.5
On HSM Door	Neutron	1.5	6.95	1.1	4.6
	Gamma	15	12.44	3.5	0.8
	Total	16.5	19.40	2.3	1.2

**Table M.5-27
ANISN Material Densities**

Element	Material Atom Densities (atoms/barn-cm)					
	Stainless Steel	Air	Lead	NS-3	Aluminum	Concrete
H	0.000E+00	0.000E+00	0.000E+00	4.597E-02	0.000E+00	7.770E-03
C	0.000E+00	0.000E+00	0.000E+00	8.253E-03	0.000E+00	0.000E+00
O	0.000E+00	5.280E-06	0.000E+00	3.780E-02	0.000E+00	4.386E-02
Al	0.000E+00	0.000E+00	0.000E+00	7.028E-03	6.026E-02	2.389E-03
Si	0.000E+00	0.000E+00	0.000E+00	1.268E-03	0.000E+00	1.581E-02
Ca	0.000E+00	0.000E+00	0.000E+00	1.484E-03	0.000E+00	2.916E-03
Fe	8.487E-02	0.000E+00	0.000E+00	1.063E-04	0.000E+00	3.128E-04
Pb	0.000E+00	0.000E+00	3.296E-02	0.000E+00	0.000E+00	0.000E+00

**Table M.5-28
1.2 kW Fuel in the HSM**

Burnup (GWd/MTU)	Initial Enrichment (wt. % U-235)	Cooling Time (years)	HSM Centerline Roof		
			neutron (mrem/hr)	gamma (mrem/hr)	Total (mrem/hr)
20	2	5	0.02	21.77	21.79
25	2.1	5	0.06	28.12	28.18
28	2.3	5	0.08	31.44	31.52
30	2.5	5	0.09	33.38	33.47
32	2.6	5	0.11	35.78	35.89
34	2.7	5	0.14	38.21	38.35
36	2.8	5	0.16	40.66	40.83
38	3.0	5	0.18	42.66	42.84
39	3.0	5	0.20	44.14	44.34
41	3.1	5	0.24	46.64	46.87
42	3.1	6	0.25	36.59	36.84
	3.8	5	0.18	44.99	45.17
43	3.2	6	0.26	37.33	37.59
	4.5	5	0.14	43.79	43.93
45	3.3	6	0.30	39.24	39.54

Bold indicates maximum calculated surface dose rate and/or source term used for design basis fuel

Table M.5-29
1.2 kW Fuel in the Transfer Cask

Burnup (GWd/MTU)	Initial Enrichment (wt. % U-235)	Cooling Time (years)	Cask Centerline Side		
			neutron (mrem/hr)	gamma (mrem/hr)	Total (mrem/hr)
20	2	5	11.66	223.68	235.33
25	2.1	5	27.81	289.62	317.43
28	2.3	5	38.35	323.53	361.88
30	2.5	5	44.37	342.99	387.36
32	2.6	5	54.36	367.86	422.21
34	2.7	5	65.56	393.23	458.79
36	2.8	5	78.04	419.09	497.13
38	3.0	5	86.66	439.24	525.89
39	3.0	5	96.41	455.35	551.76
41	3.1	5	111.88	481.92	593.80
42	3.1	6	118.75	386.55	505.31
	3.8	5	85.60	458.58	544.17
43	3.2	6	123.86	394.30	518.16
	4.5	5	67.54	441.47	509.01
45	3.3	6	141.27	415.56	556.83

Bold indicates Maximum Calculated Surface Dose Rate and/or source term used for Design Basis Fuel

**Table M.5-30
0.87 kW Fuel in the HSM**

Burnup (GWd/MTU)	Initial Enrichment (wt. % U-235)	Cooling Time (years)	HSM Centerline Roof		
			neutron (mrem/hr)	gamma (mrem/hr)	Total (mrem/hr)
20	2	5	0.02	21.77	21.79
25	2.1	5	0.06	28.12	28.18
28	2.3	5	0.08	31.44	31.52
30	2.5	5	0.09	33.38	33.47
32	2.6	6	0.11	27.30	27.41
	2.8	5	0.10	34.90	35.00
34	2.7	6	0.13	29.13	29.26
	4.9	5	0.04	31.02	31.06
36	2.8	6	0.16	30.95	31.11
38	3.0	7	0.17	26.07	26.24
	4.6	6	0.08	27.69	27.77
39	3.0	7	0.19	26.96	27.15
40	3.4	7	0.17	26.63	26.80
41	4.3	7	0.12	25.17	25.29
42	3.1	8	0.23	24.43	24.67
43	3.2	9	0.23	21.23	21.46
	3.9	8	0.17	23.16	23.33
44	3.3	9	0.24	21.63	21.87
	4.9	8	0.12	21.89	22.01
45	3.3	10	0.26	19.29	19.54
	3.9	9	0.20	20.96	21.16

Bold indicates Maximum Calculated Surface Dose Rate

**Table M.5-31
0.87 kW Fuel in the Transfer Cask**

Burnup (GWd/MTU)	Initial Enrichment (wt. % U-235)	Cooling Time (years)	Cask Centerline Side		
			neutron (mrem/hr)	gamma (mrem/hr)	Total (mrem/hr)
20	2	5	11.66	223.68	235.33
25	2.1	5	27.81	289.62	317.43
28	2.3	5	38.35	323.53	361.88
30	2.5	5	44.37	342.99	387.36
32	2.6	6	52.33	285.54	337.87
	2.8	5	47.64	357.22	404.86
34	2.7	6	63.13	305.13	368.27
	4.9	5	19.47	307.49	326.95
36	2.8	6	75.14	324.85	399.98
38	3.0	7	80.37	276.46	356.83
	4.6	6	35.87	280.63	316.50
39	3.0	7	89.42	286.81	376.22
40	3.4	7	79.60	280.67	360.27
41	4.3	7	55.93	260.02	315.95
42	3.1	8	110.12	263.50	373.62
43	3.2	9	110.60	229.81	340.41
	3.9	8	80.43	244.00	324.44
44	3.3	9	115.24	234.21	349.46
	4.9	8	55.82	225.34	281.15
45	3.3	10	121.49	210.06	331.55
	3.9	9	93.82	222.77	316.59

Bold indicates maximum calculated surface dose rate

**Table M.5-32
0.7 kW Fuel in the HSM**

Burnup (GWd/MTU)	Initial Enrichment (wt. % U-235)	Cooling Time (years)	HSM Centerline Roof		
			neutron (mrem/hr)	gamma (mrem/hr)	Total (mrem/hr)
20	2	5	0.03	21.92	21.95
25	2.1	5	0.07	28.33	28.40
28	2.3	6	0.10	24.25	24.35
	4.0	5	0.03	26.05	26.09
30	2.5	6	0.11	25.69	25.81
32	2.6	7	0.13	22.19	22.32
	4.7	6	0.04	21.98	22.02
34	2.7	8	0.16	19.76	19.92
	3.6	7	0.09	21.19	21.28
36	2.8	9	0.18	17.92	18.10
	3.4	8	0.13	19.49	19.62
38	3.0	10	0.19	16.25	16.44
	3.7	9	0.13	17.29	17.42
39	3.0	11	0.21	14.74	14.95
	3.2	10	0.19	16.41	16.60
40	3.1	11	0.22	15.05	15.26
	4.5	10	0.11	14.90	15.01
41	3.1	12	0.23	13.74	13.97
	4.1	11	0.14	14.01	14.15
42	3.1	13	0.24	12.62	12.86
	3.9	12	0.17	13.05	13.22
43	3.2	14	0.18	12.00	12.17
	3.9	13	0.24	11.52	11.76
44	3.3	15	0.25	10.57	10.81
	4.0	14	0.18	10.99	11.17
45	3.3	16	0.26	9.83	10.09
	4.0	15	0.19	10.20	10.39

Bold indicates maximum calculated surface dose rate

Table M.5-33
0.7 kW Fuel in the Transfer Cask

Burnup (GWd/MTU)	Initial Enrichment (wt. % U-235)	Cooling Time (years)	Cask Centerline Side		
			neutron (mrem/hr)	gamma (mrem/hr)	Total (mrem/hr)
20	2	5	15.63	226.35	241.98
25	2.1	5	37.29	294.11	331.40
28	2.3	6	49.58	256.64	306.21
	4.0	5	16.98	261.14	278.12
30	2.5	6	57.33	271.68	329.01
32	2.6	7	67.64	238.18	305.82
	4.7	6	20.98	222.08	243.06
34	2.7	8	78.60	214.50	293.10
	3.6	7	47.49	221.70	269.19
36	2.8	9	90.11	196.42	286.54
	3.4	8	65.75	207.62	273.36
38	3.0	10	96.37	178.68	275.05
	3.7	9	67.84	184.07	251.91
39	3.0	11	103.27	163.21	266.48
	3.2	10	95.82	179.66	275.48
40	3.1	11	108.34	166.85	275.19
	4.5	10	54.79	155.16	209.95
41	3.1	12	115.40	153.42	268.82
	4.1	11	71.35	148.38	219.73
42	3.1	13	122.52	142.01	264.52
	3.9	12	84.12	139.90	224.03
43	3.2	14	123.08	129.68	252.76
	3.9	13	89.60	129.05	218.66
44	3.3	15	123.54	118.94	242.48
	4.0	14	90.65	117.86	208.51
45	3.3	16	130.26	111.63	241.89
	4.0	15	96.03	109.78	205.81

Bold indicates maximum calculated surface dose rate

**Table M.5-34
0.63 kW Fuel in the HSM**

Burnup (GWd/MTU)	Initial Enrichment (wt. % U-235)	Cooling Time (years)	HSM Centerline Roof		
			neutron (mrem/hr)	gamma (mrem/hr)	Total (mrem/hr)
20	2	5	0.01	0.15	0.16
25	2.1	6	0.01	0.15	0.17
	3	5	0.01	0.18	0.19
28	2.3	7	0.02	0.14	0.16
	2.6	6	0.02	0.16	0.18
30	2.5	7	0.02	0.15	0.18
32	2.6	8	0.03	0.14	0.17
	5.0	7	0.01	0.10	0.11
34	2.7	9	0.03	0.14	0.17
36	2.8	11	0.03	0.13	0.17
	3.3	10	0.03	0.11	0.14
38	3.0	13	0.04	0.12	0.16
	3.1	12	0.04	0.13	0.16
	4.7	11	0.02	0.08	0.10
39	3.0	14	0.04	0.12	0.16
	3.1	13	0.04	0.13	0.16
	4.7	12	0.02	0.08	0.10
40	3.1	15	0.04	0.12	0.16
	3.3	14	0.04	0.12	0.15
	4.7	13	0.02	0.08	0.10
41	3.1	16	0.04	0.12	0.16
	3.5	15	0.03	0.11	0.14
	5.0	14	0.02	0.06	0.08
42	3.1	17	0.04	0.12	0.17
	3.7	16	0.03	0.10	0.14
43	3.2	18	0.04	0.12	0.16
	4.1	17	0.03	0.09	0.12
44	3.3	20	0.04	0.11	0.16
	3.4	19	0.04	0.11	0.16
	4.4	18	0.03	0.08	0.11
45	3.3	21	0.04	0.12	0.16
	3.7	20	0.04	0.10	0.14
	4.9	19	0.02	0.07	0.09

Bold indicates maximum calculated surface dose rate

**Table M.5-35
0.63 kW Fuel in the Transfer Cask**

Burnup (GWd/MTU)	Initial Enrichment (wt. % U-235)	Cooling Time (years)	Cask Centerline Side		
			neutron (mrem/hr)	gamma (mrem/hr)	Total (mrem/hr)
20	2	5	3.98	2.67	6.64
25	2.1	6	9.14	3.76	12.90
	3	5	4.81	3.11	7.92
28	2.3	7	12.15	4.26	16.41
	2.6	6	10.12	4.10	14.22
30	2.5	7	14.05	4.79	18.85
32	2.6	8	16.58	5.21	21.79
	5.0	7	16.58	5.21	21.79
34	2.7	9	19.27	5.73	25.00
36	2.8	11	21.28	6.00	27.28
	3.3	10	16.45	4.87	21.32
38	3.0	13	21.94	5.99	27.93
	3.1	12	21.50	5.96	27.46
	4.7	11	9.74	3.05	12.78
39	3.0	14	23.51	6.32	29.83
	3.1	13	23.06	6.28	29.33
	4.7	12	10.55	3.18	13.73
40	3.1	15	23.75	6.32	30.07
	3.3	14	22.10	5.97	28.06
	4.7	13	11.38	3.32	14.71
41	3.1	16	25.31	6.66	31.97
	3.5	15	21.22	5.69	26.91
	5.0	14	10.70	2.99	13.70
42	3.1	17	26.87	7.00	33.87
	3.7	16	20.42	5.44	25.85
43	3.2	18	27.00	6.99	33.99
	4.1	17	17.85	4.75	22.61
44	3.3	20	26.12	6.71	32.83
	3.4	19	25.76	6.65	32.41
	4.4	18	16.50	4.38	20.88
45	3.3	21	27.54	7.03	34.57
	3.7	20	23.46	6.05	29.51
	4.9	19	14.05	3.74	17.79

Bold indicates Maximum Calculated Surface Dose Rate

**Table M.5-36
0.6 kW Fuel in the HSM**

Burnup (GWd/MTU)	Initial Enrichment (wt. % U-235)	Cooling Time (years)	HSM Centerline Roof		
			neutron (mrem/hr)	gamma (mrem/hr)	Total (mrem/hr)
20	2	5	0.00	0.16	0.16
25	2.1	6	0.02	0.16	0.16
	4.7	5	0.00	0.14	0.16
28	2.3	7	0.02	0.14	0.16
	4.2	6	0.00	0.12	0.12
30	2.5	8	0.02	0.12	0.16
	3.5	7	0.02	0.12	0.12
32	2.6	9	0.02	0.12	0.16
	3.6	8	0.02	0.10	0.12
34	2.7	10	0.04	0.12	0.16
	4.5	9	0.02	0.08	0.10
36	2.8	12	0.04	0.12	0.16
	3.7	11	0.02	0.10	0.12
38	3.0	14	0.04	0.12	0.14
	3.9	13	0.02	0.08	0.10
39	3.0	15	0.04	0.12	0.16
	4.2	14	0.02	0.08	0.10
40	3.1	17	0.04	0.10	0.14
	3.2	16	0.04	0.10	0.14
	4.5	15	0.02	0.08	0.10
41	3.1	18	0.04	0.10	0.14
	3.6	17	0.04	0.10	0.12
	5.0	16	0.02	0.06	0.08
42	3.1	19	0.04	0.12	0.16
	4.0	18	0.02	0.08	0.10
43	3.2	21	0.04	0.10	0.14
	3.3	20	0.04	0.10	0.14
	4.5	19	0.02	0.06	0.10
44	3.3	22	0.04	0.10	0.14
	3.7	21	0.04	0.10	0.12
	4.9	20	0.02	0.14	0.16
45	3.3	23	0.04	0.10	0.14
	4.1	22	0.02	0.08	0.10

Bold indicates Maximum Calculated Surface Dose Rate and/or source term used for Design Basis Fuel

Table M.5-37
0.6 kW Fuel in the Transfer Cask

Burnup (GWd/MTU)	Initial Enrichment (wt. % U-235)	Cooling Time (years)	Cask Centerline Side		
			neutron (mrem/hr)	gamma (mrem/hr)	Total (mrem/hr)
20	2	5	3.98	2.66	6.64
25	2.1	6	9.14	3.76	12.90
	4.7	5	1.76	2.10	3.88
28	2.3	7	12.14	4.26	16.40
	4.2	6	3.74	2.26	5.98
30	2.5	8	13.54	4.40	17.94
	3.5	7	7.34	2.98	10.32
32	2.6	9	15.98	4.86	20.84
	3.6	8	8.90	3.18	12.08
34	2.7	10	18.58	5.40	23.98
	4.5	9	6.98	2.52	9.50
36	2.8	12	20.50	5.70	26.20
	3.7	11	12.68	3.80	16.48
38	3.0	14	21.14	5.72	26.86
	3.9	13	13.42	3.84	17.24
39	3.0	15	22.66	6.04	28.70
	4.2	14	12.46	3.54	15.98
40	3.1	17	22.06	5.80	27.86
	3.2	16	21.68	5.74	27.42
	4.5	15	11.62	3.26	14.88
41	3.1	18	23.50	6.12	29.62
	3.6	17	18.72	4.96	23.68
	5.0	16	9.96	2.82	12.78
42	3.1	19	24.96	6.44	31.40
	4.0	18	16.34	4.34	20.68
43	3.2	21	24.18	6.20	30.36
	3.3	20	23.82	6.14	29.94
	4.5	19	13.76	3.66	17.44
44	3.3	22	24.26	6.20	30.46
	3.7	21	20.62	5.32	25.92
	4.9	20	12.28	4.32	16.60
45	3.3	23	25.58	6.50	32.08
	4.1	22	18.02	4.64	22.66

Bold indicates Maximum Calculated Surface Dose Rate and/or source term used for Design Basis Fuel

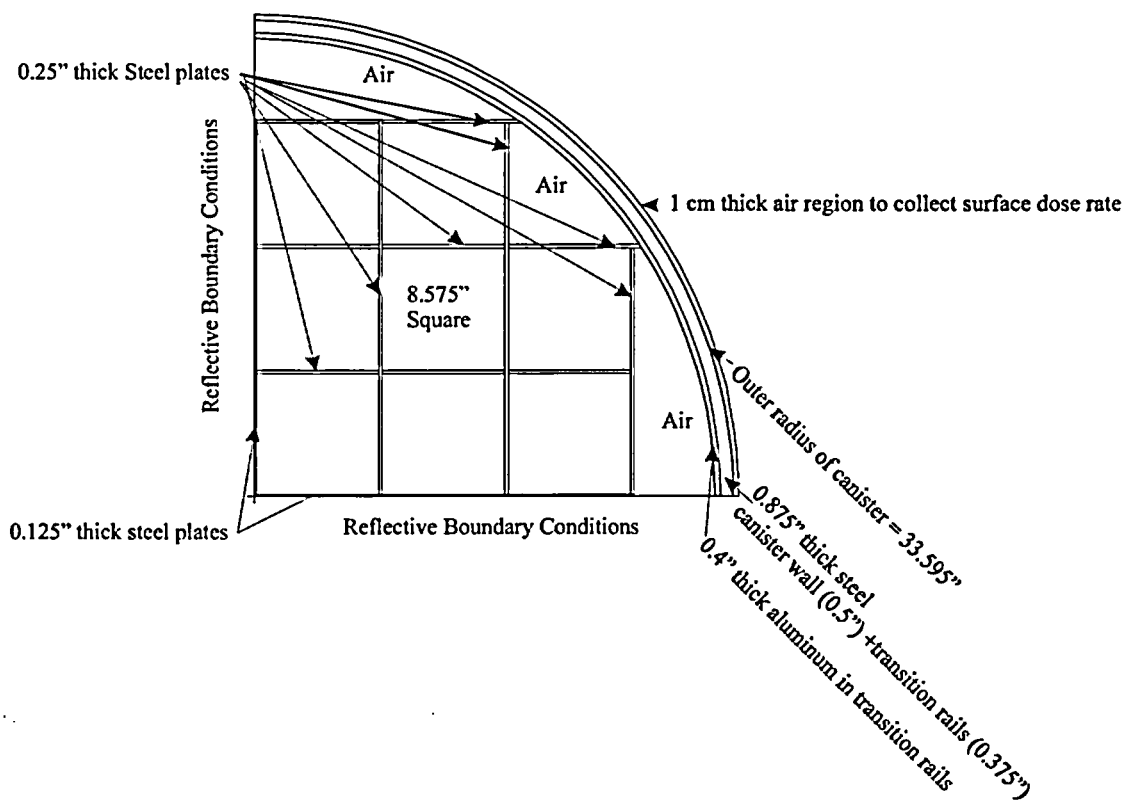
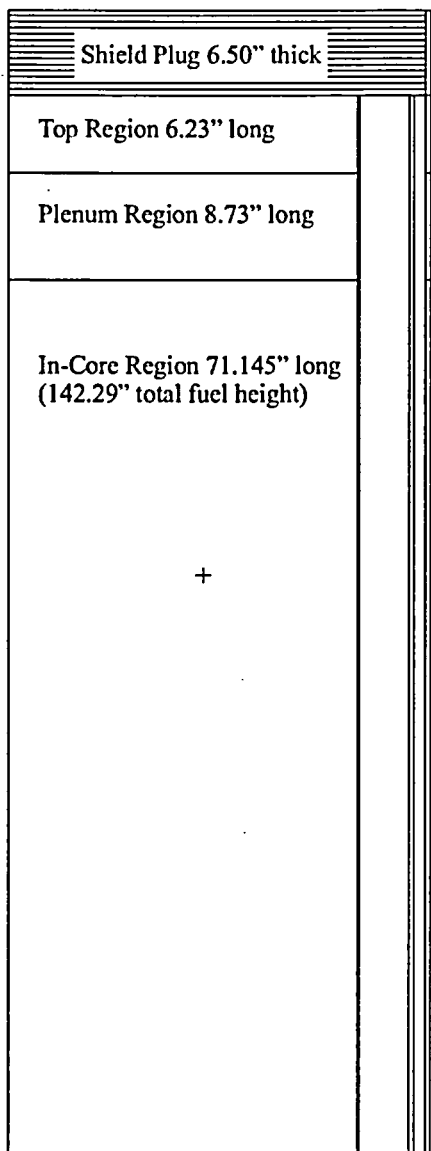


Figure M.5-1
Explicit MCNP Model – Radial View



Reflective Boundary Condition

Figure M.5-2
Explicit and Smeared MCNP Model – Axial View

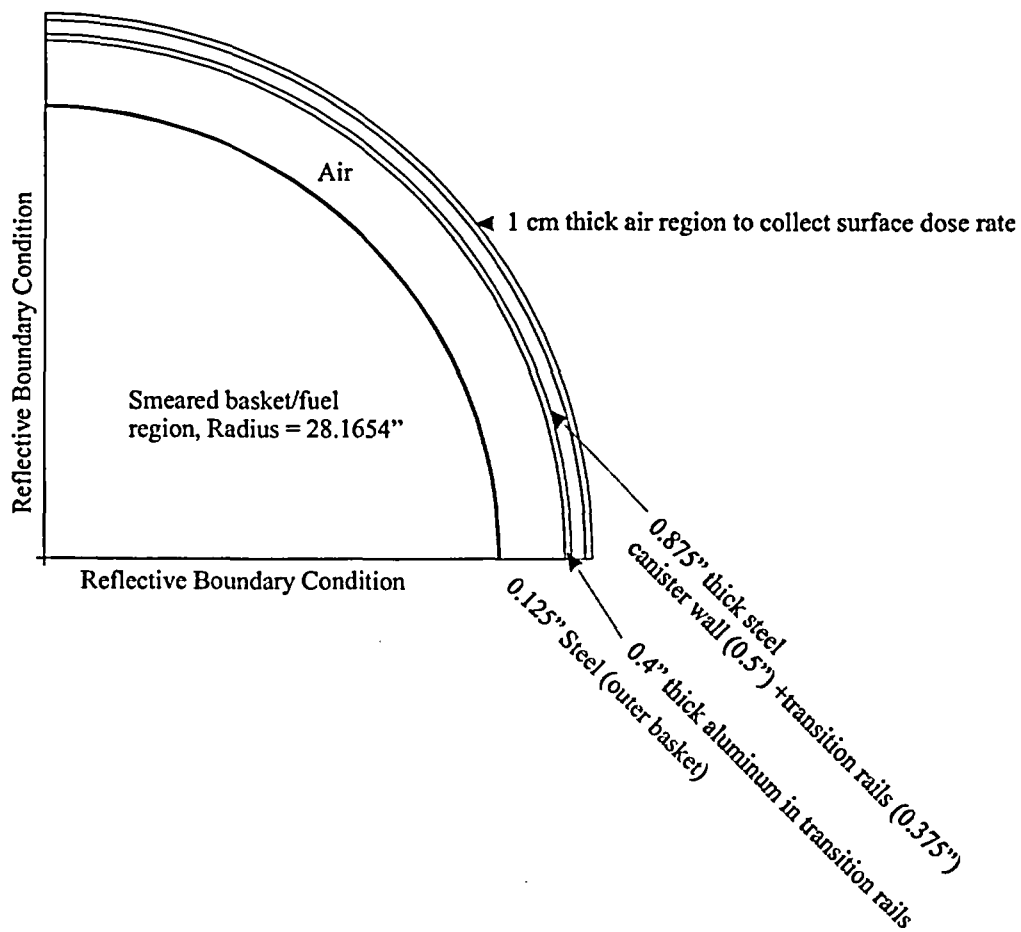


Figure M.5-3
Smeared MCNP Model – Radial View

Figure Withheld Under 10 CFR 2.390

Figure M.5-4
HSM Roof Model Geometry (32PT-S125/32PT-L125 DSC Configuration)

NUH-003
Revision 8

Page M.5-103

June 2004

Figure Withheld Under 10 CFR 2.390

**Figure M.5-5
HSM Floor Model Geometry (32PT-S125/32PT-L125 DSC Configuration)**

Figure Withheld Under 10 CFR 2.390

Figure M.5-6
HSM Side Model Geometry (32PT-S125/32PT-L125 DSC Configuration)

NUH-003
Revision 8

Page M.5-105

June 2004

Figure Withheld Under 10 CFR 2.390

Figure M.5-7
HSM Top Model Geometry (32PT-S125/32PT-L125 and 32PT-S100/32PT-L100 DSC
Configuration)

Figure Withheld Under 10 CFR 2.390

**Figure M.5-8
HSM Roof Model Geometry (32PT-S100/32PT-L100 DSC Configuration)**

**NUH-003
Revision 8**

Page M.5-107

June 2004

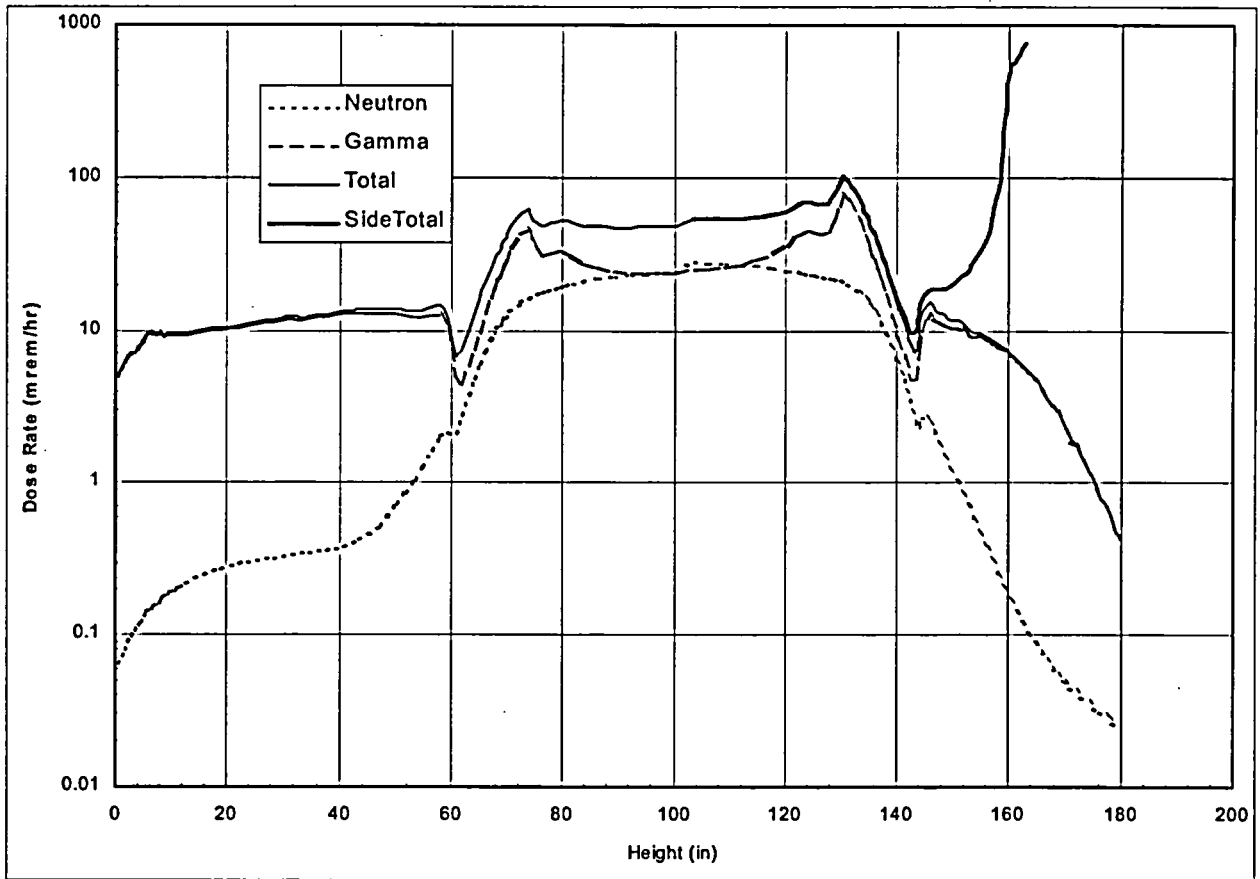


Figure M.5-9
HSM Front Wall Dose Rate Distribution (32PT-S125/32PT-L125 DSC Configuration)

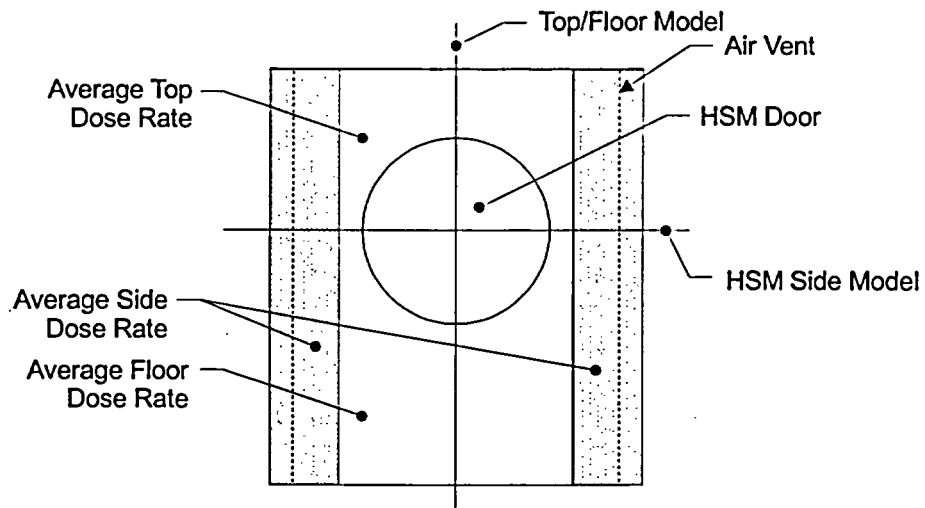
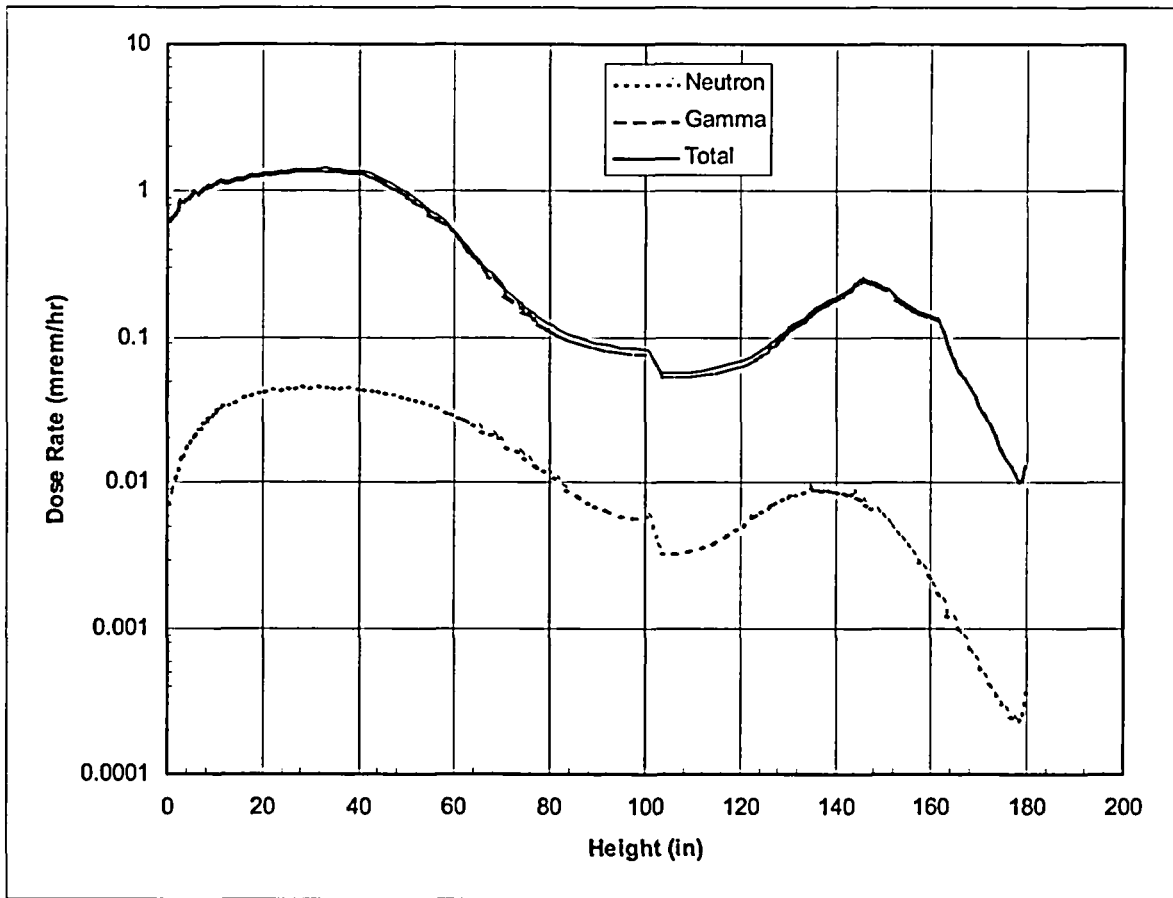


Figure M.5-10
Geometry for Front Wall Average Dose Rate Calculation



**Figure M.5-11
HSM Back Wall Dose Rate Distribution (32PT-S125/32PT-L125 DSC Configuration)**

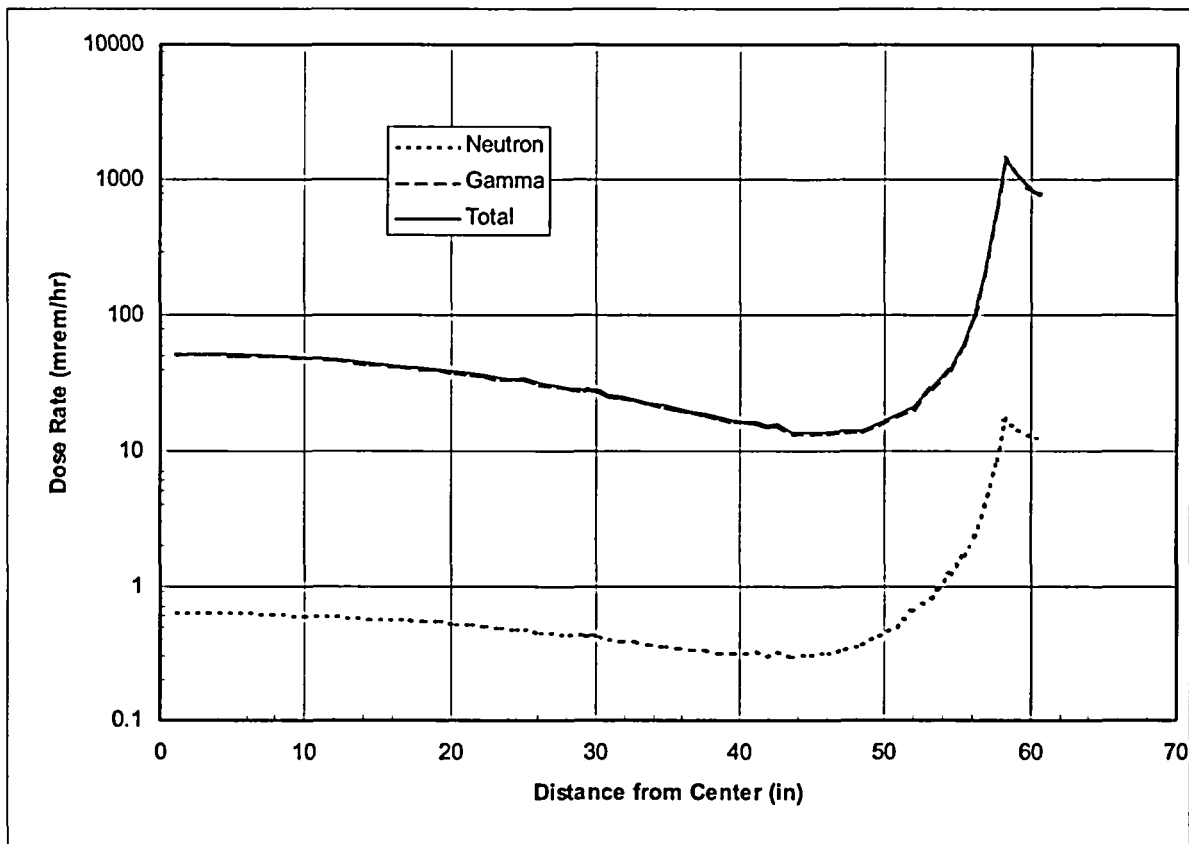


Figure M.5-12
HSM Roof Dose Rate Distribution Perpendicular to DSC Axis(32PT-S125/32PT-L125 DSC Configuration)

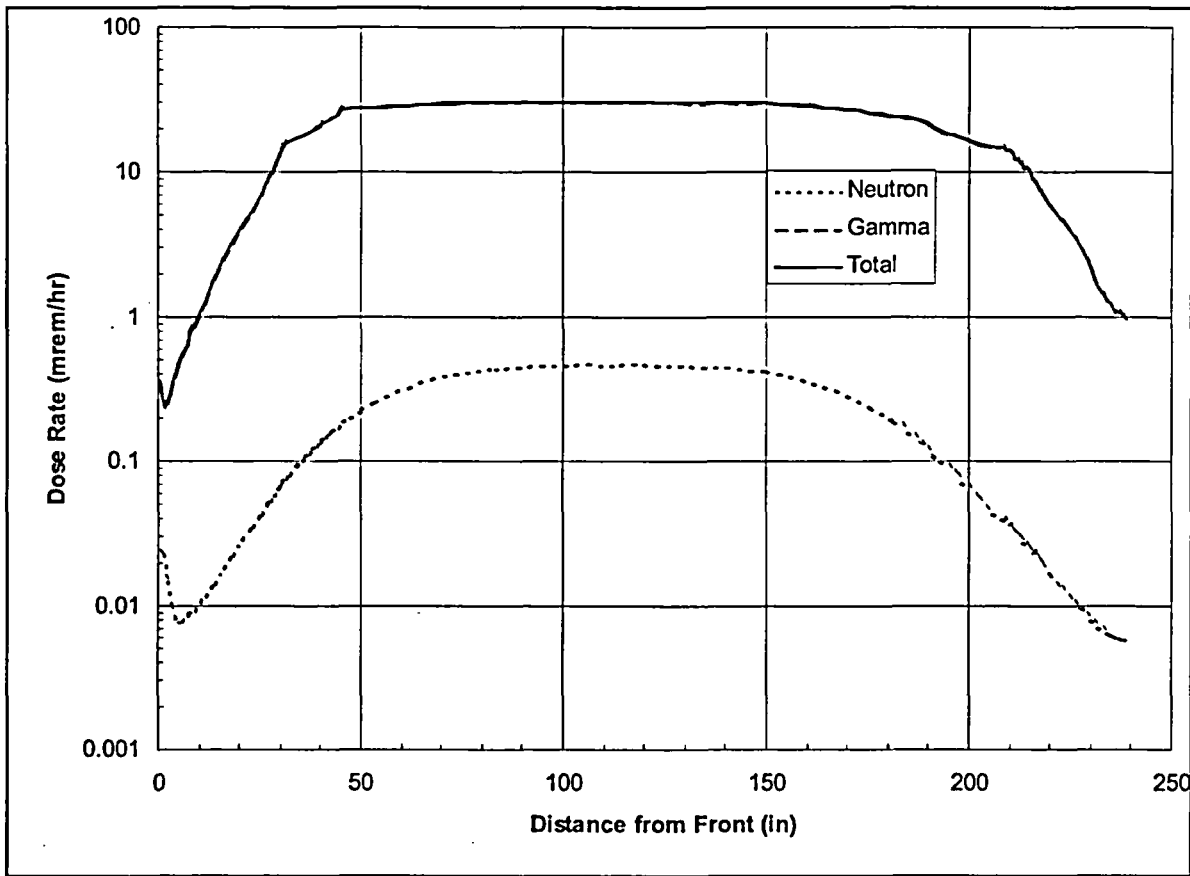


Figure M.5-13
HSM Roof Dose Rate Distribution Parallel to DSC Axis (32PT-S125/32PT-L125 DSC Configuration)

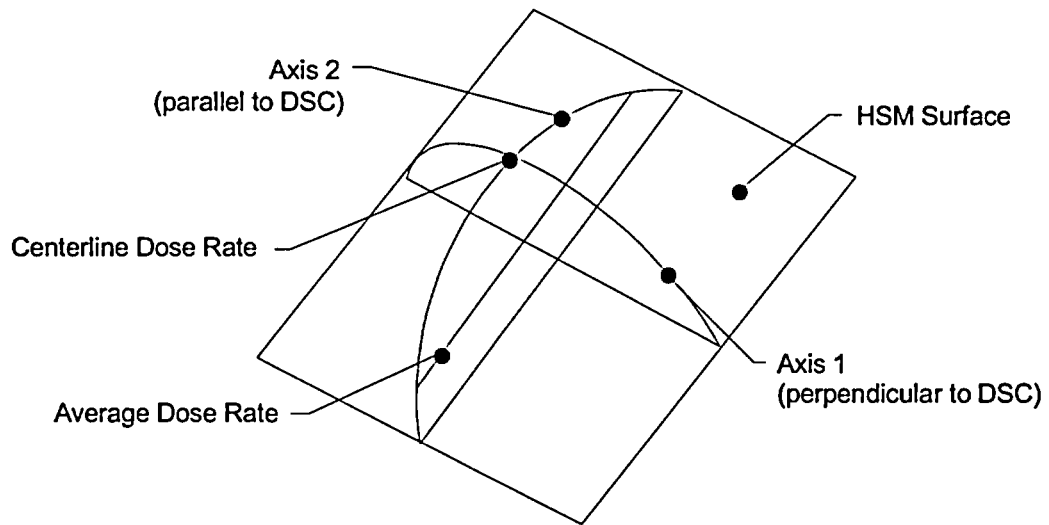


Figure M.5-14
Surface Average Calculation Geometry

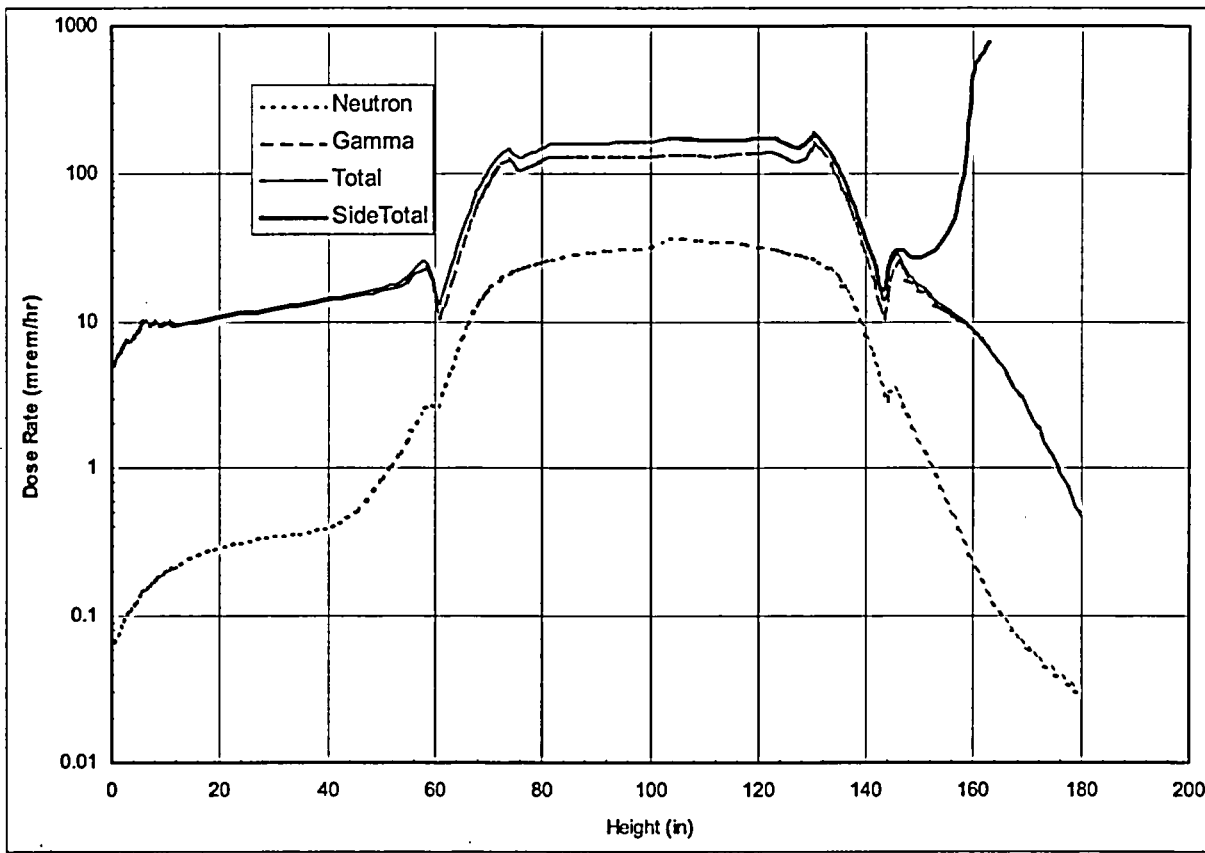


Figure M.5-15
HSM Front Wall Dose Rate Distribution (32PT-S100/32PT-L100 DSC Configuration)

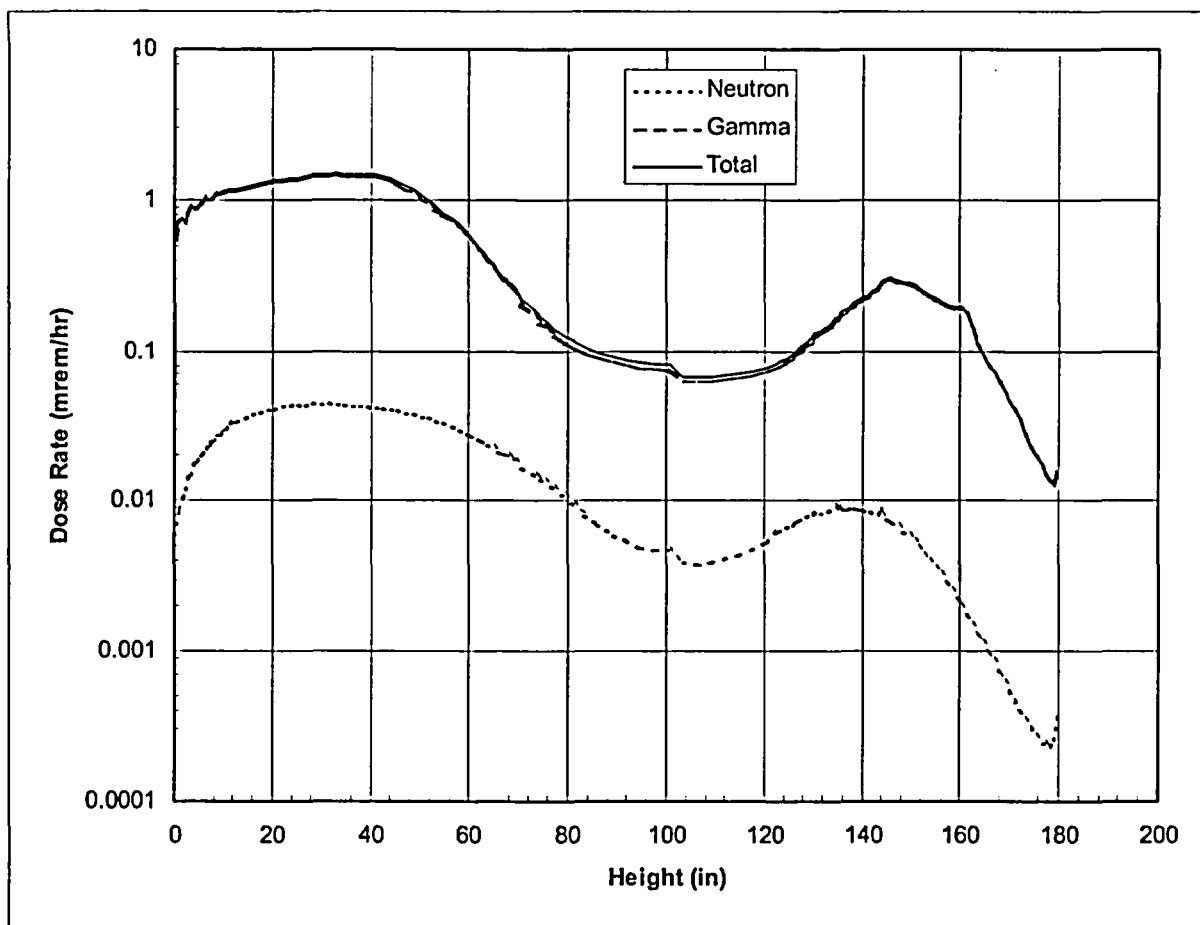


Figure M.5-16
HSM Back Wall Dose Rate Distribution (32PT-S100/32PT-L100 DSC Configuration)

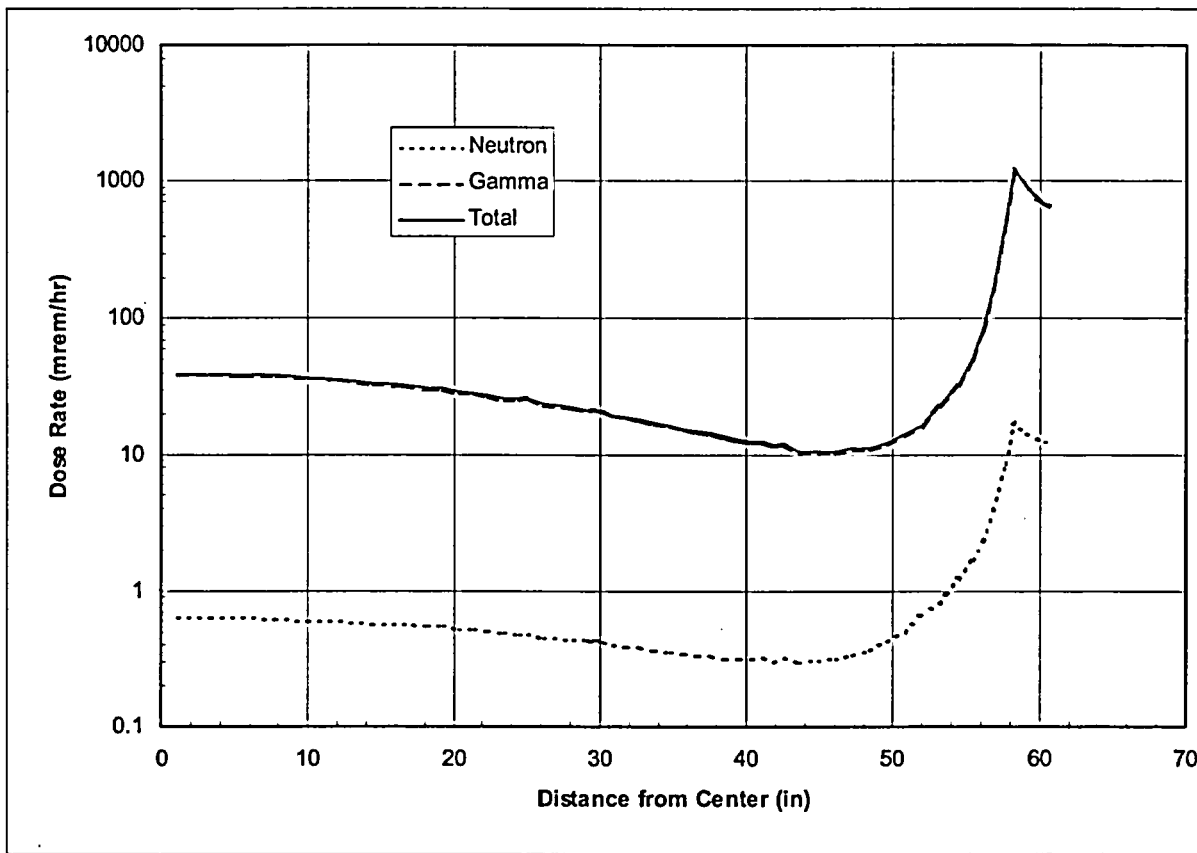


Figure M.5-17
HSM Roof Dose Rate Distribution Perpendicular to DSC Axis (32PT-S100/32PT-L100 DSC Configuration)

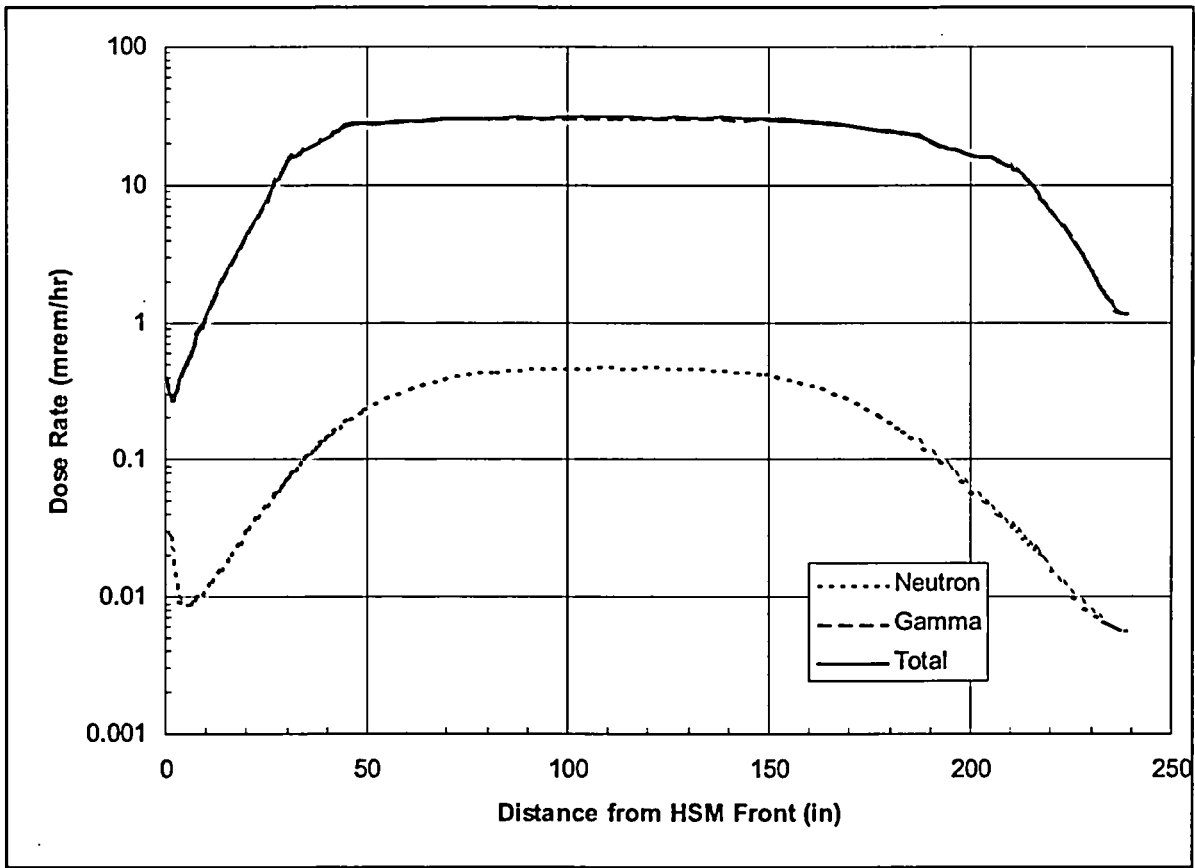


Figure M.5-18
HSM Roof Dose Rate Distribution Parallel to DSC Axis (32PT-S100/32PT-L100 DSC Configuration)

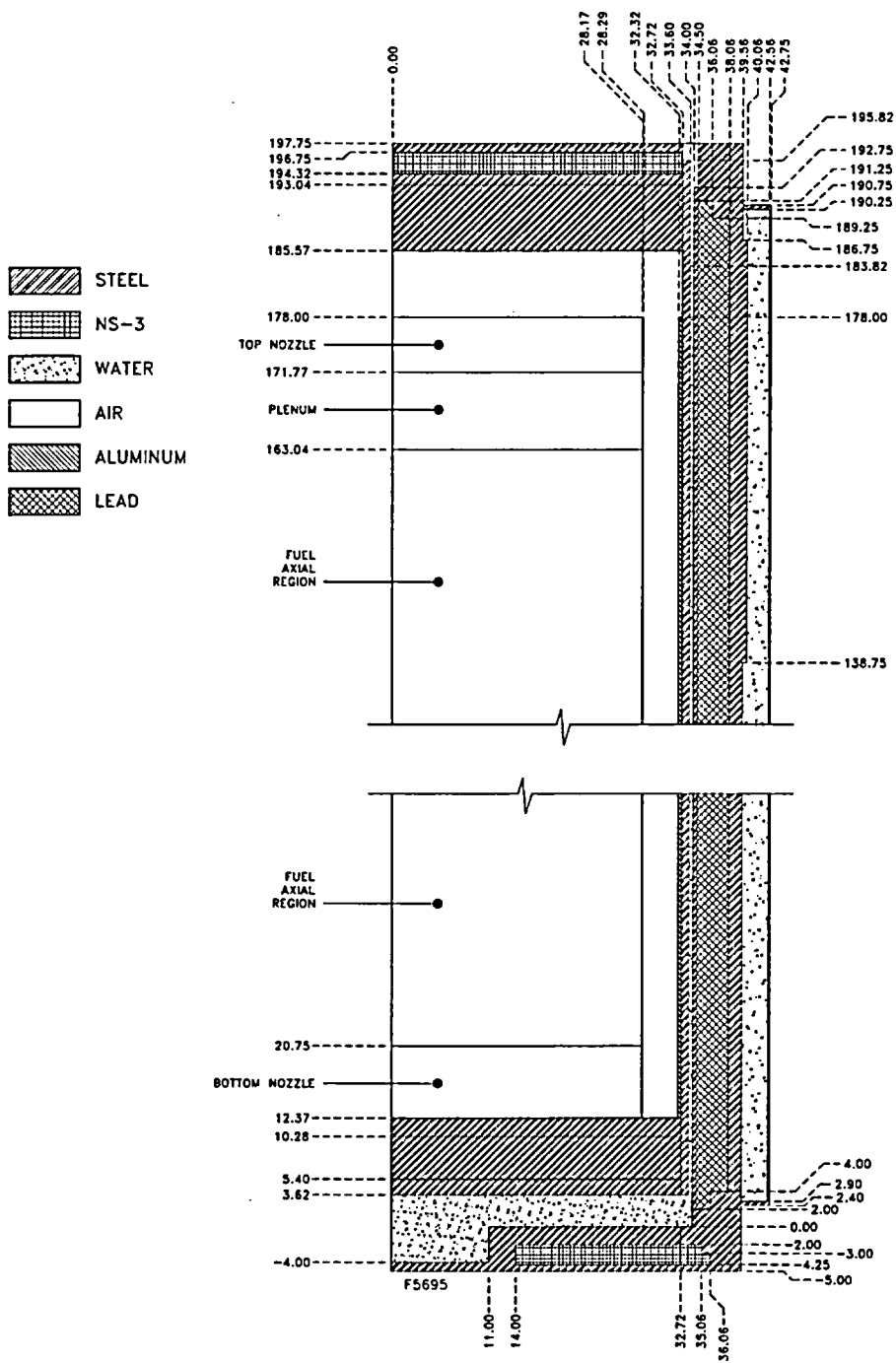


Figure M.5-19
Cask Model Geometry (32PT-S125/32PT-L125 DSC Configuration)

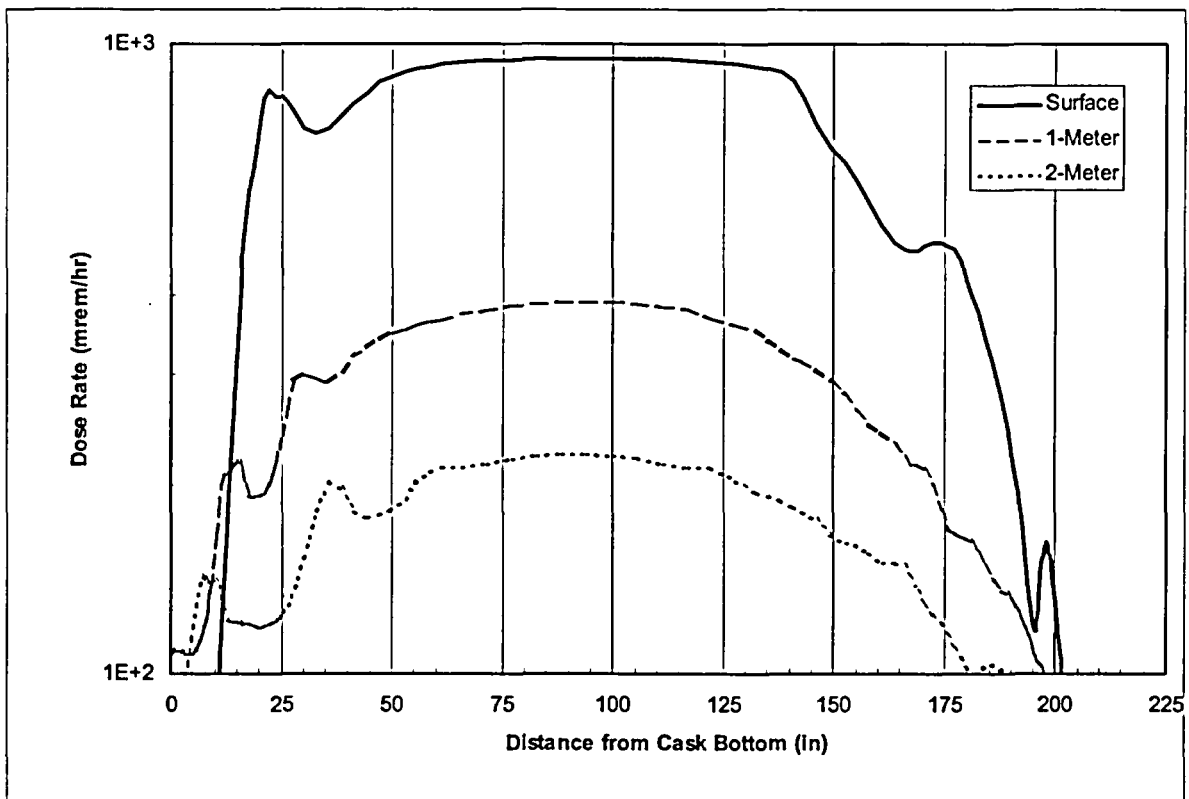


Figure M.5-20
Dose Rate Distribution Along Cask Side During Onsite Transfer (32PT-S125/32PT-L125 DSC Configuration)

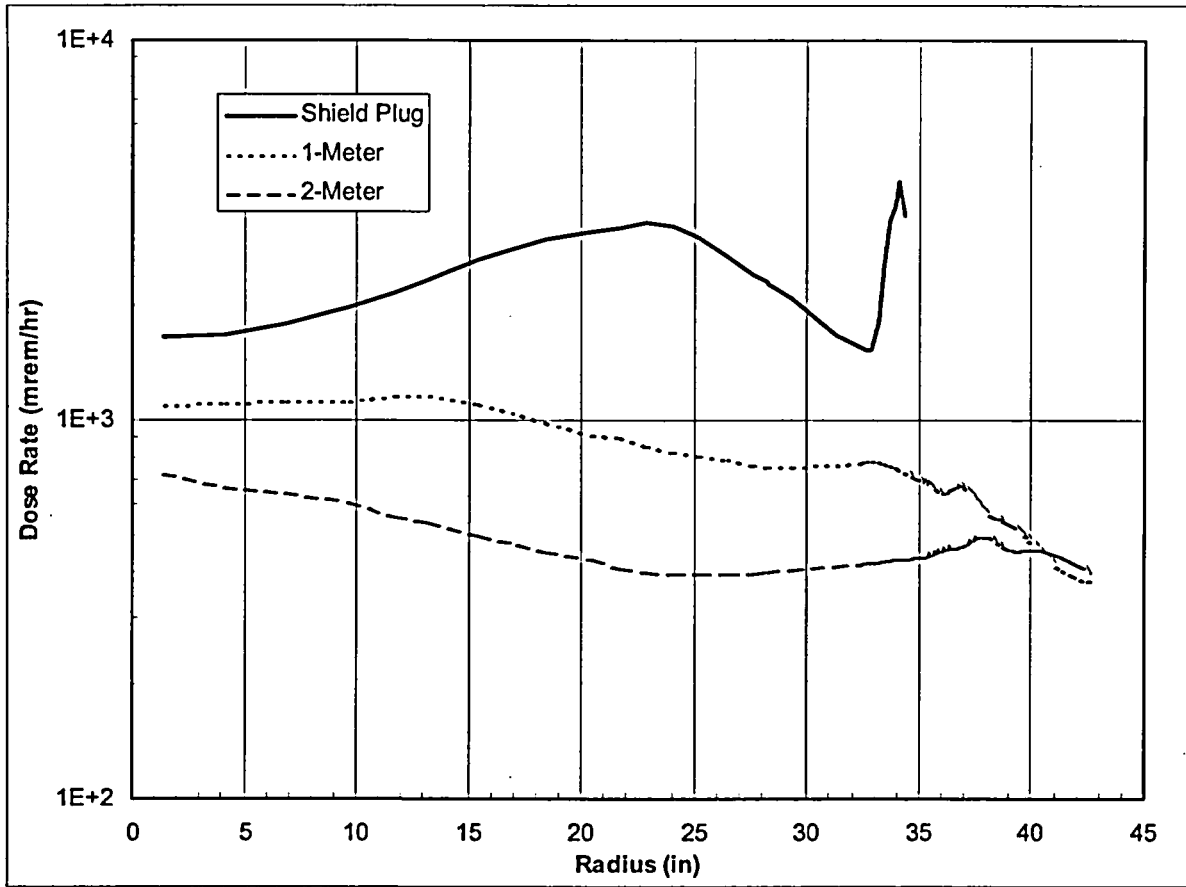


Figure M.5-21
Cask Top-End Dose Rates During Decontamination (32PT-S125/32PT-L125 DSC Configuration)

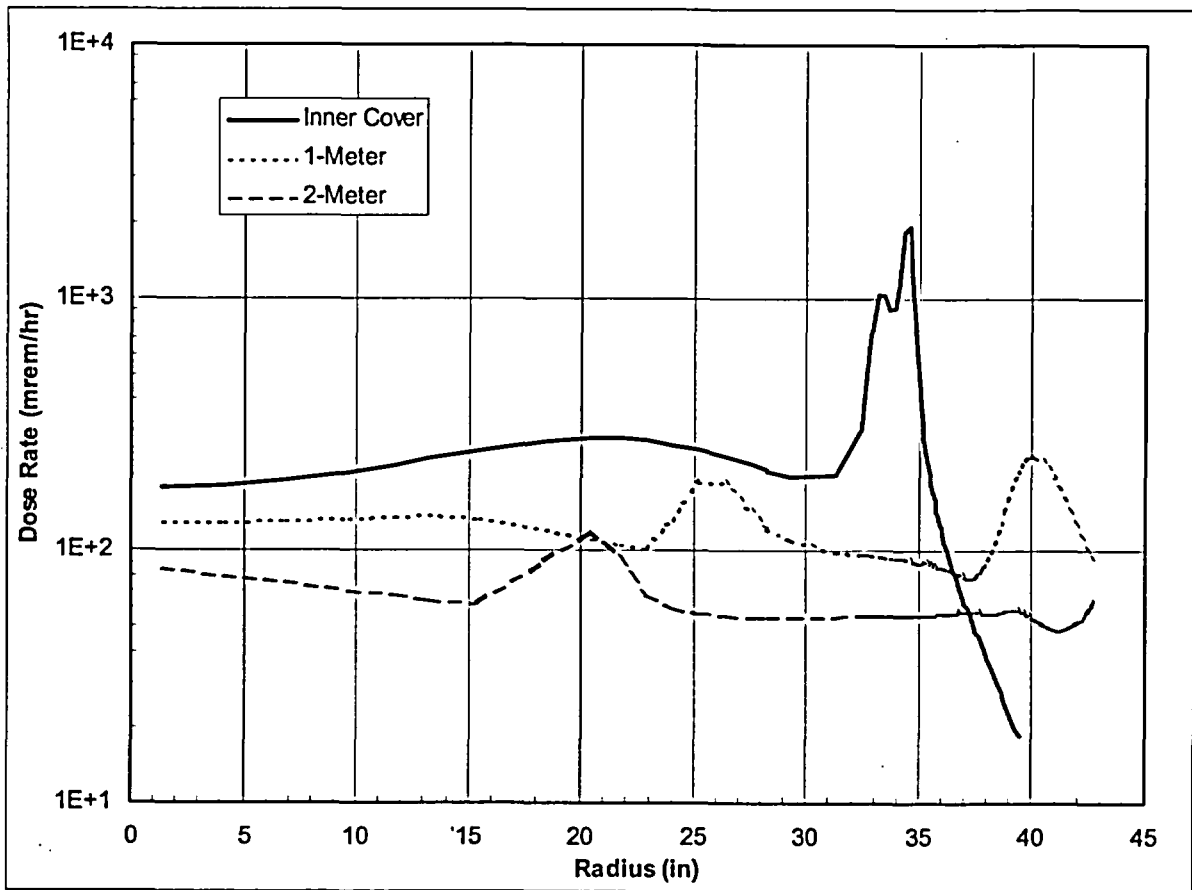


Figure M.5-22
Cask Top-End Dose Rates During Inner Cover Welding (32PT-S125/32PT-L125 DSC Configuration)

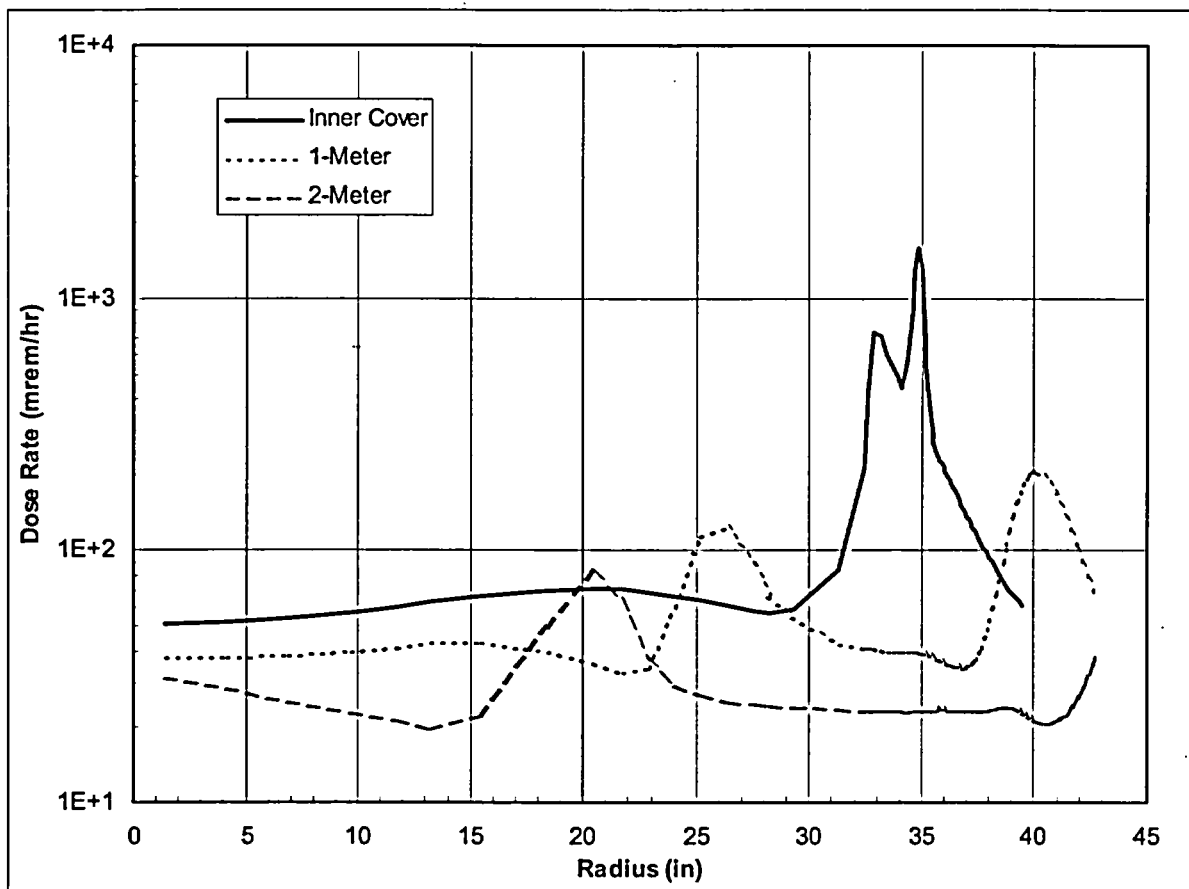


Figure M.5-23
Cask Top-End Dose Rates During Outer Cover Welding (32PT-S125/32PT-L125 DSC Configuration)

Figure Withheld Under 10 CFR 2.390

**Figure M.5-24
Cask Model Geometry (32PT-S100/32PT-L100 DSC Configuration)**

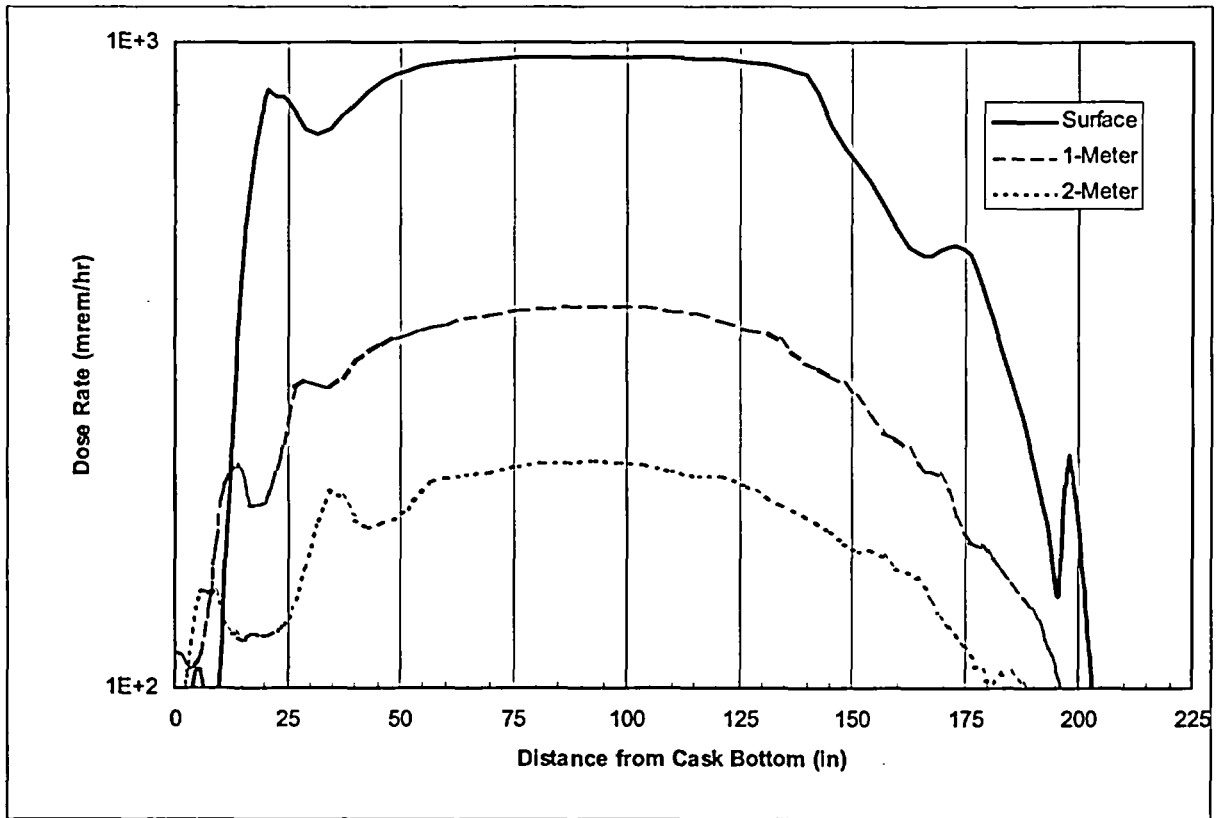


Figure M.5-25
Dose Rate Distribution Along Cask Side During Onsite Transfer (32PT-S100/32PT-L100
DSC Configuration)

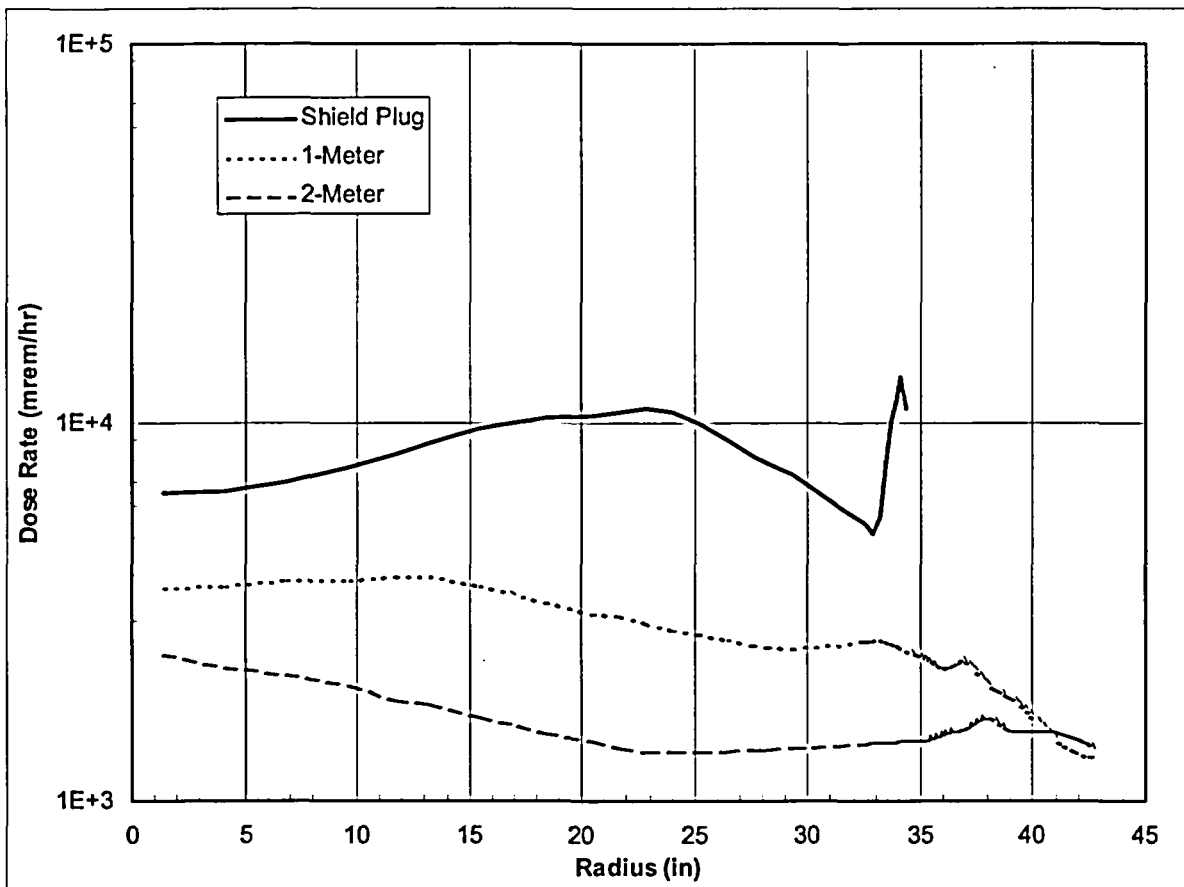


Figure M.5-26
Cask Top-End Dose Rates During Decontamination (32PT-S100/32PT-L100 DSC Configuration)

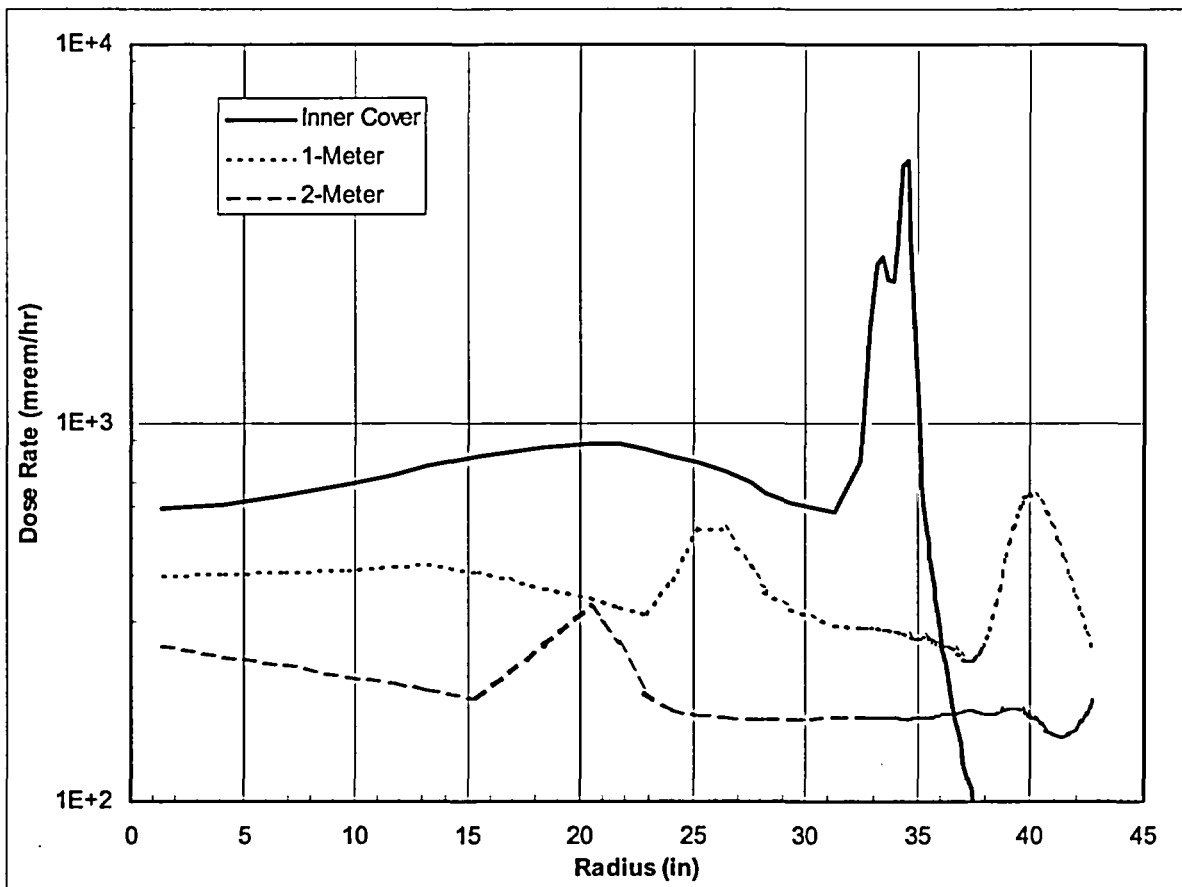


Figure M.5-27
Cask Top-End Dose Rates During Inner Cover Welding (32PT-S100/32PT-L100 DSC Configuration)

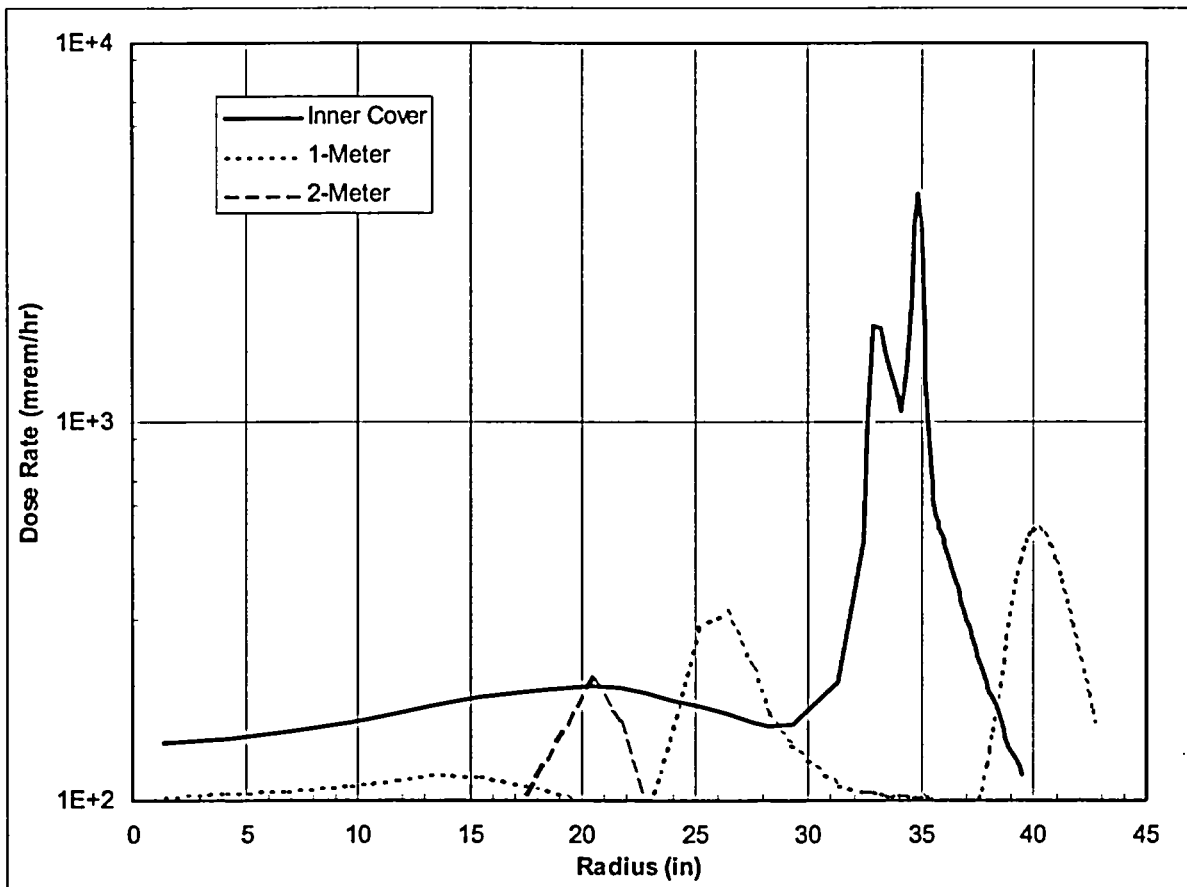


Figure M.5-28
Cask Top-End Dose Rates during Outer Cover Welding (32PT-S100/32PT-L100 DSC Configuration)

Figure Withheld Under 10 CFR 2.390

Figure M.5-29
MCNP Model – Cut Along Axial Centerline of the DSC (32PT-S100/32PT-L100 DSC
Configuration)

Figure Withheld Under 10 CFR 2.390

**Figure M.5-30
MCNP Model – Cut through the Centerline of the DSC (32PT-S100/32PT-L100 DSC
Configuration)**

Figure Withheld Under 10 CFR 2.390

**Figure M.5-31
ANISN HSM Model**

Figure Withheld Under 10 CFR 2.390

**Figure M.5-32
ANISN TC Model**

M.6 Criticality Evaluation

The design criteria for the NUHOMS[®]-32PT DSC requires that the fuel loaded in the DSC remain subcritical under normal, and accident conditions as defined in 10CFR Part 72.

The NUHOMS[®]-32PT DSC system's criticality safety is ensured by fixed neutron absorbers, soluble boron in the pool and favorable geometry. Burnup credit is not taken in this criticality evaluation. The fixed neutron absorbers are present in the form of borated metallic plates and Poison Rod Assemblies (PRAs) which are inserted in the guide tubes of certain assemblies in the basket. These materials are ideal for long-term use in the radiation and thermal environments of a DSC. The minimum required boron-10 loading for the metallic plates is 0.0070 g/cm² (90% credit taken in the criticality analysis or 0.0063 g/cm²). Metal Matrix Composites (MMCs) at a minimum areal density of 0.0070g/cm² have been qualified for use as a neutron absorber with 90% credit as justified in Section M.9.7.3.2. Similarly, Section M.9.7.3.1 provides the justification for the use of 90% credit for borated aluminum. In addition to the fixed neutron poison in the basket, PRAs may be required for the center four, eight or sixteen assemblies depending on fuel assembly design and initial enrichment. The minimum required B₄C content of the PRAs is 40% Theoretical Density (TD) with 75% credit taken in the criticality analysis or 30% TD.

Basket designations as a function of number of PRAs are as follows:

32PT DSC Basket Type	Number of PRAs
A	0
B	4
C	8
D	16

Thus, a basket with no PRAs is a Type "A" basket. Similarly, a basket that can accommodate 0, 4, 8, or 16 PRAs is a Type "A/B/C/D" basket.

M.6.1 Discussion and Results

Figure M.6-1 shows the cross section of the NUHOMS[®]-32PT DSC. The NUHOMS[®]-32PT DSC stainless steel basket consists of a welded plate or tube design. The welded plates or tubes form 32 compartments with sufficient space to accommodate aluminum or poison/aluminum inserts and a PWR fuel assembly. The fuel compartment structure is connected to perimeter transition rail assemblies as shown on the drawings in Section M.1.5. The poison/aluminum plates and aluminum plates are located inside the fuel compartments. The poison plates may be arranged in any of the following configurations: a 20 poison plate configuration (base configuration), as shown in Figure M.6-1; an alternate 16 poison plate configuration, as shown in Figure M.6-13; and another alternate 24 poison plate configuration, as shown in Figure M.6-14. Figure M.6-2 through Figure M.6-4 show the fuel compartments that must contain PRAs for loading configurations that require four, eight or sixteen PRAs. The 20 poison plate basket configuration shown in Figure M.6-1 is analyzed as a Type A/B/C/D basket while the 24 poison plate basket configurations shown in Figure M.6-14 is analyzed as an Alternate Type A/B/C/D basket. The 16 poison plate basket configuration shown in Figure M.6-13 is also analyzed as an Alternate Type A basket.

The analysis presented herein is performed for a NUHOMS[®]-32PT DSC in the NUHOMS[®] OS197/197H Transfer Casks (TCs) during normal and accident loading conditions. The NUHOMS[®] OS197/197H TCs consists of an inner stainless steel shell, lead gamma shield, a stainless steel structural shell and a hydrogenous (liquid) neutron shield. This analysis is applicable to any licensed cask of similar construction. The NUHOMS[®]-32PT DSC/TC configuration is shown to be sub-critical under normal and accident conditions of loading, transfer and storage.

The criticality analysis determines the most reactive configuration for the basket and assembly location. Then criticality calculations evaluate a variety of fuel assembly types, initial enrichments and PRA configurations. Finally, the maximum allowed initial enrichment for each assembly type/PRA configuration is determined. The maximum allowed initial enrichment for each assembly type/PRA configuration is listed in Table M.6-1. The calculations determine k_{eff} with the CSAS25 control module of SCALE-4.4 [6-1] for each assembly type/PRA configuration and initial enrichment, including all uncertainties to assure criticality safety under all credible conditions.

The results of the evaluation demonstrate that the maximum expected k_{eff} , including statistical uncertainty, will be less than the Upper Subcritical Limit (USL) determined from a statistical analysis of benchmark criticality experiments. The statistical analysis procedure includes a confidence band with an administrative safety margin of 0.05.

M.6.2 Package Fuel Loading

The NUHOMS®-32PT DSC is capable of transferring and storing PWR fuel assemblies. Table M.6-2 lists the fuel assemblies considered as authorized contents of the NUHOMS®-32PT DSC.

Table M.6-3 lists the fuel parameters for the PWR fuel assemblies. Reload fuel from other manufacture's with the same parameters are also considered as authorized contents.

For the B&W 15x15 and WE 17x17 class assemblies BPRAs are also included as authorized contents. The only change to the package fuel loading is the addition of BPRAs that are modeled as $^{11}\text{B}_4\text{C}$. Since BPRAs displace borated moderator in the assembly guide tubes, an evaluation is performed to determine the potential impact of BPRAs on the system reactivity. No credit is taken for BPRAs cladding and absorbers, rather the BPRAs are modeled as $^{11}\text{B}_4\text{C}$ in the entire guide tube of the respective design. Thus, the highly borated moderator between the guide tube and the BPRAs rodlet is modeled as $^{11}\text{B}_4\text{C}$. The inclusion of more Boron-11 and carbon enhances neutron scattering causing the neutron population in the fuel assembly to be slightly increased which increases reactivity. Therefore, these calculations bound any BPRAs design that is compatible with B&W 15x15 and WE 17x17 class assemblies. The fuel assembly dimensions reported in Table M.6-3 remain unchanged for the BPRAs cases. The models that include BPRAs only differ in that the region inside the guide tubes and instrument tube are modeled as $^{11}\text{B}_4\text{C}$ instead of moderator or PRAs.

Table M.6-4 lists the minimum B_4C contents for PRAs for the various assembly classes. The linear B_4C content per PRA rod used in the KENO V.a model is calculated by multiplying the B_4C density modeled by the cross-sectional area of the poison rod as modeled. Taking the modeled linear B_4C content and dividing by 0.75, to account for the fact that we only take credit for 75% of the B-10 in the analysis, calculates the minimum linear B_4C content per PRA rod specified in Table M.6-4. For example, the modeled B_4C density is 0.756 g/cm^3 . For the B&W 15 x15 PRA, the poison in the PRA is modeled with a radius of 0.55 cm. The cross sectional area of the poison is therefore $\pi(0.55)^2$ or 0.950 cm^2 . Therefore, the modeled linear B_4C density is 0.72 g/cm and the minimum specified B_4C density is 0.96 g/cm .

M.6.3 Model Specification

The following subsections describe the physical models and materials of the NUHOMS[®]-32PT DSC as loaded and transferred in the NUHOMS[®] OS197 or OS197H TC used for input to the CSAS25 module of SCALE-4.4 [6-1] to perform the criticality evaluation. The reactivity of canister under storage conditions is bounded by the TC analysis with zero internal moderator density case. The TC analysis with zero internal moderator density case bounds the storage conditions in the HSM because (1) the canister internals are always dry (purged and backfilled with He) while in the HSM, and (2) the TC contains materials such as steel and lead which provide close reflection of fast neutrons back into the fueled basket while the HSM materials (concrete) are much further from the sides of the DSC and thereby tend to reflect thermalized neutrons back to the canister which are absorbed in the canister materials reducing the system reactivity.

M.6.3.1 Description of Calculational Model

The TC and canister are explicitly modeled using the appropriate geometry options in KENO V.a of the CSAS25 module in SCALE-4.4. Several models are developed to evaluate the fabrication tolerances of the canister, basket, fuel clad outer diameter, fuel assembly locations, fuel assembly type, initial enrichments, PRA locations and storage of BPRAs with the B&W 15x15 and WE 17x17 assembly classes.

The first model is a full active-fuel height and full radial cross section of the canister and TC with reflective boundary conditions on the ends and sides. The model does not explicitly include the water neutron shield. However, the infinite array of TCs without the neutron shield does contain unborated water between the TCs. KENO plots of these models for each assembly class are included in Section M.6.6.2. This model is used to determine the most reactive fuel assembly for a given enrichment and without any PRAs, most reactive assembly-to-assembly pitch, and to determine the most reactive canister configuration accounting for manufacturing tolerances and fuel assembly clad outer diameter tolerances.

All calculations to determine the most reactive configuration are performed utilizing the configurations containing 20 poison plates. There is no change to the most reactive configuration due to a change in the number and orientation of the poison plates in the basket (16 poison plate and 24 poison plate configurations).

The second model is of the most reactive configuration identified above. This model is used to determine the maximum enrichment allowed for each assembly type as a function of the number of PRAs (none, four, eight and sixteen), as appropriate. In addition, the effect of BPRAs for the B&W 15x15 and WE 17x17 class assemblies for the various configurations are evaluated.

For the 24 plate poison configuration, not all fuel assembly classes are evaluated since these results are bounded by those based on the 20 poison plate configuration. Criticality calculations for the 16 poison plate and 24 poison plate configurations are carried out to ensure that the results based on the 20 poison plate configuration are bounding.

Figure M.6-5 is a sketch of each KENO V.a unit showing all materials and dimensions for each Unit and an annotated cross section map showing the assembled geometry units in the radial direction of the most reactive configuration identified in this evaluation. The bounding k_{eff} is calculated with a Westinghouse 17x17 LOPAR/Standard assembly with an initial enrichment of 3.4 wt. % U-235, with no PRAs and 32 BPRAs.

M.6.3.2 Package Regional Densities

The Oak Ridge National Laboratory (ORNL) SCALE code package [6-1] contains a standard material data library for common elements, compounds, and mixtures. All the materials used for the TC and canister analysis are available in this data library.

Table M.6-5 provides a complete list of all the relevant materials used for the criticality evaluation. The material density for the B-10 in the poison plates includes a 10% reduction and a 25% reduction for the PRAs.

M.6.4 Criticality Calculations

This section describes the analysis performed for the criticality analysis. The analyses are performed with the CSAS25 module of the SCALE system. A series of calculations are performed to determine the relative reactivity of the various fuel assembly designs evaluated and to determine the most reactive configuration without PRAs and BPRAs. The most reactive fuel for a given enrichment, as demonstrated by the analyses, is the B&W 15x15 Mark B assembly. The most reactive credible configuration is an infinite array of flooded TCs with minimum fuel compartment inner diameter, minimum basket structure thickness and minimum assembly-to-assembly pitch.

As mentioned in Section M.6.1, the NUHOMS[®]-32PT DSC (including the 16 poison plate and 24 poison plate alternate configurations) is evaluated to determine the maximum initial enrichment authorized for each assembly class without PRAs, and with four, eight and 16 PRAs, as applicable.

M.6.4.1 Calculational Method

M.6.4.1.1 Computer Codes.

The CSAS25 control module of SCALE-4.4 [6-1] is used to calculate the effective multiplication factor (k_{eff}) of the fuel in the TC. The CSAS25 control module allows simplified data input to the functional modules BONAMI-S, NITAWL-S, and KENO V.a. These modules process the required cross sections and calculate the k_{eff} of the system. BONAMI-S performs resonance self-shielding calculations for nuclides that have Bondarenko data associated with their cross sections. NITAWL-S applies a Nordheim resonance self-shielding correction to nuclides having resonance parameters. Finally, KENO V.a calculates the k_{eff} of a three-dimensional system. A sufficiently large number of neutron histories are run so that the standard deviation is below 0.0015 for all calculations.

M.6.4.1.2 Physical and Nuclear Data.

The physical and nuclear data required for the criticality analysis include the fuel assembly data and cross-section data as described below.

Table M.6-3 provides the pertinent data for criticality analysis for each fuel assembly evaluated in the NUHOMS[®]-32PT DSC.

The criticality analysis used the 44-group cross-section library built into the SCALE system. ORNL used ENDF/B-V data to develop this broad-group library specifically for criticality analysis of a wide variety of thermal systems.

M.6.4.1.3 Bases and Assumptions.

The analytical results reported in Section M.3.7 demonstrate that the TC containment boundary and canister basket structure do not experience any significant distortion under hypothetical accident conditions. Therefore, for both normal and hypothetical accident conditions the TC

geometry is identical except for the neutron shield and skin. As discussed above, the neutron shield and skin are conservatively removed and the interstitial space modeled as water.

The TC is modeled with KENO V.a using the available geometry input. This option allows a model to be constructed that uses regular geometric shapes to define the material boundaries. The following conservative assumptions are also incorporated into the criticality calculations:

1. No burnable poisons are accounted for in the fuel,
2. Water density is at optimum moderator density,
3. Unirradiated fuel – no credit taken for fissile depletion due to burnup or fission product poisoning,
4. The maximum lattice average fuel enrichment is modeled as uniform everywhere throughout the assembly. Natural uranium blankets and axial or radial enrichment zones are modeled as enriched uranium. It is assumed that the fuel assemblies are of uniform enrichment everywhere.
5. All fuel rods are filled with 100% moderator in the pellet/cladding gap,
6. Only the active fuel length of each assembly type is explicitly modeled with reflective boundary conditions on the ends; therefore the model is effectively infinitely long,
7. The neutron shield and stainless steel skin of the TC are stripped away and the infinite array of TCs are pushed close together with moderator in the interstitial spaces,
8. The least material condition (LMC) is assumed for the fuel compartment and fuel structure assemblies are pushed together toward the center maximizing reactivity; the reduction in steel thickness also reduces neutron absorption in the steel in the basket,
9. The transition rails between the basket and the canister shell are modeled as 100% aluminum. Steel and open space in the transition rails reduces reactivity because these materials have much higher absorption cross sections as compared to the aluminum,
10. Only 90% credit is taken for the B-10 in the poison plates and 75% credit for the B-10 in PRAs are credited in the KENO models,
11. Temperature is 20°C (293K),
12. Ninety six percent theoretical density for fuel which conservatively increases the total fuel content in the model, and
13. All stainless steel, including XM-19, is modeled as SS304; the small differences in the composition of the various stainless steels have no effect on results of the calculation.
14. The most reactive geometry remains unaffected for the 16 poison plate and 24 poison plate configurations.

M.6.4.1.4 Determination of k_{eff} .

The Monte Carlo calculations performed with CSAS25 (KENO V.a) use a flat neutron starting distribution. The total number of histories traced for each calculation is approximately 500,000. This number of histories is sufficient to converge the source and produce standard deviations of less than 0.15% in k_{eff} . The maximum k_{eff} for the calculation is determined with the following formula:

$$k_{\text{eff}} = k_{\text{KENO}} + 2\sigma_{\text{KENO}}.$$

M.6.4.2 Fuel Loading Optimization

Determination of the Most Reactive Fuel Type

All fuel lattices listed in Table M.6-3 are evaluated to determine the most reactive fuel assembly type with initial enrichments of 3.3 wt. % U-235. The fuel types are analyzed with water in the fuel pellet cladding annulus and are centered in the fuel compartments of the 20 poison plate configuration. Nominal basket dimensions are used in the KENO models. The effect of moderator density is also evaluated using the most reactive fuel type, B&W 15x15 Mark B.

- The canister/TC model for this evaluation differs from the actual design in the following ways:
- the boron 10 content in the poison plates is 10% lower than the minimum required,
- the neutron shield and the skin of the TC are conservatively replaced with water between the TCs, and
- the stainless steel and aluminum transition rails provide support to the fuel compartment grid are modeled as solid aluminum.

In all other respects, the model is the same as that described in Sections M.6.3.1 and M.6.1.1. KENO plots of these models are included in Section M.6.6.2.

Two typical input files are included in Section M.6.6.3, one without PRAs and one with four (4) PRAs. The results of these calculations are listed in Table M.6-6. The most reactive fuel type evaluated for the canister design for a given initial enrichment, without PRAs and without BPRAs, is the B&W 15x15 Mark B assembly.

Determination of the Most Reactive Configuration

The fuel-loading configuration of the canister/TC affects the reactivity of the package. Several series of analyses determine the most reactive configuration for the canister/TC.

For this analysis, the most reactive fuel type is used to determine the most reactive 20 poison plate configuration. The canister/TC is modeled over the active fuel height of the B&W 15x15 Mark B assembly with reflective boundary conditions on all sides. This represents an infinite array in the x-y direction of canisters/TCs that are conservatively infinite in length. The first model in this series of calculations is identical to the model used above. The canister/TC model for this evaluation differs from the actual design in the following ways:

- the boron 10 content in the poison plates is 10% lower than the minimum required,
- the stainless steel/aluminum transition rails provide support to the fuel compartment grid are modeled as various solid materials to determine the most reactive condition, and
- the neutron shield and the skin of the TC are conservatively replaced with water between the TCs.

Each evaluation is performed at 100% moderator density and again at 60% moderator density which is the most reactive moderator density as demonstrated by the results in Table M.6-6.

The first series of analyses examines the effect of the different materials used in the transition rails between the basket structure and canister shell on reactivity. The transition rails includes stainless steel and aluminum. Two cases with 2500 ppm borated water and pure water in the transition rail region are also included for completeness. The results in Table M.6-7 show a transition rail region filled with aluminum results in the most reactive condition. Therefore, all further analysis assumes solid aluminum in this region.

The second set of analysis evaluates the sensitivity of the system reactivity on fuel cladding OD. The model starts with the worst case above and the assembly cladding O.D. is varied from 0.420 to 0.440 inches. The results of this analysis demonstrate that cladding O.D. or thickness has a statistically insignificant effect on system reactivity. Therefore, the nominal clad thicknesses listed in Table M.6-3 are used for the balance of this evaluation. The results of the fuel clad OD evaluation are listed in Table M.6-8.

The third set of analyses evaluates the effect of neutron poison/aluminum plate thickness on the system reactivity. The model starts with the nominal clad OD model above. The poison plates consist of a poison/aluminum laminate. For this evaluation only the aluminum laminate thickness is varied. For the solid aluminum plate, the overall plate thickness is varied. Based on the results in Table M.6-9 the effect due to the variation in plate thickness is within the statistical uncertainty of the calculation. The nominal value, however, produced the maximum k_{eff} for both the 100 and 60% moderator density, where 60% moderator density represents the most reactive moderator density. Therefore, the nominal plate thickness is used for the balance of this evaluation.

The fourth set of analyses evaluates the effect of basket grid structure plate/tube thickness on reactivity. The model starts with the nominal poison/aluminum plate thickness above and the basket structure plate/tube thickness is varied from 0.235 to 0.26 inches. The results in Table M.6-10 show that the effect of basket structure plate/tube thickness has a statistically insignificant effect on reactivity. The most reactive calculated condition occurs with minimum basket structure plate/tube thickness because it allows the fuel assemblies to move slightly closer together. The balance of this evaluation uses the minimum basket structure plate/tube thickness because it represents the most reactive configuration.

The fifth set of analyses evaluates the effect of fuel compartment size on the system reactivity. The model starts with the minimum basket structure plate/tube thickness modeled as above because it represents the most reactive condition. For this evaluation the fuel compartment width is varied from 8.715 to 8.925 inches square. Note that these dimensions are the basket structure plate to plate distance or tube inner diameter. The actual space remaining for the fuel assembly is obtained by subtracting the poison/aluminum plate thickness. The results of the evaluation are given in Table M.6-11. The results show that the effect is within the statistical uncertainty of calculation. The most reactive configuration is with the minimum fuel compartment size because the assembly-to-assembly pitch is minimized. The balance of this evaluation use the minimum fuel compartment width because it represents the most reactive configuration.

The final series of sensitivity analyses determined the most reactive fuel assembly-to-assembly pitch. The most reactive configurations occur at the minimum assembly-to-assembly pitch. For assemblies with large cross sections such as the B&W 15x15 Mark B, however, there is little space for the assemblies to move with in the minimum fuel compartment modeled. The results in Table M.6-12 demonstrate that for the B&W 15x15 Mark B assembly the effect is within the statistical uncertainty of the calculation. For smaller assemblies such as the WE 14x14, this effect would be statistically significant because the assemblies have more space in which to move inside the fuel compartment, therefore the minimum assembly-to-assembly pitch is used for the balance of this analysis.

M.6.4.3 Studies with Radial Variation of Enrichment

The next set of analyses is for the Exxon/ANF 15x15 CE fuel assembly. These calculations justify the adequacy of the uniform maximum lattice average fuel enrichment assumed in the analysis. These calculations were carried out using a soluble boron concentration of 2500 ppm and a poison loading of 6.30 mg B-10/cm² with moderator densities (MD) varying from 40% to 100% of full density. The 16 poison plate configuration was utilized for these analyses and, the results are applicable to the 20 and 24 poison plate configuration and all basket types.

The different variable enrichments used in these calculations are shown in Table M.6-25. A plot of the fuel assembly with the radial variation in enrichment is shown in Figure M.6-17 and Figure M.6-18. The results for this evaluation are listed in Table M.6-26. Due to the higher initial enrichment values utilized to model the loading patterns 2A, 2B and 2C, the k_{eff} values shown in Table M.6-26 are higher than USL. The purpose of these calculations is to determine the sensitivity of k_{eff} due to radial variation of enrichment only and not to USL; hence, the results shown in Table M.6-26 are acceptable for these sensitivities studies.

The results demonstrate that the assumption of the uniform maximum lattice average enrichment is both appropriate and conservative. The k_{eff} of the system with the uniform maximum lattice average enrichment assumption is greater than that of the non-uniform case at all MD.

M.6.4.4 Determination of the Maximum Initial Enrichment for each Fuel Class and PRA Configuration

The most reactive configuration as determined in Section M.6.3.1 above, is with solid aluminum in the transition rail region, nominal poison/aluminum plate thickness, minimum basket structure

plate/tube thickness, minimum fuel compartment width, minimum assembly-to-assembly pitch and uniform maximum planar enrichment. The following analysis uses this configuration to determine the maximum allowed initial enrichment as a function of initial enrichment and PRA configuration for each assembly class. All three poison plate configurations (20 poison plate configuration, 16 poison plate configuration and 24 poison plate configuration) are evaluated in these calculations. Only the assembly type and PRA configuration is changed for each model. The most reactive assembly type for each assembly class is used for each evaluation. In addition, for each case the internal moderator density is varied to determine the peak reactivity for the specific configuration. The maximum initial enrichment for each assembly class and PRA configuration are provided in Table M.6-1.

The canister/TC model for this evaluation differs from the actual design in the following ways:

- the boron 10 content in the poison plates is 10% lower than the minimum required,
- the boron 10 content in the PRAs is 25% lower than the minimum required,
- the stainless steel/aluminum transition rails that provide support to the fuel compartment grid are modeled as various solid materials to determine the most reactive condition,
- BPRAs, when modeled, are modeled as solid $^{11}\text{B}_4\text{C}$ in the guide tubes and instrument tubes,
- the neutron shield and the skin of the TC are conservatively replaced with water between the TCs, and
- the worst case material conditions, as determined in Section M.6.4.2 above, are modeled.

The input file for the case with the highest calculated reactivity is included in Section M.6.6.4.

WE 17x17 Class Assemblies

The most reactive WE 17x17 class assembly is the WE 17x17 LOPAR/standard assembly as demonstrated in Table M.6-6. The results for the WE 17x17 class assembly calculations for the 20 poison plate configuration are listed in Table M.6-13 and Table M.6-14 for cases without and with BPRAs, respectively. The results for the WE 17x17 class assembly calculations for the 16 poison plate configuration are listed in Table M.6-27 and Table M.6-28 for cases without and with BPRAs, respectively. The results for the WE 17x17 class assembly calculations for the 24 poison plate configuration are listed in Table M.6-29 and Table M.6-30 for cases without and with BPRAs, respectively.

B&W 15x15 Class Assemblies

The most reactive B&W 15x15 class assembly is the B&W 15x15 Mark B assembly as demonstrated in Table M.6-6. The results for the B&W 15x15 class assembly calculations for the 20 poison plate configuration are listed in Table M.6-15 and Table M.6-16 for cases without and with BPRAs, respectively. The results for the B&W 15x15 class assembly calculations for the 16 poison plate configuration are listed in Table M.6-31 and Table M.6-32 for cases without and with BPRAs, respectively. The results for the B&W 15x15 class assembly calculations for the 24 poison plate configuration are listed in Table M.6-33 and Table M.6-34 for cases without and with BPRAs, respectively.

CE 15x15 Class Assemblies

The most reactive CE 15x15 class assembly is the CE 15x15 Palisades assembly as demonstrated in Table M.6-6. The results for the CE 15x15 class assembly calculations for the 20 poison plate configuration are listed in Table M.6-17 for cases without BPRAs. BPRAs are not authorized to be stored with CE 15x15 class assemblies.

The results for the CE 15x15 class assembly calculations for the 16 poison plate configuration are listed in Table M.6-35 for cases without BPRAs.

The results, however, shown only for the 20 poison plate and 16 poison plate configurations, are also applicable to 24 poison plate configuration.

WE 15x15 Class Assemblies

The most reactive WE 15x15 class assembly is the WE 15x15 Standard assembly as demonstrated in Table M.6-6. The results for the WE 15x15 class assembly calculations for the 20 poison plate configuration are listed in Table M.6-18 for cases without BPRAs. BPRAs are not authorized to be stored with WE 15x15 class assemblies. The results for the WE 15x15 class assembly calculations for the 16 poison plate configuration are listed in Table M.6-36 for cases without BPRAs. The results for the WE 15x15 class assembly calculations for the 24 poison plate configuration are listed in Table M.6-37 for cases without BPRAs.

CE 14x14 Class Assemblies

The most reactive CE 14x14 class assembly is the CE 14x14 Fort Calhoun assembly as demonstrated in Table M.6-6. The results for the CE 14x14 class assembly calculations for the 20 poison plate configuration are listed in Table M.6-19 for cases without BPRAs. BPRAs are not authorized to be stored with CE 14x14 class assemblies.

The results for the CE 14x14 class assembly calculations for the 16 poison plate configuration are listed in Table M.6-38 for cases without BPRAs. The results for the WE 15x15 class assembly calculations for the 24 poison plate configuration are listed in Table M.6-39 for cases without BPRAs.

WE 14x14 Class Assemblies

The most reactive WE 14x14 class assembly is the WE 14x14 ZCA/ZCB assembly as demonstrated in Table M.6-6. The results for the WE 14x14 class assembly calculations for the 20 poison plate configuration are listed in Table M.6-20 for cases without BPRAs. BPRAs are not authorized to be stored with WE 14x14 class assemblies.

The results for the CE 14x14 class assembly calculations for the 16 poison plate configuration are listed in Table M.6-40 for cases without BPRAs.

The results, however, shown only for the 20 poison plate and 16 poison plate configurations, are also applicable to 24 poison plate configuration.

M.6.4.5 Criticality Results

Table M.6-21 lists the bounding results for all conditions of storage. The highest calculated k_{eff} , including 2σ uncertainty, is for the WE 17x17 LOPAR/Standard assembly in the 20 poison plate configuration with an initial U-235 enrichment of 3.4 wt. %, no PRAs, and 24 BPRAs. The maximum allowed initial enrichment for each assembly type/PRA configuration is listed in Table M.6-1.

These criticality calculations were performed with CSAS25 of SCALE-4.4. For each case, the result includes (1) the KENO-calculated k_{KENO} , (2) the one sigma uncertainty σ_{KENO} , and (3) the final k_{eff} , which is equal to $k_{\text{KENO}} + 2\sigma_{\text{KENO}}$.

The criterion for subcriticality is that

$$k_{\text{KENO}} + 2\sigma_{\text{KENO}} \leq \text{USL},$$

where USL is the upper subcritical limit established by an analysis of benchmark criticality experiments. From Section M.6.5, the minimum USL over the parameter range is 0.9411. From Table M.6-21 for the most reactive case,

$$k_{\text{KENO}} + 2\sigma_{\text{KENO}} = 0.9389 + 2(0.0010) = 0.9409 \leq 0.9411.$$

M.6.5 Critical Benchmark Experiments

The criticality safety analysis of the NUHOMS[®] OS197/197H TC containing the NUHOMS[®] - 32PT DSC uses the CSAS25 module of the SCALE system of codes. The CSAS25 control module allows simplified data input to the functional modules BONAMI-S, NITAWL-S, and KENO V.a. These modules process the required cross-section data and calculate the k_{eff} of the system. BONAMI-S performs resonance self-shielding calculations for nuclides that have Bondarenko data associated with their cross sections. NITAWL-S applies a Nordheim resonance self-shielding correction to nuclides having resonance parameters. Finally, KENO V.a calculates the effective neutron multiplication (k_{eff}) of a 3-D system.

The analysis presented herein uses the fresh fuel assumption for criticality analysis. The analysis employs the 44-group ENDF/B-V cross-section library because it has a small bias, as determined by 121 benchmark calculations. The Upper Subcritical Limit (USL-1) was determined using the results of these 121 benchmark calculations.

The benchmark problems used to perform this verification are representative of benchmark arrays of commercial light water reactor (LWR) fuels with the following characteristics:

- (1) water moderation,
- (2) boron neutron absorbers,
- (3) unirradiated light water reactor type fuel (no fission products or "burnup credit") near room temperature (vs. reactor operating temperature),
- (4) close reflection, and
- (5) uranium oxide.

The 121 uranium oxide experiments were chosen to model a wide range of uranium enrichments, fuel pin pitches, assembly separation, concentration of soluble boron and control elements in order to test the codes ability to accurately calculate k_{eff} . These experiments are discussed in detail in Reference [6-2].

M.6.5.1 Benchmark Experiments and Applicability

A summary of all of the pertinent parameters for each experiment is included in Table M.6-22 along with the results of each run. The best correlation is observed for fuel assembly separation distance with a correlation of 0.68. All other parameters show much lower correlation ratios indicating no real correlation. All parameters were evaluated for trends and to determine the most conservative USL.

The USL is calculated in accordance to NUREG/CR-6361 [6-2]. USL Method 1 (USL-1) applies a statistical calculation of the bias and its uncertainty plus an administrative margin (0.05) to the linear fit of results of the experimental benchmark data. The basis for the

administrative margin is from Reference [6-3]. Results from the USL evaluation are presented in Table M.6-23.

The criticality evaluation used the same cross section set, fuel materials and similar material/geometry options that were used in the 121 benchmark calculations as shown in Table M.6-22. The modeling techniques and the applicable parameters listed in Table M.6-24 for the actual criticality evaluations fall within or very close the range of those addressed by the benchmarks in Table M.6-22.

M.6.5.2 Results of the Benchmark Calculations

The results from the comparisons of physical parameters of each of the fuel assembly types to the applicable USL value are presented in Table M.6-24. The minimum value of the USL is determined to be 0.9411 based on comparisons to the limiting assembly parameters as shown in Table M.6-24.

M.6.6 Appendix

M.6.6.1 References

- 6-1 Oak Ridge National Laboratory, RSIC Computer Code Collection, "SCALE: A Modular Code System for Performing Standardized Computer Analysis for Licensing Evaluations for Workstations and Personal Computers," NUREG/CR-0200, Revision 6, ORNL/NUREG/CSD-2/V2/R6.
- 6-2 U.S. Nuclear Regulatory Commission, "Criticality Benchmark Guide for Light-Water-Reactor fuel in Transportation and Storage Packages," NUREG/CR-6361, Published March 1997, ORNL/TM-13211.
- 6-3 U.S. Nuclear Regulatory Commission, "Recommendations for Preparing the Criticality Safety Evaluation of Transportation Packages," NUREG/CR-5661, Published April 1997, ORNL/TM-11936.

M.6.6.2 KENO Plots of Various Cases

The models used to determine the most reactive fuel, are reproduced below. Each model represents a different fuel assembly type. Each Unit in the KENO V.a model has a length equal to the active fuel height of the assembly modeled (see Table M.6-3) with reflective boundary conditions on the top, bottom and sides of the model.

M.6.6.3 Example CSAS25 Input Files (based on the 20 poison plate basket configuration)

The following input file listing is for the B&W 15x15 Mark B case BW15MB10.in.

```
=csas25
32P Most Reactive Fuel Analysis with B&W 15X15 Mark B, Jack Boshoven
03/29/01
44groupndf5 latticecell
uo2 1 0.96 293 92235 3.3 92238 96.7 end
zirc4 2 1.0 293 end
h2o 3 1.0 293 end
boron 3 den=0.0025 1.0 293 end
carbonsteel 4 1.0 293 end
ss304 5 1.0 293 end
al 6 1.0 293 end
al 7 0.9 293 end
b-10 7 den=0.033 1.0 293 end
b4c 8 0.3 293 end
h2o 9 1.0 293 end
pb 10 1.0 293 end
end comp
squarepitch 1.44272 0.936244 1 3 1.0922 2 0.95758 9 end
BW15MB10 2500 ppm dissolved boron; no control rods
read param
gen=500 npg=1000 nsk=5 nub=yes run=yes plt=yes
end param
read geom
unit 1 com='Fuel Rod'
cylinder 1 1 0.468122 360.172 0.0
cylinder 9 1 0.47879 360.172 0.0
cylinder 2 1 0.5461 360.172 0.0
cuboid 3 1 4p0.72136 360.172 0.0
unit 2 com='guide tube'
cylinder 3 1 0.63246 360.172 0.0
cylinder 2 1 0.6731 360.172 0.0
cuboid 3 1 4p0.72136 360.172 0.0
unit 3 com='instrument tube'
cylinder 3 1 0.56007 360.172 0.0
cylinder 2 1 0.62611 360.172 0.0
cuboid 3 1 4p0.72136 360.172 0.0
unit 4 com='top horizontal poison plate'
cuboid 7 1 2p10.71245 0.1905 0.0 360.172 0.0
cuboid 6 1 2p10.71245 0.3175 0.0 360.172 0.0
unit 5 com='bottom horizontal poison plate'
cuboid 6 1 2p10.71245 0.1270 0.0 360.172 0.0
cuboid 7 1 2p10.71245 0.3175 0.0 360.172 0.0
unit 6 com='right vertical poison plate'
```

```

cuboid      7   1  0.1905  0.0 2p10.71245  360.172 0.0
cuboid      6   1  0.3175  0.0 2p10.71245  360.172 0.0
unit 7      com='left vertical poison plate'
cuboid      6   1  0.1270  0.0 2p10.71245  360.172 0.0
cuboid      7   1  0.3175  0.0 2p10.71245  360.172 0.0
unit 8      com='horizontal aluminum plate'
cuboid      6   1  2p10.71245 0.3175  0.0  360.172 0.0
unit 9      com='vertical aluminum plate'
cuboid      6   1  0.3175  0.0 2p10.71245  360.172 0.0
unit 10     com='W17x17 Assembly up right poison'
array 1     -10.97915 -10.97915 0.0
cuboid      3   1  4p11.20775 360.172 0.0
hole        4   0.1777  10.89024 0.0
hole        6  10.89024  0.1777  0.0
cuboid      5   1  4p11.52525 360.172 0.0
unit 11     com='W17x17 Assembly up left al'
array 1     -10.66165 -10.97915 0.0
cuboid      3   1  4p11.20775 360.172 0.0
hole        8  -0.1777  10.89024 0.0
hole        9 -11.20775  0.1777  0.0
cuboid      5   1  4p11.52525 360.172 0.0
unit 12     com='W17x17 Assembly up left poison'
array 1     -10.66165 -10.97915 0.0
cuboid      3   1  4p11.20775 360.172 0.0
hole        4  -0.1777  10.89024 0.0
hole        7 -11.20775  0.1777  0.0
cuboid      5   1  4p11.52525 360.172 0.0
unit 13     com='W17x17 Assembly low left al'
array 1     -10.66165 -10.66165 0.0
cuboid      3   1  4p11.20775 360.172 0.0
hole        8  -0.1777 -11.20775 0.0
hole        9 -11.20775 -0.1777  0.0
cuboid      5   1  4p11.52525 360.172 0.0
unit 14     com='W17x17 Assembly up right'
array 1     -10.97915 -10.97915 0.0
cuboid      3   1  4p11.20775 360.172 0.0
hole        8   0.1777  10.89024 0.0
hole        9  10.89024  0.1777  0.0
cuboid      5   1  4p11.52525 360.172 0.0
unit 15     com='W17x17 Assembly low right poison'
array 1     -10.97915 -10.66165 0.0
cuboid      3   1  4p11.20775 360.172 0.0
hole        5   0.1777 -11.20775 0.0
hole        6  10.89024 -0.1777  0.0
cuboid      5   1  4p11.52525 360.172 0.0
unit 16     com='W17x17 Assembly up right'
array 1     -10.66165 -10.66165 0.0
cuboid      3   1  4p11.20775 360.172 0.0
hole        5  -0.1777 -11.20775 0.0
hole        7 -11.20775 -0.1777  0.0
cuboid      5   1  4p11.52525 360.172 0.0
unit 17     com='top row of 4 Assemblies'
array 2     -46.101  -11.52525  0.00
cuboid      5   1  2p46.101  11.84275 -11.52525  360.172 0.0
unit 18     com='left row of 4 Assemblies'
array 3     -11.52525 -46.101  0.00
cuboid      5   1  11.52525 -11.84275 2p46.101  360.172 0.0

```

```

unit 19    com='bottom row of 4 Assemblies'
array 4 -46.101  -11.52525  0.00
cuboid 5 1 2p46.101 11.52525 -11.84275 360.172 0.0
unit 20    com='left row of 4 Assemblies'
array 5 -11.52525 -46.101  0.00
cuboid 5 1 11.84275 -11.52525 2p46.101 360.172 0.0
global unit 21
array 6 -46.101  -46.1010  0.00
cylinder 6 1 84.0613 360.172 0.0
hole 17 0.0 57.62627 0.0
hole 18 -57.62627 0.0 0.0
hole 19 0.0 -57.62627 0.0
hole 20 57.62627 0.0 0.0
cylinder 5 1 85.3313 360.172 0.0
cylinder 3 1 86.36 360.172 0.0
cylinder 5 1 89.535 360.172 0.0
cylinder 10 1 97.79 360.172 0.0
cylinder 5 1 104.14 360.172 0.0
cuboid 9 1 4p104.15 360.172 0.0
end geom
read array
  com='BW 15x15 fuel assembly'
  ara=1    nux=15    nuy=15    nuz=1
  fill
    1 1 1 1 1 1 1 1 1 1 1 1 1 1 1
    1 1 1 1 1 1 1 1 1 1 1 1 1 1 1
    1 1 1 1 1 2 1 1 1 2 1 1 1 1 1
    1 1 1 2 1 1 1 1 1 1 1 2 1 1 1
    1 1 1 1 1 1 1 1 1 1 1 1 1 1 1
    1 1 2 1 1 2 1 1 1 2 1 1 2 1 1
    1 1 1 1 1 1 1 1 1 1 1 1 1 1 1
    17 1 1 1 1 1 1 3 1 1 1 1 1 1 1
    1 1 1 1 1 1 1 1 1 1 1 1 1 1 1
    1 1 2 1 1 2 1 1 1 2 1 1 2 1 1
    1 1 1 1 1 1 1 1 1 1 1 1 1 1 1
    1 1 1 2 1 1 1 1 1 1 1 2 1 1 1
    1 1 1 1 1 2 1 1 1 2 1 1 1 1 1
    1 1 1 1 1 1 1 1 1 1 1 1 1 1 1
    1 1 1 1 1 1 1 1 1 1 1 1 1 1 1
  end fill
  com='top array of Fuel'
  ara=2    nux=4    nuy=1    nuz=1
  fill
    15 15 13 16
  end fill
  com='left array of fuel'
  ara=3    nux=1    nuy=4    nuz=1
  fill
    10
    14
    15
    15
  end fill
  com='bottom array of Fuel'
  ara=4    nux=4    nuy=1    nuz=1
  fill
    10 10 11 12

```

```

end fill
com='right array of fuel'
ara=5      nux=1      nuy=4      nuz=1
fill
    12
    12
    13
    16
end fill
com='Center 4x4 Array of Fuel'
ara=6      nux=4      nuy=4      nuz=1
fill
    13 12 13 12
    15 14 15 14
    13 12 13 12
    15 14 15 14
end fill
end array
read bounds
xyf=specular
zfc=specular
end bounds
read plot
ttl='cask material plot - plan view'
pic=mat
nch=' fzmcsblxg'
xul=-85   yul=85   zul=200
xlr=85    ylr=-85  zlr=200
uax=1.0   vdn=-1.0
nax=650
end plot
end data
end

```

The following input file listing is for the B&W 15x15 Mark B case with four (4) PRAs.

```

=csas25
32P B&W 15X15 Mark B Assembly W/4 Poison Rods w/ BPRA's, Jack Boshoven
04/30/01
44groupndf5 latticecell
uo2    1 0.96 293 92235 3.9 92238 96.1 end
zirc4  2 1.0 293 end
h2o    3 0.8 293 end
boron  3 den=0.0025 0.8 293 end
carbonsteel 4 1.0 293 end
ss304  5 1.0 293 end
al     6 1.0 293 end
al     7 0.9 293 end
b-10   7 den=0.033 1.0 293 end
b4c    8 0.3 293 end
h2o    9 1.0 293 end
pb     10 1.0 293 end
b-11  11 0 1.0988-1 293 end
c      11 0 2.7470-2 293 end

```

```

end comp
squarepitch 1.44272 0.936244 1 3 1.0922 2 0.95758 9 end
BW15MB39B08 Four Poison Rods w/BPRAs 3.9 wt% U-235
read param
gen=500 npg=1000 nsk=5 nub=yes run=yes plt=no
end param
read geom
unit 1      com='Fuel Rod'
cylinder 1  1  0.468122      360.172      0.0
cylinder 9  1  0.47879       360.172      0.0
cylinder 2  1  0.5461        360.172      0.0
cuboid 3   1  4p0.72136      360.172      0.0
unit 2      com='guide tube'
cylinder 11 1  0.63246       360.172      0.0
cylinder 2  1  0.6731        360.172      0.0
cuboid 3   1  4p0.72136      360.172      0.0
unit 3      com='instrument tube'
cylinder 11 1  0.56007       360.172      0.0
cylinder 2  1  0.62611       360.172      0.0
cuboid 3   1  4p0.72136      360.172      0.0
unit 4      com='top horizontal poison plate'
cuboid 7   1  2p10.71245     0.1905  0.0 360.172 0.0
cuboid 6   1  2p10.71245     0.3175  0.0 360.172 0.0
unit 5      com='bottom horizontal poison plate'
cuboid 6   1  2p10.71245     0.1270  0.0 360.172 0.0
cuboid 7   1  2p10.71245     0.3175  0.0 360.172 0.0
unit 6      com='right vertical poison plate'
cuboid 7   1  0.1905  0.0 2p10.71245  360.172 0.0
cuboid 6   1  0.3175  0.0 2p10.71245  360.172 0.0
unit 7      com='left vertical poison plate'
cuboid 6   1  0.1270  0.0 2p10.71245  360.172 0.0
cuboid 7   1  0.3175  0.0 2p10.71245  360.172 0.0
unit 8      com='horizontal aluminum plate'
cuboid 6   1  2p10.71245  0.3175  0.0 360.172 0.0
unit 9      com='vertical aluminum plate'
cuboid 6   1  0.3175  0.0 2p10.71245  360.172 0.0
unit 10     com='BW15x15 Assembly up right poison'
array 1 -10.89027 -10.89027 0.0
cuboid 3   1  4p11.06805  360.172 0.0
hole 4    0.038  10.75054 0.0
hole 6    10.75054 0.038  0.0
cuboid 5   1  4p11.3665  360.172 0.0
unit 11     com='BW15x15 Assembly up left al'
array 1 -10.75053 -10.89027 0.0
cuboid 3   1  4p11.06805  360.172 0.0
hole 8    -0.038  10.75054 0.0
hole 9   -11.06805 0.038  0.0
cuboid 5   1  4p11.3665  360.172 0.0
unit 12     com='BW15x15 Assembly up left poison'
array 1 -10.57277 -10.89027 0.0
cuboid 3   1  4p11.06805  360.172 0.0
hole 4    -0.038  10.75054 0.0
hole 7   -11.06805 0.038  0.0
cuboid 5   1  4p11.3665  360.172 0.0
unit 13     com='BW15x15 Assembly low left al'
array 1 -10.57277 -10.57277 0.0
cuboid 3   1  4p11.06805  360.172 0.0

```



```

hole      8  -0.038  -11.06805  0.0
hole      9 -11.06805 -0.038   0.0
cuboid    5   1  4p11.3665  360.172  0.0
unit 14   com='BW15x15 Assembly up right al'
array 1 -10.89027 -10.89027  0.0
cuboid    3   1  4p11.06805  360.172  0.0
hole      8   0.038  10.75054  0.0
hole      9  10.75054  0.038   0.0
cuboid    5   1  4p11.3665  360.172  0.0
unit 15   com='BW15x15 Assembly low right poison'
array 1 -10.89027 -10.57277  0.0
cuboid    3   1  4p11.06805  360.172  0.0
hole      5   0.038  -11.06805  0.0
hole      6  10.75054 -0.038   0.0
cuboid    5   1  4p11.3665  360.172  0.0
unit 16   com='BW15x15 Assembly low left poison'
array 1 -10.75053 -10.75053  0.0
cuboid    3   1  4p11.06805  360.172  0.0
hole      5  -0.038  -11.06805  0.0
hole      7 -11.06805 -0.038   0.0
cuboid    5   1  4p11.3665  360.172  0.0
unit 17   com='BW15x15 Assembly up left poison'
array 1 -10.75053 -10.89027  0.0
cuboid    3   1  4p11.06805  360.172  0.0
hole      4  -0.038  10.75054  0.0
hole      7 -11.06805  0.038   0.0
cuboid    5   1  4p11.3665  360.172  0.0
unit 18   com='BW15x15 Assembly low left al'
array 1 -10.75053 -10.57277  0.0
cuboid    3   1  4p11.06805  360.172  0.0
hole      8  -0.038  -11.06805  0.0
hole      9 -11.06805 -0.038   0.0
cuboid    5   1  4p11.3665  360.172  0.0
unit 19   com='BW15x15 Assembly up right al'
array 1 -11.06804 -10.89027  0.0
cuboid    3   1  4p11.06805  360.172  0.0
hole      8   0.038  10.75054  0.0
hole      9  10.75054  0.038   0.0
cuboid    5   1  4p11.3665  360.172  0.0
unit 20   com='BW15x15 Assembly low right poison'
array 7 -11.06804 -10.57277  0.0
cuboid    3   1  4p11.06805  360.172  0.0
hole      5   0.038  -11.06805  0.0
hole      6  10.75054 -0.038   0.0
cuboid    5   1  4p11.3665  360.172  0.0
unit 21   com='BW15x15 Assembly w/pr low left al'
array 1 -10.75053 -10.75053  0.0
cuboid    3   1  4p11.06805  360.172  0.0
hole      8  -0.038  -11.06805  0.0
hole      9 -11.06805 -0.038   0.0
cuboid    5   1  4p11.3665  360.172  0.0
unit 22   com='BW15x15 Assembly up left poison'
array 1 -10.75053 -11.06804  0.0
cuboid    3   1  4p11.06805  360.172  0.0
hole      4  -0.038  10.75054  0.0
hole      7 -11.06805  0.038   0.0
cuboid    5   1  4p11.3665  360.172  0.0

```

```

unit 23    com='BW15x15 Assembly up right al'
array 1 -11.06804 -11.06804 0.0
cuboid   3   1 4p11.06805 360.172 0.0
hole     8   0.038 10.75054 0.0
hole     9  10.75054 0.038 0.0
cuboid   5   1 4p11.3665 360.172 0.0
unit 24    com='BW15x15 Assembly low right poison'
array 1 -11.06804 -10.75053 0.0
cuboid   3   1 4p11.06805 360.172 0.0
hole     5   0.038 -11.06805 0.0
hole     6  10.75054 -0.038 0.0
cuboid   5   1 4p11.3665 360.172 0.0
unit 25    com='BW15x15 Assembly w/pr up left poison'
array 7 -10.57277 -11.06804 0.0
cuboid   3   1 4p11.06805 360.172 0.0
hole     4  -0.038 10.75054 0.0
hole     7 -11.06805 0.038 0.0
cuboid   5   1 4p11.3665 360.172 0.0
unit 26    com='BW15x15 Assembly low left al'
array 1 -10.57277 -10.75053 0.0
cuboid   3   1 4p11.06805 360.172 0.0
hole     8  -0.038 -11.06805 0.0
hole     9 -11.06805 -0.038 0.0
cuboid   5   1 4p11.3665 360.172 0.0
unit 27    com='BW15x15 Assembly low right poison'
array 1 -10.89027 -10.75053 0.0
cuboid   3   1 4p11.06805 360.172 0.0
hole     5   0.038 -11.06805 0.0
hole     6  10.75054 -0.038 0.0
cuboid   5   1 4p11.3665 360.172 0.0
unit 28    com='BW15x15 Assembly up right al'
array 1 -10.89027 -11.06804 0.0
cuboid   3   1 4p11.06805 360.172 0.0
hole     8   0.038 10.75054 0.0
hole     9  10.75054 0.038 0.0
cuboid   5   1 4p11.3665 360.172 0.0
unit 29    com='top row of 4 Assemblies'
array 2 -45.466 -11.3665 0.00
cuboid   5   1 2p45.466 11.66495 -11.3665 360.172 0.0
unit 30    com='left row of 4 Assemblies'
array 3 -11.3665 -45.466 0.00
cuboid   5   1 11.3665 -11.66495 2p45.466 360.172 0.0
unit 31    com='bottom row of 4 Assemblies'
array 4 -45.466 -11.3665 0.00
cuboid   5   1 2p45.466 11.3665 -11.66495 360.172 0.0
unit 32    com='left row of 4 Assemblies'
array 5 -11.3665 -45.466 0.00
cuboid   5   1 11.66495 -11.3665 2p45.466 360.172 0.0
unit 33    com='guide tube with poison'
cylinder 8   1 0.55 360.172 0.0
cylinder 3   1 0.63246 360.172 0.0
cylinder 2   1 0.6731 360.172 0.0
cuboid   3   1 4p0.72136 360.172 0.0
unit 34    com='BW15x15 Assembly w/pr right al'
array 7 -10.89027 -10.89027 0.0
cuboid   3   1 4p11.06805 360.172 0.0
hole     8   0.038 10.75054 0.0

```

```

hole      9  10.75054  0.038  0.0
cuboid    5   1  4p11.3665  360.172  0.0
unit 35   com='BW15x15 Assembly w/pr low left al'
array 7 -10.75053 -10.75053 0.0
cuboid    3   1  4p11.06805  360.172  0.0
hole      8  -0.038  -11.06805  0.0
hole      9 -11.06805 -0.038  0.0
cuboid    5   1  4p11.3665  360.172  0.0
global unit 36
array 6 -45.466  -45.466  0.00
cylinder  6   1  84.0613  360.172  0.0
hole      29  0.0  56.83252  0.0
hole      30 -56.83252  0.0  0.0
hole      31  0.0  -56.83252  0.0
hole      32  56.83252  0.0  0.0
cylinder  5   1  85.3313  360.172  0.0
cylinder  3   1  86.36  360.172  0.0
cylinder  5   1  89.535  360.172  0.0
cylinder 10   1  97.79  360.172  0.0
cylinder  5   1 104.14  360.172  0.0
cuboid    9   1  4p104.15  360.172  0.0
end geom
read array
  com='BW 15x15 fuel assembly'
  ara=1      nux=15      nuy=15      nuz=1
  fill
    1 1 1 1 1 1 1 1 1 1 1 1 1 1 1
    1 1 1 1 1 1 1 1 1 1 1 1 1 1 1
    1 1 1 1 1 2 1 1 1 2 1 1 1 1 1
    1 1 1 2 1 1 1 1 1 1 1 2 1 1 1
    1 1 1 1 1 1 1 1 1 1 1 1 1 1 1
    1 1 2 1 1 2 1 1 1 2 1 1 2 1 1
    1 1 1 1 1 1 1 1 1 1 1 1 1 1 1
    1 1 1 1 1 1 1 3 1 1 1 1 1 1 1
    1 1 1 1 1 1 1 1 1 1 1 1 1 1 1
    1 1 2 1 1 2 1 1 1 2 1 1 2 1 1
    1 1 1 1 1 1 1 1 1 1 1 1 1 1 1
    1 1 1 2 1 1 1 1 1 1 1 2 1 1 1
    1 1 1 1 1 2 1 1 1 2 1 1 1 1 1
    1 1 1 1 1 1 1 1 1 1 1 1 1 1 1
    1 1 1 1 1 1 1 1 1 1 1 1 1 1 1
  end fill
  com='top array of Fuel'
  ara=2      nux=4      nuy=1      nuz=1
  fill
    27 27 21 16
  end fill
  com='left array of fuel'
  ara=3      nux=1      nuy=4      nuz=1
  fill
    10
    14
    27
    27
  end fill
  com='bottom array of Fuel'
  ara=4      nux=4      nuy=1      nuz=1

```

```

fill
    10 10 11 17
end fill
com='right array of fuel'
ara=5      nux=1      nuy=4      nuz=1
fill
    17
    17
    21
    16
end fill
com='Center 4x4 Array of Fuel'
ara=6      nux=4      nuy=4      nuz=1
fill
    13 12 18 17
    15 34 20 19
    26 25 35 22
    27 28 24 23
end fill
com='BW 15x15 fuel assembly w/pr'
ara=7      nux=15     nuy=15     nuz=1
fill
    1 1 1 1 1 1 1 1 1 1 1 1 1 1 1
    1 1 1 1 1 1 1 1 1 1 1 1 1 1 1
    1 1 1 1 1 33 1 1 1 1 33 1 1 1 1
    1 1 1 33 1 1 1 1 1 1 1 1 33 1 1
    1 1 1 1 1 1 1 1 1 1 1 1 1 1 1
    1 1 33 1 1 33 1 1 1 33 1 1 33 1 1
    1 1 1 1 1 1 1 1 1 1 1 1 1 1 1
    1 1 1 1 1 1 3 1 1 1 1 1 1 1 1
    1 1 1 1 1 1 1 1 1 1 1 1 1 1 1
    1 1 33 1 1 33 1 1 1 33 1 1 33 1 1
    1 1 1 1 1 1 1 1 1 1 1 1 1 1 1
    1 1 1 33 1 1 1 1 1 1 1 1 33 1 1
    1 1 1 1 1 1 33 1 1 1 33 1 1 1 1
    1 1 1 1 1 1 1 1 1 1 1 1 1 1 1
    1 1 1 1 1 1 1 1 1 1 1 1 1 1 1
end fill
end array
read bounds
    xyf=specular
    zfc=specular
end bounds
read plot
    ttl='cask material plot - plan view'
    pic=mat
    nch=' fzmcsblxg'
    xul=-85    yul=85    zul=200
    xlr=85     ylr=-85   zlr=200
    uax=1.0    vdn=-1.0
    nax=650
end plot
end data
end

```

M.6.6.4 Design Basis Case CSAS25 Input Deck

Model: W17STD34B07.in (based on the 20 poison plate basket configuration)

```
=csas25
32P WE17x17 LOPAR Assembly Max U235, w/ BPRAs, Jack Boshoven 04/30/01
44groupndf5 latticecell
uo2 1 0.96 293 92235 3.4 92238 96.6 end
zirc4 2 1.0 293 end
h2o 3 0.7 293 end
boron 3 den=0.0025 0.7 293 end
carbonsteel 4 1.0 293 end
ss304 5 1.0 293 end
al 6 1.0 293 end
al 7 0.9 293 end
b-10 7 den=0.033 1.0 293 end
b4c 8 0.3 293 end
h2o 9 1.0 293 end
pb 10 1.0 293 end
b-11 11 0 1.0988-1 293 end
c 11 0 2.7470-2 293 end
end comp
squarepitch 1.25984 0.81915 1 3 0.94996 2 0.83566 9 end
w17std34B07 Most Reactive w/BPRAs 3.4 wt% U-235
read param
gen=500 npg=1000 nsk=5 nub=yes run=yes plt=no
end param
read geom
unit 1 com='Fuel Rod'
cylinder 1 1 0.409575 365.76 0.0
cylinder 9 1 0.41783 365.76 0.0
cylinder 2 1 0.47498 365.76 0.0
cuboid 3 1 4p0.62992 365.76 0.0
unit 2 com='guide tube'
cylinder 11 1 0.56134 365.76 0.0
cylinder 2 1 0.60198 365.76 0.0
cuboid 3 1 4p0.62992 365.76 0.0
unit 3 com='instrument tube'
cylinder 11 1 0.5715 365.76 0.0
cylinder 2 1 0.6096 365.76 0.0
cuboid 3 1 4p0.62992 365.76 0.0
unit 4 com='top horizontal poison plate'
cuboid 7 1 2p10.71245 0.1905 0.0 365.76 0.0
cuboid 6 1 2p10.71245 0.3175 0.0 365.76 0.0
unit 5 com='bottom horizontal poison plate'
cuboid 6 1 2p10.71245 0.1270 0.0 365.76 0.0
cuboid 7 1 2p10.71245 0.3175 0.0 365.76 0.0
unit 6 com='right vertical poison plate'
cuboid 7 1 0.1905 0.0 2p10.71245 365.76 0.0
cuboid 6 1 0.3175 0.0 2p10.71245 365.76 0.0
unit 7 com='left vertical poison plate'
cuboid 6 1 0.1270 0.0 2p10.71245 365.76 0.0
cuboid 7 1 0.3175 0.0 2p10.71245 365.76 0.0
unit 8 com='horizontal aluminum plate'
cuboid 6 1 2p10.71245 0.3175 0.0 365.76 0.0
unit 9 com='vertical aluminum plate'
```

```

cuboid 6 1 0.3175 0.0 2p10.71245 365.76 0.0
unit 10 com='W17x17 Assembly up right poison'
array 1 -10.66675 -10.66675 0.0
cuboid 3 1 4p11.06805 365.76 0.0
hole 4 0.038 10.75054 0.0
hole 6 10.75054 0.038 0.0
cuboid 5 1 4p11.3665 365.76 0.0
unit 11 com='W17x17 Assembly up left al'
array 1 -10.75053 -10.66675 0.0
cuboid 3 1 4p11.06805 365.76 0.0
hole 8 -0.038 10.75054 0.0
hole 9 -11.06805 0.038 0.0
cuboid 5 1 4p11.3665 365.76 0.0
unit 12 com='W17x17 Assembly up left poison'
array 1 -10.34925 -10.66675 0.0
cuboid 3 1 4p11.06805 365.76 0.0
hole 4 -0.038 10.75054 0.0
hole 7 -11.06805 0.038 0.0
cuboid 5 1 4p11.3665 365.76 0.0
unit 13 com='W17x17 Assembly low left al'
array 1 -10.34925 -10.34925 0.0
cuboid 3 1 4p11.06805 365.76 0.0
hole 8 -0.038 -11.06805 0.0
hole 9 -11.06805 -0.038 0.0
cuboid 5 1 4p11.3665 365.76 0.0
unit 14 com='W17x17 Assembly up right al'
array 1 -10.66675 -10.66675 0.0
cuboid 3 1 4p11.06805 365.76 0.0
hole 8 0.038 10.75054 0.0
hole 9 10.75054 0.038 0.0
cuboid 5 1 4p11.3665 365.76 0.0
unit 15 com='W17x17 Assembly low right poison'
array 1 -10.66675 -10.34925 0.0
cuboid 3 1 4p11.06805 365.76 0.0
hole 5 0.038 -11.06805 0.0
hole 6 10.75054 -0.038 0.0
cuboid 5 1 4p11.3665 365.76 0.0
unit 16 com='W17x17 Assembly low left poison'
array 1 -10.75053 -10.75053 0.0
cuboid 3 1 4p11.06805 365.76 0.0
hole 5 -0.038 -11.06805 0.0
hole 7 -11.06805 -0.038 0.0
cuboid 5 1 4p11.3665 365.76 0.0
unit 17 com='W17x17 Assembly up left poison'
array 1 -10.75053 -10.66675 0.0
cuboid 3 1 4p11.06805 365.76 0.0
hole 4 -0.038 10.75054 0.0
hole 7 -11.06805 0.038 0.0
cuboid 5 1 4p11.3665 365.76 0.0
unit 18 com='W17x17 Assembly low left al'
array 1 -10.75053 -10.34925 0.0
cuboid 3 1 4p11.06805 365.76 0.0
hole 8 -0.038 -11.06805 0.0
hole 9 -11.06805 -0.038 0.0
cuboid 5 1 4p11.3665 365.76 0.0
unit 19 com='W17x17 Assembly up right al'
array 1 -11.06804 -10.66675 0.0

```

```

cuboid 3 1 4p11.06805 365.76 0.0
hole 8 0.038 10.75054 0.0
hole 9 10.75054 0.038 0.0
cuboid 5 1 4p11.3665 365.76 0.0
unit 20 com='W17x17 Assembly low right poison'
array 1 -11.06804 -10.34925 0.0
cuboid 3 1 4p11.06805 365.76 0.0
hole 5 0.038 -11.06805 0.0
hole 6 10.75054 -0.038 0.0
cuboid 5 1 4p11.3665 365.76 0.0
unit 21 com='W17x17 Assembly low left al'
array 1 -10.75053 -10.75053 0.0
cuboid 3 1 4p11.06805 365.76 0.0
hole 8 -0.038 -11.06805 0.0
hole 9 -11.06805 -0.038 0.0
cuboid 5 1 4p11.3665 365.76 0.0
unit 22 com='W17x17 Assembly up left poison'
array 1 -10.75053 -11.06804 0.0
cuboid 3 1 4p11.06805 365.76 0.0
hole 4 -0.038 10.75054 0.0
hole 7 -11.06805 0.038 0.0
cuboid 5 1 4p11.3665 365.76 0.0
unit 23 com='W17x17 Assembly up right al'
array 1 -11.06804 -11.06804 0.0
cuboid 3 1 4p11.06805 365.76 0.0
hole 8 0.038 10.75054 0.0
hole 9 10.75054 0.038 0.0
cuboid 5 1 4p11.3665 365.76 0.0
unit 24 com='W17x17 Assembly low right poison'
array 1 -11.06804 -10.75053 0.0
cuboid 3 1 4p11.06805 365.76 0.0
hole 5 0.038 -11.06805 0.0
hole 6 10.75054 -0.038 0.0
cuboid 5 1 4p11.3665 365.76 0.0
unit 25 com='W17x17 Assembly up left poison'
array 1 -10.34925 -11.06804 0.0
cuboid 3 1 4p11.06805 365.76 0.0
hole 4 -0.038 10.75054 0.0
hole 7 -11.06805 0.038 0.0
cuboid 5 1 4p11.3665 365.76 0.0
unit 26 com='W17x17 Assembly low left al'
array 1 -10.34925 -10.75053 0.0
cuboid 3 1 4p11.06805 365.76 0.0
hole 8 -0.038 -11.06805 0.0
hole 9 -11.06805 -0.038 0.0
cuboid 5 1 4p11.3665 365.76 0.0
unit 27 com='W17x17 Assembly low right poison'
array 1 -10.66675 -10.75053 0.0
cuboid 3 1 4p11.06805 365.76 0.0
hole 5 0.038 -11.06805 0.0
hole 6 10.75054 -0.038 0.0
cuboid 5 1 4p11.3665 365.76 0.0
unit 28 com='W17x17 Assembly up right al'
array 1 -10.66675 -11.06804 0.0
cuboid 3 1 4p11.06805 365.76 0.0
hole 8 0.038 10.75054 0.0
hole 9 10.75054 0.038 0.0

```

```

cuboid 5 1 4p11.3665 365.76 0.0
unit 29 com='top row of 4 Assemblies'
array 2 -45.466 -11.3665 0.00
cuboid 5 1 2p45.466 11.66495 -11.3665 365.76 0.0
unit 30 com='left row of 4 Assemblies'
array 3 -11.3665 -45.466 0.00
cuboid 5 1 11.3665 -11.66495 2p45.466 365.76 0.0
unit 31 com='bottom row of 4 Assemblies'
array 4 -45.466 -11.3665 0.00
cuboid 5 1 2p45.466 11.3665 -11.66495 365.76 0.0
unit 32 com='left row of 4 Assemblies'
array 5 -11.3665 -45.466 0.00
cuboid 5 1 11.66495 -11.3665 2p45.466 365.76 0.0
global unit 33
array 6 -45.466 -45.466 0.00
cylinder 6 1 84.0613 365.76 0.0
hole 29 0.0 56.83252 0.0
hole 30 -56.83252 0.0 0.0
hole 31 0.0 -56.83252 0.0
hole 32 56.83252 0.0 0.0
cylinder 5 1 85.3313 365.76 0.0
cylinder 3 1 86.36 365.76 0.0
cylinder 5 1 89.535 365.76 0.0
cylinder 10 1 97.79 365.76 0.0
cylinder 5 1 104.14 365.76 0.0
cuboid 9 1 4p104.15 365.76 0.0
end geom
read array
com='we 17x17 fuel assembly'
ara=1 nux=17 nuy=17 nuz=1
fill
1 1 1 1 1 1 1 1 1 1 1 1 1 1 1 1 1
1 1 1 1 1 1 1 1 1 1 1 1 1 1 1 1 1
1 1 1 1 1 2 1 1 2 1 1 2 1 1 1 1 1
1 1 1 2 1 1 1 1 1 1 1 1 1 1 2 1 1
1 1 1 1 1 1 1 1 1 1 1 1 1 1 1 1 1
1 1 2 1 1 2 1 1 2 1 1 2 1 1 2 1 1
1 1 1 1 1 1 1 1 1 1 1 1 1 1 1 1 1
1 1 1 1 1 1 1 1 1 1 1 1 1 1 1 1 1
1 1 2 1 1 2 1 1 3 1 1 2 1 1 2 1 1
1 1 1 1 1 1 1 1 1 1 1 1 1 1 1 1 1
1 1 1 1 1 1 1 1 1 1 1 1 1 1 1 1 1
1 1 2 1 1 2 1 1 2 1 1 2 1 1 2 1 1
1 1 1 1 1 1 1 1 1 1 1 1 1 1 1 1 1
1 1 1 2 1 1 1 1 1 1 1 1 1 1 2 1 1
1 1 1 1 1 2 1 1 2 1 1 2 1 1 1 1 1
1 1 1 1 1 1 1 1 1 1 1 1 1 1 1 1 1
1 1 1 1 1 1 1 1 1 1 1 1 1 1 1 1 1
end fill
com='top array of Fuel'
ara=2 nux=4 nuy=1 nuz=1
fill
27 27 21 16
end fill
com='left array of fuel'
ara=3 nux=1 nuy=4 nuz=1
fill

```



```

        10
        14
        27
        27
    end fill
    com='bottom array of Fuel'
    ara=4      nux=4      nuy=1      nuz=1
    fill
        10 10 11 17
    end fill
    com='right array of fuel'
    ara=5      nux=1      nuy=4      nuz=1
    fill
        17
        17
        21
        16
    end fill
    com='Center 4x4 Array of Fuel'
    ara=6      nux=4      nuy=4      nuz=1
    fill
        13 12 18 17
        15 14 20 19
        26 25 21 22
        27 28 24 23
    end fill
end array
read bounds
    xyf=specular
    zfc=specular
end bounds
read plot
    ttl='cask material plot - plan view'
    pic=mat
    nch=' fzmcsblxg'
    xul=-85  yul=85  zul=200
    xlr=85   ylr=-85  zlr=200
    uax=1.0  vdn=-1.0
    nax=650
end plot
end data
end

```

M.6.6.5 Example CSAS25 Input Files (based on the 16 poison plate basket configuration (we1734bP-16P250-0065.in))

```

=csas25
32P WE 17x17 Assembly, BPRA 3.4 w/o U235, Prakash 01/14/03
44groupndf5 latticecell
uo2 1 0.96 293 92235 3.4 92238 96.6 end
zirc4 2 1.0 293 end
' BORATED H2O 2500 PPM 65% Density
h2o 3 0.65 293 end
boron 3 den=0.0025 0.65 293 end
carbonsteel 4 1.0 293 end
ss304 5 1.0 293 end
al 6 1.0 293 end
' EAGLE PITCHER BORATED AL (6.30 mgB10/cm2 at 0.075")
BORON 7 DEN=2.693 0.013600 293. 5010 90.0 5011 10.0 END
AL 7 DEN=2.693 0.986400 END
b4c 8 0.3 293 end
h2o 9 1.0 293 end
pb 10 1.0 293 end
b-11 11 0 1.0988-1 293 end
c 11 0 2.7470-2 293 end
end comp
squarepitch 1.25984 0.81915 1 3 0.94996 2 0.83566 9 end
WE17 3.40 w/o with BPRA 2500 ppm dissolved boron, 16 Plates
read param
gen=500 npg=1000 nsk=5 nub=yes run=yes plt=no
end param
read geom
unit 1 com='Fuel Rod'
cylinder 1 1 0.409575 365.76 0.0
cylinder 9 1 0.41783 365.76 0.0
cylinder 2 1 0.47498 365.76 0.0
cuboid 3 1 4p0.62992 365.76 0.0
unit 2 com='guide tube'
cylinder 11 1 0.56134 365.76 0.0
cylinder 2 1 0.60198 365.76 0.0
cuboid 3 1 4p0.62992 365.76 0.0
unit 3 com='instrument tube'
cylinder 11 1 0.5715 365.76 0.0
cylinder 2 1 0.6096 365.76 0.0
cuboid 3 1 4p0.62992 365.76 0.0
unit 4 com='top horizontal poison plate'
cuboid 6 1 2p10.71245 0.1270 0.0 365.76 0.0
cuboid 7 1 2p10.71245 0.3175 0.0 365.76 0.0
unit 5 com='bottom horizontal poison plate'
cuboid 7 1 2p10.71245 0.1905 0.0 365.76 0.0
cuboid 6 1 2p10.71245 0.3175 0.0 365.76 0.0
unit 6 com='right vertical poison plate'
cuboid 6 1 0.1270 0.0 2p10.71245 365.76 0.0
cuboid 7 1 0.3175 0.0 2p10.71245 365.76 0.0
unit 7 com='left vertical poison plate'
cuboid 7 1 0.1905 0.0 2p10.71245 365.76 0.0
cuboid 6 1 0.3175 0.0 2p10.71245 365.76 0.0
unit 8 com='horizontal aluminum plate'
cuboid 6 1 2p10.71245 0.3170 0.0 365.76 0.0

```

```

unit 9      com='vertical aluminum plate'
cuboid     6  1  0.3170  0.0 2p10.71245  365.76  0.0
unit 10     com='WE 17x17 Assembly low left poison S E Quadrant'
array 1    -10.75055 -10.34923 0.0
cuboid     3  1  4p11.06805  365.76  0.0
hole       5  +0.003 -11.06805 0.0
hole       7  -11.06805 +0.003  0.0
cuboid     5  1  4p11.3665  365.76  0.0
unit 11     com='WE 17x17 Assembly low right poison S W Quadrant'
array 1    -10.66673 -10.34923 0.0
cuboid     3  1  4p11.06805  365.76  0.0
hole       5  -0.003 -11.06805 0.0
hole       6  10.75055 -0.003  0.0
cuboid     5  1  4p11.3665  365.76  0.0
unit 12     com='WE 17x17 Assembly low left poison N E Quadrant'
array 1    -10.75055 -10.75055 0.0
cuboid     3  1  4p11.06805  365.76  0.0
hole       5  +0.003 -11.06805 0.0
hole       7  -11.06805 +0.003  0.0
cuboid     5  1  4p11.3665  365.76  0.0
unit 13     com='WE 17x17 Assembly low right poison N W Quadrant'
array 1    -10.66673 -10.75055 0.0
cuboid     3  1  4p11.06805  365.76  0.0
hole       5  -0.003 -11.06805 0.0
hole       6  10.75055 -0.003  0.0
cuboid     5  1  4p11.3665  365.76  0.0
unit 20     com='WE 17x17 Assembly low left Alum S E Quadrant'
array 1    -10.75055 -10.34923 0.0
cuboid     3  1  4p11.06805  365.76  0.0
hole       8  +0.003 -11.06805 0.0
hole       9  -11.06805 +0.003  0.0
cuboid     5  1  4p11.3665  365.76  0.0
unit 21     com='WE 17x17 Assembly low right Alum S W Quadrant'
array 1    -10.66673 -10.34923 0.0
cuboid     3  1  4p11.06805  365.76  0.0
hole       8  -0.003 -11.06805 0.0
hole       9  10.75055 -0.003  0.0
cuboid     5  1  4p11.3665  365.76  0.0
unit 22     com='WE 17x17 Assembly low left Alum N E Quadrant'
array 1    -10.75055 -10.75055 0.0
cuboid     3  1  4p11.06805  365.76  0.0
hole       8  +0.003 -11.06805 0.0
hole       9  -11.06805 +0.003  0.0
cuboid     5  1  4p11.3665  365.76  0.0
unit 23     com='WE 17x17 Assembly low right Alum N W Quadrant'
array 1    -10.66673 -10.75055 0.0
cuboid     3  1  4p11.06805  365.76  0.0
hole       8  -0.003 -11.06805 0.0
hole       9  10.75055 -0.003  0.0
cuboid     5  1  4p11.3665  365.76  0.0
unit 29     com='top row of 4 Assemblies'
array 2    -45.466  -11.3665  0.00
cuboid     5  1  2p45.466  11.66495 -11.3665  365.76  0.0
unit 30     com='left row of 4 Assemblies'
array 3    -11.3665  -45.466  0.00
cuboid     5  1  11.3665  -11.66495 2p45.466  365.76  0.0
unit 31     com='bottom row of 4 Assemblies'

```

```

array 4 -45.466 -11.3665 0.00
cuboid 5 1 2p45.466 11.3665 -11.66495 365.76 0.0
unit 32 com='left row of 4 Assemblies'
array 5 -11.3665 -45.466 0.00
cuboid 5 1 11.66495 -11.3665 2p45.466 365.76 0.0
global unit 33
array 6 -45.466 -45.466 0.00
cylinder 6 1 84.0613 365.76 0.0
hole 29 0.0 56.83252 0.0
hole 30 -56.83252 0.0 0.0
hole 31 0.0 -56.83252 0.0
hole 32 56.83252 0.0 0.0
cylinder 5 1 85.3313 365.76 0.0
cylinder 3 1 86.36 365.76 0.0
cylinder 5 1 89.535 365.76 0.0
cylinder 10 1 97.79 365.76 0.0
cylinder 5 1 104.14 365.76 0.0
cuboid 9 1 4p104.15 365.76 0.0
end geom
read array
com='we 17x17 fuel assembly'
ara=1 nux=17 nuy=17 nuz=1
fill
1 1 1 1 1 1 1 1 1 1 1 1 1 1 1 1 1
1 1 1 1 1 1 1 1 1 1 1 1 1 1 1 1 1
1 1 1 1 1 2 1 1 2 1 1 2 1 1 1 1 1
1 1 1 2 1 1 1 1 1 1 1 1 1 2 1 1 1
1 1 1 1 1 1 1 1 1 1 1 1 1 1 1 1 1
1 1 2 1 1 2 1 1 2 1 1 2 1 1 2 1 1
1 1 1 1 1 1 1 1 1 1 1 1 1 1 1 1 1
1 1 1 1 1 1 1 1 1 1 1 1 1 1 1 1 1
1 1 2 1 1 2 1 1 3 1 1 2 1 1 2 1 1
1 1 1 1 1 1 1 1 1 1 1 1 1 1 1 1 1
1 1 1 1 1 1 1 1 1 1 1 1 1 1 1 1 1
1 1 2 1 1 2 1 1 2 1 1 2 1 1 2 1 1
1 1 1 1 1 1 1 1 1 1 1 1 1 1 1 1 1
1 1 1 2 1 1 1 1 1 1 1 1 1 2 1 1 1
1 1 1 1 1 2 1 1 2 1 1 2 1 1 1 1 1
1 1 1 1 1 1 1 1 1 1 1 1 1 1 1 1 1
1 1 1 1 1 1 1 1 1 1 1 1 1 1 1 1 1
end fill
com='top array of Fuel'
ara=2 nux=4 nuy=1 nuz=1
fill
23 23 22 22
end fill
com='left array of fuel'
ara=3 nux=1 nuy=4 nuz=1
fill
21
21
23
23
end fill
com='bottom array of Fuel'
ara=4 nux=4 nuy=1 nuz=1
fill

```

```

        21 21 20 20
    end fill
    com='right array of fuel'
    ara=5      nux=1      nuy=4      nuz=1
    fill
        20
        20
        22
        22
    end fill
    com='Center 4x4 Array of Fuel'
    ara=6      nux=4      nuy=4      nuz=1
    fill
        11 11 10 10
        11 11 10 10
        13 13 12 12
        13 13 12 12
    end fill
end array
read bounds
    xyf=specular
    zfc=specular
end bounds
read plot
    ttl='cask material plot - plan view'
    pic=mat
    nch=' fzmcsblxg'
    xul=-85   yul=85   zul=100
    xlr=85    ylr=-85  zlr=100
    uax=1.0   vdn=-1.0
    nax=650
end plot
end data
end

```

M.6.6.6 Example CSAS25 Input Files WE 15x15 in (based on the 24 poison plate basket configuration – worst case WE 15x15 with no BPRAs and 8 PRAs) (we1546-var-08pra-0080.in)

```
=csas25
32P WE 15x15 Std/ZC, 4.6 w/o U235, 8 PRAs Prakash 09/18/03
44groupndf5 latticecell
uo2 1 0.96 293 92235 4.6 92238 95.4 end
zirc4 2 1.0 293 end
' BORATED H2O 2500 PPM 80% Density
h2o 3 0.80 293 end
boron 3 den=0.0025 0.80 293 end
carbonsteel 4 1.0 293 end
ss304 5 1.0 293 end
al 6 1.0 293 end
' EAGLE PITCHER BORATED AL (6.30 mgB10/cm2 at 0.075")
BORON 7 DEN=2.693 0.013600 293. 5010 90.0 5011 10.0 END
AL 7 DEN=2.693 0.986400 END
b4c 8 0.3 293 end
h2o 9 1.0 293 end
pb 10 1.0 293 end
b-11 11 0 1.0988-1 293 end
c 11 0 2.7470-2 293 end
end comp
squarepitch 1.43002 0.929386 1 3 1.07188 2 0.948944 9 end
WE 15 4.60 w/o 2500 ppm dissolved boron, 24 Plates 8 PRAs
read param
gen=500 npg=1000 nsk=5 nub=yes run=yes plt=no
end param
read geom
unit 1 com='Fuel Rod'
cylinder 1 1 0.4646643 365.76 0.0
cylinder 9 1 0.474472 365.76 0.0
cylinder 2 1 0.535940 365.76 0.0
cuboid 3 1 4p0.71501 365.76 0.0
unit 2 com='guide tube'
cylinder 3 1 0.65024 365.76 0.0
cylinder 2 1 0.69342 365.76 0.0
cuboid 3 1 4p0.71501 365.76 0.0
unit 3 com='instrument tube'
cylinder 3 1 0.65532 365.76 0.0
cylinder 2 1 0.69342 365.76 0.0
cuboid 3 1 4p0.71501 365.76 0.0
unit 4 com='guide tube'
cylinder 8 1 0.55 365.76 0.0
cylinder 3 1 0.65024 365.76 0.0
cylinder 2 1 0.69342 365.76 0.0
cuboid 3 1 4p0.71501 365.76 0.0
unit 5 com='bottom horizontal poison plate'
cuboid 7 1 2p10.71245 0.1905 0.0 365.76 0.0
cuboid 6 1 2p10.71245 0.3175 0.0 365.76 0.0
unit 6 com='right vertical poison plate'
cuboid 6 1 0.1270 0.0 2p10.71245 365.76 0.0
cuboid 7 1 0.3175 0.0 2p10.71245 365.76 0.0
unit 7 com='left vertical poison plate'
```

```

cuboid 7 1 0.1905 0.0 2p10.71245 365.76 0.0
cuboid 6 1 0.3175 0.0 2p10.71245 365.76 0.0
unit 8 com='horizontal aluminum plate'
cuboid 6 1 2p10.71245 0.3170 0.0 365.76 0.0
unit 9 com='vertical aluminum plate'
cuboid 6 1 0.3170 0.0 2p10.71245 365.76 0.0
unit 10 com='WE 15x15 Assembly low left poison S E Quadrant'
array 1 -10.75055 -10.38225 0.0
cuboid 3 1 4p11.06805 365.76 0.0
hole 5 +0.003 -11.06805 0.0
hole 7 -11.06805 +0.003 0.0
cuboid 5 1 4p11.3665 365.76 0.0
unit 11 com='WE 15x15 Assembly low right poison S W Quadrant'
array 1 -10.69975 -10.38225 0.0
cuboid 3 1 4p11.06805 365.76 0.0
hole 5 -0.003 -11.06805 0.0
hole 6 10.75055 -0.003 0.0
cuboid 5 1 4p11.3665 365.76 0.0
unit 12 com='WE 15x15 Assembly low left poison N E Quadrant'
array 1 -10.75055 -10.75055 0.0
cuboid 3 1 4p11.06805 365.76 0.0
hole 5 +0.003 -11.06805 0.0
hole 7 -11.06805 +0.003 0.0
cuboid 5 1 4p11.3665 365.76 0.0
unit 13 com='WE 15x15 Assembly low right poison N W Quadrant'
array 1 -10.69975 -10.75055 0.0
cuboid 3 1 4p11.06805 365.76 0.0
hole 5 -0.003 -11.06805 0.0
hole 6 10.75055 -0.003 0.0
cuboid 5 1 4p11.3665 365.76 0.0
unit 15 com='WE 15x15 Assembly with PRA low left poison S E Quadrant'
array 7 -10.75055 -10.38225 0.0
cuboid 3 1 4p11.06805 365.76 0.0
hole 5 +0.003 -11.06805 0.0
hole 7 -11.06805 +0.003 0.0
cuboid 5 1 4p11.3665 365.76 0.0
unit 16 com='WE 15x15 Assembly with PRA low right poison S W Quadrant'
array 7 -10.69975 -10.38225 0.0
cuboid 3 1 4p11.06805 365.76 0.0
hole 5 -0.003 -11.06805 0.0
hole 6 10.75055 -0.003 0.0
cuboid 5 1 4p11.3665 365.76 0.0
unit 17 com='WE 15x15 Assembly with PRA low left poison N E Quadrant'
array 7 -10.75055 -10.75055 0.0
cuboid 3 1 4p11.06805 365.76 0.0
hole 5 +0.003 -11.06805 0.0
hole 7 -11.06805 +0.003 0.0
cuboid 5 1 4p11.3665 365.76 0.0
unit 18 com='WE 15x15 Assembly with PRA low right poison N W Quadrant'
array 7 -10.69975 -10.75055 0.0
cuboid 3 1 4p11.06805 365.76 0.0
hole 5 -0.003 -11.06805 0.0
hole 6 10.75055 -0.003 0.0
cuboid 5 1 4p11.3665 365.76 0.0
unit 20 com='WE 15x15 Assembly low left Alum S E Quadrant'
array 1 -10.75055 -10.38225 0.0
cuboid 3 1 4p11.06805 365.76 0.0

```

```

hole      8  +0.003  -11.06805  0.0
hole      9 -11.06805 +0.003   0.0
cuboid    5  1  4p11.3665  365.76  0.0
unit 21   com='WE 15x15 Assembly low right Alum S W Quadrant'
array 1 -10.69975 -10.38225 0.0
cuboid    3  1  4p11.06805  365.76  0.0
hole      8  -0.003  -11.06805  0.0
hole      9  10.75055 -0.003   0.0
cuboid    5  1  4p11.3665  365.76  0.0
unit 22   com='WE 15x15 Assembly low left Alum N E Quadrant'
array 1 -10.75055 -10.75055 0.0
cuboid    3  1  4p11.06805  365.76  0.0
hole      8  +0.003  -11.06805  0.0
hole      9 -11.06805 +0.003   0.0
cuboid    5  1  4p11.3665  365.76  0.0
unit 23   com='WE 15x15 Assembly low right Alum N W Quadrant'
array 1 -10.69975 -10.75055 0.0
cuboid    3  1  4p11.06805  365.76  0.0
hole      8  -0.003  -11.06805  0.0
hole      9  10.75055 -0.003   0.0
cuboid    5  1  4p11.3665  365.76  0.0
unit 25   com='WE 15x15 Assembly with PRA low left Alum S E Quadrant'
array 7 -10.75055 -10.38225 0.0
cuboid    3  1  4p11.06805  365.76  0.0
hole      8  +0.003  -11.06805  0.0
hole      9 -11.06805 +0.003   0.0
cuboid    5  1  4p11.3665  365.76  0.0
unit 26   com='WE 15x15 Assembly with PRA low right Alum S W Quadrant'
array 7 -10.69975 -10.38225 0.0
cuboid    3  1  4p11.06805  365.76  0.0
hole      8  -0.003  -11.06805  0.0
hole      9  10.75055 -0.003   0.0
cuboid    5  1  4p11.3665  365.76  0.0
unit 27   com='WE 15x15 Assembly with PRA low left Alum N E Quadrant'
array 7 -10.75055 -10.75055 0.0
cuboid    3  1  4p11.06805  365.76  0.0
hole      8  +0.003  -11.06805  0.0
hole      9 -11.06805 +0.003   0.0
cuboid    5  1  4p11.3665  365.76  0.0
unit 28   com='WE 15x15 Assembly with PRA low right Alum N W Quadrant'
array 7 -10.69975 -10.75055 0.0
cuboid    3  1  4p11.06805  365.76  0.0
hole      8  -0.003  -11.06805  0.0
hole      9  10.75055 -0.003   0.0
cuboid    5  1  4p11.3665  365.76  0.0
unit 29   com='top row of 4 Assemblies'
array 2 -45.466  -11.3665  0.00
cuboid    5  1  2p45.466  11.66495 -11.3665  365.76  0.0
unit 30   com='left row of 4 Assemblies'
array 3 -11.3665  -45.466  0.00
cuboid    5  1  11.3665  -11.66495 2p45.466  365.76  0.0
unit 31   com='bottom row of 4 Assemblies'
array 4 -45.466  -11.3665  0.00
cuboid    5  1  2p45.466  11.3665  -11.66495  365.76  0.0
unit 32   com='left row of 4 Assemblies'
array 5 -11.3665  -45.466  0.00
cuboid    5  1  11.66495 -11.3665  2p45.466  365.76  0.0

```



```

global unit 33
array 6 -45.466 -45.466 0.00
cylinder 6 1 84.0613 365.76 0.0
hole 29 0.0 56.83252 0.0
hole 30 -56.83252 0.0 0.0
hole 31 0.0 -56.83252 0.0
hole 32 56.83252 0.0 0.0
cylinder 5 1 85.3313 365.76 0.0
cylinder 9 1 86.36 365.76 0.0
cylinder 5 1 89.535 365.76 0.0
cylinder 10 1 97.79 365.76 0.0
cylinder 5 1 104.14 365.76 0.0
cuboid 9 1 4p104.15 365.76 0.0
end geom

```

```

read array
com='we 15x15 fuel assembly'
ara=1 nux=15 nuy=15 nuz=1
fill

```

```

1 1 1 1 1 1 1 1 1 1 1 1 1 1 1
1 1 1 1 1 1 1 1 1 1 1 1 1 1 1
1 1 2 1 1 2 1 1 1 2 1 1 2 1 1
1 1 1 1 1 1 1 2 1 1 1 1 1 1 1
1 1 1 1 2 1 1 1 1 1 2 1 1 1 1
1 1 2 1 1 1 1 1 1 1 1 1 2 1 1
1 1 1 1 1 1 1 1 1 1 1 1 1 1 1
1 1 1 2 1 1 1 3 1 1 1 2 1 1 1
1 1 1 1 1 1 1 1 1 1 1 1 1 1 1
1 1 2 1 1 1 1 1 1 1 1 1 2 1 1
1 1 1 1 2 1 1 1 1 1 2 1 1 1 1
1 1 1 1 1 1 1 2 1 1 1 1 1 1 1
1 1 2 1 1 2 1 1 1 2 1 1 2 1 1
1 1 1 1 1 1 1 1 1 1 1 1 1 1 1
1 1 1 1 1 1 1 1 1 1 1 1 1 1 1

```

```

end fill
com='top array of Fuel'
ara=2 nux=4 nuy=1 nuz=1
fill

```

```

13 13 12 12

```

```

end fill
com='left array of fuel'
ara=3 nux=1 nuy=4 nuz=1
fill

```

```

21
11
23
13

```

```

end fill
com='bottom array of Fuel'
ara=4 nux=4 nuy=1 nuz=1
fill

```

```

21 11 20 10

```

```

end fill
com='right array of fuel'
ara=5 nux=1 nuy=4 nuz=1
fill

```

```

20
10

```

```

        22
        12
    end fill
    com='Center 4x4 Array of Fuel'
    ara=6      nux=4      nuy=4      nuz=1
    fill
        11 16 10 10
        11 16 25 15
        18 28 17 12
        13 13 17 12
    end fill
    com='we 15x15 fuel assembly with PRA'
    ara=7      nux=15     nuy=15     nuz=1
    fill
        1 1 1 1 1 1 1 1 1 1 1 1 1 1 1
        1 1 1 1 1 1 1 1 1 1 1 1 1 1 1
        1 1 4 1 1 4 1 1 1 4 1 1 4 1 1
        1 1 1 1 1 1 1 4 1 1 1 1 1 1 1
        1 1 1 1 4 1 1 1 1 1 4 1 1 1 1
        1 1 4 1 1 1 1 1 1 1 1 1 4 1 1
        1 1 1 1 1 1 1 1 1 1 1 1 1 1 1
        1 1 1 4 1 1 1 3 1 1 1 4 1 1 1
        1 1 1 1 1 1 1 1 1 1 1 1 1 1 1
        1 1 4 1 1 1 1 1 1 1 1 1 4 1 1
        1 1 1 1 4 1 1 1 1 1 1 4 1 1 1
        1 1 1 1 1 1 1 4 1 1 1 1 1 1 1
        1 1 4 1 1 4 1 1 1 4 1 1 4 1 1
        1 1 1 1 1 1 1 1 1 1 1 1 1 1 1
        1 1 1 1 1 1 1 1 1 1 1 1 1 1 1
    end fill
end array
read bounds
    xyf=specular
    zfc=specular
end bounds
read plot
    ttl='cask material plot - plan view'
    pic=mat
    nch=' fzmcsblxg'
    xul=-85    yul=85    zul=100
    xlr=85     ylr=-85   zlr=100
    uax=1.0    vdn=-1.0
    nax=650
end plot
end data
end

```

**Table M.6-1
Maximum Initial Enrichment For Each Configuration**

Assembly Class	Assembly Type	Maximum Initial Enrichment, wt. % U-235			
		(Type A Basket) No PRAs	(Type B Basket) 4 PRAs	(Type C Basket) 8 PRAs	(Type D Basket) 16 PRAs
WE 17x17 ⁽¹⁾	Westinghouse 17x17 LOPAR/Std	3.40	4.00	4.50	5.00
	Westinghouse 17x17 OFA/Vantage 5,+ ⁽²⁾				
B&W 15x15 ⁽¹⁾	B&W 15x15 Mark B	3.30	3.90	Not Evaluated	5.00
CE 15x15	CE 15x15 Palisades	3.40	Not Evaluated	Not Evaluated	Not Evaluated
	Exxon/ANF 15x15 CE				
WE 15x15	Westinghouse 15x15 Std/ZC	3.40	4.00	4.60	5.00
	Exxon/ANF 15x15 WE				
CE 14x14	CE 14x14 Std/Generic	3.80	4.60	5.00	Not Evaluated
	CE 14x14 Fort Calhoun				
WE 14x14	Westinghouse 14x14 ZCA/ZCB	4.00	5.00	Not Evaluated	Not Evaluated
	Westinghouse 14x14 OFA				
	Exxon/ANF 14x14 WE				

NOTES:

- (1) With or without BPRAs in locations without PRAs
- (2) Includes all Vantage versions (5, +, ++, etc.).

**Table M.6-2
Authorized Contents for NUHOMS®-32PT System**

Assembly Type ⁽¹⁾	Array
Westinghouse 17x17 LOPAR/Standard	17x17
Westinghouse 17x17 OFA/Vantage 5	17x17
B&W 15x15 Mark B	15x15
CE 15x15 Palisades	15x15
Exxon/ANF 15x15 CE	15x15
Exxon/ANF 15x15 WE	15x15
Westinghouse 15x15 Standard/ZC	15x15
CE 14x14 Standard/Generic	14x14
CE 14x14 Fort Calhoun	14x14
Exxon/ANF 14x14 WE	14x14
Westinghouse 14x14 ZCA/ZCB	14x14
Westinghouse 14x14 OFA	14x14

NOTES:

- (1) Reload fuel from other manufacturers with these parameters are also acceptable.

**Table M.6-3
Parameters For PWR Assemblies⁽³⁾**

Manufacturer ⁽¹⁾	Array	Version	Active Fuel Length (in)	Number Fuel Rods per Assembly	Pitch (in)	Fuel Pellet OD (in)
WE	17x17	LOPAR	144	264	0.496	0.3225
WE	17x17	OFA/Van 5	144	264	0.496	0.3088
B&W	15x15	Mark B	141.8	208	0.568	0.3686
CE	15x15	Palisades	132	216	0.550	0.3580
Exxon/ANF	15x15	CE	131.8	216	0.550	0.3565
Exxon/ANF	15x15	WE	144	204	0.563	0.3565
WE	15x15	Std/ZC	144	204	0.563	0.3559
CE	14x14	Std/Gen	137	176	0.580	0.3765
CE	14x14	Ft. Calhoun	128	176	0.580	0.3815
Exxon/ANF	14x14	WE	142	179	0.556	0.3505
WE	14x14	ZCA/ZCB	144	179	0.556	0.3659
WE	14x14	OFA	144	179	0.556	0.3444

Manufacturer ⁽¹⁾	Array	Version	Clad Thickness (in)	Clad OD (in)	Guide Tube/ Instrument Tube	
					OD (in)	ID (in)
WE	17x17	LOPAR	0.0225	0.374	24@0.474 1@0.480	24@0.422 1@0.450
WE	17x17	OFA/Van 5	0.0225	0.360	24@0.482 1@0.476	24@0.450 1@0.460
B&W	15x15	Mark B	0.0265	0.430	16@0.530 1@0.493	16@0.498 1@0.441
CE	15x15	Palisades	0.0260	0.418	8@0.4135	8@0.3655
Exxon/ANF	15x15	CE	0.0300	0.417	8Guide Bars ⁽²⁾ 1@0.417	1@0.363
Exxon/ANF	15x15	WE	0.0300	0.424	20@0.544 1@0.544	20@0.510 1@0.510
WE	15x15	Std/ZC	0.0242	0.422	20@0.546 1@0.546	20@0.512 1@0.512
CE	14x14	Std/Gen	0.0280	0.440	5@1.115	5@1.035
CE	14x14	Ft. Calhoun	0.0280	0.440	5@1.115	5@1.035
Exxon/ANF	14x14	WE	0.0300	0.424	16@0.541 1@0.480	16@0.507 1@0.448
WE	14x14	ZCA/ZCB	0.0225	0.422	16@0.539 1@0.422	16@0.505 1@0.392
WE	14x14	OFA	0.0243	0.400	16@0.526 1@0.400	16@0.492 1@0.353

NOTES:

- (1) Reload fuel from other manufacturers with these parameters are also acceptable.
- (2) Guide Bars are solid Zircaloy-4 approximately 0.40 inches x 0.45 inches
- (3) All dimensions shown are nominal

**Table M.6-4
Poison Rod Assembly (PRA) Description**

Assembly Class	Minimum Number of Rods/PRA	Minimum Poison Length (cm)	Modeled B₄C Content per Rod (g/cm)	Minimum B₄C Content per Rod (g/cm)
WE 17x17	24	383.5	0.59	0.79
B&W 15x15	16	383.5	0.72	0.96
WE 15x15	20	381.0	0.72	0.96
CE 14x14	5	327.7	3.14	4.19
WE 14x14	16	381.0	0.72	0.96

**Table M.6-5
Material Property Data**

Material	Density g/cm ³	Element	Weight %	Atom Density (atoms/b-cm)
UO ₂ (Enrichment - 3.4 wt%)	10.52	U-235	3.00	8.0797E-04
		U-238	85.15	2.2666E-02
		O	11.85	4.6948E-02
UO ₂ (Enrichment - 5.0 wt%)	10.52	U-235	4.41	1.1882E-03
		U-238	83.73	2.2290E-02
		O	11.86	4.6956E-02
Zircaloy-4	6.56	Zr	98.23	4.2541E-02
		Sn	1.45	4.8254E-04
		Fe	0.21	1.4856E-04
		Cr	0.10	7.5978E-05
		Hf	0.01	2.2133E-06
Borated Water (2500 ppm Boron)	1.000	H	0.11	6.6769E-02
		O	0.89	3.3385E-02
		B-10	4.602E-04	2.7713E-05
		B-11	2.038E-03	1.1155E-04
Water	0.998	H	11.1	6.6769E-02
		O	88.9	3.3385E-02
Stainless Steel (SS304)	7.94	C	0.080	3.1877E-04
		Si	1.000	1.7025E-03
		P	0.045	6.9468E-05
		Cr	19.000	1.7473E-02
		Mn	2.000	1.7407E-03
		Fe	68.375	5.8545E-02
Aluminum	2.70	Al	100.0	6.0307E-02
		Lead	11.34	3.2969E-02
Aluminum - Boron Poison Plate (0.0063 g/cm ² B-10)	2.465	B-10	1.34	1.9847E-03
		Al	98.66	5.4276E-02
B ₄ C in PRA	0.756	B-10	14.42	6.5599E-03
		B-11	63.83	2.6405E-02
		C	21.75	8.2411E-03
¹¹ B ₄ C in BPRA	2.555	B-11	78.56	1.0988E-01
		C	21.44	2.7470E-02

**Table M.6-6
Most Reactive Fuel Type**

Manufacturer	Array	Version	k_{KENO}	1σ	k_{eff}
Most Reactive Fuel Type at 3.3 wt.% U-235, w/o PRAs, 2500 ppm Boron					
WE	17x17	LOPAR	0.8862	0.0009	0.8880
WE	17x17	OFA/Van 5	0.8579	0.0011	0.8601
B&W	15x15	Mark B	0.8932	0.0008	0.8948
CE	15x15	Palisades	0.8766	0.0009	0.8784
Exxon/ANF	15x15	CE	0.8734	0.0009	0.8752
Exxon/ANF	15x15	WE	0.8625	0.0008	0.8641
WE	15x15	Std/ZC	0.8760	0.0009	0.8778
CE	14x14	Std/Gen	0.8196	0.0009	0.8214
CE	14x14	Ft. Calhoun	0.8235	0.0009	0.8253
Exxon/ANF	14x14	WE	0.7821	0.0009	0.7839
WE	14x14	ZCA/ZCB	0.8012	0.0009	0.8030
WE	14x14	OFA	0.7638	0.0008	0.7654
B&W 15x15 Mark B - Internal Moderator Density (IMD) Evaluation					
Assembly Design	IMD Condition	k_{KENO}	1σ	k_{eff}	
B&W 15x15 Mark B	100% TD	0.8932	0.0008	0.8948	
B&W 15x15 Mark B	90% TD	0.9053	0.0008	0.9069	
B&W 15x15 Mark B	80% TD	0.9170	0.0009	0.9188	
B&W 15x15 Mark B	70% TD	0.9238	0.0009	0.9256	
B&W 15x15 Mark B	60% TD	0.9270	0.0010	0.9290	
B&W 15x15 Mark B	50% TD	0.9223	0.0008	0.9239	

**Table M.6-7
Transition Rail Material Evaluation Results**

Model Description	k_{KENO}	1σ	k_{eff}
Transition Rail Material Evaluation - 100% IMD			
Aluminum	0.8932	0.0008	0.8948
2500 ppm Borated Water	0.8873	0.0009	0.8891
Pure Water	0.8893	0.0008	0.8909
Stainless Steel	0.8918	0.0008	0.8934
Transition Rail Material Evaluation - 60% IMD			
Aluminum	0.9270	0.0010	0.9290
2500 ppm Borated Water	0.9188	0.0010	0.9208
Pure Water	0.9189	0.0011	0.9211
Stainless Steel	0.9261	0.0009	0.9279

**Table M.6-8
Fuel Clad OD Evaluation Results**

Model Description	k_{KENO}	1σ	k_{eff}
Fuel Clad O.D. Evaluation - 100% IMD			
Fuel Clad O.D. = 0.420 inches	0.8889	0.0009	0.8907
Fuel Clad O.D. = 0.422 inches	0.8884	0.0008	0.8900
Fuel Clad O.D. = 0.424 inches	0.8915	0.0010	0.8935
Fuel Clad O.D. = 0.426 inches	0.8904	0.0009	0.8922
Fuel Clad O.D. = 0.428 inches	0.8922	0.0009	0.8940
Fuel Clad O.D. = 0.430 inches	0.8932	0.0008	0.8948
Fuel Clad O.D. = 0.432 inches	0.8933	0.0008	0.8949
Fuel Clad O.D. = 0.434 inches	0.8919	0.0009	0.8937
Fuel Clad O.D. = 0.436 inches	0.8953	0.0009	0.8971
Fuel Clad O.D. = 0.438 inches	0.8948	0.0008	0.8964
Fuel Clad O.D. = 0.440 inches	0.8939	0.0009	0.8957
Fuel Clad O.D. Evaluation - 60% IMD			
Fuel Clad O.D. = 0.420 inches	0.9293	0.0009	0.9311
Fuel Clad O.D. = 0.422 inches	0.9272	0.0010	0.9292
Fuel Clad O.D. = 0.424 inches	0.9273	0.0011	0.9295
Fuel Clad O.D. = 0.426 inches	0.9268	0.0009	0.9286
Fuel Clad O.D. = 0.428 inches	0.9270	0.0008	0.9286
Fuel Clad O.D. = 0.430 inches	0.9270	0.0010	0.9290
Fuel Clad O.D. = 0.432 inches	0.9267	0.0008	0.9283
Fuel Clad O.D. = 0.434 inches	0.9258	0.0009	0.9276
Fuel Clad O.D. = 0.436 inches	0.9259	0.0009	0.9277
Fuel Clad O.D. = 0.438 inches	0.9260	0.0009	0.9278
Fuel Clad O.D. = 0.440 inches	0.9251	0.0010	0.9271

**Table M.6-9
Poison/Aluminum and Aluminum Plate Thickness Evaluation Results**

Model Description	k_{KENO}	1σ	k_{eff}
Poison/Aluminum and Aluminum Plate Thickness Evaluation - 100% IMD			
Maximum Thickness (0.135 inches)	0.8921	0.0007	0.8935
Nominal Thickness (0.125 inches)	0.8932	0.0008	0.8948
Minimum Thickness (0.115 inches)	0.8922	0.0008	0.8938
Poison/Aluminum and Aluminum Plate Thickness Evaluation - 90% IMD			
Maximum Thickness (0.135 inches)	0.9057	0.0009	0.9075
Nominal Thickness (0.125 inches)	0.9053	0.0008	0.9069
Minimum Thickness (0.115 inches)	0.9061	0.0008	0.9077
Poison/Aluminum and Aluminum Plate Thickness Evaluation - 80% IMD			
Maximum Thickness (0.135 inches)	0.9156	0.0008	0.9172
Nominal Thickness (0.125 inches)	0.9170	0.0009	0.9188
Minimum Thickness (0.115 inches)	0.9172	0.0009	0.9190
Poison/Aluminum and Aluminum Plate Thickness Evaluation 70% IMD			
Maximum Thickness (0.135 inches)	0.9232	0.0009	0.9250
Nominal Thickness (0.125 inches)	0.9238	0.0009	0.9256
Minimum Thickness (0.115 inches)	0.9245	0.0011	0.9267
Poison/Aluminum and Aluminum Plate Thickness Evaluation - 60% IMD			
Maximum Thickness (0.135 inches)	0.9261	0.0009	0.9279
Nominal Thickness (0.125 inches)	0.9270	0.0010	0.9290
Minimum Thickness (0.115 inches)	0.9257	0.0009	0.9275
Poison/Aluminum and Aluminum Plate Thickness Evaluation 50% IMD			
Maximum Thickness (0.135 inches)	0.9208	0.0009	0.9226
Nominal Thickness (0.125 inches)	0.9223	0.0008	0.9239
Minimum Thickness (0.115 inches)	0.9215	0.0010	0.9235
Poison/Aluminum and Aluminum Plate Thickness Evaluation - 40% IMD			
Maximum Thickness (0.135 inches)	0.9050	0.0010	0.9070
Nominal Thickness (0.125 inches)	0.9063	0.0012	0.9087
Minimum Thickness (0.115 inches)	0.9047	0.0008	0.9063

**Table M.6-10
Basket Grid Structure Plate/Tube Thickness Evaluation Results**

Model Description	k_{KENO}	1σ	k_{eff}
Basket Grid Structure Plate/Tube Thickness Evaluation - 100% IMD			
Maximum Thickness (0.26 inches)	0.8907	0.0010	0.8927
Nominal Thickness (0.25 inches)	0.8932	0.0008	0.8948
Minimum Thickness (0.235 inches)	0.8932	0.0008	0.8948
Basket Grid Structure Plate/Tube Thickness Evaluation - 60% IMD			
Maximum Thickness (0.26 inches)	0.9272	0.0008	0.9288
Nominal Thickness (0.25 inches)	0.9270	0.0010	0.9290
Minimum Thickness (0.235 inches)	0.9279	0.0008	0.9295

**Table M.6-11
Fuel Compartment Width Evaluation Results**

Model Description	k_{KENO}	1σ	k_{eff}
Fuel Compartment Width Evaluation - 100% IMD			
Maximum Width (8.925 inches)	0.8838	0.0008	0.8854
Nominal Width (8.825 inches)	0.8932	0.0008	0.8948
Minimum Width (8.715 inches)	0.9006	0.0008	0.9022
Fuel Compartment Width Evaluation - 60% IMD			
Maximum Width (8.925 inches)	0.9236	0.0009	0.9254
Nominal Width (8.825 inches)	0.9279	0.0008	0.9295
Minimum Width (8.715 inches)	0.9320	0.0009	0.9338

**Table M.6-12
Assembly-to-Assembly Pitch Evaluation**

Model Description	k_{KENO}	1σ	k_{eff}
Assembly-to-Assembly Pitch Evaluation - 100% IMD			
Maximum Assembly-to-Assembly Pitch	0.8983	0.0008	0.8999
Assemblies Centered in Sleeves	0.9006	0.0008	0.9022
Minimum Assembly-to-Assembly Pitch	0.9030	0.0009	0.9048
Assembly-to-Assembly Pitch Evaluation - 60% IMD			
Maximum Assembly-to-Assembly Pitch	0.9330	0.0009	0.9348
Assemblies Centered in Sleeves	0.9320	0.0009	0.9338
Minimum Assembly-to-Assembly Pitch	0.9317	0.0009	0.9335

Table M.6-13
WE 17x17 Class Assembly without BPRAs Results (20 Poison Plate)

Model Description	k_{KENO}	1σ	k_{eff}
Initial Enrichment 3.4 wt% U-235 - No PRAs, w/o BPRAs			
Internal Moderator at 100%TD	0.9099	0.0008	0.9115
Internal Moderator at 90%TD	0.9216	0.0009	0.9234
Internal Moderator at 80%TD	0.9313	0.0009	0.9331
Internal Moderator at 70%TD	0.9355	0.0010	0.9375
Internal Moderator at 60%TD	0.9369	0.0009	0.9387
Internal Moderator at 50%TD	0.9282	0.0008	0.9298
Internal Moderator at 40%TD	0.9115	0.0008	0.9131
Initial Enrichment 4.0 wt% U-235 - 4 PRAs, w/o BPRAs			
Internal Moderator at 100%TD	0.9201	0.0008	0.9217
Internal Moderator at 90%TD	0.9269	0.0008	0.9285
Internal Moderator at 80%TD	0.9322	0.0009	0.9340
Internal Moderator at 70%TD	0.9333	0.0009	0.9351
Internal Moderator at 60%TD	0.9263	0.0009	0.9281
Internal Moderator at 50%TD	0.9151	0.0009	0.9169
Internal Moderator at 40%TD	0.8913	0.0008	0.8929
Initial Enrichment 4.5 wt% U-235 - 8 PRAs, w/o BPRAs			
Internal Moderator at 100%TD	0.9262	0.0008	0.9278
Internal Moderator at 90%TD	0.9313	0.0009	0.9331
Internal Moderator at 80%TD	0.9386	0.0009	0.9404
Internal Moderator at 70%TD	0.9357	0.0010	0.9377
Internal Moderator at 60%TD	0.9283	0.0010	0.9303
Internal Moderator at 50%TD	0.9110	0.0011	0.9132
Internal Moderator at 40%TD	0.8855	0.0009	0.8873
Initial Enrichment 5.0 wt% U-235 - 16 PRAs, w/o BPRAs			
Internal Moderator at 100%TD	0.9028	0.0009	0.9046
Internal Moderator at 90%TD	0.9026	0.0010	0.9046
Internal Moderator at 80%TD	0.8986	0.0011	0.9008
Internal Moderator at 70%TD	0.8871	0.0010	0.8891
Internal Moderator at 60%TD	0.8737	0.0011	0.8759
Internal Moderator at 50%TD	0.8505	0.0009	0.8523
Internal Moderator at 40%TD	0.8193	0.0010	0.8213

Table M.6-14
WE 17x17 Class Assembly with BPRAs Results (20 Poison Plate)

Model Description	k_{KENO}	1σ	k_{eff}
Initial Enrichment 3.4 wt% U-235 - No PRAs, with BPRAs			
Internal Moderator at 100%TD	0.9256	0.0008	0.9272
Internal Moderator at 90%TD	0.9342	0.0009	0.9360
Internal Moderator at 80%TD	0.9385	0.0009	0.9403
Internal Moderator at 70%TD	0.9389	0.0010	0.9409
Internal Moderator at 60%TD	0.9357	0.0008	0.9373
Internal Moderator at 50%TD	0.9236	0.0011	0.9258
Internal Moderator at 40%TD	0.9017	0.0009	0.9035
Internal Moderator at 0%TD	0.5821	0.0005	0.5831
Initial Enrichment 4.0 wt% U-235 - 4 PRAs, with BPRAs			
Internal Moderator at 100%TD	0.9317	0.0009	0.9335
Internal Moderator at 90%TD	0.9347	0.0010	0.9367
Internal Moderator at 80%TD	0.9357	0.0009	0.9375
Internal Moderator at 70%TD	0.9314	0.0008	0.9330
Internal Moderator at 60%TD	0.9240	0.0009	0.9258
Internal Moderator at 50%TD	0.9075	0.0009	0.9093
Internal Moderator at 40%TD	0.8830	0.0009	0.8848
Initial Enrichment 4.5 wt% U-235 - 8 PRAs, with BPRAs			
Internal Moderator at 100%TD	0.9339	0.0009	0.9357
Internal Moderator at 90%TD	0.9368	0.0011	0.9390
Internal Moderator at 80%TD	0.9338	0.0009	0.9356
Internal Moderator at 70%TD	0.9257	0.0009	0.9275
Internal Moderator at 60%TD	0.9123	0.0010	0.9143
Internal Moderator at 50%TD	0.8932	0.0011	0.8954
Internal Moderator at 40%TD	0.8656	0.0010	0.8676
Initial Enrichment 5.0 wt% U-235 - 16 PRAs, with BPRAs			
Internal Moderator at 100%TD	0.9029	0.0010	0.9049
Internal Moderator at 90%TD	0.8982	0.0010	0.9002
Internal Moderator at 80%TD	0.8900	0.0010	0.8920
Internal Moderator at 70%TD	0.8785	0.0010	0.8805
Internal Moderator at 60%TD	0.8593	0.0011	0.8615
Internal Moderator at 50%TD	0.8359	0.0012	0.8383
Internal Moderator at 40%TD	0.8031	0.0008	0.8047

Table M.6-15
B&W 15x15 Class Assembly without BPRAs Results (20 Poison Plate)

Model Description	k_{KENO}	1σ	k_{eff}
Initial Enrichment 3.3 wt% U-235 - No PRAs, w/o BPRAs			
Internal Moderator at 100%TD	0.9030	0.0009	0.9048
Internal Moderator at 90%TD	0.9152	0.0009	0.9170
Internal Moderator at 80%TD	0.9249	0.0008	0.9265
Internal Moderator at 70%TD	0.9331	0.0009	0.9349
Internal Moderator at 60%TD	0.9317	0.0009	0.9335
Internal Moderator at 50%TD	0.9239	0.0009	0.9257
Internal Moderator at 40%TD	0.9078	0.0008	0.9094
Internal Moderator at 30%TD	0.8735	0.0009	0.8753
Internal Moderator at 20%TD	0.8132	0.0009	0.8150
Internal Moderator at 10%TD	0.7178	0.0007	0.7192
Internal Moderator at 0%TD	0.5676	0.0006	0.5688
Initial Enrichment 3.9 wt% U-235 - 4 PRAs, w/o BPRAs			
Internal Moderator at 100%TD	0.9200	0.0009	0.9218
Internal Moderator at 90%TD	0.9293	0.0010	0.9313
Internal Moderator at 80%TD	0.9330	0.0010	0.9350
Internal Moderator at 70%TD	0.9351	0.0010	0.9371
Internal Moderator at 60%TD	0.9326	0.0008	0.9342
Internal Moderator at 50%TD	0.9195	0.0009	0.9213
Internal Moderator at 40%TD	0.8985	0.0008	0.9001
Initial Enrichment 5.0 wt% U-235 - 16 PRAs, w/o BPRAs			
Internal Moderator at 100%TD	0.9189	0.0010	0.9209
Internal Moderator at 90%TD	0.9202	0.0010	0.9222
Internal Moderator at 80%TD	0.9176	0.0009	0.9194
Internal Moderator at 70%TD	0.9095	0.0011	0.9117
Internal Moderator at 60%TD	0.8953	0.0009	0.8971
Internal Moderator at 50%TD	0.8769	0.0010	0.8789
Internal Moderator at 40%TD	0.8450	0.0009	0.8468

**Table M.6-16
B&W 15x15 Class Assembly with BPRAs Results (20 Poison Plate)**

Model Description	k_{KENO}	1σ	k_{eff}
Initial Enrichment 3.3 wt% U-235 - No PRAs, with BPRAs			
Internal Moderator at 100%TD	0.9182	0.0009	0.9200
Internal Moderator at 90%TD	0.9272	0.0010	0.9292
Internal Moderator at 80%TD	0.9332	0.0008	0.9348
Internal Moderator at 70%TD	0.9360	0.0009	0.9378
Internal Moderator at 60%TD	0.9341	0.0010	0.9361
Internal Moderator at 50%TD	0.9213	0.0010	0.9233
Internal Moderator at 40%TD	0.9002	0.0008	0.9018
Initial Enrichment 3.9 wt% U-235 - 4 PRAs, with BPRAs			
Internal Moderator at 100%TD	0.9313	0.0008	0.9329
Internal Moderator at 90%TD	0.9382	0.0009	0.9400
Internal Moderator at 80%TD	0.9389	0.0009	0.9407
Internal Moderator at 70%TD	0.9364	0.0008	0.9380
Internal Moderator at 60%TD	0.9294	0.0009	0.9312
Internal Moderator at 50%TD	0.9139	0.0009	0.9157
Internal Moderator at 40%TD	0.8878	0.0008	0.8894
Initial Enrichment 5.0 wt% U-235 - 16 PRAs, with BPRAs			
Internal Moderator at 100%TD	0.9243	0.0010	0.9263
Internal Moderator at 90%TD	0.9228	0.0010	0.9248
Internal Moderator at 80%TD	0.9160	0.0014	0.9188
Internal Moderator at 70%TD	0.9050	0.0010	0.9070
Internal Moderator at 60%TD	0.8886	0.0008	0.8902
Internal Moderator at 50%TD	0.8683	0.0008	0.8699
Internal Moderator at 40%TD	0.8358	0.0009	0.8376

Table M.6-17
CE 15x15 Class Assembly without BPRAs Results (20 Poison Plate)

Model Description	k_{KENO}	1σ	k_{eff}
Initial Enrichment 3.4 wt% U-235 - No PRAs, w/o BPRAs			
Internal Moderator at 100%TD	0.9100	0.0009	0.9118
Internal Moderator at 90%TD	0.9188	0.0009	0.9206
Internal Moderator at 80%TD	0.9257	0.0009	0.9275
Internal Moderator at 70%TD	0.9316	0.0011	0.9338
Internal Moderator at 60%TD	0.9267	0.0009	0.9285
Internal Moderator at 50%TD	0.9177	0.0010	0.9197
Internal Moderator at 40%TD	0.8981	0.0009	0.8999

Table M.6-18
WE 15x15 Class Assembly without BPRAs Results (20 Poison Plate)

Model Description	k_{KENO}	1σ	k_{eff}
Initial Enrichment 3.4 wt% U-235 - No PRAs, w/o BPRAs			
Internal Moderator at 100%TD	0.9016	0.0009	0.9034
Internal Moderator at 90%TD	0.9149	0.0009	0.9167
Internal Moderator at 80%TD	0.9255	0.0008	0.9271
Internal Moderator at 70%TD	0.9328	0.0009	0.9346
Internal Moderator at 60%TD	0.9364	0.0009	0.9382
Internal Moderator at 50%TD	0.9308	0.0010	0.9328
Internal Moderator at 40%TD	0.9133	0.0008	0.9149
Initial Enrichment 4.0 wt% U-235 - 4 PRAs, w/o BPRAs			
Internal Moderator at 100%TD	0.9107	0.0009	0.9125
Internal Moderator at 90%TD	0.9229	0.0010	0.9249
Internal Moderator at 80%TD	0.9292	0.0010	0.9312
Internal Moderator at 70%TD	0.9307	0.0009	0.9325
Internal Moderator at 60%TD	0.9278	0.0009	0.9296
Internal Moderator at 50%TD	0.9183	0.0009	0.9201
Internal Moderator at 40%TD	0.8959	0.0008	0.8975
Initial Enrichment 4.6 wt% U-235 - 8 PRAs, w/o BPRAs			
Internal Moderator at 100%TD	0.9276	0.0009	0.9294
Internal Moderator at 90%TD	0.9325	0.0009	0.9343
Internal Moderator at 80%TD	0.9363	0.0010	0.9383
Internal Moderator at 70%TD	0.9349	0.0008	0.9365
Internal Moderator at 60%TD	0.9251	0.0009	0.9269
Internal Moderator at 50%TD	0.9130	0.0009	0.9148
Internal Moderator at 40%TD	0.8863	0.0010	0.8883
Initial Enrichment 5.0 wt% U-235 - 16 PRAs, w/o BPRAs			
Internal Moderator at 100%TD	0.8969	0.0012	0.8993
Internal Moderator at 90%TD	0.8985	0.0011	0.9007
Internal Moderator at 80%TD	0.8967	0.0010	0.8987
Internal Moderator at 70%TD	0.8894	0.0009	0.8912
Internal Moderator at 60%TD	0.8780	0.0009	0.8798
Internal Moderator at 50%TD	0.8567	0.0010	0.8587
Internal Moderator at 40%TD	0.8259	0.0009	0.8277

**Table M.6-19
CE 14x14 Class Assembly without BPRAs Results (20 Poison Plate)**

Model Description	k_{KENO}	1σ	k_{eff}
Initial Enrichment 3.8 wt% U-235 - No PRAs, w/o BPRAs			
Internal Moderator at 100%TD	0.8905	0.0011	0.8927
Internal Moderator at 90%TD	0.9078	0.0012	0.9102
Internal Moderator at 80%TD	0.9196	0.0009	0.9214
Internal Moderator at 70%TD	0.9292	0.0009	0.9310
Internal Moderator at 60%TD	0.9347	0.0010	0.9367
Internal Moderator at 50%TD	0.9309	0.0010	0.9329
Internal Moderator at 40%TD	0.9165	0.0010	0.9185
Initial Enrichment 4.6 wt% U-235 - 4 PRAs, w/o BPRAs			
Internal Moderator at 100%TD	0.9103	0.0009	0.9121
Internal Moderator at 90%TD	0.9223	0.0009	0.9241
Internal Moderator at 80%TD	0.9300	0.0010	0.9320
Internal Moderator at 70%TD	0.9371	0.0008	0.9387
Internal Moderator at 60%TD	0.9376	0.0008	0.9392
Internal Moderator at 50%TD	0.9308	0.0009	0.9326
Internal Moderator at 40%TD	0.9155	0.0010	0.9175
Initial Enrichment 5.0 wt% U-235 - 8 PRAs, w/o BPRAs			
Internal Moderator at 100%TD	0.9133	0.0009	0.9151
Internal Moderator at 90%TD	0.9199	0.0010	0.9219
Internal Moderator at 80%TD	0.9271	0.0011	0.9293
Internal Moderator at 70%TD	0.9294	0.0009	0.9312
Internal Moderator at 60%TD	0.9271	0.0008	0.9287
Internal Moderator at 50%TD	0.9181	0.0010	0.9201
Internal Moderator at 40%TD	0.8976	0.0009	0.8994

Table M.6-20
WE 14x14 Class Assembly without BPRAs Results (20 Poison Plate)

Model Description	k_{KENO}	1σ	k_{eff}
Initial Enrichment 4.0 wt% U-235 - No PRAs, w/o BPRAs			
Internal Moderator at 100%TD	0.9030	0.0011	0.9052
Internal Moderator at 90%TD	0.9148	0.0009	0.9166
Internal Moderator at 80%TD	0.9257	0.0010	0.9277
Internal Moderator at 70%TD	0.9335	0.0011	0.9357
Internal Moderator at 60%TD	0.9374	0.0010	0.9394
Internal Moderator at 50%TD	0.9343	0.0009	0.9361
Internal Moderator at 40%TD	0.9225	0.0010	0.9245
Initial Enrichment 5.0 wt% U-235 - 4 PRAs, w/o BPRAs			
Internal Moderator at 100%TD	0.9098	0.0009	0.9116
Internal Moderator at 90%TD	0.9189	0.0008	0.9205
Internal Moderator at 80%TD	0.9285	0.0009	0.9303
Internal Moderator at 70%TD	0.9348	0.0009	0.9366
Internal Moderator at 60%TD	0.9364	0.0010	0.9384
Internal Moderator at 50%TD	0.9325	0.0010	0.9345
Internal Moderator at 40%TD	0.9185	0.0010	0.9205

**Table M.6-21
Criticality Results**

STORAGE

Model Description	k_{KENO}	1σ	k_{eff}
Regulatory Requirements			
Dry Storage (Bounded by infinite array of dry casks)	0.5821	0.0005	0.5831
Normal Conditions (Wet Loading)	0.9256	0.0008	0.9272
Accident Conditions (Damaged TC while fuel still wet)	0.9389	0.0010	0.9409

**Table M.6-22
Benchmarking Results**

Run ID	U Enrich. Wt%	Pitch (cm)	H ₂ O/fuel volume	Separation of assemblies (cm)	AEG	k _{eff}	1σ
B1645SO1	2.46	1.41	1.015	1.78	32.8194	0.9967	0.0009
B1645SO2	2.46	1.41	1.015	1.78	32.7584	1.0002	0.0011
BW1231B1	4.02	1.511	1.139		31.1427	0.9966	0.0012
BW1231B2	4.02	1.511	1.139		29.8854	0.9972	0.0009
BW1273M	2.46	1.511	1.376		32.2106	0.9965	0.0009
BW1484A1	2.46	1.636	1.841	1.64	34.5304	0.9962	0.0010
BW1484A2	2.46	1.636	1.841	4.92	35.1629	0.9931	0.0010
BW1484B1	2.46	1.636	1.841		33.9421	0.9979	0.0010
BW1484B2	2.46	1.636	1.841	1.64	34.5820	0.9955	0.0012
BW1484B3	2.46	1.636	1.841	4.92	35.2609	0.9969	0.0011
BW1484C1	2.46	1.636	1.841	1.64	34.6463	0.9931	0.0011
BW1484C2	2.46	1.636	1.841	1.64	35.2422	0.9939	0.0012
BW1484S1	2.46	1.636	1.841	1.64	34.5105	1.0001	0.0010
BW1484S2	2.46	1.636	1.841	1.64	34.5569	0.9992	0.0010
BW1484SL	2.46	1.636	1.841	6.54	35.4151	0.9935	0.0011
BW1645S1	2.46	1.209	0.383	1.78	30.1040	0.9990	0.0010
BW1645S2	2.46	1.209	0.383	1.78	29.9961	1.0037	0.0011
BW1810A	2.46	1.636	1.841		33.9465	0.9984	0.0008
BW1810B	2.46	1.636	1.841		33.9631	0.9984	0.0009
BW1810C	2.46	1.636	1.841		33.1569	0.9992	0.0010
BW1810D	2.46	1.636	1.841		33.0821	0.9985	0.0013
BW1810E	2.46	1.636	1.841		33.1600	0.9988	0.0009
BW1810F	2.46	1.636	1.841		33.9556	1.0031	0.0011
BW1810G	2.46	1.636	1.841		32.9409	0.9973	0.0011
BW1810H	2.46	1.636	1.841		32.9420	0.9972	0.0011
BW1810I	2.46	1.636	1.841		33.9655	1.0037	0.0009
BW1810J	2.46	1.636	1.841		33.1403	0.9983	0.0011
EPRU65	2.35	1.562	1.196		33.9106	0.9960	0.0011
EPRU65B	2.35	1.562	1.196		33.4013	0.9993	0.0012
EPRU75	2.35	1.905	2.408		35.8671	0.9958	0.0010
EPRU75B	2.35	1.905	2.408		35.3043	0.9996	0.0010
EPRU87	2.35	2.21	3.687		36.6129	1.0007	0.0011
EPRU87B	2.35	2.21	3.687		36.3499	1.0007	0.0011
NSE71SQ	4.74	1.26	1.823		33.7610	0.9979	0.0012
NSE71W1	4.74	1.26	1.823		34.0129	0.9988	0.0013
NSE71W2	4.74	1.26	1.823		36.3037	0.9957	0.0010
P2438BA	2.35	2.032	2.918	5.05	36.2277	0.9979	0.0013

Table M.6-22
Benchmarking Results
(Continued)

Run ID	U Enrich. Wt%	Pitch (cm)	H ₂ O/fuel volume	Separation of assemblies (cm)	AEG	k _{eff}	1σ
P2438SLG	2.35	2.032	2.918	8.39	36.2889	0.9986	0.0012
P2438SS	2.35	2.032	2.918	6.88	36.2705	0.9974	0.0011
P2438ZR	2.35	2.032	2.918	8.79	36.2840	0.9987	0.0010
P2615BA	4.31	2.54	3.883	6.72	35.7286	1.0019	0.0014
P2615SS	4.31	2.54	3.883	8.58	35.7495	0.9952	0.0015
P2615ZR	4.31	2.54	3.883	10.92	35.7700	0.9977	0.0014
P2827L1	2.35	2.032	2.918	13.72	36.2526	1.0057	0.0011
P2827L2	2.35	2.032	2.918	11.25	36.2908	0.9999	0.0012
P2827L3	4.31	2.54	3.883	20.78	35.6766	1.0092	0.0012
P2827L4	4.31	2.54	3.883	19.04	35.7131	1.0073	0.0012
P2827SLG	2.35	2.032	2.918	8.31	36.3037	0.9957	0.0010
P3314BA	4.31	1.892	1.6	2.83	33.1881	0.9988	0.0012
P3314BC	4.31	1.892	1.6	2.83	33.2284	0.9992	0.0012
P3314BF1	4.31	1.892	1.6	2.83	33.2505	1.0037	0.0013
P3314BF2	4.31	1.892	1.6	2.83	33.2184	1.0009	0.0013
P3314BS1	2.35	1.684	1.6	3.86	34.8594	0.9956	0.0013
P3314BS2	2.35	1.684	1.6	3.46	34.8356	0.9949	0.0010
P3314BS3	4.31	1.892	1.6	7.23	33.4247	0.9970	0.0013
P3314BS4	4.31	1.892	1.6	6.63	33.4162	0.9998	0.0012
P3314SLG	4.31	1.892	1.6	2.83	34.0198	0.9974	0.0012
P3314SS1	4.31	1.892	1.6	2.83	33.9601	0.9999	0.0012
P3314SS2	4.31	1.892	1.6	2.83	33.7755	1.0022	0.0012
P3314SS3	4.31	1.892	1.6	2.83	33.8904	0.9992	0.0013
P3314SS4	4.31	1.892	1.6	2.83	33.7625	0.9958	0.0011
P3314SS5	2.35	1.684	1.6	7.8	34.9531	0.9949	0.0013
P3314SS6	4.31	1.892	1.6	10.52	33.5333	1.0020	0.0011
P3314W1	4.31	1.892	1.6		34.3994	1.0024	0.0013
P3314W2	2.35	1.684	1.6		35.2167	0.9969	0.0011
P3314ZR	4.31	1.892	1.6	2.83	33.9954	0.9971	0.0013
P3602BB	4.31	1.892	1.6	8.3	33.3221	1.0029	0.0013
P3602BS1	2.35	1.684	1.6	4.8	34.7750	1.0027	0.0012
P3602BS2	4.31	1.892	1.6	9.83	33.3679	1.0039	0.0012
P3602N11	2.35	1.684	1.6	8.98	34.7438	1.0023	0.0012
P3602N12	2.35	1.684	1.6	9.58	34.8391	1.0030	0.0012
P3602N13	2.35	1.684	1.6	9.66	34.9337	1.0013	0.0012
P3602N14	2.35	1.684	1.6	8.54	35.0282	0.9974	0.0013

Table M.6-22
Benchmarking Results
(Continued)

Run ID	U Enrich. Wt%	Pitch (cm)	H ₂ O/fuel volume	Separation of assemblies (cm)	AEG	k _{eff}	1σ
P3602N21	2.35	2.032	2.918	10.36	36.2821	0.9987	0.0011
P3602N22	2.35	2.032	2.918	11.2	36.1896	1.0025	0.0011
P3602N31	4.31	1.892	1.6	14.87	33.2094	1.0057	0.0013
P3602N32	4.31	1.892	1.6	15.74	33.3067	1.0093	0.0012
P3602N33	4.31	1.892	1.6	15.87	33.4174	1.0107	0.0012
P3602N34	4.31	1.892	1.6	15.84	33.4683	1.0045	0.0013
P3602N35	4.31	1.892	1.6	15.45	33.5185	1.0013	0.0012
P3602N36	4.31	1.892	1.6	13.82	33.5855	1.0004	0.0014
P3602N41	4.31	2.54	3.883	12.89	35.5276	1.0109	0.0013
P3602N42	4.31	2.54	3.883	14.12	35.6695	1.0071	0.0014
P3602N43	4.31	2.54	3.883	12.44	35.7542	1.0053	0.0015
P3602SS1	2.35	1.684	1.6	8.28	34.8701	1.0025	0.0013
P3602SS2	4.31	1.892	1.6	13.75	33.4202	1.0035	0.0012
P3926L1	2.35	1.684	1.6	10.06	34.8519	1.0000	0.0011
P3926L2	2.35	1.684	1.6	10.11	34.9324	1.0017	0.0011
P3926L3	2.35	1.684	1.6	8.5	35.0641	0.9949	0.0012
P3926L4	4.31	1.892	1.6	17.74	33.3243	1.0074	0.0014
P3926L5	4.31	1.892	1.6	18.18	33.4074	1.0057	0.0013
P3926L6	4.31	1.892	1.6	17.43	33.5246	1.0046	0.0013
P3926SL1	2.35	1.684	1.6	6.59	33.4737	0.9995	0.0012
P3926SL2	4.31	1.892	1.6	12.79	33.5776	1.0007	0.0012
P4267B1	4.31	1.8901	1.59		31.8075	0.9990	0.0010
P4267B2	4.31	0.89	1.59		31.5323	1.0033	0.0010
P4267B3	4.31	1.715	1.09		30.9905	1.0050	0.0011
P4267B4	4.31	1.715	1.09		30.5061	0.9996	0.0011
P4267B5	4.31	1.715	1.09		30.1011	1.0004	0.0011
P4267SL1	4.31	1.89	1.59		33.4737	0.9995	0.0012
P4267SL2	4.31	1.715	1.09		31.9460	0.9988	0.0016
P62FT231	4.31	1.891	1.6	5.67	32.9196	1.0012	0.0013
P71F14F3	4.31	1.891	1.6	5.19	32.8237	1.0009	0.0014
P71F14V3	4.31	1.891	1.6	5.19	32.8597	0.9972	0.0014
P71F14V5	4.31	1.891	1.6	5.19	32.8609	0.9993	0.0013
P71F214R	4.31	1.891	1.6	5.19	32.8778	0.9969	0.0012
PAT80L1	4.74	1.6	3.807	2	35.0253	1.0012	0.0012
PAT80L2	4.74	1.6	3.807	2	35.1136	0.9993	0.0015
PAT80SS1	4.74	1.6	3.807	2	35.0045	0.9988	0.0013
PAT80SS2	4.74	1.6	3.807	2	35.1072	0.9960	0.0013

**Table M.6-22
Benchmarking Results
(Continued)**

Run ID	U Enrich. Wt%	Pitch (cm)	H ₂ O/fuel volume	Separation of assemblies (cm)	AEG	k _{eff}	1σ
W3269A	5.7	1.422	1.93		33.1480	0.9988	0.0012
W3269B1	3.7	1.105	1.432		32.4055	0.9961	0.0011
W3269B2	3.7	1.105	1.432		32.3921	0.9963	0.0011
W3269B3	3.7	1.105	1.432		32.2363	0.9944	0.0011
W3269C	2.72	1.524	1.494		33.7727	0.9989	0.0012
W3269SL1	2.72	1.524	1.494		33.3850	0.9981	0.0014
W3269SL2	5.7	1.422	1.93		33.0910	1.0005	0.0013
W3269W1	2.72	1.524	1.494		33.5114	0.9966	0.0014
W3269W2	5.7	1.422	1.93		33.1680	1.0014	0.0014
W3385SL1	5.74	1.422	1.932		33.2387	1.0009	0.0012
W3385SL2	5.74	2.012	5.067		35.8818	0.9997	0.0013
Correlation	0.31	0.39	0.16	0.68	-0.03	N/A	N/A

**Table M.6-23
USL-1 Results**

Parameter	Range of Applicability	USL-1
U Enrichment (wt. % U-235)	2.4	0.9423
	2.8	0.9429
	3.3	0.9434
	3.8 – 5.7	0.9437
Fuel Rod Pitch (cm)	0.89	0.9396
	1.1	0.9407
	1.2	0.9411
	1.4	0.9418
	1.6	0.9429
	1.8 – 2.6	0.9438
Water/Fuel Volume Ratio	0.38	0.9420
	1.1	0.9425
	1.7	0.9429
	2.4 – 5.1	0.9433
Assembly Separation (cm)	1.4	0.9412
	1.6	0.9413
	4.4	0.9428
	7.1 – 21	0.9442
Average Energy Group Causing Fission (AEG)	30 – 32	0.9434
	33	0.9433
	34	0.9432
	35	0.9431
	36	0.9430
	37	0.9430

Table M.6-24
USL Determination for Criticality Analysis

Parameter	Value from Limiting Analysis	Bounding USL-1
U Enrichment (wt. % U-235)	3.4	0.9434
Fuel Rod Pitch (cm)	1.25984	0.9411
Water/Fuel Ratio	1.66	0.9425
Assembly Separation (cm)	1.4	0.9412
Average Energy Group Causing Fission (AEG)	30.8	0.9434

**Table M.6-25
Enrichment Data for Loading Pattern 1**

Radial Zone	Enrichment (wt% U-235)
Average	3.47
Radial Zone 1	3.95
Radial Zone 2	3.15
Radial Zone 3	2.73
Radial Zone 4	2.45

Enrichment Data for Loading Pattern 2

Radial Zone	Enrichment (wt% U-235) for Various Zones		
	Pattern 2A	Pattern 2B	Pattern 2C
Average	4.07	4.24	4.39
Radial Zone 1	4.42	4.56	4.78
Radial Zone 2	3.70	3.85	4.00
Radial Zone 3	2.90	3.02	3.13
Radial Zone 4	2.20	2.28	2.37

Table M.6-26
Results for the Exxon/ANF 15x15 Fuel Assembly

Model Description	k_{KENO}	1σ	k_{eff}
Exxon/ANF 15x15 CE, Uniform Maximum Lattice Average Enrichment, Loading Pattern 1			
MD=40%	0.8856	0.0009	0.8874
MD=50%	0.9074	0.0009	0.9092
MD=55%	0.9111	0.0009	0.9129
MD=60%	0.9146	0.0008	0.9162
MD=65%	0.9176	0.0007	0.9190
MD=70%	0.9169	0.0009	0.9187
MD=75%	0.9160	0.0007	0.9174
MD=80%	0.9159	0.0009	0.9177
MD=85%	0.9115	0.0008	0.9131
MD=90%	0.9081	0.0009	0.9099
MD=95%	0.9036	0.0007	0.9050
MD=100%	0.8994	0.0010	0.9014
Exxon/ANF 15x15 CE, Non-Uniform Radial Enrichment, Loading Pattern 1			
MD=40%	0.8812	0.0008	0.8828
MD=50%	0.9008	0.0008	0.9024
MD=55%	0.9052	0.0009	0.9070
MD=60%	0.9106	0.0009	0.9124
MD=65%	0.9115	0.0008	0.9131
MD=70%	0.9120	0.0009	0.9138
MD=75%	0.9109	0.0009	0.9127
MD=80%	0.9108	0.0009	0.9126
MD=85%	0.9073	0.0008	0.9089
MD=90%	0.9037	0.0009	0.9055
MD=95%	0.9000	0.0010	0.9020
MD=100%	0.8959	0.0008	0.8975
Exxon/ANF 15x15 CE, Results for the Uniform Maximum Lattice Average Enrichment Cases			
Loading Pattern 2A			
MD=60%	0.9611	0.0009	0.9629
MD=70%	0.9649	0.0008	0.9665
MD=80%	0.9628	0.0010	0.9648
MD=100%	0.9481	0.0009	0.9499
Loading Pattern 2B			
MD=60%	0.9723	0.0009	0.9741
MD=70%	0.9780	0.0009	0.9798
MD=80%	0.9742	0.0010	0.9762
MD=100%	0.9618	0.0009	0.9636

Table M.6-26
Results for the Exxon/ANF 15x15 Fuel Assembly
(Concluded)

Model Description	k_{KENO}	1σ	k_{eff}
Loading Pattern 2C			
MD=60%	0.9809	0.0008	0.9825
MD=70%	0.9866	0.0009	0.9884
MD=80%	0.9839	0.0009	0.9857
MD=100%	0.9736	0.0008	0.9752
Exxon/ANF 15x15 CE, Results for the Non-Uniform Radial Enrichment Cases			
Loading Pattern 2A			
MD=60%	0.9531	0.0008	0.9547
MD=70%	0.9602	0.0008	0.9618
MD=80%	0.9569	0.0010	0.9589
MD=100%	0.9436	0.0008	0.9452
Loading Pattern 2B			
MD=60%	0.9637	0.0009	0.9655
MD=70%	0.9683	0.0010	0.9703
MD=80%	0.9661	0.0009	0.9679
MD=100%	0.9549	0.0009	0.9567
Loading Pattern 2C			
MD=60%	0.9757	0.0010	0.9777
MD=70%	0.9801	0.0009	0.9819
MD=80%	0.9797	0.0008	0.9813
MD=100%	0.9665	0.0009	0.9683

Table M.6-27
Results for the WE 17x17 Class Fuel Assembly without BPRAs (16 Poison Plates)

Model Description	k_{KENO}	1σ	k_{eff}
Initial Enrichment 3.4 w/o U-235, No BPRAs			
MD=40%	0.9094	0.0009	0.9112
MD=50%	0.9267	0.0008	0.9283
MD=55%	0.9311	0.0009	0.9329
MD=60%	0.9320	0.0009	0.9338
MD=65%	0.9332	0.0008	0.9348
MD=70%	0.9324	0.0008	0.9340
MD=75%	0.9303	0.0009	0.9321
MD=80%	0.9256	0.0008	0.9272
MD=85%	0.9204	0.0008	0.9220
MD=90%	0.9150	0.0009	0.9168
MD=95%	0.9099	0.0010	0.9119
MD=100%	0.9038	0.0009	0.9056

Table M.6-28
Results for the WE 17x17 Class Fuel Assembly with BPRAs (16 Poison Plates)

Model Description	k_{KENO}	1σ	k_{eff}
Initial Enrichment 3.4 w/o U-235, With BPRAs			
MD=40%	0.9018	0.0009	0.9036
MD=50%	0.9208	0.0009	0.9226
MD=55%	0.9265	0.0008	0.9281
MD=60%	0.9327	0.0009	0.9345
MD=65%	0.9354	0.0009	0.9372
MD=70%	0.9340	0.0009	0.9358
MD=75%	0.9351	0.0009	0.9369
MD=80%	0.9321	0.0008	0.9337
MD=85%	0.9303	0.0008	0.9319
MD=90%	0.9284	0.0008	0.9300
MD=95%	0.9231	0.0008	0.9247
MD=100%	0.9179	0.0008	0.9195

Table M.6-29
Results for the WE 17x17 Class Fuel Assembly without BPRAs (24 Poison Plates)

Model Description	k_{KENO}	1σ	k_{eff}
Initial Enrichment 3.4 w/o U-235, No BPRAs, No PRAs			
MD=40%	0.8829	0.0009	0.8847
MD=50%	0.9030	0.0009	0.9048
MD=60%	0.9136	0.0009	0.9154
MD=70%	0.9134	0.0009	0.9152
MD=80%	0.9083	0.0009	0.9101
MD=90%	0.9008	0.0010	0.9028
MD=100%	0.8900	0.0008	0.8916
Initial Enrichment 4.0 w/o U-235, No BPRAs, 4 PRAs			
MD=40%	0.8728	0.0009	0.8746
MD=50%	0.9005	0.0010	0.9025
MD=60%	0.9176	0.0009	0.9194
MD=70%	0.9237	0.0010	0.9257
MD=80%	0.9242	0.0009	0.9260
MD=90%	0.9221	0.0009	0.9239
MD=100%	0.9153	0.0009	0.9171
Initial Enrichment 4.5 w/o U-235, No BPRAs, 8 PRAs			
MD=40%	0.8604	0.0008	0.8620
MD=50%	0.8931	0.0009	0.8949
MD=60%	0.9126	0.0010	0.9146
MD=70%	0.9240	0.0010	0.9260
MD=80%	0.9283	0.0009	0.9301
MD=90%	0.9298	0.0009	0.9316
MD=100%	0.9265	0.0010	0.9285
Initial Enrichment 5.0 w/o U-235, No BPRAs, 16 PRAs			
MD=40%	0.8023	0.0010	0.8043
MD=50%	0.8401	0.0009	0.8419
MD=60%	0.8645	0.0011	0.8667
MD=70%	0.8841	0.0011	0.8863
MD=80%	0.8974	0.0012	0.8998
MD=90%	0.9049	0.0012	0.9073
MD=100%	0.9071	0.0012	0.9095

Table M.6-30
Results for the WE 17x17 Class Fuel Assembly with BPRAs (24 Poison Plates)

Model Description	k_{KENO}	1σ	k_{eff}
Initial Enrichment 3.4 w/o U-235, with BPRAs, No PRAs			
MD=40%	0.8739	0.0009	0.8757
MD=50%	0.8960	0.0010	0.8980
MD=60%	0.9093	0.0008	0.9109
MD=70%	0.9144	0.0008	0.9160
MD=80%	0.9143	0.0009	0.9161
MD=90%	0.9117	0.0008	0.9133
MD=100%	0.9049	0.0010	0.9069
Initial Enrichment 4.0 w/o U-235, with BPRAs, 4 PRAs			
MD=40%	0.8627	0.0009	0.8645
MD=50%	0.8932	0.0008	0.8948
MD=60%	0.9115	0.0008	0.9131
MD=70%	0.9237	0.0009	0.9255
MD=80%	0.9293	0.0008	0.9309
MD=90%	0.9297	0.0010	0.9317
MD=100%	0.9256	0.0008	0.9272
Initial Enrichment 4.5 w/o U-235, with BPRAs, 8 PRAs			
MD=40%	0.8481	0.0009	0.8499
MD=50%	0.8840	0.0011	0.8862
MD=60%	0.9051	0.0011	0.9073
MD=70%	0.9205	0.0009	0.9223
MD=80%	0.9293	0.0009	0.9311
MD=90%	0.9345	0.0010	0.9365
MD=100%	0.9352	0.0011	0.9374
Initial Enrichment 5.0 w/o U-235, with BPRAs, 16 PRAs			
MD=40%	0.7905	0.0010	0.7925
MD=50%	0.8276	0.0009	0.8294
MD=60%	0.8567	0.0010	0.8587
MD=70%	0.8798	0.0011	0.8820
MD=80%	0.8937	0.0011	0.8959
MD=90%	0.9035	0.0012	0.9059
MD=100%	0.9119	0.0011	0.9141

Table M.6-31
Results for the B&W 15x15 Class Fuel Assembly without BPRAs (16 Poison Plates)

Model Description	k_{KENO}	1σ	k_{err}
Initial Enrichment 3.3 w/o U-235, No BPRAs			
MD=40%	0.9077	0.0010	0.9097
MD=50%	0.9236	0.0009	0.9254
MD=55%	0.9287	0.0008	0.9303
MD=60%	0.9291	0.0008	0.9307
MD=65%	0.9301	0.0008	0.9317
MD=70%	0.9275	0.0009	0.9293
MD=75%	0.9246	0.0008	0.9262
MD=80%	0.9215	0.0008	0.9231
MD=85%	0.9168	0.0008	0.9184
MD=90%	0.9106	0.0009	0.9124
MD=95%	0.9025	0.0009	0.9043
MD=100%	0.8975	0.0007	0.8989

Table M.6-32
Results for the B&W 15x15 Class Fuel Assembly with BPRAs (16 Poison Plates)

Model Description	k_{KENO}	1σ	k_{eff}
Initial Enrichment 3.3 w/o U-235, With BPRAs			
MD=40%	0.9003	0.0009	0.9021
MD=50%	0.9211	0.0009	0.9229
MD=55%	0.9267	0.0009	0.9285
MD=60%	0.9293	0.0008	0.9309
MD=65%	0.9321	0.0009	0.9339
MD=70%	0.9323	0.0009	0.9341
MD=75%	0.9324	0.0007	0.9338
MD=80%	0.9284	0.0010	0.9304
MD=85%	0.9260	0.0008	0.9276
MD=90%	0.9214	0.0009	0.9232
MD=95%	0.9177	0.0008	0.9193
MD=100%	0.9137	0.0008	0.9153

Table M.6-33
Results for the B&W 15x15 Class Fuel Assembly without BPRAs (24 Poison Plates)

Model Description	k_{KENO}	1σ	k_{eff}
Initial Enrichment 3.3 w/o U-235, No BPRAs, No PRAs			
MD=40%	0.8785	0.0009	0.8803
MD=50%	0.8999	0.0008	0.9015
MD=60%	0.9078	0.0009	0.9096
MD=70%	0.9077	0.0008	0.9093
MD=80%	0.9034	0.0008	0.9050
MD=90%	0.8953	0.0009	0.8971
MD=100%	0.8829	0.0010	0.8849
Initial Enrichment 3.9 w/o U-235, No BPRAs, 4 PRAs			
MD=40%	0.8794	0.0010	0.8814
MD=50%	0.9058	0.0009	0.9076
MD=60%	0.9204	0.0009	0.9222
MD=70%	0.9254	0.0009	0.9272
MD=80%	0.9275	0.0009	0.9293
MD=90%	0.9236	0.0009	0.9254
MD=100%	0.9130	0.0008	0.9146
Initial Enrichment 5.0 w/o U-235, No BPRAs, 16 PRAs			
MD=40%	0.8357	0.0008	0.8373
MD=50%	0.8704	0.0010	0.8724
MD=60%	0.8929	0.0009	0.8947
MD=70%	0.9100	0.0010	0.9120
MD=80%	0.9194	0.0011	0.9216
MD=90%	0.9233	0.0011	0.9255
MD=100%	0.9234	0.0012	0.9258

Table M.6-34
Results for the B&W 15x15 Class Fuel Assembly with BPRAs (24 Poison Plates)

Model Description	k_{KENO}	1σ	k_{eff}
Initial Enrichment 3.3 w/o U-235, with BPRAs, No PRAs			
MD=40%	0.8704	0.0009	0.8722
MD=50%	0.8953	0.0009	0.8971
MD=60%	0.9060	0.0009	0.9078
MD=70%	0.9117	0.0011	0.9139
MD=80%	0.9111	0.0008	0.9127
MD=90%	0.9050	0.0008	0.9066
MD=100%	0.8982	0.0008	0.8998
Initial Enrichment 3.9 w/o U-235, with BPRAs, 4 PRAs			
MD=40%	0.8711	0.0009	0.8729
MD=50%	0.8995	0.0009	0.9013
MD=60%	0.9167	0.0009	0.9185
MD=70%	0.9288	0.0009	0.9306
MD=80%	0.9299	0.0008	0.9315
MD=90%	0.9303	0.0010	0.9323
MD=100%	0.9257	0.0010	0.9277
Initial Enrichment 5.0 w/o U-235, with BPRAs, 16 PRAs			
MD=40%	0.8278	0.0009	0.8296
MD=50%	0.8606	0.0010	0.8626
MD=60%	0.8891	0.0008	0.8907
MD=70%	0.9062	0.0011	0.9084
MD=80%	0.9196	0.0012	0.9220
MD=90%	0.9269	0.0011	0.9291
MD=100%	0.9304	0.0010	0.9324

Table M.6-35
Results for the CE 15x15 Class Fuel Assembly without BPRAs (16 Poison Plates)

Model Description	k_{KENO}	1σ	k_{eff}
Initial Enrichment 3.4 w/o U-235, No BPRAs			
MD=40%	0.9033	0.0008	0.9049
MD=50%	0.9197	0.0008	0.9213
MD=55%	0.9232	0.0008	0.9248
MD=60%	0.9252	0.0010	0.9272
MD=65%	0.9269	0.0008	0.9285
MD=70%	0.9262	0.0008	0.9278
MD=75%	0.9231	0.0009	0.9249
MD=80%	0.9206	0.0009	0.9224
MD=85%	0.9167	0.0009	0.9185
MD=90%	0.9116	0.0008	0.9132
MD=95%	0.9061	0.0008	0.9077
MD=100%	0.9000	0.0009	0.9018
Initial Enrichment 3.5 w/o U-235, No BPRAs			
MD=40%	0.9088	0.0008	0.9104
MD=50%	0.9273	0.0009	0.9291
MD=55%	0.9314	0.0008	0.9330
MD=60%	0.9343	0.0008	0.9359
MD=65%	0.9346	0.0009	0.9364
MD=70%	0.9324	0.0009	0.9342
MD=75%	0.9327	0.0008	0.9343
MD=80%	0.9282	0.0010	0.9302
MD=85%	0.9250	0.0008	0.9266
MD=90%	0.9197	0.0010	0.9217
MD=95%	0.9142	0.0009	0.9160
MD=100%	0.9084	0.0010	0.9104

Table M.6-36
Results for the WE 15x15 Class Fuel Assembly without BPRAs (16 Poison Plates)

Model Description	k_{KENO}	1σ	k_{eff}
Initial Enrichment 3.4 w/o U-235, No BPRAs			
MD=40%	0.9129	0.0009	0.9147
MD=50%	0.9280	0.0010	0.9300
MD=55%	0.9320	0.0010	0.9340
MD=60%	0.9316	0.0008	0.9332
MD=65%	0.9321	0.0010	0.9341
MD=70%	0.9287	0.0008	0.9303
MD=75%	0.9257	0.0009	0.9275
MD=80%	0.9198	0.0008	0.9214
MD=85%	0.9158	0.0008	0.9174
MD=90%	0.9074	0.0008	0.9090
MD=95%	0.9008	0.0009	0.9026
MD=100%	0.8948	0.0009	0.8966

Table M.6-37
Results for the WE 15x15 Class Fuel Assembly without BPRAs (24 Poison Plates)

Model Description	k_{KENO}	1σ	k_{eff}
Initial Enrichment 3.4 w/o U-235, No BPRAs, No PRAs			
MD=40%	0.8847	0.0008	0.8863
MD=50%	0.9035	0.0009	0.9053
MD=60%	0.9106	0.0008	0.9122
MD=70%	0.9096	0.0008	0.9112
MD=80%	0.9040	0.0009	0.9058
MD=90%	0.8949	0.0008	0.8965
MD=100%	0.8805	0.0008	0.8821
Initial Enrichment 4.0 w/o U-235, No BPRAs, 4 PRAs			
MD=40%	0.8803	0.0009	0.8821
MD=50%	0.9049	0.0008	0.9065
MD=60%	0.9194	0.0008	0.9210
MD=70%	0.9234	0.0008	0.9250
MD=80%	0.9224	0.0010	0.9244
MD=90%	0.9174	0.0010	0.9194
MD=100%	0.9092	0.0009	0.9110
Initial Enrichment 4.6 w/o U-235, No BPRAs, 8 PRAs			
MD=40%	0.8756	0.0008	0.8772
MD=50%	0.9022	0.0010	0.9042
MD=60%	0.9234	0.0009	0.9252
MD=70%	0.9321	0.0009	0.9339
MD=80%	0.9352	0.0010	0.9372
MD=90%	0.9327	0.0009	0.9345
MD=100%	0.9270	0.0011	0.9292
Initial Enrichment 5.0 w/o U-235, No BPRAs, 16 PRAs			
MD=40%	0.8161	0.0008	0.8177
MD=50%	0.8525	0.0010	0.8545
MD=60%	0.8754	0.0010	0.8774
MD=70%	0.8927	0.0010	0.8947
MD=80%	0.9008	0.0010	0.9028
MD=90%	0.9056	0.0012	0.9080
MD=100%	0.9046	0.0012	0.9070

Table M.6-38
Results for the CE 14x14 Class Fuel Assembly without BPRAs (16 Poison Plates)

Model Description	k_{KENO}	1σ	k_{eff}
Initial Enrichment 3.8 w/o U-235, No BPRAs			
MD=40%	0.9146	0.0009	0.9164
MD=50%	0.9261	0.0008	0.9277
MD=55%	0.9269	0.0008	0.9285
MD=60%	0.9277	0.0008	0.9293
MD=65%	0.9263	0.0009	0.9281
MD=70%	0.9228	0.0009	0.9246
MD=75%	0.9147	0.0009	0.9165
MD=80%	0.9096	0.0009	0.9114
MD=85%	0.9021	0.0009	0.9039
MD=90%	0.8951	0.0008	0.8967
MD=95%	0.8871	0.0009	0.8889
MD=100%	0.8799	0.0009	0.8817
Initial Enrichment 3.9 w/o U-235, No BPRAs			
MD=40%	0.9207	0.0009	0.9225
MD=50%	0.9315	0.0008	0.9331
MD=55%	0.9356	0.0009	0.9374
MD=60%	0.9357	0.0009	0.9375
MD=65%	0.9318	0.0009	0.9336
MD=70%	0.9284	0.0009	0.9302
MD=75%	0.9243	0.0007	0.9257
MD=80%	0.9190	0.0008	0.9206
MD=85%	0.9104	0.0009	0.9122
MD=90%	0.9037	0.0010	0.9057
MD=95%	0.8952	0.0008	0.8968
MD=100%	0.8894	0.0010	0.8914

Table M.6-39
Results for the CE 14x14 Class Fuel Assembly without BPRAs (24 Poison Plates)

Model Description	k_{KENO}	1σ	k_{eff}
Initial Enrichment 3.8 w/o U-235, No BPRAs, No PRAs			
MD=40%	0.8886	0.0010	0.8906
MD=50%	0.9065	0.0011	0.9087
MD=60%	0.9094	0.0009	0.9112
MD=70%	0.9072	0.0009	0.9090
MD=80%	0.8996	0.0008	0.9012
MD=90%	0.8852	0.0009	0.8870
MD=100%	0.8716	0.0010	0.8736
Initial Enrichment 4.6 w/o U-235, No BPRAs, 4 PRAs			
MD=40%	0.8988	0.0009	0.9006
MD=50%	0.9199	0.0009	0.9217
MD=60%	0.9279	0.0010	0.9299
MD=70%	0.9285	0.0010	0.9305
MD=80%	0.9236	0.0012	0.9260
MD=90%	0.9142	0.0009	0.9160
MD=100%	0.9055	0.0009	0.9073
Initial Enrichment 5.0 w/o U-235, No BPRAs, 8 PRAs			
MD=40%	0.8883	0.0009	0.8901
MD=50%	0.9099	0.0011	0.9121
MD=60%	0.9210	0.0009	0.9228
MD=70%	0.9260	0.0009	0.9278
MD=80%	0.9234	0.0010	0.9254
MD=90%	0.9185	0.0009	0.9203
MD=100%	0.9106	0.0010	0.9126

Table M.6-40
Results for the WE 14x14 Class Fuel Assembly without BPRAs (16 Poison Plates)

Model Description	k_{KENO}	1σ	k_{eff}
Initial Enrichment 4.0 w/o U-235, No BPRAs			
MD=40%	0.9203	0.0009	0.9221
MD=50%	0.9252	0.0009	0.9270
MD=55%	0.9257	0.0009	0.9275
MD=60%	0.9254	0.0008	0.9270
MD=65%	0.9240	0.0008	0.9256
MD=70%	0.9184	0.0009	0.9202
MD=75%	0.9140	0.0010	0.9160
MD=80%	0.9098	0.0008	0.9114
MD=85%	0.9042	0.0009	0.9060
MD=90%	0.8972	0.0010	0.8992
MD=95%	0.8883	0.0010	0.8903
MD=100%	0.8758	0.0008	0.8774
Initial Enrichment 4.1 w/o U-235, No BPRAs			
MD=40%	0.9249	0.0009	0.9267
MD=45%	0.9306	0.0008	0.9322
MD=50%	0.9318	0.0010	0.9338
MD=55%	0.9320	0.0010	0.9340
MD=60%	0.9282	0.0009	0.9300
MD=65%	0.9256	0.0009	0.9274
MD=70%	0.9200	0.0010	0.9220
MD=75%	0.9144	0.0009	0.9162
MD=80%	0.9115	0.0011	0.9137
MD=85%	0.9043	0.0008	0.9059
MD=90%	0.8966	0.0010	0.8986
MD=100%	0.8820	0.0009	0.8838

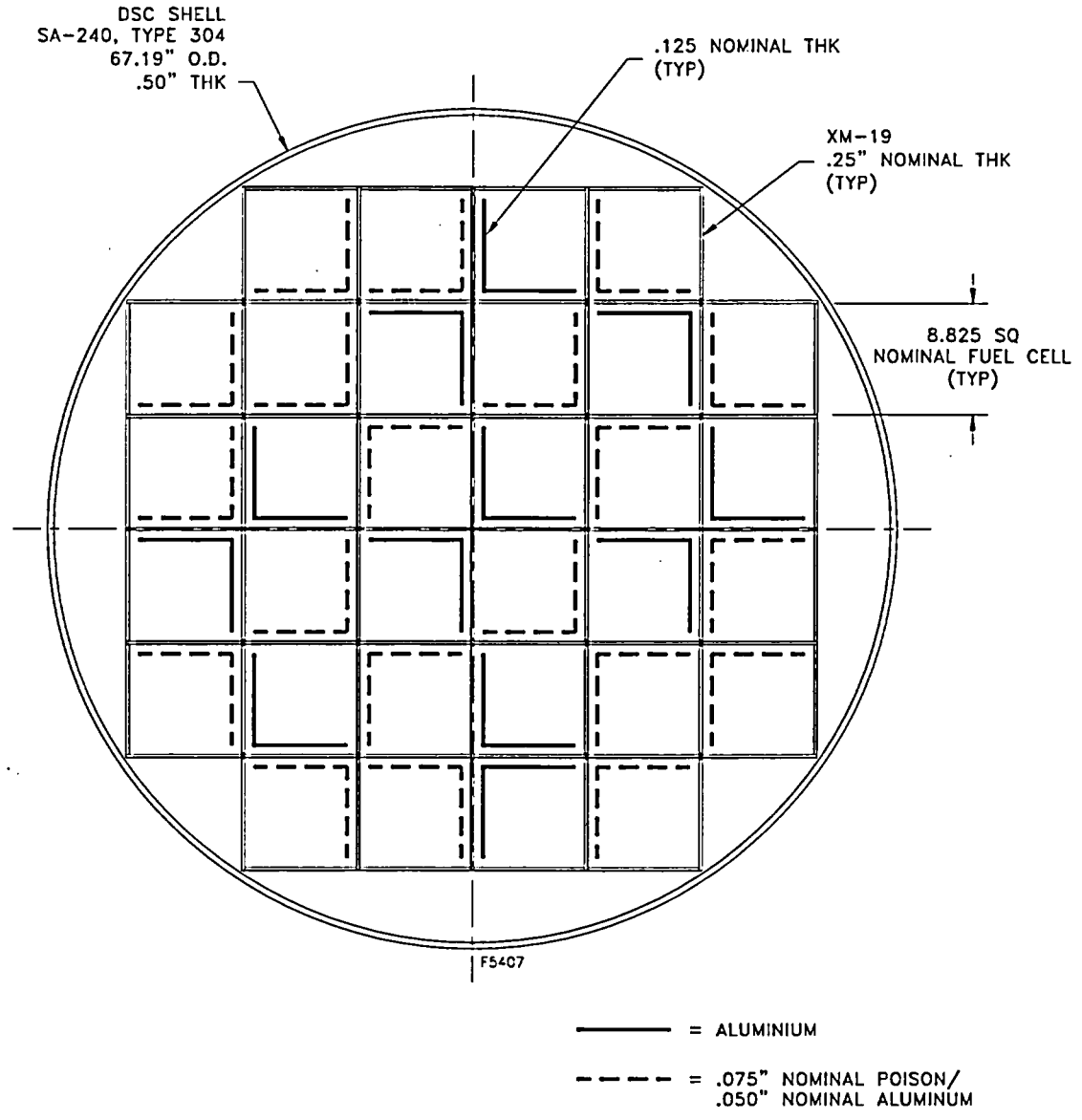


Figure M.6-1
Configuration with 20 Poison Plates
(Analyzed as Base Type A/B/C/D Basket)

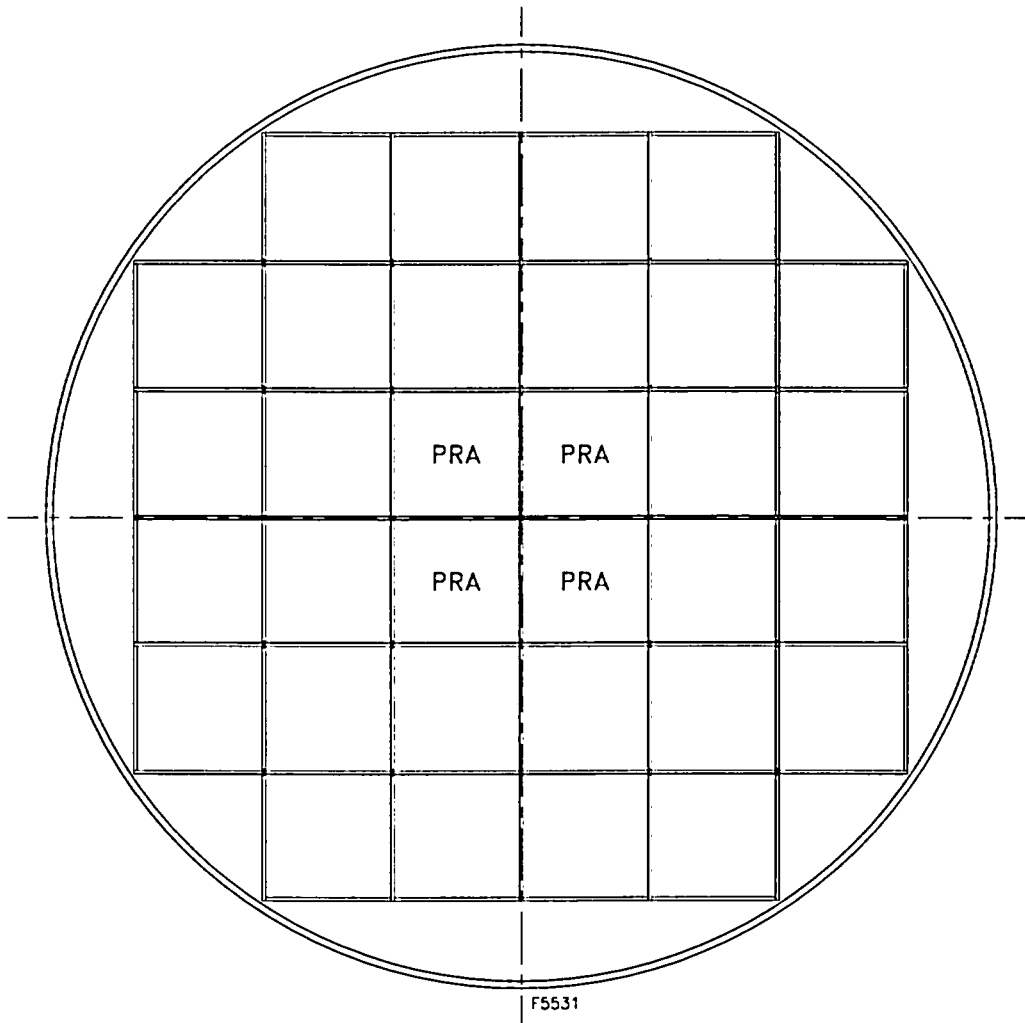
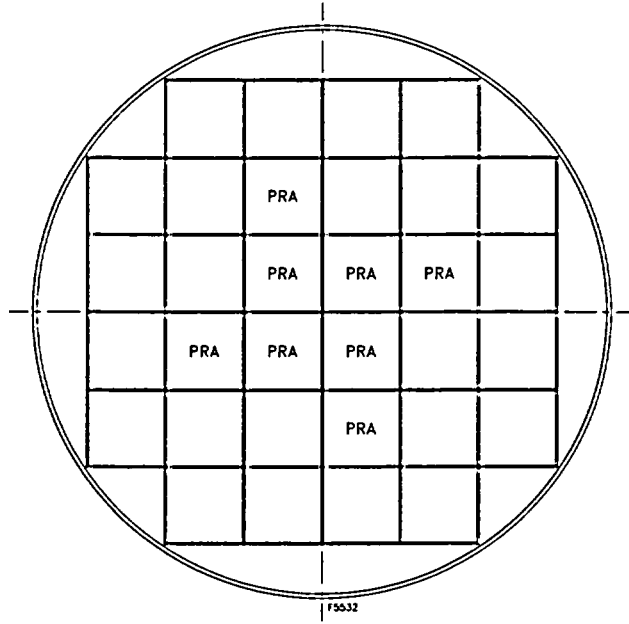


Figure M.6-2
Required PRA Locations for Configurations with Four PRAs
(Type B Basket)



OR

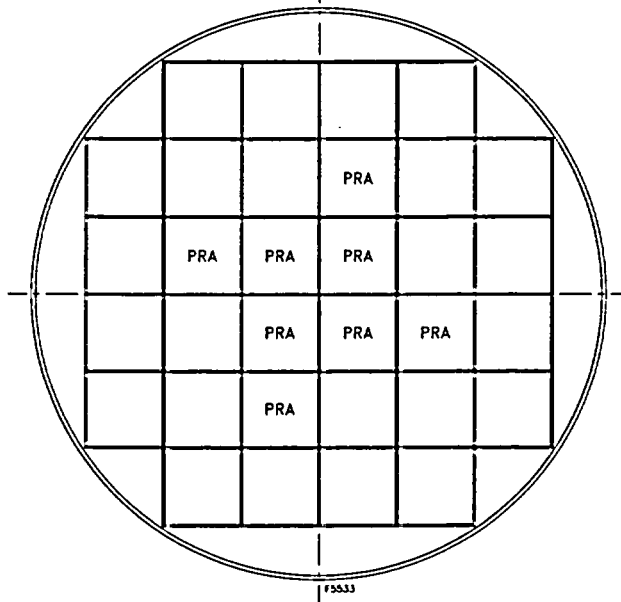


Figure M.6-3
Required PRA Locations for Configurations with Eight PRAs
(Type C Basket)

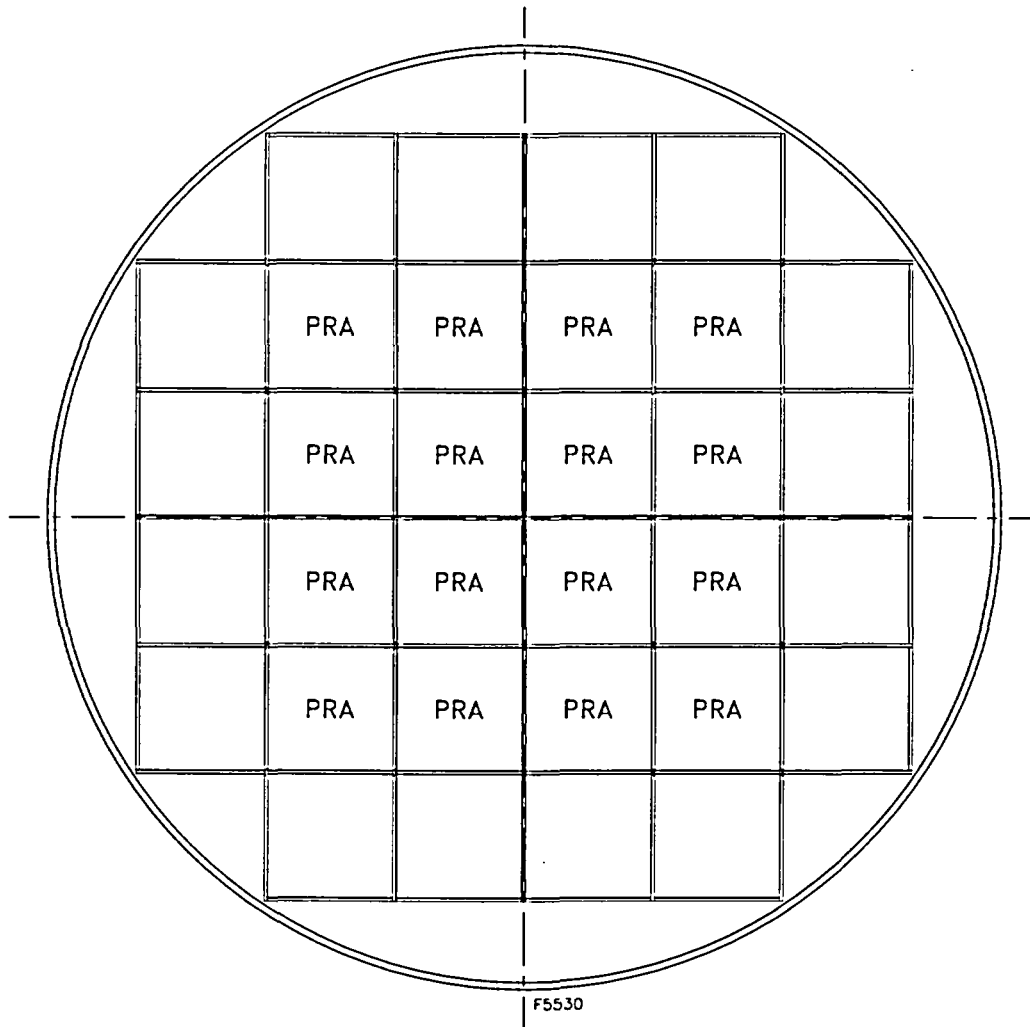
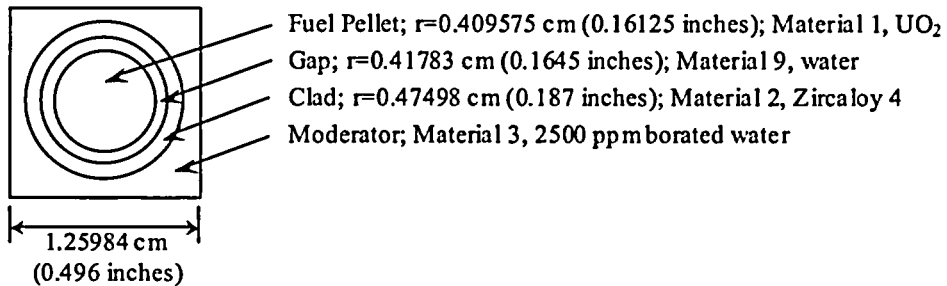
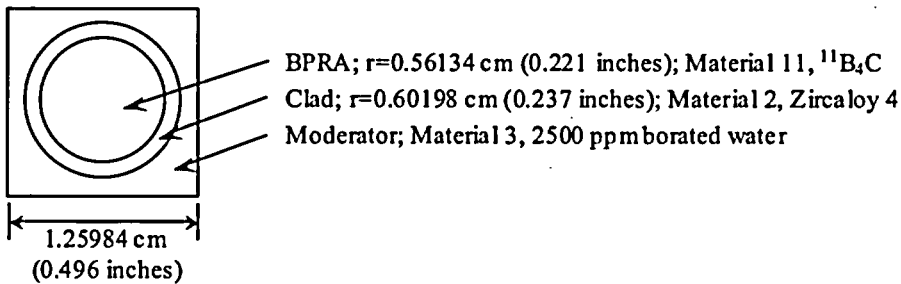


Figure M.6-4
Required PRA Locations for Configurations with Sixteen PRAs
(Type D Basket)

Unit 1 WE 17x17 Fuel Rod



Unit 2 WE 17x17 Guide Tube



Unit 3 WE 17x17 Instrument Tube

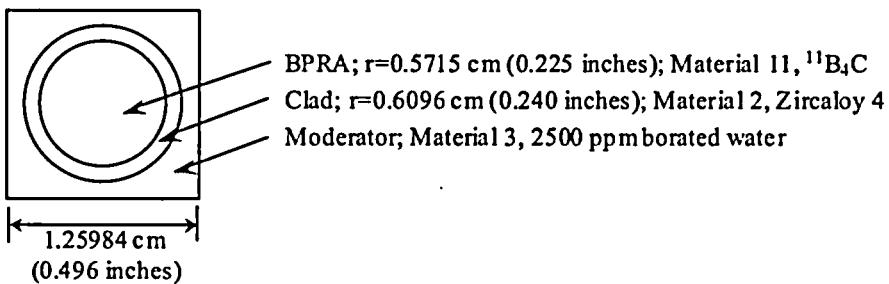
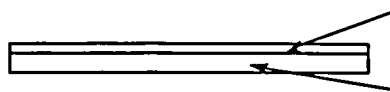


Figure M.6-5
KENO V.a units and Radial Cross Sections of the Model
Part 1 of 18 - (all units 365.76 cm (144 inches) long)

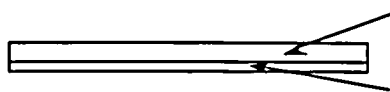
Unit 4 Top Horizontal Poison Plate



Aluminum; 21.4249 x 0.127 cm (8.435 x 0.05 inches);
Material 6, Aluminum

Poison Plate; 21.4249 x 0.1905 cm (8.435 x 0.075 inches);
Material 7, Borated Aluminum

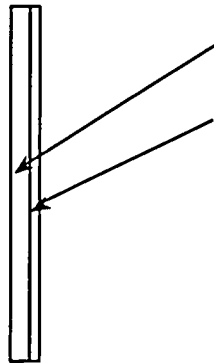
Unit 5 Bottom Horizontal Poison Plate



Poison Plate; 21.4249 x 0.1905 cm (8.435 x 0.075 inches);
Material 7, Borated Aluminum

Aluminum; 21.4249 x 0.127 cm (8.435 x 0.05 inches);
Material 6, Aluminum

Unit 6 Right Vertical Poison Plate



Poison Plate; 0.1905 x 21.4249 cm (0.075 x 8.435 inches);
Material 7, Borated Aluminum

Aluminum; 0.127 x 21.4249 cm (0.05 x 8.435 inches);
Material 6, Aluminum

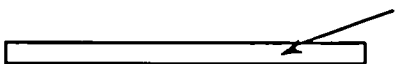
Figure M.6-5
KENO V.a units and Radial Cross Sections of the Model
Part 2 of 18 - (all units 365.76 cm (144 inches) long)

Unit 7 Left Vertical Poison Plate



Aluminum; 0.127 x 21.4249 cm (0.05 x 8.435 inches);
Material 6, Aluminum
Poison Plate; 0.1905 x 21.4249 cm (0.075 x 8.435 inches);
Material 7, Borated Aluminum

Unit 8 Top Horizontal Aluminum Plate



Aluminum; 21.4249 x 0.3175 cm (8.435 x 0.125 inches);
Material 6, Aluminum

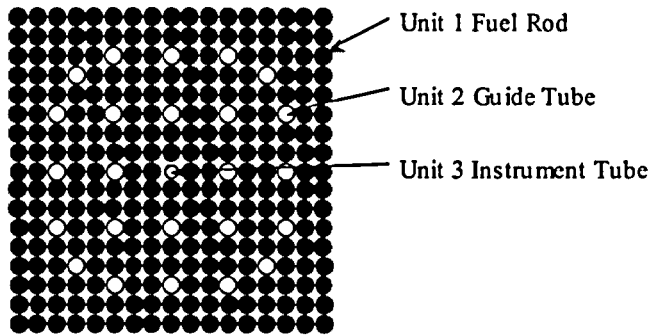
Unit 9 Left Vertical Aluminum Plate



Aluminum; 0.3175 x 21.4249 cm (1.25 x 8.435 inches);
Material 6, Aluminum

Figure M.6-5
KENO V.a units and Radial Cross Sections of the Model
Part 3 of 18 - (all units 365.76 cm (144 inches) long)

Array 1 WE 17x17 Fuel Assembly made up of a 17x17 array of Units 1 (fuel),
2 (Guide Tubes) and 3 (Instrument Tube)



Unit 10 WE 17x17 Fuel Assembly Shifted to the Upper Right in the Fuel
Compartment with Poison Plates in Upper Right

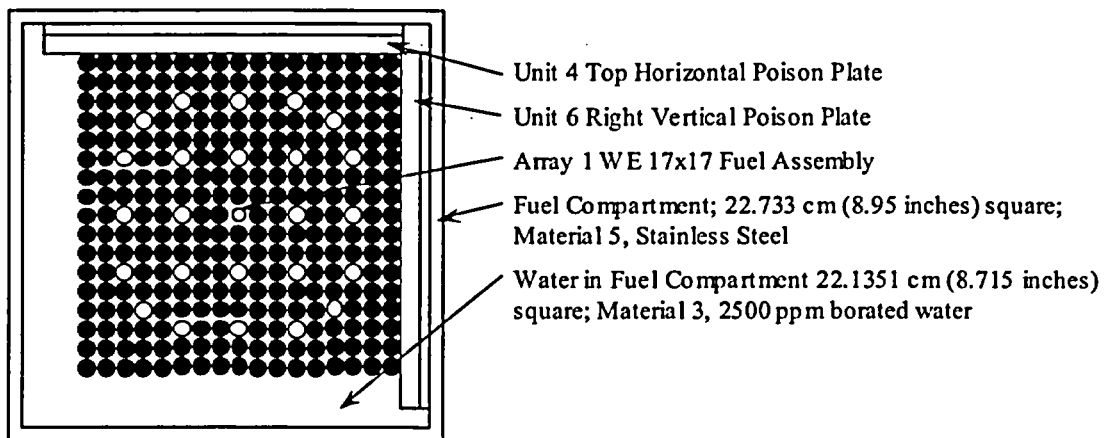
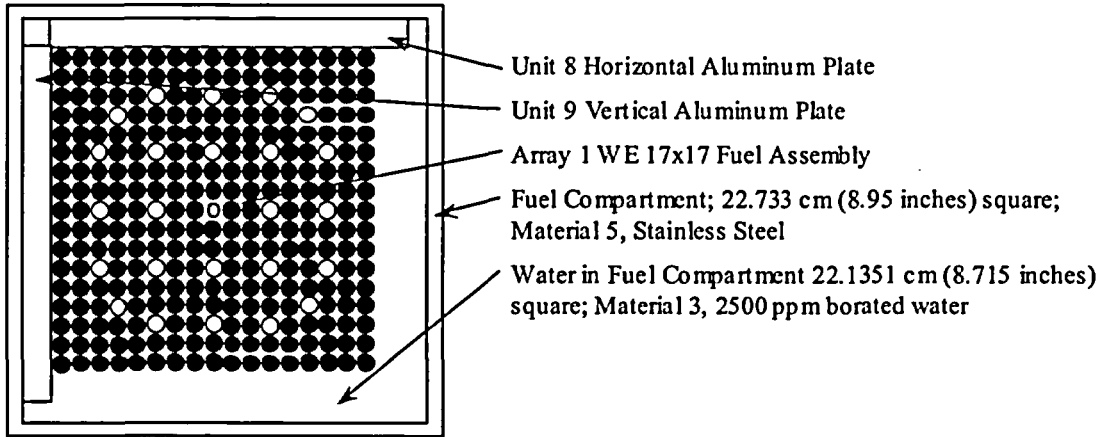


Figure M.6-5
KENO V.a units and Radial Cross Sections of the Model
Part 4 of 18 - (all units 365.76 cm (144 inches) long)

Unit 11 WE 17x17 Fuel Assembly Shifted to the Upper Left in the Fuel
Compartment with Aluminum Plates in Upper Left



Unit 12 WE 17x17 Fuel Assembly Shifted to the Upper Right in the Fuel
Compartment with Poison Plates in Upper Left

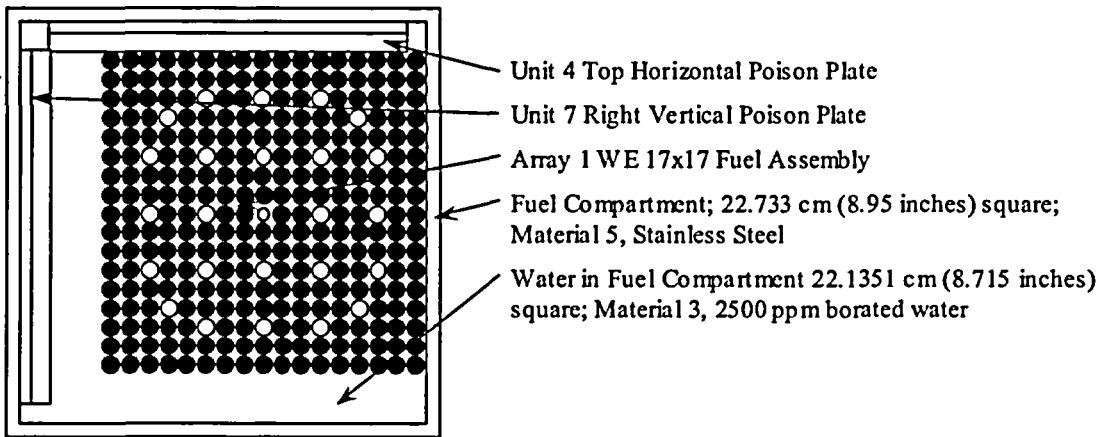
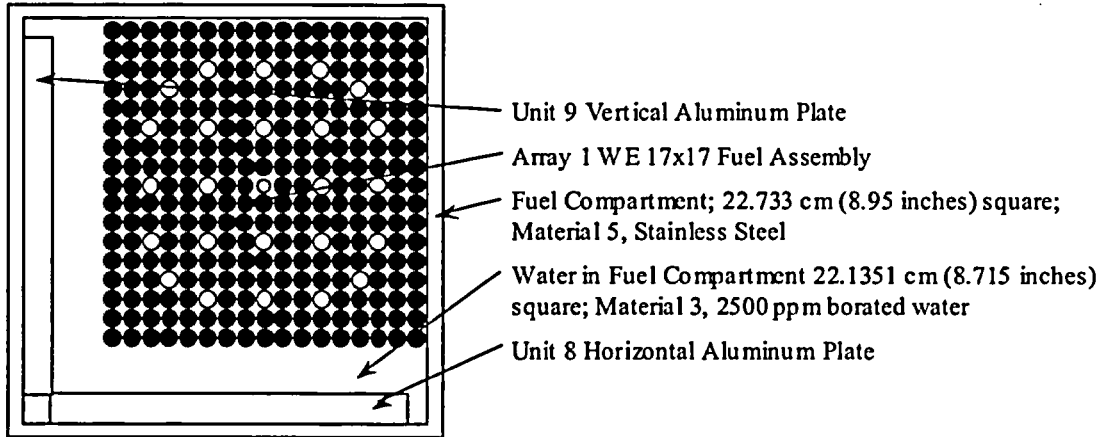


Figure M.6-5
KENO V.a units and Radial Cross Sections of the Model
Part 5 of 18 - (all units 365.76 cm (144 inches) long)

Unit 13 WE 17x17 Fuel Assembly Shifted to the Upper Right in the Fuel
Compartment with Aluminum Plates in Lower Left



Unit 14 WE 17x17 Fuel Assembly Shifted to the Upper Right in the Fuel
Compartment with Aluminum Plates in Upper Right

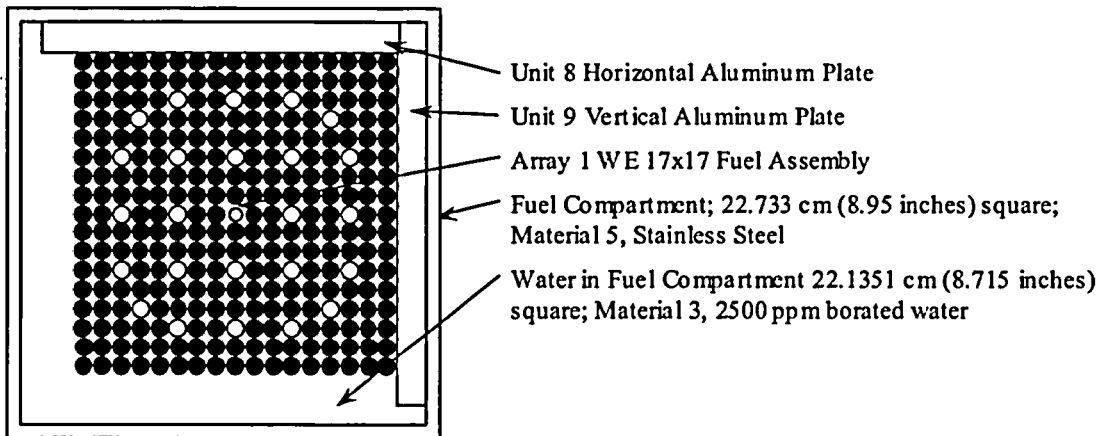
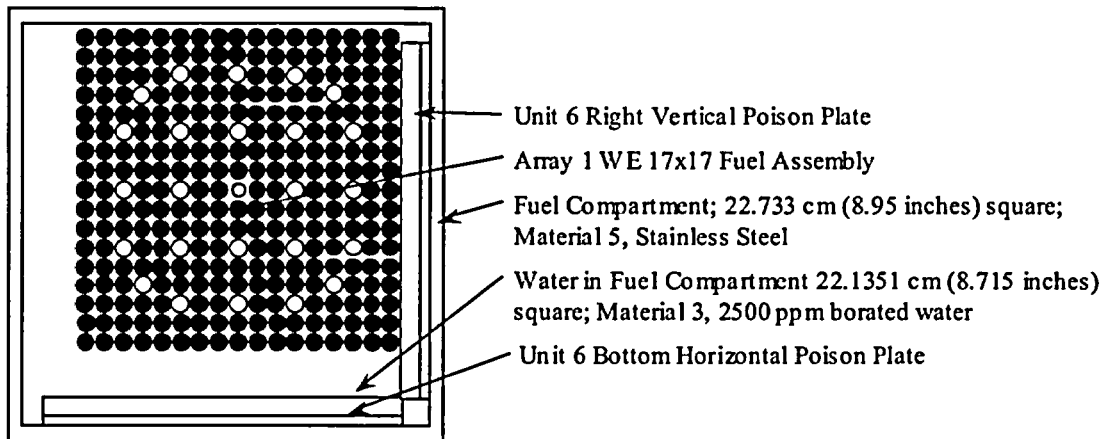


Figure M.6-5
KENO V.a units and Radial Cross Sections of the Model
Part 6 of 18 - (all units 365.76 cm (144 inches) long)

Unit 15 WE 17x17 Fuel Assembly Shifted to the Upper Right in the Fuel
Compartment with Poison Plates in Lower Right



Unit 16 WE 17x17 Fuel Assembly Shifted to the Lower Left in the Fuel
Compartment with Poison Plates in Lower Left

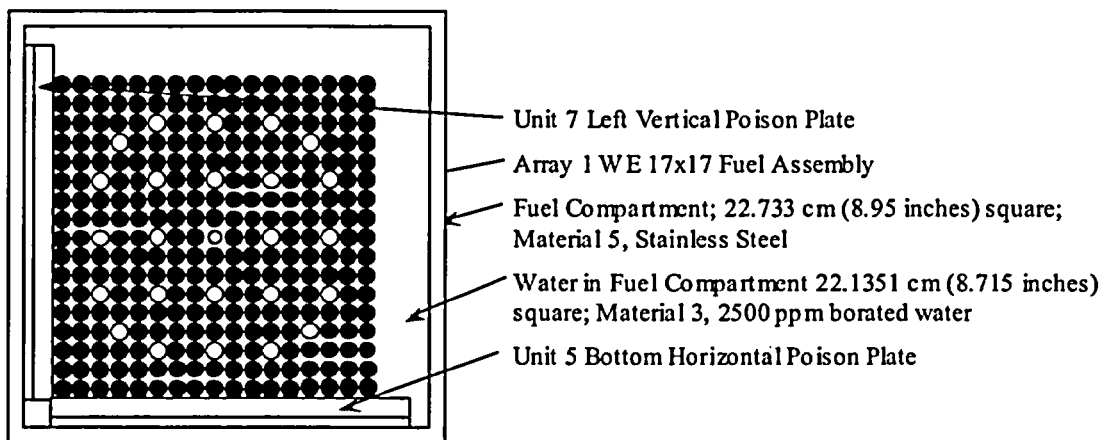
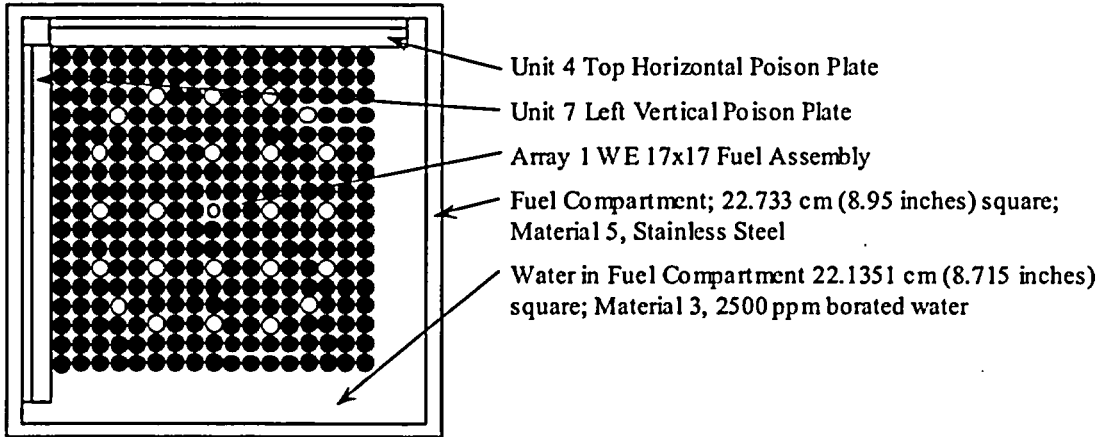


Figure M.6-5
KENO V.a units and Radial Cross Sections of the Model
Part 7 of 18 - (all units 365.76 cm (144 inches) long)

Unit 17 WE 17x17 Fuel Assembly Shifted to the Upper Left in the Fuel
Compartment with Poison Plates in Upper Left



Unit 18 WE 17x17 Fuel Assembly Shifted to the Upper Left in the Fuel
Compartment with Aluminum Plates in Lower Left

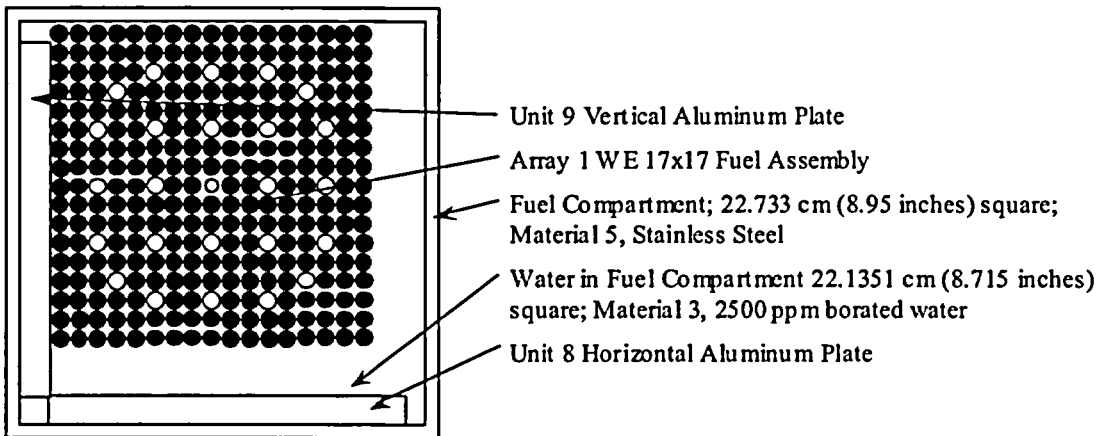
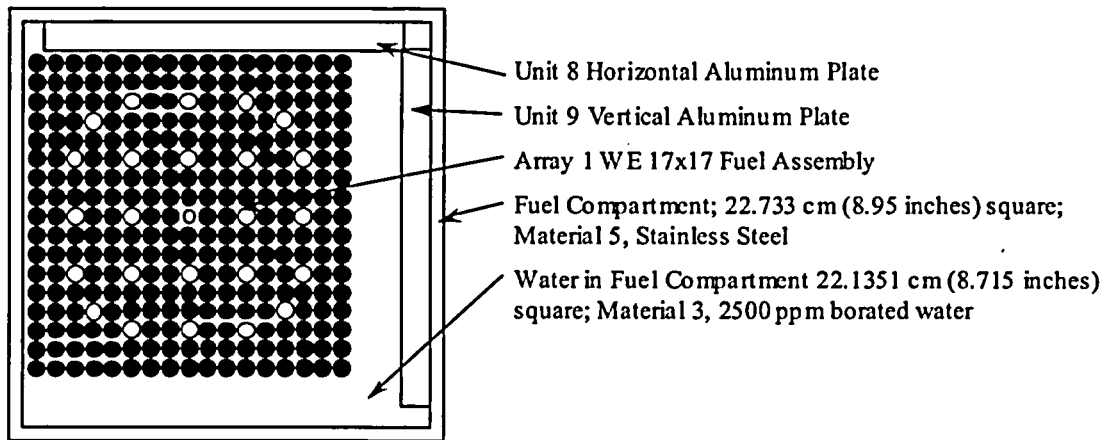


Figure M.6-5
KENO V.a units and Radial Cross Sections of the Model
Part 8 of 18 - (all units 365.76 cm (144 inches) long)

Unit 19 WE 17x17 Fuel Assembly Shifted to the Upper Left in the Fuel
Compartment with Aluminum Plates in Upper Right



Unit 20 WE 17x17 Fuel Assembly Shifted to the Upper Left in the Fuel
Compartment with Poison Plates in Lower Right

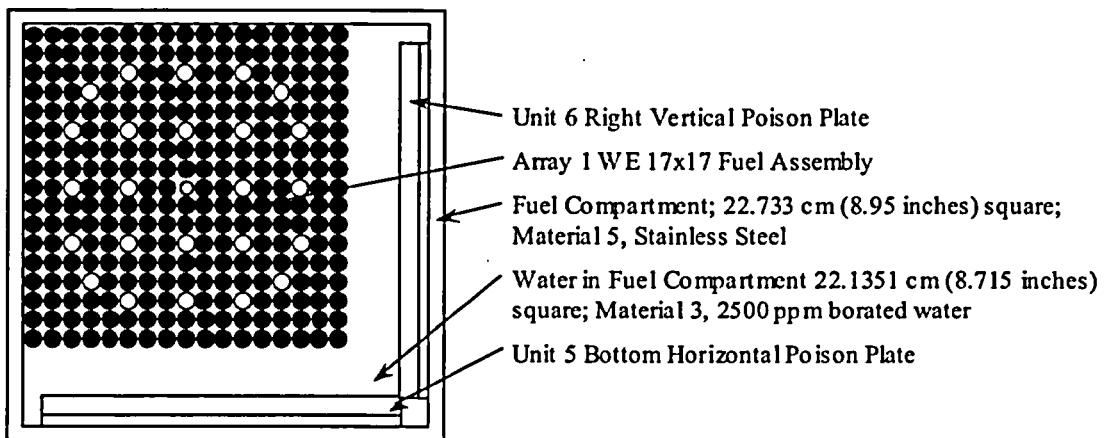
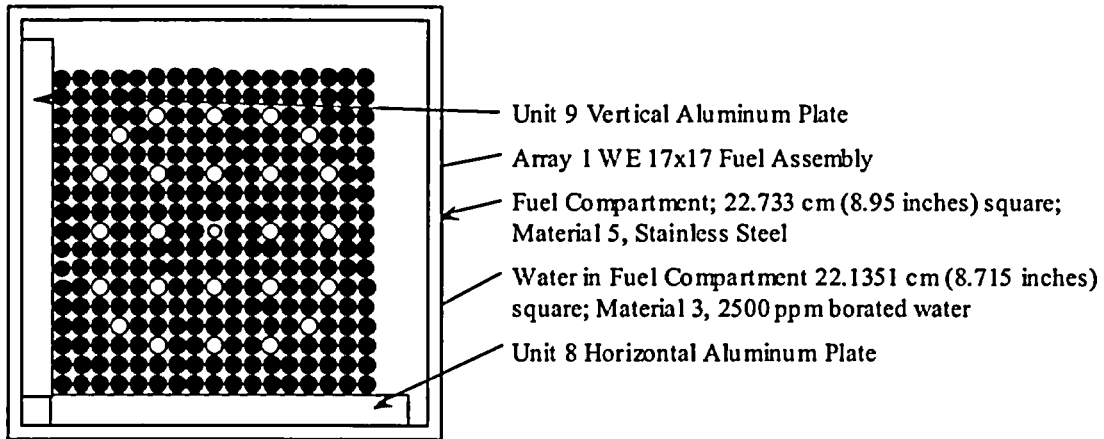


Figure M.6-5
KENO V.a units and Radial Cross Sections of the Model
Part 9 of 18 - (all units 365.76 cm (144 inches) long)

Unit 21 WE 17x17 Fuel Assembly Shifted to the Lower Left in the Fuel
Compartment with Aluminum Plates in Lower Left



Unit 22 WE 17x17 Fuel Assembly Shifted to the Lower Left in the Fuel
Compartment with Poison Plates in Upper Left

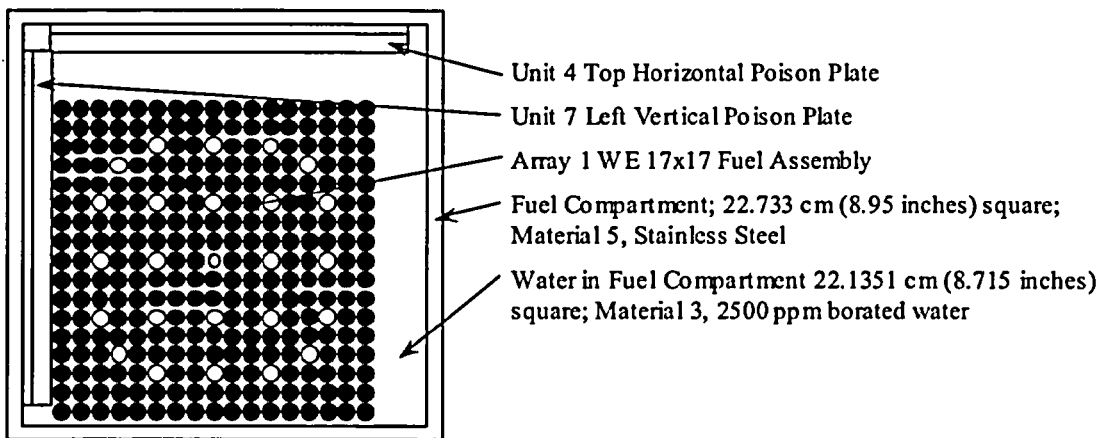
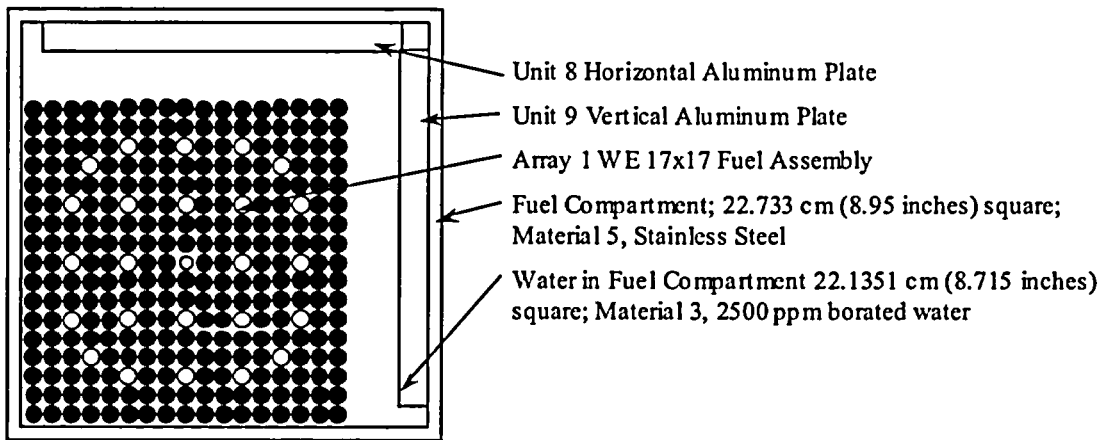


Figure M.6-5
KENO V.a units and Radial Cross Sections of the Model
Part 10 of 18 - (all units 365.76 cm (144 inches) long)

Unit 23 WE 17x17 Fuel Assembly Shifted to the Lower Left in the Fuel
Compartment with Aluminum Plates in Upper Right



Unit 24 WE 17x17 Fuel Assembly Shifted to the Lower Left in the Fuel
Compartment with Poison Plates in Lower Right

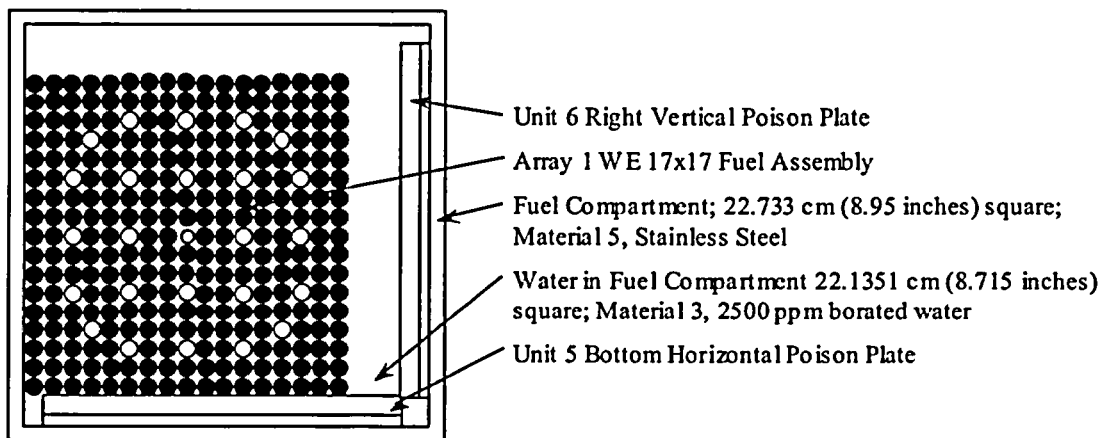
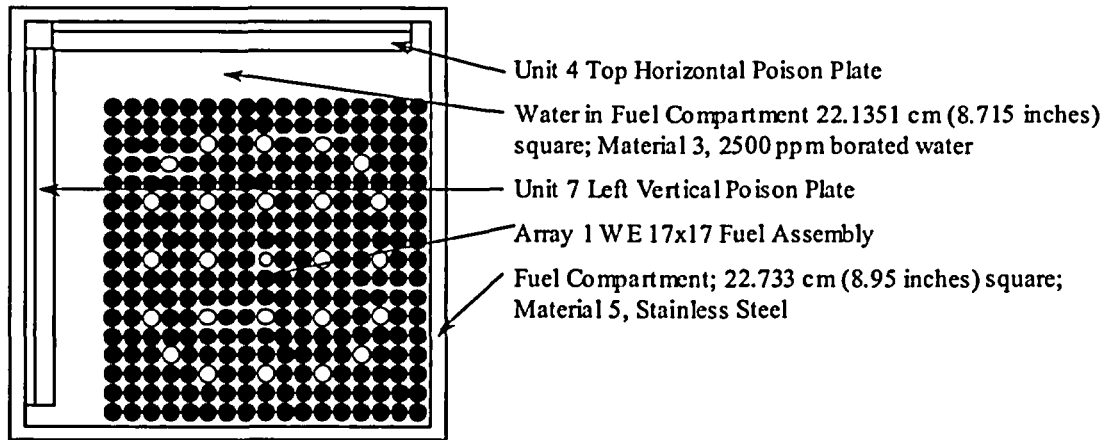


Figure M.6-5
KENO V.a units and Radial Cross Sections of the Model
Part 11 of 18 - (all units 365.76 cm (144 inches) long)

Unit 25 WE 17x17 Fuel Assembly Shifted to the Lower Right in the Fuel
Compartment with Poison Plates in Upper Left



Unit 26 WE 17x17 Fuel Assembly Shifted to the Lower Right in the Fuel
Compartment with Aluminum Plates in Lower Left

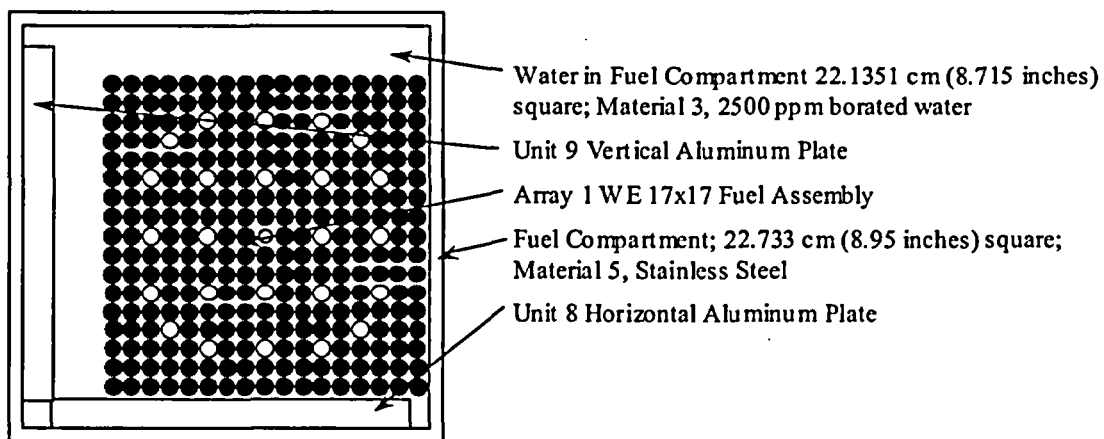
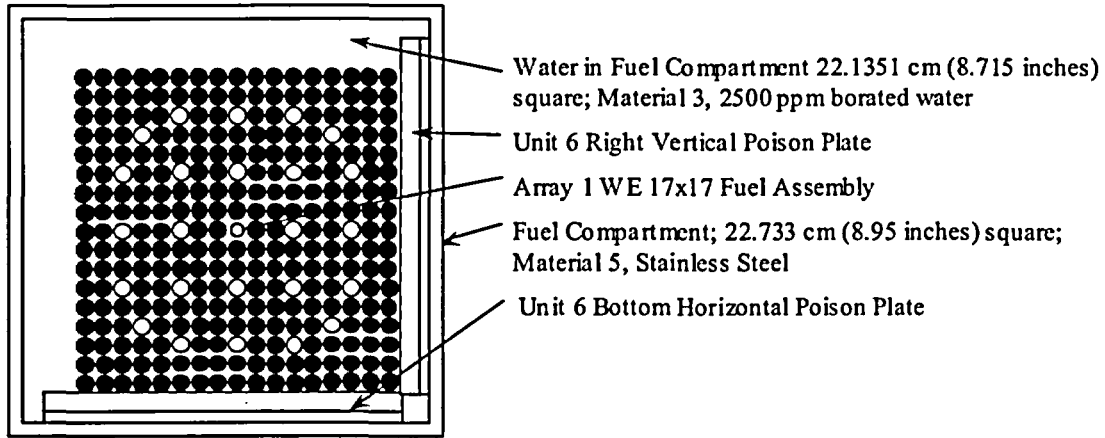


Figure M.6-5
KENO V.a units and Radial Cross Sections of the Model
Part 12 of 18 - (all units 365.76 cm (144 inches) long)

Unit 27 WE 17x17 Fuel Assembly Shifted to the Lower Right in the Fuel
Compartment with Poison Plates in Lower Right



Unit 28 WE 17x17 Fuel Assembly Shifted to the Lower Right in the Fuel
Compartment with Aluminum Plates in Upper Right

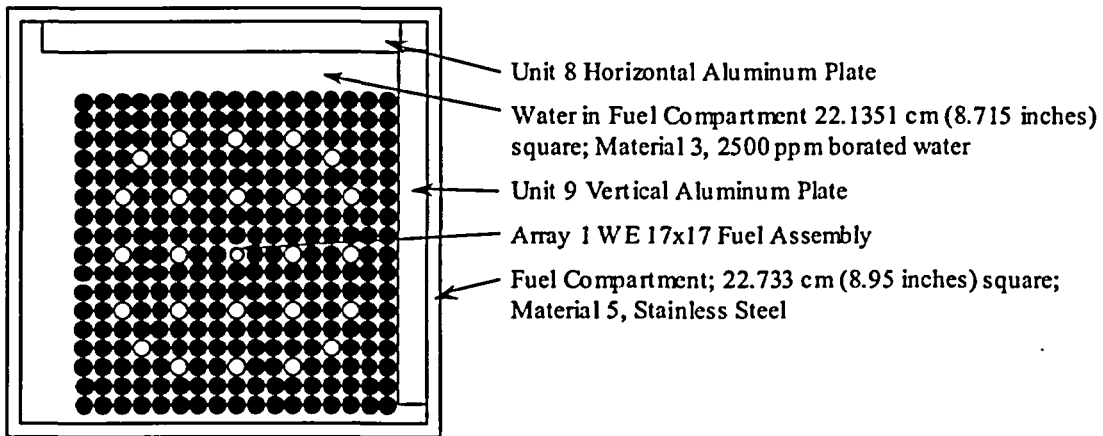
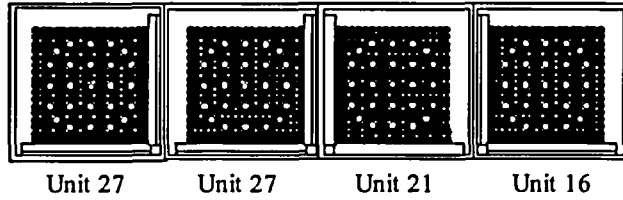


Figure M.6-5
KENO V.a units and Radial Cross Sections of the Model
Part 13 of 18 - (all units 365.76 cm (144 inches) long)

Array 2 Top Row of Assemblies made up of Units 27, 21, and 16



Array 3 Left Row of Assemblies made up of Units 10, 14, and 27

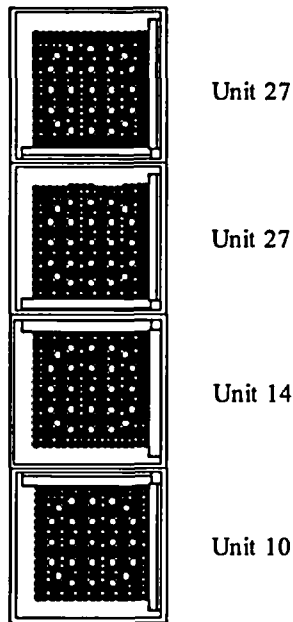
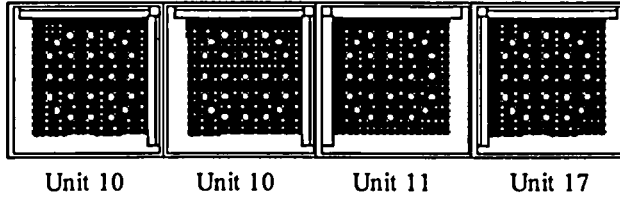


Figure M.6-5
KENO V.a units and Radial Cross Sections of the Model
Part 14 of 18 - (all units 365.76 cm (144 inches) long)

Array 4 Bottom Row of Assemblies made up of Units 10, 11, and 17



Array 5 Right Row of Assemblies made up of Units 16, 17, and 21

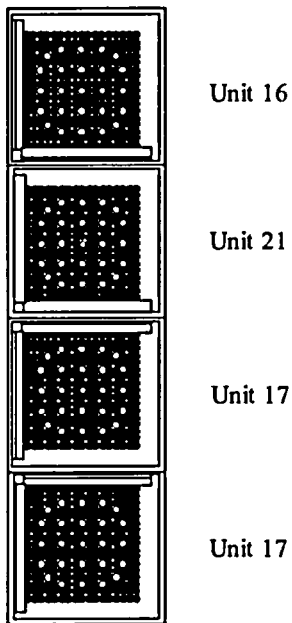


Figure M.6-5
KENO V.a units and Radial Cross Sections of the Model
Part 15 of 18 - (all units 365.76 cm (144 inches) long)

Array 6 Center 4x4 Array of Assemblies made up of Units 12 - 15, and 17 - 28

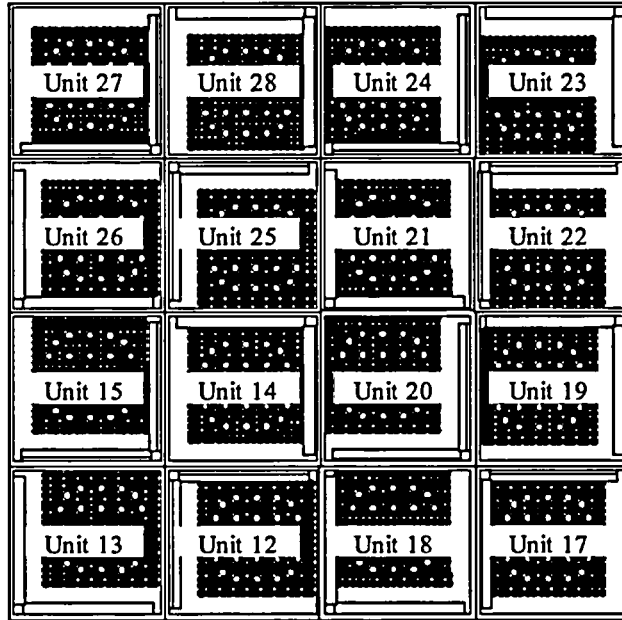
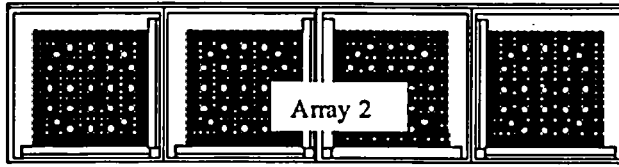
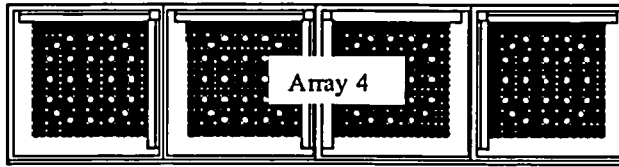


Figure M.6-5
KENO V.a units and Radial Cross Sections of the Model
Part 16 of 18 - (all units 365.76 cm (144 inches) long)

Unit 29 Top Row of Assemblies

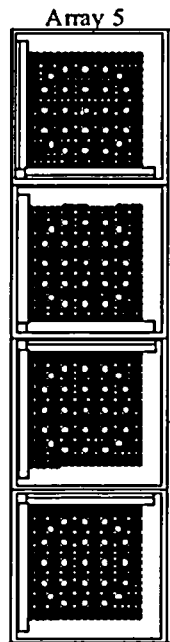


Unit 31 Bottom Row of Assemblies

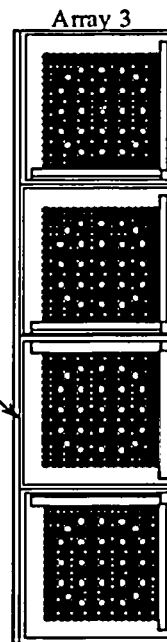


Fuel Compartment; 0.29845 cm (0.1175 inches); Material 5, Stainless Steel

Unit 32 Right Row of Assemblies



Unit 30 Left Row of Assemblies



Fuel Compartment; 0.29845 cm (0.1175 inches); Material 5, Stainless Steel

Figure M.6-5
KENO V.a units and Radial Cross Sections of the Model
Part 17 of 18 - (all units 365.76 cm (144 inches) long)

Figure Withheld Under 10 CFR 2.390

Figure M.6-5
KENO V.a units and Radial Cross Sections of the Model
Part 18 of 18 - (all units 365.76 cm (144 inches) long)

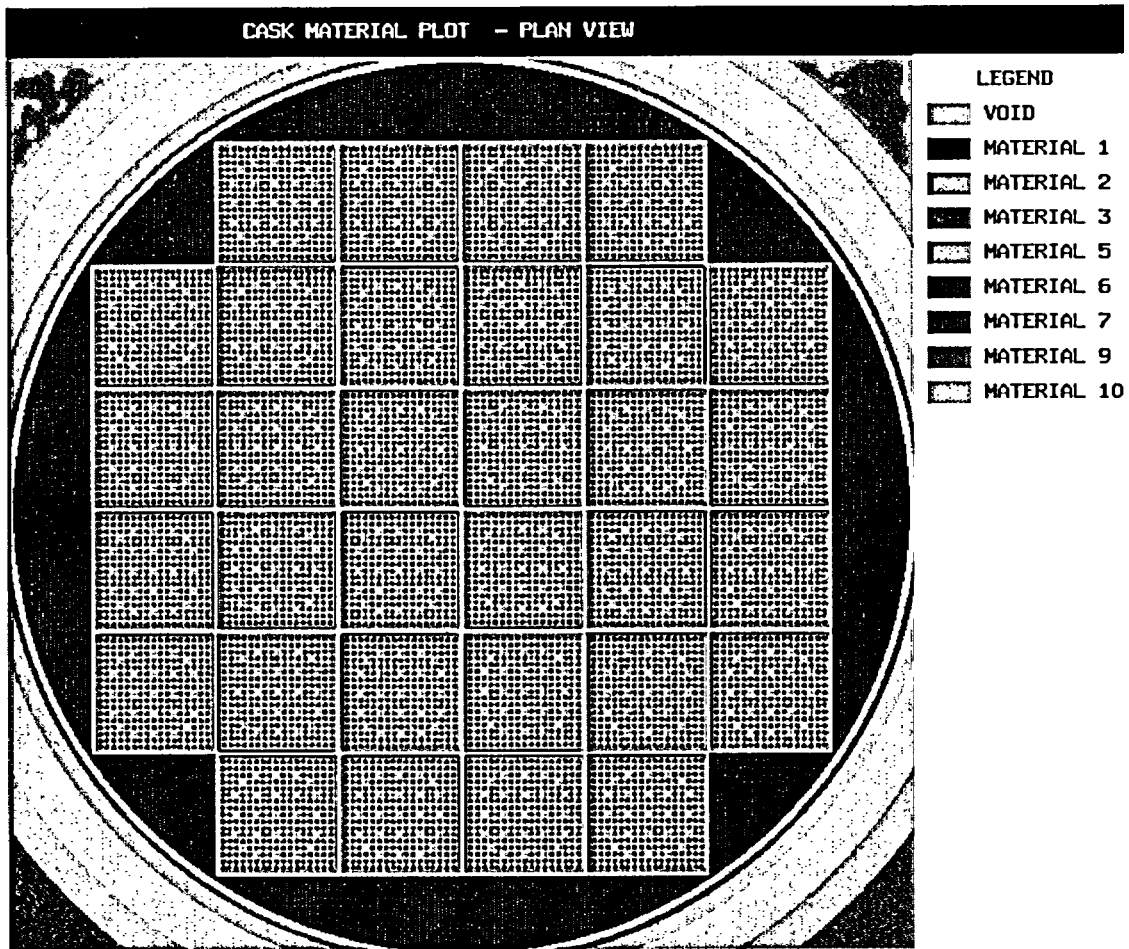


**Figure M.6-6
WE 17x17 Class Assembly**

DELETED

**Figure M.6-7
CE 16x16 Class Assembly**

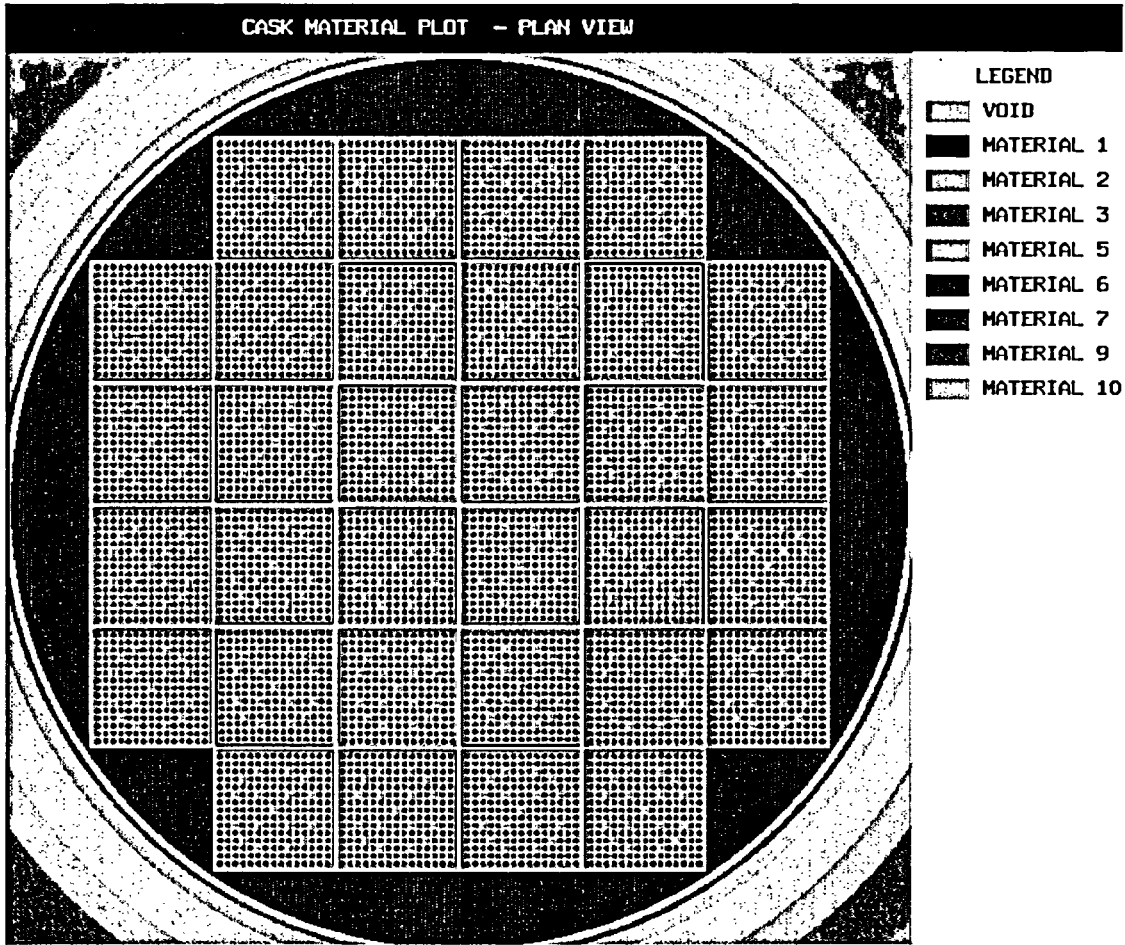


**Figure M.6-8
B&W 15x15 Class Assembly**

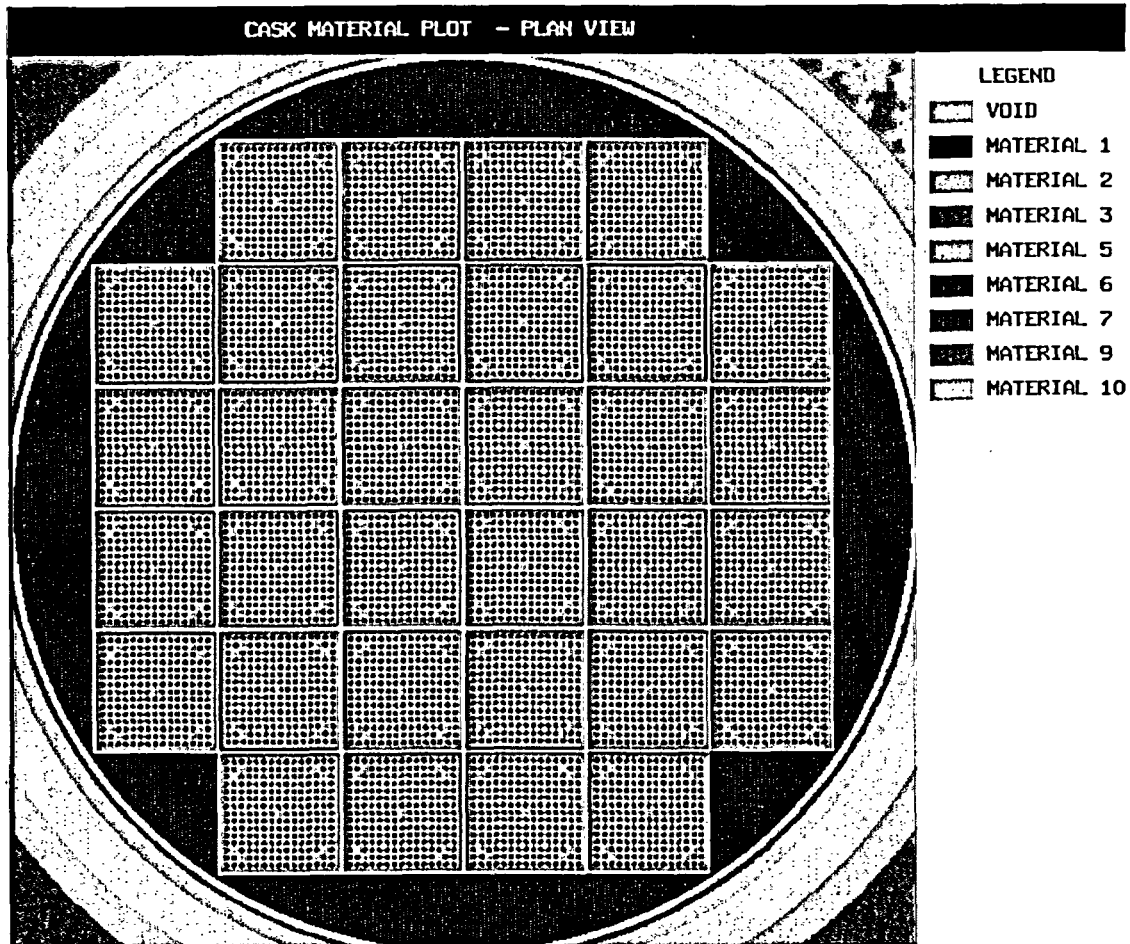


**Figure M.6-9
CE 15x15 Class Assembly**

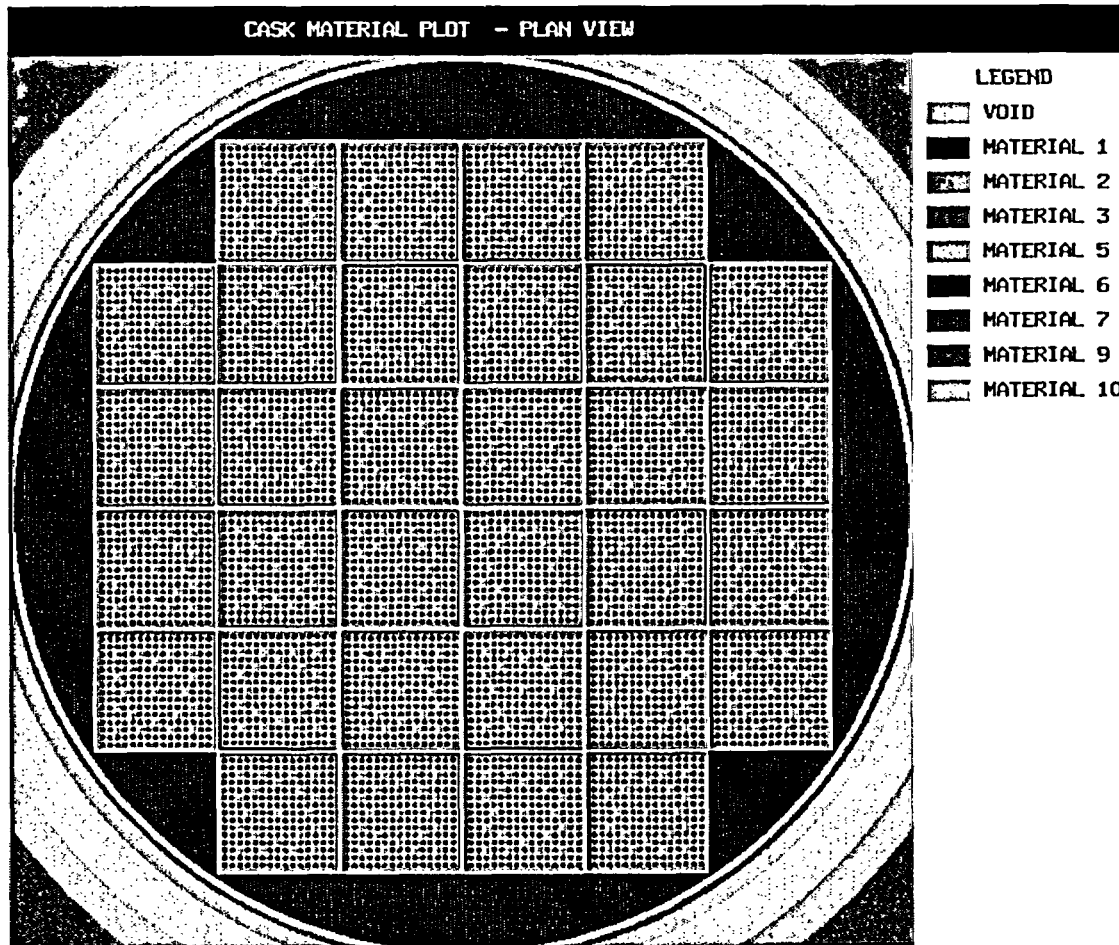


**Figure M.6-10
WE 15x15 Class Assembly**

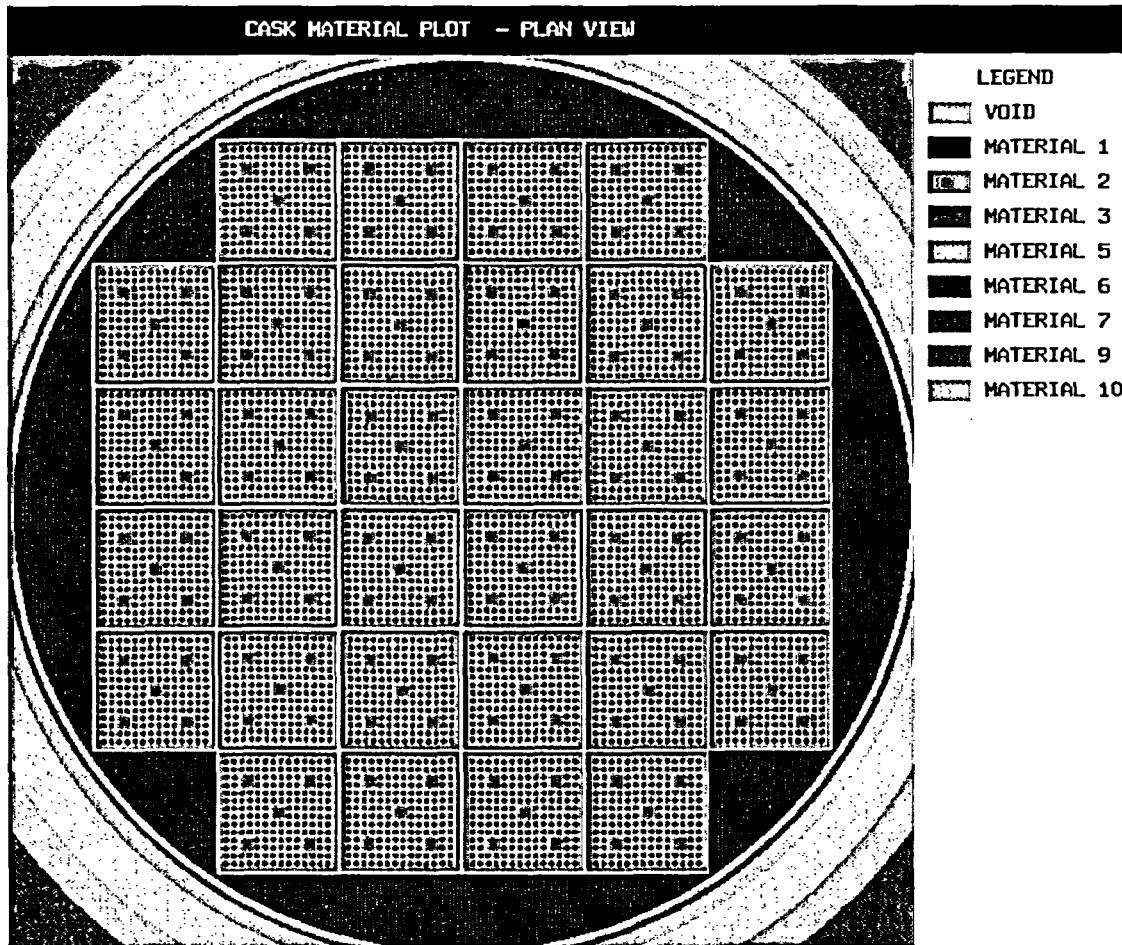


Figure M.6-11
CE 14x14 Class Assembly

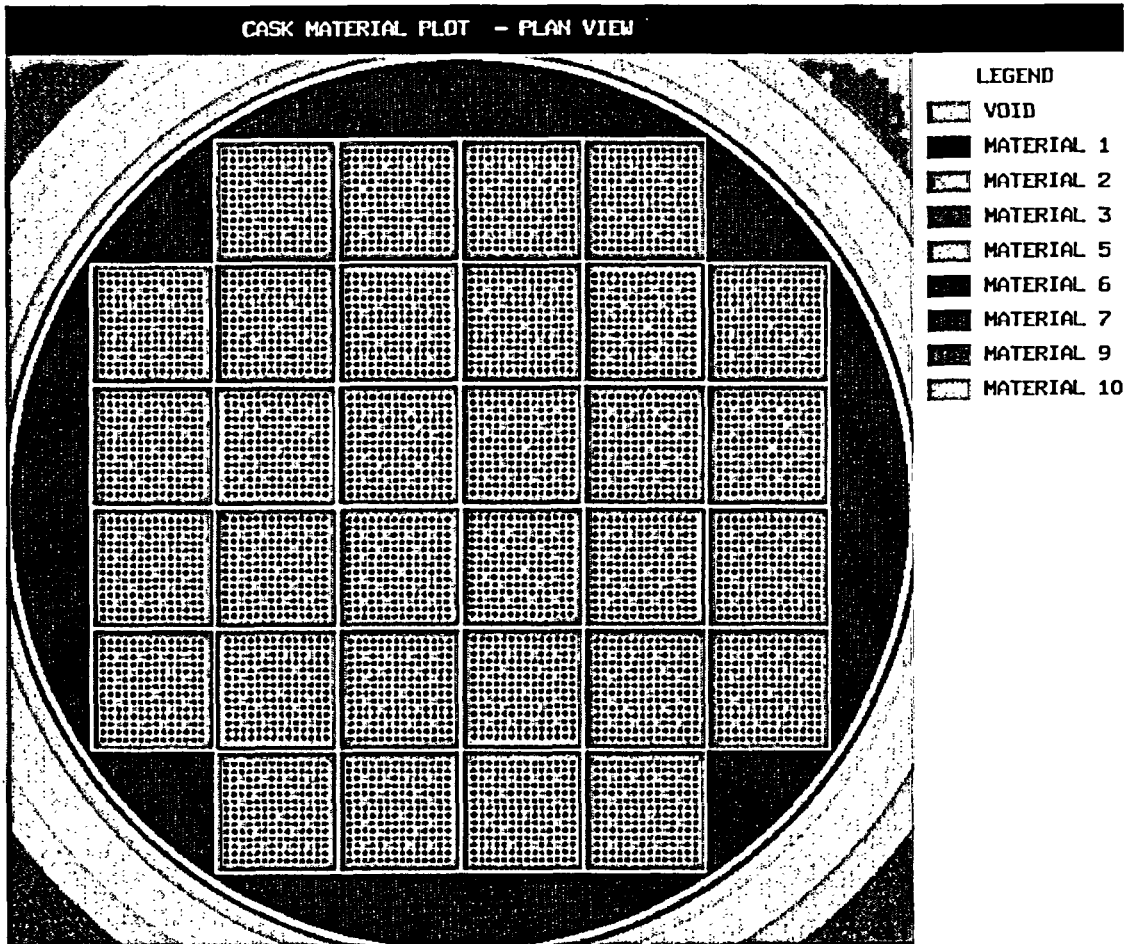


Figure M.6-12
WE 14x14 Class Assembly

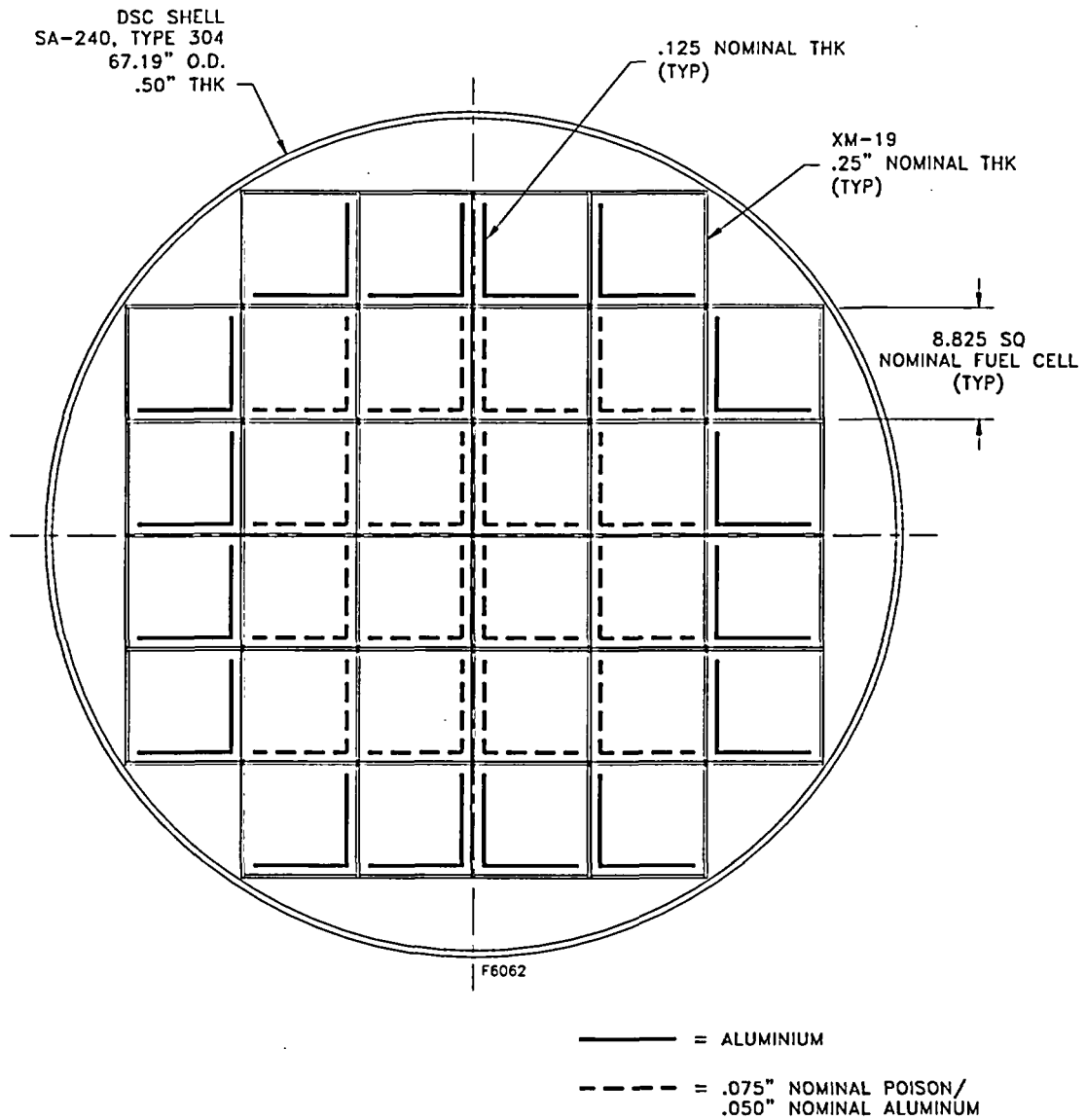


Figure M.6-13
Configuration with 16 Poison Plates
(Analyzed as Alternate Type A Basket)

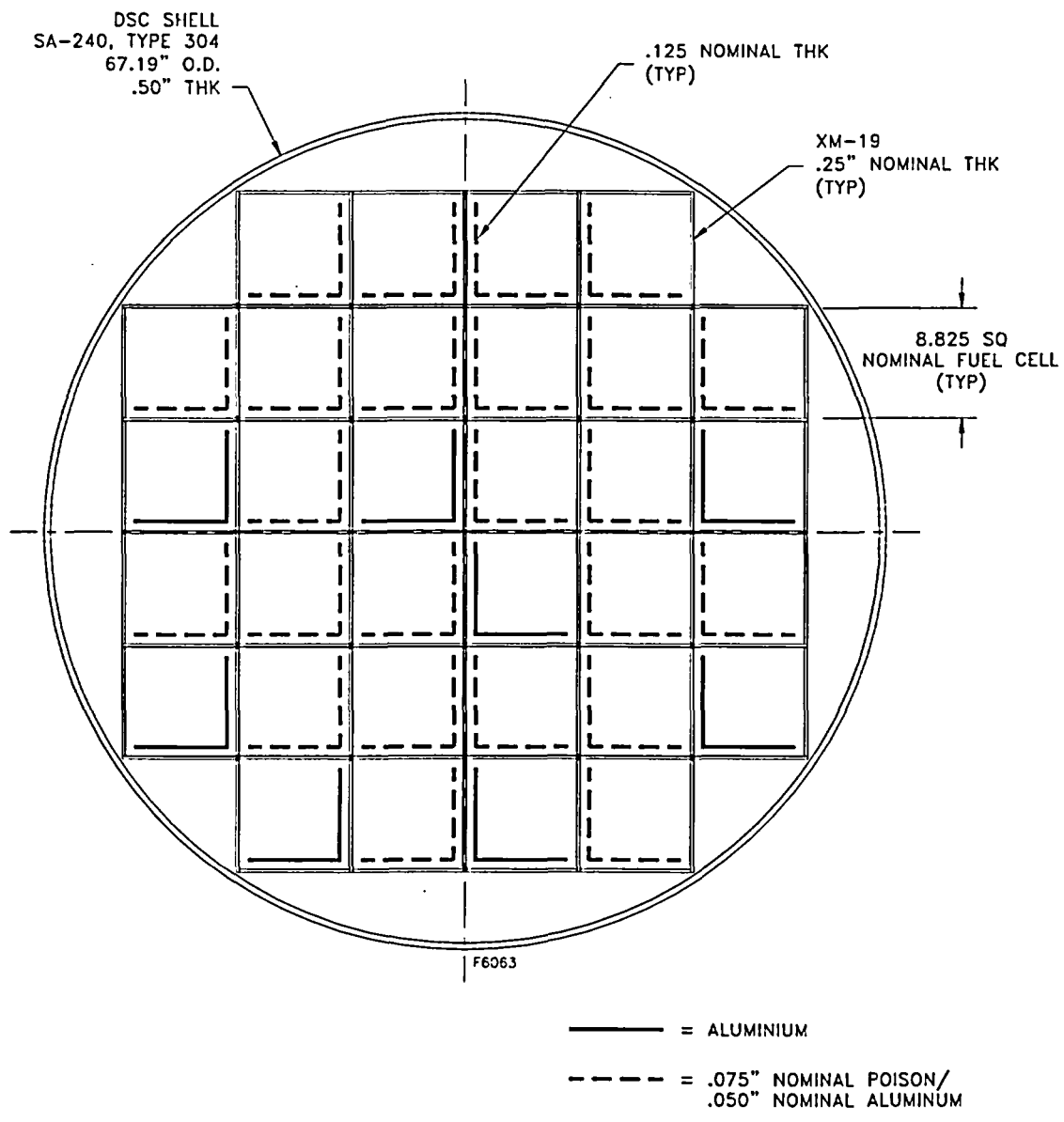


Figure M.6-14
Configuration with 24 Poison Plates
(Analyzed as Alternate Type A/B/C/D Basket)

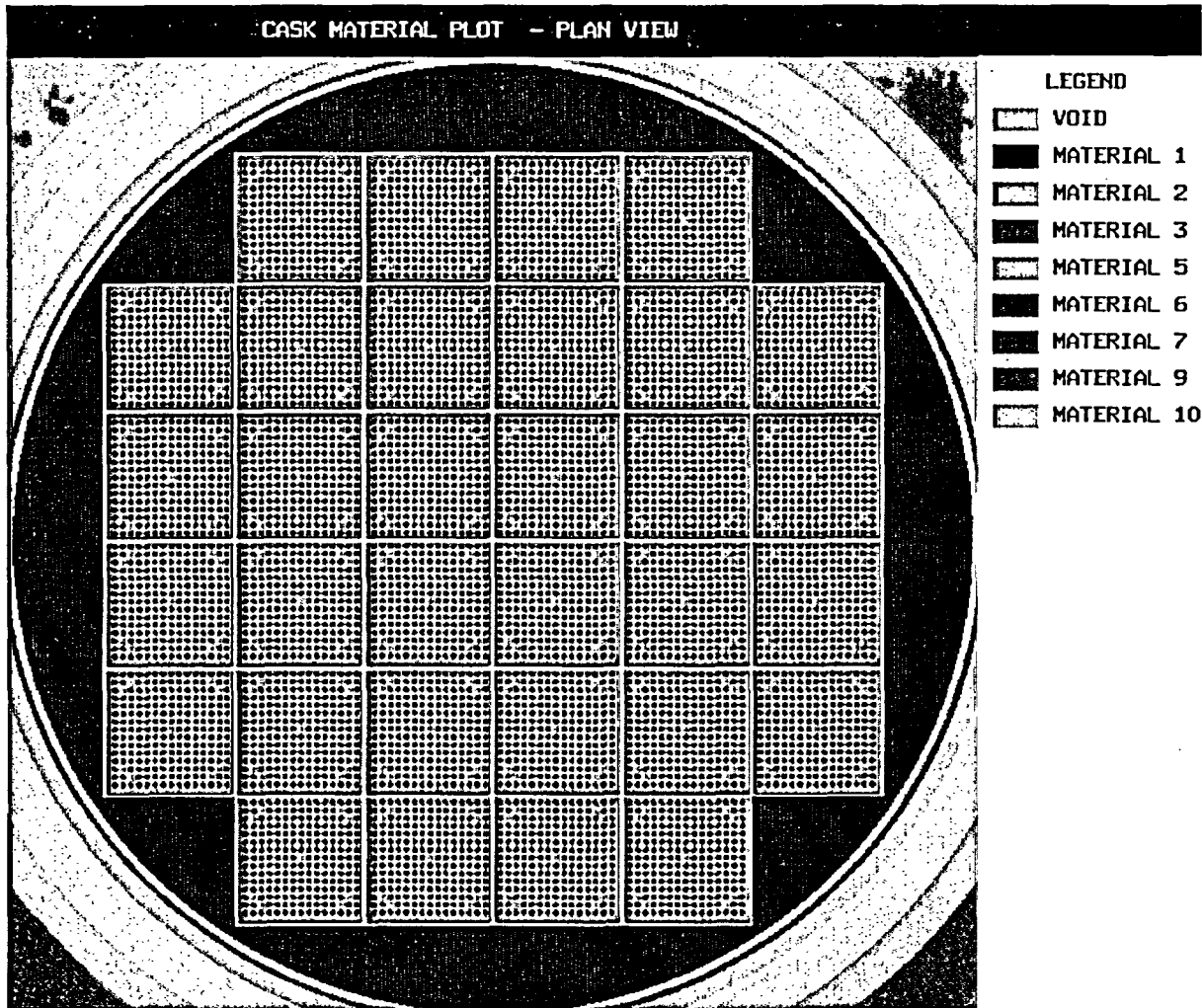


Figure M.6-15
CE 15x15 Class Fuel Assembly - 16 poison plates

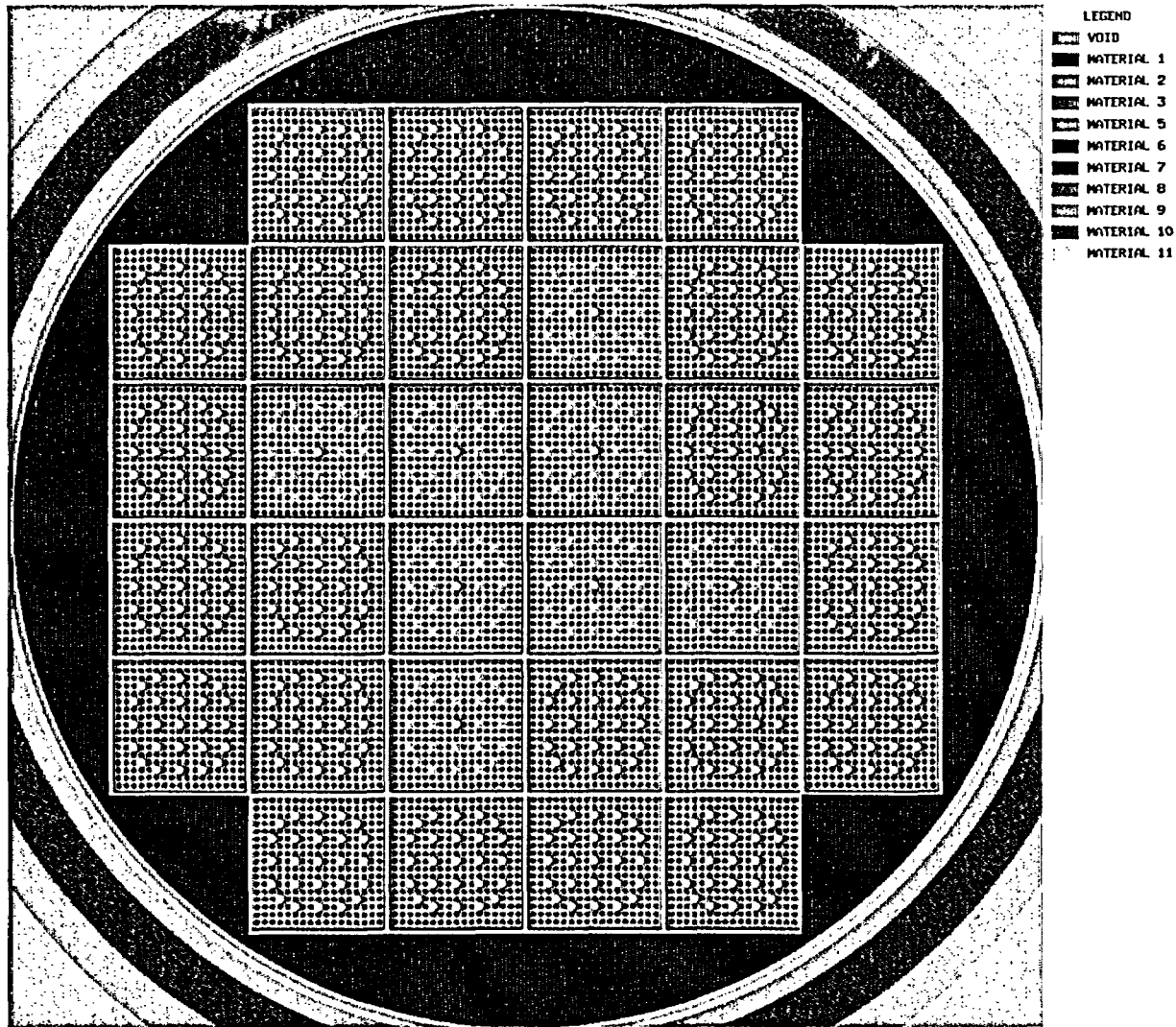


Figure M.6-16
 WE 17x17 Class Fuel Assembly – with BPRAs and 8 PRAs – 24 poison plates'

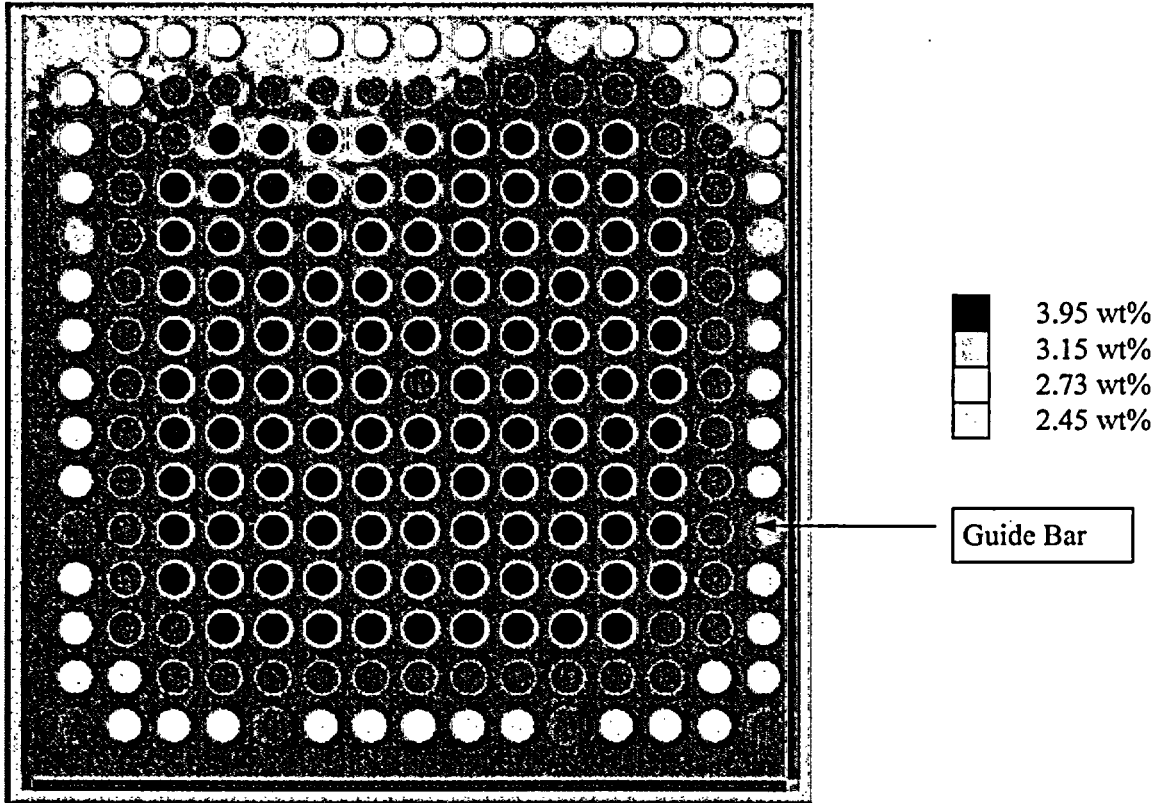
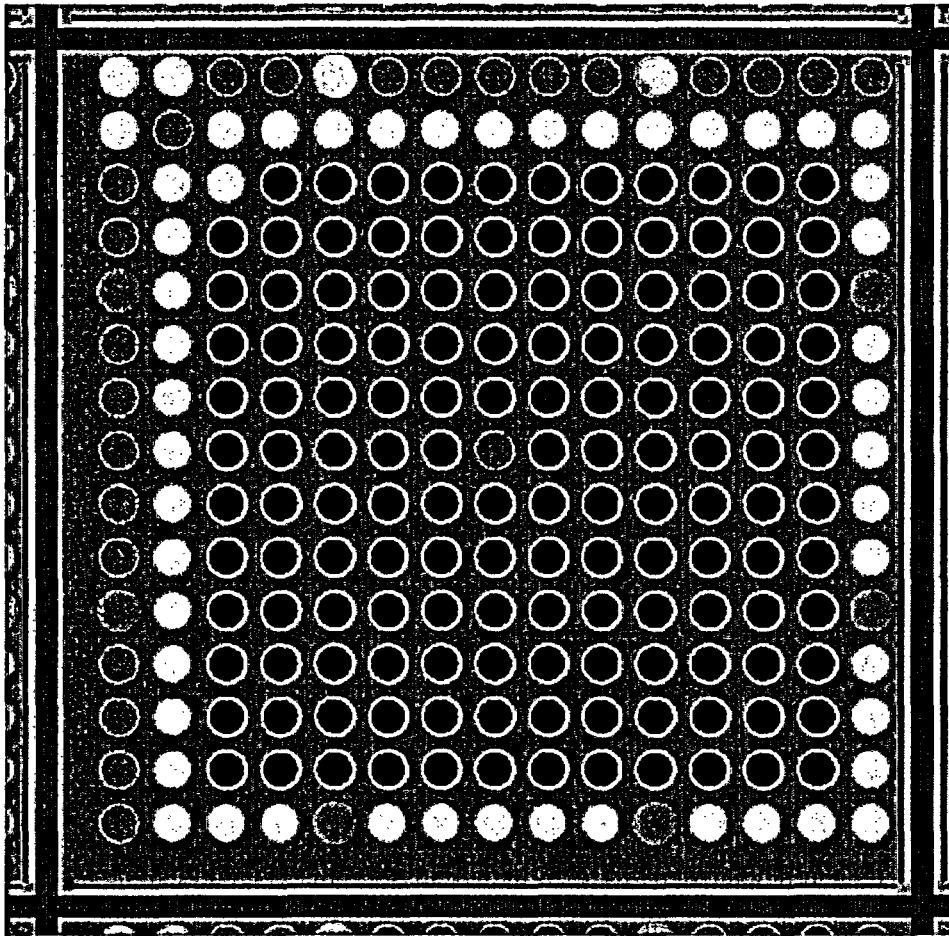


Figure M.6-17
Exxon 15x15 Fuel Assembly with Radial Variation in Enrichment (Loading Pattern 1)



Zone 1
Zone 2
Zone 3
Zone 4

Figure M.6-18
Exxon 15x15 CE Fuel Assembly with Radial Variation in Enrichment (Loading Pattern 2)

M.7 Confinement

Confinement of all radioactive materials in the NUHOMS[®]-32PT system is provided by the NUHOMS[®]-32PT DSC which is designed and tested to meet the leak tight criteria [7.1].

As discussed in Section 7.2.2, the release of airborne radioactive material is addressed for three phases of system operation: fuel handling in the spent fuel pool, drying and sealing of the DSC, and DSC transfer and storage. Potential airborne releases from irradiated fuel assemblies in the spent fuel pool are discussed in the plant's existing 10CFR50 license.

DSC drying and sealing operations are performed using procedures which prohibit airborne leakage. During these operations, all vent lines are routed to the existing radwaste systems of the plant. Once the DSC is dried and sealed, there are no design basis accidents, which could result in a breach of the DSC and the airborne release of radioactivity. Design provisions to preclude the release of gaseous fission products as a result of accident conditions are discussed in Section 8.2.9.

During transfer of the sealed DSC and subsequent storage in the HSM, the only postulated mechanism for the release of airborne radioactive material is the dispersion of non-fixed surface contamination on the DSC exterior. By filling the cask/DSC annulus with demineralized water, placing an inflatable seal over the annulus, and utilizing procedures which require examination of the annulus surfaces for smearable contamination, the contamination limits on the DSC can be kept below the permissible level for off-site shipments of fuel. Therefore, there is no possibility of significant radionuclide release from the DSC exterior surface during transfer or storage.

M.7.1 Confinement Boundary

Once inside the DSC, the SFAs are confined by the DSC shell and by multiple barriers at each end of the DSC. For intact fuel, the fuel cladding is the first barrier for confinement of radioactive materials. The fuel cladding is protected by maintaining the cladding temperatures during storage below those levels, which may cause degradation of the cladding. In addition, the SFAs are stored in an inert atmosphere to prevent degradation of the fuel, specifically cladding rupture due to oxidation and its resulting volumetric expansion of the fuel. Thus, a helium atmosphere for the DSC is incorporated in the design to protect the fuel cladding integrity by inhibiting the ingress of oxygen into the DSC cavity.

Helium is known to leak through valves, mechanical seals, and escape through very small passages because of its small atomic diameter and because it is an inert element and exists in a monatomic species. Negligible leakage rates can be achieved with careful design of vessel closures. Helium will not, to any practical extent, diffuse through stainless steel. For this reason, the DSC has been designed as a redundant weld-sealed containment pressure vessel with no mechanical or electrical penetrations.

M.7.1.1 Confinement Vessel

The confinement vessel is provided by the NUHOMS[®]-32PT DSC. The DSC is designed to provide confinement of all radionuclides under normal and accident conditions. The DSC is designed, fabricated and tested in accordance with the applicable requirements of the ASME Boiler and Pressure Vessel Code, Division 1, Section III, Subsection NB [7.2] with exceptions as discussed in Section M.3.1.2.3. The shell and inner and outer bottom cover plates are delivered to the site as an assembly. The shell and the inner bottom cover plate, which provide the confinement boundary as shown in Figure M.3-1, are tested to meet the leak tight criteria as defined in [7.1] at the fabricator. The pneumatic pressure test and leak test are performed on the finished shell and the inner cover plate during fabrication. The outer bottom cover plate provides redundant confinement boundary. The root and final layer closure welds for this redundant boundary are inspected using dye penetrant inspection methods in accordance with requirements of the ASME code [7.2].

Once the fuel assemblies are loaded in the DSC, the heavy shield plug is installed to provide radiation shielding to minimize radiation exposure to workers during DSC closure operations. The inner top cover plate is welded into place along with the vent and siphon port cover plates. These welds represent the first level of closure for the DSC. Finally, the outer top cover plate is welded into place to form the redundant confinement boundary of the DSC. The inner plate is tested using the test port in the outer top cover plate to meet the leak tight criteria [7.1]. The test port plug is then threaded into the outer top cover plate and seal welded in place. The root and final layer closure welds for this redundant boundary are inspected using dye penetrant inspection methods in accordance with requirements of the ASME code [7.2].

M.7.1.2 Confinement Penetrations

The DSC pressure boundary contains two penetrations (vent and siphon ports) for draining, vacuum drying and backfilling the DSC cavity. The vent and siphon ports are closed with welded cover plates and the outer top cover plate provides the redundant closure. The outer cover plate has a single penetration used for leak testing the closure welds. This test port plug is threaded into the outer top cover plate and seal welded in place after testing to complete the redundant closure. The DSC has no bolted closures or mechanical seals. The final confinement boundary contains no external penetrations.

M.7.1.3 Seals and Welds

The DSC cylindrical shell is fabricated from rolled ASME stainless steel plate that is joined with full penetration 100% radiographed welds. The DSC shell weldments at the inner bottom confinement boundary are also 100% volumetrically inspected welds. All top and bottom end closure welds are multiple-layer welds. This effectively eliminates a pinhole leak which might occur in a single pass weld, since the chance of pinholes being in alignment on successive weld passes is not credible. Furthermore, specific closure welds (top inner cover plate, siphon and vent block, and siphon and vent cover plate) of the pressure boundary are per ASME Code Case N-595-2. This is an alternative to the ASME Code (Reference Table M.3.1-1). These criteria insure that the weld filler metal is as sound as the parent metal of the pressure vessel. There are no bolted closures or mechanical seals.

M.7.1.4 Closure

All top end closure welds are multiple-layer welds. This effectively eliminates a pinhole leak which might occur in a single pass weld, since the chance of pinholes being in alignment on successive weld passes is not credible. Furthermore, specific closure welds (top inner cover plate, siphon and vent block, and siphon and vent cover plate) of the pressure boundary are per ASME Code Case N-595-2. This is an alternative to the ASME Code (Reference Table M.3.1-1). Finally, the inner closure welds are tested to the leak tight criteria [7.1]. There are no bolted closures or mechanical seals.

M.7.2 Requirements for Normal Conditions of Storage

M.7.2.1 Release of Radioactive Material

The NUHOMS[®]-32PT DSC is designed, fabricated and tested to meet the leak tight criteria [7.1]. Therefore, there is no release of radioactive material under normal conditions of storage. As noted in acceptance criteria IV-4 of [7.3], a closure monitoring system is not required. The confinement boundary ensures that the inert fill gas does not leak or diffuse through the weld or parent material of the DSC. The continued effectiveness of the confinement boundary is demonstrated by (a) daily visual inspections of the HSM inlets and outlets (b) daily monitoring of the HSM thermal performance (c) and the use of radiation monitors (typically TLDs) on the ISFSI boundary fence. A breach of the confinement boundary would result in an increase in the measured dose at the ISFSI fence. If an increase were detected, steps would be initiated to enable the licensee to take corrective actions to maintain safe storage conditions.

M.7.2.2 Pressurization of Confinement Vessel

The maximum internal pressures in the NUHOMS[®]-32PT DSC during transfer and storage for normal and off-normal conditions are calculated in Section M.4.4.4 and M.4.5.4. These pressures are below the design pressures of the DSC as shown in Section M.4.4 and M.4.5.

M.7.3 Confinement Requirements for Hypothetical Accident Conditions

M.7.3.1 Fission Gas Products

The analysis presented in Section M.3 demonstrates that the confinement boundary (pressure boundary) is not compromised following hypothetical accident conditions. Therefore, there is no need to calculate the fission gas products available for release.

M.7.3.2 Release of Contents

The NUHOMS[®]-32PT DSC is designed and tested to meet the leak tight criteria [7.1]. The analysis presented in Section M.11 demonstrates that the confinement boundary (pressure boundary) is not compromised following hypothetical accident conditions. Therefore, there is no release of radioactive material under hypothetical accident conditions of storage.

M.7.4 References

- 7.1 "American National Standard for Radioactive Materials – Leakage Tests on Packages for Shipment," ANSI N14.5-1997, American National Standards Institute, Inc., New York, New York, 1997.
- 7.2 ASME Boiler and Pressure Vessel Code, Section III, Division 1, Subsection NB, 1998, including 1999 addenda.
- 7.3 Interim Staff Guidance (ISG)-5, Revision; Confinement Evaluation.

M.8 Operating Systems

This Chapter presents the operating procedures for the standardized NUHOMS[®]-32PT system described in previous chapters and shown on the drawings in Section M.1.5. The procedures include preparation of the DSC and fuel loading, closure of the DSC, transport to the ISFSI using the TC, DSC transfer into the HSM, monitoring operations, and DSC retrieval from the HSM. The standardized NUHOMS[®] transfer equipment, and the existing plant systems and equipment are used to accomplish these operations. Procedures are delineated here to describe how these operations are to be performed and are not intended to be limiting. Standard fuel and cask handling operations performed under the plant's 10CFR50 operating license are described in less detail. Existing operational procedures may be revised by the licensee and new ones may be developed according to the requirements of the plant, provided that the limiting conditions of operation specified in Technical Specifications, Functional and Operating Limits of NUHOMS[®] CoC are not exceeded.

The following sections outline the typical operating procedures for the standardized NUHOMS[®] System. These generic NUHOMS[®] procedures have been developed to minimize the amount of time required to complete the subject operations, to minimize personnel exposure, and to assure that all operations required for DSC loading, closure, transfer, and storage are performed safely. Plant specific ISFSI procedures are to be developed by each licensee in accordance with the requirements of 10CFR72.24 (h) and the guidance of Regulatory Guide 3.61 [8.1]. The generic procedures presented here are provided as a guide for the preparation of plant specific procedures and serve to point out how the NUHOMS[®] System operations are to be accomplished.

M.8.1 Procedures for Loading the Cask

Process flow diagrams for the NUHOMS[®] System operation are presented Figure M.8-1 and Figure M.8-2. The location of the various operations may vary with individual plant requirements. The following steps describe the recommended generic operating procedures for the standardized NUHOMS[®] System.

M.8.1.1 Preparation of the TC and DSC

1. Prior to placement in dry storage, the candidate intact fuel assemblies shall be evaluated (by plant records or other means) to verify that they meet the physical, thermal and radiological criteria specified in Technical Specification.
2. Prior to being placed in service, the TC is to be cleaned or decontaminated as necessary to insure a surface contamination level of less than those specified in Technical Specification 1.2.12.
3. Place the TC in the vertical position in the cask decon area using the cask handling crane and the TC lifting yoke.
4. Place scaffolding around the cask so that the top cover plate and surface of the cask are easily accessible to personnel.
5. Remove the TC top cover plate and examine the cask cavity for any physical damage and ready the cask for service. If loading 32PT-S100 or 32PT-L100 DSC (qualified for 100-ton crane capacity), drain neutron shield water from the TC.
6. Examine the DSC for any physical damage which might have occurred since the receipt inspection was performed. The DSC is to be cleaned and any loose debris removed.
7. Using a crane, lower the DSC into the cask cavity by the internal lifting lugs and rotate the DSC to match the cask and DSC alignment marks.
8. Fill the cask-DSC annulus with clean, demineralized water. Place the inflatable seal into the upper cask liner recess and seal the cask-DSC annulus by pressurizing the seal with compressed air.
9. Fill the DSC cavity with water from the fuel pool or an equivalent source which meets the requirements of Technical Specification 1.2.15a.

NOTE: A TC/DSC annulus pressurization tank filled with demineralized water as described above is connected to the top vent port of the TC via a hose to provide a positive head above the level of water in the TC/DSC annulus. This is an optional arrangement, which provides additional assurance that contaminated water from the fuel pool will not enter the TC/DSC annulus, provided a positive head is maintained at all times.

10. Place the top shield plug onto the DSC. Examine the top shield plug to ensure a proper fit.

11. Position the cask lifting yoke and engage the cask lifting trunnions and the rigging cables to the DSC top shield plug. Adjust the rigging cables as necessary to obtain even cable tension.
12. Visually inspect the yoke lifting hooks to insure that they are properly positioned and engaged on the cask lifting trunnions.
13. Connect the vacuum drying system (VDS) or optional liquid pump to the siphon port of the DSC and position the connecting hose such that the hose will not interfere with loading (yoke, fuel, shield plug, rigging, etc.). A flowmeter must be installed at a suitable location as part of this connection.
14. Move the scaffolding away from the cask as necessary.
15. Lift the cask just far enough to allow the weight of the cask to be distributed onto the yoke lifting hooks. Reinspect the lifting hooks to insure that they are properly positioned on the cask trunnions.
16. Optionally, secure a sheet of suitable material to the bottom of the TC to minimize the potential for ground-in contamination. This may also be done prior to initial placement of the cask in the decon area.
17. Prior to the cask being lifted into the fuel pool, the water level in the pool should be adjusted as necessary to accommodate the cask/DSC volume. If the water placed in the DSC cavity was obtained from the fuel pool, a level adjustment may not be necessary.

M.8.1.2 DSC Fuel Loading

1. Lift the cask/DSC and position it over the cask loading area of the spent fuel pool in accordance with the plant's 10CFR50 cask handling procedures.
2. Lower the cask into the fuel pool until the bottom of the cask is at the height of the fuel pool surface. As the cask is lowered into the pool, spray the exterior surface of the cask with demineralized water.
3. Place the cask in the location of the fuel pool designated as the cask loading area.
4. Disengage the lifting yoke from the cask lifting trunnions and move the yoke and the top shield plug clear of the cask. Spray the lifting yoke and top shield plug with clean demineralized water if it is raised out of the fuel pool.
5. The potential for fuel misloading is essentially eliminated through the implementation of procedural and administrative controls. The controls instituted to ensure that fuel assemblies, BPRAs (if applicable) and Poison Rod Assemblies (PRAs), if required, are placed into a known cell location within a DSC, will typically consist of the following:
 - A cask/DSC loading plan is developed to verify that the fuel assemblies, and BPRAs, if applicable, meet the burnup, enrichment and cooling time parameters of Technical

Specification 1.2.1. If PRAs are determined to be needed by Technical Specification 1.2.1, record the number required and the DSC cell location for each of the PRAs on the loading plan.

- The loading plan is independently verified and approved before the fuel load.
 - A fuel movement schedule is then written, verified and approved based upon the loading plan. All fuel movements from any rack location are performed under strict compliance of the fuel movement schedule.
6. Prior to insertion of a spent fuel assembly (and BPRAs, if applicable) into the DSC, the identity of the assembly (and BPRAs, if applicable) is to be verified by two individuals using an underwater video camera or other means. Read and record the identification number from the fuel assembly (and BPRAs, if applicable) and check this identification number against the DSC loading plan which indicates which fuel assemblies (and BPRAs, if applicable) are acceptable for dry storage.
 7. Position the fuel assembly for insertion into the selected DSC storage cell and load the fuel assembly. Repeat Step 6 for each SFA loaded into the DSC. If applicable, insert the required number of PRAs at specific locations called out in the loading plan. After the DSC has been fully loaded, check and record the identity and location of each fuel assembly and BPRAs, if applicable, in the DSC. Also record the location of each PRA inserted in the DSC (if applicable).
 8. After all the SFAs, BPRAs, and PRAs, if applicable, have been placed into the DSC and their identities verified, position the lifting yoke and the top shield plug and lower the shield plug onto the DSC.

CAUTION: Verify that all the lifting height restrictions as a function of temperature specified in Technical Specification 1.2.13 can be met in the following steps which involve lifting of the TC.

9. Visually verify that the top shield plug is properly seated onto the DSC.
10. Position the lifting yoke with the TC trunnions and verify that it is properly engaged.
11. Raise the TC to the pool surface. Prior to raising the top of the cask above the water surface, stop vertical movement.
12. Inspect the top shield plug to verify that it is properly seated onto the DSC. If not, lower the cask and reposition the top shield plug. Repeat Steps 11 and 12 as necessary.
13. Continue to raise the TC from the pool and spray the exposed portion of the cask with demineralized water until the top region of the cask is accessible.
14. Drain any excess water from the top of the DSC shield plug back to the fuel pool.

15. Check the radiation levels at the center of the top shield plug and around the perimeter of the cask.
16. If loading 32PT-S100 or 32PT-L100 DSC (qualified for 100-ton crane capacity), drain approximately 750 gallons of water (as indicated on the flowmeter) from the DSC back into the fuel pool or other suitable location using the VDS or optional liquid pump.
17. Lift the TC from the fuel pool. As the cask is raised from the pool, continue to spray the cask with demineralized water.
18. Move the TC with loaded DSC to the cask decon area.
19. Replace the approximate 750 gallons of water removed in step 16 (as indicated on the flowmeter) from the DSC with spent fuel pool water. Fill the neutron shield with demineralized water if it was drained in Step M.8.1.1.5.
20. Verify that the transfer cask dose rates are compliant with limits specified in Technical Specification 1.2.11.

M.8.1.3 DSC Drying and Backfilling

1. Check the radiation levels along the perimeter of the cask. The cask exterior surface should be decontaminated as necessary in accordance with the limits specified in Technical Specification 1.2.12. Temporary shielding may be installed as necessary to minimize personnel exposure.
2. Place scaffolding around the cask so that any point on the surface of the cask is easily accessible to personnel.
3. Disengage the rigging cables from the top shield plug and remove the eyebolts. Disengage the lifting yoke from the trunnions and position it clear of the cask.
4. Decontaminate the exposed surfaces of the DSC shell perimeter and remove the inflatable cask/DSC annulus seal.
5. Connect the cask drain line to the cask, open the cask cavity drain port and allow water from the annulus to drain out until the water level is approximately twelve inches below the top edge of the DSC shell. Take swipes around the outer surface of the DSC shell and check for smearable contamination in accordance with the Technical Specification 1.2.12 limits.
6. Drain approximately 750 gallons of water (as indicated on a flowmeter) from the DSC back into the fuel pool or other suitable location using the VDS or an optional liquid pump.
7. Disconnect hose from the DSC siphon port.

8. Install the automatic welding machine onto the inner top cover plate and place the inner top cover plate with the automatic welding machine onto the DSC. Verify proper fit-up of the inner top cover plate with the DSC shell.
9. Check radiation levels along surface of the inner top cover plate. Temporary shielding may be installed as necessary to minimize personnel exposure.

CAUTION: Insert a 1/4 inch tygon tubing of sufficient length through the vent port such that it terminates just below the DSC shield plug. Connect the tygon tubing to a hydrogen monitor to allow continuous monitoring of the hydrogen atmosphere in the DSC cavity during welding of the inner cover plate.

10. Cover the cask/DSC annulus to prevent debris and weld splatter from entering the annulus.
11. Ready the automatic welding machine and tack weld the inner top cover plate to the DSC shell. Install the inner top cover plate weldment and remove the automatic welding machine.

CAUTION: Continuously monitor the hydrogen concentration in the DSC cavity using the tygon tube arrangement described in step 9 during the inner top cover plate cutting/welding operations. Verify that the measured hydrogen concentration does not exceed a safety limit of 2.4% [8.4]. If this limit is exceeded, stop all welding operations and purge the DSC cavity with 2-3 psig helium (or any other inert medium) via the 1/4 inch tygon tubing to reduce the hydrogen concentration safely below the 2.4% limit.

12. Perform dye penetrant weld examination of the inner top cover plate weld in accordance with the Technical Specification 1.2.5 requirements.
13. Connect the VDS to the DSC siphon and vent ports.
14. Install temporary shielding to minimize personnel exposure throughout the subsequent welding operations as required.
15. Engage the compressed air, nitrogen or helium supply and open the valve on the vent port and allow compressed gas to force the water from the DSC cavity through the siphon port.
16. Once the water stops flowing from the DSC, close the DSC siphon port and disengage the gas source.
17. Connect the hose from the vent port and the siphon port to the intake of the vacuum pump. Connect a hose from the discharge side of the VDS to the plant's radioactive waste system or spent fuel pool. Connect the VDS to a helium source.
18. Open the valve on the suction side of the pump, start the VDS and draw a vacuum on the DSC cavity. The cavity pressure should be reduced in steps of approximately 100 mm Hg, 50 mm Hg, 25 mm Hg, 15 mm Hg, 10 mm Hg, 5 mm Hg, and 3 mm Hg. After pumping down to each level, the pump is valved off and the cavity pressure monitored. The cavity pressure will rise as water and other volatiles in the cavity evaporate. When the cavity

pressure stabilizes, the pump is valved in to complete the vacuum drying process. It may be necessary to repeat some steps, depending on the rate and extent of the pressure increase. Vacuum drying is complete when the pressure stabilizes for a minimum of 30 minutes at 3 mm Hg or less as specified in Technical Specification 1.2.2.

Caution: The vacuum drying step for 32PT DSC must meet the time duration limits of Technical Specification 1.2.17a.

19. Open the valve to the vent port and allow the helium to flow into the DSC cavity.
20. Pressurize the DSC with helium to about 24 psia not to exceed 34 psia.
21. Helium leak test the inner top cover plate weld for leakage in accordance with ANSI N14.5 to a sensitivity of 1×10^{-5} atm cm³ /sec.
22. If a leak is found, repair the weld, repressurize the DSC and repeat the helium leak test.
23. Once no leaks are detected, depressurize the DSC cavity by releasing the helium through the VDS to the plant's spent fuel pool or radioactive waste system.
24. Re-evacuate the DSC cavity using the VDS. The cavity pressure should be reduced in steps of approximately 10 mm Hg, 5 mm Hg, and 3 mm Hg. After pumping down to each level, the pump is valved off and the cavity pressure is monitored. When the cavity pressure stabilizes, the pump is valved in to continue the vacuum drying process. Vacuum drying is complete when the pressure stabilizes for a minimum of 30 minutes at 3 mm Hg or less in accordance with Technical Specification 1.2.2 limits.
25. Open the valve on the vent port and allow helium to flow into the DSC cavity to pressurize the DSC to about 17.2 psia in accordance with Technical Specification 1.2.3a limits.
26. Close the valves on the helium source.
27. Decontaminate as necessary, and store.

M.8.1.4 DSC Sealing Operations

1. Disconnect the VDS from the DSC. Seal weld the prefabricated plugs over the vent and siphon ports, inject helium into blind space just prior to completing welding, and perform a dye penetrant weld examination in accordance with the Technical Specification 1.2.5 requirements.
2. Open the cask drain port valve and remove the remaining water from the cask/DSC annulus.
3. Install the automatic welding machine onto the outer top cover plate and place the outer top cover plate with the automatic welding system onto the DSC. Verify proper fit up of the outer top cover plate with the DSC shell.

4. Tack weld the outer top cover plate to the DSC shell. Place the outer top cover plate weld root pass.
5. Helium leak test the inner top cover plate and vent/siphon port plate welds using the leak test port in the outer top cover plate in accordance with Technical Specification 1.2.4a limits. Verify that the personnel performing the leak test are qualified in accordance with SNT-TC-1A [8.6].
6. If a leak is found, remove the outer cover plate root pass, the vent and siphon port plugs and repair the inner cover plate welds. repeat procedure steps from M.8.1.3 step 18.
7. Perform dye penetrant examination of the root pass weld. Weld out the outer top cover plate to the DSC shell and perform dye penetrant examination on the weld surface in accordance with the Technical Specification 1.2.5 requirements.
8. Seal weld the prefabricated plug over the outer cover plate test port and perform dye penetrant weld examinations in accordance with Technical Specification 1.2.5 requirement.
9. Remove the automatic welding machine from the DSC. Rig the cask top cover plate and lower the cover plate onto the TC.
10. Bolt the cask cover plate into place, tightening the bolts to the required torque in a star pattern.
11. Verify that the transfer cask dose rates are compliant with limits specified in Technical Specification 1.2.11.

M.8.1.5 TC Downending and Transport to ISFSI

1. If loading 32PT-S100 or 32PT-L100 DSC (qualified for 100-ton crane capacity), drain the neutron shield to an acceptable location.
2. Re-attach the TC lifting yoke to the crane hook, as necessary. Ready the transport trailer and cask support skid for service.
3. Move the scaffolding away from the cask as necessary. Engage the lifting yoke and lift the cask over the cask support skid on the transport trailer.
4. The transport trailer should be positioned so that cask support skid is accessible to the crane with the trailer supported on the vertical jacks.
5. Position the cask lower trunnions onto the transfer trailer support skid pillow blocks.
6. Move the crane forward while simultaneously lowering the cask until the cask upper trunnions are just above the support skid upper trunnion pillow blocks.
7. Inspect the positioning of the cask to insure that the cask and trunnion pillow blocks are properly aligned.

8. Lower the cask onto the skid until the weight of the cask is distributed to the trunnion pillow blocks.
9. Inspect the trunnions to insure that they are properly seated onto the skid and install the trunnion tower closure plates.
10. Fill the neutron shield, if it was drained in step M.8.1.5.1.
11. Remove the bottom ram access cover plate from the cask. Install the two-piece temporary neutron/gamma shield plug to cover the bottom ram access. Install the ram trunnion support frame on the bottom of the TC. (The temporary shield plug and ram trunnion support frame are not required with integral ram/trailer.)

M.8.1.6 DSC Transfer to the HSM

1. Prior to transporting the cask to the ISFSI, remove the HSM door using a porta-crane, inspect the cavity of the HSM, removing any debris and ready the HSM to receive a DSC. The doors on adjacent HSMs should remain in place.
2. Inspect the HSM air inlet and outlets to ensure that they are clear of debris. Inspect the screens on the air inlet and outlets for damage.

CAUTION: Verify that the requirements of Technical Specification 1.2.14, "TC/DSC Transfer Operations at High Ambient Temperatures" are met prior to next step.

3. Using a suitable heavy haul tractor, transport the cask from the plant's fuel/reactor building to the ISFSI along the designated transfer route.
4. Once at the ISFSI, position the transport trailer to within a few feet of the HSM.
5. Check the position of the trailer to ensure the centerline of the HSM and cask approximately coincide. If the trailer is not properly oriented, reposition the trailer, as necessary.
6. Using a porta-crane, unbolt and remove the cask top cover plate.
7. Back the cask to within a few inches of the HSM, set the trailer brakes and disengage the tractor. Drive the tractor clear of the trailer. Extend the transfer trailer vertical jacks.
8. Connect the skid positioning system hydraulic power unit to the positioning system via the hose connector panel on the trailer, and power it up. Remove the skid tie-down bracket fasteners and use the skid positioning system to bring the cask into approximate vertical and horizontal alignment with the HSM. Using optical survey equipment and the alignment marks on the cask and the HSM, adjust the position of the cask until it is properly aligned with the HSM.
9. Using the skid positioning system, fully insert the cask into the HSM access opening docking collar.

10. Secure the cask trunnions to the front wall embedments of the HSM using the cask restraints.
11. After the cask is docked with the HSM, verify the alignment of the TC using the optical survey equipment.
12. Position the hydraulic ram behind the cask in approximate horizontal alignment with the cask and level the ram. Remove either the bottom ram access cover plate or the outer plug of the two-piece temporary shield plug. Power up the ram hydraulic power supply and extend the ram through the bottom cask opening into the DSC grapple ring.
13. Activate the hydraulic cylinder on the ram grapple and engage the grapple arms with the DSC grapple ring.
14. Recheck all alignment marks in accordance with the Technical Specification 1.2.9 limits and ready all systems for DSC transfer.
15. Activate the hydraulic ram to initiate insertion of the DSC into the HSM. Stop the ram when the DSC reaches the support rail stops at the back of the module.
16. Disengage the ram grapple mechanism so that the grapple is retracted away from the DSC grapple ring.
17. Retract and disengage the hydraulic ram system from the cask and move it clear of the cask. Remove the cask restraints from the HSM.
18. Using the skid positioning system, disengage the cask from the HSM access opening.
19. Install the DSC axial retainer through the HSM door opening.
20. Install the HSM door using a portable crane and secure it in place. Door may be welded for security. Verify that the HSM dose rates are compliant with the limits specified in Technical Specification 1.2.7.
21. Replace the TC top cover plate. Secure the skid to the trailer, retract the vertical jacks and disconnect the skid positioning system.
22. Tow the trailer and cask to the designated equipment storage area. Return the remaining transfer equipment to the storage area.
23. Close and lock the ISFSI access gate and activate the ISFSI security measures.

M.8.1.7 Monitoring Operations

1. Perform routine security surveillance in accordance with the licensee's ISFSI security plan.
2. Perform a daily visual surveillance of the HSM air inlets and outlets to insure that no debris is obstructing the HSM vents in accordance with Technical Specification 1.3.1 requirements.

3. Perform a temperature measurement of the thermal performance, for each HSM, on a daily basis in accordance with Technical Specification 1.3.2 requirements.

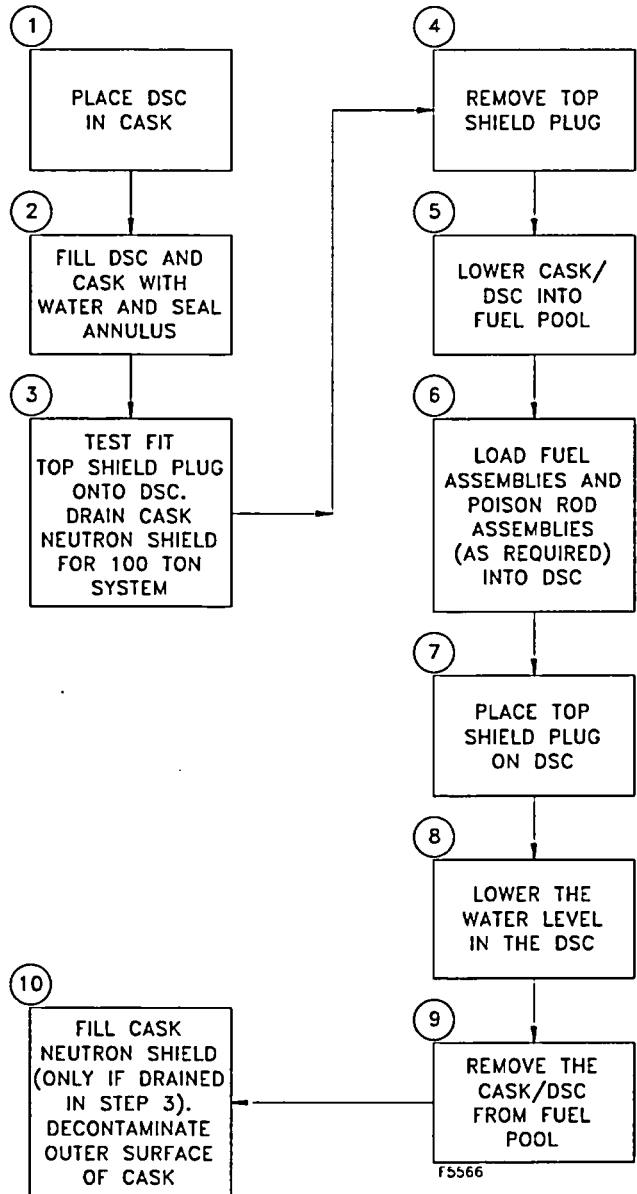


Figure M.8-1
NUHOMS® System Loading Operations Flow Chart

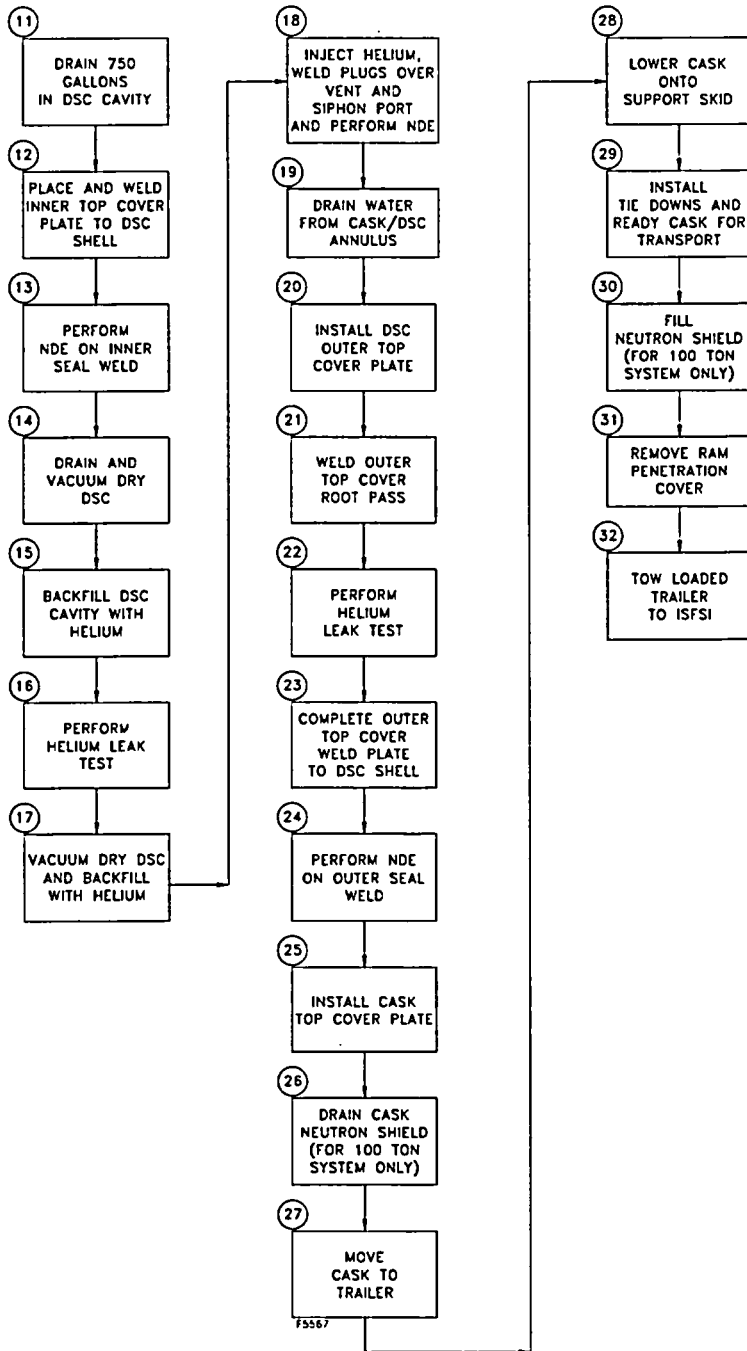


Figure M.8-1
 NUHOMS® System Loading Operations Flow Chart
 (continued)

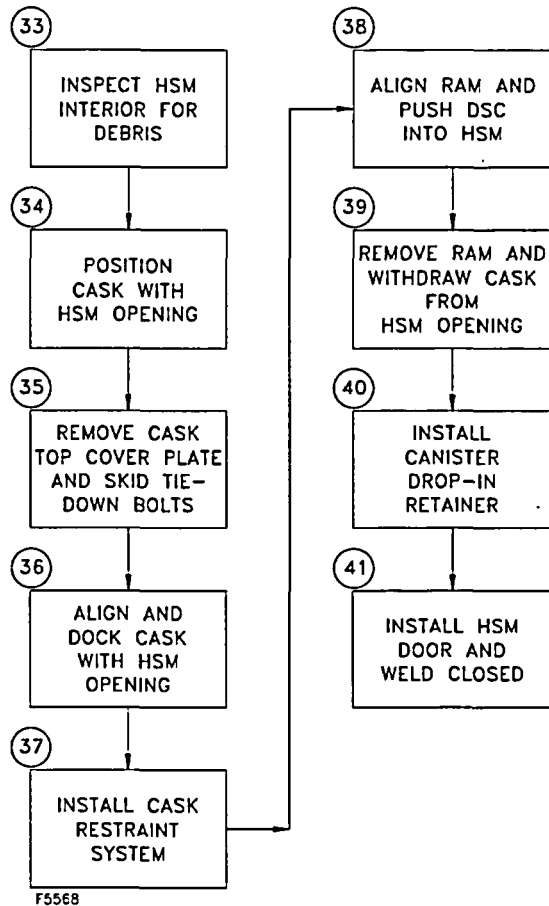


Figure M.8-1
NUHOMS® System Loading Operations Flow Chart
(concluded)

M.8.2 Procedures for Unloading the Cask

M.8.2.1 DSC Retrieval from the HSM

1. Ready the TC, transport trailer, and support skid for service and tow the trailer to the HSM.
2. Back the trailer to within a few inches of the HSM and remove the cask top cover plate.
3. Cut any welds from the door and remove the HSM door using a porta-crane. Remove the DSC drop-in retainer.
4. Using the skid positioning system align the cask with the HSM and position the skid until the cask is docked with the HSM access opening.
5. Using optical survey equipment, verify alignment of the cask with respect to the HSM. Install the cask restraints.
6. Install and align the hydraulic ram with the cask.
7. Extend the ram through the cask into the HSM until it is inserted in the DSC grapple ring.
8. Activate the arms on the ram grapple mechanism with the DSC grapple ring.
9. Retract ram and pull the DSC into the cask.
10. Retract the ram grapple arms.
11. Disengage the ram from the cask.
12. Remove the cask restraints.
13. Using the skid positioning system, disengage the cask from the HSM.
14. Install the cask top cover plate and ready the trailer for transport.
15. Replace the door on the HSM.

M.8.2.2 Removal of Fuel from the DSC

When the DSC has been removed from the HSM, there are several potential options for off-site shipment of the fuel. It is preferred to ship the DSC intact to a reprocessing facility, monitored retrievable storage facility or permanent geologic repository in a compatible shipping cask licensed under 10CFR71.

If it becomes necessary to remove fuel from the DSC prior to off-site shipment, there are two basic options available at the ISFSI or reactor site. The fuel assemblies could be removed and reloaded into a shipping cask using dry transfer techniques, or if the applicant so desires, the initial fuel loading sequence could be reversed and the plant's spent fuel pool utilized. Procedures for

unloading the DSC in a fuel pool are presented here. However, wet or dry unloading procedures are essentially identical to those of DSC loading through the DSC weld removal (beginning of preparation to placement of the cask in the fuel pool). Prior to opening the DSC, the following operations are to be performed.

1. The cask may now be transported to the cask handling area inside the plant's fuel/reactor building.
2. Position and ready the trailer for access by the crane and install the ram access penetration cover plate.
3. Attach the lifting yoke to the crane hook.
4. Engage the lifting yoke with the trunnions of the cask.
5. Visually inspect the yoke lifting hooks to insure that they are properly aligned and engaged onto the cask trunnions.
6. If unloading 32PT-S100 or 32PT-L100 DSC (qualified for 100-ton crane capacity), drain water from the neutron shield.
7. Lift the cask approximately one inch off the trunnion supports. Visually inspect the yoke lifting hooks to insure that they are properly positioned on the trunnions.
8. Move the crane backward in a horizontal motion while simultaneously raising the crane hook vertically and lift the cask off the trailer. Move the cask to the cask decon area.
9. Lower the cask into the cask decon area in the vertical position. Fill the neutron shield with water if it was drained in Step M.8.2.2.6.
10. Wash the cask to remove any dirt which may have accumulated on the cask during the DSC loading and transfer operations.
11. Place scaffolding around the cask so that any point on the surface of the cask is easily accessible to handling personnel.
12. Unbolt the cask top cover plate.
13. Connect the rigging cables to the cask top cover plate and lift the cover plate from the cask. Set the cask cover plate aside and disconnect the lid lifting cables.
14. Install temporary shielding to reduce personnel exposure as required. Fill the cask/DSC annulus with clean demineralized water and seal the annulus.

The process of DSC unloading is similar to that used for DSC loading. DSC opening operations described below are to be carefully controlled in accordance with plant procedures. This operation is to be performed under the site's standard health physics guidelines for welding, grinding, and handling of potentially highly contaminated equipment. These are to include the

use of prudent housekeeping measures and monitoring of airborne particulates. Procedures may require personnel to perform the work using respirators or supplied air.

If fuel needs to be removed from the DSC, either at the end of service life or for inspection after an accident, precautions must be taken against the potential for the presence of damaged or oxidized fuel and to prevent radiological exposure to personnel during this operation. A sampling of the atmosphere within the DSC will be taken prior to inspection or removal of fuel.

If the work is performed outside the fuel/reactor building, a tent may be constructed over the work area, which may be kept under a negative pressure to control airborne particulates. Any radioactive gas release will be Kr-85, which is not readily captured. Whether the krypton is vented through the plant stack or allowed to be released directly depends on the plant operating requirements.

Following opening of the DSC, the cask and DSC are filled with water prior to lowering the top of cask below the surface of the fuel pool to prevent a sudden inrush of pool water. Cask placement into the pool is performed in the usual manner. Fuel unloading procedures will be governed by the plant operating license under 10CFR50. The generic procedures for these operations are as follows:

15. Locate the DSC siphon and vent port using the indications on the top cover plate. Place a portable drill press on the top of the DSC. Position the drill with the siphon port.
16. Place an exhaust hood or tent over the DSC, if necessary. The exhaust should be filtered or routed to the site radwaste system.
17. Drill a hole through the DSC top cover plate to expose the siphon port quick connect.
18. Drill a second hole through the top cover plate to expose the vent port quick connect.
19. Obtain a sample of the DSC atmosphere, if necessary (e.g., at the end of service life). Fill the DSC with water from the fuel pool through the siphon port with the vent port open and routed to the plant's off-gas system.

CAUTION:

- (a) The water fill rate must be regulated during this reflooding operation to ensure that the DSC vent pressure does not exceed 20.0 psig.
 - (b) Provide for continuous hydrogen monitoring of the DSC cavity atmosphere during all subsequent cutting operations to ensure that a safety limit of 2.4% is not exceeded [8.4]. Purge with 2-3 psig helium (or any other inert medium) as necessary to maintain the hydrogen concentration safely below this limit.
20. Place welding blankets around the cask and scaffolding.
 21. Using plasma arc-gouging, a mechanical cutting system or other suitable means, remove the seal weld from the outer top cover plate and DSC shell. A fire watch should be placed on the

- scaffolding with the welder, as appropriate. The exhaust system should be operating at all times.
22. The material or waste from the cutting or grinding process should be treated and handled in accordance with the plant's low level waste procedures unless determined otherwise.
 23. Remove the top of the tent, if necessary.
 24. Remove the exhaust hood, if necessary.
 25. Remove the DSC outer top cover plate.
 26. Reinstall tent and temporary shielding, as required. Remove the seal weld from the inner top cover plate to the DSC shell in the same manner as the top cover plate. Remove the inner top cover plate. Remove any remaining excess material on the inside shell surface by grinding.
 27. Clean the cask surface of dirt and any debris which may be on the cask surface as a result of the weld removal operation. Any other procedures which are required for the operation of the cask should take place at this point as necessary.
 28. Engage the yoke onto the trunnions, install eyebolts into the top shield plug and connect the rigging cables to the eyebolts.
 29. Visually inspect the lifting hooks or the yoke to insure that they are properly positioned on the trunnions.
 30. If unloading 32PT-S100 or 32PT-L100 DSC (qualified for 100-ton crane capacity), drain approximately 750 gallons of water from the DSC. The neutron shield also needs to be drained.
 31. The cask should be lifted just far enough to allow the weight of the TC to be distributed onto the yoke lifting hooks. Inspect the lifting hooks to insure that they are properly positioned on the trunnions.
 32. Install suitable protective material onto the bottom of the TC to minimize cask contamination. Move the cask to the fuel pool.
 33. Prior to lowering the cask into the pool, adjust the pool water level, if necessary, to accommodate the volume of water which will be displaced by the cask during the operation.
 34. Lower the cask into the fuel pool leaving the top surface of the cask approximately one foot above the surface of the pool water.
 35. Fill the DSC with pool water.
 36. Position the cask over the cask loading area in the fuel pool
 37. Lower the cask into the pool. As the cask is being lowered, the exterior surface of the cask should be sprayed with clean demineralized water.

38. Disengage the lifting yoke from the cask and lift the top shield plug from the DSC.
39. Remove the fuel from the DSC and place the fuel into the spent fuel racks.
40. Lower the top shield plug onto the DSC.
41. Visually verify that the top shield plug is properly positioned onto the DSC.
42. Engage the lifting yoke onto the cask trunnions.
43. Visually verify that the yoke lifting hooks are properly engaged with the cask trunnions.
44. Lift the cask by a small amount and verify that the lifting hooks are properly engaged with the trunnions.
45. Lift the cask to the pool surface. Prior to raising the top of the cask to the water surface, stop vertical movement and inspect the top shield plug to ensure that it is properly positioned.
46. Spray the exposed portion of the cask with demineralized water.
47. Visually inspect the top shield plug of the DSC to insure that it is properly seated onto the cask. If the top shield plug is not properly seated, lower the cask back to the fuel pool and reposition the plug.
48. Drain any excess water from the top of the top shield plug into the fuel pool.
49. Lift the cask from the pool. As the cask is rising out of the pool, spray the cask with demineralized water.
50. Move the cask to the cask decon area.
51. Check radiation levels around the perimeter of the cask. The cask exterior surface should be decontaminated if necessary.
52. Place scaffolding around the cask so that any point along the surface of the cask is easily accessible to personnel.
53. Ready the DSC vacuum drying system (VDS).
54. Connect the VDS to the vent port with the system open to atmosphere. Also connect the VDS to the siphon port and connect the other end of the system to the liquid pump. The pump discharge should be routed to the plant radwaste system or the spent fuel pool.
55. Open the valves on the vent port and siphon port of the VDS.
56. Activate the liquid pump.
57. Once the water stops flowing out of the DSC, deactivate the pump.

58. Close the valves on the VDS.
59. Disconnect the VDS from the vent and siphon ports.
60. The top cover plates may be welded into place as required.
61. Decontaminate the DSC, as necessary, and handle in accordance with low-level waste procedures. Alternatively, the DSC may be repaired for reuse.

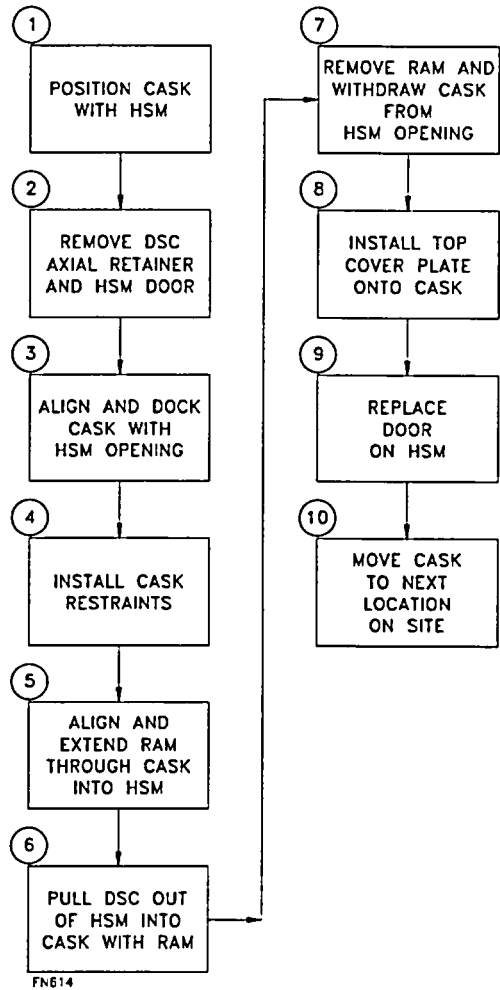


Figure M.8-2
NUHOMS® System Retrieval Operations Flow Chart

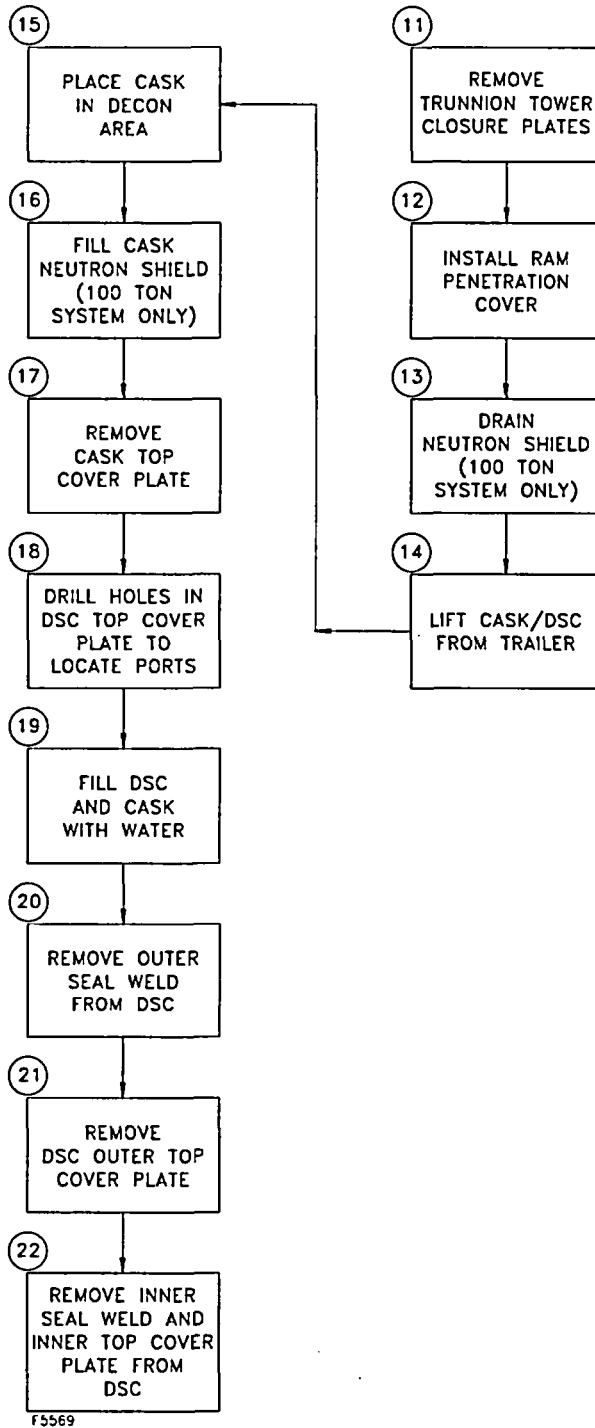


Figure M.8-2
 NUHOMS® System Retrieval Operations Flow Chart
 (Continued)

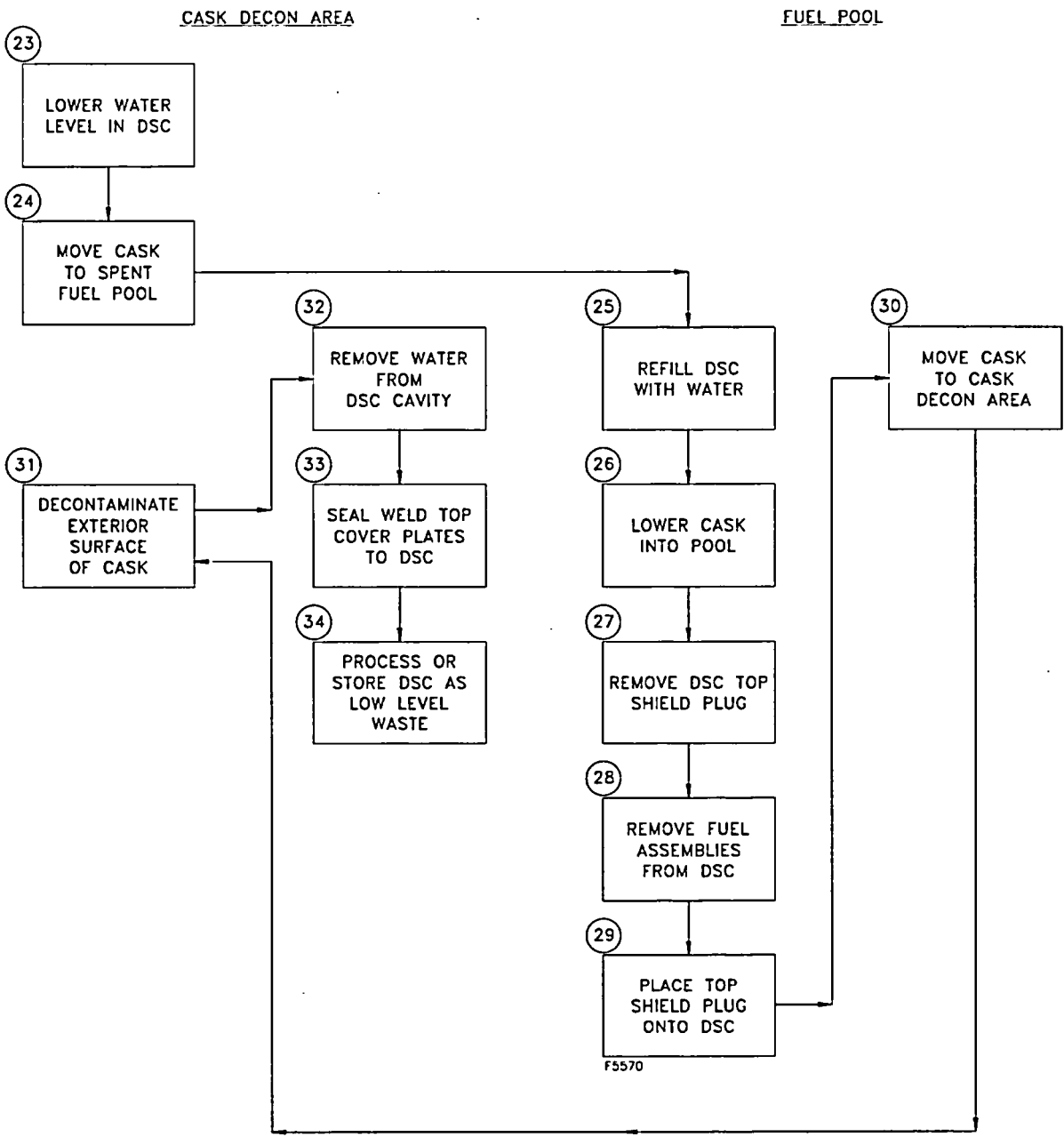


Figure M.8-2
NUHOMS® System Retrieval Operations Flow Chart
 (Concluded)

M.8.3 Identification of Subjects for Safety Analysis

No change from Section 5.1.3.

M.8.4 Fuel Handling Systems

No change from Section 5.2.

M.8.5 Other Operating Systems

No change from Section 5.3.

M.8.6 Operation Support System

No change from Section 5.4.

M.8.7 Control Room and/or Control Areas

No change from Section 5.5.

M.8.8 Analytical Sampling

No change from Section 5.6.

M.8.9 References

- 8.1 U.S. Nuclear Regulatory Commission, "Standard Format and Content for a Topical Safety Analysis Report for a Spent Fuel Dry Storage Container," Regulatory Guide 3.61 (February 1989).
- 8.2 Deleted.
- 8.3 Deleted.
- 8.4 U.S. Nuclear Regulatory Commission, Office of the Nuclear Material Safety and Safeguards, "Safety Evaluation of VECTRA Technologies' Response to Nuclear Regulatory Commission Bulletin 96-04 For the NUHOMS[®]-24P and NUHOMS[®]-7P.
- 8.5 U.S. Nuclear Regulatory Commission Bulletin 96-04, "Chemical, Galvanic or Other Reactions in Spent Fuel Storage and Transportation Casks," July 5, 1996.
- 8.6 SNT-TC-1A, "American Society for Nondestructive Testing, Personnel Qualification and Certification in Nondestructive Testing," 1992.

M.9 Acceptance Tests and Maintenance Program

M.9.1 Acceptance Tests

The acceptance requirements for the NUHOMS[®]-32PT system are given in the FSAR except as described in the following sections. The NUHOMS[®]-32PT DSC has been enhanced to provide leaktight confinement and the basket includes an updated poison plate design. Additional acceptance testing of the NUHOMS[®]-32PT DSC welds and poison plates are described.

M.9.1.1 Visual Inspection

Visual examinations are performed at the fabricator's facility to ensure that the NUHOMS[®]-32PT system components conform to the fabrication specifications and drawings.

Visual examination of all finished absorber plates and rods are done to ensure that they are free of cracks, porosity, blisters, or foreign substances. Dimensional inspections of the plates and rods are done to ensure that their functional requirements listed in M.9.17.1 are met.

M.9.1.2 Structural Tests

The NUHOMS[®]-32PT DSC confinement welds are designed, fabricated, tested and inspected in accordance with ASME B&PV Code Section III, Subsection NB [9.1] with exceptions as listed in Section M.3.1. The following requirements are unique to the NUHOMS[®]-32PT DSC:

- The inner bottom cover weld is inspected in accordance with Article NB-5231,
- The outer bottom cover weld root and cover are penetrant tested, and
- The outer top cover plate weld root and cover are penetrant tested.

The NUHOMS[®]-32PT DSC basket is designed, fabricated, and inspected in accordance with ASME B&PV Code Section III, Subsection NG [9.1] with exceptions as listed in Section M.3.1. The following requirement is unique to the NUHOMS[®]-32PT DSC basket:

- The fuel compartment welds are inspected in accordance with Article NG-5260.

M.9.1.3 Leak Tests

The NUHOMS[®]-32PT DSC confinement boundary is leak tested to verify that it is leaktight in accordance with ANSI N14.5 [9.2]. The personnel performing the leak test are qualified in accordance with SNT-TC-1A [9.14].

The leak tests are typically performed using the helium mass spectrometer method. Alternative methods are acceptable, provided that the required sensitivity is achieved.

M.9.1.4 Component Tests

No changes associated with this amendment.

M.9.1.5 Shielding Integrity Tests

No changes associated with this amendment.

M.9.1.6 Thermal Acceptance Tests

The analyses to ensure that the NUHOMS[®]-32PT DSCs are capable of performing their heat transfer function are presented in Section M.4.

M.9.1.7 Poison Acceptance

M.9.1.7.1.1 Functional Requirements of Poison Plates

The poison plates only serve as a neutron absorber for criticality control and as a heat conduction path. The NUHOMS[®]-32PT DSC safety analyses do not rely upon their mechanical strength. The radiation and temperature environment in the cask is not sufficiently severe to damage the aluminum matrix that retains the boron-containing particles. To assure performance of the plates' Important-to-Safety function, the only critical variables that need to be verified are thermal conductivity and B10 areal density as discussed in the following paragraphs.

M.9.1.7.1.2 Thermal Conductivity Testing of Poison Plates

The poison plate material shall be qualification tested to verify that the thermal conductivity equals or exceeds the values listed in Section M.4.3. Acceptance testing of the material in production may be done at only one temperature in that range to verify that the conductivity equals or exceeds the corresponding value in Section M.4.3.

Testing may be by ASTM E1225 [9.3], ASTM E1461 [9.4], or equivalent method, performed on coupons as defined in Section M.9.1.7.3.1.2.

M.9.1.7.1.3 B10 Areal Density Testing of Poison Plates

There are two poison materials qualified for the NUHOMS[®]-32PT DSC basket: Borated aluminum and boron carbide/aluminum metal matrix composites (MMCs), such as Boralyn[®], or Metamic[®], or equivalent. The B10 areal density and uniformity of the poison plates shall be verified, based on type, using approved procedures, as follows.

M.9.1.7.1.4 Borated Aluminum Using Enriched Boron, 90% B10 Credit

M.9.1.7.1.4.1 Borated Aluminum Material Description

The poison consists of wrought aluminum containing boron, which is isotopically enriched to 95 wt. % B10. Because of the negligibly low solubility of boron in solid aluminum, the boron

appears entirely as discrete second phase particles of AlB_2 in the aluminum matrix. The matrix is limited to any 1000 series aluminum, aluminum alloy 6063, or aluminum alloy 6351 so that no boron-containing phases other than AlB_2 are formed. Titanium may also be added to form TiB_2 particles, which are finer. The effect on the properties of the matrix aluminum alloy are those typically associated with a uniform fine (1-10 micron) dispersion of an inert equiaxed second phase.

The cast ingot may be rolled, extruded, or both to the final plate dimensions.

The nominal wt. % boron is 1.5 wt. %. This wt. % boron converts to areal density of B10 as follows: $(2.69 \text{ g BAl/cm}^3)(1.5 \text{ wt. \% B})(95 \text{ wt. \% B10})(0.075 \text{ inch})(2.54 \text{ cm/inch}) = 0.0073 \text{ g B10/cm}^2$, which is intentionally 4% above the design minimum of $0.0070 \text{ g B10/cm}^2$.

M.9.1.7.1.4.2 Borated Aluminum Test Coupon and Lot Definitions

Sample taken from the plate material is a test coupon. Test coupons will be removed so that there is at least one coupon contiguous with each plate. These coupons will be used for neutron transmission and thermal conductivity testing. The minimum dimension of the coupon shall be as required for the acceptance test procedures.

A lot is defined as all the plates produced from a single cast ingot, or all the plates produced from a single heat.

M.9.1.7.1.4.3 Borated Aluminum Acceptance Testing, Neutronic

Effective B10 content is verified by neutron transmission testing of these coupons. The transmission through the coupons is compared with transmission through calibrated standards composed of a homogeneous boron compound without other significant poisons, for example zirconium diboride or titanium diboride. These standards are paired with aluminum shims sized to match the scattering by aluminum in the poison plates. Uniform but non-homogeneous materials such as metal matrix composites may be used for standards, provided that testing shows them to be equivalent to a homogeneous standard.

The neutron transmission testing measurements are taken using a collimated neutron beam size of approximately 1 cm^2 . The neutron transmission test procedure shall include provisions to vary the selected measurement location along the coupon length.

The acceptance criterion for neutron transmission testing is that the B10 areal density, minus $3s$ based on the number of neutrons counted for that measurement, must be greater than or equal to the minimum value 0.007 g B10/cm^2 .

In the event that a coupon fails the single neutron transmission measurement, the associated plate is rejected. As an alternate basis for accepting that plate, four additional measurements may be made at separate random locations on the plate itself, or on coupons cut from four random locations of the plate. For each of the additional measurements, the value of areal density less $3s$ based on the number of neutrons counted must be greater than or equal to the specified minimum in order to accept the plate.

If any of those four fails, the plate associated with the measurements will be rejected. However, the average of the five measurements made is to be used as a datum in the subsequent statistical analysis conducted on the lot (see below).

Macroscopic uniformity of B10 distribution is verified by neutron radioscopy/radiography of the coupons. The acceptance criterion is that there be uniform luminance across the coupon. This inspection shall cover the entire coupon. If a coupon fails this test, the associated plate shall be rejected.

Initial sampling of coupons for neutron transmission measurements and radioscopy/radiography shall be 100%. Reduced sampling (50%) may be introduced based upon acceptance of all coupons in the first 25% of the lot. A rejection during reduced inspection will require a return to 100% inspection of the lot.

In addition, a statistical analysis of the neutron transmission results for all plates in a lot shall be performed. This analysis shall demonstrate, using a one-sided tolerance limit factor for a normal distribution with at least 95% probability, the areal density is greater than or equal to the specified minimum value of 0.007 g B10/cm^2 with 95% confidence level.

This statistical analysis shall be based on full data set for the lot, except that any data from materials which are rejected based on physical examination of the materials may be eliminated from the statistical analysis. For example, a rejection based on dimensional or surface finish inspection is ground for excluding the datum associated with that plate. Failure to meet the acceptance criterion of this statistical analysis shall result in rejection of the entire lot. Individual pieces in that lot may be accepted based on the determination of an alternate minimum thickness as follows:

All areal densities determined by neutron transmission for that lot may be converted to volume density by dividing by the thickness of the corresponding coupon. The thickness shall be measured at the same location as the neutron transmission test, or shall be an equal or larger value. The one sided lower tolerance limit of volume density with 95% probability and 95% confidence may then be determined. Finally, the minimum specified value of B10 areal density may be divided by the 95/95 lower tolerance limit of B10 volume density to arrive at a minimum plate thickness. Then, all plates which have any location (other than local pits) thinner than this minimum shall be rejected, and those equal to or thicker may be accepted.

M.9.1.7.1.4.4 Justification for Acceptance Test Requirements, Borated Aluminum

According to NUREG/CR-5661 [9.5]:

“Limiting added poison material credit to 75% without comprehensive tests is based on concerns for potential ‘streaming’ of neutrons due to nonuniformities. It has been shown that boron carbide granules embedded in aluminum permit channeling of a beam of neutrons between the grains and reduce the effectiveness for neutron absorption.”

Furthermore:

“A percentage of poison material greater than 75% may be considered in the analysis only if comprehensive tests, capable of verifying the presence *and uniformity* of the poison, are implemented.” [emphasis added]

The calculations in Section M.6 use boron areal densities that are 90% of the minimum value of 0.007 g B10/cm². This is justified by the following considerations:

- a) The coupons for neutronic inspection are removed contiguous to every finished plate. As such, they are taken from locations that are representative of the finished product.
- b) Statistical analysis of the neutron transmission results on the coupons demonstrates that at any location in the plates, the B10 areal density will meet or exceed the specified minimum with 95% confidence and 95% probability.
- c) Neutron radiography/radioscopy across the entire coupon will detect macroscopic non-uniformities in the B10 distribution which could be introduced by the fabrication process. The use of neutron transmission and neutron radiography/radioscopy of the coupons, satisfies the “and uniformity” requirement emphasized in NUREG/CR-5661 on both the microscopic and macroscopic scales.
- d) The recommendations of NUREG/CR-5661 are based upon testing of a poison with boron carbide particles averaging 85 microns. The boride particles in the borated aluminum are much finer (5-10 microns). Both the manufacturing process and the neutron radiography assure that they are uniformly distributed. For a given degree of uniformity, fine particles will be less subject to neutron streaming than coarse particles. Furthermore, because the material reviewed in the NUREG was a sandwich panel, the thickness of the boron carbide containing center could not be directly verified by thickness measurement. The alloy specified here is uniform throughout its thickness.

M.9.1.7.1.5 Metal Matrix Composites (MMCs) Boralyn[®], Metamic[®], or Equivalent; 90% B10 credit

M.9.1.7.1.5.1 MMC Material Description

The MMC poison plates (Boralyn[®], Metamic[®], or Equivalent) consist of a composite of aluminum with boron carbide particulate reinforcement. The material is formed into a billet by powder metallurgical processes and either extruded, rolled, or both to final dimensions. The finished product has near-theoretical density and metallurgical bonding of the aluminum matrix particles. It is “uniform” blend of powder particles from face to face, i.e.; it is not a “sandwich” panel.

The nominal volume % boron carbide is 10.7 volume %. This volume % boron carbide corresponds to a B10 areal density of 0.107(2.52 g/cm³ B₄C)(0.782 gB/gB₄C)(0.185 g B10/gB)(0.075 in)(2.54 cm/in) = 0.0074 g B10/cm², which is intentionally 6% above the design and specification minimum of 0.007 g B10/cm².

The maximum areal density that will be permitted for use in Boralyn[®] corresponds to a maximum 15 volume % B₄C composition for which Boralyn[®] was originally qualified. This corresponds to a maximum B10 areal density for Boralyn[®] of $(15.0 \text{ volume \% B}_4\text{C}) / (10.7 \text{ volume \% B}_4\text{C}) * 0.0074 \text{ gB10/cm}^2 = 0.0104 \text{ g B10/cm}^2$.

Similarly, the maximum areal density that will be permitted for use in Metamic[®] corresponds to a maximum 40.0 volume % B₄C composition for which Metamic[®] was originally qualified. This corresponds to a maximum B10 areal density for Metamic[®] of $(40.0 \text{ volume \% B}_4\text{C}) / (10.7 \text{ volume \% B}_4\text{C}) * 0.0074 \text{ gB10/cm}^2 = 0.0277 \text{ g B10/cm}^2$.

Typical MMC processing steps consist of:

- blending of boron carbide powder with aluminum alloy powder,
- billet formed by vacuum hot pressing (Boralyn[®]) or cold isostatic pressing followed by vacuum sintering (Metamic[®]),
- billet extruded to intermediate or to final size,
- hot roll, cold roll and flatten as required, and
- anneal (optional).

M.9.1.7.1.5.2 MMC Qualification Test Program

The process specifications for the Boralyn[®] or Metamic[®] have been subjected to qualification testing to demonstrate that the process results in a material that:

- has a uniform distribution of boron carbide particles in an aluminum alloy with few or none of the following: voids, oxide-coated aluminum particles, B₄C fracturing, or B₄C/aluminum reaction products,
- meets the requirements for B10 areal density and thermal conductivity, and
- will be capable of performing its Important-to-Safety functions under the thermal and radiological environment of the NUHOMS[®]-32PT DSC over its 40-year lifetime.

These qualification programs consisted of:

1. Fast neutron irradiation of the material to a fluence of about $8 \times 10^{15} \text{ n/cm}^2$ or more, with dimensional measurements, transmission electron microscopic (TEM) examination, and /or mechanical testing to evaluate differences in the as-produced and irradiated conditions.
2. Exposure to temperatures in the range of 700°F or greater for periods of 30 days or more, again with dimensional measurements, transmission electron microscopic (TEM) examination, and /or mechanical testing to evaluate differences in the as-produced and irradiated conditions.
3. Evaluation of corrosion or hydrogen generation rates.
4. Verification of uniformity of B10 distribution by neutron radiography or by statistical analysis of neutron transmission measurements together with quantitative metallography.

The results of these qualification test programs have been previously presented to the NRC in the license applications for the TN-68 dry storage cask [9.12], the NUHOMS[®] 61BT DSC (Appendix K), and the NUHOMS[®] MP-197 transport packaging [9.13].

The qualification testing described above demonstrated, as would be expected from the properties of aluminum and boron carbide alone, that the materials suffer insignificant damage from the levels of radiation and temperature experienced in dry storage or transport of irradiated fuel. These materials also demonstrate corrosion characteristics very similar to the aluminum matrix.

Boralyn[®] qualification testing was performed on a 15 volume % boron carbide / 1000 series aluminum composite, and Metamic[®] qualification testing was performed on 15, 31 and 40 volume % boron carbide / 6000 series aluminum composites. The boron carbide content of material produced for the NUHOMS[®]-32PT DSC will not exceed the volume percent subjected to qualification testing for that material, unless it is subjected to additional testing as described in the following sections.

The production of MMC plates for use in the NUHOMS[®]-32PT DSC is consistent with the process used to produce the qualification test material. Processing changes may be incorporated into the production process, only if they are reviewed and approved by the holder of an NRC-approved QA plan who is supervising fabrication, in accordance with the following criteria:

Major processing changes, such as billet formation by processes other than hot vacuum pressing or CIP/vacuum sintering, or direct rolling of the billet (elimination of extrusion) shall be subject to a complete program of qualification testing including the four areas of radiation exposure, thermal exposure, hydrogen generation / corrosion, and B10 uniformity described above for the original Boralyn[®] and Metamic[®] qualification programs. Other examples of major changes which require qualification testing are:

- B₄C content of > 15 volume % for Boralyn[®] or equivalent, or
- B₄C content of > 40 volume % for Metamic[®] or equivalent, or
- Product theoretical density < 98%, or
- More than 5 % of B₄C powder ≥ 40 microns, and more than 20 % of B₄C powder ≥ 25 microns.

Minor processing changes that do not have an adverse effect on the particle bonding, microstructure or uniformity of the B₄C particle distribution may be accepted by engineering review without testing. Examples of such changes include reduction of B₄C content in the MMC, increased billet forming pressure, and changes in mechanical processing variables such as extrusion speed. Changes that have an uncertain or a small adverse effect on the microstructure shall be subjected to limited additional testing such as microscopic metallurgical examination in the as-built condition of the plates. Examples of such changes are increased billet forming temperature and small increases in the B₄C content (within the maximum limits listed above).

The basis for acceptance shall be that the changes do not have an adverse effect on either the durability or neutron absorption effectiveness of the material. These characteristics are

determined by the bonding and uniformity of the B₄C particle distribution. The evaluation may consist of an engineering review, or it may consist of additional testing.

M.9.1.7.1.5.3 MMC Test Coupon and Lot Definitions

Coupon removal for MMC's is the same as for borated aluminum. A lot shall be defined as all plates made from a single billet, or from a group of billets, all processed from the same batch of blended powder, and compacted into billets during a single production campaign.

M.9.1.7.1.5.4 MMC Acceptance Testing, Neutronic

The acceptance criteria for neutron transmission testing of MMC plates and the alternate acceptance criteria in the event that a MMC coupon fails an acceptance criteria are the same as those discussed in Section M.9.1.7.3.1.3.

M.9.1.7.1.6 Justification for Acceptance Test Requirements, MMCs

The justification for the test requirements and 90% B10 credit for MMCs is the same as those for borated aluminum, except that the boron carbide particles in a MMC are typically in the range of 1-25 microns.

M.9.1.7.1.7 B₄C Linear Density Testing for Poison Rod Assemblies (PRAs)

The PRAs are shown in Figure M.1-2, and additional physical requirements are listed in Table M.2-4. The B₄C poison is inserted into the stainless steel tubes shown in Figure M.1-2. Table M.2-4 specifies the minimum B₄C content per unit length in the axial direction of the rods for the various PRA designs. The minimum B₄C content per unit length is consistent with the criticality analysis (Section M.6) with an additional 25% margin.

Pellets or powder representing each powder lot shall be tested per ASTM C751 [9.6] or ASTM C750 (Type 2) [9.7] (or equivalent). Density and diameter shall be measured to verify conformance to the specification requirements.

Deviations from the specified dimensions or density may be accepted, so long as the resulting minimum B₄C mass per unit length is maintained.

Justification for Durability of B₄C Pellets:

B₄C is essentially inert and will not be attacked even by hot hydrofluoric or nitric acids[9.8]. It is insoluble in water [9.9], resistant to steam at temperatures of 200 to 300°C [9.10] and has a melting point of 2450°C [9.10]. Mechanically, B₄C is extremely hard (Mohs hardness of 9.3 vs. 10 for diamond) and is used in abrasion- and wear-resistant applications and in bullet-proof tiles. It has a compressive strength of 398,000 psi. In the PRAs, the B₄C pellets are sealed within stainless steel. With this configuration there is nothing that could cause the material to degrade. In the unlikely event that a pellet were to crack or break, the total mass would be confined by the steel to the same dimensions.

The irradiation-induced swelling is due to neutron capture by the ^{10}B isotope. Using data from [9.11] and by determining the neutron absorption in the B_4C (^{10}B capture) from the shielding analyses, the swelling is determined to be negligible $\sim 0.00002\%$. Finally, according to [9.11], the first intergranular cracks do not start to appear until fluences are 5.5 orders of magnitude greater than those calculated for 50 year operation.

M.9.2 Maintenance Program

NUHOMS[®]-32PT system is a totally passive system and therefore requires little, if any, maintenance over the lifetime of the ISFSI. Typical NUHOMS[®]-32PT system maintenance tasks are performed in accordance with the FSAR.

M.9.3 References

- 9.1 ASME Boiler and Pressure Vessel Code, Section III, 1998 Edition including 1999 addenda.
- 9.2 ANSI N14.5-1997, "American National Standard for Leakage Tests on Packages for Shipment of Radioactive Materials," February 1998.
- 9.3 ASTM E1225, "Thermal Conductivity of Solids by Means of the Guarded-Comparative-Longitudinal Heat Flow Technique."
- 9.4 ASTM E1461, "Thermal Diffusivity of Solids by the Flash Method."
- 9.5 NUREG/CR-5661, "Recommendations for Preparing the Criticality Safety Evaluation of Transportation Packages," 1997.
- 9.6 ASTM C751, "Standard Specification for Nuclear-Grade Boron Carbide Pellets."
- 9.7 ASTM C750, "Standard Specification for Nuclear-Grade Boron Carbide Powder."
- 9.8 The Merck Index, 9th edition, Merck & Co., 1976.
- 9.9 Grant (ed.), Hackh's Chemical Dictionary, 4th edition, McGraw-Hill, 1969.
- 9.10 Lipp, A., "Boron Carbide: Production, Properties, Application," Reprint from Technische Rundschau, Nos. 14, 28, 33 (1995) and 7 (1966).
- 9.11 Stoto, T. et al., "Swelling and Microcracking of Boron Carbide Subjected to Fast Neutron Irradiations," Journal of Applied Physics, Vol. 68, No.7, October 1, 1990, pp. 3198-3206.
- 9.12 Transnuclear Inc., TN-68 Dry Storage Cask, Final Safety Analysis Report, Revision 0, Hawthorne, NY, 2000 (Docket No. 72-1027).
- 9.13 Transnuclear Inc., NUHOMS[®] - MP197 Transportation Packaging, Safety Analysis Report (Docket No. 71-9302).
- 9.14 SNT-TC-1A, "American Society for Nondestructive Testing, Personnel Qualification and Certification in Nondestructive Testing," 1992.

M.10 Radiation Protection

Section 7.4.1 discusses the anticipated cumulative dose exposure to site personnel during the fuel handling and transfer activities associated with utilizing one NUHOMS[®] HSM for storage of one DSC. Chapter 5 describes in detail the NUHOMS[®] operational procedures, several of which involve potential exposure to personnel.

M.10.1 Occupational Exposure

The expected occupational dose for placing a canister of spent fuel into dry storage is based on the operational steps outlined in Table 7.4-1. The total exposure for the occupational dose due to placing a single NUHOMS[®]-32PT DSC into storage is conservatively estimated to be 1.8 person-rem (32PT-S125/32PT-L125 DSC configuration) and 3.8 person-rem (32PT-S100/32PT-L100 DSC configuration). This is a very conservative estimate because the dose rates on and around the 32PT DSC used in these calculations are based on very conservative assumptions for the design-basis source terms (32PT-S100/32PT-L100 DSC with Heat Loading Zoning Configuration 2 from Chapter M.2). As in Section M.5, no credit is taken for the thicker door described in Section 8.1.1.6 or for any steel liners around the vent openings for the occupational exposure analysis. The calculated exposures for both configurations are due mainly to the expected gamma dose rate during preparation for welding. The increased calculated exposure for the 32PT-S100/32PT-L100 configuration is due to the thinner shield plug and due to draining the NUHOMS[®]-32PT DSC to meet a 32PT-S100/32PT-L100 DSC weight limit as described in Section M.8.

The NUHOMS[®]-32PT System loading operations, the number of workers required for each operation, and the amount of time required for each operation are presented in Table M.10-1 and Table M.10-2 for the 32PT-S125/32PT-L125 DSC and 32PT-S100/32PT-L100 DSC configurations respectively. This information is used as the basis for estimating the total occupational exposure associated with one fuel load. This evaluation is performed for the storage of one design-basis NUHOMS[®]-32PT DSC in an HSM. The dose rates applicable for each operation are based on the results presented in Section M.5.4 for loading operations. Engineering judgment and operational experience are used to estimate dose rates that were not explicitly evaluated. This evaluation assumes that a transfer trailer/skid with an integral ram is used for the DSC transfer operations. Licensees may elect to use different equipment and/or different procedures. Unique steps are sometimes necessary at the individual site to load the canister, complete closure operations and place the canister in the HSM. Specifically, the licensee may choose to modify the sequence of operations in order to achieve reduced dose rates for a larger number of steps, with the end result of reduced total exposure. The only requirement is that the licensee practice ALARA with respect to the total exposure received for a loading campaign. These estimated durations, manloading and dose rates are not limits.

The amount of time required to complete some operations is sometimes far greater than the actual amount of time spent in a radiation field. The process of vacuum drying the DSC includes setting up the vacuum drying system (VDS), verifying that the VDS is operating correctly, evacuating the DSC cavity, monitoring the DSC pressure, and disconnecting the VDS from the DSC. Of these tasks, only setup and removal of the VDS require a worker to spend time near the DSC. The most time consuming task, evacuating the DSC, does not require anyone to be present at all. The total exposure calculated for each task is therefore not necessarily equal to the

number of workers multiplied by the time required multiplied by a dose rate. The exposure estimation for each task accounts for cases such as vacuum drying correctly, and assumes that good ALARA practices are followed.

The results of the evaluations are presented in Table M.10-1 and Table M.10-2 for the 32PT-S125/32PT-L125 DSC and 32PT-S100/32PT-L100 DSC configurations, respectively.

M.10.2 Off-Site Dose Calculations

Calculated dose rates in the immediate vicinity of the NUHOMS[®]-32PT system are presented in Section M.5 which provides a detailed description of source term configuration, analysis models and bounding dose rates. Dose rates at longer distances (off-site dose rates and doses) are presented in this section. This evaluation determines the neutron and gamma-ray off-site dose rates including skyshine in the vicinity of the two generic ISFSI layouts containing design-basis fuel in the NUHOMS[®]-32PT DSCs. The first generic ISFSI evaluated is a 2x10 back-to-back array of HSMs loaded with design-basis fuel, including BPRAs, in NUHOMS[®]-32PT DSCs (32PT-S100/32PT-L100 DSC with Configuration 2 from Chapter M.2). The second generic layout evaluated is two 1x10 front-to-front arrays of HSMs loaded with design-basis fuel, including BPRAs, in NUHOMS[®]-32PT DSCs (32PT-S100/32PT-L100 DSC with Configuration 2 from Chapter M.2). This calculation provides results for distances ranging from 6.1 to 600 meters from each face of the two arrays of HSMs. As in Section M.5, no credit is taken for the thicker door described in Section 8.1.1.6 or for any steel liners around the vent openings for the site dose analysis.

The total annual exposure for each ISFSI layout as a function of distance from each face is given in Table M.10-3 and plotted in Figure M.10-1. The total annual exposure assumes 100% occupancy for 365 days.

The Monte Carlo computer code MCNP [3.1] calculated the dose rates at the specified locations around the arrays of HSMs. The results of this calculation provide an example of how to demonstrate compliance with the relevant radiological requirements of 10CFR20 [3.2], 10CFR72 [3.3], and 40CFR190 [3.4] for a specific site. Each site must perform specific site calculations to account for the actual layout of the HSMs and fuel source.

The assumptions used to generate the geometry of the two ISFSIs for the MCNP analysis are summarized below.

- The 20 HSMs in the 2x10 back-to-back array are modeled as a box enveloping the 2x10 array of HSMs including the six inch gaps between modules and the 2-foot shield walls on the two sides of the array. MCNP starts the source particles on the surfaces of the box.
- The 20 HSMs in the two 1x10 front-to-front arrays are modeled as two boxes which envelope each 1x10 array of HSMs including the six inch gaps between modules and the 2-foot shield walls on the two sides and back of each array. MCNP starts the source particles on the surfaces of one of the boxes.
- The ISFSI approach slab is modeled as concrete. Because the ground composition has, at best, only a secondary impact on the dose rates at the detectors, any differences between this assumed layout and the actual layout would not have a significant affect on the site dose rates.
- For the 2x10 array, the interiors of the HSMs and shield walls are modeled as air. Most particles that enter the interiors of the HSMs and shield walls will therefore pass through unhindered.

- For the two 1x10 arrays, the interiors of the HSMs and shield walls modeled the 1x10 array in which the source is as air. Most particles that enter the interiors of these HSMs and shield walls will therefore pass through unhindered. Model the other 1x10 array as concrete to simulate the shielding provided by the second array of HSMs for the direct radiation from the front of the opposing 1x10 array.
- The “universe” is a sphere surrounding the ISFSI. To account for skyshine radius of this sphere ($r=500,000$ cm) is more than 10 mean free paths for neutrons and 50 mean free paths for gammas greater than that of the outermost surface, thus ensuring that the model is of a sufficient size to include all interactions, including skyshine, affecting the dose rate at the detectors.

The assumption used to generate the HSM surface sources for the MCNP analysis is summarized below.

- The HSM surface sources are bootstrapped (input to provide an equivalent boundary condition) using the HSM surface average dose rates calculated in Section M.5.4.

The assumptions used for the MCNP analysis are summarized below.

MCNP starts the source particles on the ISFSI array surface with initial directions following a cosine distribution. Radiation fluxes outside thick shields such as the HSM walls and roof tend to have forward peaked angular distributions; therefore, a cosine function is a reasonable approximation for the starting direction distribution. Vents through shielding regions such as the HSM vents tend to collimate particles such that a semi-isotropic assumption would not be appropriate.

Point detectors determine the dose rates on the four sides of the ISFSI as a function of distance from the ISFSI. All detectors represent the dose rate at three feet above ground level.

Source information required by MCNP includes gamma-ray and neutron spectra for the HSM array surfaces, total gamma-ray and neutron activities for each HSM array face and total gamma-ray and neutron activities for the entire ISFSI. The neutron and gamma-ray spectra are determined using a 1-D ANISN [3.6] run through the HSM roof using the design-basis in-core neutron and gamma fuel sources. Use of the roof is conservative because it represents the thickest cross section of the HSM shield. The thicker shield increases the dose rate importance of the higher energy neutrons and gamma-rays from the fuel because the thicker shield filters out the lower energy particles. Therefore, use of the thickest part of the shield results in a harder spectrum for all of the other surfaces. The HSM spectra as determined from ANISN are normalized to a one mrem/hour source using the flux-to-dose-factors from Reference [3.5]. These normalized spectra are then input in the MCNP ERG source variable.

The probability of a particle being born on a given surface is proportional to the total activity of that surface. The activity of each surface is determined by multiplying the sum of the normalized group fluxes, calculated above, by the average surface dose rate, by the area of the surface and by a flux-to-current conversion factor. This calculation is performed for the roof, sides, back and front of the HSM. The sum of the surface activities is then input as the tally

multiplier for each of the MCNP tallies to convert the tally results to fluxes (particles per second per square centimeter).

Gamma-ray spectrum calculations for the HSM are shown in Table M.10-4. The group fluxes on the HSM roof are taken from the ANISN run. The dose rate contribution from each group is the product of the flux and the flux-to-dose factor. The "Input Flux" column in Table M.10-4 is simply the roof flux in each group, divided by the total dose rate and represents the roof flux normalized to one mrem per hour. Similar calculations for neutrons are shown in Table M.10-5.

M.10.2.1 Activity Calculations

2x10 Back-to-Back Array

A box that envelops the HSM array and shield walls, as modeled in MCNP, approximates the 2x10 back-to-back array of HSMs. The dimensions of the box also include the width of the HSM end shield walls. As discussed above, the total activity of each face of the box is calculated by multiplying the flux per mrem/hr by the average dose rate of the face and by the area of the face.

Two 1x10 Front-to-Front Arrays

A box that envelops the HSM array and shield walls, as modeled in MCNP, approximates the two 1x10 arrays of HSMs. The dimensions of the box also include the width of the HSM end and back shield walls. As discussed above, the total activity of each face of the box is calculated by multiplying the flux per mrem/hr by the average dose rate of the face and by the area of the face.

The HSM surface activities are summarized in Table M.10-6.

M.10.2.2 Dose Rates

Dose rates are calculated for distances of 6.1 meters (20 feet) to 600 meters from the edges of the two ISFSI designs. The HSM is modeled in MCNP as a box, representing the HSM arrays.

Neutron and gamma-ray sources are placed on each HSM, with shield walls, surface using the spectra and activities determined above. The angular distribution of source particles is modeled as a cosine distribution. The contribution of capture gamma-rays has been neglected, as has the contribution of bremsstrahlung electrons. The inclusion of coherent scattering greatly increases the variance in a problem with point detector tallies without improving the accuracy of the calculation. Thus, coherent scattering of photons is ignored.

The MCNP models of the two ISFSI layouts are described herein. For the 2x10 back-to-back array of HSMs with end shield walls the "box", dimensions are as follows. The total width is 1158 cm. The length of the "box" is 3220 cm and the height of the "box" is 457 cm.

For the two 1x10 front-to-front arrays of HSMs with end and back shield walls the "box", dimensions for each array are as follows. The total width is 640 cm. The length of the "box" is

3220 cm and the height of the "box" is 457 cm. The two 1x10 arrays are 1066 cm (35 feet) apart.

Point detectors are placed at the following locations as measured from each face of the "box": 6.095 m (20 feet), 10 m, 20 m, 30 m, 40 m, 50 m, 60 m, 70 m, 80 m, 90 m, 100 m, 200 m, 300 m, 400 m, 500 m, and 600 m. Each point detector is placed 91.4 cm (3 feet) above the ground.

The MCNP results for each detector from the front of 2x10 back-to-back array are summarized in Table M.10-7. The MCNP results as a function of distance from the back of the two 1x10 front-to-front arrays are summarized in Table M.10-8. The MCNP results as a function of distance from the side of the 2x10 back-to-back array and the two 1x10 front-to-front arrays are summarized in Table M.10-9. The results from Table M.10-7, Table M.10-8 and Table M.10-9 are plotted in Figure M.10-1.

M.10.3 References

- 3.1 "MCNP 4 - Monte Carlo Neutron and Photon Transport Code System," CCC-200A/B, Oak Ridge National Laboratory, RSIC Computer Code Collection, File Number QA040.215.0002, October 1991.
- 3.2 Title 10, "Energy," Code of Federal Regulations, Part 20, "Standards for Protection Against Radiation."
- 3.3 Title 10, "Energy," Code of Federal Regulations, Part 72, "Licensing Requirements for the Independent Storage of Spent Nuclear Fuel and High-Level Radioactive Waste."
- 3.4 Title 40, "Protection of Environment," Part 190, "Environmental Radiation Protection Standards for Nuclear Power Operations."
- 3.5 "American National Standard Neutron and Gamma-Ray Fluence-to-Dose Factors," ANSI/ANS-6.1.1-1977, American Nuclear Society, La Grange Park, Illinois, March 1977.
- 3.6 "ANISN-ORNL - One-Dimensional Discrete Ordinates Transport Code System with Anisotropic Scattering," CCC-254, Oak Ridge National Laboratory, RSIC Computer Code Collection, April 1991.

**Table M.10-1
Occupational Exposure Summary
(32PT-S125/32PT-L125 DSC configuration)**

Task	Number of Workers	Completion Time (hours)	Dose Rate (mrem/hr)	Exposure (mrem)
Location: Auxiliary Building and Fuel Pool				
Ready the DSC and Transfer Cask for Service ⁽¹⁾	2	4	0	-
Place the DSC into the Transfer Cask ⁽¹⁾	3	1	2	6
Fill the Cask/DSC Annulus with Clean Water and Install the Inflatable Seal	2	2	2	8
Fill the DSC Cavity with Water ⁽²⁾	1	6	2	1
Install Shield Plug and Connect VDS	2	0.5	2	2
Place the Cask Containing the DSC in the Fuel Pool	5	0.5	2	5
Verify and Load the Candidate Fuel Assemblies into the DSC	3	8	2	48
Place the Top Shield Plug on the DSC	2	1	2	4
Raise the Cask/DSC to the Fuel Pool Surface	5	0.5	2	5
Remove the Cask/DSC from the Fuel Pool and Place them in the Decon Area	2	0.5	20	20
Location: Cask Decon Area				
Decontaminate the Outer Surface of the Cask (on the hook) ⁽³⁾	3	1	varies	65
Cask Decontamination (in the decon area) ⁽³⁾	3	1	varies	110
Remove the Cask/DSC Annulus Seal and Set-up Welder ⁽³⁾	2	1.5	varies	88
Drain the DSC Cavity ⁽³⁾	2	0.5	varies	33
Weld the Inner Top Cover to the DSC Shell and Perform NDE ⁽³⁾	2	6	varies	71
Vacuum Dry and Backfill the DSC with Helium ⁽³⁾	2	16	varies	33
Helium Leak Test the Shield Plug Weld	2	1	2	4
Seal Weld the Prefabricated Plugs to the Vent and Siphon Port and Perform NDE	1	1	241	241
Drain Cask/DSC Annulus ⁽³⁾	1	0.25	varies	23
Install DSC Outer Top Cover Plate ⁽³⁾	2	1	varies	209
Weld the Outer Top Cover Plate to DSC Shell and Perform NDE ⁽³⁾	2	16	varies	112
Install the Cask Lid	2	1	15	30
Location: Reactor /Fuel Building Bay				
Ready the Cask Support Skid and Transport Trailer for Service ⁽¹⁾	2	2	0	-
Place the Cask Onto the Skid and Secure ⁽²⁾	3	0.5	225	225
Location: ISFSI Site				
Ready the HSM and Hydraulic Ram System for Service ⁽¹⁾	2	2	0	-
Transport the Cask to the ISFSI ⁽¹⁾	6	1	0	-
Position the Cask in Close Proximity with the HSM ⁽¹⁾	3	1	0	-
Remove the Cask Lid	3	1	25	75
Align and Dock the Cask with the HSM	2	0.25	225	113
Position and Align Ram with Cask ⁽³⁾	2	0.5	varies	28
Remove the RAM Access Cover Plate	2	0.25	121	61
Transfer the DSC from the Cask to the HSM ⁽¹⁾	3	0.5	0	-
Un-Dock the Cask from the HSM	2	0.083	752	125
Install the HSM Access Door	2	0.5	63	63
Total		80		1,808

Total estimated dose is 3.8 person-rem per canister load

Total estimated completion time is 80 hrs

- (1) Performed away from any significant radiation sources.
- (2) Personnel are not present throughout this activity.
- (3) Dose rates and locations vary during this task.

**Table M.10-2
Occupational Exposure Summary
(32PT-S100/32PT-L100 DSC configuration)**

Task	Number of Workers	Completion Time (hours)	Dose Rate (mrem/hr)	Exposure (mrem)
Location: Auxiliary Building and Fuel Pool				
Ready the DSC and Transfer Cask for Service ⁽¹⁾	2	4	0	-
Place the DSC into the Transfer Cask ⁽¹⁾	3	1	2	6
Fill the Cask/DSC Annulus with Clean Water and Install the Inflatable Seal	2	2	2	8
Fill the DSC Cavity with Water ⁽²⁾	1	6	2	1
Install Shield Plug and Connect VDS	2	0.5	2	2
Place the Cask Containing the DSC in the Fuel Pool	5	0.5	2	5
Verify and Load the Candidate Fuel Assemblies into the DSC	3	8	2	48
Place the Top Shield Plug on the DSC	2	1	2	4
Raise the Cask/DSC to the Fuel Pool Surface	5	0.5	2	5
Drain Water from DSC Cavity	1	1	100	100
Remove the Cask/DSC from the Fuel Pool and Place them in the Decon Area	2	0.5	20	20
Location: Cask Decon Area				
Decontaminate the Outer Surface of the Cask (on the hook) ⁽³⁾	3	1	varies	680
Fill Cask Neutron Shield and DSC Cavity	1	0.1	57	6
Cask Decontamination (in the decon area) ⁽³⁾	3	1	varies	112
Remove the Cask/DSC Annulus Seal and Set-up Welder ⁽³⁾	2	1.5	varies	191
Drain the DSC Cavity ⁽³⁾	2	0.5	varies	84
Weld the Inner Top Cover to the DSC Shell and Perform NDE ⁽³⁾	2	6	varies	139
Vacuum Dry and Backfill the DSC with Helium ⁽³⁾	2	16	varies	84
Helium Leak Test the Shield Plug Weld	2	1	2	4
Seal Weld the Prefabricated Plugs to the Vent and Siphon Port and Perform NDE	1	1	650	650
Drain Cask/DSC Annulus ⁽³⁾	1	0.25	varies	58
Install DSC Outer Top Cover Plate ⁽³⁾	2	1	varies	527
Weld the Outer Top Cover Plate to DSC Shell and Perform NDE ⁽³⁾	2	16	varies	214
Install the Cask Lid	2	1	25	50
Location: Reactor /Fuel Building Bay				
Ready the Cask Support Skid and Transport Trailer for Service ⁽¹⁾	2	2	0	-
Place the Cask Onto the Skid and Secure ⁽²⁾	3	0.5	226	226
Location: ISFSI Site				
Ready the HSM and Hydraulic Ram System for Service ⁽¹⁾	2	2	0	-
Transport the Cask to the ISFSI ⁽¹⁾	6	1	0	-
Position the Cask in Close Proximity with the HSM ⁽¹⁾	3	1	0	-
Remove the Cask Lid	3	1	27	81
Align and Dock the Cask with the HSM	2	0.25	226	113
Position and Align Ram with Cask ⁽³⁾	2	0.5	varies	50
Remove the RAM Access Cover Plate	2	0.25	274	137
Transfer the DSC from the Cask to the HSM ⁽¹⁾	3	0.5	0	-
Un-Dock the Cask from the HSM	2	0.083	788	131
Install the HSM Access Door	2	0.5	96	96
Total		81		3,831

Total estimated dose is 1.8 person-rem per canister load

Total estimated completion time is 80 hrs

(1) Performed away from any significant radiation sources.

(2) Personnel are not present throughout this activity.

(3) Dose rates and locations vary during this task.

**Table M.10-3
Total Annual Exposure**

Two 1x10 Front To Front Array

Distance (meters)	Back Total Dose (mrem)	1 σ Error (mrem.hr)	MCNP Relative Error
6.1	7680	46	0.006
10	6435	71	0.011
20	4250	61	0.014
30	2909	30	0.010
40	2182	26	0.012
50	1673	33	0.020
60	1345	21	0.016
70	1034	11	0.011
80	846	10	0.012
90	703	8	0.011
100	616	11	0.019
200	134	3	0.023
300	42	2	0.040
400	14	0.8	0.056
500	5	0.3	0.063
600	2	0.1	0.067

Distance (meters)	Side Total Dose (mrem)	1 σ Error (mrem.hr)	MCNP Relative Error
6.1	65241	179	0.003
10	32798	129	0.004
20	10346	64	0.006
30	5145	44	0.009
40	3185	42	0.013
50	2172	32	0.015
60	1569	29	0.019
70	1234	44	0.036
80	947	19	0.020
90	759	16	0.021
100	623	12	0.019
200	132	6	0.044
300	35	2	0.046
400	14	2	0.143
500	4	0.5	0.106
600	2	0.1	0.051

2x10 Back To Back Array

Distance (meters)	Front Total Dose (mrem)	1 σ Error (mrem.hr)	MCNP Relative Error
6.1	199520	374	0.002
10	116793	259	0.002
20	43196	120	0.003
30	21328	82	0.004
40	12338	60	0.005
50	7805	35	0.004
60	5441	35	0.006
70	3902	44	0.011
80	2985	65	0.022
90	2231	19	0.009
100	1756	18	0.010
200	287	4	0.015
300	82	3	0.033
400	27	1	0.038
500	10	0	0.051
600	3.7	0.1	0.029

Distance (meters)	Side Total Dose (mrem)	1 σ Error (mrem.hr)	MCNP Relative Error
6.1	9802	79	0.008
10	6848	51	0.007
20	4101	83	0.020
30	2622	24	0.009
40	1979	62	0.031
50	1520	46	0.030
60	1160	15	0.013
70	963	33	0.034
80	767	12	0.016
90	639	12	0.019
100	528	10	0.018
200	117	5	0.041
300	36	2	0.056
400	11	0	0.045
500	5	1	0.127
600	1.8	0.4	0.192

**Table M.10-4
HSM Gamma-Ray Spectrum Calculation Results**

Group Number	E _{upper} (MeV)	E _{mean} (MeV)	Flux-Dose ANSI/ANS-6.1.1-1977 (mR/hr)/(γ/cm ² -sec)	Roof Flux (γ/cm ² -sec)	Dose Rate (mR/hr)	Input Flux (γ/cm ² -sec per mrem/hr)
23	10	9	8.77E-03	5.35E-01	4.69E-03	5.74E-03
24	8	7.25	7.48E-03	4.49E+00	3.36E-02	4.82E-02
25	6.5	5.75	6.37E-03	5.60E+00	3.57E-02	6.01E-02
26	5	4.5	5.41E-03	7.30E+00	3.95E-02	7.82E-02
27	4	3.5	4.62E-03	1.97E+01	9.09E-02	2.11E-01
28	3	2.75	3.96E-03	3.67E+01	1.46E-01	3.94E-01
29	2.5	2.25	3.47E-03	4.13E+02	1.43E+00	4.43E+00
30	2	1.83	3.02E-03	3.49E+02	1.06E+00	3.75E+00
31	1.66	1.495	2.63E-03	1.41E+03	3.72E+00	1.52E+01
32	1.33	1.165	2.21E-03	2.98E+03	6.57E+00	3.19E+01
33	1	0.9	1.83E-03	2.74E+03	5.02E+00	2.94E+01
34	0.8	0.7	1.52E-03	4.19E+03	6.38E+00	4.49E+01
35	0.6	0.5	1.17E-03	6.61E+03	7.75E+00	7.09E+01
36	0.4	0.35	8.76E-04	4.53E+03	3.97E+00	4.86E+01
37	0.3	0.25	6.31E-04	6.18E+03	3.90E+00	6.63E+01
38	0.2	0.15	3.83E-04	1.41E+04	5.42E+00	1.52E+02
39	0.1	0.08	2.67E-04	3.97E+03	1.06E+00	4.26E+01
40	0.05	0.03	9.35E-04	1.14E+01	1.07E-02	1.23E-01
			Totals	4.76E+04	4.66E+01	5.10E+02

**Table M.10-5
HSM Neutron Spectrum Calculations**

Group Number	E _{upper} (MeV)	E _{mean} (MeV)	Flux-Dose ANSI/ANS-6.1.1-1977 (mR/hr)/(n/cm ² -sec)	Roof Flux (n/cm ² -sec)	Dose Rate (mR/hr)	Input Flux (n/cm ² -sec per mrem/hr)
1	1.49E+01	1.36E+01	1.94E-01	7.41E-05	1.44E-05	1.57E-04
2	1.22E+01	1.11E+01	1.60E-01	5.41E-04	8.65E-05	1.15E-03
3	1.00E+01	9.09E+00	1.47E-01	1.86E-03	2.74E-04	3.94E-03
4	8.18E+00	7.27E+00	1.48E-01	1.47E-02	2.17E-03	3.11E-02
5	6.36E+00	5.66E+00	1.53E-01	4.15E-02	6.37E-03	8.79E-02
6	4.96E+00	4.51E+00	1.51E-01	3.88E-02	5.84E-03	8.21E-02
7	4.06E+00	3.54E+00	1.39E-01	4.56E-02	6.33E-03	9.64E-02
8	3.01E+00	2.74E+00	1.28E-01	1.11E-01	1.43E-02	2.35E-01
9	2.46E+00	2.41E+00	1.25E-01	1.04E-01	1.30E-02	2.20E-01
10	2.35E+00	2.09E+00	1.26E-01	1.66E-01	2.10E-02	3.52E-01
11	1.83E+00	1.47E+00	1.29E-01	2.58E-01	3.33E-02	5.47E-01
12	1.11E+00	8.30E-01	1.17E-01	2.71E-01	3.17E-02	5.73E-01
13	5.50E-01	3.31E-01	6.52E-02	3.90E-01	2.54E-02	8.26E-01
14	1.11E-01	5.72E-02	9.19E-03	6.55E-01	6.02E-03	1.39E+00
15	3.35E-03	1.97E-03	3.71E-03	3.15E-01	1.17E-03	6.66E-01
16	5.83E-04	3.42E-04	4.01E-03	3.79E-01	1.52E-03	8.01E-01
17	1.01E-04	6.50E-05	4.29E-03	3.17E-01	1.36E-03	6.72E-01
18	2.90E-05	1.96E-05	4.48E-03	2.30E-01	1.03E-03	4.86E-01
19	1.01E-05	6.58E-06	4.57E-03	3.12E-01	1.42E-03	6.59E-01
20	3.06E-06	2.09E-06	4.54E-03	2.80E-01	1.27E-03	5.92E-01
21	1.12E-06	7.67E-07	4.37E-03	2.98E-01	1.30E-03	6.31E-01
22	4.14E-07	2.12E-07	3.71E-03	1.65E+01	6.14E-02	3.50E+01
			Totals	2.08E+01	2.36E-01	4.395E+01

**Table M.10-6
Summary of ISFSI Surface Activities**

2x10 Back-To-Back Array

Source	Area (cm ²)	Neutron Activity (neutrons/sec)	Gamma-Ray Activity (γ/sec)
Roof	3,730,366.7	1.233x10 ⁸	1.038x10 ¹¹
Front 1	1,472,513.2	5.915x10 ⁸	6.493x10 ¹⁰
Front 2	1,472,513.2	5.915x10 ⁸	6.493x10 ¹⁰
Side 1	529,547.3	1.092x10 ⁶	4.649x10 ⁸
Side 2	529,547.3	1.092x10 ⁶	4.649x10 ⁸
Total		1.308x10 ⁹	2.346x10 ¹¹

Two 1x10 Font-To-Front Array

Source	Area (cm ²)	Neutron Activity (neutrons/sec)	Gamma-Ray Activity (γ/sec)
Roof	2,061,518.5	6.813x10 ⁷	5.734x10 ¹⁰
Front	1,472,513.2	5.915x10 ⁸	6.493x10 ¹⁰
Back	1,472,513.2	1.081x10 ⁶	3.615x10 ⁸
Side 1	292,644.6	6.032x10 ⁵	2.569x10 ⁸
Side 2	292,644.6	6.032x10 ⁵	2.569x10 ⁸
Total		6.619x10 ⁸	1.232x10 ¹¹

**Table M.10-7
MCNP Front Detector Dose Rates for 2x10 Array**

Distance (meters)	Gamma Dose Rate (mrem/hr)	Gamma MCNP 1 σ error	Neutron Dose Rate (mrem/hr)	Neutron MCNP 1 σ error	Total Dose Rate (mrem/hr)	Combined MCNP 1 σ error
6.10E+00	2.01E+01	0.0019	2.72E+00	0.0071	2.28E+01	0.0019
1.00E+01	1.18E+01	0.0022	1.56E+00	0.0092	1.33E+01	0.0022
2.00E+01	4.36E+00	0.0026	5.67E-01	0.0134	4.93E+00	0.0028
3.00E+01	2.16E+00	0.0033	2.76E-01	0.0217	2.43E+00	0.0038
4.00E+01	1.25E+00	0.0051	1.56E-01	0.0166	1.41E+00	0.0049
5.00E+01	7.97E-01	0.0047	9.41E-02	0.0149	8.91E-01	0.0045
6.00E+01	5.53E-01	0.0055	6.85E-02	0.0382	6.21E-01	0.0065
7.00E+01	4.00E-01	0.0122	4.55E-02	0.0238	4.45E-01	0.0112
8.00E+01	2.98E-01	0.0096	4.30E-02	0.1590	3.41E-01	0.0218
9.00E+01	2.29E-01	0.0090	2.59E-02	0.0271	2.55E-01	0.0085
1.00E+02	1.80E-01	0.0106	2.00E-02	0.0322	2.00E-01	0.0101
2.00E+02	2.99E-02	0.0161	2.90E-03	0.0240	3.28E-02	0.0148
3.00E+02	8.40E-03	0.0354	9.88E-04	0.0765	9.38E-03	0.0327
4.00E+02	2.66E-03	0.0406	3.85E-04	0.1035	3.04E-03	0.0378
5.00E+02	9.51E-04	0.0546	1.54E-04	0.1436	1.11E-03	0.0511
6.00E+02	3.59E-04	0.0326	5.90E-05	0.0639	4.18E-04	0.0294

Table M.10-8
MCNP Back Detector Dose Rates for the Two 1x10 Arrays

Distance (meters)	Gamma Dose Rate (mrem/hr)	Gamma MCNP 1 σ error	Neutron Dose Rate (mrem/hr)	Neutron MCNP 1 σ error	Total Dose Rate (mrem/hr)	Combined MCNP 1 σ error
6.10E+00	6.75E-01	0.0048	2.01E-01	0.0203	8.77E-01	0.0059
1.00E+01	5.69E-01	0.0113	1.66E-01	0.0302	7.35E-01	0.0111
2.00E+01	3.80E-01	0.0142	1.05E-01	0.0419	4.85E-01	0.0144
3.00E+01	2.68E-01	0.0098	6.42E-02	0.0341	3.32E-01	0.0103
4.00E+01	2.04E-01	0.0114	4.47E-02	0.0410	2.49E-01	0.0119
5.00E+01	1.60E-01	0.0213	3.09E-02	0.0488	1.91E-01	0.0195
6.00E+01	1.30E-01	0.0151	2.33E-02	0.0589	1.53E-01	0.0156
7.00E+01	1.02E-01	0.0113	1.61E-02	0.0312	1.18E-01	0.0107
8.00E+01	8.34E-02	0.0116	1.31E-02	0.0428	9.65E-02	0.0116
9.00E+01	7.02E-02	0.0122	1.00E-02	0.0324	8.03E-02	0.0115
1.00E+02	6.06E-02	0.0175	9.76E-03	0.0776	7.03E-02	0.0185
2.00E+02	1.37E-02	0.0250	1.60E-03	0.0375	1.53E-02	0.0227
3.00E+02	4.09E-03	0.0403	6.70E-04	0.1367	4.76E-03	0.0396
4.00E+02	1.32E-03	0.0387	3.10E-04	0.2436	1.63E-03	0.0559
5.00E+02	4.96E-04	0.0737	9.42E-05	0.0526	5.90E-04	0.0625
6.00E+02	2.03E-04	0.0663	5.02E-05	0.2098	2.53E-04	0.0675

**Table M.10-9
MCNP Side Detector Dose Rates**

2x10 Back-to-Back Array

Distance (meters)	Gamma Dose Rate (mrem/hr)	Gamma MCNP 1 σ error	Neutron Dose Rate (mrem/hr)	Neutron MCNP 1 σ error	Total Dose Rate (mrem/hr)	Combined MCNP 1 σ error
6.10E+00	8.97E-01	0.0047	2.22E-01	0.0357	1.12E+00	0.0080
1.00E+01	6.25E-01	0.0053	1.57E-01	0.0303	7.82E-01	0.0074
2.00E+01	3.68E-01	0.0152	1.00E-01	0.0763	4.68E-01	0.0202
3.00E+01	2.44E-01	0.0089	5.49E-02	0.0320	2.99E-01	0.0093
4.00E+01	1.89E-01	0.0368	3.66E-02	0.0322	2.26E-01	0.0313
5.00E+01	1.38E-01	0.0108	3.54E-02	0.1406	1.74E-01	0.0299
6.00E+01	1.12E-01	0.0130	2.01E-02	0.0409	1.32E-01	0.0127
7.00E+01	9.14E-02	0.0188	1.85E-02	0.1785	1.10E-01	0.0339
8.00E+01	7.49E-02	0.0136	1.26E-02	0.0750	8.75E-02	0.0159
9.00E+01	6.20E-02	0.0166	1.10E-02	0.0809	7.30E-02	0.0186
1.00E+02	5.14E-02	0.0156	8.90E-03	0.0854	6.03E-02	0.0183
2.00E+02	1.18E-02	0.0455	1.49E-03	0.0752	1.33E-02	0.0413
3.00E+02	3.55E-03	0.0635	5.46E-04	0.0691	4.09E-03	0.0558
4.00E+02	9.93E-04	0.0312	2.52E-04	0.1845	1.25E-03	0.0449
5.00E+02	4.70E-04	0.1499	9.21E-05	0.1116	5.62E-04	0.1267
6.00E+02	1.37E-04	0.0522	7.31E-05	0.5412	2.10E-04	0.1916

Two 1x10 Front-To-Front Arrays

Distance (meters)	Gamma Dose Rate (mrem/hr)	Gamma MCNP 1 σ error	Neutron Dose Rate (mrem/hr)	Neutron MCNP 1 σ error	Total Dose Rate (mrem/hr)	Combined MCNP 1 σ error
6.10E+00	6.52E+00	0.0026	9.26E-01	0.0123	7.45E+00	0.0027
1.00E+01	3.27E+00	0.0041	4.72E-01	0.0126	3.74E+00	0.0039
2.00E+01	1.02E+00	0.0057	1.59E-01	0.0272	1.18E+00	0.0061
3.00E+01	5.03E-01	0.0081	8.44E-02	0.0358	5.87E-01	0.0086
4.00E+01	3.12E-01	0.0123	5.16E-02	0.0553	3.64E-01	0.0132
5.00E+01	2.10E-01	0.0112	3.78E-02	0.0740	2.48E-01	0.0147
6.00E+01	1.56E-01	0.0205	2.36E-02	0.0439	1.79E-01	0.0187
7.00E+01	1.21E-01	0.0365	2.02E-02	0.1223	1.41E-01	0.0358
8.00E+01	9.28E-02	0.0177	1.53E-02	0.0934	1.08E-01	0.0202
9.00E+01	7.53E-02	0.0210	1.14E-02	0.0866	8.66E-02	0.0215
1.00E+02	6.26E-02	0.0192	8.43E-03	0.0755	7.11E-02	0.0191
2.00E+02	1.36E-02	0.0477	1.46E-03	0.0817	1.51E-02	0.0438
3.00E+02	3.53E-03	0.0503	4.63E-04	0.1043	3.99E-03	0.0461
4.00E+02	1.10E-03	0.0358	4.86E-04	0.4612	1.59E-03	0.1434
5.00E+02	4.14E-04	0.1238	7.30E-05	0.0603	4.87E-04	0.1056
6.00E+02	1.43E-04	0.0393	4.37E-05	0.1767	1.87E-04	0.0511

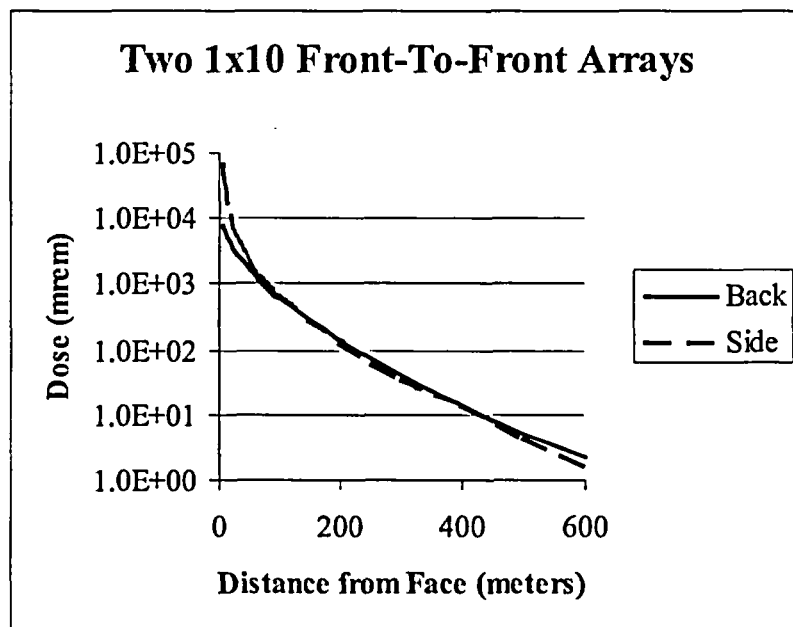
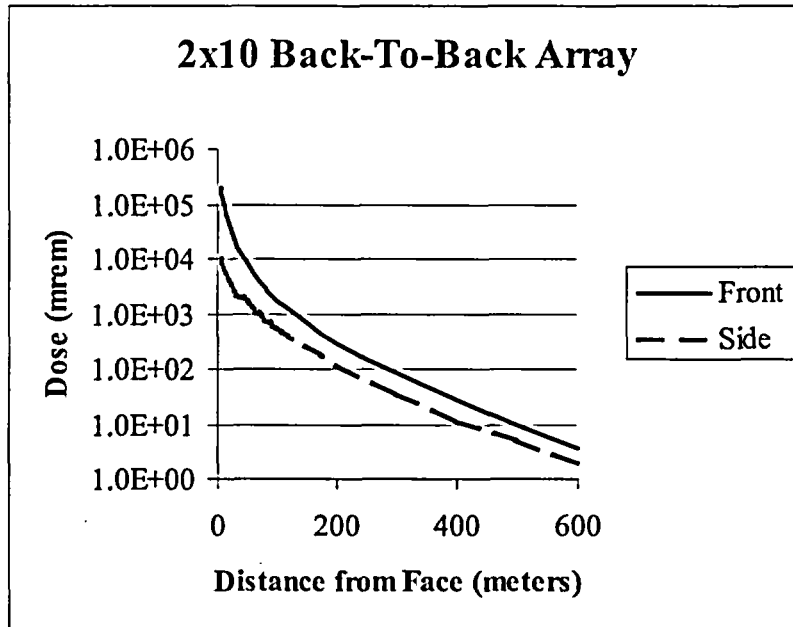


Figure M.10-1
Annual Exposure from the ISFSI as a Function of Distance

M.11 Accident Analyses

This section describes the postulated off-normal and accident events that could occur during transfer and storage of the NUHOMS[®]-32PT DSC. Sections which do not affect the evaluation presented in Chapter 8 are identified as “No change.” Detailed analysis of the events are provided in other sections and referenced herein.

M.11.1 Off-Normal Operations

Off-normal operations are design events of the second type (Design Event II) as defined in ANSI/ANS 57.9 [11.1]. Off-normal conditions consist of that set of events that, although not occurring regularly, can be expected to occur with moderate frequency or on the order of once during a calendar year of ISFSI operation.

The off-normal conditions considered for the NUHOMS[®]-32PT DSC are off-normal transfer loads, extreme temperatures and a postulated release of radionuclides.

M.11.1.1 Off-Normal Transfer Loads

No change. The limiting off-normal event is the jammed DSC during loading or unloading from the HSM. This event is described in Section 8.1.2. Other off-normal events are bounded by the jammed DSC.

M.11.1.1.1 Postulated Cause of Event

See Section 8.1.2. The probability of a jammed DSC does not increase with the NUHOMS[®]-32PT DSC, since the outside diameter of the DSC is the same as the NUHOMS[®]-24P.

M.11.1.1.2 Detection of Event

No change. See Section 8.1.2.

M.11.1.1.3 Analysis of Effects and Consequences

A detailed evaluation of this event is presented in Section M.3.6.2 and is summarized below. The NUHOMS[®]-32PT DSC has a 0.5 inch shell wall thickness, while the NUHOMS[®]-24P and -52B have 0.62 inch thick shells. Therefore, the stresses in the canister shell are increased. The DSC shell stress due to the 2,690 in-kip moment due to axial sticking of the DSC is $S_{mx} = 1.55$ ksi. This magnitude of stress is negligible when compared to the allowable membrane stress of 17.5 ksi.

The DSC shell stress due to the 1,400 pound axial load during the binding of the DSC is 15.7 ksi. As stated in Section M.3.6.2.1, this stress is considered secondary and is enveloped by other handling stresses.

The evaluation of the basket due to normal and off-normal handling and transfer loads is presented in Section M.3.6.1.3.

M.11.1.1.4 Corrective Actions

No change. See Section 8.1.2.

M.11.1.2 Extreme Temperatures

No change. The off-normal maximum ambient temperature of 125°F is used in Section 8.1.2.2. For the NUHOMS®-32PT system, a maximum ambient temperature of 117°F is used. Therefore, the analyses in Section 8.1.2.2 bound the NUHOMS®-32PT system.

M.11.1.2.1 Postulated Cause of Event

No change. See Section 8.1.2.2.

M.11.1.2.2 Detection of Event

No change. See Section 8.1.2.2.

M.11.1.2.3 Analysis of Effects and Consequences

The thermal evaluation of the NUHOMS®-32PT system for off-normal conditions is presented in Section M.4.5. The 100°F normal condition with insolation bounds the 117°F case without insolation for the DSC in the TC. Therefore the normal condition maximum temperatures are bounding. The 117°F case with the DSC in the HSM is not bounded by the normal conditions.

The structural evaluation of the 32PT DSC for off-normal temperature conditions is presented in Section M.3.6.2.2. The structural evaluation of the basket due to off-normal thermal conditions is presented in Section M.3.4.4.

M.11.1.2.4 Corrective Actions

Restrictions for onsite handling of the TC with a loaded DSC under extreme temperature conditions are presented in Technical Specifications 1.2.13 and 1.2.14. There is no change to this requirement as a result of addition of the NUHOMS®-32PT DSC.

M.11.1.3 Off-Normal Releases of Radionuclides

The NUHOMS®-32PT DSC is designed and tested to the leak tight criteria of ANSI N14.5 [11.2]. Therefore the estimated quantity of radionuclides expected to be released annually to the environment due to normal or off-normal events is zero.

M.11.1.3.1 Postulated Cause of Event

In accordance with the Standard Review Plan, NUREG-1536 [11.3] and ISG-5 Rev. 1 [11.4] for off-normal conditions, it is conservatively assumed that 10% of the fuel rods fail.

M.11.1.3.2 Detection of Event

Failed fuel rods would go undetected, but are not a safety concern since the canister is designed and tested to leak tight criteria.

M.11.1.3.3 Analysis of Effects and Consequences

The bounding off-normal pressure for the NUHOMS[®]-32PT DSC is calculated with the DSC in either the HSM or in the TC in Section M.4.5.4 as 15.2 psig. The NUHOMS[®]-32PT DSC stresses due to these pressures are below the allowable stresses for off-normal conditions, as shown in M.3.6.

The NUHOMS[®]-32PT DSC is designed and tested to the leak tight criteria of ANSI N14.5. Therefore the estimated quantity of radionuclides expected to be released annually to the environment due to normal or off-normal events is zero.

M.11.1.3.4 Corrective Actions

None required.

M.11.1.4 Radiological Impact from Off-Normal Operations

The NUHOMS[®]-32PT DSC is designed and tested to the leak tight criteria of ANSI N14.5. The off-normal conditions have been evaluated in accordance with the ASME B&PV code [11.5]. The resulting stresses are below the allowable stresses. There will be no breach of the confinement boundary due to the off-normal conditions. Therefore, the estimated quantity of radionuclides expected to be released annually to the environment due to off-normal events is zero.

M.11.2 Postulated Accidents

M.11.2.1 Reduced HSM Air Inlet and Outlet Shielding

M.11.2.1.1 Cause of Accident

No change. See Section 8.2.1.1.

M.11.2.1.2 Accident Analysis

There are no structural consequences that affect the safe operation of the NUHOMS[®]-32PT system resulting from the separation of the HSMs. The thermal effects of this accident results from the blockage of HSM air inlet and outlet openings on the HSM side walls in contact with each other. This would block the ventilation air flow provided to the HSMs in contact from these inlet and outlet openings. The increase in spacing between the HSM on the opposite side from 6 inches to 12 inches, will reduce the ventilation air flow resistance through the air inlet and outlet openings on these side walls, which will partially compensate the ventilation reduction from the blocked side. However, the effect on the NUHOMS[®]-32PT DSC, HSM and fuel temperatures is bounded by the complete blockage of air inlet and outlet openings described in Section M.11.2.7. The radiological consequences of this accident are described in the paragraph below.

M.11.2.1.3 Accident Dose Calculations

The off-site radiological effects that result from a partial loss of adjacent HSM shielding is an increase in the air scattered (skyshine) and direct doses from the 12 inch gap between the separated HSMs. The air scattered (skyshine) and direct doses are reduced from the gap between the HSMs that are in contact with each other. On-site radiological effects result from an increase in the direct radiation during recovery operations and increased skyshine radiation. Table 8.2-2 shows the comparisons of the increased dose rate as a function of distance due to the reduced shielding effects of the adjacent HSM for the 24P DSC with 5-year cooled design basis fuel. Table M.11-1 provides a similar table for 32PT-S100/32PT-L100 DSC with Configuration 2, from Chapter M.2, of the NUHOMS[®]-32PT System. For the NUHOMS[®]-32PT System, the dose received by a person located 100 meters away from the NUHOMS[®] installation for eight hours a day for five days (estimated recovery time) would be 32 mrem. The increased dose to an off-site person for 24 hours a day for five days located 2000 feet away would be about 0.02 mrem. Thus, the 10CFR72 requirements for this postulated event are met.

M.11.2.1.4 Corrective Actions

No change. See Section 8.2.1.4.

M.11.2.2 Earthquake

M.11.2.2.1 Cause of Accident

No change. See Section 8.2.3.1.

M.11.2.2.2 Accident Analysis

Section 8.2.3.2 describes the analyses performed to demonstrate that the NUHOMS[®] System withstands the design basis seismic event. Section M.3.7.3 presents the changes to this analysis resulting from the addition of NUHOMS[®]-32PT DSC. As documented in Chapter 8 the HSM and the TC have been evaluated for a payload that bounds the 32PT DSC payload, and thus these two components are not affected by the 32PT DSC. Therefore, only those analyses documented in Chapter 8 that are affected by the increased weight of the 32PT DSC are addressed in Section M.3.7.3. The results of this analysis show that seismic stresses are well below allowables and, thus, the leak-tight integrity of the canister is not compromised.. The basket stresses are also low and do not result in deformations that would prevent fuel from being unloaded from the canister.

M.11.2.2.3 Accident Dose Calculations

The design earthquake does not damage the NUHOMS[®]-32PT system. Hence, no radioactivity is released and there is no associated dose increase due to this event.

M.11.2.2.4 Corrective Actions

After a seismic event, the NUHOMS[®] HSMs and TC would be inspected for damage. Any debris would be removed. An evaluation would be performed to determine if the cask were still within the licensed design basis.

M.11.2.3 Extreme Wind and Tornado Missiles

M.11.2.3.1 Cause of Accident

The determination of the tornado wind and tornado missile loads acting on the HSM are detailed in Section 8.2.2.

M.11.2.3.2 Accident Analysis

An evaluation of the HSM and TC with respect to tornado winds and tornado missiles is presented in Section 8.2.2. Changes to this analysis, as a result of the addition of the NUHOMS[®]-32PT DSC, are presented in Section M.3.7.2. The analysis presented in Section 8.2.2 is bounding.

M.11.2.3.3 Accident Dose Calculations

The NUHOMS[®]-32PT DSC is designed and tested as a leak-tight containment boundary. Tornado wind and tornado missiles do not breach the containment boundary. Therefore, there is no increase in site boundary dose due to this accident event.

M.11.2.3.4 Corrective Actions

After excessive high winds or a tornado, the HSM's and TC would be inspected for damage. Any debris would be removed. Any damage resulting from impact with a missile would be evaluated to determine if the system was still within the licensed design basis.

M.11.2.4 Flood

M.11.2.4.1 Cause of Accident

No change. See Section 8.2.4.1.

M.11.2.4.2 Accident Analysis

The HSM is evaluated for flooding in Section 8.2.4. This evaluation is bounding for the NUHOMS[®]-32PT DSC as described in Section M.3.7.4. The canister is designed and tested to be leak tight. The stresses in the canister due to the design basis flood are well below the allowable stresses for Service Level C of the ASME Code Subsection NB [11.5]. Therefore, the NUHOMS[®]-32PT DSC will withstand the design basis flood without breach of the confinement boundary.

M.11.2.4.3 Accident Dose Calculations

The radiation dose due to flooding of the HSM is negligible. The NUHOMS[®]-32PT DSC is designed and tested as a leak-tight containment boundary. Flooding does not breach the containment boundary. Therefore radioactive material inside the DSC will remain sealed in the DSC and, therefore, will not contaminate the encroaching flood water. See also Section 8.2.4.3.

M.11.2.4.4 Corrective Actions

No change. See Section 8.2.4.4.

M.11.2.5 Accidental TC Drop

M.11.2.5.1 Cause of Accident

See Section M.3.7.5.1.

M.11.2.5.2 Accident Analysis

The evaluation of the NUHOMS[®]-32PT DSC shell and basket assemblies due to an accidental drop is presented in Section M.3.7.5. As documented in Chapter 8 the TC have been evaluated for a payload that bounds the 32PT DSC payload, and therefore is not affected by the 32PT DSC. As shown in Section M.3.7.5, the DSC shell and basket stress intensities are within the appropriate ASME Code Service Level D allowable limits and maintain their structural integrity.

For the case of a liquid neutron shield, a complete loss of neutron shield was evaluated at the 100°F ambient condition with full solar load. It is conservatively assumed that the neutron shield jacket is still present but all the liquid is lost. The maximum DSC shell temperature is 520°F. The maximum cask inner shell, cask outer shell, and cask neutron shield jacket temperatures are bounded by analyses presented in Section 8.1.3.3 which are 393°F, 384°F and 238°F respectively. The DSC shell temperatures and hence fuel cladding temperature are bounded by the HSM plugged vent case shown in Table M.4-14. Accident thermal conditions, such as loss of the liquid neutron shield, need not be considered in the load combination evaluation. Rather the peak stresses resulting from the accident thermal conditions must be less than the allowable fatigue stress limit for 10 cycles from the appropriate fatigue design curves in Appendix I of the ASME Code. Similar analyses of other NUHOMS® TCs have shown that fatigue is not a concern. Therefore, these stresses in a TC with a liquid neutron shield need not be evaluated for the accident condition.

M.11.2.5.3 Accident Dose Calculations for Loss of Neutron Shield

The postulated accident condition for the on-site TC assumes that after a drop event, the water in the neutron shield is lost. The loss of neutron shield is modeled using the normal operation models described in Section M.5.4 by replacing the neutron shield with air.

The accident condition dose rates for Configuration 2, from Chapter M.2, are summarized in Table M.11-2 and Figure M.11-1 for the bounding 32PT-L100 DSC loaded with design basis fuel plus BPRAs.

A comparison of the results in Table M.11-2 and Table M.5-3, demonstrates a maximum cask surface contact dose rate increase from 9.50E+02 mrem/hr to 4.63E+03 mrem/hr. These dose rates are approximately 2.2 times those reported in Section 8.2.5.3.2. Therefore, one would expect that the additional dose rate to an average on-site worker at an average distance of fifteen feet would also increase from 310 mrem/hr to 700 mrem/hr. Similarly the exposure to off-site individuals at a distance of 2000 feet would also be expected to increase from 0.04 mrem for an assumed eight hour exposure to 0.09 mrem. This exposure is still well within the limits of 10CFR72 for an accident condition. This corresponds to the exposure to an individual at a distance of 100 meters of approximately 42 mrem for the assumed eight hour duration also well within the limits of 10CFR72 for an accident condition.

M.11.2.5.4 Corrective Action

No change. See Section 8.2.5.4.

M.11.2.6 Lightning

No change. The evaluation presented in Section 8.2.6 is not affected by the addition of the NUHOMS®-32PT DSC to the NUHOMS® System.

M.11.2.7 Blockage of Air Inlet and Outlet Openings

This accident conservatively postulates the complete blockage of the HSM ventilation air inlet and outlet openings on the HSM side walls.

M.11.2.7.1 Cause of Accident

No change. See Section 8.2.7.1.

M.11.2.7.2 Accident Analysis

This event is evaluated in Section 8.2.7.2 . The section below describes the additional analyses performed to demonstrate the acceptability of the system with the NUHOMS[®]-32PT DSC. The thermal evaluation of this event is presented in Section M.4.6. The temperatures determined in Section M.4.6 are used in the structural evaluation of this event, which is presented in Sections M.3.7.7 and M.3.4.4.3.

M.11.2.7.3 Accident Dose Calculations

There are no off-site dose consequences as a result of this accident. The only significant dose increase is that related to the recovery operation. This is bounded by the evaluation of the NUHOMS[®] System with the 24P canister. See Section 8.2.7.3 .

M.11.2.7.4 Corrective Action

No change. See Section 8.2.7.4.

M.11.2.8 DSC Leakage

The NUHOMS[®]-32PT DSC is designed as a pressure retaining containment boundary to prevent leakage of contaminated materials. The analyses of normal, off-normal, and accident conditions have shown that no credible conditions can breach the DSC shell or fail the double seal welds at each end of the DSC. The NUHOMS[®]-32PT DSC is designed and tested to be leak tight. Therefore DSC leakage is not considered a credible accident scenario. See Section M.7.3.

M.11.2.9 Accident Pressurization of DSC

M.11.2.9.1 Cause of Accident

The bounding internal pressurization of the NUHOMS[®]-32PT DSC is postulated to result from cladding failure of the spent fuel in combination with the transfer accident case with the loss of sunshield and liquid neutron shield in the transfer cask under extreme ambient temperature conditions of 117°F and maximum insolation, and the consequent release of spent fuel rod fill gas and free fission gas. The evaluation conservatively assumes that 100% of the fuel rods have failed.

M.11.2.9.2 Accident Analysis

The pressure due to this case is evaluated in Section M.4.6. The maximum pressure calculated is 102.9 psig. The accident pressure is conservatively assumed to be 105 psig in the structural load combinations presented in Table M.2-15.

M.11.2.9.3 Accident Dose Calculations

There is no increase in dose rates as a result of this event.

M.11.2.9.4 Corrective Actions

This is a hypothetical event. Therefore no corrective actions are required. The canister is designed to withstand the pressure as a Level D condition. There will be no structural damage to the canister or leakage of radioactive material as a result of this event.

M.11.2.10 Fire and Explosion

M.11.2.10.1 Cause of the Accident

Combustible materials will not normally be stored at an ISFSI. Therefore, a credible fire would be very small and of short duration such as that due to a fire or explosion from a vehicle or portable crane.

However, a hypothetical fire accident is evaluated for the NUHOMS[®]-32PT System based on a fuel fire. The source of fuel is postulated to be from a ruptured fuel tank of the TC transporter tow vehicle. The bounding capacity of the fuel tank is 300 gallons and the bounding hypothetical fire is an engulfing fire around the TC. Direct engulfment of the HSM is highly unlikely. Any fire within the ISFSI boundary while the DSC is in the HSM would be bounded by the fire during TC movement. The HSM concrete acts as a significant insulating fire wall to protect the 32PT-DSC from the high temperatures of the fire.

M.11.2.10.2 Accident Analysis

The evaluation of the hypothetical fire event is presented in Section M.4.6.3. The fire thermal evaluation is performed primarily to demonstrate the confinement integrity and fuel retrievability of the 32PT-DSC. This is assured by demonstrating that the DSC temperatures and internal pressures will not exceed those of the blocked vent condition (see Section M.11.2.7) during the fire scenario. Peak temperatures for the NUHOMS[®]-32PT System components are summarized in Table M.4-16.

M.11.2.10.3 Accident Dose Calculations

The 32PT-DSC confinement boundary will not be breached as a result of the postulated fire/explosion scenario. Accordingly, no 32PT-DSC damage or release of radioactivity is postulated. Because no radioactivity is released, no resultant dose increase is associated with this event.

The fire scenario may result in the loss of TC neutron shielding should the fire occur while the 32PT-DSC is in the cask. The effect of loss of the neutron shielding due to a fire is bounded by that resulting from a cask drop scenario. See Section M.11.2.5.3 for evaluation of the dose consequences of a cask drop.

M.11.2.10.4 Corrective Actions

Evaluation of HSM or TC neutron shield damage as a result of a fire is to be performed to assess the need for temporary shielding (for HSM or cask, if fire occurs during transfer operations) and repairs to restore the TC and HSM to pre-fire design conditions.

M.11.3 References

- 11.1 American Nuclear Society, ANSI/ANS-57.9, Design Criteria for an Independent Spent Fuel Storage Installation (Dry Storage Type), 1992.
- 11.2 N14.5-1997, "Leakage Tests on Packages for Shipment," February 1998.
- 11.3 NUREG-1536, "Standard Review Plan for dry Storage Casks, Final Report," US Nuclear Regulatory Commission, January 1997.
- 11.4 ISG-5, Rev. 1, Confinement Evaluation.
- 11.5 American Society of Mechanical Engineers, ASME Boiler and Pressure Vessel Code, Section III, 1998 including 2000 addenda.

Table M.11-1
Comparison of Total Dose Rates for HSM with and without Adjacent HSM Shielding Effects

Distance from Nearest HSM Wall, 2x10 Array (meters)	Normal Case Dose Rate ⁽¹⁾ (mrem/hr)	Accident Case Dose Rate ⁽¹⁾ (mrem/hr)
10	27	54
100	0.4	0.80
500	1.1×10^{-3}	4.4×10^{-3}
600	4.2×10^{-4}	1.7×10^{-3}

⁽¹⁾ Air scattered plus direct radiation

**Table M.11-2
TC Bounding Accident Dose Rate Results**

Cask			
	Side (mrem/hr)	Top (mrem/hr)	Bottom (mrem/hr)
Neutron	3.78E+03	4.06E+01	9.54E+02
Gamma	1.07E+03	9.48E+01	7.58E+02
Total	4.64E+03	1.08E+02	1.70E+03
1-Meter from Cask			
	Side (mrem/hr)	Top (mrem/hr)	Bottom (mrem/hr)
Neutron	1.29E+03	1.26E+01	9.10E+01
Gamma	3.88E+02	1.70E+01	1.85E+02
Total	1.67E+03	2.65E+01	2.76E+02
2-Meters from Cask			
	Side (mrem/hr)	Top (mrem/hr)	Bottom (mrem/hr)
Neutron	6.43E+02	6.33E+00	3.03E+01
Gamma	2.34E+02	8.89E+00	8.07E+01
Total	8.77E+02	1.46E+01	1.11E+02

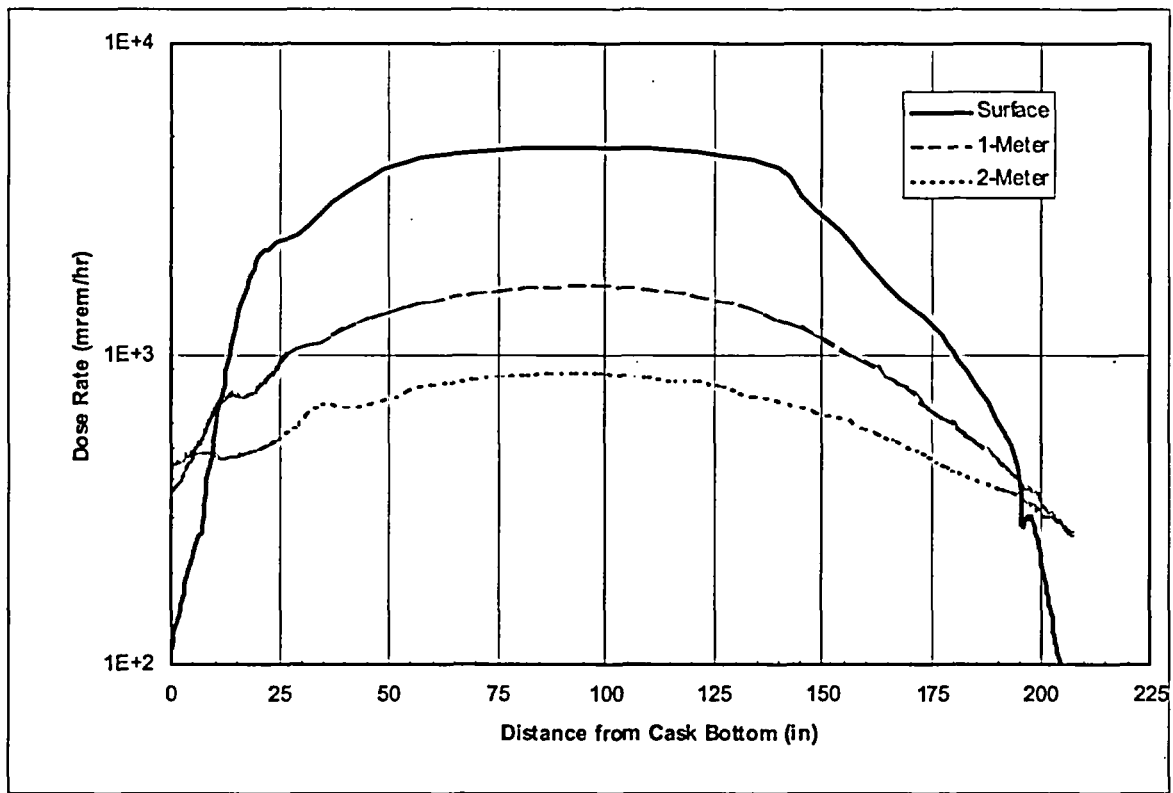


Figure M.11-1
TC Bounding Accident Dose Rate Distribution

M.12 Conditions for Cask Use - Operating Controls and Limits or
Technical Specifications

The Technical Specification changes, due to the addition of 32PT DSC to the NUHOMS® System, are included in Attachment A to NUHOMS® CoC 1004 Amendment No. 5.

M.13 Quality Assurance

Chapter 11.0 provides a description of the Quality Assurance Program to be applied to the safety related and important to safety activities associated with the standardized NUHOMS® System. For the 32PT DSC system, the following is added to clarify the contents of Section 11.2:

“In lieu of the requirements listed in paragraphs A through H, Category A items may also be procured as commercial grade items and dedicated by in accordance with the guidelines of EPRI NP-5652.”

M.14 Decommissioning

There is no change from the decommissioning evaluation presented in Section 9.6 due to the addition of 32PT DSC to the NUHOMS® System.